Human S100A8 and S100A9 Scavenge Pro-inflammatory Hypohalous Acids in Disease

Author:
Gomes, Lincoln Henry

Publication Date:
2012

DOI:
https://doi.org/10.26190/unsworks/15681

Human S100A8 and S100A9 Scavenge Pro-inflammatory Hypohalous Acids in Disease

by

Lincoln Henry Gomes

A thesis submitted in fulfillment of the requirements
for the degree of Doctor of Philosophy

Faculty of Medicine
The University of New South Wales
2012

THE UNIVERSITY OF NEW SOUTH WALES
Thesis/Dissertation Sheet

Surname or Family name: Gomes
First name: Lincoln **Other name/s:** Henry
Abbreviation for degree as given in the University calendar: PhD
School: Medical Sciences **Faculty:** Medicine
Title: S100A8 and S100A9 scavenge pro-inflammatory hypohalous acids in disease

Abstract 350 words maximum: (PLEASE TYPE)

S100A8, S100A9 and S100A12 are generally considered pro-inflammatory proteins because their expression is elevated in chronic inflammatory disorders. Hypohalous acids generated by activated phagocytes are scavenged by murine S100A8 and S100A9, suggesting a protective role in oxidative stress, but effects on human recombinant S100A8 and S100A9 are undefined. Hypohalous acids at low molar ratios (1:1) promoted structural changes in human S100A8 and S100A9 *in vitro*, generating two novel post-translational modifications on Cys_{42} in S100A8, defined as oxathiazolidine-oxide and dioxide. Particular methionine residues in S100A9 were also modified.

S100A8 and S100A9 are increased in respiratory diseases in which reactive oxygen species are implicated and anti-oxidant mechanisms compromised. Oxidized S100A8 (oxS100A8) was prominent in asthmatic lung and significantly elevated in sputum, compared to controls, whereas S100A8 or S100A9 levels were not. Monomeric oxS100A8 was the major component in asthmatic sputum; modifications were similar to those generated by hypochlorous acid (HOCl) *in vitro*. Oxidized $Met_{63/81/94}$ were variously present in S100A9 from asthmatic sputum, only oxidized Met_{63} was seen in control sputum. oxS100A8 and oxS100A9 did not form heterocomplexes and neutrophil adhesion to fibronectin, properties typical of the native complex, and antimicrobial activity was significantly compromised.

Inflammation is associated with increased risk of cardiovascular disease in chronic autoimmune diseases such as systemic lupus erythematosus (SLE) and with asthma. Serum levels of S100A8, S100A9 and S100A8/A9 were similar in patients with SLE and controls. Native and oxS100A8 were not apparent in Western blots of serum, and were located in HDL, possibly due to interaction with ApoAI. Carotid artery extracts indicated oxidant scavenging by S100A8 and S100A9. S100A8 protection of lipid-free ApoAI against oxidation by HOCl was Cys_{42}-dependent. S100A8 and S100A9 reduced generation of hypochlorite-oxidized proteins in endothelial cells, suggesting a protective role for these proteins in the vasculature.

Results have broad implications in diseases where hypohalous acid oxidants are generated and support the notion that oxidant scavenging and subsequent post-translational modifications are functionally important, emphasizing a role for S100A8 and S100A9 in redox homeostasis in inflammation.

ORIGINALITY STATEMENT

‘I hereby declare that this submission is my own work and to the best of my knowledge it contains no materials previously published or written by another person, or substantial proportions of material which have been accepted for the award of any other degree or diploma at UNSW or any other educational institution, except where due acknowledgement is made in the thesis. Any contribution made to the research by others, with whom I have worked at UNSW or elsewhere, is explicitly acknowledged in the thesis. I also declare that the intellectual content of this thesis is the product of my own work, except to the extent that assistance from others in the project's design and conception or in style, presentation and linguistic expression is acknowledged.’

Signed …….....

Date …….....

Dedicated to Shirley Meades and Ann Gomes. You have given me many precious memories and inspired me to live a meaningful life. You will never be forgotten.

TABLE OF CONTENTS

LIST OF FIGURES

LIST OF TABLES

ABBREVIATIONS

$[Ca^{2+}]_i$	intracellular calcium concentration
°C	degree Celcius
4-HNE	4-hydroxynonenal
A	absorbance
AA	arachidonic acid
ABCA1	ATP-binding cassette transporter member 1
ACPA	anti-citrullinated peptide antibodies
ADAMTS	a disintegrin and metalloproteinase with thrombospondin motifs
AFM	atomic force microscopy
Ala	alanine
ALE	lipid peroxidation end product
AMP	antimicrobial peptides
ANOVA	analysis of variance
ApoAI(HDL)	ApoAI in HDL
ApoE/AI/B-100	apolipoprotein E/AI/B-100
Arg	arginine
Asn	asparagine
Asp	aspartic acid
ARDS	acute respiratory distress syndrome
BAEC	bovine aortic endothelial cell
BALF	bronchoalveolar lavage fluid
BCA	bicinchoninic acid

bHLH	basic helix-loop-helix
BILAG	The British Isle's Lupus Assessment Group 2004
CAD	coronary artery disease
cAMP	cyclic AMP
C/EBP	CCAAT/enhancer-binding proteins
CF	cystic fibrosis
CFU	colony forming unit
CGD	chronic granulomatous disease
CHO	Chinese hamster ovary
CIA	collagen-induced arthritis
CK	casein kinase
cNOS	constitutive nitric oxide synthase
CO	carbon monoxide
COPD	chronic obstructive pulmonary disease
COX	cyclooxygenase
CRP	C-reactive protein
Cys	cysteine
Cys_{42}-Ala_{42}S100A8	S100A8 protein where Cys_{42} is substituted with Ala
CVD	cardiovascular disease
Da	Dalton; kDa, kilodalton
DAMPS	damage-associated molecular patterns
Dex	dexamethasone
DMSO	dimethyl sulfoxide

DOPA	3,4-dihydroxyphenylalanine
dpc	days post-coitum
dsRNA	double stranded RNA
DTPA	diethylenetriamine pentaacetic acid
DTT	dithiothreitol
e.g.	for example
EGF	epidermal growth factor
ELISA	enzyme-linked immunosorbent assay
eNOS	endothelial nitric oxide synthase
EPC	ectoplacental cone
EPO	eosinophil peroxidase
ERK	extracellular signal-regulated kinase
ESI-MS	electrospray ionization mass spectrometry
et al.	et alia; and others
FA	fatty acid
FEV1	forced expiratory volume
FGF	fibroblast growth factor
fMLP	formyl-methionine-leucine-phenylalanine
FPLC	fast protein liquid chromatography
FVC	forced vital capacity
GAG	glycosaminoglycan
GC	glucocorticoids
G-CSF	granulocyte colony-stimulating factor

GFAP	glial fibrillary acidic protein
Gln	glutamine
Glu	glutamic acid
Gly	glycine
GM-CSF	granulocyte-macrophage colony-stimulating factor
GPx	glutathione peroxidase
Grx	glutaredoxin
GST	glutathione-S-transferase
GSH	glutathione
GSSG	oxidized glutathione
h	human, when referring to hS100 protein
HCl	hydrochloric acid
HDL	high-density lipoprotein
His	histidine
His(+16)	histidine with addition of one oxygen
HMEC	human microvascular endothelial cells
HMGB1	high-mobility group protein B1
$HO^{\cdot}$	hydroxyl radical
HO-1	heme oxygenase-1
HOBr	hypobromous acid
HOCl	hypochlorous acid
HOP	hypochlorite oxidized proteins
HOI	hypoiodous acid
HOSCN	hypothiocyanous acid

hrs	hours
HSA	human serum albumin
HUVEC	human umbilical vein endothelial cells
IBD	inflammatory bowel disease
IBS	irritable bowel syndrome
ICAM-1	intracellular adhesion molecule-1
IDA	information-dependent acquisition
i.e.	id est; that is to say
IF	intermediate filament
IFN	interferon
IL	interleukin
iNOS	inducible nitric oxide synthase
IPF	idiopathic pulmonary fibrosis
i.p. injection	intraperitoneal injection
IPTG	isopropyl-β-D-thiogalactosidase
l	liter (ml, milliliter; µl, microliter)
LAT	linker for activation of T cells
LC/MS	liquid chromatography-mass spectrometry
LDL	low-density lipoprotein
LPS	lipopolysaccharide
Lys	lysine
m	murine, when referring to mS100 protein
mAb	monoclonal antibody
MAPK	mitogen-activated protein kinase

MARCKS	myristoylated alanine-rich C kinase substrate
mBSA	methylated bovine serum albumin
MC	mast cell
MCP-1	monocyte chemotactic protein-1
M-CSF	monocyte colony-stimulating factor
MDA	malondialdehyde
MDSC	myeloid-derived suppressor cells
Met	methionine
Met(O)	methionine sulfoxide
MF	microfilament
MIC	minimum inhibitory concentration
MIF	migration inhibitory factor
min	minute
MIP	macrophage inhibitory protein
MMP	matrix metalloproteinase
MPO	myeloperoxidase
MRP-8	MIF-related protein-8
MRP-14	MIF-related protein-14
MS	mass spectrometry
MS/MS	tandem mass spectrometry
MSR	methionine sulfoxide reductase
MT	microtubule
NADPH	nicotinamide adenine dinucleotide phosphate
NEM	N-ethylmaleimide

NET	neutrophil extracellular trap
NMR	nuclear magnetic resonance
nNOS	neuronal nitric oxide synthase
NO	nitric oxide
NOX	NADPH oxidase when referring to the NOX family of enzymes
$O_2^{\cdot -}$	superoxide anion
$ONOO^-$	peroxynitrite
o-Tyr	hydroxyphenylalanine
oxLDL	oxidized low density lipoproteins
ox	oxidized, when referring to S100 proteins or ApoAI/ApoAI(HDL)
PAF	platelet activating factor
PAGE	polyacrylamide gel electrophoresis
PAMP	pathogen-associated molecular protein
PBS	phosphate buffered saline
PBMC	peripheral blood mononuclear cell
PDGF	platelet-derived growth factor
PGE2	prostaglandin E2
pH	power of hydrogen; log (1/[H+]
PI3K	phosphotidylinositol 3-kinase
PKA	protein kinase A
PKC	protein kinase C
PKR	protein kinase R
PMA	phorbol 12-myristate 13-acetate
PMN	polymorphonuclear leukocytes

Poly I:C	polyinosinic acid-polycytidylic acid
PON1	paraoxonase 1
Pro	proline
Prx	peroxiredoxin
PtdlnsP	3-phosphorylated phosphatidylinositols
PVDF	polyvinylidene difluoride (membrane)
RA	rheumatoid arthritis
RAGE	receptor for advanced glycation end-products
rec	recombinant
RCC	reactive carbonyl compounds
RCT	reverse cholesterol transport
ROS	reactive oxygen species
RNA	ribonucleic acid (mRNA, messenger RNA)
RNS	reactive nitrogen species
RP-HPLC	reverse-phase high performance liquid chromatography
RSOH	sulfenic
RSO_2H	sulfinic
RSO_3H	sulfonic
RT	room temperature
s	second
S100A9*	truncated S100A9 isoform
S100A9-GSH	glutathionylated S100A9 by S-nitrosoglutathione
S100A9-SSG	S-glutathionylated S100A9

S100A15-S/L	S100A15 long/short isoform
SDS-PAGE	sodium dodecyl sulphate polyacrylamide gel electrophoresis
SELDI-TOF	surface-enhanced laser desorption/ionization – time of flight
Ser	serine
siRNA	small interfering RNA
SLE	systemic lupus erythematosus
SLEDAI	systemic lupus erythematosus activity index
SMC	smooth muscle cells
SNO	S-nitrosylated, when referring to protein
SOD	superoxide dismutase
STAT	signal transducer and activator of transcription
TBS	tris-buffered saline
TGF	transforming growth factor
Thr	threonine
TLR	toll-like receptor
TMB	tetramethylbenzidine
TNF	tumour necrosis factor
TOF	time of flight
Trp	tryptophan
Trp(+16)	tryptophan with addition of one oxygen
Trx	thioredoxin
Tween 20	polyoxyethylenesorbitan monolaurate
Tyr	tyrosine

UV	ultraviolet light
V	volt
VCAM-1	vascular cell adhesion molecule-1
VP	ventral prostate, when referring to S100 ventral prostate

ACKNOWLEDGEMENTS

Completion of this thesis would not have been possible had it not been for the support of a great number of people.

To my supervisor, Prof. Carolyn Geczy, I am indebted to you for giving me the opportunity to undertake this project. I am extremely grateful for your patience, guidance and support.

To my co-supervisor, Dr. Ken Hsu, thank you for providing advice and technical support during my PhD and making the lab a great place to work.

To A/Prof. Mark Raftery, your support and kindness are truly appreciated. Your knowledge of mass spectrometry and protein chemistry is awe-inspiring and it has been a privilege to learn from you over the years. Your input has been invaluable.

To my collaborators, Prof. Paul Thomas, Prof. Hazel Mitchell, Prof. Roland Stocker, Dr. Shane Thomas, Dr. Cacang Suarna and Thuan Thai, thank you for allowing me into your labs, and for teaching me new techniques. You all made me feel part of your labs and I greatly appreciate the level of trust and freedom afforded to me while I worked with you all.

To past members of our research group, Dr. Jing Zhao, Dr. Weixing Yan, Drs. Yasumi and Ikuko Endoh, and Georgia Margalit, it is rare to work with so many kind and friendly people willing to offer advice and support. A particular thanks to Drs. Jesse Goyette and Esther Lim, your friendship, advice and help in the lab were invaluable. I hope I did not ask you too many questions. To current members of our lab, thank you for providing a friendly and pleasant environment to work in, your friendship is invaluable.

To all my friends who have ridden the highs and lows with me over the years, your friendship is priceless.

To my family, your love, support and encouragement is very much appreciated. To my mother and father, thank you for providing me with a stable environment to grow up in and allowing me the freedom to pursue my interests.

Lastly, to my wife Yuen Ming, words cannot express how much you have inspired me to be positive and selfless. I would not have been able to complete this thesis without you.

PUBLISHED WORK AND AWARDS FROM THIS THESIS

Publications

1) Geczy, C.L., Tessier, P.A., **Gomes, L.** Calgranulins in Inflammation, in the Neutrophils: New Outlook for Old Cells (3rd Edition); DI Gabrilovich, (ed.), Imperial College Press; in the press (2012).

2) **Gomes, L.***, Raftery, M.*, Yan, W.X., Goyette, J., Mitchell, H., Thomas, P.S., Geczy, C.L., S100A8 and S100A9 - Oxidant scavengers in inflammation. * Equal first author. Manuscript in preparation.

3) **Gomes, L.**, Raftery, M., Suarna, C., Lim, S.Y., Thai, T., Thomas, S., Stocker, R., Geczy, C.L., S100A8: Implications for new protective mechanisms in atherogenesis. Manuscript in preparation.

Abstracts (as presenting author)

1) **Gomes, L.**, Raftery, M., Zhao, J., Yan, W.X., Thomas, P.S., Geczy, C.L. Novel post-translational oxidative modifications in S100A8 in sputum from stable asthmatics. Poster presented at the 38th Australasian Society for Immunology Annual Scientific Meeting, Canberra, ACT (December, 2008).

2) **Gomes, L.**, Raftery, M., Zhao, J., Yan, W.X., Thomas, P.S., Geczy, C.L. Novel post-translational oxidative modifications in S100A8. Poster presented at the 5th Joint Meeting of the Societies for Free Radical Research Australasia and Japan, Sydney University, NSW (December 2009).

3) **Gomes, L.**, Raftery, M., Zhao, J., Yan, W.X., Thomas, P.S., Geczy, C.L. S100A8 – An oxidant scavenger and immune modulator in allergic inflammation. Poster presented at the 39th Australasian Society for Immunology Annual Scientific Meeting, Gold Coast, QLD (December 2009).

4) **Gomes, L.**, Raftery, M., Zhao, J., Lim, S.Y., Yan, W.X., Mitchell, H., Thomas, P.S., Geczy, C.L. An oxidant scavenger and immune modulator in allergic inflammation. Poster presented at the 14th International Congress of Immunology, Kobe, Japan (August, 2010).

Awards

Awarded “The International Journal of Biochemistry and Cell Biology Young Investigator Award” for best poster. Poster presented at the 5th Joint Meeting of the Societies for Free Radical Research Australasia and Japan, Sydney University, NSW (December 2009).

ABSTRACT

S100A8, S100A9 and S100A12 are proposed as damage-associated molecular pattern molecules (DAMPs) due to their modulation of inflammatory responses via interaction with the receptor for advanced glycation end products and toll-like receptor-4, and are generally considered pro-inflammatory because of their elevated expression in chronic inflammatory disorders.

However, emerging evidence suggests that S100A8 and S100A9 may have pleiotropic roles in inflammation, and recent studies implicate anti-inflammatory functions. For example, LPS induction of S100A8 in murine macrophages and human macrophages and monocytes is dependent on the anti-inflammatory cytokine IL-10 and anti-inflammatory glucocorticoids induce or amplify expression.

S100A8 and S100A9 are constitutively expressed in neutrophils and induced in activated macrophages, cells that produce high amounts of reactive oxygen species (ROS), which, in excess, can cause oxidative tissue damage. Hypohalous acids are scavenged by murine S100A8 and S100A9 resulting in post-translational modifications. Hypochlorous acid generates inter- and intra-molecular sulfinamide bonded murine S100A8, suggesting a protective role in oxidative stress. More recently, S100A8 was shown to become S-nitrosylated by NO donors, and this adduct suppressed mast cell activation and leukocyte adhesion and extravasation induced by mast cell activation in rat mesenteric microcirculation. S100A9 can undergo S-glutathionylation, and this significantly increased leukocyte adhesion to fibronectin, whereas in the presence of S100A8, adhesion was significantly decreased. Together these results suggest that post-translational modifications of S100A8 and S100A9 may negatively regulate inflammatory responses. However, effects of hypohalous acids on S100A8 and S100A9 are undefined.

Chapter 3 shows that a 1:1 molar ratio of HOCl:S100A8 was sufficient to generate the oxidized monomer and dimer, resistant to DTT reduction. Exposure to the same molar ratio of HOBr only generated monomeric oxidized S100A8. A 2-fold excess of HOCl caused aggregation demonstrating the sensitivity of S100A8 to HOCl. HOCl-oxidation of a Cys_{42}-Ala_{42}S100A8 mutant failed to produce oxidized dimer, suggesting a Cys_{42}-dependent mechanism. S100A9 was less sensitive to HOCl, generating oxidized monomer and disulfide-linked dimer. Structural changes in human S100A8 and S100A9 after exposure to hypohalous acids *in vitro* were examined by mass spectrometry (MS). In S100A8, HOCl oxidation of Met_{78} to Met_{78} sulfoxide ($Met_{78}(O)$) was observed, together

with oxidation of Trp_{54} and $His_{17/27/83}$ (addition of one oxygen; +16 Da) and two novel post-translational modifications on Cys_{42}, defined as oxathiazolidine-oxide and dioxide. In HOBr-oxidized S100A8, only Cys_{42}-sulfonic acid and oxidized Trp_{54} (addition of one oxygen; +16 Da) adducts were obvious. S100A8 oligomers were investigated, but there was no compelling evidence for chlorination of Tyr residues or amino acid carbonylation. $Met_{63/81/83/94}$ were modified to Met(O) in HOCl-oxidized S100A9, with no compelling evidence for Cys_3 modification. Results confirmed active scavenging of low molar ratios (1:1) of hypohalous acids *in vitro*.

S100A8 and S100A9 are increased in respiratory diseases in which ROS are implicated, and anti-oxidant mechanisms compromised. Chapter 4 shows that oxidized S100A8 was prominent in asthmatic lung and significantly elevated in sputum, compared to patients with bronchiectasis or healthy controls, whereas, S100A8, S100A9 and S100A12 levels were not. Oxidized monomeric S100A8 was the major component in enriched fractions of asthmatic sputum and modifications were similar to those generated by HOCl *in vitro*. Met_1(O) was identified in control and asthmatic sputum; Met_1 is not present in the recombinant S100 proteins. Oxidized $Met_{63/81/94}$ were variously present in S100A9 enriched from asthmatic sputum; only Met_{63}(O) was seen in control sputum. Oxidized S100A8 and S100A9 did not form heterocomplexes and neutrophil adhesion to fibronectin, typical of the native complex, was compromised following HOCl oxidation, contrasting with the strong adhesion observed with fMLP-treated neutrophils. Interestingly, pre-incubation of neutrophils with either native or oxidized S100A8 and S100A9 reduced fMLP-induced adhesion to fibronectin, uncovering a new anti-inflammatory function. Oxidation of S100A8 and S100A9 also significantly compromised the ability of the heterocomplex to reduce *Escherichia coli* growth.

Inflammation is associated with increased risk of cardiovascular disease in chronic autoimmune diseases such as systemic lupus erythematosus (SLE) and with asthma. Chapter 5 shows that serum levels of S100A8, S100A9 and S100A8/A9 were similar in patients with SLE and controls. Native and oxidized S100A8 were not apparent in Western blots of serum, and were located in HDL, possibly due to interaction with ApoAI. Our group previously showed that S100A8/oxidized S100A8 and S100A9 were present in macrophages, foam cells and neovessels in human atheroma. In this thesis, analysis of S100A8 from carotid artery extracts enriched by RP-HPLC indicated some oxidant scavenging by S100A8 and S100A9. MPO binds ApoAI, and chronic excesses of ROS promote formation of dysfunctional, pro-inflammatory HDL, via oxidation of

ApoAI. Presently, S100A8 protected lipid-free ApoAI against oxidation by HOCl in a Cys_{42}-dependent manner, indicating that the single Cys residue was largely responsible for oxidant scavenging. S100A8 and S100A9 also reduced generation of hypochlorite-oxidized proteins in endothelial cells, suggesting a protective role for these proteins in the vasculature.

Taken together, these results have broad implications in diseases where hypohalous acid oxidants are generated, and support the notion that oxidant scavenging and subsequent post-translational modifications are functionally important, emphasizing a role for S100A8 and S100A9 in redox homeostasis in inflammation.

CHAPTER 1: INTRODUCTION

1.1 THE S100 PROTEIN FAMILY

1.1.1 NOMENCLATURE

The first member of the S100 protein family was isolated from a mixture of proteins purified from bovine brain by Moore in 1965 [1]. The protein was given the name “S100” because of its solubility in 100% ammonium sulphate solution at neutral pH [1]. Since their discovery, the nomenclature has undergone significant revision and redefinition, particularly by Schäfer *et al.* [2]. This was based around the relative chromosomal location of the S100 proteins. The prefix S100A denotes those genes on the 1q21 locus, and the numbered suffix indicates their relative position in the cluster. S100 genes lying outside this locus are given the suffix S100, followed by a different letter, for example, S100G [3]. This was designed to indicate homologies within the S100 family and to indicate that some genes are located within different loci of the genome. Non-functional pseudogenes are designated by the symbol of the functional homologue suffixed with P, such as S100A11P [4]. Genes that are highly similar to a known gene, but of unknown functional relevance, are assigned the suffix L, for example, S100A7L1 to L4 represent newly-identified copies of the S100A7 gene [5, 6]. As with many systems of classification there are situations where these rules may not apply. For example, S100A12 lies between S100A8 and S100A9, but because it was discovered after the whole gene family was classified, the name has remained. Ravasi *et al.*, described three new S100 genes, S100A15, S100A16 and S100A17, all of which were conserved in the rodent and human genomes [7].

S100A8, S100A9 (the focus of this thesis) and S100A12 have had several acronyms since their discovery. Initially, S100A8 and S100A9 were commonly known as migration inhibitory factor (MIF)-related proteins-8 and -14 (MRP8 and MRP14). These proteins were purified as MIF and annotated according to their masses (kDa) [8]. However, the acronyms of MRP8 and MRP14 are now understood by some authors to mean ‘myeloid-related’ proteins, a name that still persists [8]. The acronym ‘calgranulin’ refers to these neutrophil-derived proteins and their calcium-binding properties. S100A8 is also known as calgranulin A, S100A9 as calgranulin B and S100A12 as calgranulin C. The heterocomplex S100A8/A9 is widely known as calprotectin to reflect its antimicrobial effects [9] (Table 1.1).

The nomenclature defined by Schäfer *et al.* [2] and Marenholz *et al.* [3] will be used in this thesis. For S100A8, S100A9 and S100A12, the collective name of ‘calgranulins’ will be used for these three inflammation-related proteins, and calprotectin for the S100A8/A9 complex where relevant.

Table 1.1: The S100 protein family

Gene name	Synonyms	Discovery (year)	Refs.
S100A1	S100A, S100, S100α	Isolated from bovine brain (1965)	[1, 10]
S100A2	S100L, CaN19	Identified by sequence homology with S100A10 in bovine lung (1989)	[11]
S100A3	S100E	Sequence analysis of S100 gene cluster (1993)	[12]
S100A4	MTS1, CAPL, p9Ka, pEL98, 18A2, 42A	cDNA isolated from cultured murine fibroblasts (1983)	[13]
S100A5	S100D	Sequence analysis of S100 gene cluster (1993)	[12]
S100A6	CACY, 2A9, CABP, 5B10, PRA	Isolated from cDNA clones of growth factor-inducible mRNAs (1986)	[14]
S100A7	PSOR1	Identified in psoriatic skin (1991)	[15]
S100A7L2	S100A7b	Identified as a copy of S100A7 gene (2003)	[6]
S100A7L3	S100A7d	Identified as a copy of S100A7 gene (2003)	[6]
S100A7L4	S100A7e	Identified as a copy of S100A7 gene (2003)	[6]
S100A8	CAGA, MRP-8, P8, CGLA, MIF, NIF, L1Ag, MA387, 60B8AG, CFAG, CP-10	Purified from myeloid cells (1983)	[7, 16] [17-19]
S100A9	CAGB, MRP-14, P14, CGLB, MIF, NIF, L1Ag, MAC387, 60B8AG, CFAG	Purified from myeloid cells (1983)	[7, 16] [17, 18]
S100A10	ANX2LG, CAL1L, CLP11, ANX2L, p11, p10, 42C, GP11	Identified in bovine intestinal epithelium as a potential substrate for Epidermal Growth Factor (EGF)-receptor tyrosine kinase (1985)	[20]

Gene name	Synonyms	Discovery (Year)	Refs.
S100A11	S100C, MLN70, calgizzarin	Smooth muscle cells of chicken gizzard (1991)	[21]
S100A11P	S100A14	Analysis of chromosome 7q22 (2001)	[4]
S100A12	CAAF1, CGRP, MRP-6, p6, ENRAGE	Pig granulocytes (1994)	[22]
S100A13		Identified by cDNA sequence homologies with other S100 proteins (1996)	[23]
S100A14	BCMP84, S100A15	Identified from a lung cancer cell line cDNA library (2002)	[24]
S100A15	S100A7L1, S100A7a	Identified as a copy of S100A7 gene after transcriptome database search (2003)	[6]
S100A16	S100F, DT1P1A7, MGC17528	Identified in tumours(2004)	[5]
S100B	S100β, neural extension factor (NEF)	Isolated from bovine brain (1965)	[1]
S100P		Isolated from human placenta (1992)	[25]
S100Z		Identified from a human prostate cDNA library (2001)	[26]
S100G	Calbindin D9K, CaBP9k, CABP1	Isolated from rat intestinal mucosa (1967)	[27]

Adapted from [7].

1.1.2 S100 GENE STRUCTURE

The S100 protein family is the largest subgroup within the super-family of proteins that contain the Ca^{2+}-binding EF-hand motif [5]. The EF-hand is a basic functional and evolutionarily conserved domain that consists of 29 amino acids arranged in a helix-loop-helix conformation [28].

1.1.2.1 Chromosome location

Of the human genes, twenty are located within the epidermal differentiation complex, tightly clustered in region 1q21 of human chromosome 1 (reviewed in [29]). In the mouse, an analogous cluster is located at region 3F2 of mouse chromosome 3 where 16 of the 19 genes are located [7, 10, 30], and in the rat at position 2q34 [5, 7]. Interestingly, within the 1q21 gene cluster, there are further subgroups of closely arranged S100 genes. For example a contiguous stretch of 15 kb genomic sequence contains four S100 genes (S100A3, A4, A5, and A6). In addition, S100A1 neighbours S100A13, and S100A15, S100A7, S100A8, S100A12, S100A9 map within a short distance. Remarkably, S100A10, S100A11 and S100A16 are positioned 1.5 Mb away from the core gene cluster, separated by epidermal differentiation genes (Fig. 1.1) [2, 7, 10, 26, 31-34]. There are four exceptions in the human genome, S100G (Xp22), S100B (21q22), S100P (4p16) and S100Z (5q13) (gene locations are summarized in Table 1.2) [2, 7, 10, 23, 24, 26, 31, 32, 35, 36].

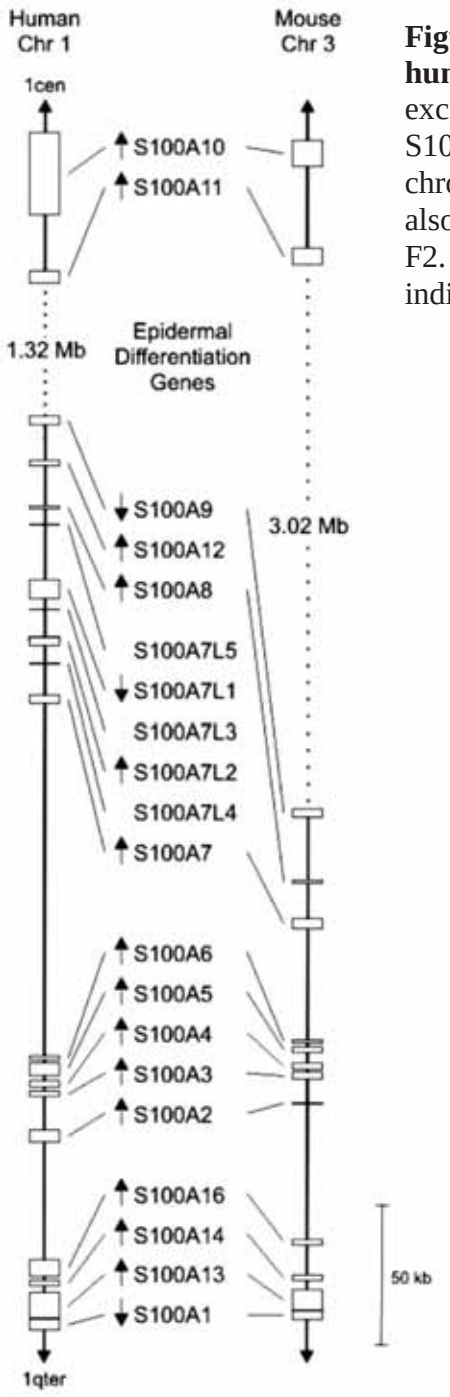

Figure 1.1: Chromosomal location of human and mouse S100 genes. With the exception of S100B, S100P, S100Z and S100G, S100 genes are closely clustered on chromosome 1q21. Mouse S100 proteins are also closely clustered on chromosome 3F1-F2. Transcriptional direction of the genes is indicated by arrows [5].

Table 1.2: S100 gene location

S100 proteins	Human	Mouse	Rat
S100A1	1q21	3F1	2q34
S100A2	1q21	3F1	Not present
S100A3	1q21	3F1	2q34
S100A4	1q21	3F1	2q34
S100A5	1q21	3F1	2q34
S100A6	1q21	3F1	2q34
S100A7	1q21	Not present	Not present
S100A7/L2	1q21	Not present	Not present
S100A7/L3	1q21	Not present	Not present
S100A7/L4	1q21	Not present	Not present
S100A8	1q21	3F1	2q34
S100A9	1q21	3F1	2q34
S100A10	1q21	3F2	2q34
S100A11	1q21	3F2	2q34
S100A11P	7q22-q31	Not present	Not present
S100A12	1q21	Not present	Not present
S100A13	1q21	3F1	2q34
S100A14	1q21	3F1	2q34
S100A15	1q21	Not present	Not present
S100A16	1q21	3F1	2q34
S100B	21q22	10C1	20p12
S100G	Xp22	XF4	Xq21
S100P	4p16	Not present	Not present
S100Z	5q14	13D1	Not present

Adapted from [5, 7].

1.1.2.2 Genomic organization and S100 isoforms

The majority of S100 proteins typically consist of three exons and two introns; the first exon is non-coding. The coding sequence is within the second and third exons [32, 37]. Only four genes have distinctly different coding and non-coding regions. S100A4 and S100A5 genes have four exons [38, 39] with coding sequences in exons 3 and 4. The coding regions of the S100A11 [40] and S100A14 [24] genes are located within exon 3 (Fig. 1.2).

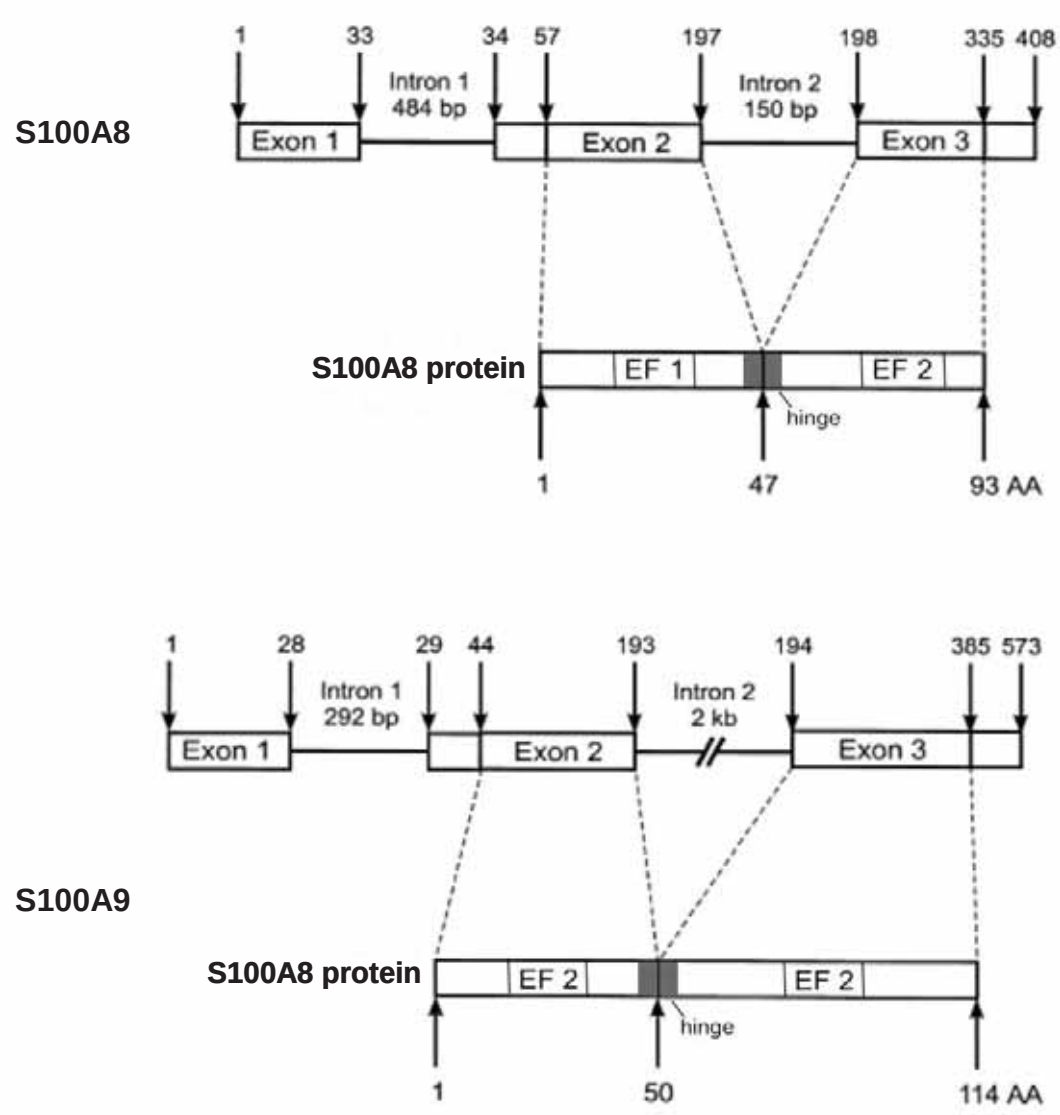

Figure 1.2: Genomic organization of S100A8 and S100A9. The S100 genome typically consists of three exons and two introns. The sequence within exons 2 and 3 encode the two EF hands, whereas intron 2 codes for the hinge region. Adapted from [41].

Isoforms of some S100 proteins are reported, but little is known concerning their functional significance. For example, S100A4 and S100A15 have two distinct isoforms. S100A4 isoforms are the result of alternate splicing of the first two exons. The long transcript encodes all four exons, whereas the short transcript lacks the second exon [42]. The only difference between the two isoforms is the 5' untranslated region, and both transcripts have the same RNA stability. The long transcript is mainly expressed in HeLa cells, whereas the short transcript was found in lung carcinoma cell lines. In RNase protection assays, the short transcript was more efficiently transcribed [42].

S100A15 also has splice variants. Interestingly, it has 93% amino acid sequence homology to S100A7. In its normal form, S100A15 has 101 amino acids containing two potential EF-hand motifs [43]. The differences between S100A15 and S100A7 are related to amino acids important for the structure of the EF-hand domain (Gly for Arg at amino acid position 22, Gly for Asp at position 25) or in the Ca^{2+}-binding (Glu for Asp at position 28) [43]. The splice variants of S100A15 include long (S100A15-L) and short (S100A15-S) isoforms generated by alternate splicing of the 3' and 5' untranslated regions [43]. Both S100A15 transcripts were seen in non-lesional and lesional psoriatic skin compared with normal skin [43] and expression levels of the short isoform were increased >20-fold in lesional skin, whereas the long form is >70-fold higher, compared to normal tissue [43]. Many studies suggest that S100A15-L is more abundant, although this is still debated [44].

Human S100A9 (hS100A9) has two isoforms; the truncated (S100A9*) isoform is translated from an alternate start codon (Met_5). This does not exist in murine S100A9 (mS100A9) [45-47].

Finally, S100A5 has two Met start codons. The first translates to a 12,813 Da protein, the second to a 10,744 Da protein. Of the two, the shorter one is most likely to be present in tissues [12, 39].

1.1.2.3 Phylogeny and evolution of S100 proteins

EF-hand proteins, such as troponin C, are found in invertebrates and in calmodulin in protozoa [5]. S100 proteins may have evolved from a calmodulin-type ancestor by domain swapping and subsequent loss of two EF- hands [7, 48, 49]. S100 proteins have so far only been isolated from vertebrates, *Squalus acanthias* is the lowest organism known to express S100 protein. This organism contains a protein closely related to S100A1, suggesting that S100A1 is the ancestral member [7]. Analysis of available

genomes of non-vertebrate eukaryotes such as nematodes, insects and protozoa yielded no S100-like sequences [5]. Until recently, the majority of publications focus on mammalian family members [50]. In 2008, data mining studies in the teleost fish indicated that the S100 family predates the diversion of bony and cartilaginous fish [50]. Given the clustered organization and conserved gene structure, it is realistic to hypothesize that S100 genes evolved from a common ancestor (Fig. 1.3) [5].

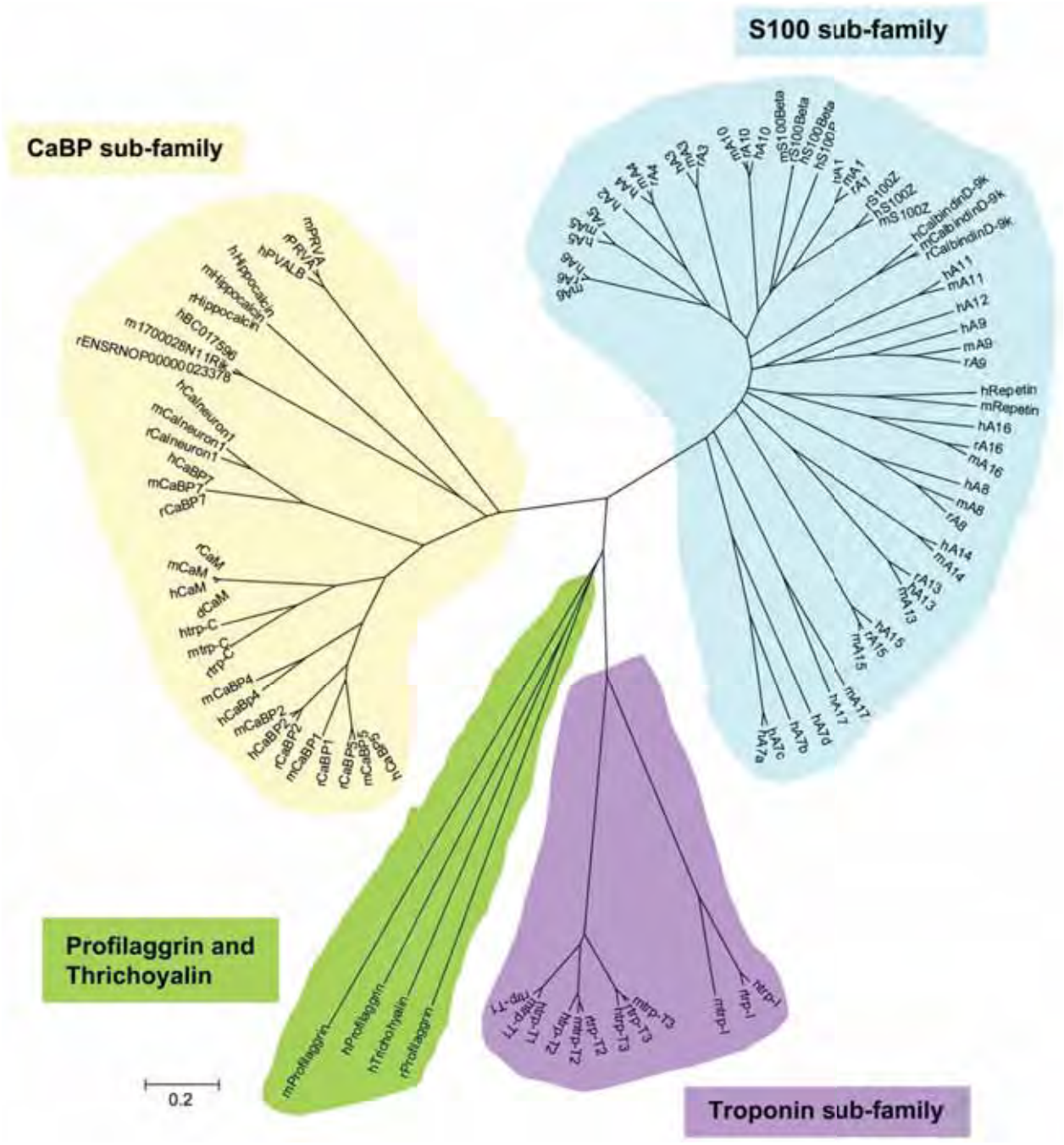

Figure 1.3: Phylogeny of the EF-hand family. A schematic representing the four distinct groups belonging to the EF-hand family, illustrating that the S100, CaBP, troponin and profilaggrin and thrichoyalin sub-families evolved from a common ancestor. From [7].

The sequence divergence in the S100A8 and S100A9 murine and human genes indicates rapid evolution of these genes, despite their presumed recent origin, possibly resulting from modular evolution – a process whereby conserved domains are swapped by homologous recombination of exons and by gene duplication. This allows proteins to evolve rapidly and at a molecular level it may generate a protein with a new function [7].

There are several examples of rapid diversification. S100A7 is 93% homologous with S100A15, but there is no rodent equivalent of S100A7 suggesting that these two genes diverged recently [43]. After extensive phylogenetic tree reconstructions on the basis of sequence alignments of the human, mouse and rat genes, Marenholz *et al.* suggests four major subgroups of S100 proteins in mammals that evolved from a common protein through multiple duplication events [5]. The first consists of S100B, S100A1, S100P and S100Z, with S100A10 and S100A11 closely related to it. The second subgroup consists of S100A2, S100A3, S100A4, S100A5 and S100A6. The phylogenetic distances between the proteins in this group are the smallest suggesting recent gene duplication. The third group includes S100A8, S100A9 and S100A12. The fourth subgroup comprises S100A13, S100A14 and S100A16 (Fig. 1.4) [5].

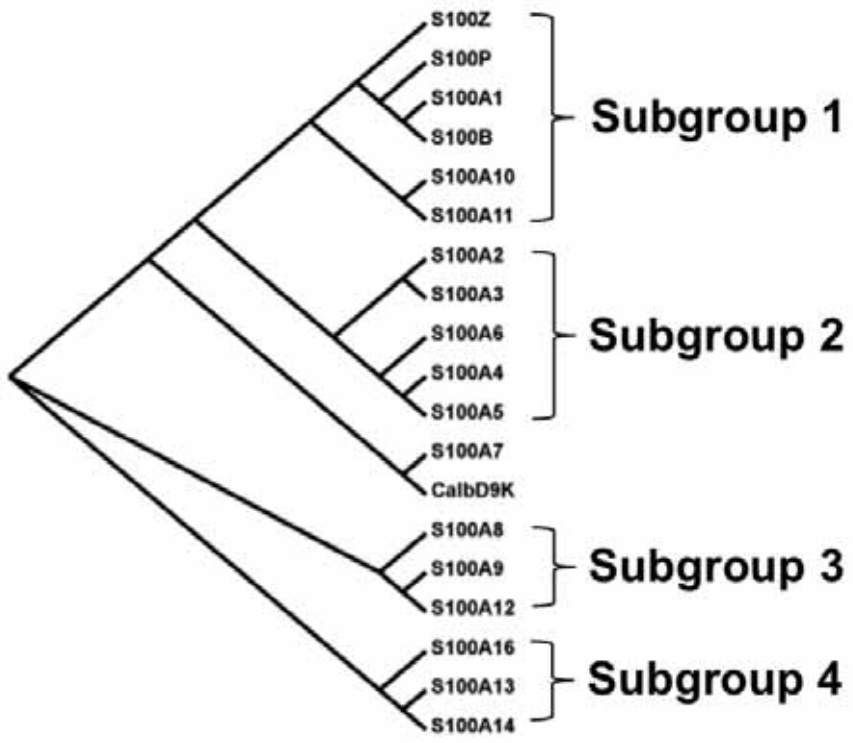

Figure 1.4: Phylogenetic tree of S100 proteins. S100 proteins can be divided into four major branches, which comprise evolutionary related S100 proteins. Adapted from [5].

The similarities between amino acid sequences of rodent and human S100 proteins have been well examined. For S100s with rodent orthologues, the proteins generally exhibit well-conserved amino acid sequence identity between rodent and human (~90% amino acid identity), with the exception of S100A8, S100A9 (~60% amino acid homology), and S100A15 (32% sequence identity) [7]. Of interest is the lack of S100A12, S100A2, S100A7 or S100P in the rodent genome [7, 51]. The duplication and divergence seen in the human genome support the idea of rapid evolution and subsequent expansion of the S100 protein family, and may also explain why S100A12, S100A2, S100A7 and S100P are absent in the rodent and mouse [7]. Isoforms of S100A7 genes may be largely non-functional in humans.

One explanation is that pathogenic microorganisms may influence diversity of antigen-recognition molecules. By analyzing the mean divergence of 14 different families of host-defense proteins, Murphy showed that the most divergent groups (relative to the human-rodent split) were those proteins related to extracellular or transmembrane components of intracellular signalling systems. More specifically, those dedicated to the development and/or activation of lymphocytes and phagocytic cells that mediate the inflammatory response and defense of the host against microbial infection [52]. This subset of proteins includes interleukins, interferons, colony-stimulating factors, chemoattractants and chemokines [52]. Hence, the differing sequence homologies of some S100 proteins in rodent and man could result from selective pressure brought on by exposure of these proteins to a multitude of bacterial pathogens. The calgranulins and S100A7/A15 are involved in several aspects of inflammatory responses, and because the host is potentially exposed to frequent assault by pathogens, host defense proteins and receptors are more commonly less conserved between species compared to those proteins and receptors involved in regular physiological processes [52]. This may explain the sequence divergence seen in the calgranulins and S100A7/A15 due to their importance in host defense, whereas other S100 proteins may be more conserved because their roles are not consistently challenged.

Another explanation for inter-species variation could be because of rapid evolution and expansion as a result of modular evolution, whereby, conserved domains were swapped by homologous recombination of exons, and by gene duplication [53, 54].

There is, however, one rodent S100 protein that has no human ortholog, S100VP (S100 ventral prostate, also known as S100RVP, S100 rat ventral prostate) [55, 56]. Rat S100VP is ~55% similar and ~33% identical to the amino acid sequence of human and

mouse S100A13, and human S100A7 (~53% similarity, ~24% identity) [55]. S100VP is expressed in rat ventral prostate epithelial cells and is regulated by androgens [55], but its function is still largely unknown. Oram *et al.* propose that it may be involved in Ca^{2+} homeostasis [55] however its function in humans is unknown, due to its absence.

1.1.3 S100 PROTEIN STRUCTURE

1.1.3.1 EF-hands

The S100 protein family constitutes one of 45 distinct subfamilies of EF-hand proteins [30]. Unlike other members of the EF-hand superfamily that contain variable numbers of EF-hand motifs (for example calmodulin, which contains four [57]), S100 proteins specifically contain two. They are characterized by proteins of relatively low mass (~10-14 kDa), generally with sequence length between 79 and 114 amino acid residues [5, 58]. The EF-hand domain, or calmodulin fold [28], is a basic functional and evolutionarily-conserved domain consisting of 29 amino acids arranged in a helix-loop-helix formation [28]. For simplicity, the EF-hand domain can be thought of as a human right hand. The index finger symbolises the first α-helix, with the Ca^{2+} loop represented by a clenched middle finger and a second α-helix symbolised by the thumb [28]. In S100 proteins there are two EF-hands, each EF-hand consists of an α-helix, E, a loop around the Ca^{2+} ion and a second α-helix, F (Fig.1.5).

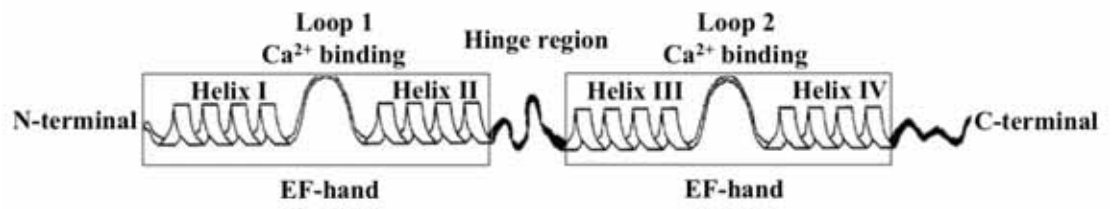

Figure 1.5: Schematic representation of secondary structure of an S100 protein. Each Ca^{2+}-binding loop (Loop I and Loop II) is flanked by α-helices. The hinge region connects helices II and III. The hinge region and the C-terminal extension have the least amount of sequence homology that may confer functional specificity. Adapted from [81].

The two distinct EF-hand motifs are encoded by separate exons; the second intron splits the coding sequence at the hinge region between the two. The second exon encodes the N-terminal EF-hand, whereas the third exon encodes the C-terminal EF-hand (Fig. 1.2) [32].

The EF-hands are flanked by hydrophobic regions and are separated by a central hinge region with significant amino acid sequence divergence [59]. The C-terminal EF-hand is also structurally divergent and rich in acidic amino acids and contains a calcium ion-binding loop encompassing 12 amino acids. The N-terminal EF-hand is rich in basic amino acids, consisting of 14 amino acids [60, 61]. The C-terminal EF-hand binds Ca^{2+} with higher affinity that the non-conventional 'pseudo EF-hand' in the N-terminal domain [62]. The pseudo EF-hand resembles a Ca^{2+}-bound conformation, with two additional amino acids and conserved residues surrounding the domain accounting for its low Ca^{2+}-binding affinity [63]. In addition, the backbone rather than side-chain oxygen atoms bind Ca^{2+} [57, 64, 65].

Because of differences in Ca^{2+} affinities in the N- and C-terminal EF-hands S100 proteins allow binding of two Ca^{2+} ions, with different affinities [63]. The N-terminal EF-hand may only be occupied after a rise in intracellular Ca^{2+}. Extracellularly, the Ca^{2+} ion concentration would be at sufficiently high levels to ensure that S100s remain in a Ca^{2+}-loaded state, allowing functionally-relevant extracellular roles for some [59]. Recently, nuclear magnetic resonance and X-ray crystallography showed that several S100 proteins change structure in response to Ca^{2+} in the apo- (Ca^{2+}-free), Ca^{2+}-loaded (Fig. 1.6), and target protein-bound states [66]. These studies demonstrate that the structural changes that occur in response to Ca^{2+}-binding in S100 proteins are distinct from those that occur in calmodulin [67].

It should be noted however, that levels of Ca^{2+}-binding and the degree of conformational change varies between S100s. For example, S100A10 and the N-terminal EF-hand of S100A7 resemble the Ca^{2+}-bound state, suggesting that these proteins could interact with targets in the absence of Ca^{2+} [68, 69].

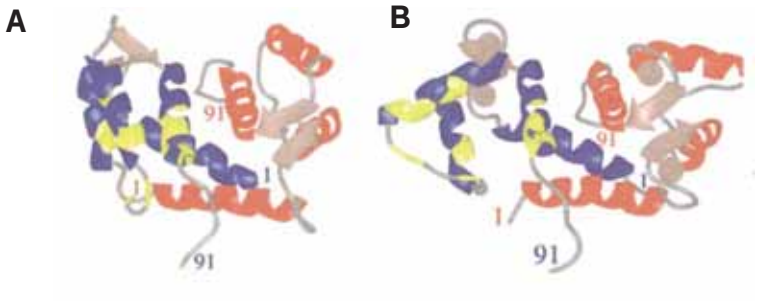

Figure 1.6: S100B in two different states. S100B is represented in the (**A**) Ca^{2+}-free and (**B**) Ca^{2+}-loaded state. Red and blue represent the helices of each subunit of S100B. Grey represents the beta strands, the loops and Ca^{2+} ions. From [66].

Other examples include modest Ca^{2+}-induced structural changes observed in S100A6 that may not strongly influence protein-target interactions [32]. Similarly, S100A7 only binds one Ca^{2+}/monomer and little conformational change noted [59]. On the other hand, when Ca^{2+} binds S100A11, a hydrophobic surface is exposed that facilitates protein-protein interactions [70]. S100A10 is unique because it remains in the Ca^{2+}-loaded conformation, despite an inability to bind Ca^{2+} [71]. S100A3 has a very low affinity for Ca^{2+} highlighting that it may function independently of Ca^{2+}[72, 73].

1.1.3.2 Zinc and copper binding

Some S100 proteins also bind zinc (Zn^{2+}). The earliest reports showed that S100A1 and S100B had Zn^{2+}-binding sites structurally distinct from the Ca^{2+}-binding sites [74]. There are two putative Zn^{2+}-binding sites in S100 proteins. In the S100B dimer, the His residues in one subunit are in close proximity to one-another, and are involved in binding neighbouring His and Cys residues in the other subunit. These residues are conserved in the N- and C-terminal regions of the majority of S100s. A second proposed motif comprises His residues (His-X-X-X-His) in the N- or C-terminal regions, present in S100A7, S100A8, S100A9 and S100A12 [75].

As with Ca^{2+}, binding affinities and numbers of cations chelated can vary and Zn^{2+}-binding can modify affinities for Ca^{2+}. For example, S100B can bind four Zn^{2+} ions with high affinity (1 μM) but binding reduces affinity for Ca^{2+} from 500 to 40 μM [76]. The S100A12 dimer binds two Ca^{2+}/dimer with low affinity and two Zn^{2+} ions with high affinity and upon Zn^{2+}-binding, two high affinity Ca^{2+}-binding sites are induced [22]. Interestingly, S100A3 has a low affinity for Ca^{2+} but it binds eight Zn^{2+}. Binding does not

increase affinity for Ca^{2+} [72]. Zn^{2+}-binding may also modify Ca^{2+}-induced interactions with other proteins, for example, S100A8/A9 [77]. S100A8/A9 binding of Zn^{2+} and Mn^{2+} is discussed in Section 1.3.6.7.

Some S100 proteins also bind copper (Cu^{2+}), although this aspect has not been thoroughly studied. The S100B dimer binds four Cu^{2+} ions, and this can be inhibited by Zn^{2+}, suggesting that the two ions share the same binding site [77]. Given the high abundance of S100B in the brain, it is possible that it protects against oxidative damage and plays a role in Cu^{2+} homeostasis [59]. The dimer of S100A5 can bind four Cu^{2+} ions, which strongly inhibits its ability to bind Ca^{2+} suggesting that the two ions share the same binding motifs [39]. S100A12 also has Cu^{2+}-binding properties, proposed to be essential for early immune response in host-parasite defense [78].

1.1.3.3 Dimer formation and its effects on function

A unique feature of most S100 proteins is their ability to form dimers or higher-order compounds either as homo- or hetero complexes. All form covalent or non-covalent anti-parallel homo- or heterodimers in the presence of Ca^{2+}, except for S100G. Most form anti-parallel homodimers in which the monomers are held together by non-covalent interactions and are oriented by a two-fold axis of rotation to create a hydrophobic interface that may bind target proteins (Fig. 1.7) [68, 79, 80].

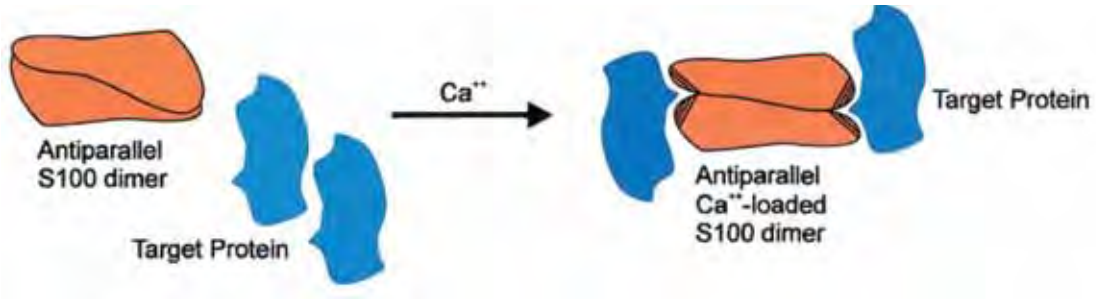

Figure 1.7: S100 dimer formation with target proteins. S100 proteins exist as anti-parallel dimers. Increases in Ca^{2+} concentration may cause conformational changes in the dimer, exposing a cleft, which forms the target protein binding site. From [413].

Typical S100 heterodimers include, S100B/S100A1 and S100A8/S100A9 [80]. Donato suggests that most S100 proteins form dimers because monomers are insufficient for binding a target protein, or target protein binding occurs with reduced strength

(reviewed in [81]). Yeast two-hybrid screens identified novel interactions of S100B with S100A6 and S100A11, and of S100A4 with S100A1 [80]. S100 dimers contain two monomers packed in an antiparallel conformation. Within each monomer of an S100 dimer, the surface defined by residues in the hinge region, helices III and IV, and the C-terminal extension are exposed to solvent upon Ca^{2+}-binding. The N-terminal helix (helix I) of the other monomer of the dimer contributes to the formation of the binding surface on each side of the dimer [71, 82, 83]. Charged residues in the monomers of an S100 dimer contribute to stabilization of heterocomplexes comprising two S100 proteins and two target proteins [84, 85].

Many S100s also form oligomeric complexes, which are generally dependent upon binding Ca^{2+} and/or Zn^{2+} [86-92]. The calgranulins, for example, S100A8/A9 form Ca^{2+}-dependent trimers and tetramers [91]. S100A12 forms quatramers [93] and hexamers (Fig. 1.8), arranged as a trimer of dimers [86, 90-94].

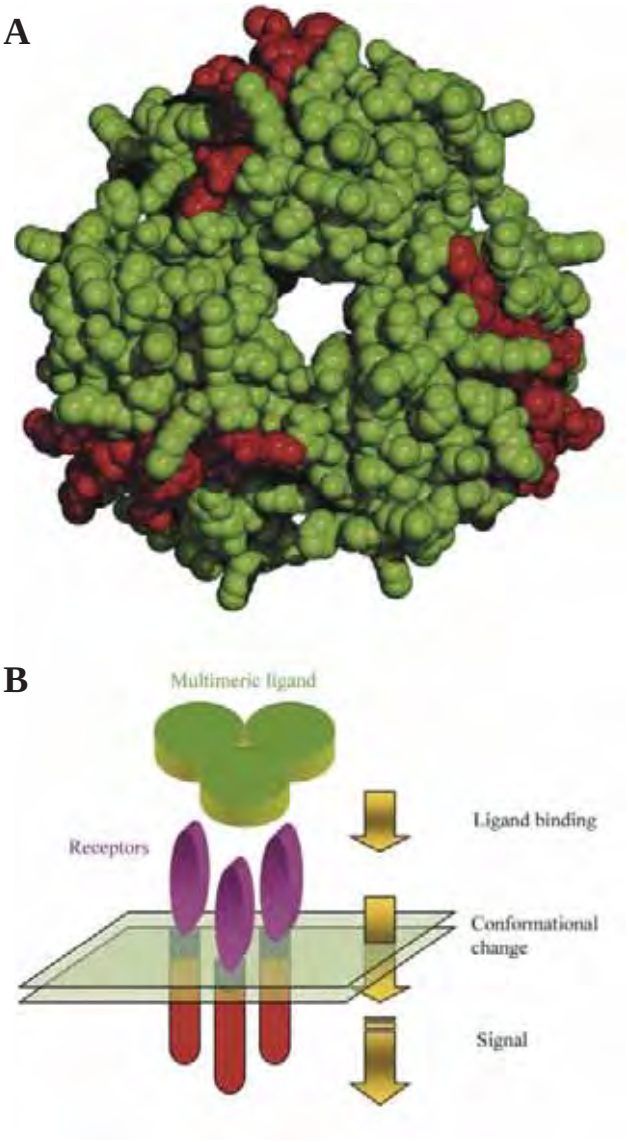

Figure 1.8: Receptor binding of hexameric S100A12. (**A**) Surface representation of the S100A12 hexamer. Red residues indicate target binding residues (residues 1-11, 40-46 and 79-85). (**B**) Hexameric S100A12 receptor binding. Extracellular domains of the receptor are indicated in purple, transmembrane domains in blue and cytoplasmic domains in red, with multimeric ligand in green. Transparent surface represents the cell surface. From [93].

S100A2, S100A3, S100A4, S100A16, S100B, S100P can also form homotetramers [87-89, 95-97]. S100 oligomers are functionally important. For example, S100A4 tetramers and higher-order oligomers stimulate neurite outgrowth and links between S100A4 oligomers and rheumatoid arthritis (RA) have been reported. S100A3 tetramers form following citrullination and are proposed to deliver Ca^{2+} to maturing hair cuticles [98]. S100A8/A9 and S100A12 oligomers are discussed in more detail in Sections 1.3.1.1 and 1.3.6.5 respectively.

1.1.4 EXPRESSION OF S100 PROTEINS

1.1.4.1 S100 expression profiles

Table 1.3 summarizes S100 expression in normal human tissues.

Table 1.3: S100 expression profile

S100 proteins	Expression in normal cells	Refs.
S100A1	Kidney (renal tubule cells), testes, lung, pancreas, aorta, brain, glial cells, skeletal, smooth (slow twitch) and cardiac muscle, satellite cells of sensory, sympathetic and enteric ganglia, supporting cells of the adrenal medulla, Schwann cells, peripheral neurons, Meissner and Pacinian corpuscles, subcutis adipose tissue, uterus, ovarian epithelium, brown fat	[62, 99-106]
S100A2	Cytoplasm and nucleus from lung and kidney, sheath epithelium of hair follicles, eccrine duct, myoepithelium and secretory coil of sweat glands, brain, nucleus of smooth muscle, liver, cardiac muscle, breast epithelium, oesophageal epithelial cells	[99, 100, 102, 107-110]
S100A3	Skin – inner root sheath cuticle of selected hair follicles, brain	[73, 99, 111, 112]
S100A4	Fibroblasts, brain, cytosol of sarcoplasmic reticulum and actin stress fibers, bone marrow, spleen, keratinocytes, melanocytes, Langerhan's cell and sweat glands, ovary and prostate, human fetal hippocampus and temporal cortex, myloepithelial cells	[99, 102, 107, 113-115]
S100A5	Olfactory bulb and terminals in a subset of glomeruli, brain, cells and fibers of the polymorphic, pyramidal and molecular layers of the hippocampus, temporal cortex, kidney, colon	[39, 99, 115, 116]
S100A6	Melanocytes, Langerhans' cells, cells of sweat glands, brain, sarcoplasmic reticulum and cell nucleus of smooth muscle, fibroblasts, epithelial cells, neuronal cells	[99, 100, 102, 109, 117]
S100A7	Epithelial cells, keratinocytes and breast epithelial cells	[107, 118]
S100A8	Neutrophils, macrophages and endothelial cells, tongue, oesophagus, uterine cervix, bone, dendritic cells, platelets	[119-124]
S100A9	Neutrophils, macrophages and endothelial cells, tongue, oesophagus, bone, dendritic cells, platelets	[107, 119-124]
S100A10	Cytoplasm of fibroblasts, placenta, basal layer of epidermis, epithelium	[107, 125-127]
S100A11	Smooth and heart muscle, fibroblasts, lung, mammary duct, renal tubule, prostate, uterus, testes, stomach, small intestine, colon, thyroid, bladder, ovary	[107, 128, 129]
S100A12	Cytoplasm of granulocytes, brain, oesophageal epithelial cells, neutrophil cytoplasm, lung	[99, 107, 109, 130, 131]
S100A13	Skeletal muscle, heart, kidney, pancreas, ovary, spleen, small intestine, prostate, testes, colon, brain, thymus, lung, liver and placenta, hippocampus and temporal cortex	[35, 115, 132]

S100 proteins	Expression in normal cells	Refs.
S100A14	Colon, thymus, kidney, liver, small intestine, lung, breast, ovary, prostate, rectum, stomach, thyroid, uterus	[24]
S100A15	Epidermal keratinocytes, keratinocytes, melanocytes, Langerhans' cells, dendritic cells, smooth muscle cells, internal and external root sheath of hair follicles, sebaceous gland, smooth muscle layer of blood vessel endothelium	[133, 134]
S100B	Brain, white fat, testes, extracellular and cytoplasm from glial and Schwann cells, chondrocytes, brain, Langerhans' cells, vascular dendritic cells, interdigitating reticulum cells	[62, 105, 107, 135-138]
S100G	Cytoplasm of intestine	[107, 139]
S100P	Oesophageal epithelial cells, placenta	[109, 140]
S100Z	Heart, placenta, skeletal muscle, colon, brain, kidney, thymus, testes, liver, lung, leukocytes, prostate, pancreas, spleen, small intestine	[26]

From Table 1.3, it should be noted that although particular S100 proteins generally exhibit tissue and/or cell-specific expression, there are exceptions. For example, S100A1 and S100A13 are expressed in the brain, kidney, testes and pancreas [105, 106, 132, 141]. In contrast, some have very limited expression. For example, S100A7 has only been detected in epithelial cells and keratinocytes, and S100G in the cytoplasm of intestinal epithelial cells [107, 139].

1.1.4.2 S100 protein and mRNA induction by extracellular stimuli

Importantly, S100 expression in some cells is regulated by extracellular/environmental stimuli (for example, growth factors, cytokines, drugs) (reviewed in [120]), and/or cell cycle progression and differentiation. For example, dexamethasone (Dex) increases S100B mRNA expression in cultured hippocampal astrocytes (reviewed in [142]). Murine S100A8 (mS100A8) mRNA and protein are induced in macrophages by lipopolysaccharide (LPS) from *Escherichia coli* (*E. coli*). This is controlled at the transcriptional level and S100A9, generally co-ordinately expressed with human S100A8 (hS100A8), is not induced by LPS under the same conditions in murine macrophages [143]. In addition, LPS can synergize with interleukin (IL)-10 so that mRNA and protein levels of mS100A8 are markedly increased [144]. Regulation and expression of S100A8 and S100A9 are described in more detail in Sections 1.3.1.2 and 1.3.1.3 respectively.

S100A10 protein is reduced in response to retinoic acid in bronchial epithelial cells whereas mRNA levels are unchanged, possibly the result of increased activity of the proteasome pathway protein causing degradation. When the proteasome activity is inhibited, basal levels of S100A10 increase, suggesting that it is under steady-state post-translational control by the ubiquitin-proteasome pathway [145, 146].

1.2 FUNCTIONS OF S100 PROTEINS

1.2.1 INTRACELLULAR FUNCTIONS

In general, intracellular functions of S100 proteins can be grouped according to modulation of cell growth and differentiation, regulation of Ca^{2+} homeostasis and enzyme activities, particularly regulation of phosphorylation mediated by protein kinases, and interactions with cytoskeletal components and transcription factors.

1.2.1.1 Cell growth and differentiation

A number of S100s regulate cell growth and differentation, with expression associated with many cancers (see Section 1.3.3.5). S100B interacts with p53, blocking its oligomerization and may cause growth arrest and apoptosis, suggesting a role in the regulation of cell growth [147]. However, this finding is controversial as some report that S100B is involved in p53-dependent tumour suppressor activity [148, 149], but others report tumour-promoting activity [81, 150]. For example, cytoplasmic accumulation of S100B in cultured glioma C6 cells correlates with contact-dependent inhibiton of growth, differentiation and increased sensitivity of the cells to UV-induced apoptosis [149, 151, 152]. S100B effects on apoptosis may provide a link between the over-expression of S100B seen in neurodegenerative diseases such as Alzheimer's disease [149]. That is, the oxidative stress-induced by UV exposure is similar to that which causes oxidative stress-induced DNA damage *in vivo*. DNA damage may activate the S100B apoptosis pathway contributing to the death of glial cells in neurodegenerative diseases [149]. However, although S100B is normally expressed in the brain, it is upregulated in various cell types, and an inhibitory effect on p53 would correlate better with its expression in cancer.

S100A2 and S100A11 may inhibit growth of some cells. S100A2 is markedly downregulated in breast tumour biopsies but re-expressed in mammary carcinoma cells by azadeoxycytidine treatment [153]. Similarly, S100A11 is downregulated in immortalized, compared to normal fibroblasts and exogenous S100A11 localized in the nuclei of HeLa cells (an epithelial cell line) inhibited DNA synthesis, suggesting a role in contact inhibition of cell growth [154].

S100A4 interacts with amino acid residues 360-393 of the C-terminal domain of p53 [155]. S100A4 associates with stress fibers, F-actin and tropomyosin, regulating cell motility and cytoskeletal dynamics [155-157]. This interaction affects phosphorylation of p53 by protein kinase C (PKC) and its DNA binding capacity *in vitro* [155-157]. The

interaction between p53 and S100A4 may induce apoptotic responses depending on environment and cell type [155-157].

S100A6 may regulate fibroblast proliferation [158]. When an NIH 3T3 fibroblast cell line was transfected with small interfering RNA (siRNA) against S100A6, these fibroblasts showed altered cell morphology and reduced proliferation, compared to untransfected cells [158]. S100A8 and S100A9-mediated cell growth and differentiation are discussed in more detail in Section 1.3.4.

1.2.1.2 Regulation of calcium homeostasis

Regulation of Ca^{2+} homeostasis by S100s can be attributed to their affinities for Ca^{2+}. $[Ca^{2+}]_i$ during a Ca^{2+} wave is ~ 1 μM [159]. Roles in Ca^{2+} homeostasis include interactions of S100A1 with the ryanodine receptor, a receptor present in skeletal muscle sarcoplasmic reticulum [160]. The C-terminus of S100A1 can augment contractile performance of fast- and slow-twitch skeletal muscle fibers based on enhanced sarcoplasmic reticulum Ca^{2+} efflux, suggesting that S100A1 may serve as an endogenous enhancer of sarcoplasmic reticulum Ca^{2+} release, and therefore relevant in the process of excitation-contraction coupling in skeletal muscle [160].

A mixture of S100A1 and S100B consisting of ~20% S100A1 and ~80% S100B caused similar effects, suggesting regulation of Ca^{2+} homeostasis through S100A1, and possibly S100B activation of the ryanodine receptor [161, 162]. Interestingly, glial cells from neonatal S100B-null mice display enhanced Ca^{2+} transients in response to KCl or caffeine [163], suggesting a role of S100B in cytosolic Ca^{2+} buffering [164]. This is despite the fact that S100B has relatively low affinity for Ca^{2+} *in vitro* [62].

1.2.1.3 Regulation of enzyme activities

Although there are no S100 proteins that have enzymatic activity, several may regulate activities of enzymes. These include enzymes involved in regulation of energy metabolism, the cell cycle, myeloid cell maturation, anti-inflammatory activity and muscle contraction (reviewed in [29, 81, 147]). Table 1.4 summarizes some enzyme activities modulated by the different S100 proteins.

Table 1.4: Regulation of enzyme activities by S100 proteins

S100 proteins	Enzymes	Effects	Suggested functions	Refs.
S100B	Fructose-1,6-biphosphate aldolase	Stimulation	Regulation of energy metabolism	[165]
	Phosphoglucomutase	Stimulation	Regulation of energy metabolism	[166]
	Twitchin kinase	Stimulation	Muscle contraction	[167]
	Ndr	Stimulation	Regulation of cell cycle	[168]
	Adenylate cyclase	Inhibition	Unknown	[169, 170]
	Membrane-bound guanylate cyclase	Stimulation	Dark adaptation of photoreceptors	[171-173]
S100A1	Fructose-1,6-biphosphate aldolase	Stimulation	Regulation of energy metabolism	[165]
	Phosphoglucomutase	Inhibition	Regulation of energy metabolism	[166]
	Titin	Inhibition	Regulation of elasticity	[174]
	Glycogen phosphorylate	Inhibition	Regulation of energy metabolism	[175]
	Twitchin kinase	Stimulation	Muscle contraction	[167]
	F_1 subunit of ATPase	Stimulation	Regulation of cell cycle	[176]
	Adenylate cyclase	Stimulation	Unknown	[169, 173]
	Membrane-bound guanylate cyclase	Stimulation	Dark adaption of photoreceptors	[169, 173]
S100A8/A9	Casein kinase I and II	Inhibition	Myeloid cell maturation	[177]
	NADPH oxidase	Activation	Phagocyte oxidative burst	[178-182]
S100A8	Telomerase	Inhibition	Keratinocyte differentiation	[183]
S100A10	Phospholipase A	Inhibition	Anti-inflammatory activity	[184]
	Plasminogen activator	Stimulation	Anti-coagulant activity	[185]
S100A11	Actomyosin ATPase	Inhibition	Unknown	[186]

Adapted from [29].

1.2.1.4 Regulation of protein phosphorylation

Some S100 proteins inhibit protein phosphorylation by interacting with kinase substrates, blocking access to kinases (reviewed in [81]). Others inhibit protein phosphorylation regulating specific steps in those signalling pathways in which S100 target proteins have a role. For example, S100B is induced in rat myocardium post-infarction, concomitant with down-regulation of skeletal α-actin [187]. Transfection of S100B into cultured neonatal rat cardiomyocytes induces β-PKC-mediated inhibition of skeletal α-actin and embryonic β-myosin heavy chain. This implies that S100B may negatively regulate hypertrophic responses after myocardial infarction by inhibiting β-PKC-dependent phosphorylation of an as yet unidentified protein [187, 188]. Targets of S100 phosphorylation are summarized in Table 1.5.

Table 1.5: Regulation of protein phosphorylation by S100 proteins

S100 proteins	Targets	Suggested functions	Refs.
S100B	Tau proteins	Inhibition of tau phosphorylation by protein kinase II	[189]
	Myristoylated alanine-rich C kinase substrate (MARCKS)	Unknown	[190]
	Annexin II	Unknown	[191]
	GAP-43 (neuromodulin)	Unknown	[192, 193]
	Neurogranin	Unknown	[190]
	MARCKS-like retinal phosphoprotein p80	Unknown	[172]
	Caldesmon	Reversal of caldesmon-dependent inhibition of actomyosin ATPase activity	[194, 195]
	GFAP, vimentin	Unknown	[196]
	p53	Stimulation/inhibition of p53-dependent activities	[197]
S100A1	MyoD	Inhibition of MyoD phosphorylation and DNA binding	[198, 199]
	Tau proteins	Unknown	[200]
S100A4	Myosin heavy chain	Modulation of the cytoskeleton dynamics in metastatic cells	[201-203]
	p53	Inhibition of p53-dependent activities	[155]
S100A10	Annexin II	Regulation of annexin II interaction with membranes	[204]
S100A11	Annexin I	Regulation of annexin I interaction with membranes	[83, 205]

Adapted from [29, 81].

1.2.1.5 Interaction with cytoskeletal components

Three major constituents of the cytoplasmic cytoskeleton – microtubules (MT), intermediate filaments (IF) and microfilaments (MF), and tropomyosin and myosin may be regulated by S100 proteins [102, 206-208] (summarized in Table 1.6). S100B may reduce excess tubulin polymerization and/or remodelling of MTs following elevation of cytosolic Ca^{2+}, due to its association with axonal MTs, centrioles, basal bodies, mitotic spindles, and centrosomes [206]. Similarly, S100A1 inhibits tubulin assembly. S100A1 and S100B also inhibit desmin and glial fibrillary acidic protein (GFAP) assemblies by sequestering unassembled IF subunits [209-211]. In contrast, S100A6 and S100A10 do not bind desmin or affect GFAP assembly [209, 212]. S100A1 associates with twitchin

kinase (involved in regulation of ATP-binding), a member of the Ca^{2+}-regulated protein kinase superfamily, in a Ca^{2+} and Zn^{2+}-enhanced manner [167]. Interestingly, S100A6, S100A10 and calbindin failed to activate this kinase, despite showing Ca^{2+}-dependent binding, suggesting both Ca^{2+} and Zn^{2+} are required for activation [213].

Conversely, S100A4 may modulate actin/myosin cytoskeletal dynamics, via inhibition of PKC-dependent phosphorylation [201] and may contribute to metastatic invasiveness by inhibiting PKC-dependent phosphorylation of the heavy chain of non-muscle myosin-II [201], which regulates metastatic invasiveness of some tumour cells [214]. S100A4 binds tropomyosin, which can bind some actin filaments and regulate different isoforms of myosin and may impart Ca^{2+} sensitivity to tropomyosin regulation of ATPase activity [156]. In addition, S100A2, which undergoes transient, Ca^{2+}-dependent translocation from the cytoplasm to microvilli, might prevent association of tropomyosin to MFs in microvilli (reviewed in [29]). Thus S100A2 plays an important role in the organization of the actin cytoskeleton through tropomyosin interaction in LLC PK1 cells (a kidney proximal tubule cell line) [208]. The calgranulins are discussed in more detail in Section 1.3.5.5.

Table 1.6: Interaction of S100 proteins with cytoskeletal components

S100 proteins	Cytoskeletal elements	Suggested functions	Refs.
S100B	Microtubules	Inhibition of assembly via sequestration of tubulin and stimulation of Ca^{2+} sensitivity of preformed microtubules	[215-217]
	Type III intermediate filaments	Inhibition of assembly and stimulation of disassembly by sequestration of unassembled subunits	[209, 210]
	Caldesmon	Reversal of caldesmon-dependent inhibition of actomyosin ATPase activity	[194, 195, 218]
	Calponin	Reversal of calponin-dependent inhibition of actomyosin ATPase activity	[219, 220]
S100A1	CapZα	Unknown	[221, 222]
	Microtubules	Inhibition of assembly by sequestration of tubulin and stimulation of Ca^{2+} sensitivity of preformed microtubules	[206, 216, 217]
	Type III intermediate filaments	Inhibition of assembly and stimulation of disassembly by sequestration of unassembled subunits	[209, 210]
	Microfilaments	Unknown	[102, 200, 207]
S100A2	Tropomyosin	Organization of the actin cytoskeleton in microvilli via its interaction with tropomyosin	[208]
S100A4	Myosin	Regulation of the dynamics of myosin filaments in relation to metastatic cells	[223-227]
	Tropomyosin	Regulation of Ca^{2+} sensitivity to tropomyosin modulation of actomyosin ATPase activity	[156]
	Microfilaments	Unknown	[157]
S100A6	Tropomyosin	Unknown	[228]
	Caldesmon	Reversal of caldesmon-dependent inhibition of actomyosin ATPase activity	[229]

S100 proteins	Cytoskeletal elements	Suggested functions	Refs.
S100A8/ S100A9	Type III intermediate filaments Keratin filaments	Modulation of Ca^{2+}-dependent interactions between intermediate filaments and membranes during migration, chemotaxis, degranulation, phagocytosis and respiratory burst of activated granulocytes and monocytes Modulation of wound healing	[230-232] [233]
S100A10	Unknown	Stimulation of annexin II translocation, F-actin bundling activity of annexin II, and enhancement of annexin II stimulation of GFAP polymerization	[212, 234]
S100A11	F-actin Microtubules	Inhibition of actin-activated myosin ATPase activity Formation of comified envelope	[186] [235]
S100A12	Undefined cytoskeleton elements	Modulation of Ca^{2+}-dependent interactions between cytoskeleton elements and membranes	[120, 236]

Adapted from [81].

1.2.1.6 Interaction with transcription factors

Basic helix-loop-helix (bHLH) proteins are a group of transcription factors involved in differentiation and other important cell processes. Calmodulin and certain S100 proteins are involved in the differential regulation of bHLH proteins (HLH protein sequences). S100A1 and S100B dimers, and calmodulin, have distinct bHLH protein preferences, determined by particular basic sequences and the N-terminal sequence. For example, the bHLH protein, E12ΔN is more sensitive to calmodulin and the S100A1 dimer than to the S100A1/S100B heterocomplex or S100B dimer. However, like calmodulin, these S100 proteins inhibit bHLH functions by binding to the basic sequence, and inhibiting DNA binding (reviewed in [81]).

S100A4 appears to activate and integrate pathways that generate phenotypic responses characteristic of cancer [237]. In particular, intracellular S100A4 regulates proliferation and differentiation via p53 regulation (by binding its C-terminal regulatory region) and regulates other transcription factors [237]. Similarly, in head and neck squamous cell carcinomas, where it is abundantly expressed, S100A2 binds the C-terminus of p53 in a Ca^{2+}-dependent manner, increasing its transcriptional activity, and may modulate proliferation [238]. Interestingly however, S100A2 also has anti-mitogenic effects and arrested hepatocellular carcinoma cell growth and proliferation [239]. Overall these data suggest that the S100 protein family act in several ways to regulate cell growth and differentiation, in health and disease, and differences may relate to particular cell types and may be tightly regulated.

1.2.2 EXTRACELLULAR FUNCTIONS OF S100 PROTEINS

S100 proteins lack signal peptide sequences required for classical ER-Golgi-mediated secretion and mechanisms of secretion are poorly understood. Some may regulate secretion of other proteins with extracellular functions. For example, fibroblast growth factor (FGF)-1 associates with synaptotagmin 1 and S100A13, and is secreted from fibroblasts following stress [240]. Importantly, the complex must be formed before the aggregate can be exported across the plasma membrane, via an intact filament network [241, 242]. A tubulin-dependent pathway is proposed for secretion of the S100A8/A9 heterocomplex [230]. Secretion of S100A8/A9 is energy-dependent, relying on activation of monocytes by PKC and an intact microtubule network [230].

Recent evidence indicates another mechanism of calgranulin secretion. Neutrophil

extracellular traps (NETs) comprise histones, DNA and >20 granular and cytoplasmic proteins [243]. *Candida*, *Aspergillus sp* or phorbol myristate acetate (PMA) trigger NET release. NET formation occurs over several hours, and NETs contain S100A8/S100A9 following neutrophil death and membrane rupture. S100A12 was also found in NETs [243]. Table 1.7 summarizes some extracellular functions of several S100s, and their proposed mechanisms.

Table 1.7: Extracellular functions of human S100 proteins

S100 proteins	Effects	Suggested mechanisms	Refs.
S100B	Neurite extension activity and pro-survival effects on neurons	Nuclear translocation of NF-κB via Receptor for Advanced Glycation End Products (RAGE)-dependent activation of the Ras/MAP kinase and the cdc42/Rac pathways and stimulation of Bcl-2 expression	[244-259]
	Stimulation of astrocyte proliferation	Unknown	[260]
	Neuronal apoptosis	RAGE-dependent, cytochrome C-mediated activation of caspase-3 and down-regulation of Bcl-2 expression; stimulation of Ca^{2+} influx in neurons and upregulation of expression of c-fos, c-jun, bax, bcl-x, p-15, and p-21, stimulation of nitric oxide (NO) release by astrocytes	[249, 261-264]
	Stimulation of IL-6 secretion by neurons	Nuclear translocation of a novel NFκB-binding factor expressed in neurons	[265]
	Stimulation of NO secretion by microglia, astrocytes and astrocyte apoptosis	Induction of inducible nitric oxide synthase (iNOS) in astrocytes via nuclear translocation of NF-κB or binding of RAGE	[261, 262, 266, 267]
	Modulation of synaptic plasticity	Depression of long term potentiation	[268]
	Inhibition of myogenesis	Inactivation of extracellular signal-regulated kinase (ERK)1/2, Akt and p38 in a RAGE-independent manner	[269-273]

S100 proteins	Effects	Suggested mechanisms	Refs.
S100A1	Neurite extension activity and pro-survival effects on neurons	Nuclear translocation of NF-κB via RAGE-dependent activation of the Ras/MAP kinase and the cdc42/Rac pathways	[249]
	Inhibition of ventricular cardiomyocyte apoptosis	Activation of ERK 1/2 pathway	[274]
S100A2	Chemotactic for eosinophils; inhibition of tumour cell motility	Unknown; regulation of actin cytoskeletal polymerization and dynamics	[275, 276]
S100A4	Neurite extension activity and stimulation of angiogenesis	Activation of the ERK1/2 signalling pathway in neurons (receptor unknown)	[96]
	Pro-survival effects on cardiac myocytes	Activation of the ERK1/2 signalling pathways	[277]
	Induction of capillary-like tube formation in endothelial cells	Annexin II-binding and tissue plasminogen activation and induction of matrix metalloproteinase (MMP)-13 via RAGE-independent nuclear translocation of NF-κB	[42]
	Stimulation of astrocytic tumor cell motility	Decreased expression of polymerized F-actin, RhoA, mDia and profilin	[278-280]
S100A6	Neuronal apoptosis	RAGE-dependent activation of JNK and caspase-3 and -7	[281]
S100A7	Chemotactic for $CD4^+$ lymphocytes	Interaction with Jab 1	[282, 283]
	Inhibition of bacterial growth	Zn^{2+}-dependent mechanism	[284]
S100A8	Refer to Table 1.15		
S100A9	Refer to Table 1.15		
S100A10	Inhibition of extrinsic pathway of blood coagulaiton	Binding to plasminogen and stimulation of tissue-type plasminogen activator-dependent plasminogen activation	[185]

S100 proteins	Effects	Suggested mechanisms	Refs.
S100A11	Stimulation of keratinocyte proliferation	Induction of EGF proteins via RAGE-dependent nuclear translocation of NF-κB and the cyclic AMP (cAMP) response element-binding protein signalling	[285, 286]
	Stimulation of type X collagen and IL-8 production in reticular chrondrocytes	RAGE-dependent activation of p38 signalling	[287, 288]
S100A12	Refer to Table 1.15		
S100P	Stimulation of fibroblasts, proliferation of colon and pancreatic cancer cells	Nuclear translocation of NF-κB via RAGE-dependent activation of ERK1/2 signalling	[289, 290]

Adapted from [29, 81].

1.2.2.1 Receptors for S100 proteins

A diverse range of receptors is reported for extracellular S100 proteins and RAGE is implicated as a receptor for several. RAGE belongs to the immunoglobulin super-family, and is a multi-ligand receptor interacting with ligands of different structures, probably by cell surface oligomerization [291]. The extracellular portion of RAGE binds S100B, S100A1, S100A2, S100A5, S100A6 and S100A12 via the V immunoglobulin-like domain. S100A4, S100A7, S100A8/A9, S100A11, S10013 and S100P are also reported to bind RAGE but the binding domain is unknown (Fig. 1.9) [291].

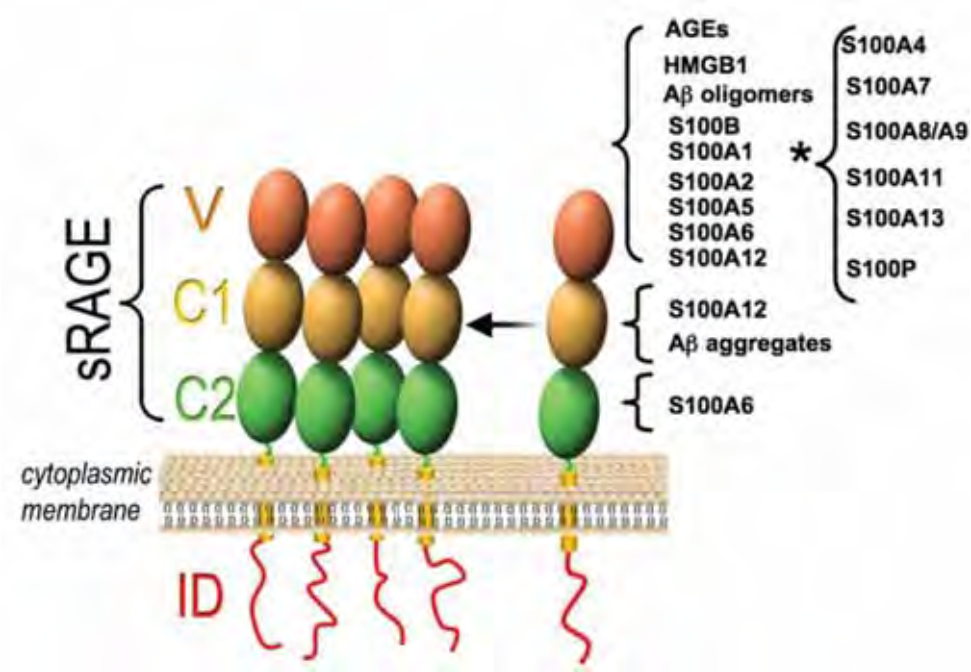

Figure 1.9: A schematic representation of RAGE. The extracellular portion of RAGE consists of three immunoglobulin-like domains – V, C1 and C2. A single transmembrane helix links the extracellular domain with the intracellular domain (ID). RAGE ligands bind the extracellular domain. * indicates S100 proteins for which the RAGE binding domain is unknown. Adapted from [291].

Given the diverse tissue expression of S100 proteins, RAGE ligation results in equally diverse functions. For example, S100B, S100A1, S100A6, S100A7, S100A11, S100A8, S100A9, S100A12, S100A13 and S100P activate intracellular signalling pathways such as MAPK and NF-κB, to promote cell activation, proliferation and/or survival [133, 289, 291-294]. Ligation of S100A8/A9 with RAGE is discussed in Section 1.3.8.4

Some S100 proteins interact with receptors distinct from RAGE. S100A1 and

S100B appear to interact with neuronal receptor/s. Although S100A15 co-evolved with S100A7 and is structurally similar (>90% amino acid sequence homology) [295], it does not appear to interact with RAGE, but through a G protein-coupled receptor [133]. Similarly, bovine S100A2 (on guinea pig eosinophils) [275], mS100A8 [296], hS100A9 [297] and hS100A12 [298] may also exert extracellular chemotactic activities via a G protein-coupled receptor. Other receptors implicated in binding of the calgranulins will be discussed in Section 1.3.8.

1.2.2.2 Neurotrophic and neurotoxic effects

S100B is expressed in the nervous system and may have neurotrophic and neurotoxic effects. S100B induces trophic effects in RAGE-expressing cells, such as neuronal survival through NF-κB activation [249, 253], stimulation of neurite outgrowth [299] and astrocyte proliferation [260] at nanomolar concentrations. Similar concentrations also negatively regulate astrocytic and microglial responses to neurotoxic agents [299]. On the other hand, micromolar concentrations of S100B, in response to injury, induce apoptosis in an oxidant-dependent manner, but only in cells expressing full-length RAGE. This suggests that RAGE is a signal-transducing receptor for both trophic and toxic effects of S100B [249]. Neurotrophic activity is also induced by S100A1, dependent on RAGE activation of the Ras/MAPK pathway and oligomeric S100A4 secreted by astrocytes stimulates neuronal differentiation and outgrowth via activation of ERK1/2 (reviewed in [300]).

1.2.2.3 Apoptotic properties

A defining feature of the S100 protein family is their ability to influence apoptosis. S100B promotes apoptosis in PC12 cells (derived from a pheochromocytoma of the rat adrenal medulla [301]), through induction of intracellular Ca^{2+} channels, which cause a rapid rise of $[Ca^{2+}]_i$ and a progressive increase in cell degeneration and death [261]. Intriguingly, S100A6, which is structurally similar to S100B, triggers apoptosis at micromolar levels, but unlike S100B, not cellular proliferation [281], despite evidence for S100A6-mediated proliferation of fibroblasts under certain conditions (see Section 1.2.1.1). Both S100 proteins promote reactive oxygen species (ROS) generation, although S100B recruited phosphatidylinositol 3-kinase/Akt and NF-κB, whereas S100A6 activated JNK [281]. S100A8/A9 also induces apoptosis in various tumour cell lines in a

Zn^{2+}-dependent manner [302], possibly through Zn^{2+} chelation. Zn^{2+} ions inhibit apoptotic nucleases and caspase activation [303, 304]. Zn^{2+} deficiency causes induction of nuclease and caspase activity, initiating apoptosis [305-308].

Extracellular S100A1 inhibits apoptosis in ventricular cardiomyocytes via activation of ERK1/2 [274], suggesting that injury dependent-release of S100A1 from cardiomyocytes may promote survival of the myocardium *in vivo* [274]. S100A4, which has metastasis-promoting properties, can sensitize osteosarcoma cells to interferon (IFN)-γ mediated induction of apoptosis, which was ROS dependent but independent of caspase activation [309]. Interestingly, S100A4 inhibits apoptosis during injury to the myocardium [277], indicating the complex nature of tissue-specific expression of S100 proteins and their subsequent effects on function and outcome during pathology.

1.2.2.4 Mitogenic activities

Several S100 proteins are mitogenic, including S100B, S100A2, S100A6 and S100P [158, 259, 260, 289, 310]. S100B promotes astrocyte [259] and myoblast proliferation [273] by activating mitogenic kinase Akt and stimulating the Ras-MEK-ERK1/2 pathway. S100B also stimulates proliferation of rat C6 glioma cells and primary astrocytes, primarily through upregulation of *c-myc* and *c-fos* proto-oncogene [260]. S100P also stimulated proliferation and survival of 3T3 cells in a RAGE-dependent manner [289].

1.2.2.5 Host defense against infection

In a study aiming to identify early mediators of host defense against *Pseudomonas aeruginosa* (*P. aeruginosa*), several S100 proteins were among the most differentially-expressed in epithelial cells [311]. These included S100A2, S100A6, S100A8 and S100A9. The authors proposed that the S100 proteins might either strengthen the physical epithelial barrier or deprive the microenvironment of essential nutrients, thereby starving microorganisms of nutrients essential to survival [311].

S100 proteins may modulate host defense by other mechanisms. For example, S100A7 protects human skin from *E. coli* infection, possibly through Zn^{2+} chelation [312] although, a recent study by Michalek *et al*. showed that at pH <6, S100A7 has pore-forming activity that disrupts microbial membranes. Killing is pH dependent, with Gram-negative bacteria such as *E. coli*, and these are killed without compromising its membrane

at pH 7.4. However at low pH, only the Gram-positive bacterium *Bacillus megaterium* was killed by permeabilization of its cytoplasmic membrane [313] suggesting that S100A7 has pH-dependent target specificity.

Anti-infective and anti-invasive functions of the calgranulins, S100A8, S100A9 and S100A12 will be discussed in Section 1.3.6.7.

1.2.2.6 Chemotactic activity

In 1991, mS100A8 (then known as CP-10) was the first S100 protein shown to have chemotactic activity [314], a function subsequently ascribed to bovine S100A2, hS100A7, hS100A8, hS100A8/S100A9, hS100A12 and bovine S100B (see Table 1.8).

Table 1.8: Chemotactic activities of S100 proteins

S100 proteins	Responsive cells	Optimal concentrations	Refs.
Bovine S100A2	Guinea pig eosinphils	10^{-10} M	[275]
Human S100A7	Human neutrophils, monocytes and $CD4^+$ T cells	10^{-11}-10^{-8} M	[133, 282]
Human S100A15	Human neutrophils and monocytes	10^{-9} M	[133]
Murine S100A8	Murine neutrophils and monocytes	10^{-13}-10^{-11} M	[314-316]
Murine S100A8 hinge region ($S100A8_{42-55}$)	Murine neutrophils and monocytes	10^{-11}-10^{-10} M	[315, 317]
Human S100A8, S100A9 and S100A8/A9	Neutrophils	10^{-12}-10^{-9} M	[316]
Human $S100A8_{21-45}$	Human periodontal ligament cells	10^{-12} M	[318]
Human S100A12	Human monocytes, neutrophils, mast cells and THP-1 cells	10^{-12}-10^{-8} M	[298, 319, 320]
Human S100A12 hinge region ($S100A12_{38-53}$)	Human mast cells, monocytes and murine mast cells	10^{-12}-10^{-9} M	[298]
Bovine S100B	Murine smooth muscle cells	Not determined	[321]

Adapted from [120].

Although the chemotactic receptors for these have not been characterized, studies

indicate that the binding domains of mS100A8 [296, 315] and hS100A12 [298] are within the hinge regions and G-proteins are possible ligands. hS100A8, hS100A9 and hS100A12 are the main focus of this thesis and their chemotactic activities will be discussed more fully in Section 1.3.6.3.

Bovine S100A2, earlier referred to as S100L is chemotactic for guinea pig eosinophils but did not elicit for guinea pig neutrophils or monocytes [275]. The receptor implicated is a G protein-coupled receptor, as pre-treatment of eosinophils with pertussis toxin caused inhibition [275].

Infiltration of neutrophils and T lymphocytes are common in inflammatory skin disorders such as psoriasis. At concentrations of 10^{-11} M *in vitro*, S100A7 is chemotactic for neutrophils and $CD4^+$ T lymphocytes [282]. Although S100A7 and S100A15 share almost identical amino acid sequences, and both are chemoattractants, they have activity for distinct leukocyte subsets [133]. For example, S100A15 is chemotactic for monocytes and granulocytes, but not lymphocytes [133]. In contrast, S100A7 is chemotactic for these three leukocyte populations [133]. When combined and administered by intraperitoneal injection (i.p injection) in C57BL/6 wild type mice, S100A7 and S100A15 potentiate inflammation [133].

1.2.3 S100 PROTEINS AND HUMAN DISEASE

Diseases associated with altered expression of S100 proteins can be classified into six main categories, summarized in Table 1.9. The reason for this clustering may result from their evolutionary history. Marenholz *et al.* suggests four evolutionary subgroups [5] (see Fig. 1.4), but the phylogenetic organization of this family does not necessarily indicate disease associations. For example, the calgranulins, are primarily involved in inflammatory responses, but play roles in infection and cancer (discussed in detail in Sections 1.3.3.1 and 1.3.3.5).

Table 1.9: S100 proteins and disease

S100 proteins	Disease association
S100A1	Cardiomyopathies
S100A1, S100A2, S100A3, S100A4, S100A5, S100A6, S100A8, S100A9 S100A10, S100A11 S100P, S100B	Cancer
S100A7, S100A15	Psoriasis
S100A4, S100A8, S100A9, S100A12	Inflammatory disorders
S100B	Neurodegenerative
S100A4, S100A7, S100A8, S100A9, S100A11, S100A12, S100A13, S100A15	Infection

Adapted from [5, 18, 134, 139, 322-327].

Several diseases are associated with altered S100 gene expression. Re-arrangements on human chromosome 1q21 form the basis of several cancers. It is likely that for S100A2, S100A4 and S100A6, deletions, translocations and/or duplications in the 1q21 region may alter their differential expression [328].

For ease of reference, individual S100 proteins are listed in Table 1.10 with associated pathological conditions.

Table 1.10: S100 proteins and associated diseases

S100 proteins	Disease association	Refs.
S100B	Melanoma, amyotrophic lateral sclerosis, epilepsy, Alzheimer's disease, Down syndrome	[142, 329-333]
S100A1	Lung carcinoma, acute myocardial ischemia, right ventricular hypertrophy, cardiomyopathies	[334-337]
S100A2	Pilomatrixoma, squamous cell lung carcinoma, breast cancer, non-small cell lung cancer, gastric cancer, ovarian cancer, melanoma, epithelial tumours of the skin, lymphoma, Barrett's adenocarcinomas, pancreatic cancer	[337-349]
S100A3	Hair follicle damage, bronchial cysts, craniopharyngiomas, pilomatrixoma	[348, 350]
S100A4	Lung carcinoma, breast cancer	[277, 337, 351-354]
S100A5	Meningioma	[355-357]
S100A6	Acute renal failure, craniopharyngiomas, osteosarcoma, branchial cysts, pilomatrixoma, pancreatic cancer, colorectal adenocarcinoma, hepatocellular carcinoma, gastric cancer, Barrett's adenocarcinoma, lung cancer, breast cancer, melanoma	[99, 337, 338, 348, 350, 358-369]
S100A7	Psoriasis, lichen sclerosis, atopic dermatitis, mycosis, fungoides, Darier's disease, breast cancer	[134, 283, 370-376]
S100A8/S100A9	see Section 1.3.3	
S100A10	Inflammation and depression	[377, 378]
S100A11	Skin diseases, breast cancer, ocular melanoma, prostate cancer, pancreatic cancer	[119, 325, 379-383]
S100A12	see Section 1.3.3	
S100A13	Unknown	[384, 385]
S100A15	Breast cancer, psoriasis	[295, 374]
S100G	Vitamin D deficiency, abnormal mineralization	[32]
S100P	Pancreatic tumours, breast cancer, lung adenocarcinomas	[337, 338, 386]

Adapted from [5, 32].

1.3 INFLAMMATION-ASSOCIATED S100 PROTEINS

This thesis focuses primarily on S100A8 and S100A9, and because S100A12 is also an inflammation-associated calgranulin constitutively present in neutrophils, a more in-depth review of these proteins is presented.

1.3.1 S100A8 AND S100A9

1.3.1.1 Structure

Although the structures of S100A8 and S100A9 are fairly well studied, there is still debate concerning the composition of the biologically active complexes, primarily due to the limitations of analytical techniques. For example, gel filtration lacks the desired accuracy, polyacrylamide gel electrophoresis (PAGE) often destroys non-covalent interactions, and cross-linking can produce artificial results. In addition, light scattering experiments require knowledge of the shape of proteins, and analytical ultracentrifugation gives only limited information about the exact complex composition [47].

The following examples illustrate disparities between studies. Pröpper *et al.* propose that heterodimerization of S100A8 and S100A9 is the strongly preferred form of the human and murine proteins. However, using the yeast two-hybrid system, they showed striking differences in homodimer formation between the murine and human proteins. mS100A8 and mS100A9 readily formed homodimers whereas hS100A8 and hS100A9 did not [90].

Experiments using atomic force microscopy (AFM) may provide new insights into the structures. Imaging in buffer using tapping-mode, liquid-cell AFM of S100A8, S100A9 and S100A12 identified experimental monomeric molecular volumes consistent with the volumes calculated from thier molecular weights [387]. Moreover, in solution S100A8 existed as a non-covalently linked dimer, consistent with observations by Ishikawa *et al*. [388]. S100A9 exists as four dimers, consistent with the reported crystal structure [69], which coalesced in a clover leaf-like structure [387].

S100A8 and S100A9 form stable heterodimers and Ca^{2+}-dependent heterotrimers (also known as L1 antigen) [47, 69, 92, 388, 389]. They may also form heterotetramers, as well as their respective homodimers, through hydrophobic interactions between paired monomers [47, 69, 92, 388, 389]. In addition, Strupat *et al*. showed that the number of Ca^{2+} ions bound to individual tetramers is eight for the non-phosphorylated forms. S100A9 can be phosphorylated on Thr_{113} at the C-terminal site [91]. Approximately 1.2

Ca^{2+} ions bound the phosphorylated form, possibly binding more phosphate groups in the tetramers [91].

The functional relevance of S100A8 and S100A9 homodimers is still being unravelled. Much early work was based on analysis using the monoclonal antibody (mAb) 27E10, which recognizes a trans-dimer epitope specific for the heterodimer [390]. Heteronuclear nuclear magnetic resonance (NMR) experiments indicated that a specific, well-packed heterodimer is formed only in equimolar mixtures of the two proteins. A unique complementarity at the interface of the S100A8/S100A9 complex is indicated, and this cannot be fully reproduced in the S100A8 homodimer, as it is not soluble at high concentrations [391]. However, crystallographic studies show that S100A8 forms a stable homodimer [388]. mS100A8 also forms homodimers in non-denaturing solvent when analyzed by electrospray ionization mass spectrometry (ESI-MS) and chemical cross-linking [389]. Interestingly a recent study indicates that the S100A8/A9 heterodimer adopts a structure like that of the S100A8 homodimer, which is more stable than the S100A9 homodimer [392].

The crystal structures of S100A8 and S100A9 homodimers are similar; with each monomer being stabilized by a hydrophobic core of conserved amino acids (Fig. 1.10) [388]. These homodimers are unusual in that the four Ca^{2+}-binding sites are all occupied, which is different from most other S100 proteins as the N-terminal EF-hand generally represents a pseudo-Ca^{2+}-binding site with extremely weak affinity [159]. Homodimer formation is mainly stabilized by interactions of hydrophobic side-chains within helices I and IV [392].

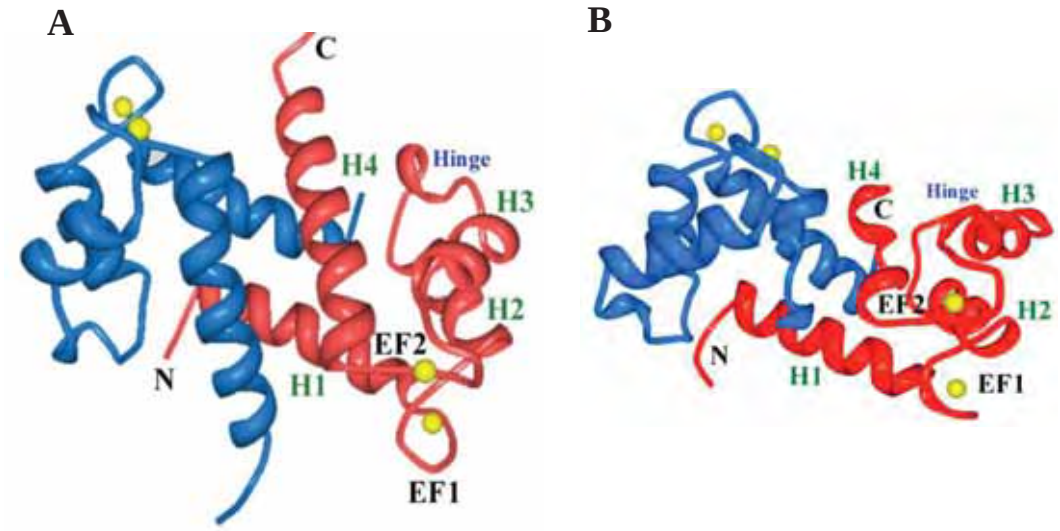

Figure 1.10: Ribbon diagrams of hS100A8 and hS100A9 dimers. (**A**) A ribbon representation of the S100A8 dimer. The two monomers are illustrated in blue and red, with each monomer able to bind two Ca^{2+} ions (yellow spheres). (**B**) S100A9 is represented in a similar manner, and like the S100A8 dimer, each S100A9 monomer can bind two Ca^{2+} ions. The N- and C-terminal domains, helices (H1-H4), EF-hands (EF1-EF2) and the hinge region of both proteins are indicated as labelled. Models are viewed parallel to the two-fold symmetry axis and were drawn by Dr. Esther Lim, using the program PDB Protein Workshop v3.4. Adapted from [388].

Diffusion of xenon into the crystal of S100A8 revealed a cavity between the two α-helices (helices IV and IV') in the homodimer which may be a binding site for hydrophobic molecules [388].

Although homodimerization of the individual S100A8 and S100A9 proteins is well understood on the structural level, little is known concerning precise mechanisms of hetero-oligomer formation, which may be preferred under some physiological conditions and crucial for many pathophysiological functions, such as that of calprotectin.

In the absence of Ca^{2+} the heterodimer of S100A8/S100A9 is the preferred form [393]. This is a non-covalently-associated anionic complex [394]. The heterodimer can chelate Zn^{2+} through a His-Glu-X-X-His motif in the C-terminal region of S100A9 (residues 91-95) and a His-X-X-X-His motif with a proximal upstream Glu in S100A8 (residues 83-87-91) [394]. These particular binding sites are present in the α-helices. The differing extent of crystallographically-ordered conformation in the C-terminal α-helix IV of both subunits may be important for heterodimer formation [392].

Zn^{2+} addition can induce S100A8/S100A9$_2$-tetramers, through Zn^{2+}- specific binding sites independent of the Ca^{2+}-specific EF-hands [395]. Interestingly, the heterotetramer has two different putative Zn^{2+}-binding sites at the S100A8/S100A9 subunit interface. One corresponds to a high affinity arrangement of three His residues and one Asp side-chain (His_{83} and His_{87} from S100A8 and His_{20} and Asp_{30} from S100A9), which is unique to the heterotetramer, and this may contribute to the Zn^{2+}-binding activity of calprotectin [392]. Korndorfer *et al.* showed that the quaternary structure of the $(S100A8/S100A9)_2$ heterotetramer may result from reduced exposure of solvent-accessible residues in both proteins, particularly in S100A9, forming a dimer of heterodimers [392]. The main contributors to tetramer association are the Ca^{2+}-binding loops in the C-terminals of the two proteins [392].

A Ca^{2+}-dependent trimer of S100A8/S100A9$_2$ is also proposed because of its elution characterized from size exclusion chromatography [86]. However Foell *et al*. suggest that this could be an artifact because trimer formation is contradicted by structural data obtained by NMR analysis [91, 391, 393].

New insights are emerging regarding the functional importance of Ca^{2+} and Zn^{2+}-binding in S100A8 and S100A9, which undergo metal-mediated amyloid oligomerization and fibrillation *in vitro*. These were seen in prostate cancer lesions and may contribute to the amyloidogenic processes in prostate cancer patients [396]. Hetero-oligomeric complexes of S100A8/A9 are characterized by significant stability and protease resistance. In protease-rich environments, for example at sites of inflammation, this protease resistance could favour accumulation and conversion to amyloid structures [396].

1.3.1.2 Regulation of S100A8 and S100A9

S100A8 and S100A9 are constitutively co-expressed in human neutrophils [397], monocytes [397], myeloid dendritic cells [398], platelets [124], osteoclasts and hypertrophic chondrocytes [122]. Many regions upstream and downstream of the transcription initiation site regulate the promoter activity of the murine and human genes. Myeloid-related protein regulatory elements [399], CCAAT/enhancer-binding proteins (C/EBPα and β) and putative STAT binding sites [400, 401] may regulate S100A8 and S100A9 transcription in a myeloid differentiation- and activation-dependent manner.

Deletion analysis of the mS100A8 gene promoter indicates several distinct regulatory regions downstream and upstream of the transcription initiation site that may activate or repress promoter activity [402]. Elements essential for LPS induction in myeloid cells and glucocorticoid enhancement are located within the region -178 to -1 [402]. Consensus motifs for transcription factors are located within these regions, and include TATA, NF1, E box, GC box, NF-κB, SPE, IRE, Ets box, Myb and AP-1 [399-403]. These factors are associated with basal, tissue-specific differentiation, activation and inflammation [402]. Importantly, the promoter region of the hS100A8 gene is essentially similar to that of mS100A8, in particular the common regulatory motifs such as TATA box, NF1 and E-box. These factors are associated with basal, tissue-specific, developmental, and inducible expression of genes, including many associated with myeloid and lymphoid-specific differentiation, activation and inflammation [402]. The sequence AAAAGCAGCTGA, located at position -27 immediately 3' to the TATA box is assumed to regulate S100 gene expression. Its location in mS100A8 and hS100A8 genes suggests a role in the formation of the transcription initiation complex [402].

Analysis of proximal promoter regions of S100A9 indicate many common binding sites for distinct transcription factors, such as AP-1, NF-κB and C/EBP [18, 403]. In addition, epithelial and myeloid-specific DNA elements regulate S100A9 gene transcription in a cell type-specific manner [403]. The promoter regions of S100A8 and S100A9 also contain several potential STAT3 binding sites (TTCCC G/A G/T AA). STAT3 signalling pathway is implicated in myeloid cell differentiation and macrophage activation [404]. STAT3 immunoprecipitated from 32D myeloid cells interacted with the promoter regions of both S100A8 and S100A9 genes, suggesting that STAT3 regulates their transcription under certain circumstances [404].

1.3.1.3 Expression of S100A8 and S100A9

S100A8 and S100A9 are constitutively co-expressed in a number of cell types. These proteins are also expressed in stratified squamous epithelia of the tongue, oesophagus and buccal cells [397]. Although there is relatively low expression in monocytes, tissue macrophages do not constitutively express these [405]. This restricted constitutive expression pattern suggested that expression is tightly regulated during myeloid cell differentiation. These proteins are not constitutively expressed in lymphocytes or basophils (see Table 1.11) [397].

Table 1.11: Expression of S100A8 and S100A9 in various cell types

Cell type	Mouse S100A8	Mouse S100A9	Human S100A8	Human S100A9	Refs.
Neutrophils	Constitutive	Constitutive	Constitutive	Constitutive	[86, 397]
Macrophages	Inducible	Nil	Inducible	Inducible	[143, 144, 406, 407]
Myeloid dendritic cells	ND	ND	Constitutive	Constitutive/ Inducible	[398]
Monocytes	Inducible	Nil	Constitutive	Constitutive	[143, 397]
Eosinophils and basophils	ND	ND	Nil	Nil	[408, 409]
Lymphocytes	ND	ND	Nil	Nil	[408]
Platelets	ND	ND	Constitutive	Constitutive	[124]
Endothelial cells	Inducible	Inducible	Inducible	Inducible	[410, 411]
Keratinocytes	Inducible	Nil	Inducible	Inducible	[412-416]
Embryonic stem cells	Inducible	Inducible	ND	ND	[404]
Microglia	ND	ND	Nil	Inducible	[417, 418]
Osteoclasts	Constitutive	Constitutive	Constitutive	Constitutive	[122]
Fibroblasts	Inducible	Nil	ND	ND	[419]
Hypertrophic chondrocytes	Constitutive	Constitutive	Constitutive	Constitutive	[122]
Trophoblasts	Transient	Nil	ND	ND	[420]

Adapted from [120].

Induction of hS100A8 is generally a late response, occurring maximally after 24 hrs, suggesting a requirement for other induced factors. Antiviral defense and MyD88-dependent/independent signalling is mediated by protein kinase R (PKR) [421] and reviewed in [422]. Induction of S100A8 by the Toll-like receptor (TLR)-4 agonist LPS and the TLR-3 agonist polyinosinic acid-polycytidylic acid (Poly I:C, a double stranded RNA (dsRNA) mimetic) involved p38 and ERK MAPK pathways, possibly mediated by PKR, with induction largely dependent on generation of IL-10 [400]. S100A8 is not directly induced by IL-10, but induction of S100A8 by LPS and Poly I:C is abolished by anti-IL-10 and is absent in IL-$10^{-/-}$ macrophages. Prostaglandin E_2 (PGE_2) and cAMP (cyclooxygenase (COX)-2 metabolites) synergize with LPS to enhance S100A8 expression [144]. Unlike LPS-provoked responses, dsRNA-induced S100A8 was independent of COX-2 metabolites because COX-2 gene expression had no effect on mRNA levels [400]. S100A8 is also induced by tumour necrosis factor (TNF)-α, IFN-γ, and Poly I:C [144, 406, 407].

Interestingly, mS100A9 is not induced in macrophages, fibroblasts or keratinocytes by the same stimuli that induce mS100A8. However mS100A9 is upregulated by IL-1β and TNF-α, in microvascular endothelial cells, whereas induction of mS100A8 by IL-1β and TNF-α is dependent on LPS activation, suggesting common and distinct regulatory pathways for mS100A8 and mS100A9 induction in microvascular endothelial cells [411]. In contrast to murine macrophages, in human monocytes and macrophages, S100A9 induction, like S100A8 is enhanced by IL-10 and reduced by antibodies to IL-10, indicating similarities in regulation of the human genes, but divergence in expression patterns in rodents and humans [400]. Inducers, enhancers and suppressors of the S100A8 gene are summarized in Table 1.12.

Table 1.12: Inducers, enhancers and suppressors of S100A8 gene expression

Cell types	Inducers	Enhancers	Suppressors	Refs.
Murine cell lines				
Macrophages/monocytes (RAW 264.7)	LPS	GC, IL-10, cAMP, PGE_2, TGF-β	IL-4, IL-13	[143, 406]
	Poly(I:C)	LPS, IL-10	-	[400]
	CpG	IL-10, PGE_2	-	*
Fibroblasts (NIH/3T3)	LPS	Dex (GC)	-	[406]
	FGF-2, IL-1β	Heparin	TGF-β	[419]
Microvascular endothelial cells (bEND3)	LPS, IL-1	TNF-α	-	[411]
	LPS	Dex (GC)	IL-4, IL-13	[407]
Keratinocytes (PAM212)	UVA, H_2O_2, LPS+IL-10+TNF-α	-	SOD_3 catalase	[416]
(PMK-R3)	PMA	-	Dex (GC)	[423]
Primary murine cells				
Fibroblasts	LPS	Dex (GC)	-	[406]
	FGF-2, IL-1β	Heparin	-	[419]
Elicited macrophages	LPS, TNF-α, IFN-γ, Poly I:C	IL-10, TGF-β, GC	IL-4, IL-13	[144, 400]
Keratinocytes	UVA	-	-	[416]
	PMA	-	Dex	[423]
Human cell lines				
Monocyte/macrophages (differentiated HL-60)	$VitD_3$	-	PMA	[231]
	PMA	-	-	[424]
Monocytic cells (Monomac 6)	$VitD_3$, LPS	IL-10, PGE_2, cAMP	-	*
(U937)	$VitD_3$, DMSO, Dex (GC), PMA, Retinoic acid, Norepinephrine			[425, 426]

Cell types	Inducers	Enhancers	Suppressors	Refs.
Primary human cells				
Monocytes	LPS, IL-1, TNFα	IL-10, GC	IL-10, IL-14	[427, 428]
	LPS, Dex (GC)			[406]
	PMA, LPS, GM-CSF			[230]
	Poly(I:C)			[400]
Dendritic cells	IL-10			[398]
Keratinocytes	TNF-α, IL-1β, IFN-γ			[429]

GC: glucocorticoids, TGF: transforming growth factor, PMA: phorbol 12-myristate 13-acetate, GM-CSF: granulocyte-macrophage colony-stimulating factor, SOD: superoxide dismutase, DMSO: dimethyl sulfoxide *unpublished data from our laboratory.

mS100A8 upregulation in macrophages, fibroblasts and microvascular endothelial cells by LPS is amplified by GCs [406]. GCs increased mS100A8 gene transcription and mRNA half-life. Dex does not induce mS100A8 directly, but does induce this gene in human monocytes. Moreover, synergy between LPS and Dex involves ERK1/2 and p38 mitogen-activated protein kinase (MAPK) pathways and required *de novo* protein synthesis, which was subsequently reduced by anti-IL-10 IgG indicating involvement of IL-10 induction is also important [406]. In addition, protein kinase A (PKA) positively, and PKC negatively regulated this process, suggesting that these pathways provide an additional level of control system.

Importantly, macrophages expressed hS100A8 and hS100A9 (although macrophage numbers were not significant) in the synovium from patients with rheumatoid arthritis (RA), following treatment with high dose corticosteroids, supporting S100A8 and S100A9 generation *in vivo* by GCs [406]. In mice, mS100A8 was detected in lung lavage fluid, and in infiltrating neutrophils in mice pre-treated with Dex, then given LPS intraperitoneally [430]. Interestingly, Dex repressed mS100A8 and mS100A9 expression in phorbol ester-induced skin inflammation, but only in wild type mice, not *c-fos*$^{-/-}$ mice, suggesting negative regulation of the two proteins by *c-fos*/AP-1-target proteins [423]. Repression may be due to negative interference between the activated glucocorticoid receptor and transcription factors such as AP-1, NF-κB and NF-IL-6 involved in inflammatory responses [423]. Thus synergy/repression of mS100A8 gene expression by GCs may be dependent on the cell type and/or mediator responsible for induction.

Because S100A8 expression in monocytes and macrophages is dependent on IL-10 and enhancement by GC [400, 406], the protein may have anti-inflammatory functions important in the resolution of inflammation.

Growth factors such as FGF-2 and TGF-β regulate fibroblast function, differentiation and proliferation. LPS, IFN-γ, TNF and TGF-β did not induce the S100A8 gene in murine 3T3 fibroblasts, whereas FGF-2 was a strong inducer [419]. This response was amplified by heparin. Heparin sulfate is a component of the extracellular matrix and can bind FGFs and this complex may be functionally important [431]. In addition, IL-1β either alone, or together with FGF-2/heparin also enhanced mRNA induction. In contrast, S100A9 mRNA was not upregulated by any treatment. Moreover, rat dermal wounds contained numerous S100A8-positive fibroblast-like cells 2 to 4 days after injury, but

were not detected in healed wounds [419]. S100A8 may play a role in fibroblast differentiation and proliferation, and in wound healing and repair, because of its upregulation by FGF-2/IL-1β, down-regulation by TGF-β and its time-dependent expression in wound fibroblasts [419].

Keratinocytes within the dermis of patients with psoriasis and squamous cell carcinomas express S100A8 and S100A9, whereas, normal keratinocytes do not [119, 121, 432, 433]. Murine and human S100A8 and S100A9 are also over-expressed in keratinocytes in inflamed skin in chronic inflammatory skin conditions such as lichen planus and systemic lupus erythematosus (SLE) [432, 434, 435]. In the human epidermis, epithelial cells express antimicrobial peptides (AMPs). In keratinocytes, AMPs are regulated in part by bacteria, through induction of IL-1α [436]. Addition of IL-1α to HaCaT cells (an immortalized keratinocyte cell line) promoted time- and dose-dependent increases in S100A8 and S100A9 gene expression, implying that these may impact on innate epithelial cell immunity [436]. In some cases, expression in keratinocytes may be mediated by stress responses via ROS and UVA exposure. mS100A8 is induced in keratinocytes by UVA, which promotes generation of ROS in the cell membrane *in vitro* and *in vivo*. mS100A8 induction was suppressed by the application of catalase and SOD during irradiation or 4-hydroxy-tempol (a SOD-mimicking agent) application prior to UVA irradiation of mouse skin, possibly through scavenging of $O_2^{\cdot -}$ and H_2O_2 *in vitro* or *in vivo*. This indicates that UVA-induced S100A8 expression in keratinocytes occurs through generation of ROS [416]. In humans, mild skin insults, such as tape stripping, are sufficient to induce S100A8 and S100A9 in the human epidermis [437].

1.3.2 REGULATION AND EXPRESSION OF S100A12

S100A12 has a different expression profile to S100A8 and S100A9. It constitutes ~5% of total cytoplasmic protein in neutrophils. It is also expressed in monocytes, but not lymphocytes, and expression occurs at a later stage of myeloid cell differentiation than the other calgranulins [438]. S100A12 is only seen in human oesophageal epithelial cells undergoing differentiation and only keratinocytes with no proliferating activity expressed S100A12. In contrast, immature proliferating cells in the epithelium did not produce S100A12 [130]. This suggests that S100A12 has a distinct regulatory role in differentiation and proliferation. S100A12 regulation and expression in smooth muscle cells (SMC) is described in more detail in Section 1.3.5.7.

S100A12 can be induced in several cell types by pro-inflammatory stimuli The S100A12 gene is transiently upregulated in monocytes by TNF-α after 4 hrs, whereas LPS causes more sustained expression. Treatment of phorbol ester-differentiated THP-1 macrophages with IL-6 induced S100A12 [439]; maximal induction was earlier than induction of mS100A8 [143], and in the Jurkat T cell line by anti-CD3/CD28 cross-linking [440]. Although no expression is seen in circulating eosinophils, eosinophils in airway tissue from asthmatic patients express S100A12 [131] but regulators mediating this are not characterized. These results imply distinct mechanisms of upregulation of the S100A12 gene that generally indicate a pro-inflammatory role even though there is emerging evidence that S100A12 has some protective roles in inflammation (discussed in Section 1.3.6.5).

1.3.3 CALGRANULINS IN DISEASE

In normal cells, the calgranulins have distinct expression patterns, but when normal processes are improperly regulated, expression of the calgranulins are often seen in cells that normally have no constitutive expression. The calgranulins are often elevated in plasma and/or serum during acute inflammation, likely due to secretion from neutrophils and/or activated macrophages (reviewed in [18, 441]). Similarly, calgranulin expression is elevated in patients with chronic inflammatory disorders, such as RA, inflammatory bowel disease, atherosclerosis and respiratory conditions such as asthma and bronchiectasis [131, 410, 442-445]. Conditions associated with altered calgranulin expression in tissues, serum and other bodily fluids are summarized in Table 1.13.

Table 1.13: Calgranulins in Disease

Diseases	S100 expression	Refs.
Infectious diseases		
Periodontitis	S100A8, S100A9	[446, 447]
Onchocerca infection	S100A8, S100A9	[448, 449]
Tuberculosis	S100A8, S100A9	[450]
Cat scratch disease	S100A8, S100A9	[451]
Malaria	S100A8, S100A9	[452]
Leishmaniasis	S100A9	[453]
HIV-1	S100A8, S100A9	[454-456]
Helmithic infections	S100A12	[457]
Bacterial abscesses	S100A8, S100A9	[458]
Influenza	S100A8	[400]
Leprosy	S100A8, S100A9	[459]
Autoimmune diseases		
Rheumatoid arthritis	S100A8, S100A9, S100A12	[442]
Psoriatic arthritits	S100A8, S100A9, S100A12	[460]
Juvenile idiopathic arthritis	S100A8, S100A9, S100A12	[442]
Systemic-onset juvenile idiopathic arthritis	S100A8, S100A9, S100A12	[442]
Systemic sclerosis	S100A8, S100A9	[401]
Sjogren's syndrome	S100A8, S100A9	[401]
Autoimmune polyneuropathies	S100A8, S100A9, S100A12	[461]
Crohn's disease	S100A8, S100A9, S100A12	[462]
Ulcerative colitis	S100A8, S100A9, S100A12	[462]
Multiple sclerosis	S100A8, S100A9	[463]
Inflammatory bowel disease (IBD)	S100A8, S100A9, S100A12	[444, 445]
Autoimmune keratitis	S100A12	[464-471]
Systemic lupus erythematosus	S100A8, S100A9	[472]
Kawasaki disease	S100A8, S100A9, S100A12	[470]
Skin diseases		
Psoriasis	S100A8, S100A9, S100A12	[370, 473-476]
Contact dermatitis	S100A8, S100A9, S100A12	[477]
Erythroderma	S100A8, S100A9	[472]
Sarcoidosis	S100A8, S100A9	[408]
Leprosy	S100A8, S100A9, S100A12	[408]
Lichen planus	S100A8, S100A9, S100A12	[478]
Contact eczema	S100A8, S100A9	[479]
Vascular diseases		
Atherosclerosis	S100A8, S100A9, S100A12	[410]
Ischemic heart disease	S100A8, S100A9	[124]
Kawasaki disease	S100A8, S100A9, S100A12	[470, 480]
Obesity	S100A8, S100A9	[481]
Giant cell arteritis	S100A8, S100A9, S100A12	[482]
Unstable angina	S100A8, S100A9	[483]

Diseases	S100 expression	Refs.
Respiratory diseases		
Cystic fibrosis (CF)	S100A8, S100A9, S100A12	[484-492]
Chronic bronchitis	S100A8, S100A9	[493]
Pneumonia	S100A8, S100A9, S100A12	[494]
Asthma	S100A12	[131]
Acute respiratory distress syndrome (ARDS)	S100A8, S100A9, S100A12	[495, 496]
Chronic obstructive pulmonary disease (COPD)	S100A8, S100A9, S100A12	[496]
Idiopathic pulmonary fibrosis (IPF)	S100A9	[497]
Others		
Alzheimer's disease	S100A9, S100A12	[418]
Cerebral malaria	S100A8, S100A9	[498]
Cerebral infarction	S100A8	[499]
Brain aging and injury	S100A8, S100A9	[100, 500]
Gout	S100A8, S100A9, S100A12	[501]
Osteroarthritis	S100A8, S100A9	[502]
Renal allograft rejection	S100A8, S100A9	[503]
Type II diabetes	S100A12	[504]
Hyperzincemia/	S100A8, S100A9	[505]
Hypercalprotectinaemia	S100A9	[506]
Autism		
Eye disorders	S100A8, S100A9	[507-509]
Irritable bowel sydrome (IBS)	S100A12	[510]

1.3.3.1 Expression in infectious diseases

S100A8, S100A9 and S100A12 are proposed as possible markers of disease and/or disease progression. Calgranulins are implicated in the host response against bacterial infection and invasion (see Section 1.3.6.7).

Normal human skin forms a barrier to resisting infection by pathogenic microbes. This protective function is partly mediated by AMPs (see Section 1.3.1.3). Human foreskin-derived epidermal keratinocytes exposed to Gram-negative bacteria such as *E. coli* or *P.aeruginosa* have increased amounts of S100A8 and S100A9, implicating a role in barrier defense of skin (see Section 1.3.5.6) [511]. S100A8 and S100A9 were observed in murine abscesses induced by i.p injection of *E. coli*, with high levels of these proteins found throughout abscess development. S100A8 and S100A9 was monomeric (one-third of protein amount), with no evidence of heterodimer formation. Moreover, S100A8 from abscesses was chemotactic, implicating a role for leukocyte recruitment [19]. In abscesses induced by *Staphylococcus aureus*, calprotectin was shown to inhibit growth by Mn^{2+} and Zn^{2+}, suggesting a role in the innate immune response to infection [512]. Similarly, calgranulins are found in cell-free fluid from human abscesses. In humans, high levels of calgranulins are also found in gingival crevicular fluid from patients with periodontitis [447].

Elevated S100A8 and S100A9 expression has also been reported in viral conditions. High levels were found in immunodeficient, HIV-1 seropositive patients [456] and calprotectin was significantly raised in serum from HIV patients at stages II and III (clinically asymptomatic and symptomatic stages, respectively, defined by the Centres for Disease Control and Prevention); the highest levels were found in patients with stage III, and acute ongoing opportunistic infections [513]. Only S100A9 was significantly raised in HIV stage III individuals with acute clinical events but was not related to $CD4^+$ T-cell numbers [513]. Importantly, S100A8 from cervico-vaginal secretions, and recombinant S100A8/A9, activate HIV replication in lymphocytes indicating that these proteins may contribute to the disease process [514, 515]. S100A8 was expressed in lungs of influenza-infected mice and was maximal at day eight in epithelial cells lining the airways and mononuclear cells. As IL-10 is implicated in viral persistence, and S100A8/S100A9 levels are likely to be maintained in conditions where IL-10 is raised, these proteins may contribute to persistence in patients with RNA viruses [400].

Infection with the malarial parasite *Plasmodium falciparum*, causes parasitaemia and fever episodes, and systemic S100A8 and S100A9 concentrations correlated well with these clinical manifestations [448, 452, 516].

1.3.3.2 Respiratory diseases

Early studies analyzing proteins in serum/plasma from patients with CF found a unique protein then called the cystic fibrosis antigen [517], subsequently identified as the S100A8/S100A9 heterocomplex [484]. S100A8/A9 levels are elevated in serum, plasma, sputum and bronchoalveolar lavage fluid (BALF) from patients with CF, and S100A12 is elevated in sputum and BALF [443, 485, 493, 496, 518]. S100A8 was confirmed in BALF from patients with CF using surface-enhanced laser desorption/ionization – time of flight (SELDI-TOF) analysis, highlighting the value of a proteomics study of biological fluids [519]. Increased levels may result from secretion from recruited neutrophils that characterize the chronic airway inflammation in this disease [485, 517]. Interestingly, lungs of mice carrying the G551D mutation in CF transmembrane conductance regulator have S100A8 mRNA levels three to four times higher than control mice [520]. Upon administration of LPS, S100A8 mRNA was also greater than controls. Its subsequent accumulation and localization in the lung indicate that it may be a marker for neutrophil accumulation. Macrophages from these mice were also hypersensitive to LPS [520], triggering over-expression of mS100A8 and TNF-α. S100A8 is proposed to contribute to the pathogenesis of CF by mounting an excessive inflammatory response to infection [520]. Thus, high serum levels of S100A8 and S100A9 are not just a consequence of chronic inflammation, but possibly also of macrophage hyper-reactivity.

S100A12 is also implicated in CF. Foell *et al.* found S100A12 in infiltrating neutrophils from lung specimens from patients with end-stage CF, and elevated S100A12 levels in serum from patients with acute infectious exacerbations [486]. This was corroborated by elevated S100A12 levels in sputum from CF patients. The authors suggest S100A12 as a putative marker of acute infectious exacerbations in CF [486].

Pulmonary fiborosis, defined as an overgrowth of fibroblasts and extracellular matrix deposition, is the end stage of many chronic inflammatory interstitial lung diseases [521], including sarcoidosis and IPF. S100A9 stimulates fibroblast proliferation *in vitro* and is expressed in granulomas from sarcoidosis patients [521]. S100A9 levels are elevated in BALF from IPF and sarcoidosis patients and these are associated with disease

severity, suggesting it as a marker for interstitial lung diseases [521]. Another study found an inverse relationship between S100A9 and forced vital capacity (FVC) and diffusion capacity of the lung for carbon monoxide (CO) in patients with IPF, suggesting that S100A9 may be involved in the evolution and progression of IPF [497]. Calgranulins and their association with asthma will be discussed in detail in Chapter 4.

1.3.3.3 Expression in vascular diseases

S100A8 and S100A9 are absent in normal arteries, but expressed in human giant cell arteritis [482], macrophages [479, 522], foam cells [410, 523] and neovessels in human atheroma and are also suggested markers of acute coronary syndromes. S100A8/A9 is elevated in the circulation prior to markers of myocardial necrosis and may be a suitable candidate for identification of unstable plaques and treatment of acute coronary syndromes [524]. Moreover, the risk of a repeat cardiovascular event increased with increasing S100A8/A9, and patients with the highest levels had a two-fold increased risk of a recurrent event [525]. Microarray analysis also indicated increased expression of platelet S100A9 mRNA in patients with acute ST-segment-elevation (relative to the isoelectric line as determined by electrocardiogram [526]) in myocardial infarction compared to stable coronary artery disease (CAD) [124].

In Apolipoprotein E $(ApoE)^{-/-}$ mice (develop advanced atherosclerotic lesions under a normal chow diet), mS100A9, but not mS100A8 was found in macrophages from atherosclerotic lesions [527]. In addition, mS100A8 recruited macrophages with a proatherogenic phenotype [523]. Mice deficient in S100A9 and ApoE had attenuated atherosclerotic lesion development and macrophage accumulation compared to mice deficient in ApoE alone fed a high fat diet [528]. Thus, S100A9 may regulate vascular inflammation and, by promoting leukocyte recruitment, responses to vascular injury (discussed in more detail in Chapter 5) [528].

Significantly higher S100A12 levels were detected in sera from CAD patients compared to controls and this may be secreted into the circulation from ruptured plaques; S100A12 levels correlated positively with levels of C-reactive protein (CRP) [529]. S100A12 was apparent in macrophages with some co-localization with RAGE, foam cells and around neovessels in atherosclerotic lesions [529]. In post-mortem samples, S100A12 was expressed in human coronary artery SMCs in ruptured plaques, and was more prominent in plaque from diabetic patients [530]. Increased plasma S100A12 was also elevated in hemodialysis patients with atherosclerosis and a role in disease acceleration

suggested [531]. Pro-inflammatory cytokines such as TNF-α and IL-1β contribute to atherogenesis [532], but in contrast to a previous study testing bovine S100A12 on a murine microglial cell line [440], our lab showed that S100A12 did not induce these cytokines in human monocytes or macrophages [529].

1.3.3.4 Expression in autoimmune diseases

S100A8, S100A9 and S100A12 are highly expressed in inflammatory and autoimmune arthritis [533] and reviewed in [441]. In RA, these proteins are highly expressed in activated phagocytes, and in infiltrating inflammatory cells in the synovium [442]. Expression is strongest at the cartilage-pannus junction; the primary site of cartilage and bone erosion in arthritis [442]. Synovial fluid from patients with juvenile RA, psoriatic arthritis or RA is rich in S100A8 and S100A9, with significantly higher concentrations than in patient-matched serum [460, 534]. S100A9 levels in serum from RA patients also correlated with body mass index; S100A8 levels were associated with S100A9 levels, anti-citrullinated peptide antibodies (ACPA) and rheumatoid factor [533]. Their expression is proposed to be associated with inflammation of synovial tissue where they activate the endothelium to propagate recruitment of inflammatory leukocytes into synovial tissue [442].

S100A12 levels are increased in synovial fluid and serum from RA patients, and disease severity correlates well with these [533, 535], and with ACPA, history of diabetes and serum S100A9 levels [533]. In contrast, S100A12 was undetectable in synovia from patients with osteoarthritis or in RA patients who responded to treatment [319, 535]. Interestingly, individuals with a Gly-Ser substitution at amino acid position 82 in RAGE have increased susceptibility to RA development. Cells expressing the serine residue have enhanced binding of S100A12 and cytokine/MMP generation compared to cells expressing the glycine residue. Serine was proposed to increase the binding affinity of RAGE, thereby contributing to the inflammatory phenotype seen in RA patients [536].

Another autoimmune disease with associated expression of S100A8 and S100A9 is SLE, characterized by the systemic involvement of several organs. Serum levels of S100A8/A9 were reported to correlate with the Systemic Lupus Erythematosus Activity Index (SLEDAI), and it was suggested as a potential marker of disease activity [468]. Interestingly, those patients presenting with arthritis in addition to SLE had higher S100A8/A9 levels [468, 472]. In SLE, higher levels of S100A8/A9 are suggested to be

due to active secretion by neutrophils at sites of inflammation (discussed in detail in Chapter 5).

Elevated amounts of S100A8, S100A9 and S100A12 are found in serum and mucosa in patients with IBD. Serum S100A8/A9 levels correlated with S100A12 levels and with disease activity, in children. These proteins are particularly evident throughout the lamina propria and epithelium in inflamed mucosa and were proposed to contribute to pathogenesis [444]. Similarly, S100A12 levels are elevated in other chronic inflammatory intestinal conditions, such as ulcerative colitis and Crohn's disease – both characterized by increased number of neutrophils in the intestinal mucosa [537]. Several studies suggest the value of S100A12 levels in faeces as a diagnostic marker of IBS and IBD [444, 510, 538, 539]. Faecal S100A12 can distinguish between active IBD and healthy controls with a sensitivity of ~86% and a specificity of ~100%, and between IBD and IBS with a sensitivity of ~86% and a specificity of ~96% [510]. S100A12 provokes activation of mast cells which are prominent in the intestinal mucosa, and may contribute to inflammation by promoting pro-inflammatory cytokine production [320].

1.3.3.5 Expression in cancer

Increasing evidence suggests that changes in the expression and/or function of S100 proteins may be critical during cancer development [403]. Genomic mutations within the chromosome 1q21, where many S100 genes are located, are associated with development of human epithelial tumours such as, lung, breast, oesophagus, colorectal and liver [540-548] and with tumours of soft tissue and bone [549-553]. Chromosomal positions 1q21-q23 are also target regions for transcriptional activation in common human epithelial malignancies [554, 555]. S100A8 and S100A9 are strongly upregulated in breast, lung, gastric, colorectal, pancreatic and prostate cancer [403], and altered S100A9 expression in carcinomas can lead to chemoresistance [556]. Paradoxically, S100A12, associated with regulation of pro-inflammatory pathways is not over-expressed in ovarian adenocarcinoma, breast adenocarcinoma, brain cancer, lymphoma, prostate adenocarcinoma, lung cancer or melanoma [338], and S100A12's involvement in cancer development is unclear.

In prostatic intraepithelial neoplasia, S100A8 and S100A9 expression is elevated in high-grade adenocarcinomas, particularly in lesions with a high degree of stromal invasion. S100A9 serum levels are significantly elevated in prostate cancer patients compared to healthy controls or those with benign prostatic hyperplasia [327]. The

heterocomplex induced activation of NF-κB and increased phosphorylation of p38 and p44/42 MAPKs in LNCaP cells, an androgen-sensitive human prostate adenocarcinoma cell line [557]. Extracellular S100A8/A9 also stimulated migration of benign prostatic cell *in vitro* [557]. Thus, enhanced S100A8 and S100A9 expression may be an early event in prostate tumorigenesis, which may contribute to its development and/or progression.

S100A8 and S100A9 may regulate proliferation and differentiation of some tumours. Growth of the breast cancer cell lines MCF-7 and MDA-MB-231 are promoted by low levels of the heterocomplex, in a MAPK-dependent pathway via RAGE ligation and NF-κB activation [294]. Conversely, in MCF-7 cells, oncostatin M strongly inhibits growth via the STAT3 signalling cascade, and this induced S100A9 gene expression. In cells expressing a dominant-negative mutant of STAT3, S100A9 induction was markedly reduced [558] and inhibition of S100A9 expression with siRNA reduced oncostatin M-induced growth supression [558]. The promoter region of S100A9 contains two oncostatin-M responsive regions; deletion of the 5'-flanking region from -1000 to -203 reduced two thirds of the oncostatin M activity and deletion to -106 completely eliminated the effects of oncostatin M, indicating that S100A9 may regulate oncostatin M-mediated breast cancer cell growth [558].

S100A9 may also regulate differentiation of some carcinomas. Its expression in invasive ductal breast carcinoma is associated with poor tumour differentation [408, 559]. Myeloid-derived suppressor cells (MDSC) are important in reducing the host response in cancer. In these cells there is a STAT3-inducible upregulation of S100A9, which subsequently prevents differentiation to dendritic cells and macrophages [404]. S100A9 also inhibits MDSCs implicated in suppression of T cell responses, and induction of T cell tolerance in cancer [560, 561]. $S100A9^{-/-}$ mice have reduced numbers of MDSC, reduced tumour size and increased tumour rejection when these mice were injected with EL-4 lymphoma cells [404]. MDSC accumulation promoted by mS100A9 expression may contribute to suppression of anti-tumour immune responses and promotion of tumour growth. These effects may be due to production of ROS in myeloid progenitor cells possibly by S100A9-dependent NADPH oxidase activation [404].

During cancer, macrophages and haematopoietic bone-marrow progenitors contribute to metastasis of the primary tumour [562, 563]. For example, primary tumours promote expression of MMP-9 in lung macrophages and endothelial cells, and promoted

subsequent invasion of lung tissue [563]. S100A8 and S100A9 expression in the lung is upregulated by distant tumours. As S100A8 is chemotactic, it may attract Mac 1^+-myeloid cells in premetastatic lung cancer. Neutralizing antibodies to S100A8 and S100A9 abrogated tumour cell migration and morphological changes to Mac 1^+-myeloid cells, suggesting that they contribute to tumour cell metastasis [564].

1.3.3.6 Expression in skin diseases

S100A8, S100A9 and S100A12 are either absent or expressed at low levels in normal epidermis but are highly expressed in inflammatory skin dermatoses such as lichen planus (a chronic mucocutaneous disease that affects the skin, tongue, and oral mucosa), psoriasis vulgaris and SLE. [432, 434, 473]. Expression profiles of calgranulins are summarized in Table 1.14.

Table 1.14 Calgranulin expression in inflammatory dermatoses

S100 proteins	Normal epidermal expression	Expression in skin diseases	Refs.
S100A8	UVA-induced in epidermis, minimal expression in epidermis,	Basal and suprabasal keratinocytes in psoriasis	[370, 416, 423, 474, 565]
S100A9	Minimal expression in epidermis	Psoriasis	[87, 370, 423, 474, 565, 566]
S100A12	Basal keratinocytes, suprabasal keratinocytes, Langerhan's cells	Lesional psoriasis, melanoma, Spitz nevi	[473, 474, 567]

Adapted from [413].

UVA induced-oxidative stress in murine keratinocytes increases S100A8 protein and mRNA but there is no evidence of S100A9 induction [416]. Mild insult by external stimuli in human skin caused strong expression of S100A8 and S100A9 in the epidermis (reviewed in [435]). Hence, in the skin, S100A8 and S100A9 are believed to be stress-related proteins and may have a protective role in wound healing, contrasting with their proposed pro-inflammatory functions in phagocytes [421].

S100A8 and S100A9 expression are associated with altered or abnormal pathways of epithelial cell differentation. These proteins are present in keratinocytes in the hyper-thickened epidermis of acute murine and human wounds, and of human ulcers. The altered expression of the proteins is most likely related to the activation keratinocytes and not to the inflammation itself. Cultured keratinocytes efficiently secrete the S100A8/A9 complex and may regulate the hyperproliferative state in the epidermis [565].

1.3.4 DIFFERENTIATION AND DEVELOPMENT

1.3.4.1 S100A8 and S100A9 in development

S100A8 and S100A9, although co-expressed during a number of cellular events, appear to have clearly distinct roles during fetal development. S100A8 mRNA is expressed in two sites – in extra-embryonic tissue, specifically, the ectoplacental cone (EPC) at 6.5-7.5 days post-coitum (dpc) and in myeloid cells in the developing liver at 11.5 dpc [420]. The EPC and the extra-embryonic ectoderm, from which many differentiated secondary tropoblast cell types arise, resemble granulocytes and macrophages [420]. They appear to be capable of phagocytosis and express the gene encoding the receptor for colony stimulating factor-1, also expressed in macrophages [568]. In contrast, S100A8 mRNA was detected in a very small subset of cells that delineate the external perimeter of the EPC. By 7.5 dpc, S100A8 forms a ring of cells surrounding the EPC as well as at the tip [420]. By 8.5 dpc, no S100A8 mRNA expression around the EPC was seen, but was still present at high levels in trophoblasts and trophoblast giant cells [420]. At 10.5-11.0 dpc, S100A8 mRNA expression was detected in cells associated with the vasculature at the maternal face of the placenta [420].

Deletion of mS100A8 is embryonic lethal [420]. At 6.5 and 7.5 dpc, intact embryos were indistinguishable from normal embryos. However, at 9.5 and 10.5 dpc, there is overt embryo resorption [420]. Homozygous null embryos contain cells of maternal genotype [420], suggesting that S100A8 may have a role in fetal-maternal interactions, because the decidual reaction to embryo implantation is essentially a form of acute inflammation. That is, the process of blastocyst attachment is similar to an acute inflammatory reaction [569]. For example, both processes involve elevated concentrations of prostaglandins, increased vascular permeability, production of ROS, tissue remodelling, including collagen degradation, and neutrophil infiltration [570]. Thus the absence of S100A8 may allow maternal cell infiltration, resulting in resorption of the embryo in $S100A8^{-/-}$ mice [420].

S100A9 is co-expressed with S100A8 in myeloid cells in the liver at 11.5 dpc [420] but is not detected in the EPC at any stage, except in decidual neutrophils [420]. Interestingly, although the S100A9 $^{-/-}$ gene results in somewhat compromised neutrophil function, it is not embryonic lethal [571, 572]. This suggests that S100A8 and S100A9 have roles independent of their heterodimers. Some functional implications of S100A9 deletion are discussed further in Section 1.3.6.10.

1.3.4.2 S100A8 and S100A9 in differentiation

In human bone marrow, S100A8/S100A9 expression is observed, first, at the metamyelocyte stage of neutrophil development whereas, those cells committed to monocyte development, express the complex at an earlier stage, therefore, approximately 50% of bone marrow monoblasts express S100A8/S100A9 [397]. In mouse bone marrow, however, expression of S100A8/S100A9 overlaps the leukocyte integrin CD11b/Mac-1, suggesting that mouse bone marrow cells have a function closer to mature myeloid cells [397].

S100A8 and S100A9 are clustered on human chromosome 1q21 – a region defined as the differentiation complex [33]. These genes are expressed during differentiation of human leukemia HL-60 cells (which do not express these proteins) into macrophage-like cells after vitamin D_3 treatment, with maximal expression two days post-treatment [573]. S100A8 and S100A9 expression is tightly regulated during monocyte-macrophage and granulocyte differentiation [402, 574]. Proliferating HL60 cells are terminally differentiated into non-proliferating monocytes after treatment with PMA [574], and within 24 hrs S100A8 and S100A9 mRNA levels are undetectable [574]. In contrast, when HL60 cells are differentiated to the granulocytic lineage with DMSO, high levels of S100A8 and S100A9 mRNA were observed after 24hrs [574], reminiscent of their constitutive expression patterns.

In murine myelomonocytic cell lines, expression of S100A8 and S100A9 is somewhat similar; expression is restricted to granulocytes and distinct stages of macrophage differenatiation [575]. Goebeler *et al*. demonstrated the tightly regulated nature of S100A8 and S100A9 expression during monocyte differentiation to mature macrophages. Using myeloid cell lines as representatives of different stages of differentiation, decreased S100A8 and S100A9 expression was found as these cells progressed to a “mature” macrophage phenotype [575]. Manitz *et al*. also showed that more S100A9-null bone marrow cells responded to granulocyte colony-stimulating factor

(G-CSF) or monocyte colony-stimulating factor (M-CSF), suggesting a shift to more mature myeloid precursor cells in S100A9-deficient bone marrow [572].

S100A9 is implicated in regulation of myeloid derived suppressor cells in cancer. Hematopoietic progenitor cells from wild type mice cultured with GM-CSF resulted in reduced differentiation of dendritic cells and macrophages and substantially increased the production of Gr-1^{+}CD$11b^{+}$ myeloid derived suppressor cells. This was not the case for cells cultured from the knockout mice, indicating that S100A9 prevents the defective differentiation of tumour cell-conditioned medium treated myeloid cells [404].

1.3.5 INTRACELLULAR FUNCTIONS OF CALGRANULINS

1.3.5.1 Modulation of intracellular calcium

S100s are implicated in the Ca^{2+}-dependent regulation of a variety of intracellular activities (see Section 1.2.1). The abundance of S100A8/S100A9 in particular (the most abundant Ca^{2+}-binding complex in neutrophils), may act as a "calcium sink" to protect cells from the harmful effects of prolonged elevation of Ca^{2+} following neutrophil activation [576].

S100A9 has a marked influence on intracellular Ca^{2+} and subsequent Ca^{2+}-dependent activities. For example, S100$A9^{-/-}$ neutrophils, which also have less S100A8, are less responsive to some chemoattractants and their ability to upregulate CD11b [572] in Ca^{2+}-free buffers. When extracellular Ca^{2+} is added *in vitro*, normal CD11b surface expression returns [572]. It is suggested, that deletion of the human S100A9 gene significantly alters Ca^{2+} homeostasis [572].

In mS100$A9^{-/-}$ bone marrow neutrophils, basal $[Ca^{2+}]_i$ are higher than wild type whereas in peritoneal granulocytes, basal levels were similar in both [577]. Stimulation by low concentrations of macrophage inflammatory protein-2 (MIP-2) reduced $[Ca^{2+}]_i$ by 40% compared to wild type cells, although chemotactic responses, induction of the respiratory burst, phagocytosis and neutrophilic apoptosis remained unchanged [571]. This implies that although S100A9 levels may regulate $[Ca^{2+}]_i$, its functions are not necessarily dependent Ca^{2+} flux. However, in peritoneal granulocytes, stimulated with platelet activating factor, there were no differences in the rise of $[Ca^{2+}]_i$ seen in S100$A9^{-/-}$ neutrophils, although ATP enhanced $[Ca^{2+}]_i$ levels in S100A9-null cells, but did not alter ATP-induced adhesion of neutrophils to endothelium [577]. Unlike MIP-2 stimulation, the ATP-induced oxidative burst was diminished in S100A9-deficient neutrophils, suggesting that purinergic receptors mediate these processes [577]. Phenotype and

functions relating to S100A9-deficient mice are discussed in Sections 1.3.6.9 and 1.3.6.10.

1.3.5.2 Regulation of enzyme activity

In myeloid cells, the activity of casein kinase (CK) I and II is inhibited by the S100A8/A9 heterocomplex, but PKC, cAMP-dependent protein kinase, insulin receptor tyrosine kinase or v-abl tyrosine kinase are unaffected [177]. CKII is implicated in phosphorylation of substrates such as nuclear oncogenes, RNA polymerase II and topoisomerase, which are necessary for normal cellular transcription and translation (reviewed in [397]). Metabolic events are terminated through inhibition of CK, which for short-lived and terminally-differentiated neutrophils and activated macrophages is of particular importance (reviewed in [397])[578]. S100A8/S100A9 may induce terminal myeloid cell differentiation in this manner (reviewed in [29, 397]). This function may provide an insight as to why the longer-lived tissue macrophages do not express S100A8/A9, whereas neutrophils, which have a defined lifespan, do (reviewed in [397]).

1.3.5.3 Fatty acid metabolism and transport

The heterocomplex binds a number of unsaturated fatty acids (FA) with high affinity [579]. FA binding by the complex has been found in neutrophils and keratinocytes [178, 579, 580]; α-linoleic, γ-linolenic and arachidonic acids bind most effectively. Saturated FA such as palmitic and stearic acids, and monounsaturated FA are poor competitors [579, 580]. FA binding appears to be Ca^{2+}-dependent, with one Ca^{2+} bound to each of the four EF-hands present in the heterodimer [581]; lowering free Ca^{2+} levels reduces the FA-binding capacity [579].

Arachidonic acid (AA) binding is abrogated by other bivalent cations such as Zn^{2+} and Cu^{2+} in the presence of Ca^{2+}, whereas Mg^{2+}, does not [581]. Interestingly, the inhibitory effects of Zn^{2+} and Cu^{2+} are not due to reduced formation of the S100A8/A9 heterocomplex. Each cation promotes a different conformational change that affects the subsequent Ca^{2+}-induced formation of the AA binding pocket within the complex [581]. Importantly, the inhibitory effect of Zn^{2+} occurs at physiological serum concentrations, suggesting that the heterocomplex may transport AA at sites of inflammation, but not within the blood compartment [581]. Post-translational modifications such as

phosphorylation of S100A9 may also affect heterocomplex formation but this did not affect AA binding properties [580].

When neutrophils were stimulated with opsonised zymosan, the FA-S100A8/A9 complex translocates to the membrane [582]. Stimulation of neutrophil-like HL-60 cells with PMA, leads to secretion of the complex, with concomitant release of bound AA. However, when $[Ca^{2+}]_i$ levels were elevated with A23187, arachidonic acid was released without secretion of S100A8/A9, suggesting an important role for the heterocomplex in mediating Ca^{2+} signalling and AA effects [580].

The interaction of the heterocomplex with AA and the metabolite eicosanoid, may mediate monocyte and neutrophil functions, for example, adhesion to the endothelium. Direct binding of AA to the heterocomplex also contributes to activation of nicotinamide adenine dinucleotide phosphate (NADPH) oxidase (see Section 1.3.5.4) [583].

1.3.5.4 Regulation of NADPH oxidase activity

Phagocytes play important roles in host defense against microbial infection, through production of ROS, which are dependent on NADPH oxidase, which is dormant in resting phagocytes (see Section 1.4.1.5) [465]. High concentrations of AA (50-100 μM) can activate NADPH oxidase by direct interaction between the components $p47^{phox}$ and $p22^{phox}$ [465]. At low AA concentrations, phosphorylated $p47^{phox}$ binds $p22^{phox}$ and activates the oxidase [465].

The S100A8/A9 heterocomplex, which binds AA, is also a novel partner of NADPH oxidase. S100A8/A9 transfers AA to NADPH oxidase, primarily via S100A8 binding to $p67^{phox}$ and Rac. In contrast, S100A9 does not interact with either $p67^{phox}$ or $p47^{phox}$ [178]. A mutant form of the heterocomplex, unable to bind AA, cannot enhance NADPH oxidase activity. Thus, the heterocomplex plays an important role in phagocyte NADPH oxidase activation [178].

NADPH oxidase activity is impaired by reducing S100A9 expression in neutrophil-like NB4 cells, and in bone marrow neutrophils from $S100A9^{-/-}$ mice. Similarly, impaired oxidase activation ocurred following pretreatment of neutrophil cytosol with an S100A9-specific antibody [178]. In addition, the S100A9 residue Thr_{113}, which, when phosphorylated, promotes S100A8/A9 translocation to the plasma membrane, is important in NADPH oxidase activity [584]. S100A9 mutants lacking this

residue have reduced ability to promote NADPH oxidase activity in HaCaT keratinocytes [584].

1.3.5.5 Regulation of cytoskeletal dynamics

S100 proteins regulate the three major constituents of the cytoskeleton (Section 1.2.1.5). When cytosolic $[Ca^{2+}]_i$ are elevated following neutrophil activation (by zymosan), S100A8, S100A9 and S100A12 translocate from the cytosol to the plasma membrane and vimentin IFs in monocytes and granulocytes, and to keratin IFs in epithelial cells [231, 233, 585]. Translocation of S100A8 requires prior complexation with S100A9 [231]. The heterocomplex is believed to modulate Ca^{2+}-dependent interactions between IFs and membranes, and when PKC is activated in monocytes, the heterocomplex is translocated to the cytoskeleton and interacts with MTs, IFs, or F-actin, suggesting that they modulate cytoskeletal rearrangement and/or dynamics central to phagocytosis, exocytosis and/or migration [29, 230, 231, 585-587]. There is, however, no information to show that S100A8 and/or S100A9 does or does not affect IF dynamics and IF interactions with membranes and/or other cytoskeletal components and the accompanying functional implications are unknown.

Phosphorylation of S100A9 at residue Thr_{113} [588], when in complex with S100A8, by p38 MAPK, inhibits S100A8/A9 induced tubulin polymerization [232], implying that phosphorylation modulates phagocyte migration. *In vitro* studies with neutrophils and *in vivo* work using $S100A9^{-/-}$ mice showed reduced recruitment of neutrophils into granulation tissue during wound healing [232]. $S100A9^{-/-}$ neutrophils also contained significantly less polymerized tubulin [232]. S100A8 and S100A9 form non-covalently linked tetramers upon binding to Ca^{2+} [47]. Tetramer formation of S100A8/A9 promotes MT polymerization and bundling and cross-linking to F-actin [589], important processes in leukocyte migration. Neutrophils from $S100A9^{-/-}$ mice have reduced levels of polymerized tubulin, and there is diminished granulocyte recruitment and altered phagocyte migration *in vivo* [232].

1.3.5.6 Antimicrobial and anti-invasive activity

The extracellular antimicrobial functions of S100A8/A9 are well documented and described in Section 1.3.6.7. However, intracellular roles for S100A8/A9 are also proposed.

Mucosal keratinocytes are frequently exposed to endogenous and exogenous invading microorganisms. Cells that express S100A8/A9 resist bacterial adherence and invasion. For example, KB cells (a cell line derived from a human carcinoma of the nasopharynx), transfected with calprotectin had 40-50% fewer internalised *P. gingivalis* compared to sham controls [590]. Similarly, the transfected cell line resisted invasion by *L. monocytogenes* and *S. enterica* [591], suggesting that calprotectin not only has innate immune functions, but also enhances barrier protection to bacterial invasion. However, *L. monocytogenes* can grow in the cytoplasm, and appears to circumvent the intracellular antimicrobial activity of S100A8/S100A9 [592]. Using TR146 epithelial cells (a human buccal tumour cell line), Zaia *et al*. found that after exposure of TR146 epithelial cells to *L. monocytogenes*, calprotectin mobilised from the cytoplasm to MTs, facilitating intraepithelial survival of the bacterium [592].

Keratinocyte resistance to bacterial invasion depends on the Ca^{2+}-binding domains within S100A9 in the intracellular heterocomplex [593]. S100A9 has an extended C-terminal region identical to the N-terminal region of neutrophil immobilizing factor (NIF) [588, 594]. This region has a suggested putative antimicrobial Zn^{2+}-binding motif and a phosphorylation site. A His-rich sequence in $S100A9_{103-105}$ is reported to bind Zn^{2+} [595], however, deletion of this did not affect anti-*Listeria* activity [593]. Interestingly, deletion of C-terminal residues 113 and 114 enabled invasion by *Listeria* and *Salmonella*, suggesting that these regulate mechanisms that facilitate internalization [593]. $S100A9_{113}$ is the only phosphorylation site in S100A9, and regulates MT-dependent translocation of the S100A8/A9 complex to the plasma membrane [596], binding [580, 581] and release of AA [597]. Deletion of this residue may disrupt calprotectin localization in the plasma membrane, subsequently causing tubulin cytoskeletal dysfunction, thereby disrupting binding and internalization of bacteria [593].

Moreover, mutation of both Ca^{2+}-binding loops in S100A9 (complexed with native S100A8) failed to promote epithelial cell resistance to bacterial invasion by *Listeria monocytogenes* (*L. monocytogenes*) and *Salmonella typhimurium,* suggesting that Ca^{2+}-binding loops I and II promote resistance to bacterial invasion in keratinocytes [593].

Intracellular calgranulins also mediate host protection in wound healing. For example, in mice with wounds from free-electron laser or scalpel incision S100A8 and S100A9 expression levels were elevated in the epidermis. Low S100A8 and S100A9 expression correlated with reduced wound healing, and higher levels of MMP-13, which

breaks down extracellular matrix, and the high S100A8 and S100A9 levels found in the dermal wound margin may assist in wound healing [598]. Some report that S100A8/A9 inhibits MMP activity by Zn^{2+} sequestration [599] and is protease resistant [600], and Greenlee *et al*. suggest that S100A8 and S100A9 are substrates for MMP-2 and MMP-9 [601]. More research is required to illucidate the mechanisms of MMP interaction, and how S100A8 and S100A9 regulate their expression.

TGF-β is implicated in the healing process of dermal wounds [602, 603]. S100A8 mRNA and protein induced by FGF-2/heparin was suppressed in fibroblasts co-stimulated with TGF-β, possibly by decreasing S100A8 mRNA stability. TGF-β is associated with apoptosis and accumulation of extracellular matrix in cataracts [604]. In later stages of wound healing, TGF-β is active. Down-regulation of fibroblast-derived S100A8 is consistent with reduced inflammation in scar tissue [419].

As S100A8 is an avid oxidant scavenger [410, 605, 606], it is proposed that induction in UVA irradiated murine keratinocytes protects against excessive ROS-induced damage. Therefore, calprotectin may reduce microbial invasion and support repair of damaged tissues [18]. Extracellular functions of the heterocomplex are discussed in Section 1.3.6.7.

1.3.5.7 Intracellular functions of S100A12

Intracellular functions of S100A12 are poorly studied. In the absence of Ca^{2+}, S100A12 was found in the cytosol. Upon addition of Ca^{2+}, S100A12 translocates to the membrane and cytoskeletal components [236, 482, 495]. S100A12 does not associate with S100A8 or S100A9 *in vivo*, despite their close amino acid sequence homologies [438]. Hatakeyama *et al*. found that S100A12 binds several intracellular mammalian proteins, including isocitrate dehydrogenase (IDH), fructose-1,6-bisphosphate aldolase A, glyceraldehyde-3-phosphate dehydrogenase (GAPDH), and annexin V. Of these binding partners, annexin V was strictly Ca^{2+}-dependent, whereas binding of GAPDH and IDH was only weakly Ca^{2+}-dependent [607]. Results suggest that mammalian S100A12 may have a chaperone/anti-chaperone-like function [608].

S100A12 is associated with coronary atherosclerotic plaque rupture. S100A12 promotes transformation of contractile vascular SMCs to cells with reduced expression of contractile fibers, increased production of ROS, IL-6 and TGF-β [609]. Recently, vascular smooth muscle S100A12 was implicated in acceleration of atherosclerosis and

atherosclerosis osteogenesis – a feature of plaque instability [610]. ApoE-null mice, with the S100A12 transgene, showed increased expression of bone morphogenic protein-2 and osteoblastic genes, for example Runx-2 and Dmp-1 were increased in aorta and cultured vascular SMCs. Moreover, inhibition of NADPH oxidase attenuated S100A12-mediated osteogenesis in cultured vascular SMCs, suggesting that a pro-inflammatory environment was required to induce osteoblastic differentiation and vascular calcification [610].

1.3.6 EXTRACELLULAR FUNCTIONS OF CALGRANULINS

1.3.6.1 Extracellular functions of calgranulins

S100A8 and S100A9 are found in the extracellular space in inflammatory lesions and systemically in many clinical conditions. Although many extracellular functions are reported (summarized in Table 1.15), some findings are somewhat conflicting. Variations in observations may be due to protein preparations. For example, recombinant proteins purified from *E. coli* can be contaminated by endotoxin. In addition, correct protein folding and post-translational modifications, particularly from reactive oxygen intermediates, may also alter extracellular activity. Levels of Ca^{2+}, Zn^{2+} and Cu^{2+}, can also influence complex formation and thereby influence extracellular functions. In addition, species differences also make functional analysis difficult. For example, hS100A8 does not possess the same chemotactic properties as mS100A8 [420], although both proteins are implicated in inflammatory responses. Some studies report the use of heterologous systems (i.e. testing S100A12 on murine cells) that could lead to spurious results.

Table 1.15: Extracellular functions of S100A8, S100A9, S100A8/A9 and S100A12

S100 proteins	Extracellular functions	Proposed mechanisms	Refs.
Human S100A8	Phagocyte migration	Induction of Mac-1 and L-selectin shedding, suppression of S100A9-mediated integrin activation	[297, 316, 611]
	Chemotaxis	G protein-coupled mechanism	[297, 316-318]
	Fugetaxis	Oxidation-dependent mechanism	[612]
	Protection against oxidants	Scavenging of ROS and reactive nitrogen species (RNS)	[410, 605, 606, 613]
	Phagocyte activation	Activation of TLR-4	[421]
Human S100A9	Phagocyte migration and adhesion	Induction of Mac-1 (CD11b/CD18) and L-selectin shedding, upregulation of Mac-1, stimulation of neutrophil adhesion to fibrinogen and fibronectin	[297, 316, 611]
	Chemotaxis	G protein-coupled mechanism	[297, 316]
	Fugetaxis	Oxidation-dependent mechanism	[614]
	Fibrin formation	Inhibition of fibrin formation due to homology with high molecular weight kininogen	[615]
	Anti-nociceptive activity	Secretion of S100A9 into the extracellular millieu	[616, 617]
	Modulation of macrophage function	Inhibition of $O_2^{\cdot -}$ and H_2O_2 release from activated macrophages	[618]
Human S100A8/S100A9	Phagocyte migration	Induction of Mac-1 (CD11b/CD18) and L-selectin shedding, upregulation of Mac-1	[297, 316, 611]
	Chemotaxis	G protein-coupled mechanism	[316]
	AA transport	Delivery of AA to endothelial cells via CD36-mediated uptake	[619]

S100 proteins	Extracellular functions	Proposed mechanisms	Refs.
	Antimicrobial and antifungal activities	Sequestration of Zn^{2+} and Mn^{2+}	[512, 620, 621]
	Anti-invasive activities	Ca^{2+}-binding loops I and II of S100A9	[593]
	Tumour cell lines apoptosis	Sequestration of Zn^{2+}, activation of caspase-3, mitochondrial release of pro-apoptotic proteins	[302, 622]
	Endothelial cell activation	Induction of pro-inflammatory genes and adhesion molecules via NF-κB activation by RAGE-MAPK	[623]
	Regulation of MMP activity	Sequestration of Zn^{2+}	[599, 624, 625]
Murine S100A8	Activation and recruitment of neutrophils and macrophages	Nuclear translocation of MyD88, activation of NF-κB, and secretion of TNF-α via TLR-4 ligation, induction of NO production via inducible nitric oxide synthase (iNOS) in macrophages	[421, 626]
	Chemotaxis of neutrophils and monocytes	G protein-coupled mechanism	[296, 314]
	Regulation of cartilage destruction	Upregulation of MMP-2, -3 and -9 expression	[625, 627]
	Protection against oxidants	Scavenging of ROS and RNS	[605, 606, 628]
Murine S100A9	Anti-nociceptive activity mediated by inhibition of adherent peritoneal cells	Secretion of S100A9 from activated neutrophils	[629, 630]
	Modulation of macrophage function	Inhibition of $O_2^{\cdot -}$ and H_2O_2 release from activated macrophages, neutralization of mS100A8-dependent stimulation of TLR-4, inhibition of macrophage spreading and phagocytosis	[421, 618]

S100 proteins	Extracellular functions	Proposed mechanisms	Refs.
Murine S100A8/S100A9	Suppression of nitrogen oxide from activated neutrophils and/or macrophages	Suppression of IL-6 and NO production	[631]
S100A12	Pro-inflammatory activity on inflammatory and endothelial cells	Binding to RAGE on inflammatory cells, nuclear translocation of NF-κB, secretion of cytokines, activation of MAPK pathway	[440]
	Neurite extension activity	Binding to RAGE and stimulation of phospholipase C (PLC), PKC, MAPK and Ca^{2+}/calmodulin-dependent kinase II activities in neurons	[464]
	Regulation of MMP activity	Zn^{2+}-induced S100A12 hexamer formation	[529]
	Monocytoid chemotaxis	Positive regulation of actin polymerization	[320]
	Mast cell degranulation and activation	Ligation of an unknown G-protein coupled receptor	[131]
	Monocyte and mast cell chemotaxis	G protein-coupled mechanism	[298, 320]
	Antimicrobial, antifungal and antiparasitic activities	Zn^{2+}-dependent mechanism, binding to nematode paramyosin	[632]
	Phagocyte migration	Binding to RAGE, upregulation of Mac-1 affinity and L-selectin shedding	[319]
	Suppression of MMP activity	Sequestration of Zn^{2+}	[529]

Adapted from [120].

1.3.6.2 Secretion of the calgranulins

S100A8 and S100A9 lack structural requirements for secretion via the classical endoplasmic reticulum/Golgi route [230, 633]. Secretion of S100A8 and S100A9 appears to be cell specific. That is, in murine and human microvascular endothelial cells (HMEC), fibroblasts and keratinocytes these proteins appear to be principally cell-associated [411, 416, 419], whereas stimulated neutrophils and monocytes/macrophages secrete S100A8 [144, 230, 400, 407]. Secretion of S100A8/A9 can occur as a result of cell disruption or death [633]. Human neutrophil calprotectin is only secreted after incubation with live *Candida albicans* (*C. albicans),* and its secretion correlates with loss of neutrophil viability [633].

When human monocytes are activated by PKC, S100A8 and S100A9 secretion is energy-dependent. As expected, inhibitors designed to block the reticulum/Golgi route do not prevent secretion [230]. Secretion of the complex is inhibited by MT-depolymerizing agents, demecolcine and nocodazole, indicating a requirement for intact tubulin network [230]. This observation was corroborated by Kido *et al.* in their study of *Porphyromonas gingivalis* lipopolysaccharide (P-LPS)-induced secretion of calprotectin from human neutrophils [634]. Secretion was inhibited by anti-CD14 and anti-TLR-2 antibodies that would negate P-LPS binding and by inhibitors of MT and MF polymerization. In this case, heterocomplex secretion may occur via the CD14-TLR2-NF-κB signalling pathway [634].

Chemotaxins such as C5a, formyl-methionine-leucine-phenylalanine (fMLP), and PKC also promote S100A8/A9 secretion [230, 635]. C5a and fMLP induce secretion in a dose-dependent manner [635] and is dependant on ligation of G protein-coupled receptors. LPS [144, 407] or dsRNA [400] induce relatively high amounts of S100A8 in murine macrophages that are readily secreted in the absence of S100A9.

1.3.6.3 Phagocyte migration

mS100A8 was the first S100 to have a well defined chemotactic function, with potent activity for neutrophils and monocytes at concentrations of 10^{-13} and 10^{-11} M *in vitro* [314]. The chemotactic portion of mS100A8 corresponds to the hinge region: $mS100A8_{42-55}$. Chemoattractants such as fMLP, C5a and IL-8 are defined as ‘classical’ chemoattractants because they stimulate phagocyte activation and migration, and a Ca^{2+} influx, whereas some chemoattractants, including TGF-β, and some S100s promote only

actin polymerization without causing Ca^{2+} influx or altering adhesion molecule expression [296, 315]. The receptor through which mS100A8 exerts its function is possibly a pertussis toxin sensitive, G protein-coupled receptor [296].

When mS100A8 was injected into the footpad of mice, it caused a mild, but sustained response with mixed cellular infiltrate: predominantly polymorphonuclear leukocytes (PMN) 4 hr post-injection, and PMN and mononuclear cells 24 hrs post-injection [317], similar to that of mild delayed type hypersensitivity skin reaction [317]. The murine hinge region caused a transient inflammatory response, with little infiltrate after 24 hrs [317], indicating additional, but as yet unidentified, structural domains essential for leukocyte recruitment. Neutrophils recruited by intraperitoneal mS100A8 injection expressed high levels of β_2 integrin Mac-1, suggesting that it may modulate leukocyte adhesion [636].

Chemotactic activators of hS100A8 and hS100A9 are slightly more controversial. Newton and Hogg found that S100A8 and S100A9 did not have chemotactic activity for human neutrophils [297]. In addition, studies with the hinge region of S100A8 (residues 43-56) did not elicit significant chemotactic responses on murine PMN and WEHI 265 cells [317]. In contrast, Ryckman *et al.* showed upregulation and activation of Mac-1, shedding of L-selectin and Mac-1-mediated neutrophil adhesion to fibrinogen in response to S100A8, S100A9 and S100A8/A9 [316]. They found that these proteins provoked neutrophil chemotaxis at concentrations of 10^{-12}-10^{-9} M [316]. Ryckman *et al*. also reported that chemotactic activity, as with mS100A8 [605] was inactivated by oxidation [316]. NaOCl-treated hS100A8 inhibited neutrophil adhesion to fibrinogen by >95%. In contrast, oxidation of hS100A9 and the heterocomplex had no effect on chemotaxis [316]. This suggests that some of the differences in observations between groups may be the result of oxidation during protein purification and/or storage. We found that S100A8 spontaneously oxidizes to the dimer (inactive in chemotaxis) if not stored under argon.

Ryckmann *et al*. reported that hS100A9 and hS100A8/A9 were also chemotactic, for neutrophils *in vivo* and *in vitro*. These proteins stimulated L-selectin shedding and upregulation of CD11b, inducing neutrophil adhesion to fibrinogen via CD11b and increasing affinity [316] via a pertussin toxin-sensitive, G protein-coupled receptor. However, in another study, addition of S100A8 to S100A9 and subsequent dimerization inhibited this function [297]. S100A9 alone stimulates neutrophil adhesion to fibronectin [611, 637], and monocyte adhesion to the endothelium *in vitro* [638]. S100A8/A9 also

upregulate adhesion molecules, intracellular adhesion molecule-1 (ICAM-1) and vascular cell adhesion molecule-1 (VCAM-1) on endothelial cells, which may promote further leukocyte recruitment [623]. Injection of hS100A8/A9 or the individual subunits into the murine air pouch resulted in accumulation of neutrophils, which was negated by neutralizing antibodies to these proteins [639].

mS100A9 is implicated in leukocyte infiltration to sites of inflammation. For example, in acute pancreatitis, induced with supramaximal injections of caerulein, there were large differences between wild type and S100A9-null mice affected with pancreatitis; S100A9-null mice had less leukocyte infiltration and myeloperoxidase (MPO) activity in lungs and pancreas [640]. Moreover, serum amylase, lipase activities and intrapancreatic trypsinogen activation peptide-levels were reduced. The authors suggest that leukocyte infiltration into the pancreas depends on S100A9 secreted from PMN [640].

The Hogg group showed that neutrophils from S100A9-null mice have reduced responses to some chemoattractants because of defective chemoattractant-induced Ca^{2+} signalling [641], confirming earlier observations by Manitz *et al*. [572]. Although the response to fMLP in $S100A9^{-/-}$ neutrophils was unaffected, sub-optimal levels of MIP-2α, MIP-1α, PKC, C5a and platelet activating factor (PAF) decreased the Ca^{2+} flux required for optimal chemotactic responses [571, 641]. Moreover, bone marrow neutrophils from $S100A9^{-/-}$ mice have reduced responsiveness to chemotactic signals such as IL-8 and LTB_4 *in vitro,* and IL-8 failed to upregulate CD11b [572]. S100A9-null neutrophils contain less polymerized tubulin, suggesting that deficiencies in their migration are due to dysregulation of cytoskeletal dynamics [572].

mS100A9 is also suggested to be critical in responses to vascular injury, by moderating leukocyte recruitment and proliferation [528]. Femoral artery wire injury in S100A9-deficient mice showed significantly reduced leukocyte accumulation, proliferation of intimal and medial cells and neointimal formation, compared to wild type mice [528]. In another model, induction of vasculitis with LPS and subsequent TNF-α injection in $S100A9^{-/-}$ or wild type mice indicated that S100A8/S100A9 complexes regulate neutrophil-dependent thrombohemorrhagic vasculopathy [528]. S100A9-null mice had 59% less hemorrhagic lesion severity and ~82% less hemorrhagic area compared to wild type mice. Moreover, skin edema was reduced by ~26% in S100A9-null mice and neutrophil accumulation in the vascular wall and skin fell by ~45% [528].

However, mS100A9 is apparently not essential for all inflammatory processes. For example, although cytoskeletal dysfunction resulting from the absence of S100A9 led to diminished responses to wound healing *in vivo* [232]**,** injection of IL-8 into the ear pouch of S100A9 null mice, caused neutrophil infiltration similar to wild type. In addition, thioglycolate recruitment of leukocytes was similar in S100A9-null and wild type mice [572]. Similarly, myeloid cell functions, *in vitro* indicated no difference in terms of phagocytosis, superoxide burst, and apoptosis. This indicates that S100A8 and S100A9 are not absolutely necessary for many myeloid functions.

S100A12 is chemotactic for monocytes [298] and mast cells [131] at nanomolar to picomolar concentrations, and is weakly chemotactic for neutrophils *in vitro*. The function of S100A12 is attributed to the hinge region (residues 38-53), that has a very similar in amino acid sequence to the hinge region of murine S100A8 [298]. Amino acid residues Asn_{46} and Ile_{47}, are conserved at similar positions and are required for chemotactic activity. In mice, S100A12 is chemotactic for monocytes, mast cells and neutrophils [131, 298, 320]. Neutrophil adhesion to fibrinogen is induced by S100A12 via upregulation of Mac-1 at concentrations similar to those found in synovial fluids from patients with inflammatory arthritis [319]. Expression of ICAM-1 and VCAM-1 on endothelial cells were also upregulated by S100A12 [440], which might facilitate neutrophil adhesion and extravasation in the vasculature.

1.3.6.4 Mast cell function

Activation of mast cells is important in the early events following infection and autoimmune diseases, and is modulated by inflammation [642, 643], but characterization of non-IgE-mediated activation, or how these processes are modulated, is only now emerging [131].

S100A8 is implicated in the pathogenesis of inflammatory diseases (reviewed in [435]) and is elevated in respiratory diseases (see Section 4.1, Chapter 4). However in contrast to its pro-inflammatory functions, mS100A8 reduced mast cell degranulation, and IL-6, IL-4 and GM-CSF release, in response to IgE cross-linking *in vitro*. In contrast, Cys_{42}-Ala_{42}S100A8 failed to suppress degranulation, and the active Cys residue in

mS100A8 reduced intracellular ROS [644][1] required for signalling through linker for activation of T cells (LAT) [645]. In a murine model of acute asthma, S100A8, but not Cys_{42}-Ala_{42}S100A8, reduced mast cell degranulation and generation of eosinophil chemoattractants, and reduced mucus production in the lungs, indicating a protective role in allergic inflammation through oxidant scavenging [644].

S100A8 can also be S-nitrosylated (S100A8-SNO) (see Section 3.1, Chapter 3). S100A8-SNO also suppressed mast cell degranulation *in vitro* and inflammation provoked by mast cell activation in the rat mesenteric circulation [613]. NO suppresses mast cell degranulation, via modification of acceptor proteins [646, 647]. S100A8-SNO is an NO donor and can transfer NO [613], indicating the mechanism underlying the observed effects. S100A12-mediated effects on mast cells are discussed in Section 1.3.7.

1.3.6.5 Regulation of MMPs

Emerging evidence suggests that the calgranulins may mediate MMP activities. A murine chondrocyte cell line H4 stimulated with TNF-α, IL-1β, IL-17 and IFN-γ expressed S100A8 mRNA and protein, and to a lesser extent, S100A9. When these cells were stimulated with S100A8, there was significant upregulation of MMP-2, MMP-3, MMP-9, MMP-13, A Disintegrin And Metalloproteinase with Thrombospondin Motifs (ADAMTS)-4 and ADAMTS-5 mRNA, suggesting that S100A8 mediates matrix degradation through MMP production [627]. $S100A9^{-/-}$ mice with antigen-induced arthritis had reduced cartilage destruction and leukocyte infiltration [625], implying that S100A9 contributed to pathogenesis by increasing leukocyte recruitment and modulating MMPs. MMP-3, -9 and -13 mRNA levels were significantly less in arthritic synovial tissue from $S100A9^{-/-}$ mice than normal. However, the activities and/or protein levels of these MMPs are not tested and mRNA levels do not indicate their functional capacities.

Paradoxically, S100A8/A9 inhibits MMP activity by Zn^{2+} sequestration [599] and/or by scavenging oxygen radicals that mediate MMP activation [625, 627], highlighting the need for further research. Moreover, S100A8/A9 attentuated avridine-induced arthritis in a rat model, implying that increased local concentrations of calprotectin were protective, and when reduced, severity of injury increased [648].

---

[1] In this report recombinant mS100A8 was used. Recombinant murine S100A8 does not contain the first Met residue as it is removed by thrombin cleavage from the GST fusion protein [927]. However, in Chapter 4 we showed S100A8, *in vivo*, retains Met_1. To avoid confusion between *in vitro* and *in vivo* analysis, all subsequent amino acid sequences for mS100A8 are analyzed assuming Met_1 is retained.

S100A12 forms a hexamer in the presence of Zn^{2+}. In acute coronary syndrome, ruptured plaque releases S100A12 into the coronary circulation. In contrast to previous studies, S100A12 failed to stimulate pro-inflammatory cytokines in human monocytes or macrophages. Moreover, S100A12 stimulated macrophages failed to induce MMP gene expression. When S100A12 chelated zinc, MMP-2, MMP-9 and MMP-3 activities were significantly inhibited, and the hexameric form of S100A12 was co-expressed in plaque with MMP-9 indicating Zn^{2+}-sequestration from MMP-9 *in vivo*. This indicates that S100A12 may protect advanced atherosclerotic lesions from rupture by inhibiting excessive MMP activity through Zn^{2+} chelation [529].

1.3.6.6 Anti-nociceptive activity

Originally described as neutrophil immobilizing factor [594], the C-terminus (amino acids 92-112) of mS100A9 inhibits hyperalgesia induced by jararhagin, a metalloprotease [629]. The C-terminus also inhibited thermal hyperalgesia [629] and MPO activity induced by carrageenan [649]. Hyperalgesia induced by the serine protease, protease-activated receptor-2 was also abrogated by this peptide suggesting that the C-terminal domain may interfere with control mechanisms of inflammatory pain [649]. Ca^{2+} flux into the dorsal root ganglia neurons induced by KCl is inhibited by the C-terminus, suggesting that these analgesic properties are independent of opioid receptor signalling [649]. Inhibition of nociception was not due to depletion intracellular Ca^{2+} stores or chelation and may function by inhibiting activation of N-type voltage-operated Ca^{2+} channels [649].

A role for S100A8 in hyperalgesia is also proposed. Hyperalgesia induced by carrageenan causes rapid and sustained increases in S100A8 and S100A9 in rat hind paws [650]. Peripheral inflammation leads to neutrophil migration in the vasculature of brain and pituitary gland, with possible diffusion of S100A8 and S100A9 through the endothelial blood-brain barrier [650]. It is proposed that S100A8 and S100A9 may relay disease or tissue damage from peripheral cells to the central nervous system [650].

1.3.6.7 Antimicrobial and anti-invasive activity

S100A8/A9 was originally called calprotectin because of its bacteriostatic activity. Calprotectin was also known as the calcium binding leukocyte L1 protein, although this comprises one light chain (8.2 kDa, S100A8) and two heavy chains (13.3 kDa, S100A9) [9]. The individual subunits lack activity at concentrations up to 50 μM,

whereas heterodimeric S100A8/A9 inhibits *C. albicans* growth at concentrations >2 μM [9, 620, 621].

The antimicrobial activity attributed to the calprotectin extends beyond its effects first reported for *C. albicans* [9, 620, 621]. van Zoelen *et al*. showed that S100A8/S100A9 levels are elevated in murine and human sepsis [651]. In an *E. coli*-induced abdominal sepsis model in mice there was enhanced expression of mS100A8/S100A9 in peritoneal lavage fluid, plasma in lung and liver homogenates after 6 and 20 hrs [651]. Similarly, S100A8/A9 is increased in bacterial abscesses in mice [19]. In humans, LPS elevates hS100A8/S100A9 levels in plasma of healthy subjects as early as 1.5 hrs post-injection and is sustained for 24 hrs [651]. S100A8/S100A9 was also released primarily at the site of infection [651].

The heterodimer has reported effects on cerebrospinal fluid isolates of *Cryptococcus neoformans* [9]. Minimum inhibitory concentrations (MIC) for blood isolates of *E. coli, Klebsiella* spp*, Staphylococcus aureus,* and *Staphlycoccus epidermidis* range from 64-256 mg/l. Antimicrobial activity is strongly influenced by the nature of the culture medium [9]. Direct contact between the S100A8/A9 complex and microbes is unnecessary for growth inhibition [652] and Ca^{2+} is not critical for antimicrobial activity. Deprivation of the essential nutrient Zn^{2+} by high affinity chelation may be the mechanism [9, 620, 621]. At present it is unclear if the effect of Zn^{2+} chelation is a direct or indirect factor for affecting microbial growth. For example, although Zn^{2+} is an essential nutrient, it is unclear whether Zn^{2+} chelation alters other factors important for microbial growth, such as pH. For example, uropathogenic *E. coli* isolated from patients with diabetes appear sensitive to pH changes. When the pH of urine was changed from pH 5.5 to pH 5.0, *E. coli* growth was less (though not significant) [653].

The antifungal effects are best achieved when S100A8 and S100A9 as a complex. Although S100A9 has a mild antifungal effect, S100A8 exhibits no antifungal activity [620, 621]. S100A8 and S100A9 contain HEXXH Zn^{2+}-binding sites and the heterocomplex exhibits Zn^{2+}-reversible, antimicrobial activity [621]. Although the heterodimer retains some antimicrobial activity after truncation of the C-terminal GHHHKPGLGEGTP tail of S100A9, it is less than the intact form, supporting the proposal that an intact Zn^{2+}-binding site is required for optimal antimicrobial activity [621]. Although the C-terminal region of S100A9 contains three consecutive histidine residues ($S100A9_{103\text{-}105}$) thought to be involved in Zn^{2+}-binding, the HXXXH Zn^{2+}-binding motifs of S100A8 and S100A9 ($S100A8_{83\text{-}87}$ and $S100A9_{91\text{-}95}$) are specifically

implicated [620, 621].

Recent research also implicates Cu^{2+}, Mn^{2+}[654] and Mg^{2+} chelation (specific for S100A9) [655]) in growth inhibition of several fungal species. In addition, the heterocomplex can restrict mycelial growth and glucose incorporation by *C. albicans*, suggesting that chelation of essential nutrients is not the sole mechanism [620]. Substitution of Met_{63} or Met_{83} of S100A9 resulted in loss of antifungal activity, and substitution of Cys_{42} to Ala in S100A8 reduced its ability to enhance S100A9's antifungal effect [655]. It is proposed that S100A8/A9 exerts an anti-inflammatory activity in the healthy state and that conditions associated with oxidative stress may activate the antifungal activity of S100A8/A9 [655].

The heterocomplex also has antiparasitic properties. In an experimental murine model of cutaneous leishmaniasis, infection caused accumulation of macrophages expressing S100A8 and S100A9. S100A8/A9 adhered to amastigotes in skin lesions from these mice and S100A9 adhered in a Ca^{2+} and Zn^{2+} dependent manner to *L. amazonensis* amastigotes propagated *in vitro* in the macrophage cell line J774G8 [453]. S100A9 also adhered to promastigotes, suggesting that S100A9 receptors are expressed in both stages of parasite development. Roles for S100A8 and S100A9 in granulomatous response during parasite infection are proposed, but mechanisms are unclear [453].

Similarly, injection of synthetic hemozoin, a parasite metabolite involved in malarial infection, into BALB/c mice induced S100A8, S100A9 and S100A8/A9 in air pouch exudates [516]. On the other hand, S100A8 and S100A9 transcripts were repressed upon *Leishmania major (L. major)* administration to human macrophages [656]. The S100A8/A9 heterocomplex plays a role in NADPH oxidase activation in phagocytes (see Section 1.3.5.4), an essential component of intracellular parasite killing. Inhibition of S100A8/A9 expression by *L. major* may be a critical mechanism to avoid ROS-mediated killing [656].

The C-terminal region of S100A12 has antimicrobial activity against Gram negative bacteria [312], and antifungal activity, which is enhanced by Zn^{2+}-binding [632]. S100A12 also inhibits nematode motility in Ca^{2+} and Zn^{2+}-dependent complex formation with paramyosin which is involved in muscle contraction and which ultimately promotes nematode death [98].

1.3.6.8 Apoptosis

S100A8/A9 complex promotes apoptosis of several tumour cell lines. Rat S100A8/A9 causes apoptosis of murine lymphoma, carcinoma, hepatoma, thymoma, fibrosarcoma, melanoma, human mammary adenocarcinoma and leukaemic, rat osteosarcoma cell lines and normal bone marrow cells, and macrophages from C3H/HeN mice [302, 657]. S100A8 lacks cytotoxic characteristics [658] and S100A9 may be responsible for the cytotoxic activity of the complex; S100A8 may enhance its effects. These observations suggest S100A8/A9 is a negative regulator of growth and/or survival of normal and tumour cells [659]. It could be argued that testing rat S100A8/A9 on human cell lines from different species could yield confounding results because of the low sequence homologies between rodent and human calgranulins [7]. However, high concentrations of hS100A8/A9 (20 μM) induces apoptosis of human endothelial cells, MOLT-4 defined leukemia and MCF-7 mammary carcinoma cell lines [302, 657].

Early studies implicate Zn^{2+} exclusion from target cells [302, 660]. The heterocomplex also induces activation of apoptotic caspases-3 and -9, DNA fragmentation and membrane phosphatidylserine translocation to outer membranes of target cells, independent of death receptor signalling [622]. Caspase-9 is an essential component of the mitochondrial pathway of apoptosis. Once activated, it cleaves and activates the effector caspase-3 [622]. Similarly, S100A8/A9 inhibits proliferation and differentiation of myoblasts via activation of caspase-3, suggesting that during the course of inflammatory myopathies, activated macrophages may promote destruction and impair regeneration of myocytes by secreting S100A8/A9 [661].

More recently, S100A8/A9-induced cell death was proposed to involve Bak, a pro-apoptotic protein, and selective release of caspase activators, Smac/DIABLO and Omi/HtrA2 from mitochondria [662]. Moreover, recent reports suggest that the promoter region of S100A9 contains several putative p53-binding sites which indicate a partly p53-dependent apoptosis pathway. S100A9 mRNA and protein expression can be positively regulated in a p53-dependent manner and knockdown of S100A9 in the oesophageal squamous cell carcinoma cell line, YES2, impaired p53-induced apoptosis [663].

1.3.6.9 Studies with S100A8 ($S100A8^{-/-}$) and S100A9 knockout ($S100A9^{-/-}$) mice

Several functions of S100A8 and S100A9 are dependent on their heterocomplex formation, but studies with $S100A8^{-/-}$ and $S100A9^{-/-}$ mice confirm functions independent of formation. In 2003, two independent $S100A9^{-/-}$ murine models were generated.

An S100A9$^{-/-}$ mouse was generated by Hobbs *et al*. In contrast to S100A8$^{-/-}$ mice, S100A9$^{-/-}$ mice displayed no obvious phenotype and were fertile [571]. Chemotactic reponses in these mice are described in Section 1.3.6.3. In a murine model generated by Manitz *et al.*, [572], S100A9 protein was undetectable in the blood neutrophils and bone marrow leukocytes. There were no morphological alterations observed in the brain, thymus, heart, lung, kidney, spleen, lymph nodes, small and large intestines, and skin from wild type or knockout mice [572]. The morphology of peripheral leukocytes was also unaltered [572].

S100A9$^{-/-}$ mice are often reported as mS100A8$^{-/-}$, particularly relating to neutrophil function. Nacken *et al*. noted that S100A9 deficiency results in a ~30% reduction of S100A8-positive cells in the bone marrow, which after 2 days of culture increased to ~60% reduction. However, after i.p. injection of thioglycollate, numbers of S100A8+ve cells in bone marrow from S100A9$^{-/-}$ mice were similar to those of wild type mice [572]. Interestingly, mS100A8 mRNA, is found in myeloid cells of S100A9$^{-/-}$ mice, although protein levels are reduced and it is proposed that the stability of S100A8 in neutrophils is dependent on S100A9 [571, 572]. However in other systems, such as in activated murine macrophages, mS100A8 is stable and generally produced in the absence of mS100A9 [144, 406, 407]. It is detected intracellularly and in supernates, making its lack of stability an unlikely explanation, although it is possible that S100A8 is more readily secreted in the absence of S100A9. Moreover, monocytes and activated macrophages from S100A9$^{-/-}$ mice have not been thoroughly investigated, and more work is required to fully understand the extent of S100A8 expression in myeloid cells deficient in S100A9.

1.3.6.10 Functional consequences of S100A9 deficiency

Elevated diacylglycerol inhibited chemokine-induced signalling in S100A9-null cells, suggesting that S100A9 may regulate an as yet unmapped signalling pathway, explaining why leukocyte influx is disrupted in only select *in vivo* models [641]. Some examples are given below (for clarity, Table 1.16 summarizes many features of S100A9$^{-/-}$ mouse phenotype).

The role of S100A9 in acute and chronic models of inflammatory arthritis was investigated in S100A9$^{-/-}$ mice. Acute inflammatory arthritis was induced by K/BxN serum transfer to wild type or S100A9$^{-/-}$ mice; collagen-induced arthritis (CIA) was used for the chronic inflammatory arthritis model [664]. In acute arthritis, S100A9-null mice

had similar disease, as indicated by paw swelling and clinical index, to wild type mice with no apparent differences in the presence or severity of joint damage or bony erosions. In the CIA model, paw swelling and clinical index were mildly increased, but only paw swelling was statistically significantly more in S100A9 null mice and no differences in joint damage or bony erosions were seen [664]. On the other hand, van Lent *et al.* describe development of arthritis in response to methylated bovine serum albumin (mBSA) [625] and showed that in $S100A9^{-/-}$ mice, arthritis induction and proteoglycan depletion from cartilage was significantly lower [625]. The K/BxN and CIA models involved a booster injection directly into the joint that leads to chronic destructive localized arthritis [664]. This may explain some of the differences reported in the two studies.

Other studies indicate that S100A9 has no role in host defense against *E. coli* in the urinary tract system [665]. Dessing *et al*. showed that bacterial outgrowth, neutrophilic infiltrate and inflammatory mediators in the bladder and kidney were not significantly different following administration of uropathogenic *E. coli* transurethrally in wild type and $S100A9^{-/-}$ mice [665]. Oddly, mice lacking S100A9 were protected against *E. coli*-induced abdominal sepsis [421]. Moreover, $S100A9^{-/-}$ phagocytes from mouse bone marrow cells were resistant to stimulation by LPS, with genes encoding for TNF-α, MIP-2, chemokine receptor 1, $gp91^{phox}$ (also known as NADPH oxidase 2) and MAPK-activated protein kinase-2, downregulated 4 hrs after LPS administration, suggesting absence of S100A9 is protective [421].

S100A9 was recently identified as a novel target for treatment of autoimmune disease by binding to quinoline-3-carboxamides [666]. Quinoline-3-carboxamides inhibited TNF-α release in an S100A9-dependent model *in vivo*. Antibodies against the quinoline-3-carboxamide-binding domain of S100A9 also caused inhibition, highlighting S100A9 as a novel target for treatment of autoimmune disease [666].

Table 1.16: Characterization of S100A9$^{-/-}$ mouse phenotype

Processes	S100A9$^{-/-}$ phenotype	Refs.
Myeloid cell functions		
Myeloid cell differentiation	- No differences in morphology or numbers of circulating leukocytes - Mildly reduced numbers of bone-marrow granulocytes and reduced colony forming potential of bone marrow cells stimulated with IL-13 - GM-CSF failed to reduce differentiation of hematopoietic progenitor cells	[404, 571, 572]
Neutrophil migration	- No effect on neutrophil migration in response to MIP-2, PKC or fMLP *in vitro* - Reduced migration to IL-8 and leukotriene B4 *in vitro* - IL-8 failed to upregulate CD11b levels on S100A9$^{-/-}$ granulocytes - Activation of p38 did not enhance migration in S100A9$^{-/-}$ granulocytes - see Section 1.3.6.3	[232, 571, 572, 641]
Oxidative burst	- No change in phorbol ester-stimulated oxidative burst of neutrophils - Decreased ATP- and PAF-stimulated oxidative burst of neutrophils	[571, 577]
S100A8 levels	- Normal levels of S100A8 mRNA - Low levels of intracellular S100A8 in neutrophils - ~30% bone marrow neutrophils contain S100A8 - see Section 1.3.8.3	[571, 572, 577]
Intracellular Ca^{2+} signalling	- No change in fMLP-stimulated Ca^{2+} influx in neutrophils - Increased ATP-stimulated Ca^{2+} influx - Decreased Ca^{2+} influx in neutrophils stimulated with suboptimal levels of MIP-2, KC, MIP-1α, C5a and PAF	[571, 577, 641]
Intracellular Zn^{2+}	- No change in basal or NO-stimulated labile $[Zn^{2+}]_i$ in neutrophils	[577]
Cytoskeletal dynamics	- Reduced basal levels of tubulin - Reduced p38-dependent activation of Rac1 and cdc42 in granulocytes - Abnormal polarization in unstimulated neutrophils	[232, 572]
Phagocytosis	- No change in phagocytosis of *E. coli* by monocytes or neutrophils	[571]
Apoptosis	- No change in proportion of apoptotic neutrophils induced by ionomycin, thapsigargin, gliotoxin, TNF-α or staurosporine	[571]

Processes	S100A9$^{-/-}$ phenotype	Refs.
In vivo models		
Leukocyte recruitment	- No change in rate of neutrophil, monocyte, eosinophil, B cell, CD4 or CD8 T cell influx in thioglycollate-induced peritonitis - No change in rate of neutrophil or monocyte influx after LPS injection into airpouch - No change in neutrophil accumulation after subcutaneous injection of IL-8 - Reduced infiltration of granulocytes to skin wounds - Reduced leukocyte recruitment and cellular proliferation of intimal and medial cells after femoral wire injury - see Section 1.3.6.3	[528, 571, 572, 640]
LPS stimulation	- Reduced expression of pro-inflammatory cytokines in S100A9$^{-/-}$ bone marrow cells stimulated with LPS - S100A9$^{-/-}$ mice exposed to LPS-induced septic shock lived significantly longer - Reduction in hemorrhagic lesion severity, area and edema in the skin from LPS-induced vasculitis with subsequent injection of TNF-α	[421, 528]
Bacterial infection	- No differences in bacterial outgrowth, neutrophilic infiltrate and inflammatory mediators in the bladder and kidney during *E. coli*-induced urinary tract infection - S100A9 null mice protected against *E. coli*-induced abdominal sepsis	[421, 665]
Cancer	- S100A9 null mice rejected injected lymphoma and C3 sarcoma tumour cells	[404]
Autoimmune disease	- Severity of experimental autoimmune encephalomyelitis was greater in S100A9-null mice	[666]
Ischemia	- Lesion volume in S100A9$^{-/-}$ mice was significantly smaller when exposed to focal cerebral ischemia - see Section 1.3.8.3	[667]
Antigen-induced arthritis	- Reduced joint-swelling, proteoglycan depletion and cellular mass in joint cavity and synovial layer in mBSA-induced arthritis - Significantly increased paw swelling in S100A9 null mice in a CIA model - No differences in joint damage and bony erosions in acute arthritis	[625, 664]
Caerulein-induced pancreatitis	- Reduced leukocyte infiltration and reduced serum amylase and lipase - see Section 1.3.6.3	[640]

1.3.7 EXTRACELLULAR FUNCTIONS OF S100A12

S100A12 is a monocyte chemoattractant [320, 440] and also sequesters mast cells (MC) [298] (see Section 1.3.6.4). RAGE was proposed to propagate inflammation and monocyte recruitment by engaging with S100A12 [440]. S100A12-induced edema and leukocyte rolling, adhesion and transmigration in the rat mesenteric microcirculation are MC-dependent. An antagonist to RAGE partially blocked the S100A12 response, but MC did not express mRNA or protein, suggesting a receptor distinct from RAGE [131].

The MC-dependent leukocyte rolling observed in the rat suggested that S100A12 may contribute to the pathogenesis of asthma and allergic inflammation, by triggering mast cell degranulation [131]. S100A12 potentiated IgE-mediated MC degranulation and induction of a cytokine profile indicative of a role in innate/Th1-mediated responses [131]. Activation of mast cells is initiated by FcεRI-bound IgE cross-linking with an antigen triggering degranulation and release of mediators such as histamine, leukotrienes and prostanoids [642]. S100A12 activates human cord blood-derived MC to produce a number of cytokines that propagate inflammation, including IL-6, IL-8, monocyte chemotactic protein-1 (MCP-1) and MIP-1β [131]. These effects were attributed to the hinge domain of S100A12 and S100A12 was suggested to exacerbate allergic inflammation and asthma [131].

Sensitised transgenic mice expressing human S100A12 in vascular SMCs driven by the SM22α promoter [668] challenged with ovalbumin indicate that S100A12 is protective. These mice had reduced peribronchial and perivascular inflammation, mucus production and eosinophilia and attenuated airway hyper-reactivity compared to wild type [669]. Transgenic mice showed thinning of the airway smooth muscle, a possible explanation for the attenuated response. The authors propose that reduced airway responsiveness was due to S100A12-induced Fas expression and activation of caspase-3 (observed in cultured airway SMCs) that may trigger myocyte apoptosis and cause thinning of airway smooth muscle [669]. Unexpectedly, S100A12 over-expression in mice did not exacerbate lung inflammation. Moreover, the elevated S100A12 in BALF from asthmatics did not significantly mediate pulmonary inflammation [669]. However results may be difficult to interpret because mice do not have large numbers of MC in the lung.

Recent work suggests that S100A12 may have a pleiotropic role in atherogenesis [529]. In human atherosclerotic carotid artery, strong anti-S100A12 immunoreactivity

was observed in foam cells and around neovessels and $CD68^+$ macrophages [529] (see Section 1.3.6.5).

Unlike S100A8 and S100A9, S100A12 has no Cys or Met residues (which modifies function; see Section 3.1, Chapter 3). Furthermore, S100A12 lacks tryptophan (Trp), an amino acid susceptible to oxidation and important in myeloperoxidase-mediated loss of cholesterol acceptor activity of Apolioprotein AI (ApoAI) [670]. Hence, S100A12 may be more resistant to oxidant-induced modification during inflammatory episodes where HOBr and HOCl may occur in high concentrations. Table 1.17 summaries the varied extracellular functions of S100A12 and suggested mechanisms.

Table 1.17 Extracellular functions of S100A12

Suggested functions	Suggested mechanisms	Refs.
Chemotactic for mast cells and monocytes	Ligation of a G protein-coupled receptor, active hinge region (residues 38-53)	[298, 320]
Degranulation of mucosal and tissue mast cells, amplifies IgE-mediated responses	Ligation to an unknown receptor	[131]
Induces neutrophil adhesion to fibrinogen via Mac-1 upregulation	Assumed ligation with RAGE	[319]
Stimulation of IL-1β and TNF-α production in BV-2 murine microglial cells; IL-2 production from peripheral blood mononuclear cells (PBMCs), induction of ICAM-1 and VCAM-1 on endothelial cells**	Ligation of RAGE	[440]
Filariacidal activity, inhibition of filial growth and motility	Immobilization of nematode parasite by direct binding	[457, 671]
C-terminal is antimicrobial and antifungal	Activity is enhanced in the presence of $ZnCl_2$	[632]
Stimulates neurite outgrowth in rat hippocampal neurons	Ligation of RAGE and activation of PLC, PKC, Ca^{2+} fluxes, calmodulin-dependent kinase II, and MAPK pathways	[464]
Inhibition of MMP-2 and MMP-9	Zn^{2+} chelation	[529]

** Our lab recently showed human S100A12 in human macrophages failed to induce pro-inflammatory cytokines IL-1β or TNF-α mRNA. PBMCs stimulated with S100A12 did to induce IL-6, IL-8 or TNF-α [529].

1.3.8 RECEPTORS FOR S100A8, S100A9 AND S100A12

Several receptors for S100A8, S100A9 and S100A12 are implicated and fall into four main categories: N-glycans and glycosaminoglycans (GAGs), CD36, TLR-4 and RAGE. It is within these categories that putative receptors for S100A8, S100A9, the heterocomplex and S100A12 will be discussed.

1.3.8.1 Glycosaminoglycans

S100A8/A9 binds with high affinity to heparin and heparan sulfate GAGs on endothelial cells [431]. GAGs are implicated in cell-cell and cell-extracellular matrix adhesion, provide a reservoir for growth factors and chemokines, and act as co-receptors [672-674]. S100A8/A9 bind GAGs [431, 675]. Binding of S100A9 and S100A8/A9 to the HMEC-1 required Ca^{2+} and Zn^{2+} but was independent of Mg^{2+}, suggesting that only the Ca^{2+} and Zn^{2+} bound conformation of S100A9 bound endothelial cell surfaces [431]. These results were further confirmed by binding assays; S100A8/A9 bound T lymphoblasts, neutrophils, myeloid cells and Chinese hamster ovary (CHO) cells. CHO cells deficient in GAGs did not bind the proteins [431].

S100A8/A9 was also identified as a binding partner for carboxylated N-glycans on endothelial cells. Purified hS100A8/A9 bound immobilised bovine lung carboxylated glycans in a carboxylate-dependent manner [675]. The heterocomplex also recognized a subset of mannose-labelled endothelial glycoproteins immunoprecipitated by mAb GB3.1, a mAb that recognizes these novel glycans [675]. These observations suggest that carboxylated glycans play a role in leukocyte trafficking by interacting with proteins which influence extravasation [675]. More recently, S100A8/A9 were found to bind carboxylated N-glycans expressed on RAGE and other cell surface glycoprotein receptors on MDSCs. The complex may promote MDSC migration as an anti-carboxylated glycan antibody reduced MDSC levels in blood and secondary lymphoid organs in mice with metastatic lesions. This implies that S100A8/A9 may sustain accumulation of MDSC via an autocine feedback loop [676].

Interestingly, some solvent-exposed hydrophobic residues in the S100A9 homodimer may contribute to the specific binding of target molecules such as endothelial heparan sulphate proteoglycans or the cell surface proteins CD36 and RAGE [405, 677].

1.3.8.2 CD36

CD36 is part of the free FA transporter family of proteins implicated in uptake of FAs by endothelial cells [619, 678]. S100A8/A9 are secreted from phorbol ester-stimulated neutrophil like HL-60 cells, and transports AA [580] (see Section 1.3.5.3). A subsequent study by the same group showed that in the presence of S100A8/A9, AA was rapidly taken up by human umbilical vein endothelial cells (HUVEC) in a saturable and energy-dependent manner [619]. Uptake of exogenous AA by HUVECs was mediated by CD36 (confirmed by immunoprecipitation experiments using fusion proteins and partially-purified membrane protein from platelets (rich in CD36) and HUVECs). This interaction may promote host responses at sites of inflammation [619].

In contrast to HUVEC, HMEC-1 cells express little CD36 and no detectable RAGE, suggesting that S100A8/A9 binding to these cells is dependent on another binding partner, possibly GAGs (see Section 1.3.8.1) [431]. Differences could be due to the type of endothelial cell used, i.e. HMEC [431], or HUVECs, which have some distinct physiological characteristics [619].

1.3.8.3 TLR-4

TLRs are important receptors that recognize pathogen-associated molecular patterns (PAMPs) in the innate immune system. TLR-4, for example recognizes LPS, a component of Gram-negative cell walls (reviewed in [679, 680]).

S100A8 was reported by Vogl *et al*. as a TLR-4 ligand, confirmed by surface plasmon resonance studies *in vitro*, which showed that S100A8, but not S100A9 specifically interacted with TLR-4, thus representing an endogenous ligand of TLR-4 [421]. Only, mS100A8, but not mS100A9 or the mS100A8/A9 heterocomplex, stimulated TNF-α production from LPS-stimulated $S100A9^{-/-}$ bone marrow cells. S100A9 suppressed the S100A8-mediated response but the heterocomplex enhanced TNF-α secretion in the presence of LPS [421]. $S100A9^{-/-}$ mice were protected from endotoxin-induced lethal shock and *E. coli*-induced abdominal sepsis [421].

The study by Vogl *et al*. used $S100A9^{-/-}$ (assumed to be $S100A8^{-/-}$) mouse bone marrow cells, which comprises ~30% neutrophils. These may have died during the culture period (4 hrs), and could result in S100A8 and S100A9 release [633] and presumably competition with the exogenously-added S100A8. $S100A9^{-/-}$ mice are not totally deficient in mS100A8, as the protein is present in bone marrow cells, although it is

~30% less than in normal cells [572]. TNF-α could have been produced in response to bone marrow cell necrosis. Dead/dying cells release ATP, which can activate purinergic receptors on neutrophils, monocytes and macrophages [681]. Therefore, TNF-α production may have resulted from loss of viability of the neutrophils rather than a direct effect of S100A8.

A subsequent study showed that stimuation of chondrocytes with S100A8 and S100A9 caused strong upregulation of MMP-1, -3, -9 and -13, and IL-6, IL-8 and MCP-1, and down-regulation of anabolic markers (aggrecan and collagen type II), indicating that S100A8 and S100A9 facilitate cartilage breakdown. This was blocked by an intracellular small molecule inhibitor, TAK242, which blocked TLR-4. The catabolic effect of S100A8 and S100A9 was also observed in chondrocytes from osteoarthritis patients [682]. Thus, S100A9 was also implicated in TLR-4 binding.

Loser *et al*. propose that both S100A8 and S100A9 were TLR-4 ligands. In a murine autoimmune model, $S100A9^{-/-}$ showed delayed onset and significantly reduced severity of autoimmune dermatitis, lower autoantibody concentrations and reduced nephritis and proteinuria compared to wild type [683]. S100A8 and S100A9 were observed to be essential for induction of autoreactive $CD8^{+}$ T cells, and subsequent development of systemic autoimmunity. Furthermore, these effects were mediated by TLR-4, and increased IL-17 expression, implicating S100A8 and S100A9 in the development of autoreactive lymphocytes and development of systemic autoimmunity [683].

$S100A9^{-/-}$ mice with focal cerebral ischemia had significantly smaller lesion volumes, less brain swelling and reduced macrophage/microglia cell numbers compared to wild type mice [667]. It was proposed that both S100A8 and S100A9 were endogenous TLR-4 agonists mediating TLR-activation in cerebral ischemia. The absence of S100A9 with concomitant reduction in inflammation suggests that it contributes to neuroinflammation and progression of ischemic damage [667].

Other studies are more cautious in defining a specific receptor for S100A8 and S100A9. For example, Simard *et al*. describe enhanced bactericidal activity of human neutrophils via S100A9-dependent enhancement of phagocytosis. The authors acknowledged associations with TLR-4 and RAGE but did not favour one or the other as the definitive receptor, preferring to assert that the receptor may still be unknown [684].

In contrast to the above, Ikemoto *et al.*, suggest that the S100A8/A9 complex has an anti-inflammatory role in liver injury induced by LPS in rats [631]. Specifically, serum concentrations of IL-6 and nitrite were significantly decreased in rats injected intraperitoneally with LPS. I.p injection of S100A8/S100A9 1 or 3.5 hrs after LPS significantly reduced serum IL-6 and nitrite levels, whereas treatment with anti-S100A8/A9 IgG 1 hr after injection with LPS increased IL-6. The authors suggest that the hetercomplex bound non-specifically to pro-inflammatory cytokines and this subsequently reduced NO levels [631]. Unfortunately, Ikemoto's study used hS100A8/A9 and its partner antibody, and the S100s have different amino acid sequence homologies to rat S100A8 and S100A9.

1.3.8.4 RAGE

Several groups have identified RAGE as a potential ligand for S100A8 and S100A9, however RAGE binding to S100A8/A9 remains poorly understood. For example, immunofluorescence experiments on LNCaP cells (androgen-sensitive human prostate adenocarcinoma cells) showed co-localization of S100A8/A9 and RAGE after increasing cytosolic Ca^{2+} levels and incubating with extracellular S100A8/A9 [557]. Immunoprecipitation experiments indicate *in vitro* interactions between RAGE and S100A8/A9 and S100A8/A9 is thought to promote tumour cell growth via p38 MAPK and p44/42 kinase activation [294]. RAGE is also implicated as the receptor for S100A8 and S100A9 homodimers, and S100A8/A9, in MC38 colon tumor cells from mice [685].

Binding of S100A8/A9 to RAGE may be cell dependent. For example, RAGE-specific antibodies and siRNA blocked proliferation of MDA-MB231 (human estrogen receptor-negative breast cancer) cells induced by S100A8/A9 [294]. Similarly, S100A8/A9-mediated cardiomyocyte dysfunction is blocked by anti-RAGE [686]. In prostate cancer cell lines, S100A8/A9 co-localized with RAGE, but the lack of suppression after addition of anti-RAGE antibodies to block S100A8/A9-induced NF-κB activation suggests RAGE-independent signalling [327]. This apparent disparity may be explained by the presence or absence of carboxylated N-glycans on RAGE whereby binding may be dependent on carboxylated N-glycans, rather than to RAGE directly [675].

Interaction of S100s with RAGE may also be influenced by other factors. It is also possible that observations involving RAGE, NF-κB and subsequent activation of various

responses may, in some cases, be due to contamination. For example, Tian and colleagues highlight that high-mobility group protein B1 (HMGB1) purified from *E. coli* is a potent activator of plasmacytoid dendritic cells, whereas HMGB1 protein purified from calf thymus, which contains minimal DNA or RNA, does not [687].

Some authors assert another hypothesis; that S100A8/A9 may not have a specific receptor, in part, because Ghavami *et al*. indicated that calprotectin-induced apoptosis of HT29/219 cells (colon carcinoma cell line) and SW742 cells (adenocarcinoma cell line) was not due to a specific cell surface receptor [688]. In addition, Nakatani *et al*. suggest a mechanism independent of Zn^{2+} exclusion (a second mechanism proposed for calprotectin-induced apoptosis) because calprotectin-induced apoptosis of the MM46 cell line (an MM 3 antigen -positive tumour cell line) was particularly insensitive to removal of Zn^{2+} [514]. Zali *et al*. suggest that the pro-apoptotic property of the heterocomplex may be initiated through non-specific internalization, independent of Zn^{2+} concentration. This hypothesis is called the internal target hypothesis [504]. Zali *et al.* surmise that instead of a specific calprotectin receptor on the cell surface, it may bind the membrane non-specifically and become internalised, possibly in an energy-consuming process such as pinocytosis [504]. This may explain why a specific receptor for calprotectin is still debated. Despite theoretical models predicting cell survival behaviour by the internal target hypothesis [504], further research needs to be completed to confirm this.

RAGE was reported as a receptor for S100A12. Hofmann *et al.* found that bovine S100A12 bound to RAGE on endothelium, mononuclear phagocytes and lymphocytes, triggering activation [440]. However, the majority of the work involved murine models, for example, IL-1β and TNF-α induction in BV-2 cells (a murine microglial cell line) by bovine S100A12 [440]. This work is problematic because S100A12 is not present in rodents [7, 51] and our work with hS100A12 and human macrophages showed that S100A12 did not induce IL-1β or TNF-α mRNA. Similarly, PBMCs stimulated with S100A12 failed to induce IL-6, IL-8 or TNF-α [529]. Importantly, the recombinant S100A12 used for these experiments was active in chemotaxis assays and provoked mast cell-dependent edema in mice [131], confirming its functional capacity.

The hinge domain of S100A12 (residues 38-53) has increased helical structure in hydrophobic environments, which are necessary to promote monocyte chemotaxis *in vitro* and generation of edema *in vivo* [298]. Yan *et al*. proposed that the hydrophobic environment of a cell membrane allows residues of the S100A12-hinge domain to align

on one face of an α-helix, facilitating receptor interaction [298]. Data from our lab suggests that a G protein-coupled mechanism may be facilitating many of the features of S100A12-induced edema, and leukocyte and MC recruitment [131, 298], rather than RAGE ligation, although more research is required to characterize this. Other studies also implicate a G protein-coupled receptor in the chemotactic responses of mS100A8 [296, 298, 320].

1.3.9 S100A8, S100A9 AND S100A12 AS DAMAGE-ASSOCIATED MOLECULAR PATTERNS (DAMPs)

S100A8, S100A9 and S100A12 were described as DAMPs molecules, because of their ability to mediate inflammatory responses and recruit inflammatory cells to sites of tissue damage [393]. DAMPs act in a similar manner to PAMPs, engaging TLRs and RAGE, leading to NF-κB activation [319], that stimulates innate immune cells to generate inflammatory responses. DAMPs may also be released from injured tissue and exert anti-inflammatory effects to counteract excessive tissue damage. One such DAMP is galectin-1, a member of the galectin family of 15 proteins [689-692]. Galectin-1 inhibits iNOS activity and NO production in response to LPS treatment of rat macrophages [690] and suppresses leukocyte rolling and extravasation in experimental inflammation, suggesting an anti-inflammatory role [691].

We propose that S100A8 and S100A9 can also be considered anti-inflammatory DAMPs under some circumstances. They appear to have pleiotropic roles, which may depend on their extracellular levels, and the extent of tissue damage and repair. For example, upregulation of S100A8 by FGF-2/IL-1β, and down-regulation by TGF-β, and its time dependent expression in wound fibroblasts suggest a role in fibroblast differentiation at sites of inflammation and repair (see Section 1.3.5.6) [419]. Moreover, as S100A8 and S100A9 scavenge ROS/RNS, these proteins may facilitate restoration of redox balance during resolution of inflammation. Interestingly, several DAMPs are susceptible to oxygen-mediated inactivation [693], and the redox state may also modulate the activities of S100A8 and S100A9. For example, NO mediates processes involved in vascular homeostasis, SMC function and antimicrobial defense [694]. S-nitrosylation (covalent coupling of NO to Cys thiols) regulates functions of S100A8 and S100A9, with S100A8 preferentially modified in the heterocomplex [613].

Transmigrating leukocytes deposit S100A8 and S100A9 on the microvasculature.

We propose that S-nitrosylation of S100A8, by NO produced by endothelial nitric oxide synthase (eNOS) may regulate blood flow during inflammation (see Section 3.1, Chapter 3) [613]. S100A8/A9 was reported to induce iNOS in macrophages [626], but our laboratory failed to replicate these results (reviewed in [695].

Glutathione (GSH) is an abundant anti-oxidant, and can reduce oxidative damage by scavenging oxidants. S100A8 and S100A9 undergo S-glutathionylation *in vitro*, but, only S100A9 is S-glutathionylated *in vivo*. S-glutathionylated S100A9 promoted neutrophil adhesion to fibronectin but this activity is lost upon complex formation with S100A8. S-glutathionylation of S100A9 may protect it against further oxidation by RNS/ROS, and reduce neutrophil binding. S-glutathionylation may mediate the magnitude of neutrophil accumulation in the extravasculature (see Section 3.1, Chapter) [637]. Taken together, oxidative modifications to S100A8 and S100A9 represent novel mechanisms by which these proteins exert particular functions.

1.4 CALGRANULINS AND OXIDATION

Many cellular functions depend on the maintanence of ROS/RNS and anti-oxidant defenses are important in maintaining intracellular redox and cellular homeostasis [696, 697]. Although production of ROS/RNS are an essential part of the inflammatory process, excess leads to oxidative stress, resulting in modification of lipids [698], proteins or DNA, generated primarily as a result of apoptosis [699]. The following sections provide an overview of how ROS/RNS are generated in phagocytes, and anti-oxidant defense systems. Effects of ROS/RNS on lipids and proteins and their associated effects on protein, DNA and lipid function will be discussed.

1.4.1 ROS/RNS AND NADPH OXIDASE REGULATION

1.4.1.1 Generation of ROS/RNS

ROS/RNS encompass a variety of diverse chemical species. These include superoxide anions, hydroxyl radicals ($HO^{\cdot}$), H_2O_2 as well as NO and peroxynitrite ($ONOO^-$) [700]. Superoxides and $HO^{\cdot}$ are particularly unstable, whereas H_2O_2 is freely diffusible and relatively long-lived [700]. These species can either be generated from exogenous sources, intracellularly from different sources [701] or as a result of anti-oxidant defense systems (summarized in Fig. 1.11) [700]. In many cell types, most intracellular ROS are derived from the mitochondria, the result of side-products of

electron transfer [701]. ROS are also generated following phagocyte activation and via biological reactions with AA. In the latter, $O_2^{\cdot -}$ is generated via side chain reaction during AA conversion by lipooxygenase and COX, to prostaglandins and leukotrienes [701-703].

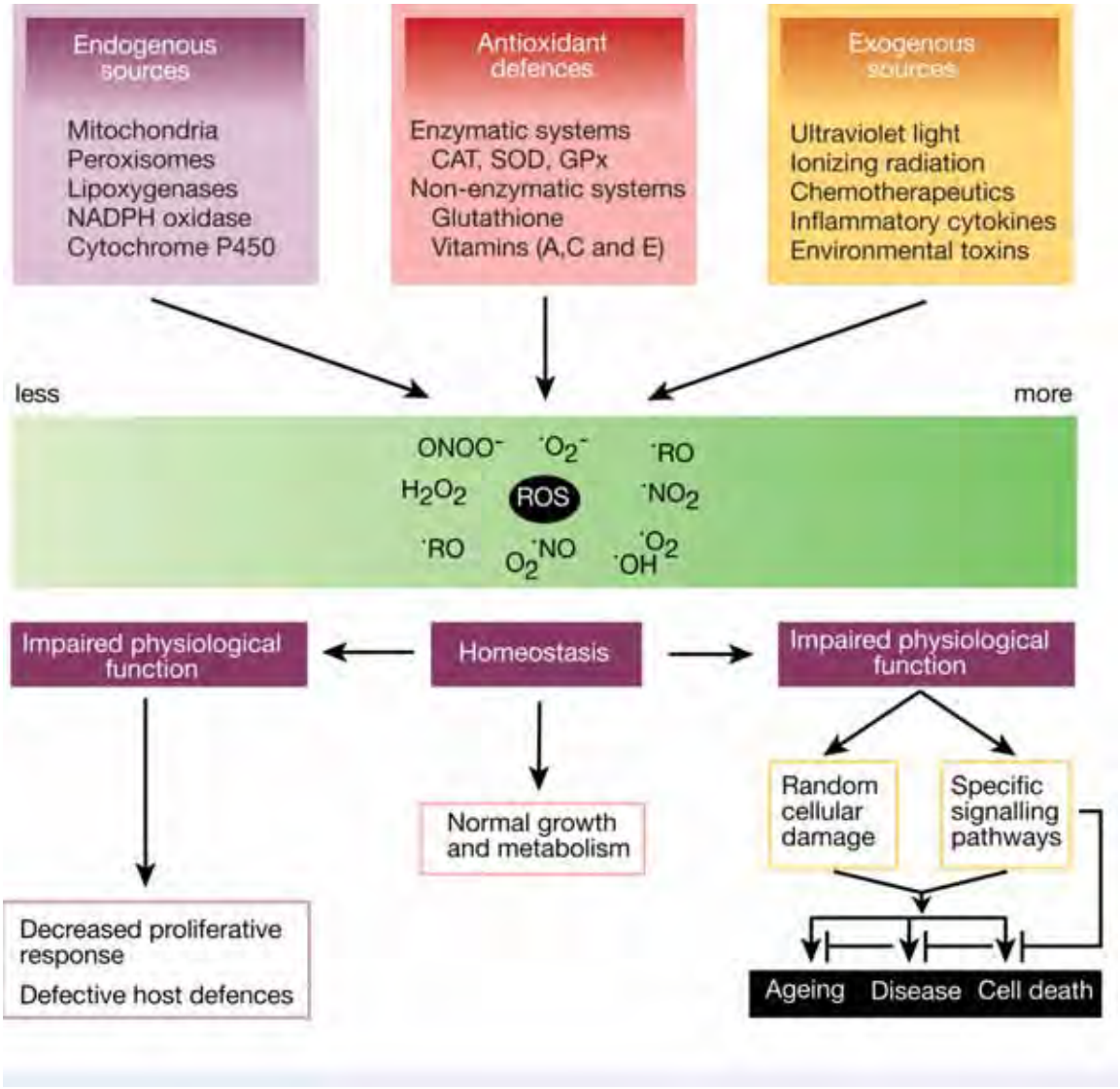

Figure 1.11: Sources and cellular responses to ROS. Oxidants are generated during normal intracellular metabolism in the mitochondria, peroxisomes and cytosolic enzyme systems. Enzymatic and non-enzymatic anti-oxidant defense systems regulate the amount of ROS, maintaining physiological homeostasis. Lowering of ROS may disrupt cell proliferation and host defense. Increased generation of ROS may cause cell death or accelerated ageing. Elevated levels of ROS may cause a stress signal, activating redox-signalling pathways with potentially damaging or protective functions. From [700].

Mitochondrial superoxide radicals are produced at two discrete points in the electron transport chain – complex I (NADPH dehydrogenase) and complex III (ubiquinone-cytochrome *c* reductase) [704]. During normal metabolic conditions, complex III is the main site for generation of ROS. Its action is summarized in Fig. 1.12 [700]. $O_2^{\cdot -}$ is rapidly eliminated by mitochondrial SOD, and may only have minor effects on overall levels of ROS in cells.

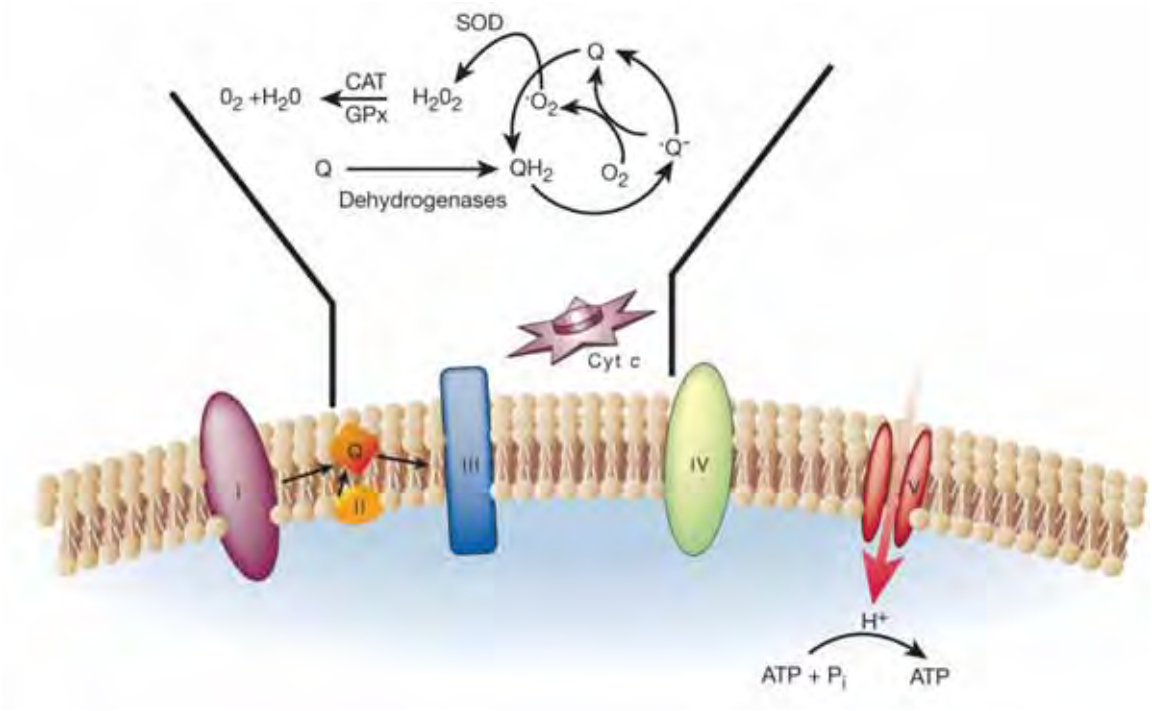

Figure 1.12: Complex III is the major source of mitochondrial ROS production. Electrons from complex I or II dehydrogenases are transferred to coenzyme Q. QH_2, the reduced form of coenzyme Q, undergoes two sequential one-electron reductions using oxidized and reduced forms of cytochrome *b* and *c*. The unstable intermediate ·Q can cause superoxide formation via transfer of electrons to molecular oxygen. These superoxides can be enzymatically dismutated by SOD, forming H_2O_2. H_2O_2 can be metabolised by enzymes such as glutathione reductase to generate water and molecular oxygen. Superoxide generation is non-enzymatic, therefore, the higher the rate of metabolism, the greater ROS production. From [700].

1.4.1.2 The NADPH oxidase complex

Cytosolic enzyme systems contributing to oxidative stress include the NADPH oxidase family of oxidases. This is a superoxide-generating system first described in neutrophils [700]. The NADPH oxidase system is a critical component of innate immunity, responsible for generation of antimicrobial ROS in phagocytes [705].

The NADPH oxidase system is also present in B lymphocytes, keratinocytes and other non-phagocytic cells [706]. Superoxide-generating homologues known as NADPH oxidase (NOX) enzymes producing "incidental" levels of ROS in other cell types contribute to the regulation of distinctive cell functions relating to innate immunity, signal transduction and modification of the extracellular matrix [706]. For example, several barrier cells express NOX enzymes, primarily colon epithelium (NOX1), kidney epithelium (NOX4), keratinocytes (NOX1) and lung epithelium (dual oxidase 1) suggesting roles in defense at these sites, similar to phagocytes (reviewed in [706]).

Gene deletion studies of the NOX family in mice confirm the diverse functions of these oxidases. For example, NOX1 promotes proliferation of hepatic stellate cells, accelerating development of fibrosis following bile duct ligation-induced liver injury [707]. NOX2 knockout mice have heightened T cell-mediated allergic responses with increased airway inflammation, suggesting that NOX2 regulates T-cell mediated airway inflammation [708]. NOX3 is critical in mediating vestibular effects, allowing for proper perception of motion and gravity [709]. NOX4 has functions similar to NOX2, mediating production of ROS and regulating epithelial cell death in pulmonary fibrosis [710]. Knockout studies with NOX5 are not possible as the gene is absent in the rodent genome. It is proposed that humans lacking the NOX5 gene are not viable, although no firm evidence is available [711].

Superoxide formation is largely regulated by the specific NADPH oxidase expressed in particular cells. For example, depending on the oxidase, non-phagocyte NADPH oxidases can either trigger cellular transformation or replicative senescence, using generation of ROS to regulate normal cellular signalling and homeostasis [700].

Generation of ROS by the NADPH oxidase system is a complex, coordinated process, represented in Fig. 1.13. The complex consists of membrane-bound flavocytochrome b_{558} (composed of glycosylated $gp91^{phox}$ and non-glycosylated $p22^{phox}$). The complex also contains cytosolic proteins $p47^{phox}$, $p67^{phox}$, $p40^{phox}$ and Rac1/2 G protein. When neutrophils are exposed to microorganisms or inflammatory mediators (reviewed in [706]) flavocytochrome b_{558} becomes activated. Subsequently, $p47^{phox}$,

p67^{phox} and p40^{phox} are phosphorylated and translocate to flavocytochrome b_{558}, which assist in activation of the complex [712]. For NADPH oxidase to be activated, p67^{phox} must interact with gp91^{phox}, mediated by the G protein Rac. O_2 is then reduced to $O_2^{\cdot -}$ by NADPH. This can either be converted to H_2O_2 by spontaneous or enzymatic dismutase, or $O_2^{\cdot -}$ transformed to $HO^{\cdot}$ in the presence of H_2O_2 and a transition metal [705, 712]. S100A9, in complex with S100A8 is also implicated in regulation of the NADPH oxidase complex (see Section 1.3.5.4).

MPO, eosinophil peroxidase (EPO) and heme peroxidases are also found in phagocytes and are responsible for generating hypochlorous (HOCl) or hypobromous acid (HOBr), when H_2O_2 is in the presence of a halogen [713] and reviewed in [714]. These enzymes are discussed in more detail in Chapter 3, Section 3.1.

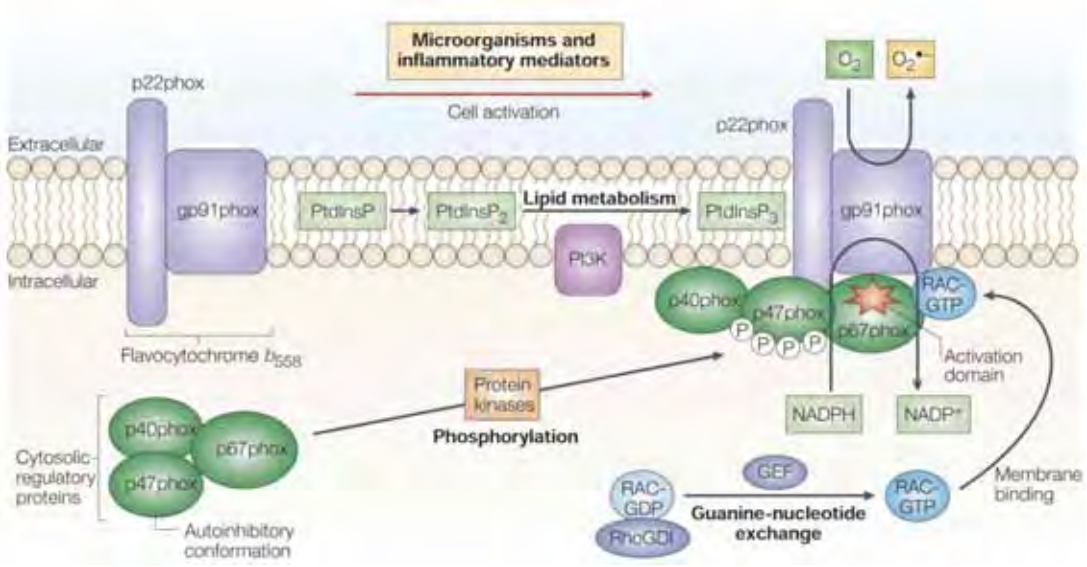

Figure 1.13: Activation of the NADPH oxidase complex. Phosphorylation of cytoplasmic p47^{phox}, p67^{phox} and p40^{phox} by protein kinases (for example PKC and AKT) activate the NADPH oxidase complex in phagocytes. The phosphorylated protein is translocated to the plasma membrane to interact with cytochrome b_{558}. Phosphotidylinositol 3-kinase (PI3K) and phospholipase D produce 3-phosphorylated phosphatidylinositol (PtdInsP) and phosphatidic acid respectively. This enables binding of p47^{phox} and p40^{phox} to plasma membrane lipids. Post-translational modifcation of RAC-GDP to RAC-GTP via guanine-nucleotide exchange is necessary for activation. RAC-GTP dissociates from RhoGDI translocating to the NADPH complex at the plasma membrane. From [706].

1.4.1.3 NO and RNS

NO plays a vital role in a number of elements of the immune system. The following section is a short overview of NO and RNS and their role in cellular redox. Its ubiquitous nature is attributed to its production in leukocytes (e.g. macrophages, dentritic cells, natural killer cells, microglia, eosinophils and neutrophils), and a number of other cell types that depend on its production to regulate homeostasis in neurotransmission, immune responses (reviewed in [715]), vascular function and host defense (reviewed in [716]). RNS also play a critical role in cell signalling, regulating neutrophil functions and modulating transcription factors such as NF-κB, as well as membrane receptors, ion channels and protein and lipid kinases (reviewed in [717]).

NO is derived enzymatically from the amino acid L-arginine by either iNOS, eNOS or neuronal NOS (nNOS) [718]. nNOS and eNOS isoforms are known collectively as constitutive NOS (cNOS), as they are usually constitutively expressed in particular cells and are regulated by Ca^{2+} fluxes and binding of calmodulin [719].

The function of NO is largely dependent on cell type and enzyme isoform. eNOS produces most of the vascular NO present in endothelial cells, subsequently modulating vascular tone and inhibiting platelet aggregation [720]. iNOS, induced in macrophages, generates NO, which serves as an antimicrobial agent [721]. NO generated by nNOS, is present in the brain, and mediates synaptic signalling and long term potentiation (a process underlying learning and memory in the brain) [722, 723].

Once NO is produced it can react with $O_2^{\cdot -}$, produced by NADPH oxidase. The subsequent product is $ONOO^-$, a microbicidal molecule [716]. NO can also interact with O_2 and metal ions to produce a diverse range of RNS, for example nitrogen dioxide and nitrosyl anion, however, their slow rate of reaction make these compounds unlikely to contribute to significant nitrosative stress [724].

When compounds such as $ONOO^-$ reach excessive levels, cellular redox and protein function can be altered and NO-dependent activation of apoptotic pathways in mitochondria induced [725, 726].

1.4.1.4 ROS/RNS in redox signalling

Although ROS/RNS are heavily involved in pathogen defense and regulation of redox homeostasis, several new studies highlight its importance in regulating signalling pathways in host defense, signal transduction and in Ca^{2+} signalling in vascular

pathophysiology [727-729]. For example, ROS/RNS regulate several tyrosine kinases such as p56/59^{hck} and p72^{syk} [730, 731] and can influence functions of SHP-1 and CD45 (protein tyrosine phosphatases), which influence tyrosine kinase-induced phosphorylation [732]. Importantly, tyrosine phosphorylation-dependent pathways are involved in antimicrobial and host defense functions in leukocytes, hence ROS/RNS generated by these cells may regulate pathways in host defense [733] as well as being directly antimicrobial.

Ligand-stimulated generation of ROS plays a role in signal transduction [704]. Mediators such as platelet-derived growth factor (PDGF), EGF, angiotensin II and many cytokines trigger rapid production of intracellular ROS [704] when they bind their relevant cell targets. Inhibition (by catalase) of ROS following ligand addition inhibits, among other pathways, the ability of EGF to stimulate tyrosine phosphorylation of the EGF receptor and phospholipase C-γ1 [734]. Similarly, inhibition of H_2O_2, in response to PDGF stimulation of rat vascular SMCs inhibited tyrosine phosphorylation, MAPK stimulation, DNA synthesis and chemotaxis, indicating that H_2O_2 is a signal-transducing molecule in these cells [735]. Similarly, endogenous ROS activate tyrosine kinases in human neutrophils [731].

In addition to modulating protein tyrosine kinases, protein phosphatases and MAPKs, ROS are important regulators of intracellular Ca^{2+} homeostasis and RhoA/Rho kinase signalling via angiotensin II [729]. ROS increase vascular $[Ca^{2+}]_i$ by stimulating inositol triphosphate-mediated Ca^{2+} mobilization, by increasing cytosolic Ca^{2+} accumulation through sarcoplasmic/endoplasmic reticulum Ca^{2+}-ATPase inhibition and by stimulating Ca^{2+} influx through Ca^{2+} channels [729]. Increased levels of ROS can also enhance Ca^{2+} signalling and upregulate RhoA/Rho kinase, altering vascular contractility and tone [729]. Similarly, nNOS-derived NO is necessary to induce synaptic detachment from motor neurons, resulting in activation of RhoA/Rho kinase signalling, leading to myosin activation and actomyosin contraction. Importantly, actomyosin contraction is believed to contribute to axon retraction, which is common in neurodegenerative diseases [736]. Hence, ROS/RNS play important roles in regulating pathological processes.

1.4.1.5 ROS/RNS and HOBr/HOCl-induced antimicrobial activity by phagocytes

Phagocyte-derived ROS and RNS are important in mediating host resistance to microbial pathogens. The two most important components of antimicrobial systems in

phagocytic cells are *phox*, and iNOS, which generate superoxide and NO respectively (reviewed in [721]; summarized in Fig. 1.14).

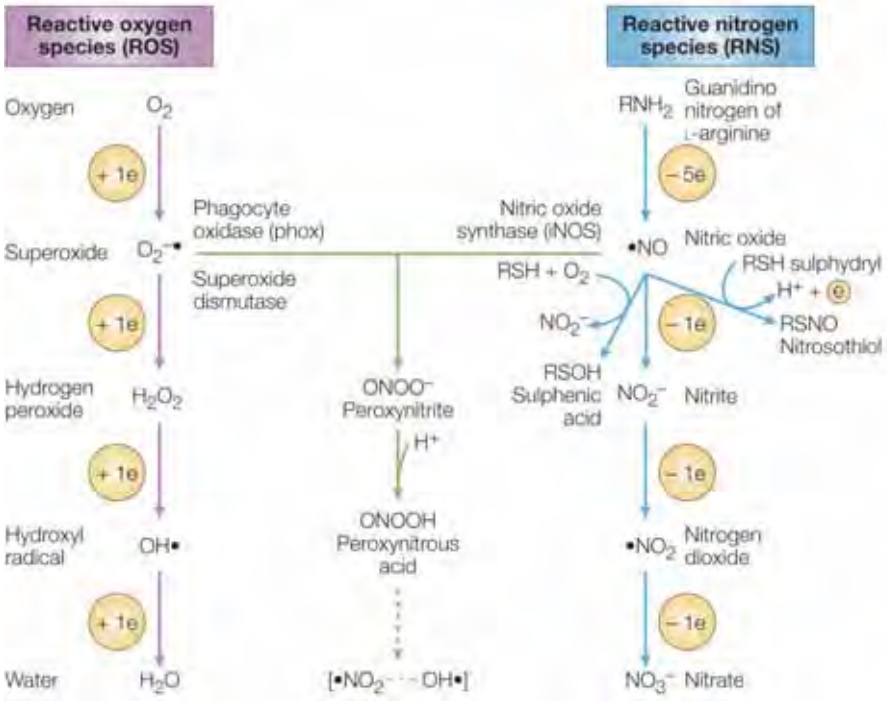

Figure 1.14: RNS and ROS production in mammalian cells. The product of the reaction catalyzed by *phox* is superoxide. The product catalyzed by iNOS is nitric oxide. However, subsequent spontaneous, or catalyzed reactions involving superoxide and nitric oxide can result in the formation of additional intermediates such as H_2O_2, $HO^\cdot$, nitrogen dioxide or peroxynitrite. From [721].

Superoxide is converted to H_2O_2 by SOD. Low concentrations of H_2O_2 are responsible for ROS-dependent DNA damage of *E. coli*, which results in antibacterial activity [737, 738]. DNA damage is mediated by iron, forming toxic intermediates, such as $HO^\cdot$ or ferryl radicals [739]. Oxidative damage to DNA bases generates 8-hydroxyguanine, urea, hydroxymethyl urea and thymine glycol, perpetuating oxidative damage (reviewed in [721]). Oxidative damage to membrane lipids may be an important factor contributing to damage in eukaryotic pathogens [740].

Perhaps the most profound effect of *phox* dependent production of superoxide is apparent in patients with chronic granulomatous disease, caused by a deficiency of any one of the four *phox* subunits. The majority of patients (~70%) have a mutation in $gp91^{phox}$ (NOX2) [741, 742]. NOX2 is responsible for transferring electrons from

cytosolic NADPH to molecular oxygen, releasing superoxide into the phagosomal lumen [743]. This product (superoxide) can dismutate to H_2O_2, and ultimately forms HOCl, $HO^{\cdot}$ and singlet oxygen [744]. These products are critical for mounting an immune response against bacteria and fungi. Because these patients fail to produce a respiratory burst in their phagocytes, the majority suffer from severe recurrent infections [741].

RNS are abundant in activated macrophages and less so in activated neutrophils. RNS production requires *de novo* synthesis of iNOS, generally via co-signals such as IFN-γ and LPS or TNF-α. NO can diffuse across membranes, where, in the lumen, ROS convert NO to different RNS (including nitrogen dioxide, $ONOO^-$, dinitrogen trioxide, dinitrosyl iron complexes, nitrosothiols and nitroxyl radicals) (reviewed in [721]). RNS-mediated antimicrobial actions are more complicated than ROS-mediated activities. NO and S-nitrosothiols induce reversible inhibition of bacterial DNA replication via Zn^{2+} mobilization [745]. NO itself inhibits bacterial respiration [746, 747], which may account for induced dormant states of microbes such as *Mycobacterium tuberculosis* [748, 749]. Ribonucleotide reductase is responsible for synthesis and repair of DNA. NO and tyrosyl radicals inihibit this activity, representing another mechanism to inhibit microbial growth [750].

MPO generates a number of ROS based on the attached halide (i.e. HOX, X= Cl, Br). HOCl and HOBr can interact with a number of targets in a microbial cell, including thiols, metal centres, protein tyrosines, nucleotide bases and lipids [751] (summarized in Fig. 1.15).

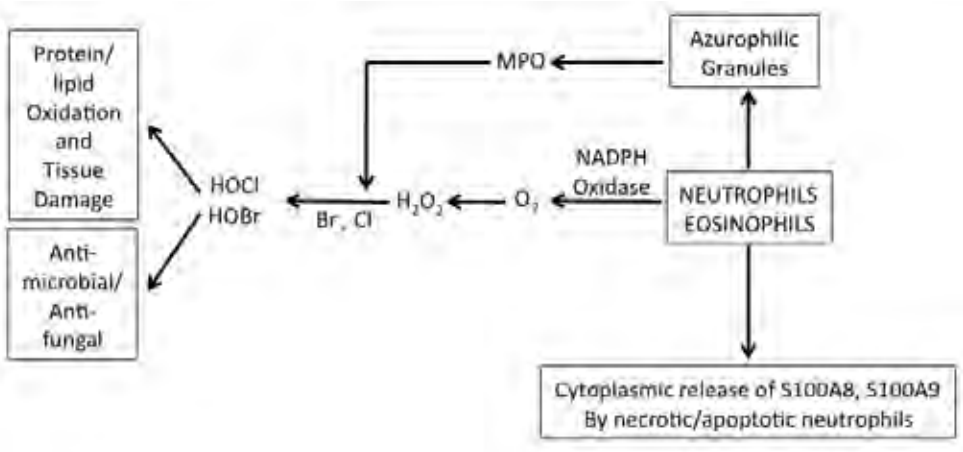

Figure 1.15: Production of HOCl via MPO. During inflammation, activated neutrophils generate HOCl via the NADPH oxidase system and MPO. HOCl may oxidize surrounding tissue causing excess tissue damage.

HOCl is strongly bactericidal [752]. *In vitro*, the MPO-H_2O_2-halide system oxidizes bacterial thiols, releases sulfide from iron-sulfur centres and inhibits respiration [753, 754]. Other groups susceptible to oxidation include sulfur-ether groups, heme groups and unsaturated fatty acids. As such, HOCl can cause loss of microbial membrane transport [755], interrupt the membrane electron transport chain [756], dissipate adenylate energy reserves [757], and suppress bacterial DNA synthesis [758], ultimately causing impaired bacterial cell viability and death.

HOBr, generated by activated eosinophils, also has antimicrobial effects [759]. Interestingly, formation of HOBr is not restricted to EPO; recent reports implicate MPO in formation of this hypohalous acid, due to interactions between HOCl and Br^- [760, 761]. HOBr (10^{-6} M) at pH 5.0 has significant bactericidal activity against *E. coli* whereas HOCl in the same system was less efficient, and a concentration of 10^{-4} M was required to cause death [762]. HOBr can also react rapidly with a variety of cellular and extracellular targets [763] and sulfur-containing compounds [764], altering protein structure and function, resulting in disruption of the extracellular matrix and cell lysis [765-768].

1.4.1.6 ROS/RNS and inflammation

The role of ROS/RNS in inflammation extends well beyond the classical view of antimicrobial activity and induced dysfunction of protein, DNA and lipids. Extracellular ROS/RNS produced by activated phagocytes promotes expression of cell adhesion molecules on the endothelium, induction of pro-inflammatory chemokines, cytokines and acute phase proteins, generally via redox-sensitive transcription factors, such as NF-κB [769, 770]. ROS/RNS are involved in LPS-induced and/or TNF-α-mediated NF-κB activation [771, 772]. For example, short bursts of NO enhance activation of NF-κB in LPS or TNF-α-stimulated cells [773, 774]. Conversely, long-term exposure to NO inhibits NF-κB, serving as a negative-feedback signal [775-777]. Similar plieotrophic functions were found with H_2O_2; low levels enhance NF-κB [778, 779], whereas higher concentrations (>100 μM) inhibit activity [775-777] Inhibition of NF-κB may also occur as a consequence of HOCl-mediated oxidation of IκB [780]. Hence, ROS and RNS regulate the expression of inflammatory genes, and consequently, the immune response. Therefore, oxidative stress can contribute to the upregulation of molecules that, as a bi-product of normal activity, produce greater amounts of ROS. Examples of NADPH

oxidase-derived superoxide production in the pathogenesis of chronic inflammatory diseases include its implication in vascular dysfunction, atherosclerosis, hypertension, diabetic vasculopathy and heart failure [781].

For example, H_2O_2 promotes endothelial dysfunction by stimulating $O_2^{\cdot-}$ production via xanthine and NADPH oxidases and mitochondria [782], decreasing the bioavailability of agonist-induced $^{\cdot}NO$, thereby contributing to vascular dysfunction [782]. Similarly, inactivation of NO by ROS can damage the endothelium [781]. Iron-derived ROS released by erythrocytes are also implicated in endothelial dysfunction [783]. When hemoglobin in plasma is oxidized, heme is transferred to endothelium and lipoprotein [783], in turn upregulating expression of adhesion moleules ICAM-1 and VCAM-1. Hemin, the pro-inflammatory molecule of heme can also increase migration and activation of neutrophils, thereby propagating inflammation [784].

1.4.1.7 Lipid, DNA and protein products of oxidation

Polyunsaturated FA (PUFA) are susceptible to oxidation by ROS such as $HO^{\cdot}$, forming lipid radicals. Interaction with O_2 can generate lipid peroxyl radicals, which can auto-oxidize surrounding PUFAs, potentially damaging the plasma membrane [785]. Lipid peroxyl radicals induced by oxidants and oxidative stress generate a number of lipid peroxidation products, including stable products such as ketones and alkanes [785]. Aldehydes also react with cell and tissue proteins forming advanced lipid peroxidation end-products that can cause protein dysfunction and alter cellular processes, summarized in Fig. 1.16 [785].

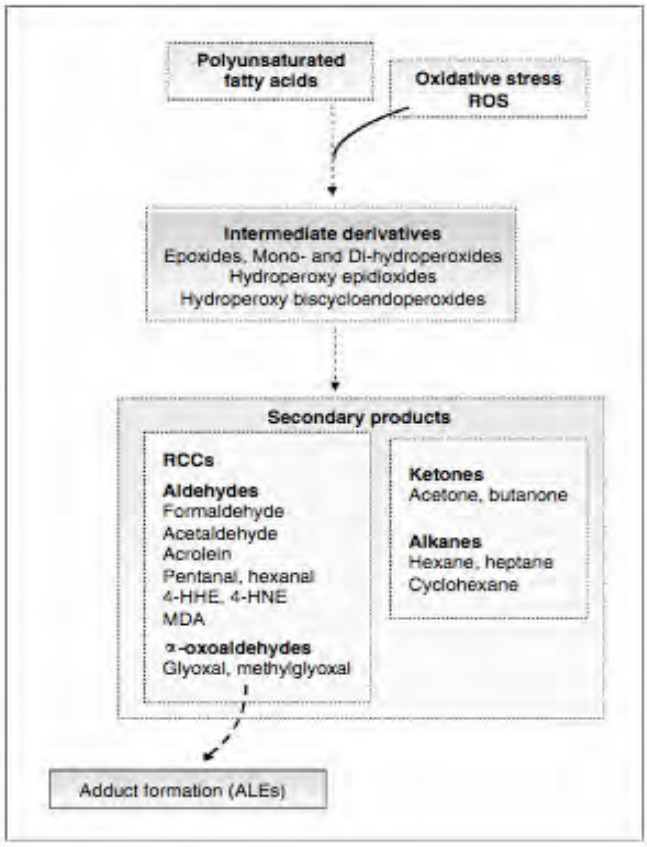

Figure 1.16: Schematic steps of lipid peroxidation. PUFA interact with ROS generated through oxidative stress, resulting in formation of intermediate derivatives. Derivatives can form secondary products. Reactive carbonyl compounds (RCCs) can react with proteins and other biological molecules, forming advanced lipid peroxidation end products (ALEs). Stable products (alkanes) do not react with proteins. From [785].

Structural damage can also occur following peroxidation of membrane FA such as docosahexaenoate, which is highly susceptible to auto-oxidation. In addition, lipid peroxyl radicals can be converted to hydroperoxide, which is less reactive, but can also cause auto-oxidation and propagate inflammation in the presence of metal ions iron and Cu^{2+} [786]. This process can be prevented by glutathione peroxidase (GPx), which the converts hydroperoxide to a harmless hydroxy FA, or by Vitamin E via free-radical scavenging [787]. However, vitamin E can have pro-oxidant effects, particularly in cigarette smokers, where Vitamin E prolongs mean LDL oxidation lag time and also increases F_2-isoprostanes (biologically active prostanoids formed by free radical-initiated rearrangement of AA). Importantly, F_2-isoprostanes are vasoactive and increase platelet activation, which may increase the risk of cardiovascular disease [788].

Lipid peroxide radicals can also decompose, forming highly reactive fragments

such as malonaldehyde which can form cross-links with free amino groups of proteins, phospholipids and nucleic acids, producing high molecular weight polymers. These are unable to interact with enzymes in cellular and subcellular membranes and can change function [787].

Advanced lipid peroxidation end products play significant roles in development of several pathologies, including cardiovascular disease (CVD), neurodegenerative diseases, cancer and chronic inflammatory diseases [785]. In CVD, oxidation of low-density lipoprotein (LDL) by 4-hydroxynonenal (4-HNE) and malondialdehyde (MDA) (released in response to oxidation of LDL, which contribute to auto-oxidation) within plaque could constitute a new prognostic indicator of cardiovascular disease (reviewed in [785]).

HOCl mediated oxidation of lipids also contributes cardiovascular disease (reviewed in [789]). Phospholipids, FA, sterols and sphingolipids are targets. Alkenes in aliphatic residues of esterified and nonesterified FAs and the double bond in cholesterol are oxidized to chlorohydrins [790-797]. Chlorohydrins have the potential to disrupt cell membranes, resulting in cell lysis and death and may represent putative biomarkers of neutrophil/monocyte-induced oxidative damage [791]. In addition, primary amine groups in ethanolamine and serine glycerophospholipids can be oxidized to chloramines, dichlorinated amines, chorimines and nitriles [798, 799], contributing to atherosclerosis and myocardial ischemia (reviewed in [789]). Kinetic studies of HOCl with phospholipid headgroups found in LDL demonstrated that HOCl reacted more strongly with phosphotidyl-ethanolamine and phosphotidyl-serine (forming chloramines) compared to phosphotidyl-choline and 3-pentenoic acid (double bonded unsaturated FA) (reviewed in [789]). Furthermore, chloramines formed on the lipid headgroups decompose, forming radicals and may contribute to further lipid peroxidation [800].

In contrast, HOBr appears to have a different kinetic profile to HOCl; bromamines and bromohydrins were detected on LDL and isolated phospholipids after exposure to HOBr [801, 802]. Second-order rate constants for HOBr reactions with the amine headgroups of phosphotidyl-serine and phosphotidyl-ethanolamine are ~30-50-fold greater than HOCl [803]. Moreover, the rate of rection with 3-pentanoic acid is ~1000-fold greater than that for HOCl, and consistent with the greater reactivity of double bonds to HOBr. This may explain the increased concentrations of halohydrins in phospholipid micelles, liposomes, LDL and red blood cells when treated with HOBr, compared to HOCl [801, 802, 804-806].

In neurodegenerative diseases, it is unclear whether oxidation is a cause or

consequence of neuronal death. In Alzheimer's, Parkinson's and Creutzfeldt-Jakob disease, 4-HNE may play a central role in accumulation of modified proteins that contribute to neuronal death [807-812].

In chronic inflammatory diseases, MDA and 4-HNE (considered mutagenic, as it forms adducts on guanine, and is carcinogenic for hepatocytes [813]) adducts contribute to cartilage degradation by modifying type II collagen [814]. 4-HNE alters osteoblast activity [815]. Oxidative damage and lipid peroxidation contribute to asthma, acute lung inflammation and allergic airway inflammation, although precise mechanisms are not yet established [816, 817].

Damage caused by ROS can have a direct effect on nuclear and mitochondrial DNA. Much oxidant-induced DNA damage is associated with $HO^{\cdot}$, its reactivity is so great that it does not diffuse more than a few molecular diameters before reacting with susceptible compounds [818]. As such, it is likely that H_2O_2 serves as a diffusible form of $HO^{\cdot}$ produced following reaction with a metal ion (for example Fe^{2+}) near susceptible DNA molecules [819, 820]. Intermediates of oxygen reduction attack bases or the deoxyribosyl backbone of DNA [821]. Oxygen radicals can also generate reactive compounds by reacting with lipids that couple to DNA bases [821]. Interestingly, levels of oxidative DNA damage in human tissues or in animal models of carcinogenesis are greater than the levels of DNA damage observed in lesions induced by exogenous carcinogens. Moreover, HOCl and N-chloramines that chlorinate genetic material may contribute to development of inflammation-associated cancers [822] illustrating the profound effect of oxidation induced-DNA damage [821].

1.4.1.8 Anti-oxidant defense systems

Excess production of ROS/RNS in phagocytes is moderated by the anti-oxidant defense system which consists of micronutrients (vitamin C and E), or enzymes dependent on dietary micronutrients (SOD1 and SOD2), or produced by specific endogenous pathways [823]. These examples are defined as direct anti-oxidants. However, other components can act indirectly by modulating direct agents or by regulating the biosynthesis of anti-oxidant proteins [823], and are known as pro-anti-oxidants. SODs are probably the most important line of anti-oxidant enzyme defense, particularly against superoxide anion radicals [824]. These enzymes are present in mitochondria, cytoplasm and extracellular compartments and can rapidly remove $O_2^{\cdot -}$

generated during mitochondrial respiration, and by NADPH oxidase, by converting it to H_2O_2 [824].

Three isoforms of SOD have been identified. Two have Cu^{2+} and Zn^{2+} in their catalytic centres, and localize to either intracellular cytoplasmic compartments (CuZn-SOD, also known as SOD1) or to extracellular elements (EC-SOD, also known as SOD3) [824]. Mice deficient in SOD1 have a reduced lifespan and increased incidence of neoplastic changes in the liver [825]. A third isoform has manganese as a cofactor and localizes in mitochondria of aerobic cells (Mn-SOD or SOD2) [824]. SOD2 plays a major role in promoting cell differentiation and/or tumorigenesis and in protecting against hypoxia-induced pulmonary toxicity [824]. Homozygous null mutant mice die within the first 10 days of life, and display dilated cardiomyopathy, accumulation of lipid in liver and skeletal muscle and metabolic acidosis [826]. Moreover, these mice have severely reduced succinate dehydrogenase (complex II) and aconitase (a tricarboxylic acid cycle enzyme) activities in the heart [826]. This indicates that SOD2 is required for normal functions of tissues by maintaining the integrity of mitochondrial enzymes susceptible to direct inactivation by superoxide [826].

Catalase is found in peroxisomes (a cell organelle which contains catalase and oxidase, that catalyze the production and breakdown of H_2O_2) and in the cytoplasm of most tissues. Catalase works in harmony with SOD, by reducing H_2O_2 generated by SOD, to H_2O and O_2 (reviewed in [827]). A null mutation of catalase in mice produces animals that are healthy up to 1 year of age and have normal fertility [827]. Similarly, their hematological profile is normal, as is the susceptibility of their lungs to hypoxia, and lenses of the eye to photochemical reaction. However, mitochondria in the brain have impaired oxidative phosphorylation after trauma [828]. In contrast, when catalase is overexpressed in mitochondria, lifespan of the mice was increased ~20%, with cardiac pathology and cataract development delayed [829], confirming its importance redox homeostasis.

Peroxiredoxins (Prx) are a family of thiol peroxidases that scavenge peroxides in cells. Prxs use Cys at their active site to convert H_2O_2 to sulfenic acid (reviewed in [830]). Prxs are very abundant, accounting for ~1% of soluble cellular protein [831], indicating that they have a central role in responses of cells to oxidative stress.

Within the Prx family, thioredoxin (Trx) and glutaredoxin (Grx) regulate redox status by changing the structure and activity of a broad spectrum of target proteins [832]. These proteins function by reducing disulfide bridges in target oxidized proteins

(summarized in Fig. 1.17), releasing the reduced target and oxidized redoxin protein [832].

Trx is a low molecular weight protein (12-18 kDa) with an active thiol/disulfide site and oxidoreductase activity (reviewed in [833]). Trx has two isoforms, cytosolic Trx1 and mitochondrial Trx2 [834]. Both contribute to anti-oxidant cell defense by repairing the catalytic activity of peroxiredoxins and glutathione peroxidases by decomposing hydroperoxides and H_2O_2 [835]. In addition, both isoforms are a sink for $HO^{\cdot}$ radicals [836]. Knockout of either isoform is embryonic lethal; lethality in Trx2 knockout mice occurs in the middle of development. The main cause of death in these mice is due to increased levels of ROS, confirming this as a critical component of anti-oxidant defense (reviewed in [833]).

Trx1 has diverse functions. For example, it acts as a growth factor and as an enzyme cofactor of peroxiredoxin [835], ribonucleotide reductases, methionine sulfoxide reductases, and is involved in DNA repair [837]. Moreover, C57BL/6 transgenic mice overexpressing Trx1 have increased life spans compared to wild type mice, with resistance to cerebral infarction [838], pneumonia [839] and renal ischemia-reperfusion [840]. Importantly Trx1 overexpressing mice embryos develop normally under conditions of oxidative stress, highlighting its role in oxidant defense [841].

In yeast, Trx2 reduces the oxidized form of mitochondrial peroxiredoxin (Prx3), in turn, reducing peroxides; yeast cells difficient in Trx2 are more sensitive to H_2O_2 [842]. Over-expression of Trx2 facilitates resistance to ROS-induced apoptosis [843].

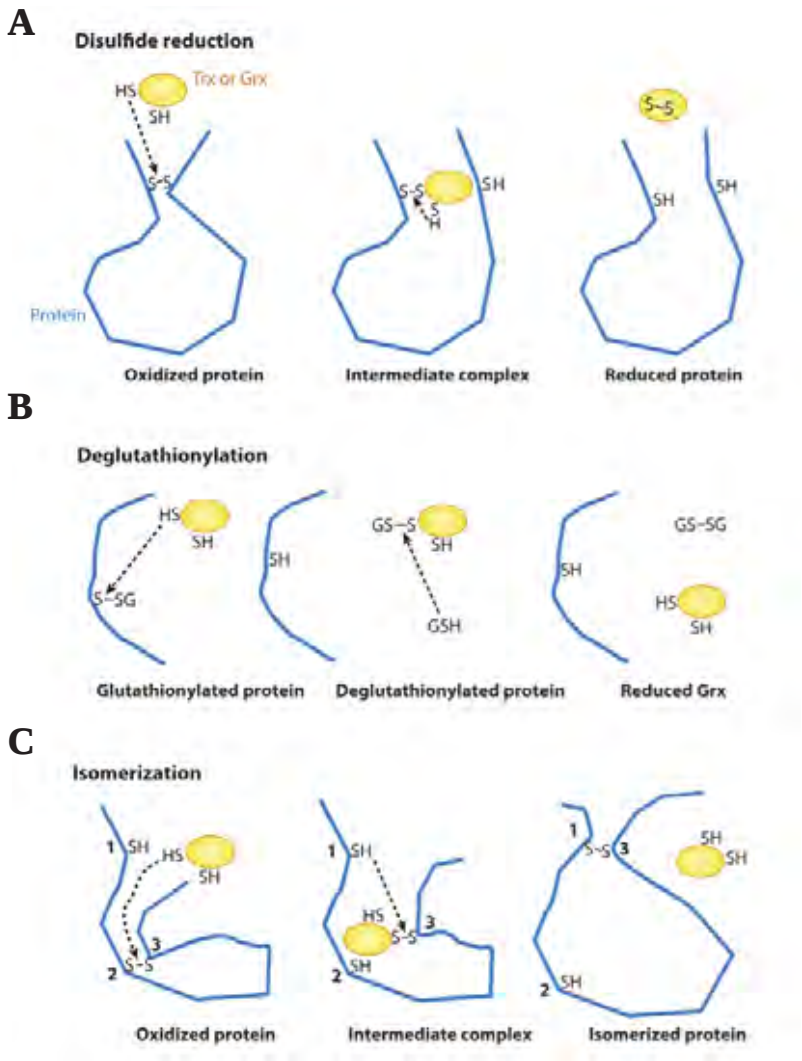

Figure 1.17: Mechanisms for regulating Trx or Grx target proteins by dithiol-disulfide exchange. (**A**) The reduced form of dithiol Trx or Grx is responsible for the disulfide reduction. The disulfide group is reduced to the sulfhydryl. (**B**) Deglutathionylation is catalyzed by dithiol or monothiol Grx. Glutathione bound to the target protein is released by reduction. The protein then exists in the sulfhydryl state. (**C**) Isomerization by a dithiol or monothiol Trx or Grx. The redox state of the target protein is unchanged, but the position of the disulfide bond is altered. From [832].

In contrast, glutaredoxins are low molecular weight (9-14 kDa), GSH-dependent oxidoreductases; electron transfer occurrs via NADPH-dependent glutathione reductase to the oxidized glutathione to form GSH, which reduces oxidized glutaredoxin. Disulfides and mixed disulfides are the main substrates, and disulfide reduction is mediated by one (monothiol) or two (dithiol) Cys residues in the active centre (reviewed in [833]).

In humans, three Grx exist, Grx1 (cytosolic), Grx2 and Grx5 (mitochondrial) [844, 845]. Grx1 reduces disulfides and is implicated in thiol-disulfide exchange [846]. Grx1 is involved in cell differentiation [847], regulation of transcription factors [848-850] and apoptosis [851, 852]. Grx1 is proposed to play a protective function in atherosclerosis; macrophages in regions of atheroma express high levels of the Grx1 gene [853]. ROS-dependent activation of Ras is one of the main causes of atherogenesis and restenosis [854]. Over-expression of the Grx1 gene promotes deglutathionylation of Ras, thereby inhibiting its activation [855]. Grx2 catalyzes deglutathionylation of protein mixed disulfides [856] and regulates mitochondrial ROS levels by catalysis of reversible S-glutathionylation of proteins in mitochondrial complex I [857, 858] and reversible glutathionylation of inner membrane proteins [857]. Over-expression of Grx2 in HeLa cells decreases their sensitivity to apoptosis and prevents oxidation of cardiolipin, and also inhibits activation of caspases [859]. Grx5 is implicated in iron homeostasis and reduces mixed protein and protein disulfides [845, 860-862] and is required for haem synthesis [845]. Together, Trx and Grx play essential roles in cellular redox homeostasis and in redox-dependent regulation of proliferation, differentiation and apoptosis.

Glutathione peroxidases (the general name for a family of multiple isozymes) are physiologically important anti-oxidant enzymes. In mammals, seven isoenzymes have been described. GPx1 is present in red blood cells, liver, lung and kidney. GPx2 is restricted to the gastrointestinal tract, whereas GPx3 and GPx4 exhibit wide tissue distribution [863, 864]. The precise function of GPx5 is not well understood. GPx6 is expressed exclusively in the olfactory epithelium, whereas GPx7 appears to mitigate oxidative stress in breast cancer cells [864]. The primary function of the glutathione peroxidase family is to catalyze reduction of H_2O_2 or organic hydroperoxides to water or alcohols via reduced glutathione or selenium (reviewed in [863]). Impaired function of these isoenzymes leads to a variety of maladies; for example, low level activity of GPx1 predicts increased risk of cardiovascular events [865] and is associated with acute myelogenous leukemia, Hodgkin's disease and visceral cancers [866]. GPx3 deficiency increases the risk of arterial ischemic stroke [867].

Non-enzymatic anti-oxidants include glutathione and ergothioneine-2-mercapto-*N*α-trimethyl-L-histidine. These scavenge free radicals and activated oxygen species in the cytosolic, mitochondrial and nuclear aqueous compartments [868-870]. Conversely, hydrophobic scavengers are found in lipoproteins and membranes and function by either interrupting the propagation step of lipid peroxidation by destroying peroxyl radicals, or blocking formation of hydroperoxides from singlet oxygen [869]. Hydrophobic anti-oxidants include Vitamin E, carotenoids and ubiquinol, also known as the reduced form of coenzyme Q. Of these, Vitamin E is the most efficient scavenger of peroxyl radicals in phospholipid bilayers, because it is preferentially incorporated into the membrane of mammalian cells (reviewed in [869, 871]).

As mentioned, anti-oxidant defense systems can be divided into two categories: anti-oxidants and pro-anti-oxidants. The most prominent pro-anti-oxidant is heme oxygenase-1 (HO-1). This enzyme catabolizes heme into three products: CO, biliverdin (rapidly converted to bilirubin) and free iron (later converted to ferritin), all of which have anti-inflammatory, anti-oxidative and cytoprotective activities [872, 873]. CO suppresses pro-inflammatory responses of macrophages, and may contribute to controlling the balance of inflammation. When these cells are stimulated with LPS or other TLR agonists, cytokines such as TNF-α and IL-10 are produced [872]. However, when these cells are exposed to CO *in vitro* before stimulation with LPS, the pro-inflammatory response (TNF-α production) is markedly inhibited and IL-10 (anti-inflammatory) production is enhanced [874]. CO also suppressed production of ROS and NO [874, 875].

Bilirubin and biliverdin stabilize vitamin A and β-carotene during intestinal uptake. Interestingly, animals with low plasma bilirubin show early symptoms of vitamin E deficiency [873]. Unconjugated bilirubin scavenges singlet oxygen and is a reducing agent for peroxidizes such as horseradish peroxidase and prostaglandin H synthase [876-879]. In addition, bilirubin in its free, albumin-bound and conjugated forms has a pair or reactive hydrogen atoms which function in carbonate H-ion donation, producing subsequent anti-oxidant activity. When bilirubin is bound to albumin it acts as a peroxyl radical scavenger, protecting FA transported on albumin [880]. Finally, ferritin appears to substitute for HO-1 action. Ferritin was believed to be the mechanism by which HO-1 conferred resistance to oxidative stress in endothelial cells, and hypoxic lung injury [881-884].

1.4.2 POST-TRANSLATIONAL OXIDATIVE MODIFICATION OF PROTEINS BY ROS/RNS

1.4.2.1 Reversible protein modifications generated by ROS/RNS

ROS may generate various modifications to particular targets, but it is important to understand the significance of reversible and irreversible modifications in a functional context.

One postulate is that reversible modifications protect proteins against irreversible oxidation. Transient modifications can be reversed by reductases such as glutathione reductases, Met sulfoxide reductases, Prxs or changes in intracellular redox potential [885]. One example is glutathione, a major anti-oxidant recycling thiol in mammalian cells [886]. Reversible disulfide bond formation, and mixed disulfides between protein cysteines and glutathione can stabilize extracellular proteins and protect against irreversible oxidation of critical cysteine residues [886].

S-thiolation of proteins can occur within minutes after stimulation of an oxidative burst in neutrophils, and can neutralize partially-oxidized protein cysteine residues [886]. Strong oxidants irreversibly oxidize Cys residues to sulfinic and/or sulfonic acid derivatives [887]. Sulfinic acid was believed to be an irreversible modification although, recent work by Biteau *et al.*, reports an enzyme in yeast that reduces sulfinic acid derivatives. This enzyme, known as sulfiredoxin, reduces oxidized proteins via its intrinsic phosphotransferase and thioltransferase activity [888].

RNS also generate reversible modifications in proteins, for example, S-nitrosylation, the covalent coupling of a NO group to Cys thiols [694]. S-nitrosylation of proteins is dependent on the structure surrounding Cys residues and the local environment hence few proteins are targets of this modification (reviewed in [695]). The most likely mechanism regulating S-nitrosylation may be via an acid-base catalyzed SNO/SH exchange between the susceptible Cys residue, and the basic and acidic amino acids which surround it [889]. S-nitrosylation is reversible because it readily dissociates or can be cleaved by specific enzymes. Transition metals or transnitrosation can accelerate denitrosylation [890]. The transient nature of the S-nitrosylated modification means that it can regulate protein function and redox-dependent signalling, such as seen for NF-κB [891]. S-nitrosylated proteins may also act as NO donors, to facilitate NO transport to different targets [613, 890, 892].

Met residues modified by ROS can be reduced by methionine sulfoxide reductase

(MSR). This enzyme can restore regular function to many proteins with oxidized methionine residues. For example, HIV-2 protease is inactivated after of oxidation of Met_{76} and Met_{95} residues to Met sulfoxide. MSR partially restores function [893].

In summary, reversibility of the modifications described are critical in determining protein function and in modulating particular pathways of cell signalling [894-896].

1.4.2.2 Irreversible protein modifications by ROS

Characterizations of irreversible protein modifications are important in understanding dysfunction of biological pathways, but this area of research is relatively understudied. Irreversible modifications are generally associated with loss of function and can lead to accumulation of damaged proteins (reviewed in [886]).

Protein carbonylation is the most common and best-studied irreversible protein modification and occurs when carbonyl groups (for example reactive aldehydes and ketones) are introduced into protein by oxidation of amino acid side chains [897]. Oxidative cleavage of protein by α-amidation or by oxidation of glutamyl side chains also leads to carbonylation [897].

Carbonylated proteins react with 2,4-dinitrophenylhydrazine to form hydrazines, via direct oxidation of side chains of Lys, Arg, Pro and Thr residues [898, 899]. These residues are the most susceptible amino acids and when modified can trigger oxidation-induced cleavage and subsequent protein degradation by the proteasome [900]. Carbonylation also generates high mass aggregates that may accumulate as damaged or unfolded proteins that can inhibit proteasome activity [900].

The build-up of protein aggregates and complexes may contribute to the pathogenesis of many chronic inflammatory diseases. The brain is particularly susceptible to the damaging effects of ROS, because of its high metabolic rate and reduced capacity for regeneration compared to other organs [901]. Accumulation of proteolysis-resistant aggregates is also associated with the pathogenesis of several neurodegenerative diseases [900]. For example, carbonylated proteins were found in brains affected by Alzheimer's disease [902], suggesting that accumulation of oxidized proteins contributes to the pathogenesis of neurodegenerative conditions.

The NADPH complex and MPO generate HOCl from H_2O_2 (see Section 1.4.1.2). Excessive HOCl can cause severe protein oxidation and generate complexes and

aggregates. Oxidation of LDL with HOCl *in vitro* resulted in formation of higher-order complexes in a concentration-, temperature-, and time-dependent manner; complexes were stable to dithiothreitol (DTT) reduction, suggesting alternate covalent bonded, cross-linking [903]. Importantly, LDL peptides treated with HOCl form sulfinamide bonded peptides [904], a similar modification generated by HOCl in mS100A8 [606].

Like carbonylated proteins, HOCl-induced oxidation can produce high mass aggregates. For example, oxidation of LDL peptides may generate intra- and inter-molecular protein cross-linking that may contribute to aggregate formation in the artery wall [904]. Interestingly, HOCl-oxLDL was effective as a ligand for loading mouse peritoneal macrophages *in vitro*, suggesting that HOCl also contributes to generation of atherogenic forms of lipoproteins [903].

The implications of Tyr nitration are relatively poorly defined. Tyr nitration occurs via reactions with $ONOO^-$ [905, 906] and can be mediated by MPO, via Compound I (reviewed in [907]). Like S-nitrosylation, Tyr nitration is similarly selective and appears to be structure-dependent, requiring one or more acidic residues near the nitratable Tyr, a nearby turn-inducing amino acid (for example Pro or Gly), and exclusion of sulfur-containing Met and Cys residues [908]. Links between protein Tyr nitration and mechanisms involved in formation of numerous pathological conditions, ranging from post-radiation responses, tumour vascularization and chronic obstructive pulmonary disease are proposed [909]. Tyr nitration was initially thought to be irreversible but studies analyzing nitration of mitochondrial proteins indicate that Tyr residues can undergo denitration [910, 911]. This suggests that the modification exhibits many characteristics found for some redox switches in classical signalling pathways: reversibility, responsiveness on a physiological time scale and selectivity [909]. Tyr nitration is implicated in regulation of p53 [912], IκBα [913], ERK1/2 [914] and Akt [914, 915], possibly by affecting transcriptional activity, independent of DNA damage signalling, and signalling pathways.

Tyrosine is also susceptible to bromination and chlorination [761]. Originally 3-chlorotyrosine and 3-bromotyrosine were thought to be specific biomarkers of MPO [916, 917] and EPO [918, 919]; elevated levels of EPO and brominated tyrosine residues were both detected in sputum from patients with asthma relative to controls [918, 920, 921]. However, *in vitro* experiments showed that at physiological concentrations of bromide and chloride, MPO generated HOBr and HOCl, and levels of 3-bromotyosine in human

serum albumin (HSA) increased to 16-fold higher levels than that of 3-chlorotyrosine under the same conditions [761]. This is unsurprising as HOBr reacts some 5000-fold faster with Tyr than HOCl [922]. Because of these observations the ratio of 3-chlorotyrosine:3-bromotyrosine may not reflect activities of HOCl and HOBr in disease processes [761].

Chlorination of amino acids can have profound effects on basic physiological functions and immune system regulation. Chlorination of Tyr promotes a range of products (see Section 5.1, Chapter 5). Perhaps the most widely-studied protein that is sensitive to Tyr chlorination is ApoAI. Chlorination of Tyr_{192} in ApoAI is associated with altered reverse cholesterol transport (RCT) because it interfers with ATP-binding cassette transporter member 1 (ABCA1) function, thereby increasing the risk of coronary artery disease (reviewed in [907]) (see Section 5.1, Chapter 5 for discussion of Tyr chlorination).

Taurine, a semi-essential amino acid not incorporated into proteins, is ubiquitous and the most abundant free amino acid in leukocytes [923]. Taurine scavenges HOCl to form the more stable and less toxic taurine chloramine [924]. Although considered stable, taurine chloramines can decompose thermally to sulphoacetaldehyde [925]; decomposition increases at low pH [926]. Taurine chloramines can downregulate pro-inflammatory mediator production in human leukocytes, for example, by inhibiting NF-κB activation by oxidizing IκBα at Met_{45} [924]. Similar effects were observed with glycine chloramine, indicating that chloramines can affect cell-regulatory pathways [780].

1.4.3 S100A8 AND S100A9 IN REDOX BALANCE

S100A8 and S100A9 may have dual roles in inflammation. At low concentrations (picomolar levels) they may modulate leukocyte recruitment. However, there is accumulating evidence for pleiotropic functions in response to oxidant scavenging [612-614, 631, 655, 695], even though S100A8/A9 may be important in generation of ROS by regulating NADPH oxidase activation (see Section 1.3.5.4). Oxidant-induced structural modifications to S100A8 and S100A9, and their functional consequences, are discussed in detail in Chapter 3. Chapters 4 and 5 of this thesis will describe novel oxidative modifications of hS100A8 and hS100A9, and investigate some functional effects of these.

1.4.4 HYPOTHESIS AND AIMS

1.4.4.1 Hypothesis

We propose that oxidation of S100A8 and/or S100A9 represent important feed-back mechanisms, mediating downregulation of pro-inflammatory activities through post-translational oxidative modification.

1.4.4.2 Aims

The aim of this thesis was to investigate putative post-translational oxidative modifications to S100A8 and S100A9 after exposure to hypohalous acids, *in vitro*, confirm the presence of these modifications in chronic inflammatory diseases, *in vivo* and assess the impact of these modifications on some relevent functions. Specifically, we aimed to:

Chapter 3-

1. Determine oxidative modifications to recombinant (rec)-hS100A8 and rec-hS100A9 by HOCl and HOBr *in vitro*.

Chapter 4-

2. Determine whether S100A8, oxidized S100A8 (oxS100A8) and/or S100A9 were expressed in asthmatic lung.
3. Quantitate levels of S100A8, oxS100A8, S100A9 and S100A12 in sputum from patients with asthma and bronchiectasis.
4. Characterize putative oxidative modifications in the S100 proteins from asthmatic sputum.
5. Illustrate oxidation by HOCl modifies functions of rec-hS100A8, rec-hS100A9 and rec-hS100A8/S100A9, *in vitro*.

Chapter 5-

6. Quantitate levels of S100A8, S100A9 and S100A8/S100A9 in serum from patients with SLE.
7. Investigate whether S100A8 complexes with lipoproteins in serum from healthy controls and from patients with SLE.
8. Investigate potential interactions between rec-hS100A8 and ApoAI.
9. Characterize potential oxidative modifications to S100A8 and S100A9 in carotid artery extracts.
10. Determine whether rec-hS100A8 protects ApoAI from oxidation by HOCl *in vitro*.

11. Determine whether rec-hS100A8, rec-hS100A9 and/or rec-hS100A8/S100A9 reduce formation of oxidized protein in endothelial cell extracts after exposure to MPO/H_2O_2.

CHAPTER 2: MATERIALS AND METHODS

Methods common to several sections of this thesis are described here. Specific experimental protocols are described in the appropriate Chapters. Reagents used are described in Appendix I.

2.1 EXPERIMENTAL PROCEDURES

2.1.1 PREPARATION OF RECOMBINANT PROTEIN

Recombinant hS100A8, hS100A9, hS100A12 and $hCys_{42}$-Ala_{42}S100A8 mutant, where the single Cys residue is replaced with Ala, were produced as described [320]. PCR-amplified S100 cDNA generated from the SuperScript™ Preamplification System (Invitrogen, CA, USA) was digested by *Bam*HI, cloned into the glutagene pGEX-2T bacterial expression vector (Pharmacia, NY, USA) and expressed in *E. coli* strain BL21 [927]. *E. coli* cells were streaked onto Lennox broth (LB) agar plates containing ampicillin (50 μg/ml; Sigma, MO, USA) and grown overnight at 37°C. A single colony was selected and transferred under sterile conditions to 200 ml LB-Lennox media containing 50 μg/ml ampicillin (Sigma, MO, USA) and grown to saturation at 37°C overnight with shaking (220 rpm). The culture was then transferred into 800 ml pre-warmed LB containing ampicillin (50 μg/ml) and shaken (220 rpm) for 60 min at 37°C, after which isopropyl-β-thiogalactosidase (Invitrogen, CA, USA; 25 mg/l culture) was added, and culture incubated for another 4 hrs at 37°C, with shaking (220 rpm).

Bacteria were pelleted by centrifugation for 10 mins at 4°C, resuspended in 40 ml TBS and pelleted again by centrifugation. Supernatant was discarded and bacteria resuspended in 5 ml chilled wash buffer (TBS with 0.1% Triton X-100 (Sigma, MO, USA) and 0.5 mM ethylene glycol bis (β-aminoethyl ether) N, N'-tetraacetic acid (EGTA; Sigma, MO, USA), and sonicated at 50% power for 2.5 min using a Branson sonicator (Branson Ultrasonic; CT, USA). The suspension was diluted further with another 20 ml chilled-wash buffer and sonicated for 2.5 min at 50% power.

Insoluble material was separated from soluble protein by centrifugation and supernatants filtered through a 0.45 μm filter (Millipore, MA, USA), then incubated with glutathione-conjugated agarose (210 mg; Sigma, MO, USA) for 30 min at room temperature (RT) to allow Glutathione-S-transferase (GST)-S100A8, S100A9 or

S100A12 to bind. Beads were washed 3 times with chilled wash buffer, then 3 times with TBS before a final wash in 50 mM Tris pH 8.5. GST-S100 fusion proteins were incubated with thrombin (20 U for S100A8 and S100A9, 100 U for S100A12; Sigma, MO, USA). The tube was purged with argon gas prior to sealing and incubation at RT (S100A8 and S100A12 overnight, S100A9 for 2 hrs).

S100 proteins were then eluted from the beads with 2 x 4 ml elution buffer (TBS and 10mM DTT; Bio-Rad, CA, USA; incubated for 15 min at RT), then eluates filtered through a 0.22 μm Millex-GP filter unit (Millipore, MA, USA). Cleaved recS100 protein was separated using a preparative C8 column (300 Å, 20 μm particle size, 10 x 100 mm, Aquapore, Varian Inc., CA, USA) by reverse-phase high performance liquid chromatography (RP-HPLC). Purity was confirmed by analytical C4-RP-HPLC column (300 Å, 5 μm particle size, 250 x 4.6 mm, supplied by Vydac, Separations Group, CA, USA) and by SDS-PAGE and silver staining, for all recombinant preparations.

Protein concentrations for rec-hS100A8, S100A9 and S100A12 were determined by measuring $A_{280\ nm}$ (for rec-hS100A8 and S100A9) or $A_{205\ nm}$ (for rec-hS100A12) using the Nanodrop ND-1000 Spectrophotometer (Thermo Fisher Scientific, Waltham, MA, USA) and plate reader (in a quatz cuvette, SpectroMax M5, Molecular Devices Inc., CA, USA), respectively. Concentrations were determined using Beer's Law ($A=\varepsilon bc$, where ε is the extinction co-efficent, b is the pathlength and c is the concentration. The extinction coefficient of 1.56 L g-1 cm-1 (rec-hS100A8), 0.527 L g-1 cm-1 (rec-hS100A9) or 28 (rec-hS100A12) was used. Final concentrations of all recombinant S100 protein preparations were determined by taking the average concentration at $A_{280\ nm}$ or $A_{205\ nm}$ and the area under the peak at $A_{214\ nm}$ (after separation by C4-RP-HPLC).

All S100 proteins were stored in RP-HPLC eluate (~45% acetonitrile, 0.1% trifluoroacetic acid) in polyethylene tubes at -80°C, under argon, until required. The method of lyophilization and reconstitution of S100 proteins depended on the final use. Generally, S100 protein was diluted with appropriate buffer and lyophilized to leave only residual salts and protein. Protein was then reconstituted to final working concentration in appropriate buffer.

2.1.2 PROTEIN A PURIFICATION OF ANTIBODIES AND BIOTINYLATION

Rabbit polyclonal antibodies produced in-house by immunizing New Zealand white rabbits intradermally with 50 μg rec-hS100A8, rec-hS100A9, rec-hS100A12 or oxidized rec-hS100A8 were available for use [928].

Pre-immune IgGs were unreactive in Western blotting/immunohistochemistry. Anti-S1008, -oxS100A8 and -S100A9 IgG were immunospecific. Anti-oxS100A8 IgG reacted more strongly with oxS100A8 than S100A8 using ELISA [410]. Anti-S100A9 IgG recognized the S100A8/S100A9 heterodimer, whereas anti-S100A8 did not. These antibodies only reacted with the immunogen and not other S100s.

IgG in antisera was purified using Protein A Sepharose CL-4B affinity (Pharmacia, CA, USA). Gel with a packed volume of 0.5 ml was poured into a column (3 ml total volume) and equilibrated with 25 mM Tris, 150 mM NaCl pH 7.5 (TBS) at RT. Antisera were passed through the column 5 times, followed by 5 x 2 ml washes with TBS. Bound IgG was eluted with 0.1 M glycine (MP Biomedicals, OH, USA), 150 mM NaCl, pH 3.0 and collected in 10 x 1 ml fractions, each containing 35 μl 1M Tris, pH 9.0 to neutralize the eluates to pH 7.5. IgG concentrations were quantitated by measuring A_{280nm} and concentration calculated according to Beer-Lamberts law ($A=\varepsilon bc$, where A is absorbance, ε is the extinction coefficient, b is pathlength and c is concentration); the extinction coefficient of 1.4 L g^{-1} cm^{-1} for IgG was used. Fractions containing abundant IgG were combined, dialysed against PBS (1 L) overnight at 4°C and the final concentration measured by absorbance.

To generate biotinylated anti-S100A8, anti-S100A9 and anti-S100A12 IgG, 1 mg/ml IgG was incubated with 0.35 mM EZ-link®sulfo-NHS-LC-biotin (Pierce, IL, USA) for 2 hrs on ice. Unreacted biotin was removed by dialysis overnight at 4°C against two changes of PBS.

2.1.3 SODIUM DODECYL SULPHATE POLYACRYLAMIDE GEL ELECTROPHORESIS (SDS-PAGE) AND WESTERN BLOTTING

SDS-PAGE was performed using the Bio-Rad Mini Protean II electrophoresis apparatus (Bio-Rad, CA, USA) and a Tris-Tricine buffer system [929]. Samples were heated with sample buffer to 100ºC for 3 min and SDS-PAGE performed according to Schagger *et al.* [930] using 10% polyacrylamide gels under non-reducing or reducing conditions (5-100 mM DTT as required and detailed in the appropriate sections). Proteins

were silver-stained [931] or transferred to polyvinylidenedifluoride (PVDF) membranes (0.22 μm; Millipore, MA, USA) using a Bio-Rad transfer apparatus (45 min at 75 V) for Western blot analysis.

For Western blotting, membranes were blocked at RT for 2 hrs with 5% (w/v) skim milk in TBS, pH 7.4, washed 2x10 min with 0.05% Tween 20-TBS and 10 min with TBS, then incubated for 2 hrs with IgG antibodies to S100s (1-2 μg/ml in 1% skim milk in TBS). Membranes were washed 2x10 min with 0.05% Tween 20-TBS, 10 min with TBS then incubated for 2 hrs with HRP-conjugated goat anti-rabbit IgG (1:2000 (v/v); Bio-Rad, CA, USA, in 1% skim milk in TBS). After 2x10 min washes in 0.05% Tween 20-TBS and once in TBS, membranes were processed with Western Lightning-ECL enhanced chemiluminescence substrate (Perkin Elmer, Waverly, Australia) according to the manufacturer's instructions. Blots were visualized using a Fujifilm LAS-3000 CCD camera and the ImageGauge software (Tokyo, Japan).

2.1.4 RP-HPLC

Liquid chromatographic separation was performed with a Waters 996 photodiode array detector using a non-metallic LC626 HPLC system (Waters, MA, USA) and UV absorbance monitored at $A_{214\ nm}$ and $A_{280\ nm}$ with a Waters 996 photodiode array detector. Analytical RP-HPLC was performed using an analytical C4 column and a gradient of 25-75% acetonitrile (0.1% trifluoroacetic acid), eluted at 1 ml/min over 30 min. Preparative RP-HPLC was performed using a semi-preparative C8 column and a gradient of 35-65% acetonitrile in 0.1% trifluoroacetic acid eluted at 3 ml/min over 30 minutes. Fractions with large $A_{214\ nm}$ were manually collected. All buffers were purged with helium to remove dissolved oxygen.

2.1.5 PREPARATION OF OXS100A8 AND OXS100A9

For HOCl oxidation and generation of a predominantly oxidized monomer, 10 nmol rec-hS100A8 (100 μg) or rec-hS100A9 (140 μg) in 100 μl PBS was treated with 10 nmol HOCl (Sigma, MO, USA; molar ratio, 1:1), for 15 min on ice; ratios of 1:2 and 1:4 S100A8:HOCl were also used [606]. All incubations were for 15 min on ice, then L-Met (Sigma, MO, USA;100 mM in PBS) added to quench oxidation. Products were eluted from C4-RP-HPLC (25-70% acetonitrile/water); oxS100A8 monomer and dimer eluted at 14.4 min and 14.8 min; oxS100A9 monomer and dimer at 14.8 min and 15.7 min. Peaks

(0.5 μg) were separated by SDS-PAGE (100 mM DTT) and silver stained (see Section 2.1.3) to confirm separation of oxidized monomers and dimers.

Protein concentrations for HOCl-oxidized rec-hS100A8 and S100A9 were determined by measuring $A_{280\ nm}$ using the Nanodrop ND-1000 Spectrophotometer (Thermo Fisher Scientific, Waltham, MA, USA). Concentrations were determined using Beer's Law ($A=\varepsilon bc$, where ε is the extinction co-efficent, b is the pathlength and c is the concentration. The extinction coefficient of 1.56 L g-1 cm-1 (rec-hS100A8), 0.527 L g-1 cm-1 (rec-hS100A9) was used. Purified protein was stored under argon at -80°C to prevent oxidation.

2.1.6 ENZYME-LINKED IMMUNOSORBENT ASSAY (ELISA) FOR S100A8, S100A9 AND S100A12

A double sandwich enzyme-linked immunosorbent assay (ELISA) was used for S100A8, S100A9 and S100A12 detection. Flat-bottom 96 well plates (Maxisorp; Nunc, Roskilde, Denmark) were coated with anti-S100A12 IgG (2 μg/ml), anti-S100A8 IgG or anti-S100A9 IgG (4 μg/ml) in 0.05 M sodium carbonate buffer, pH 9.6 at 50 μl/well overnight at RT. Plates were washed 3 times with wash buffer (PBS, 0.05% Tween 20) and blocked with 1% BSA in PBS (200 μl/well) for 1 hr at RT. Serial dilutions (250 - 3.9 ng/ml) of rec-hS100s in PBS were used to create a standard curve. Samples and standards (100 μl/well) were incubated for 2 hrs at RT, wells washed 3 three times with 0.05% Tween 20-PBS then biotinylated anti-S100A8, anti-S100A9 (5 μg/ml) or anti-S100A12 (2 μg/ml) IgG added (100 μl/well) and plates incubated for 1 hr. Visualization was with 100 μl/well streptavidin-horseradish peroxidase conjugated (1:1500 (v/v), 30 min at RT; R&D Systems, MN, USA) and reactivity was developed with 100 μl/well substrate 3,3,5,5-tetramethylbenzidine (TMB; Pierce, IL, USA) solution for 20 min at RT in the dark. The reaction was stopped with 50 μl/well 2 N H_2SO_4 and $A_{450\ nm}$ measured with a plate reader (Titertec Multiscan MCC/340; Labsystem, Helsinki, Finland). Values for duplicate samples were calibrated against the standard curve.

2.1.7 SAMPLE PREPARATION FROM SDS-PAGE FOR MASS SPECTROMETRY

In-gel digestion of proteins separated and visualized by silver-staining were prepared using the following method. Protein bands of interest were excised and dehydrated with 100 μl acetonitrile, lyophilized, reduced with 10 mM DTT in 20 mM

NH_4HCO_3 (100 µl) at 56ºC for 1 hr, then alkylated with 100 µl 55 mM iodoacetamide (Sigma, MO, USA) in 20 mM NH_4HCO_3, in the dark at RT for 45 min. Gel slices were rinsed in 20 mM NH_4HCO_3 (100 µl) for 10 min at RT, dehydrated in acetonitrile then washed twice in NH_4HCO_3 (10 min). To generate peptide fragments for mass spectrometry (MS), gel slices were resuspended in 100 µl 20 mM NH_4HCO_3 overnight with either 200 ng trypsin (Roche Diagnostics, Mannheim, Germany) or 100 ng of endoproteinase AspN (Roche Diagnostics) at 37ºC, then digestion stopped with 50 µl 0.1% formic acid for 15 min at RT. Supernatants were collected, and gel slices treated with 50 µl 0.1% formic acid in 50% acetonitrile in water for 15 min and supernatants collected. Finally, 50 µl acetonitrile was added to the gel slices for 15 min, supernatants pooled (total volume, 250 µl) and then lyophilized [931] using the SpeediVac Concentrator Savant SCIIOA (Thermo Electron Corporation, Waltham, MA, USA). Peptide sequencing by MS was conducted on the LTQ-FT and QStar Mass Spectrometers by A/Prof Mark Raftery (UNSW, Australia), as described in Section 2.1.8.

2.1.8 MASS SPECTRAL ANALYSIS

Mass spectra data were acquired in collaboration with A/Prof. Mark Raftery Protein mass measurements were acquired using an API QStar Pulsar i hybrid tandem mass spectrometer (Applied Biosystems, Vic, Australia). Lyophilized samples (1-5 pmol) were dissolved in water:acetonitrile (50:50 (v/v), 0.1% acetic acid), loaded into nanospray needles (Proxeon, Denmark) with the tip positioned ~10 mm from the orifice. Nitrogen was used as curtain gas and a potential of 900 V applied to the needle. A time of flight (TOF)-MS scan was acquired (m/z 250-2000, 1 s) and accumulated for ~30 s into a single file. Spectra were deconvoluted using the Bayesian reconstruct algorithm. In some cases, spectra were recorded using liquid chromatography-mass spectrometry (LC/MS) with an 1100 MSD as described [637].

Digest peptides were separated by nano-LC using an Ultimate HPLC and Famos autosampler system (LC-Packings/Dionex, NSW, Australia). Samples (~200 fmol) were concentrated and desalted onto a micro C18 pre-column (500 µm x 2 mm, Michrom Bioresources) with H_2O:CH_3CN (98:2, 0.05 % HFBA) at 20 µl/min. After a 4 min wash the pre-column was switched (Switchos, LC Packings) into line with a fritless nano-column manufactured according to Gatlin *et al*. [932]. Peptides were eluted using a linear gradient of H_2O:CH_3CN (98:2, 0.1 % formic acid) to H_2O:CH_3CN (36:64, 0.1 % formic

acid) at ~300 ml/min over 30 min. High voltage (2300 V) was applied to low volume tee (Upchurch Scientific, WA, USA) and a column tip positioned ~ 1 cm from the orifice of an API QStar Pulsar i hybrid tandem mass spectrometer (Applied Biosystems, Vic, Australia). Positive ions were generated by electrospray and the QStar operated in information-dependent acquisition mode (IDA). A TOF-MS survey scan was acquired (m/z 350-1700, 1 s). The 2 largest multiply charged ions (counts > 15) were sequentially selected by Q1 for tandem mass spectrometry (MS/MS) analysis. Nitrogen was used as collision gas and an optimum collision energy chosen (based on charge state and mass). MS/MS spectra were accumulated for 2.5 s (m/z 65-2000) with up to two repeat spectra before dynamic exclusion for 45 s.

Peak lists were generated using Mascot Distiller (Matrix Science, MA, USA) using the default parameters, and submitted to the database search program Mascot (version 2.2, Matrix Science). Manual inspection identified Cys-containing peptides with additions of m/z +30 and +46 Da and modifications containing these mass additions created, added to the Mascot server and searches repeated. Search parameters were: precursor and product ion tolerances of ± 0.25 and 0.2 Da respectively; Met(O), Cys-carboxyamidomethylation, sulfenic, sulfinic acid, oxathiazolidine-oxide +30, oxathiazolidine-dioxide +46. After appropriate training by A/Prof. Mark Raftery, protein modifications including Met-sulfone, di-tyrosine, chlorotyrosine derivatives, carbonylation of Lys, Pro, Arg, Thr, bromination of Lys, His, Arg, Asn and Gln residues and oxidation (addition of oxygen, +16 Da) of His and Trp (for analysis of recS100A8 and recS100A9 protein only) were analyzed as variable modifications to assist in characterizing other oxidation products that could potentially form cross-linked structures. Analysis of chloramines was not performed; these modifications are relatively unstable and chloramine formation was not observed after ESI-MS analysis. Some samples were run using an LTQ FT Ultra as described [933]. Weaker or poorer quality data were obtained from less abundant samples, but the spectra were consistent with the formation of the unusual adducts. This data was obtained from samples where the enzyme used was not specified. Non-specified enzyme searches were used to characterize peptide fragments that may have formed independently of enzyme specific cleavage. Oxidant scavenging potential of S100A8 and S100A9 *in vitro* and *in vivo* was based on generation of oxidation products (identified by MS spectra of peptides) using different molar ratios of oxidants:S100 proteins. For S100A8, a Cys_{42}-Ala_{42} mutant preparation subjected to the same treatments confirmed oxidant-scavenging activity and provided proof-of-concept.

CHAPTER 3: OXIDATION OF S100A8 AND S100A9 BY HYPOHALOUS ACIDS

3.1 INTRODUCTION

MPO and EPO are mammalian heme peroxidase enzymes that play a role in a wide range of human pathologies [934]. The bactericidal activity of leukocytes is attributed to MPO [934] and EPO. MPO is released by activated neutrophils from intracellular granules and accounts for 5% of their dry mass [935]. MPO is present in smaller amounts in monocytes and tissue macrophages [936].

EPO is released by activated eosinophils [920]. It is the major granule protein of eosinophils, specialized phagocytic cells that play a role in elimination of parasites and related organisms [937]. Neutrophils phagocytose target organisms then release MPO into phagolysosomal compartments. In contrast, eosinophils exocytose granule contents onto the surface to which they are attached, for example, parasites. EPO has ~70% amino acid homology with MPO and these share many structural similarities. They are both cationic enzymes with a modified iron protoporphyrin IX heme active site [938]. The heavy and light chains of EPO are also analogous to MPO [939]. Not surprisingly, MPO and EPO occupy adjacent positions on chromosome 17 and have similar intron-exon structures, suggesting that they were derived from a common ancestor [940].

Activation of phagocytes is a vital process in the immune response to invading pathogens. Activation promotes assembly of the NOX2 enzyme complex at the plasma membrane (see Section 1.4.1.2, Chapter 1). A subsequent respiratory burst ensues, resulting in reduction of O_2 to a superoxide radical, $O_2^{\cdot-}$ [934]. The oxygen radical is then catalyzed by SOD to H_2O_2. Enzymatic reactions between MPO, H_2O_2 and halides (Cl^-, Br^-, I^-) or pseudohalide (SCN^-) ions generate hypohalous acids: HOCl, HOBr, hypoiodous acid (HOI), and hypothiocyanous acid (HOSCN) [714, 941]. These oxidants are widely believed to be responsible for the antibactericidal activity of neutrophils.

The ROS generated not only promote antibactericidal activity, but are vital in regulating signalling pathways in host defense (see Section 1.4.1.5, Chapter 1), signal transduction and mediating Ca^{2+} signalling in vascular pathophysiology [728, 729]. ROS are also implicated in the regulation of tyrosine kinases, protein tyrosine phosphatases and tyrosine phosphorylation-dependent pathways involved in antimicrobial and host defense in leukocytes [731, 732].

Apart from their antibactericidal properties (see Section 1.4.1.5), HOCl and HOBr can interact with proteins to generate several products. HOCl oxidation of Cys residues generates several post-translational modifications, for example sulfonic acid, via sulfenic and sulfinic acid intermediates [942], or disulfide linked complexes when a second Cys residue is present [943, 944]. Sulfenyl chloride intermediates can produce further oxidation products, for example sulfenamide, sulfinamide and sulfonamides [904] by interactions with nitrogen centres. In contrast, oxidation of Met is less complex and Met sulfoxide is the principle oxidation product [943].

Less stable products, such as mono- and di-chloroamines, can be produced by HOCl, particularly on Lys side chains or terminal α-amino groups; chloroamines situated at an α-amino site decompose to form aldehydes [945]. Lys-derived chloroamines can form inter- or intra-molecular cross-links after undergoing hydrolysis to aldehydes [946, 947]. His residues can also form HOCl-mediated aggregates (reviewed in [948]). HOCl also causes DTT-resistant protein aggregation (for example fibronectin [949]) and fragmentation after backbone chloramides undergo hydrolysis [950, 951].

HOBr brominates aromatic amino acid residues in proteins, such as 3-bromotyrosine and 3,5-dibromotyrosine [918, 952-954]; minor products such as protein carbonyls, di-tyrosine and 3,4-dihydroxyphenylalanine (DOPA) such as observed in BSA can also form [760]. Amino acid side chains are more reactive than backbone amide groups; Cys, Met, Trp, His, Tyr and Lys side-chains and cystine residues are the most reactive [922]. As with HOCl, increasing amounts of HOBr cause protein fragmentation and aggregation in some proteins [760].

However, excessive ROS contribute to the pathogenesis of chronic inflammatory diseases (Section 1.4.1.7). Anti-oxidant defense systems, such as SOD and peroxiredoxins, thioredoxin and glutaredoxin counter over-production of ROS (Section 1.4.1.8), in particular superoxide and H_2O_2. Excess production of MPO-derived $HO^{\cdot}$, can be countered by several physiological anti-oxidants, including Vitamin C and E, uric acid, reduced glutathione and ubiquinone (reviewed in [955]), that reduce oxidation of available halides such as Cl^- and Br^-.

There is increasing evidence that S100 proteins may contribute to anti-oxidant defense (reviewed in [695]). S100A8 and S100A9 are abundantly expressed in neutrophils and induced in activated macrophages and other cells by inflammatory mediators (see Section 1.3.6.2, Chapter 1) [407, 411]. Both are increased in chronic

inflammatory lesions, such as in atherosclerotic plaque, rheumatoid synovium and inflamed bowel (see Section 1.3.3, Chapter 1). We propose that one function of these proteins is to control excessive oxidation induced by hypohalous acids released from activated phagocytes.

Met and Cys residues are highly conserved within S100 homologues. Met residues are present in all S100s (except S100A12) and the Cys residue is only absent in three (S100A12, S100A13 and calbindin) [3]. mS100A8 has three such residues – $Met_{37/74}$ and Cys_{42} and hS100A8 has two, Met_{78} and Cys_{42}. Both proteins have a Met residue at position 1, but this is not present in recombinant protein [927]. mS100A8 is very sensitive to oxidation; low levels of HOCl (40 μM) converted 70-80% to the disulfide-linked homodimer. The homodimer was also identified in lung lavage fluid from mice treated with LPS [605]. MS analysis of HOCl-oxidized mS1008 identified Met sulfoxides ($Met_{37/74}$) and novel, DTT resistant, inter- and intra-molecular sulfinamide bonds. Sulfinamide bond formation occurs between the thiol group in Cys_{42} and the ε-amine groups of Lys residues following formation of a sulfenic acid and/or sulfinyl chloride intermediate.

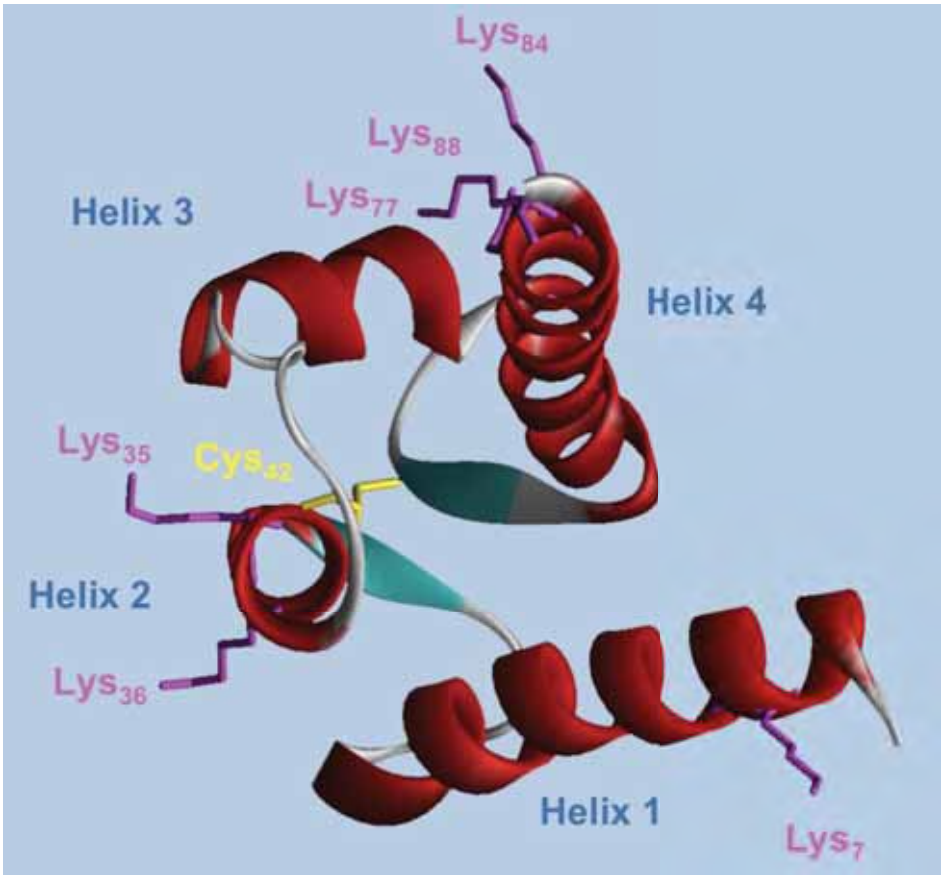

Figure 3.1: Ribbon diagram of mS100A8. 3D reconstruction of mS100A8 demonstrates the close proximity of $Lys_{35/36}$ to Cys_{42}, facilitating formation of sulfinamide bonds after oxidation by HOCl. $Lys_{7/88}$ are also implicated but these residues are distant to Cys_{42}, making sulfinamide bond formation less likey. Diagram was drawn using the PDB ProteinWorkshop v3.4.

$Lys_{35/36}$ are structurally most favourable for inter-chain sulfinamide cross-linking, although $Lys_{7/88}$ are implicated in inter-molecular cross-linking (Fig. 3.1) [606][2].

Recently our lab showed that S100A8 and S100A9 are targets for S-nitrosylation [613, 637]. S100A8 is preferentially nitrosylated in the S100A8/A9 complex. Unlike S100A8, S-nitrosylation of S100A9 is Ca^{2+}-dependent. S100A8 is found in normal human neutrophils, and S100A8-SNO increases after treatment of these cells with the NO-donor S-nitroso-*N*-acetylpenicillamine [613].

Met residues undergo a two-electron oxidation to Met sulfoxide (Met(O)). This can be reduced by Met(O) reductases, and may represent a mechanism whereby particular

[2] In this report rec-mS100A8 was used. rec-mS100A8 and rec-hS100A8 do not contain the first Met residue as it is removed by thrombin cleavage from the GST fusion protein [927]. However, in Chapter 4 we show that hS100A8 isolated from an *in vivo* source retains Met_1. To avoid confusion between *in vitro* and *in vivo* analysis, all subsequent amino acid sequences are analyzed assuming that Met_1 is retained.

functional Met residues are transiently deactivated by ROS [956]. $Met_{37/74}$ are readily oxidized to Met(O) in mS100A8, however, methionine oxidation of hS100A8 has not been characterized. mS100A9 has seven Met residues – $Met_{9/41/50/64/81/82/84}$, and three Cys residues – $Cys_{80/91/111}$. hS100A9 has five Met residues – $Met_{5/63/81/83/94}$ and a single Cys residue at position 3. Native mS100A9 has an intra-molecular disulfide bond between Cys_{80} and Cys_{91}; oxidation by HOCl does not promote disulfide or sulfinamide bond formation, at the free Cys_{111} [957][3]. Oxidative modifications of Met residues in mS100A9 have not been characterized, but higher mass monomers form with increasing amounts of HOCl, ranging from 14-16 kDa [605], indicating sequential, concentration-dependent Met oxidation. Interestingly, when low amounts of OCl^- are added to equimolar mixtures of mS100A8 and mS100A9 combined, only low levels of the disulfide-linked heterodimer were detected. In this case, S100A8 is predominantly oxidized to the 20 kDa homodimer and S100A9 is converted to a higher mass (~16 kDa), monomeric form [605].

In hS100A9, Cys_3 is not always present; full-length and truncated S100A9 is found in monocytes; in neutrophils full-length S100A9 comprises ~70% of S100A9 in cytosol [637]. Relative expression levels of these adduct would affect S100A9's susceptibility to oxidation, and possibly regulation of intracellular redox. Thus, each isoform may have distinct and common functions, particularly as Cys_3 is redox-reactive. Modifications indicate disulfide-linked S100A9 and Cys-sulfonic acid, Met(O) and an unusual Met-sulfone derivative [637] in cytosol from activated neutrophils, although functions are not characterized. Due to its abundance, Met oxidation of S100A9 in neutrophils may protect other proteins from modification following activation. Oxidation of Met(O) to Met-sulfone is rare and irreversible [958]; its generation is linked to the pathogenesis of Parkinson's and Alzheimer's disease [959].

S-nitrosoglutathione (GSNO) preferentially generates glutathionylated S100A9 (S100A9-GSH) [637], whereas it S-nitrosylates S100A8, suggesting roles in maintaining glutathione and NO following neutrophil activation [613].

Glutathionylation of S100A9 causes structural changes that increase surface hydrophobicity upon Zn^{2+}-binding, and reduce its ability to form non-covalent complexes with S100A8 [637]. S100A9 may be glutathionylated *in vivo*. S100A9-SSG was found in the cytosol of PMA-activated neutrophils and S100A9 and glutathione co-localized in

[3] In this report rec-mS100A9 was used. rec-mS100A9 and rec-hS100A9 do not contain the first Met residue as it is removed by thrombin cleavage from the GST fusion protein [927]. For consistency, all subsequent amino acid sequences are analyzed assuming that Met_1 is retained.

neutrophils particularly around phagosomes that had engulfed activated zymosan [637]. Thus, glutathionylation of S100A9, particularly following phagocyte activation may regulate intracellular redox processes and may maintain glutathione levels after an oxidative burst.

The aim of this study was to characterize modifications generated by HOCl using rec-hS100A8 and rec-hS100A9. HOBr-induced modifications to rec-hS100A8 were also characterized to compare the products, particularly as HOBr is generated in asthmatic lung by EPO from activated eosinophils. Characterization of putative modifications in tissue and/or samples from two sources known to contain high levels of calgranulins: human lung disorders [496] (Chapter 4) and human atheroma (Chapter 5) [410, 529] was performed to confirm oxidant scavenging in inflammation *in vivo*.

Here, we show that rec-hS100A8 and rec-hS100A9 readily form oxidized monomers and dimers after hypohalous acid oxidation. Novel adducts to S100A8 were identified after exposure to HOCl, but not HOBr, illustrating differences in hypohalous acid reactivity. However, sulfinamide bond formation, as occurs in rec-mS100A8, was not apparent in multimeric oxidized hS100A8 and further work is required to characterize mechanisms of covalent complex formation.

3.2 EXPERIMENTAL PROCEDURES

3.2.1 GENERATION OF HOBR-OXS100A8

For HOBr oxidation (1:1 or 1:10 molar ratios), OBr^- solutions were generated within 30 min of use by mixing equimolar amounts of OCl^- with Br^- at pH 9 in sterile, de-ionised water [804]. Because of HOBr/OBr^- instability, solutions were adjusted to pH 7.4 with HCl immediately before use; the p*K* of HOBr is 8.7, and at pH 7.4 is mostly HOBr [804]. All incubations were for 15 min on ice then L-Met (100 mM in PBS) added to quench oxidation. Products were eluted from C4-RP-HPLC (25-70% acetonitrile/water); oxS100A8 monomer eluted at 15.7 min. Peaks (0.5 μg) were separated by SDS-PAGE (100 mM DTT) and silver-stained (Section 2.1.3) to confirm separation of the oxidized monomer. Purified protein was stored under argon at -80°C to prevent generation of unwanted oxidation products (Section 2.1.5).

3.2.2 GENERATION OF OXCYS$_{42}$-ALA$_{42}$S100A8

To investigate the requirement for Cys_{42} on dimer formation in oxS100A8, the Cys_{42}-Ala_{42}S100A8 mutant was oxidized as described in Section 2.1.5, with one amendment; Cys_{42}-Ala_{42}S100A8 was separated by SDS-PAGE under non-reducing conditions and silver-stained to confirm the absence of dimer.

3.2.3 GENERATION OF MULTIMERIC OXS100A8 BY HOCl

To examine the nature of complexes generated by HOCl, S100A8 (10 μg) was lyophilized, suspended in 10 μl PBS and HOCl added in molar ratios of 1:1 or 1.5:1 (HOCl:S100A8) and incubated on ice for 15 min. A second preparation of 1:1 (HOCl:S100A8) was incubated for 30 min on ice to determine whether multimeric complexes increased. Equimolar amounts of L-Met (relative to HOCl) were then added to quench oxidation. Final preparations were divided into 5 μg aliquots, and 100 mM DTT (final concentration) added to one aliquot. Samples were immediately separated by SDS-PAGE and gels silver-stained (Section 2.1.3).

3.2.4 PEPTIDE GENERATION BY IN-GEL DIGESTION

To investigate oxidative modifications, S100A8 and oxS100A8 (4 μg, prepared with 100 mM DTT) were separated by SDS-PAGE and silver stained (Section 2.1.3).

Components separating at 10 kDa, 20 kDa or 30 kDa were excised and digested as described in Section 2.1.7. Digested samples were analyzed as described in Section 2.1.8.

3.2.5 PEPTIDE GENERATION BY IN-SOLUTION DIGESTION

Because conventional analysis of in-gel digests with trypsin was unsuccessful, the following protocol was developed to detect putative modifications generated in S100A8 and S100A9 *in vitro*. Recombinant oxS100A8 and oxS100A9 monomers and dimers were eluted from C4-RP-HPLC (25-70% acetonitrile/water); oxS100A8 monomer and dimer eluted at 14.4 min and 14.8 min, respectively; oxS100A9 monomer and dimer at 14.8 min and 15.7 min, respectively. Protein peaks (5 μg) were lyophilized, suspended in 20 mM NH_4HCO_3 (100 μl), digested for 4 hrs at 37°C with 50 ng AspN or trypsin and analyzed by MS (see Section 2.1.8, Chapter 2). AspN was chosen as a second enzyme to compare its effectiveness with trypsin in in-solution cleavage.

3.2.6 OXIDATION AND CHARACTERIZATION OF MULTIMERIC REC-OXS100A8

Enrichment of carotid artery samples by RP-HPLC and Western blotting with anti-oxS100A8 IgG confirmed the presence of multimeric oxS100A8 (Chapter 5), not seen in other biological samples (e.g. asthmatic sputum, see Chapter 4). Previous attempts to characterize post-translational oxidative modifications by in-gel digests had been troublesome (see Section 3.3.2). A new protocol was developed to increase peptide yield; 10 μg S100A8 was lyophilized with 10 μl PBS. Protein was suspended in MilliQ H_2O (10 μl) and HOCl added to a final molar ratio of 1:1.5 (S100A8:HOCl) then left on ice for 15 min, then DTT added to a final concentration of 200 μM and incubated for a further 5 min at 37°C. Then, iodoacetamide (final concentration 400 μM) was added for 5 min in the dark. SDS-PAGE loading buffer was added, samples heated for 3 min at 100°C, then immediately separated by SDS-PAGE. Gels were stained for 30 min with Coomassie solution (2.5% Brilliant Blue R (Sigma, MO, USA), 10% acetic acid, 40% methanol) then destained (40% methanol, 10% acetic acid) for 20 min. Destaining solution was removed and repeated until bands were optimal. Unoxidized native S100A8 migrated at 10 and 20 kDa; oxS100A8 contained three major bands at 10, 20 and 30 kDa. These were excised and digested as described in Section 3.2.4 and peptides analyzed as described in Section 2.1.8.

3.3 RESULTS

3.3.1 CHARACTERIZATION OF OXIDATION PRODUCTS OF S100A8

Conditions were established to generate oxidized monomeric and dimeric products from rec-hS100A8. The exquisite sensitivity of S100A8 with a 1:1 molar ratio of HOCl was indicated by changes in elution times. oxS100A8 eluted as two broad peaks at elution maxima 14.4 and 14.8 min (Fig. 3.2A, profile 2) from C4-RP-HPLC, which differed from S100A8 (Fig. 3.2A, profile 1) that eluted as a single peak after 13.5 min. Peaks 1 and 2 of oxS100A8[4] were silver-stained to indicate putative products after SDS-PAGE separation. Monomeric oxS100A8 was observed in peak 1 (14.4 min). Monomeric and dimeric oxS100A8 (resistant to reduction by DTT) eluted in peak 2 (elution time 14.8 min) (Fig. 3.2B) but monomeric S100A8 in this fraction could not be separated further. Complete resolution of the two forms was not achieved using C4-RP-HPLC using a range of gradients (not shown).

Oxidation of the Cys_{42}-Ala_{42}S100A8 mutant with a 1:1 molar ratio of HOCl did not alter its elution time from C4-RP-HPLC (not shown) and no dimer was obvious after SDS-PAGE and silver staining (Fig. 3.2C), indicating that dimer formation in native S100A8 after oxidation with HOCl may be dependent on Cys_{42} but may not be disulfide in nature.

Increasing HOCl concentrations generated multimeric complexes that were resistant to reduction, possibly by forming DTT-resistant inter-chain sulfinamide bonds such as occurs in rec-mS100A8 [606]. DTT-resistant complexes, defined in this thesis as covalent complexes with uncharacterized bonds, were generated (see Fig. 3.10, Section 3.3.4), confirming previous observations by McCormick *et al*. [410]. Doubling the time for oxidation did not enhance multimer levels suggesting that 15 min was sufficient to oxidize S100A8 with an equimolar amount of HOCl (not shown). Higher molar ratios of 2:1 (Fig. 3.2A, profile 3) HOCl:S100A8, produced aggregates (covalently-associated S100A8 of high molecular mass) that could not be resolved by C4-RP-HPLC.

HOBr appeared less reactive than HOCl; 1:1 molar ratios generated principally monomeric oxS100A8 with elution maximum at 15.1 min (Fig. 3.2D, profile 2), much

[4] In this section, abbreviations such as oxS100A8 denote those peaks collected from HOCl/HOBr-oxS100A8 after C4-RP-HPLC, and is not intended to indicate that confirmation of oxidation products was by inspection of RP-HPLC elution times. Confirmation of HOCl-modified Cys and Met residues in S100A8 are discussed in Sections 3.3.2 and 3.3.3. Hereafter, the term oxS100A8 denotes hypohalous-acid modified protein confirmed by MS analysis.

later than native S100A8 (13.5 min; Fig. 3.2D, profile 1) and this migrated as a single 10 kDa band in SDS-PAGE (Fig. 3.2E). A small peak with elution maximum at 15.6 min was observed, but was not characterized due to insufficient protein (Fig. 3.2D, profile 2), whereas 10-fold more HOBr promoted aggregation (Fig. 3.2D, profile 3).

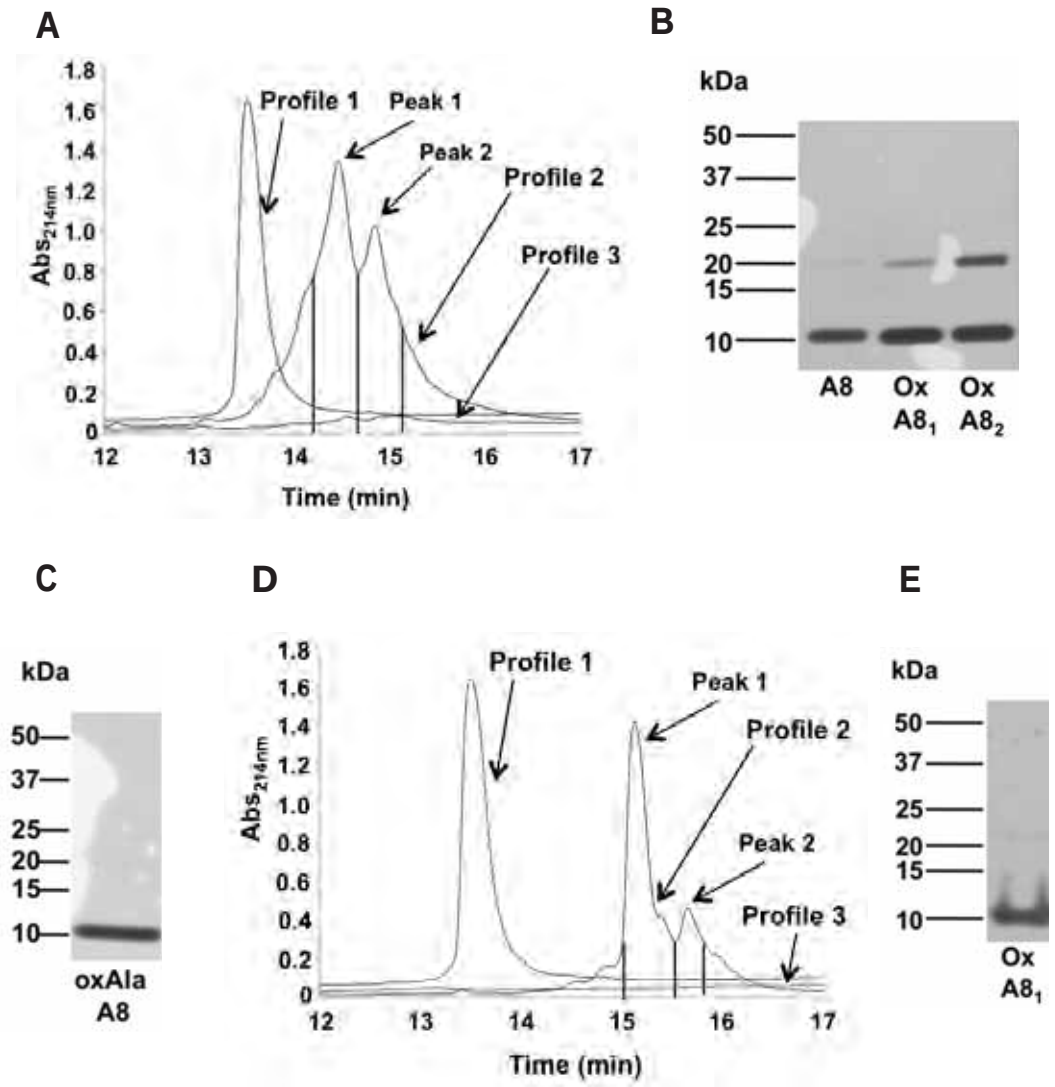

Figure 3.2: Hypohalous acids generate structural changes in rec-hS100A8 that alter RP-HPLC retention profiles. (**A**) 100 μg S100A8 eluted from C4-RP-HPLC at 13.5 min (profile 1). Profile 2 shows separation of S100A8 oxidized with an equimolar amount of HOCl. Two peaks eluted at 14.4 and 14.8 min. Profile 3 highlights the susceptibility of S100A8 to form aggregates using a 2:1 molar ratio of HOCl:S100A8 that could not be separated by C4 RP-HPLC. (**B**) SDS-PAGE separation (under reducing conditions) and silver staining of oxidized peaks confirmed that mostly monomeric S100A8 ($oxA8_1$) eluted at 14.4 min. Dimeric S100A8 ($oxA8_2$) also contained monomeric protein; this could not be separated further by C4-RP-HPLC. Unmodified S100A8 separated by SDS-PAGE was silver stained for comparative analysis. (**C**) Non-reducing SDS-PAGE indicated that a 1:1 ratio of HOCl:Cys_{42}-Ala_{42}S100A8 (oxAlaA8) did not generate dimer, suggesting that Cys_{42} was involved in dimer formation after exposure to HOCl. (**D**) Profile 1 shows 100 μg S100A8 eluting from C4-RP-HPLC at 13.5 min. S100A8 oxidized with HOBr:S100A8 (equimolar ratio) had a major peak with retention time 15.1 min, and a second minor peak at 15.6 min (profile 2). The minor peak eluting at 15.6 min contained insufficient protein and could not be characterized. Profile 3 shows that 10-fold more HOBr caused aggregation. (**E**) Silver staining of PAGE gels (run under reducing conditions) of HOBr-oxidized peak 1 (profile 2, 15.1 min) indicated mostly monomeric oxS100A8 ($oxA8_1$).

Deconvoluted mass analysis of unmodified recS100A8 showed a single, multiply-charged ion, as expected (Fig. 3.3A). Masses of monomeric (Fig. 3.2A, peak 1, profile 2) and dimeric (Fig. 3.2A, peak 2, profile 2; not protease cleavage products) S100A8 produced by HOCl were determined using ESI-MS and compared to theoretical values calculated from the derived cDNA sequence. These spectra showed several different series of multiply-charged ions, confirming the presence of oxidation products (Table 3.1 and Fig. 3.3B). In monomeric samples, mass additions of +48 Da (10,892 Da) were readily observed, and based on kinetic studies [960] were most probably Cys_{42}-sulfinic acid + Met(O) or Cys_{42}-sulfonic acid. Sulfinic acid adducts are intermediates in the formation of the more stable Cys_{42}-sulfonic acid oxidation product (reviewed in [948] and were not always evident as unique products. Other possible modifications included Met(O) (10,860 Da; +16 Da) and a m/z +64 modification; possibly a combination of Met(O) and Cys_{42}-sulfonic acid. A mass addition of m/z +80 was also observed, corresponding to addition of five oxygens. An unusual m/z +30 modification (10,874 Da; +30 Da) was identified, possibly corresponding to Cys_{42} and Met(O) oxidation products, but these were not plentiful and could not be characterized fully by MS. Monomeric oxS100A8 also contained small quantities of unmodified S100A8 indicating that the amounts of HOCl used in these experiments possibly represented mild oxidation of the recombinant protein.

Dimeric samples contained a mixture of monomeric and dimeric species, in agreement with products collected at 14.8 mins (Fig. 3.2A, peak 2, profile 2 and Fig. 3.2B). In dimeric oxS100A8, two unknown modifications of low abundance were observed, with mass additions of m/z +130 and +26.

A

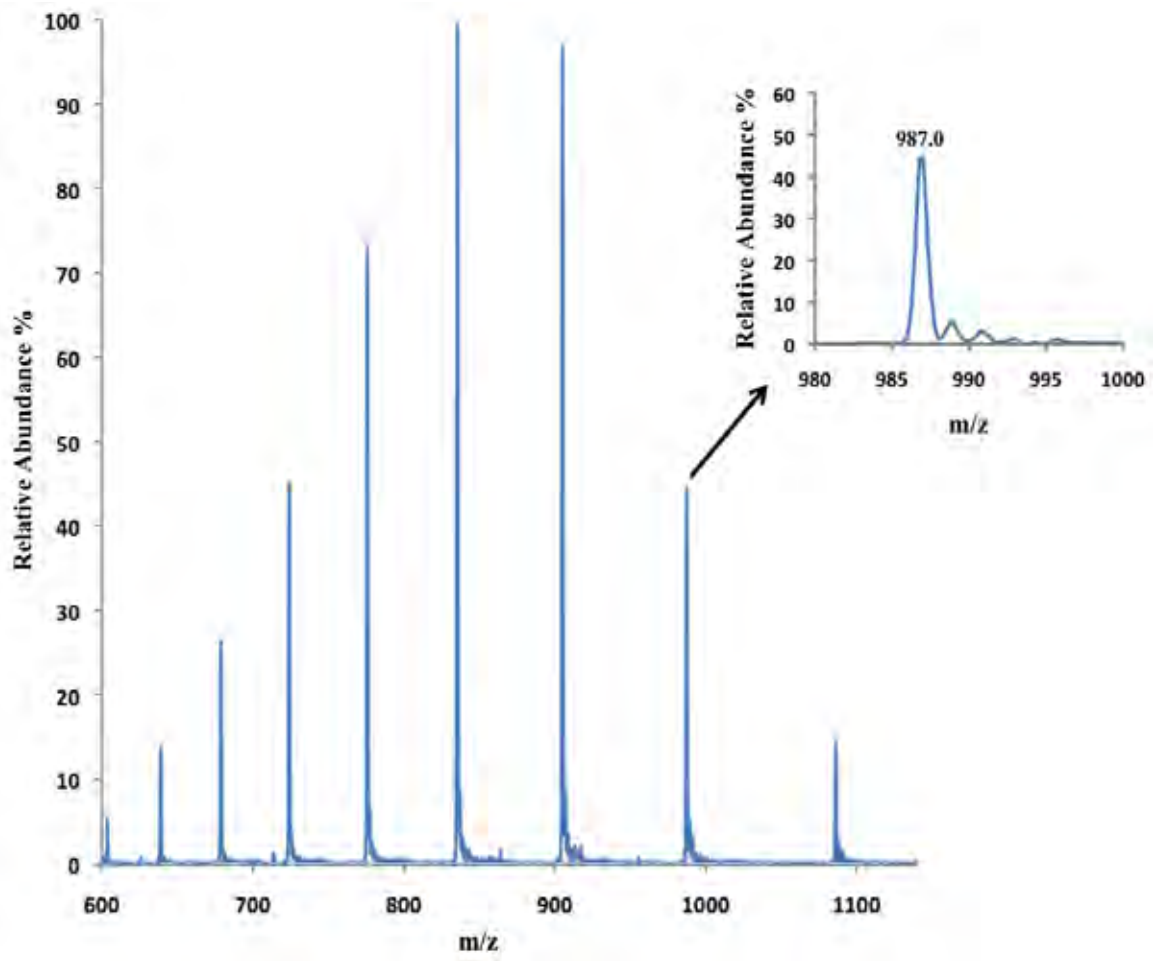

B

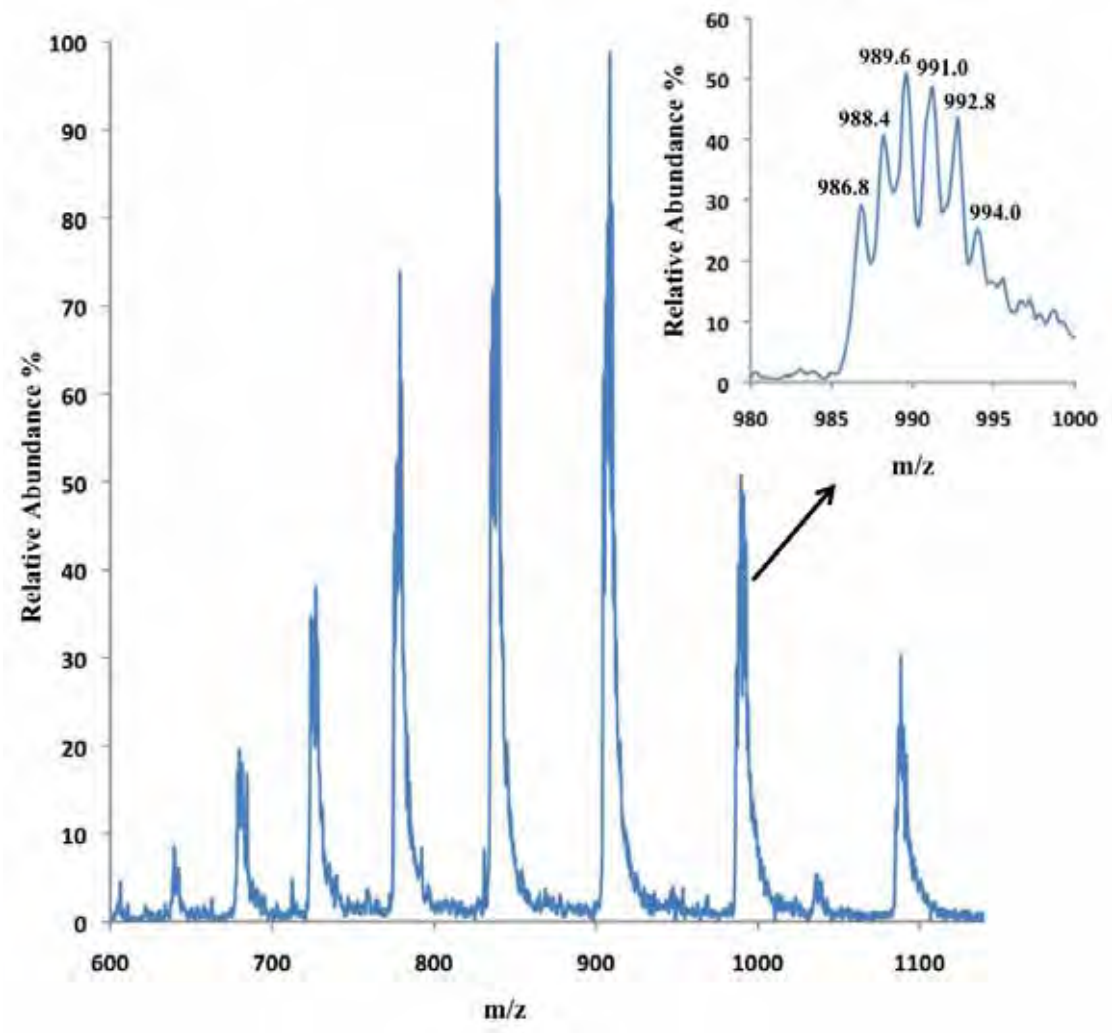

Figure 3.3: ESI-MS of unmodified and HOCl-modified S100A8. (**A**) ESI-MS of unmodified S100A8. ESI-MS of monomeric products collected after C18-RP-HPLC (equivalent to peak 1, profile 1, Fig. 3.2A) showed a single multiply-charged ion (insert is an expanded region around m/z 990 $[M+11H]^{11+}$ ions). This was S100A8 (m/z 987.0). (**B**) ESI-MS of S100A8 oxidation products. ESI-MS of monomeric oxidation products collected after C18-RP-HPLC (equivalent to peak 1, profile 2, Fig. 3.2A) showed a series of multiply-charged ions corresponding to S100A8. Insert is the expanded region around m/z 990 showing various oxS100A8 $[M+11H]^{11+}$ ions. These are: S100A8 (m/z 986.8), S100A8 + 16 (Met(O), m/z 988.4), S100A8 + 30 (Cys_{42}- and Met(O) oxidation products, m/z 989.6), S100A8 + 48 (sulfinic acid + Met(O) or

Table 3.1: Deconvoluted masses of recombinant HOCl-oxS100A8

Sample	Mass addition (Da)	Relative abundance (%)*	Possible modification
HOCl-oxS100A8 (monomer)	+48 (10,892 Da)	100	Cys_{42}-sulfinic acid and Met(O) or Cys_{42}-sulfonic acid
	+64 (10,908Da)	86.34	Met(O) and Cys_{42}-sulfonic acid
	+30 (10,874 Da)	78.43	Cys_{42}- and Met(O) oxidation products
	+16 (10,860Da)	77.76	Met(O)
	0 (10,844 Da)	60.74	Full length S100A8
	+80 (10,924 Da)	26.54	Addition of 5 oxygens
HOCl-oxS100A8 (dimer)	**Oxidized Monomer**		
	+48 (10,892 Da)	100	Cys_{42}-sulfinic acid and Met(O) or Cys_{42}-sulfonic acid
	+64 (10,908 Da)	66.45	Met(O) and Cys_{42}-sulfonic acid
	+30 (10,874 Da)	43.82	Cys_{42}- and Met(O) oxidation products
	0 (10,844 Da)	38.57	Full length S100A8
	+16 (10,860 Da)	33.93	Met(O)
	Oxidized Dimer		
	+64 (21,752 Da)	100	Met(O) and Cys_{42}-sulfonic acid
	+96 (21,784 Da)	86.42	Addition of 6 oxygens
	+48 (21,736 Da)	46.74	Cys_{42}-sulfinic acid and Met(O) or Cys_{42}-sulfonic acid
	+130 (21,818 Da)	34.94	Unknown modification
	+26 (21,714 Da)	34.30	Unknown modification

* Relative abundance of protein products is calculated by adding the integrated signals of contributing ions for each protein isoform in the ESI-MS. The most abundant signals/proteins are assigned 100%. All other ion signals are expressed as a percentage of this, and these measurements reflect an estimation of the relative abundance of isoforms in solution.

Due to the high abundance of Cys_{42}-sulfonic acid and Met(O) ions in monomeric samples (Fig. 3.3B), and the complexity of dimeric samples (Table 3.1), combined with the capabilities of the 1100 MSD mass spectrometer used to analyze intact protein masses, it was not possible to reliably identify all ions with small mass differences such as sulfinamides (m/z + 14) [606].

3.3.2 IN VITRO CHARACTERIZATION OF OXS100A8 BY IN-GEL DIGESTS

Only information on abundantly modified forms present in the oxidized sample was possible from SDS-PAGE and MS of the intact proteins. No information was obtained concerning the precise identities and locations of these modifications. SDS-PAGE separated proteins were digested with trypsin and the identities of modified peptides proposed from MS, MS/MS experiments, Mascot database searches and *de novo* sequencing. The major HOCl oxidation product of oxS100A8 was monomeric (elution time 14.1-14.6 min, 10 kDa) although this fraction contained a very small amount of dimer observed by SDS-PAGE, which could not be reduced by 100 mM DTT (20 kDa) (Fig. 3.2B). Both bands were excised and MS analysis of tryptic, in-gel digests showed little evidence of the oxidative modifications that were seen in ox-mS100A8 as described by Raftery *et al*. [606]. Spectra searched using Mascot included the Cys_{42} oxidation products sulfenic, sulfinic and sulfonic acids and sulfinamide as variable modifications. Bands migrating at 10 kDa only indicated sulfonic acid formation; an irreversible modification affecting the single Cys_{42} residue and corresponding to a mass addition of m/z +48 Da. The same modification was seen in the component migrating at 20 kDa, the dimer resistant to DTT reduction. This suggests formation of non-disulfide, Cys-dependent dimers.

Unoxidized S100A8 separated at 10 kDa and contained some Cys_{42}-sulfonic acid adducts, suggesting spontaneous oxidation during SDS-PAGE (Table 3.2). MS analysis is not quantitative, and estimation of relative amounts of sulfonic acid in native and oxidized samples is difficult, but because the elution time from C4-RP-HPLC differed from the oxidized products, and the sizes of the peaks were markedly different, we conclude that only minor amounts were oxidized in the native S100A8 preparation and oxidation products found in HOCl-treated samples were predominately generated by HOCl.

Table 3.2 Oxidative modifications in recombinant HOCl-oxS100A8 identified by MS after in-gel digest

Sample	Mass Addition (Da)	Modification
Native S100A8 (10 kDa)		
LLETECPQYIR	+48 (10,892 Da)	Cys_{42}-sulfonic acid
oxS100A8 (1:1) (10 kDa)		
LLETECPQYIR	+48 (10,892 Da)	Cys_{42}-sulfonic acid
oxS100A8 (1:1) (20 kDa)		
LLETECPQYIR	+48 (10,892 Da)	Cys_{42}-sulfonic acid

Because S100A8 had been stored under argon, and mass validation before the experiment confirmed the mass of the unmodified protein, these results suggest that the process of SDS-PAGE and/or of in-gel digestion was sufficient to partially oxidize unmodified S100A8. Another problem was that only a small number of peptides were identified by Mascot search and manual inspection, despite SDS-PAGE separation of 4 μg of protein from each peak collected after C4-RP-HPLC. To overcome some of these problems, all subsequent *in vitro* and *in vivo* analysis of oxidized S100 proteins was carried out using the in-solution method outlined in Section 3.2.5, in an attempt to increase the yield of oxidized S100 peptides for analysis.

3.3.3 NOVEL OXATHIAZOLIDINE-DIOXIDE MODIFICATIONS IN OXS100A8

Protein fractions were digested with trypsin or AspN to more precisely identify the sites and types of modifications present in S100A8 after HOCl treatment. AspN was used because this had facilitated characterization of the sulfinamide bond in mS100A8 [606]. Monomeric ox-hS100A8 (C4-RP-HPLC, Fig. 3.2A, profile 2, elution time 14.1-14.6 min) digested with AspN or trypsin yielded sufficient amounts of oxidized peptides for more complete analysis. Spectra were searched using Mascot, with mass tolerances of 0.25 for MS and 0.2 for MS/MS. Met(O), Cys_{42}-sulfenic acid (m/z +16), Cys_{42}-sulfinic acid (m/z +32), Cys_{42}-sulfonic acid (m/z +48) were specified as variable modifications. Three additional modifications, $+O\text{-}H_2$ (m/z +14) $+O_2\text{-}H_2$ (m/z +30) and $O_3\text{-}H_2$ (m/z +46), were added to the Mascot search program and included the possibility of neutral losses of SO_2 or SO_3.

Trypsin digestion of monomeric HOCl-oxS100A8 generated peptides with spectra containing the same Cys_{42}-sulfinic and -sulfonic acid modifications identified in the oxidized protein (Table 3.1). No evidence for inter-molecular sulfinamide bonds (m/z

+14) was found. On the other hand, many spectra contained the unusual mass addition of m/z +30 on Cys-containing peptides, originally observed in deconvoluted spectra (Fig. 3.3B). A second novel adduct, of m/z +46 Da not apparent in HOCl-oxidized mS100A8 was also identified.

Figures 3.4A-F show extracted ion chromatograms and masses of modified forms of LLETECPQYIR in tryptic digests and the time when MS/MS spectra were acquired. Comparisons of these MS/MS spectra with those of sulfinamide-containing murine peptides generated by similar methods [606] indicated different modifications for two reasons. Firstly, there were no Lys residues in several peptides analyzed, making sulfinamide formation, as described previously, impossible; secondly, prominent neutral losses of m/z -64 (corresponding to neutral loss of SO_2, from peptides with m/z +30 additions) and m/z -80 (corresponding to neutral loss of SO_3, from peptides with m/z +46 additions) were observed in MS/MS spectra of these ions. Based on the fragmentation pattern, the novel m/z +30 was denoted oxathiazolidine-oxide, and the m/z +46 addition defined as oxathiazolidine-dioxide. A possible reaction mechanism is discussed in Section 3.4.3.

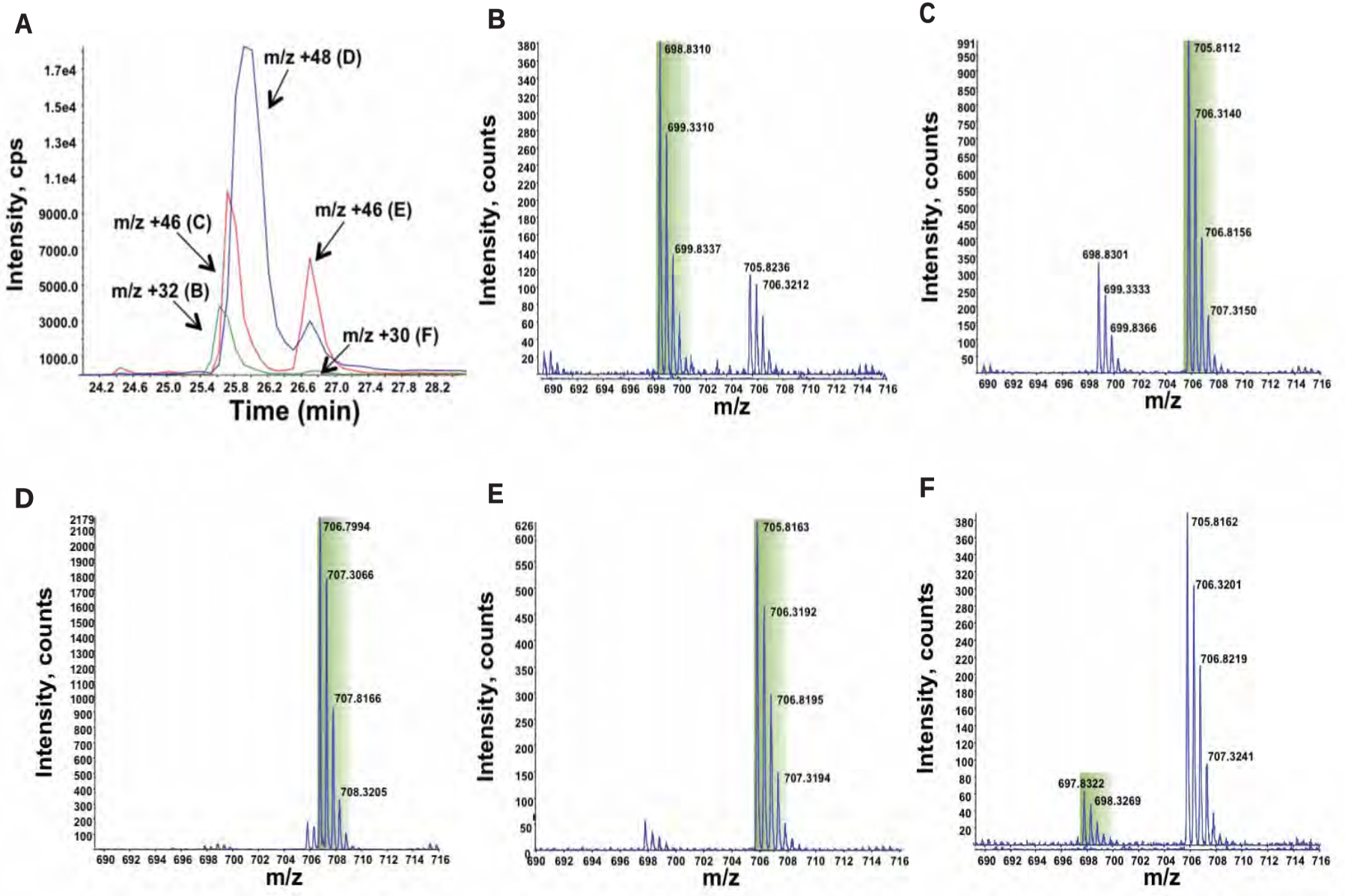
A
m/z +48 (D)
m/z +46 (C)
m/z +46 (E)
m/z +32 (B)
m/z +30 (F)
Intensity, cps
Time (min)
B
698.8310
699.3310
699.8337
705.8236
706.3212
Intensity, counts
m/z
C
705.8112
706.3140
706.8156
698.8301
699.3333
699.8366
707.3150
Intensity, counts
m/z
D
706.7994
707.3066
707.8166
708.3205
Intensity, counts
m/z
E
705.8163
706.3192
706.8195
707.3194
Intensity, counts
m/z
F
705.8162
706.3201
706.8219
707.3241
697.8322
698.3269
Intensity, counts
m/z

Figure 3.4: Extracted ion chromatograms and masses of modified forms of LLETECPQYIR. (**A**) Extraction ion chromatograms from nano-LC MS of $[M+2H]^{2+}$ ions of LLETECPQYIR modified by O_2-H_2 (+30), O_2 (+32), O_3-H_2 (+46), or O_3 (+48). Partial TOF-MS of individual precursor ions: (**B**) m/z +32, $+O_2$; (**C**) m/z +46, $+O_3$-H_2; (**D**) m/z +48, $+O_3$; (**E**) m/z +46, $+O_3$-H_2; (**F**) m/z +30, $+O_2$-H_2 at retention times indicated by arrows in (**A**). Two forms of m/z +46, O_3-H_2 were separated (TOF-MS shown in (**C**) and (**E**)) and these were attributed to isomeric oxathiazolidine-dioxides. Each modified form of S100A8 separated sufficiently well by nano-LC MS to ensure MS/MS selection of the desired precursor only (selection windows are shown as shaded colour boxes). The switch to MS/MS occurred early in the elution profile with a threshold of 10 counts. This also assisted in ensuring isolation of a single precursor ion m/z.

MS/MS of oxS100A8 trypsin-derived peptide LLETECPQYIR was performed as illustrated in the extracted ion chromatograms from sample; Fig. 3.4A, B, D. Although a definitive assignment of Cys modifications was not possible, the oxidation products observed most likely correspond to Cys_{42}-sulfinic acid and Cys_{42}-sulfonic acid. When Pro is present in a peptide sequence, fragmentations adjacent to Pro predominate. N-terminal peptide cleavage results in preferential formation of an abundant y-ion on this residue [961], demonstrated by intense fragment abundance on Pro_{43} (labelled as ion y_5; Figure 3.5A, B). The same approach was used to confirm the presence of the novel +30 and +46 mass additions as these were observed only in ions that contained the Cys residue (Fig. 3.6A, B) observed in Fig. 3.4A, C, E, F.

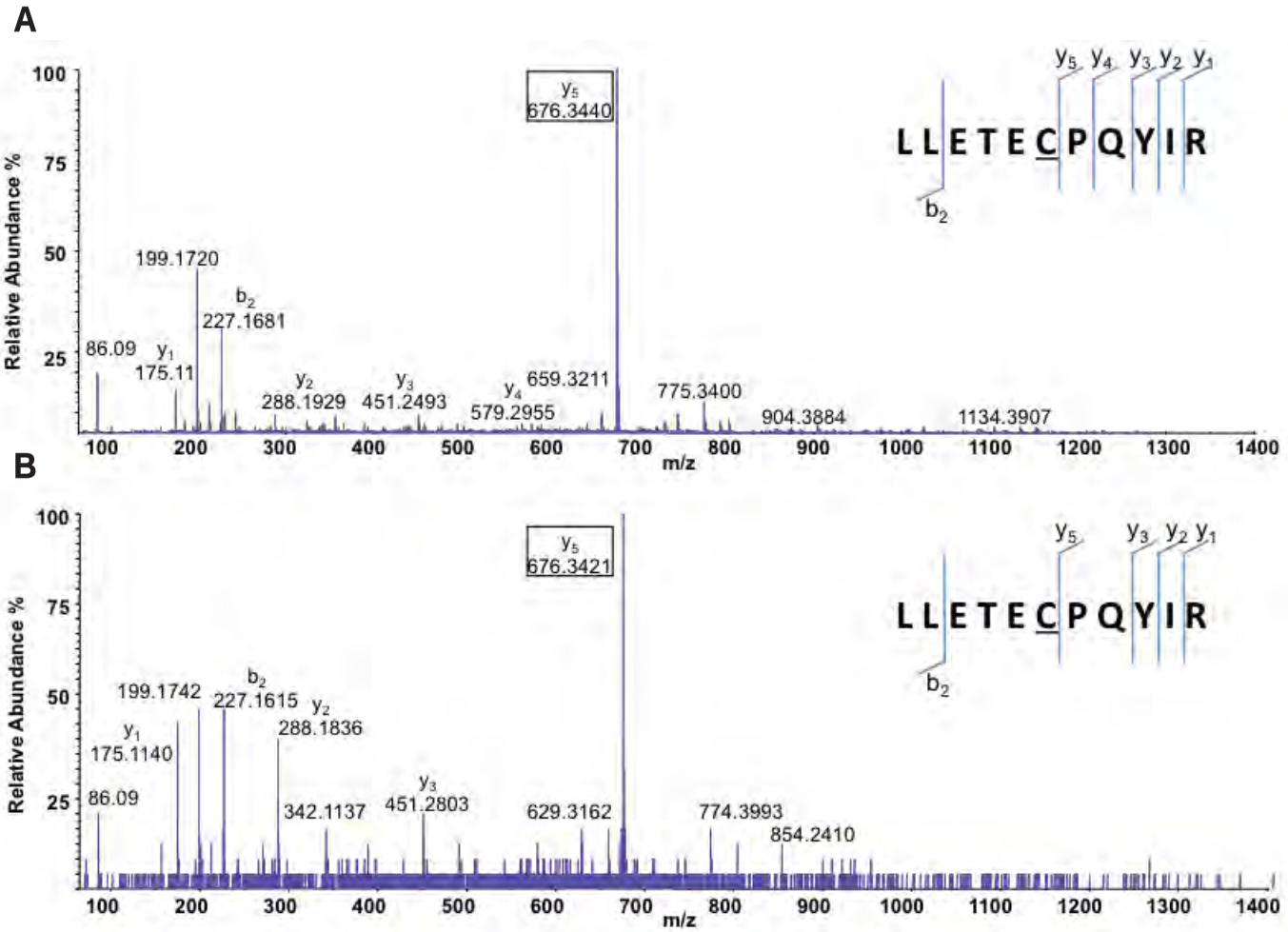

Figure 3.5: Annotated MS/MS of modified S100A8 tryptic peptides of LLETECPQYIR. (A) MS/MS of $S100A8_{37\text{-}47}$ most likely containing a m/z +32 addition (Cys_{42}-sulfinic acid) at retention time = 25.08 (as calculated by nano-LC MS). **(B)** MS/MS of $S100A8_{37\text{-}47}$ containing a probable m/z +48 addition (Cys_{42}-sulfonic acid). Sequence-specific ions are labelled and an intense fragment ion y_5 was observed on Pro_{43} (highlighted in box), as expected.

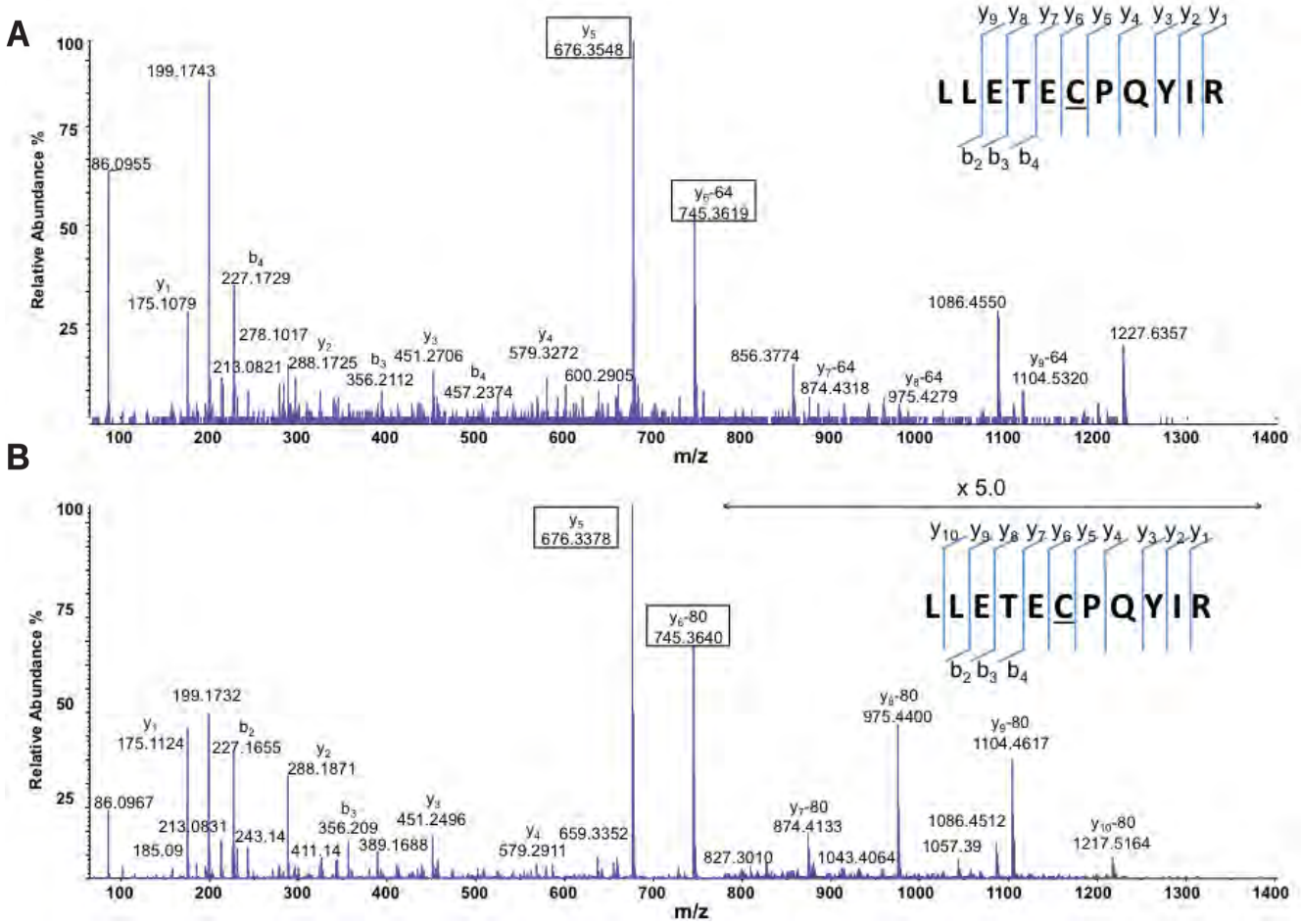

Figure 3.6: Annotated MS/MS of modified S100A8 tryptic peptides of LLETECPQYIR. (**A**) MS/MS of $A8_{37-47}$ containing a m/z +30 addition (retention time = 25.808 min, as calculated by nano-LC MS). (**B**) MS/MS of $A8_{37-44}$ containing a m/z +46 addition (retention time = 26.74 min, as calculated by nano-LC MS) and corresponding to the second eluting peak (a very similar MS/MS spectrum was recorded for $[M+2H]^{2+}$ ions eluting at 25.67 min, as calculated by nano-LC MS). Sequence-specific ions are labelled. Intense fragment ion y_5 (Pro residue; shown in box) are observed, as expected. Only ions containing Cys show loss of m/z -64 or -80 (shown in box).

MS/MS of the modified S100A8 AspN-derived peptide DDLKKLLETECPQYIRKKGA indicated a potential Cys_{42}-sulfinic acid modification (Fig. 3.7A); an intense fragment on Cys_{42} (labelled as ion y_{10}) identified in peptides containing Cys_{42}-sulfonic acid (Fig. 3.7B) and the novel +46 mass addition (Fig. 3.7C, D). The latter was also observed in the peptide ETECPQYIRKKGA (Fig. 3.8). The novel +30 mass addition was not obvious in AspN digests, possibly because of the lower abundance of this modification.

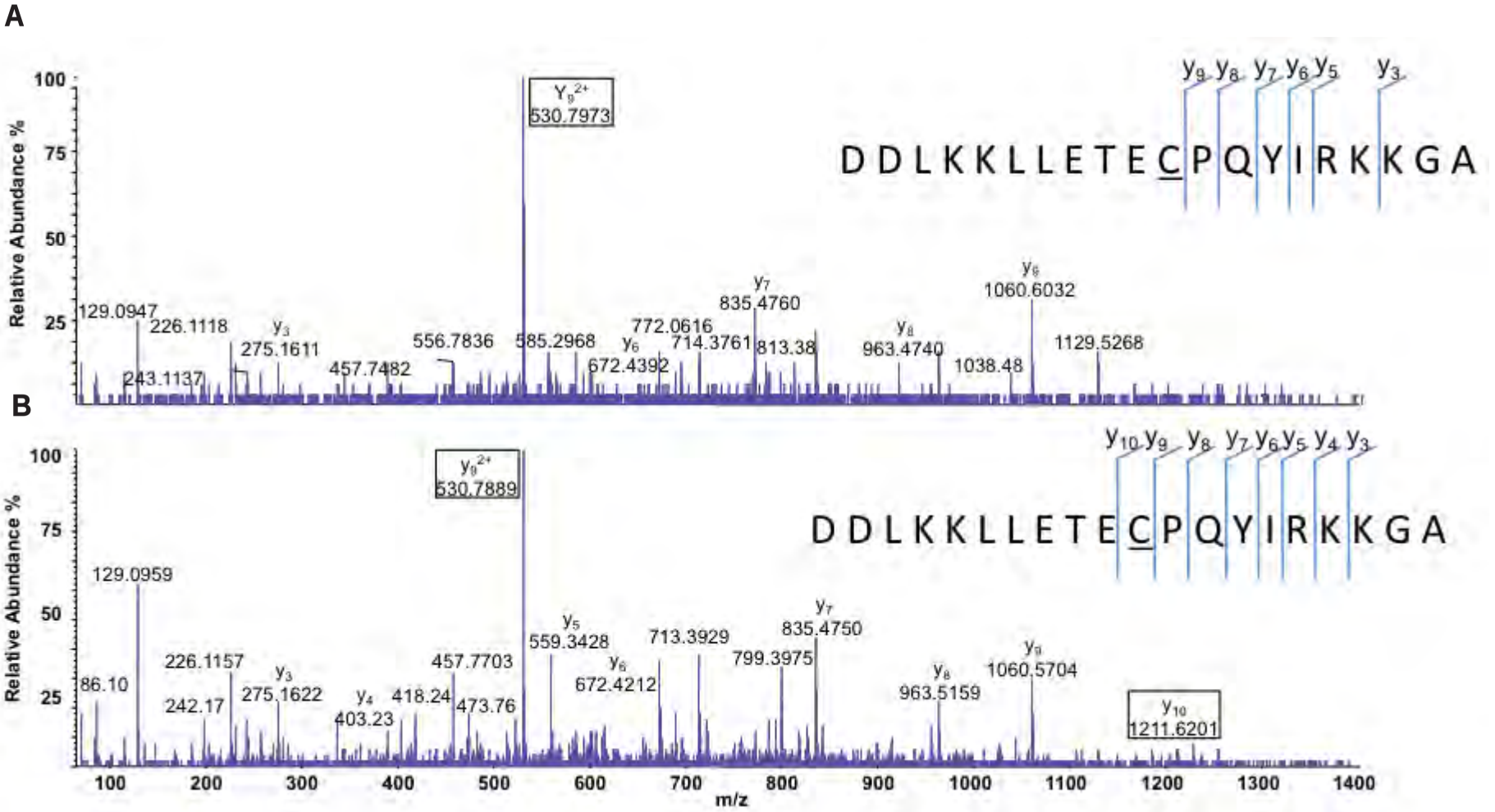
A
Relative Abundance %
100
75
50
25
Y_9^{2+}
530.7973
y_9 y_8 y_7 y_6 y_5 y_3
D D L K K L L E T E C P Q Y I R K K G A
129.0947
226.1118
y_3
275.1611
243.1137
457.7482
556.7836
585.2968
y_6
672.4392
772.0616
714.3761
y_7
835.4760
813.38
y_8
963.4740
1038.48
y_9
1060.6032
1129.5268
B
Relative Abundance %
100
75
50
25
y_9^{2+}
530.7889
y_{10} y_9 y_8 y_7 y_6 y_5 y_4 y_3
D D L K K L L E T E C P Q Y I R K K G A
129.0959
86.10
226.1157
242.17
y_3
275.1622
y_4
403.23
418.24
457.7703
473.76
y_5
559.3428
y_6
672.4212
713.3929
y_7
835.4750
799.3975
y_8
963.5159
y_9
1060.5704
y_{10}
1211.6201
100 200 300 400 500 600 700 800 900 1000 1100 1200 1300 1400
m/z

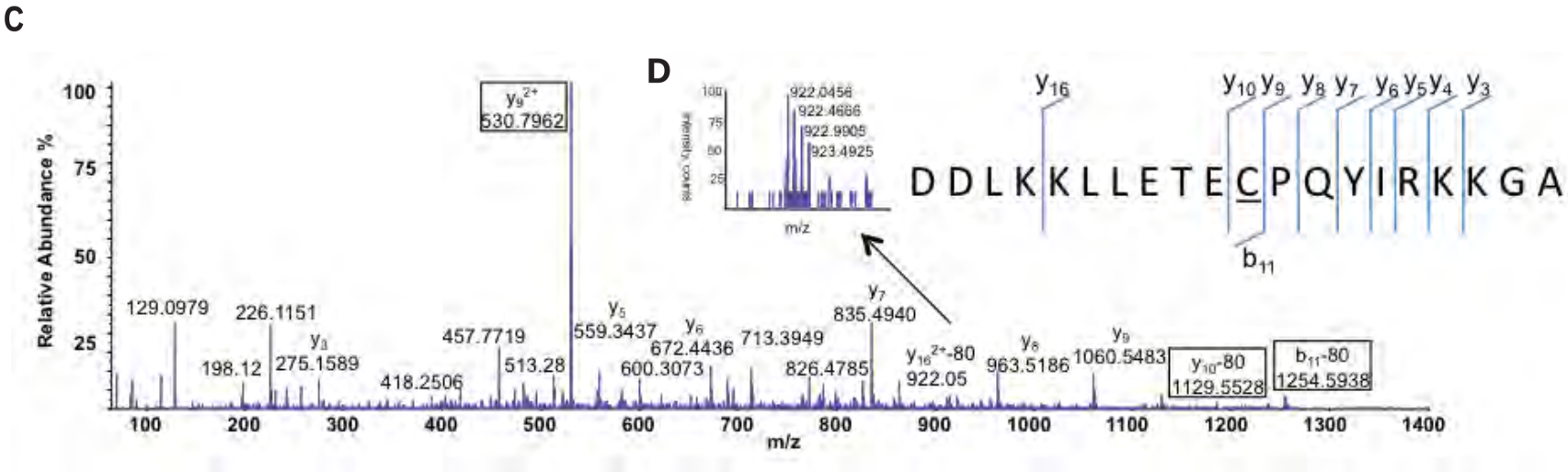

Figure 3.7: Annotated MS/MS of modified S100A8 AspN digest peptides. (**A**) MS/MS of $A8_{32-51}$ containing a m/z +32 addition. (**B**) MS/MS of $A8_{32-51}$ containing a m/z +48 addition (identified as y_{10}; shown in box). (**C**) MS/MS of $A8_{32-51}$ containing a m/z +46 addition (identified as b_{11} and y_{10} -80 ion; shown in box). Sequence-specific ions are labelled. Intense fragment ion y_9^{2+} (Pro residue, m/z 530.7962, shown in box) observed, as expected. (**D**) Identity of $[M+2H]^{2+}$ as y_{16}-80 ion confirmed by m/z 0.5 separation between isotopes.

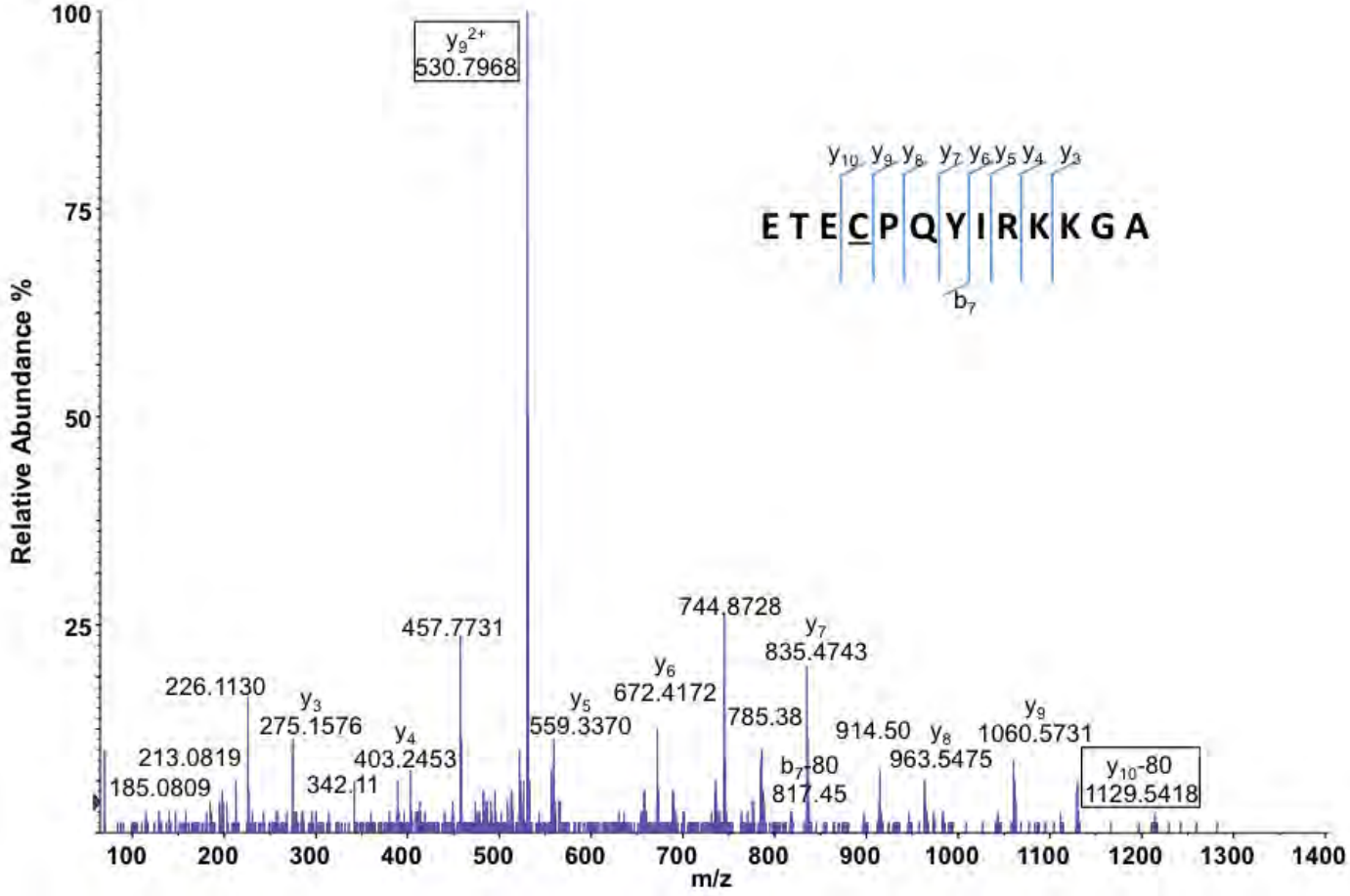

Figure 3.8: Annotated MS/MS of modified S100A8 AspN digest peptide. MS/MS of $A8_{39\text{-}51}$ containing a m/z +46 addition and sequence specific ions are labelled. Intense fragment ion y_9^{2+} at m/z 530.7968 (Pro residue, shown in box) observed as expected. The series of ions allows almost complete sequencing with only ions containing Cys_{42} showing loss of m/z -80 (at m/z 1129.5418, shown in box).

Post-translational modifications observed in dimeric oxS100A8 samples were difficult to identify precisely. No indication of sulfinamide bond formation was observed, suggesting that sulfinamide-dependent dimer formation was unlikely. No modifications were identified within the peptide digest samples corresponding to the unusual mass additions observed in the dimer (+26 [21,714 Da] and +130 [21,818Da]; Table 3.1) and these samples were not characterized further.

An attempt was made to identify other possible modifications generated by HOCl, using Mascot searches selecting the following modifications, and performing variable modification searches (Met(O)/sulfone, di-tyrosine, chlorotyrosine derivatives, carbonylation of Lys, Pro, Arg, Thr, oxidation of His and Trp to His(+16) or Trp(+16) (corresponding to addition of one oxygen) and (for HOBr specifically), bromination of Lys, His, Arg, Asn and Gln residues. Modifications were selected based on their presence in proteins oxidized by ROS (Section 1.4.2.2) and because no prior examination of these products had been performed in our studies.

Oxidation of Met_{78} to Met_{78}(O) was obvious in peaks eluting at 14.4 and 14.8 min by C4-RP-HPLC after AspN digest. Trypsin digests identified only one peptide ($S100A8_{78-85}$) suggesting some oxidation of Met_{78} to Met_{78}-sulfone (Mowse score[962]: 65)[5], an irreversible modification. Despite identification of several Tyr-containing peptides, only one ($S100A8_{7-18}$) indicated chlorination of Tyr_{16} to 3-chloroTyr (Mowse score: 35). These modifications were only found in monomeric samples, suggesting that they did not contribute to dimer formation. Analaysis of His and Trp in these samples was complicated by a lack of Trp containing peptides, however, in these samples there was no evidence for His oxidation.

[5] The Mowse score is a similarity score that calculates the probably of matching "N" peaks by random chance. It is a scoring method that provides higher scores when there are more matched peaks. Conversely, low scores indicate few matched peaks [962].

Several Tyr-containing peptides were identified in AspN digests of monomeric and dimeric oxS100A8. Oxidation of Tyr_{19} to 3-chlorotyrosine was apparent in one peptide ($S100A8_{14-31}$) (Mowse score: 20), indicating a weak spectrum; there was no evidence that this modification was present in the oxidized dimer. Met_{78}-sulfone was not apparent in the oxS100A8 monomer or dimer digests. Taken together, the relative abundance of these modifications was much less compared to the amounts of novel oxathiazoldine adducts identified on Cys_{42}, suggesting that even under favourable conditions, oxidative modifications to Tyr residues, or oxidation of Met_{78}(O) to Met_{78}-sulfone are less favourable compared to oxidation of Cys or Met_{78}. No carbonyl-adducts were observed in any Mascot searches from any spectra.

There was evidence for addition of one oxygen on the single Trp residue at position 54 and $His_{17/27}$ in monomeric oxS100A8. Similar products were observed in the oxidized dimer. Additional Mascot searches were performed using the same data because some non-specific peptide-bond cleavages were observed. Non-enzyme specified searches indicated addition of one oxygen to His_{83} in monomeric and dimeric samples.

HOBr was a less efficient oxidant than HOCl; deconvoluted masses of monomeric S100A8 oxidized with HOBr (1:1, HOBr:S100A8) only showed two adducts, which, based on kinetic studies [922], likely correspond to Met(O) or Trp_{54}(+16) (10,860 Da, +16 Da) and Met(O)/Trp_{54}(+16) and Cys_{42}-sulfinic acid or Cys_{42}-sulfonic acid (10,892 Da, +48 Da; Fig. 3.9 and Table 3.3). Protein amounts of oxS100A8, derived after treatment with a 10 molar excess of HOBr, were insufficient to allow analysis of deconvoluted masses and amounts ranging from 1:1 – 1:5 S100A8:HOBr may be required to assess changes.

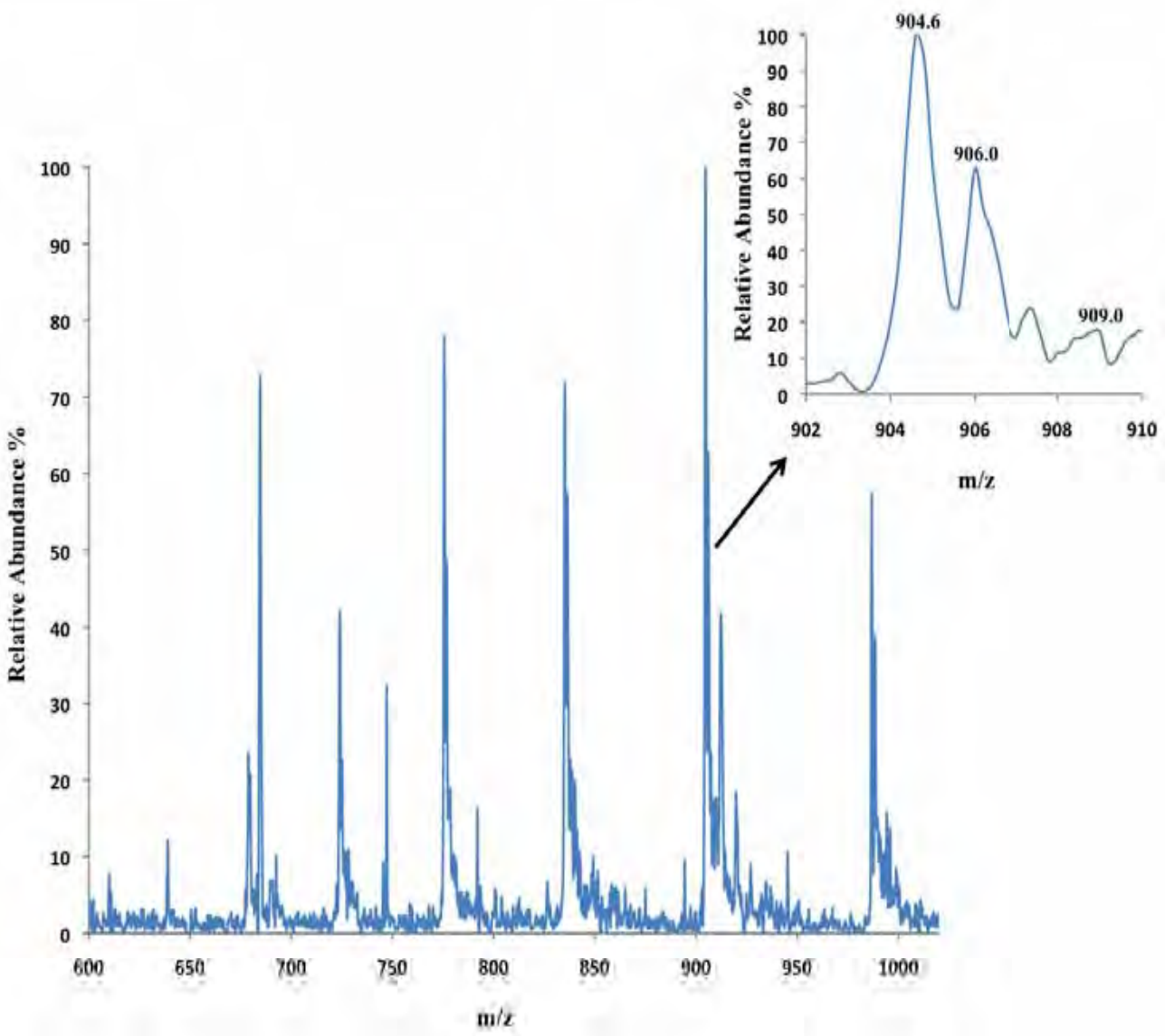

Figure 3.9: ESI-MS of HOBr-oxS100A8 products. ESI-MS of oxidation products collected after C18-RP-HPLC (equivalent to peak 1, profile 2, Fig. 3.2D) showed a series of multiply-charged ions. Insert shows expanded region around m/z 906 and shows various oxS100A8 $[M+12H]^{12+}$ ions. These are: S100A8 (m/z 904.6), S100A8+16 (met(O)/Trp_{54}(+16), m/z 906.0), S100A8+48 (sulfinic acid + Met(O)/Trp_{54}(+16) or sulfonic acid, m/z 909.0). The mass accuracy and resolution of the 1100 MSD was insufficient to identify ions with other mass differences, in the presence of these abundant ions.

Table 3.3: Deconvoluted masses of recombinant HOBr-oxS100A8

Sample	Mass addition (Da)	Relative abundance (%)	Possible modification
HOBr-oxidized S100A8 (monomer)	0 (10,844 Da) +16 (10,860 Da) +48 (10,892Da)	100 69.43 19.67	Full length S100A8 Met(O)/ Trp_{54}(+16) Met(O)/ Trp_{54}(+16) and Cys_{42}-sulfinic acid or Cys_{42}-sulfonic acid

MS/MS analysis identified sulfonic acid intermediates and Trp_{54}(+16) residue in AspN digests of the oxS100A8 monomer (peak 1, profile 2, Figure 3.2D). A summary of the major products identified in HOCl- and HOBr-oxS100A8 peptides is given in Table 3.4.

Table 3.4: Summary of major oxidative modifications in rec-oxS100A8 identified by MS

Sample	Mass addition (Da)	Modification
HOCl-oxidized S100A8 (1:1)		
AspN digest		
DDLKKLLETE<u>C</u>PQYIRKKGA	+32 (10,876 Da)	Cys_{42}-sulfinic acid
ETE<u>C</u>PQYIRKKGA		
DDLKKLLETE<u>C</u>PQYIRKKGA	+48 (10,892 Da)	Cys_{42}-sulfonic acid
ETE<u>C</u>PQYIRKKGA		
DDLKKLLETE<u>C</u>PQYIRKKGA	+46 (10,890 Da)	Cys_{42}-oxathiazolide-dioxide
ETE<u>C</u>PQYIRKKGA		
EFLILVIK<u>M</u>GVAAHKKSHE	+16 (10,860 Da)	Met_{78}(O)
DV<u>W</u>FKEL	+16 (10,860 Da)	Trp_{54}(+16)
DVY<u>H</u>KYSLIKGNFHAVYR	+16 (10,860 Da)	His_{17}(+16)
DVYHKYSLIKGNF<u>H</u>AVYR	+16 (10,860 Da)	His_{27}(+16)
GVAA<u>H</u>KKSHEESHKE*	+16 (10,860 Da)	His_{83}(+16)
Trypsin digest		
LLETE<u>C</u>PQYIR	+30 (10,874 Da)	Cys_{42}-oxathiazolidine-oxide
	+46 (10,890 Da)	Cys_{42}-oxathiazolidine-dioxide
	+48 (10,892 Da)	Cys_{42}-sulfonic acid
HOBr-oxidized S100A8 (1:1)		
AspN digest		
ETE<u>C</u>PQYIRKKGA	+48 (10,892 Da)	Cys_{42}-sulfonic acid
DV<u>W</u>FKEL	+16 (10,860 Da)	Trp_{54}(+16)

TABLE 3.4: Modifications identified in peptides derived from recS100A8 oxidized with HOCl or HOBr at the molar ratios indicated. Oxidation products on Cys_{42} in S100A8 were identified in in-solution digests by peptide mapping and MS/MS; Oxathiazolidine-oxide (+30 m/z) and -dioxide, (+46 m/z) adducts were obvious, the former was only seen in tryptic peptides. The oxathiazolidine-dioxide derivative was plentiful in peptides from all HOCl-oxidized samples. Masses of modifications are indicated in parentheses, expressed in daltons (Da). Oxidized peptides marked with * indicate sequences identified in non-enzyme specified samples. Modifications observed in these peptides were consistent with modifications identified in enzyme-specified searches.

3.3.4 SULFINAMIDE CROSS-LINKS WERE NOT FOUND IN MULTIMERIC OXS100A8

We observed DTT-resistant bands in silver-stained SDS-PAGE of HOCl-oxS100A8. A variety of cross-links are possible, but no evidence for these was found using in-solution digests, and we attempted to characterize these components further. The dimer and trimer were analyzed because this cross-linking was typical of HOCl-oxS100A8 [410] but has not been characterized. To ensure only oligomers were isolated S100A8 was oxidized with HOCl (Section 3.2.6), and separated by SDS-PAGE under DTT-reducing conditions and then Coomassie-stained. An important difference between these experiments and our earlier attempts (Section 3.3.2) to characterize modified S100A8 from gels was the quantity of protein separated (10 μg) and the type of staining. Protein bands excised from Coomassie-stained PAGE gels showed more diverse modifications, compared to modifications observed in protein excised from silver-stained PAGE gels, most likely due to the increased amounts of digested sample analyzed, rather than increases in molar concentration of HOCl.

Native S100A8 separated predominantly as a monomer with lower amounts of oligomers. oxS100A8 migrated as monomer (10 kDa), dimer (20 kDa) and some trimer (30 kDa) (Fig. 3.10). Bands were excised as described in Section 3.2.4, digested with trypsin and peptides analyzed by MS.

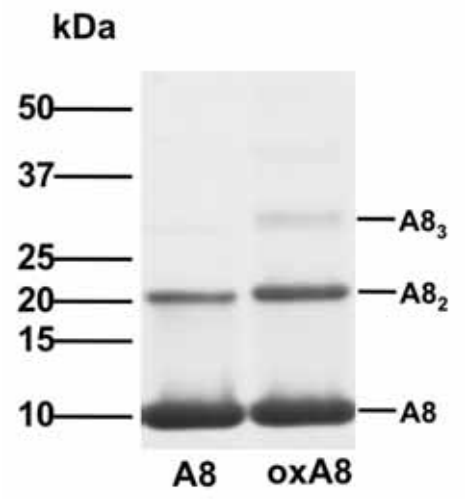

Figure 3.10: Formation of multimeric oxS100A8. Coomassie-stained S100A8 or oxS100A8 showed covalent complex formation following oxidation with HOCl (1:1.5 molar ratio of S100A8:HOCl). Native S100A8, under reducing conditions, migrated at 10 kDa; some dimer was obvious. When oxidized, S100A8 migrated at 10 kDa; dimers and trimers were obvious, indicating complexing, similar to that shown in Fig. 5.9B, C (Chapter 5) and previously reported [410].

Sulfonic acid in the peptide LLETECPQYIR ($S100A8_{37-47}$) was evident in the unoxidized S100A8 monomer, as was oxidation of Met_{78} to $Met_{78}(O)$ in 2/2 preparations. The peptide LLETECPQYIR ($S100A8_{37-47}$) was also identified in digests of the 20 kDa; the same Cys_{42}-sulfonic acid modification was observed in 2/2 preparations and Cys_{42}-

oxathiazolidine-dioxide was apparent in dimer digests of 1/2 preparations (Table 3.5). Cys_{42}-oxathiazoldine-dioxide observed in preparation 2 was unexpected in native preparations. The native S100A8 dimer contained Cys_{42}-oxathiazolidine-dioxide, and was separated in the lane adjacent to oxS100A8, and may have become contaminated during loading or excision of gel slices. There was no evidence for oxidation of His and Trp in native preparations. Notwithstanding, these results suggest that, as discussed in Section 3.3.2, the handling, separation and processes such as lyophilization may cause protein oxidation that is independent of oxidation caused by HOCl.

Table 3.5: Summary of oxidative modifications in native S100A8

Sample	Mass addition (Da)	Modification
Monomeric S100A8		
Preparation 1		
MGVAAHK	+16 (10,860 Da)	Met_{78}(O)
LLETECPQYIR	+48 (10,892 Da)	Cys_{42}-sulfonic acid
Preparation 2		
MGVAAHK	+16 (10,860 Da)	Met_{78}(O)
LLETECPQYIR	+48 (10,892 Da)	Cys_{42}-sulfonic acid
Dimeric S100A8		
Preparation 1		
LLETECPQYIR	+48 (10,892 Da)	Cys_{42}-sulfonic acid
Preparation 2		
LLETECPQYIR	+48 (10,892 Da)	Cys_{42}-sulfonic acid
LLETECPQYIRK		
LLETECPQYIR	+46 (10,890 Da)	Cys_{42}-oxathiazolidine-dioxide

Peptides derived from in-gel digests of native, unoxidized S100A8 treated with trypsin.

Following oxidation with HOCl the oxidized monomer migrated in a similar fashion to the native monomer. The peptide MGVAAHK ($S100A8_{78-84}$) from monomeric S100A8 contained Met_{78}(O) in 2/2 preparations, not consistently observed in oxS100A8 peptides derived from in-solution digests (Section 3.3.3). Cys_{42}-sulfonic acid, and the novel adduct Cys_{42}-oxathiazolidine-dioxide were observed in peptides from 2/2 preparations. Oxidation of Met_{78} to Met_{78}-sulfone was observed in 2/2 preparations (Mowse scores: 24 and 32 respectively), but only one peptide ($S100A8_{78-85}$) contained this modification indicating low abundance. Conversion of Tyr_{30} to 3-chlorotyrosine was apparent in peptides from 1/2 preparations (Mowse score: 38), in one peptide ($S100A8_{24-31}$), again indicating low abundance. No oxidation of $Tyr_{16/19}$ to 3-chlorotyrosine (see Section 3.3.3) was seen. Monomeric samples indicated oxidation of Trp_{54} and $His_{17/27}$ in 1/2 preparations; oxidation of Trp_{54} and His_{17} was indicated in another preparation. In the band migrating at 20 kDa and corresponding to oxS100A8 dimer, Cys_{42}-sulfonic acid and Cys_{42}-oxathiazolidine-dioxide-containing peptides were identified in 2/2 preparations, in peptide sequences that were identical to those from the oxidized monomer ($S100A8_{37-37}$ and $S100A8_{37-48}$, respectively). The trimer only generated peptides with Cys_{42}-sulfonic acid in one preparation, probably because of the low amount of material present in this band.

Results of all peptides with major modifications are summarized in Table 3.6. Free Cys residues were converted to Cys_{42}-carbamidomethyl, confirming reactivity of several free Cys residues with iodoacetamide. This again indicates that the complexes observed in gels were unlikely to be disulfide-linked. There was no evidence of protein carbonylation, or formation of di-tyrosine, modifications involved in cross-linking of some proteins. Formation of cross-linked oxS100A8 may be different to the Cys-Lys cross-linking typical of HOCl-oxidized mS100A8. Moreover, oxidized Trp and His residues were not found in dimeric and trimeric samples, but more work is required to elucidate the effect that oxidation of Trp and His residues in the monomer might have on formation of S100A8 dimers and higher mass covalent complexes. The presence of Cys_{42}-oxathiazolidine-dioxide in oxidized dimer suggests that dimer formation may be due to intra-molecular Cys_{42}-oxathiazolidine-dioxide formation. This possibility requires further characterization.

Table 3.6: Summary of major oxidative modifications in HOCl-oxS100A8 oligomers

Sample	Mass addition (Da)	Modification
Monomeric oxS100A8		
Preparation 1		
MGVAAHK	+16 (10,860 Da)	Met_{78}(O)
LLETECPQYIR	+48 (10,892 Da)	Cys_{42}-sulfonic acid
LLETECPQYIRK	+48 (10,892 Da)	Cys_{42}-sulfonic acid
	+46 (10,890 Da)	Cys_{42}-oxathiazolidine-dioxide
GADVWFK	+16 (10,860 Da)	Trp_{54}(+16)
ALNSIIDVYHK	+16 (10,860 Da)	His_{17}(+16)
GNFHAVYR	+16 (10,860 Da)	His_{27}(+16)
Preparation 2		
MGVAAHK	+16 (10,860 Da)	Met_{78}(O)
LLETECPQYIR	+48 (10,892 Da)	Cys_{42}-sulfonic acid
LLETECPQYIRK	+48 (10,892 Da)	Cys_{42}-sulfonic acid
	+46 (10,890 Da)	Cys_{42}-oxathiazolidine-dioxide
KLLETECPQYIR	+48 (10,892 Da)	Cys_{42}-sulfonic acid
GADVWFK	+16 (10,860 Da)	Trp_{54}(+16)
ALNSIIDVYHK	+16 (10,860 Da)	His_{17}(+16)
Dimeric oxS100A8		
Preparation 1		
LLETECPQYIR	+48 (10,892 Da)	Cys_{42}-sulfonic acid
	+46 (10,890 Da)	Cys_{42}-oxathiazolidine-dioxide
LLETECPQYIRK	+46 (10,890 Da)	Cys_{42}-oxathiazolidine-dioxide
KLLETECPQYIR	+48 (10,892 Da)	Cys_{42}-sulfonic acid
Preparation 2		
LLETECPQYIR	+48 (10,892 Da)	Cys_{42}-sulfonic acid
	+46 (10,890 Da)	Cys_{42}-oxathiazolidine-dioxide
LLETECPQYIRK	+46 (10,890 Da)	Cys_{42}-oxathiazolidine-dioxide
KLLETECPQYIR	+48 (10,892 Da)	Cys_{42}-sulfonic acid
Trimeric oxS100A8		
Preparation 1		
LLETECPQYIR	+48 (10,892 Da)	Cys_{42}-sulfonic acid
KLLETECPQYIR		
Preparation 2		
No oxidized peptides		

Peptides derived from in-gel digests of rec-oxS100A8 with trypsin.

3.3.5 CHARACTERIZATION OF HOCl-OXS100A9

S100A9 had a retention time of 14.1 min (Fig. 3.11A, profile 1) from C4-RP-HPLC; two peaks were generated with S100A9:HOCl (1:1 molar ratio; Fig. 3.11A, profile 2), with longer retention times of 14.8 and 15.7 min respectively. Silver-staining of oxS100A9 showed that peak 1 contained monomeric oxS100A9 and some disulfide-linked dimer. Peak 2 contained monomeric S100A9 and disulfide-linked dimer, which was reduced after reduction with DTT (Fig. 3.11B). As for S100A8, use of the abbreviation oxS100A9 denotes oxS100A9 collected after C4-RP-HPLC. Hereafter, oxS100A9 refers to oxS100A9 confirmed by MS.

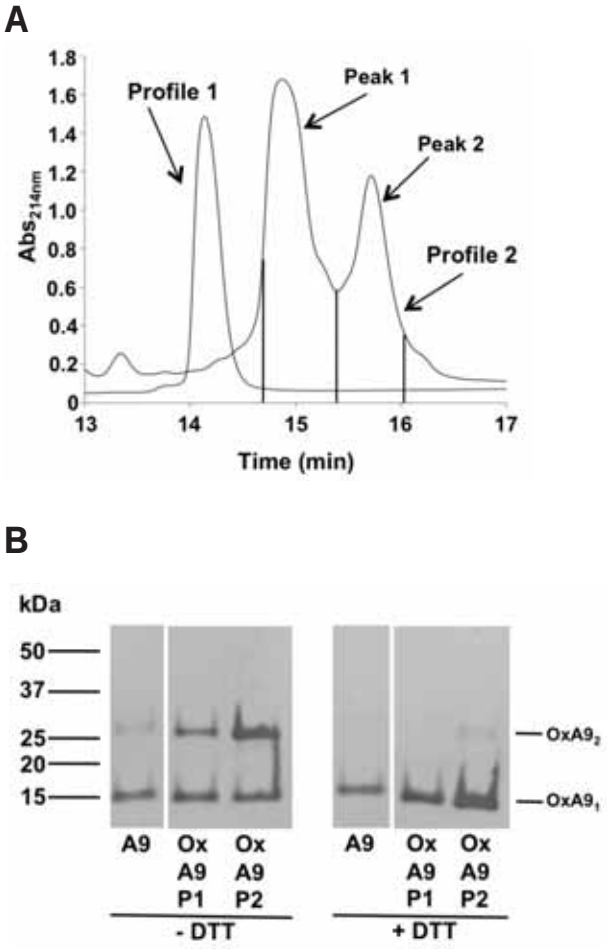

Figure 3.11: HOCl generates structural changes in S100A9 that alter RP-HPLC retention profiles. (**A**) S100A9 eluted from C4-RP-HPLC at 14.1 min (Profile 1); S100A9 oxidized with equimolar ratios of S100A9:HOCl eluted as two peaks, retention times 14.8 and 15.7 min. (**B**) SDS-PAGE separation (under non-reducing conditions) and silver staining of oxidized peaks showed that monomeric and dimeric S100A9 ($oxA9_1$) eluted at 14.8 min. Protein eluting at 15.7 min ($oxA9_2$) contained monomer and more dimer compared to $oxA9_1$. Silver staining of PAGE gels run under reducing conditions (100 mM DTT) showed that dimeric S100A9 from both peaks was reduced, indicating that the protein migrating at 20 kDa was disulfide-linked dimer. Unmodified S100A9 (0.5 μg) was silver-stained for comparative analysis.

Deconvoluted masses of unmodified S100A9 (Fig. 3.11A, profile 1), monomeric (Fig. 3.11A, peak 1, profile 2) and dimeric (Fig. 3.11A, peak 2, profile 2) oxS100A9 products were determined by ESI-MS. ESI-MS of recombinant S100A9 indicated a single, multiply-charged ion, confirming unmodified monomer (Fig. 3.12A). Monomeric oxS100A9 showed three multiply-charged ions (Fig. 3.12B). Unmodified monomer was a major product, possibly indicating more resistance to HOCl oxidation. A mass addition of +28 Da (13,281Da), possibly corresponds to unknown Cys_3 and/or Met oxidation products. A third product had a mass addition of +112 Da (13,365) corresponding to addition of seven oxygens, indicating possible Cys_3 and Met oxidation products (Fig. 3.12B).

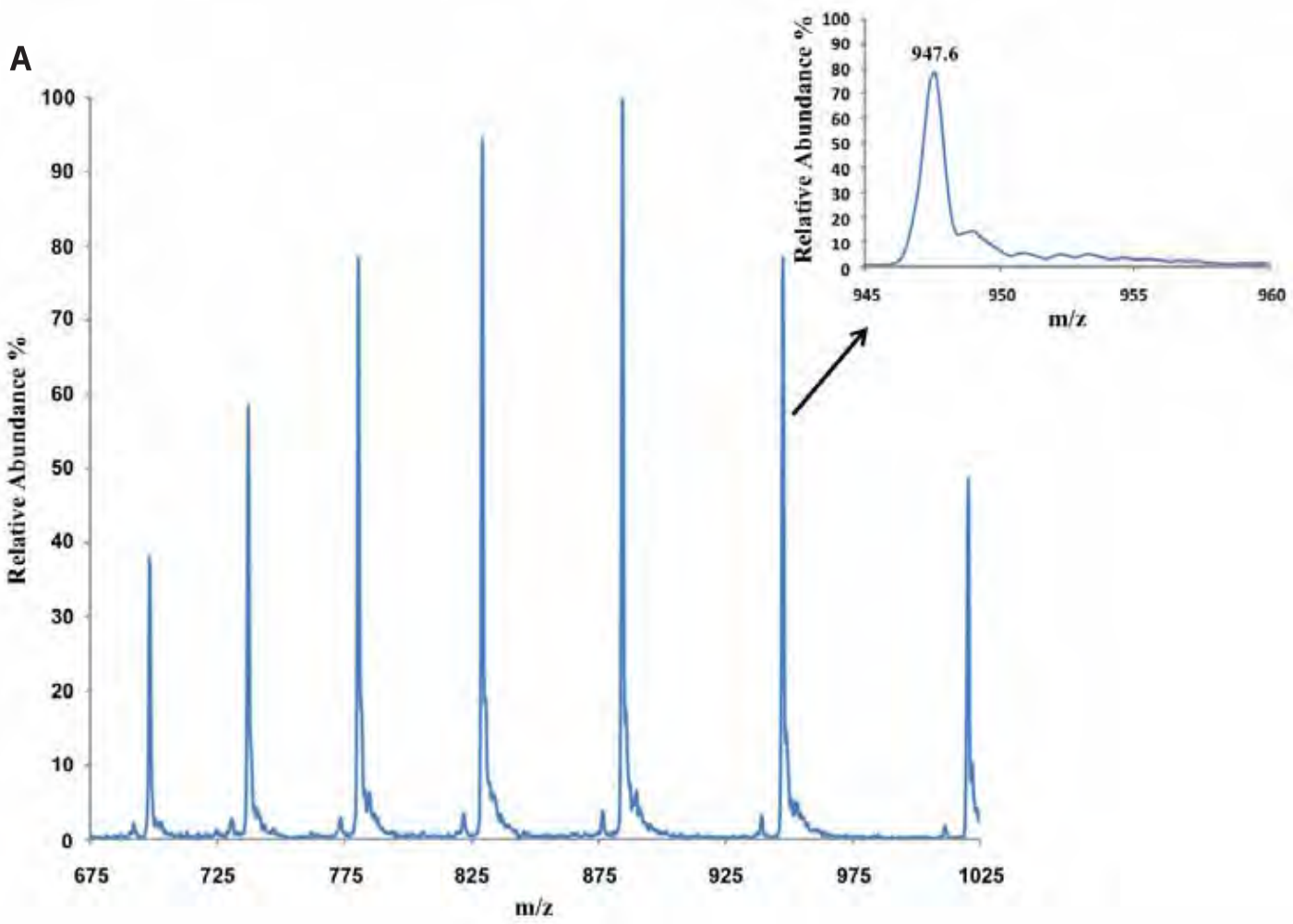
A
Relative Abundance %
100
90
80
70
60
50
40
30
20
10
0
675
725
775
825
875
925
975
1025
m/z
947.6
Relative Abundance %
100
90
80
70
60
50
40
30
20
10
0
945
950
955
960
m/z

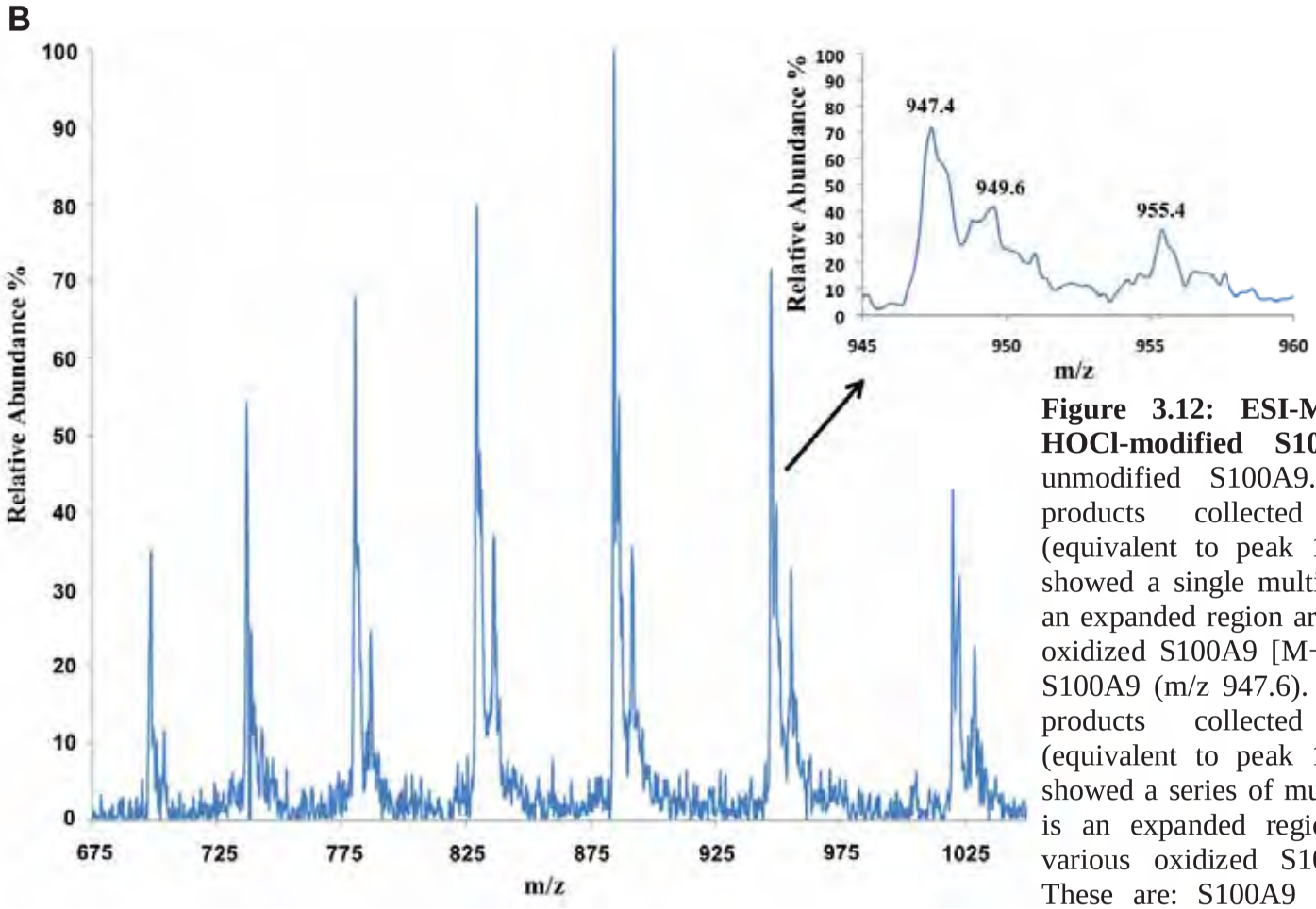

Figure 3.12: ESI-MS of unmodified and HOCl-modified S100A9. (**A**) ESI-MS of unmodified S100A9. ESI-MS of oxidation products collected after C18-RP-HPLC (equivalent to peak 1, profile 1, Fig. 3.11A) showed a single multiply-charged ion (insert is an expanded region around m/z 950 and various oxidized S100A9 $[M+14H]^{14+}$ ions). This was S100A9 (m/z 947.6). (**B**) ESI-MS of oxidation products collected after C18-RP-HPLC (equivalent to peak 1, profile 2, Fig. 3.11A) showed a series of multiply-charged ions (insert is an expanded region around m/z 950 and various oxidized S100A9 $[M+14H]^{14+}$ ions). These are: S100A9 (m/z 947.4), S100A9+28 (Cys_3 and Met oxidation products, m/z 949.6), S100A9+112 (addition of seven oxygens, m/z 955.4). The mass accuracy and resolution of the 1100 MSD was insufficient to identify ions with other mass differences in the presence of these abundant ions.

Dimeric samples contained an abundance of disulfide-linked dimer, with no obvious mass additions (not shown), suggesting that any potential modifications were too low in abundance to be measured. The mass additions are summarized in Table 3.7.

Table 3.7: Deconvoluted masses of recombinant HOCl-oxS100A9

Sample	Mass addition (Da)	Relative abundance (%)	Possible modifications
HOCl-oxidized S100A9 (monomer)	0 (13,252 Da) +28 (13,280Da) +112 (13,364Da)	100 51.69 31.95	Full-length S100A9 Oxidized Cys and Met products Addition of 7 oxygens
HOCl-oxidized S100A9 (dimer)	0 (26,504 Da)	100	Full-length S100A9 disulfide-linked dimer

In-solution AspN digests of monomeric oxS100A9 (elution maximum 14.8 min, Fig 3.11A, peak 1, profile 2) and subsequent MS analysis revealed no compelling evidence of oxidation of the single Cys_3 residue in peptide searches. The predicted addition of seven oxygens identified by ESI-MS could not be accurately confirmed by MS/MS of digested samples. Sequence coverage of peptides was not 100%, although some peptides containing Cys_3 and Met_5 were identified in non-enzyme specified searches from one sample (MS/MS analysis was performed on 3 individual samples). This modification was in low abundance, making positive identification of the weak spectra difficult. Because of the difficulty in characterizing Cys modifications, oxidation of recS100A9 with HOBr was not attempted. However, $Met_{63/81/83/94}$ in monomeric rec-oxS100A9 were converted to Met(O) by HOCl (Fig. 3.13-3.16). Conversion of Met_{81} to Met_{81}-sulfone was observed in only one peptide (S100A9 $_{71\text{-}91}$; Mowse score: 32) from monomeric oxS100A9 and the very low abundance suggests that this was a relatively unfavourable reaction with the quantity of HOCl used. The oxidized disulfide-linked dimer of S100A9 (Fig. 3.11A, peak 2, 15.7 min, profile 2) only generated one peptide, EKVIEHI<u>M</u>, and confirmed oxidation of to Met_{63}(O). However, these samples contained a mixture of monomeric and dimeric oxS100A9. MS analysis cannot discriminate between oxidation products in oxidized monomers and dimers. Therefore, it was difficult to conclude if this product was derived from the monomer or the dimer. Similarly, MS

analysis of oxidation on Trp and His residues was difficult to characterize accurately and requires further work to accurately characterize potential oxidation products. Isolated peptides and their major modifications are summarized in Table 3.8.

Table 3.8: Summary of major oxidative modifications in HOCl-oxS100A9 identified by MS

Sample	Mass addition (Da)	Modification
HOCl-oxidized S100A9 (1:1) (Fig. 3.11A, peak 1, 14.8 min)		
AspN digest		
EKVIEHIM	+16 (13,268 Da)	$Met_{63}(O)$
EEFIMLMARLTWASH	+16	$Met_{81}(O)$
EEFIMLMARLTWASH	+16	$Met_{83}(O)$
EEFIMLMARLTWASHEKMHEG	+16	$Met_{94}(O)$
HOCl-oxidized S100A9 (1:1) (Fig. 3.11A, peak 2, 15.7 min)		
EKVIEHIM	+16 (13,268 Da)	$Met_{63}(O)$

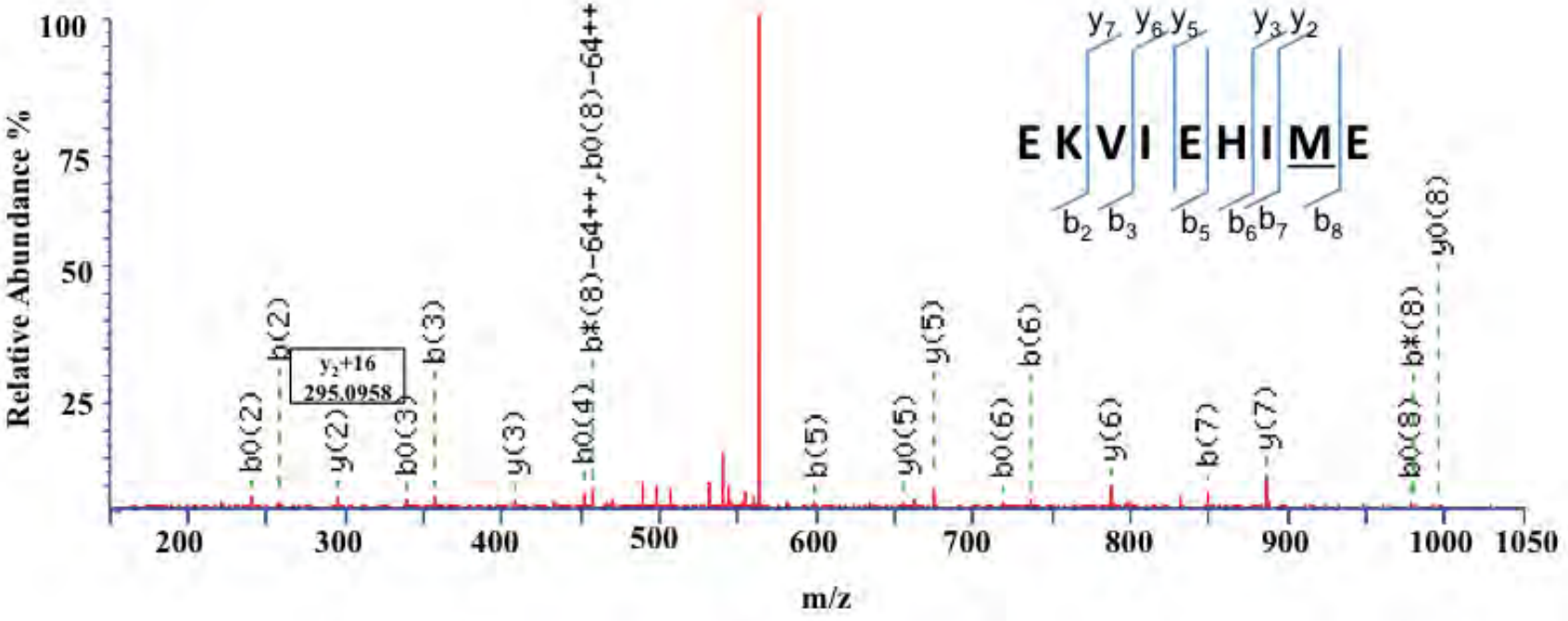
Relative Abundance %
100
75
50
25
200
300
400
500
600
700
800
900
1000
1050
m/z
y2+16
295.0958
b0(2)
b(2)
y(2)
b0(3)
b(3)
y(3)
b0(4) - b*(8)-64++, b0(8)-64++
b(5)
y0(5)
y(5)
b0(6)
b(6)
y(6)
b(7)
y(7)
b0(8) - b*(8)
y0(8)
y7 y6 y5 y3 y2
E K V I E H I M E
b2 b3 b5 b6 b7 b8

#	b	Seq.	y	#
1	130.0499	**E**		**9**
2	***258.1448***	**K**	1014.5288	**8**
3	***357.2132***	**V**	***886.4339***	**7**
4	470.2973	**I**	***787.3655***	**6**
5	***599.3399***	**E**	***674.2814***	**5**
6	***736.3988***	**H**	545.2388	**4**
7	***849.4829***	**I**	***408.1799***	**3**
8	***996.5183***	**M**	***295.0958***	**2**
9		**E**	148.0604	**1**

Figure 3.13: Annotated MS/MS of monomeric rec-oxS100A9 Met_{63}-containing AspN digest peptide. MS/MS of $S100A9_{56-64}$ sequence-specific ions (either as y or b ions) are labelled. Only fragment ion b_8 and y_2 (Met_{63}) showed gain of m/z +16 (y_2 ion shown in box), confirming oxidation of Met_{63} to $Met_{63}(O)$. Masses of individual amino acids are listed in the table. Amino acids in bold italics are those contributing to Mowse scores of isolated peptides.

E E F I M L M A R L T W A S H
b2
b8
y6
y4
y3
y2
b10
Relative Abundance %
100
75
50
25
200
400
600
800
1000
1200
1400
1600
m/z
y0(2)
y(2)
y(4)++,b0(4)++
b(2)
y(5)++,b(5)-64++
y(3)
y(7)++
y(8)++
y(4)
b0(4)
b(9)-64++,y(9)++
b*(9)++,b0(9)++
b(10)-64++,y(10
b0(11)++,y(11)++
b*(11)++
y0(12)++,y(6)
y(12)++
b*(12)++,b0(6)
b*(13)++,b0(13)++
y(13)++
b(13)++
b0(14)++,b*(14)++
b0(7)
b0(8)
b(8)
b0(9)
b*(9)
b0(10)
b*(10)
b(10),y0(11)-64
y*(11)-64
y*(11)
b0(11)
b*(11)

#	b	Seq.	y	#
1	130.0499	**E**		**15**
2	***259.0925***	**E**	1721.8502	**14**
3	406.1609	**F**	1592.8076	**13**
4	519.2449	**I**	1445.7392	**12**
5	666.2803	**M**	1332.6551	**11**
6	779.3644	**L**	1185.6197	**10**
7	910.4049	**M**	1072.5357	**9**
8	***981.4420***	**A**	941.4952	**8**
9	1137.5431	**R**	870.4581	**7**
10	***1250.6272***	**L**	***714.3570***	**6**
11	1351.6749	**T**	601.2729	**5**
12	1537.7542	**W**	***500.2252***	**4**
13	1608.7913	**A**	***314.1459***	**3**
14	1695.8233	**S**	***243.1088***	**2**
15		**H**	156.0768	**1**

Figure 3.14: Annotated MS/MS of monomeric rec-oxS100A9 Met_{81}-containing AspN digest peptide. MS/MS of $S100A9_{77-91}$ sequence specific ions (either as y or b ions) are labelled. Only fragment ion b_5 and y_{11} (Met_{81}) showed gain of m/z +16, confirming oxidation of Met_{81} to $Met_{81}(O)$. Masses of individual amino acids are listed in the table. Amino acids in bold italics are those contributing to Mowse scores of isolated peptides.

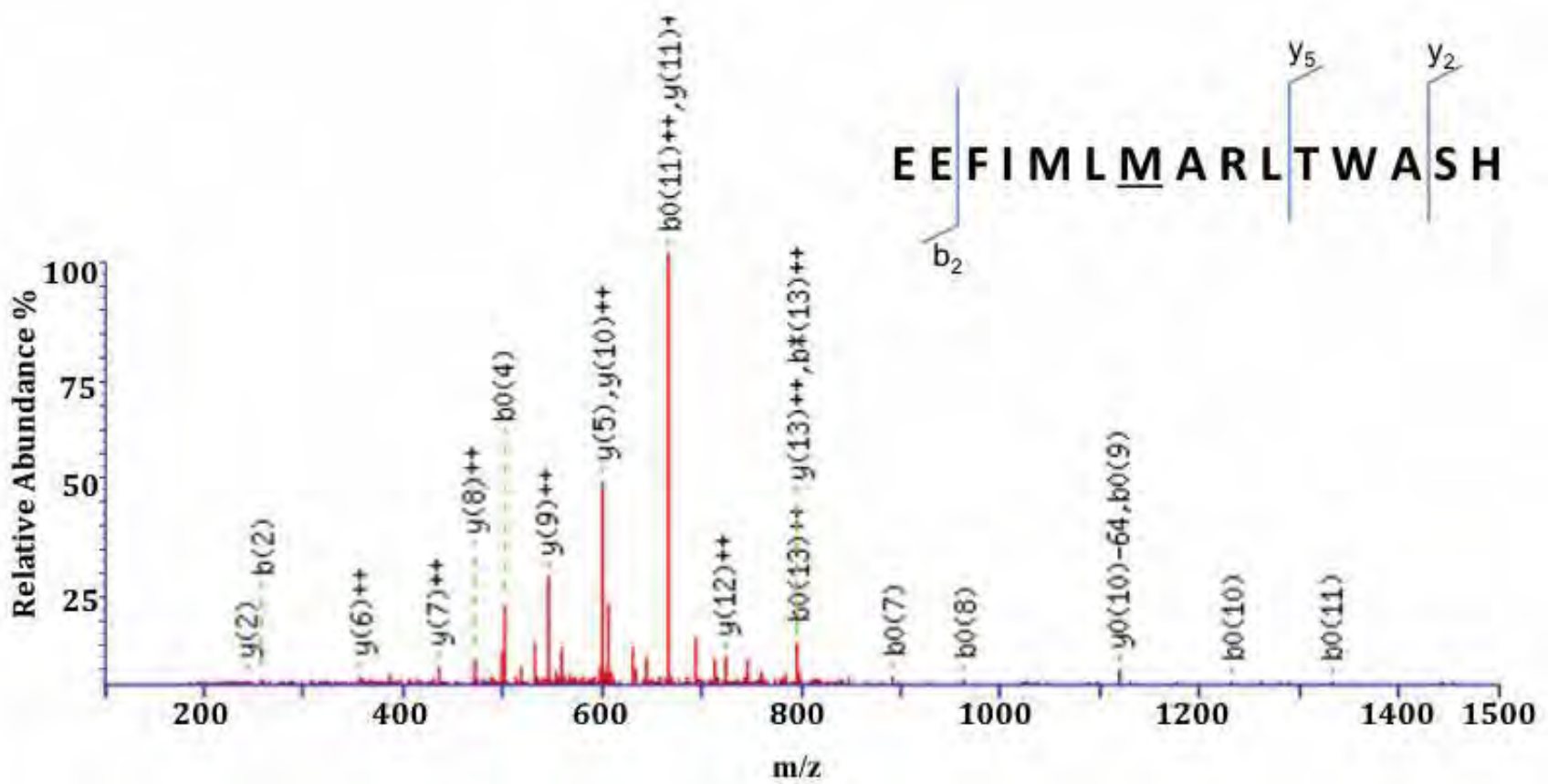
E E F I M L M A R L T W A S H
y5
y2
b2
Relative Abundance %
100
75
50
25
200
400
600
800
1000
1200
1400
1500
m/z
y(2)
b(2)
y(6)++
y(7)++
y(8)++
b0(4)
y(9)++
y(5),y(10)++
b0(11)++,y(11)+
y(12)++
b0(13)++
y(13)++,b*(13)++
b0(7)
b0(8)
y0(10)-64,b0(9)
b0(10)
b0(11)

#	b	Seq.	y	#
1	130.0499	**E**		**15**
2	***259.0925***	**E**	1721.8502	**14**
3	406.1609	**F**	1592.8076	**13**
4	519.2449	**I**	1445.7392	**12**
5	650.2854	**M**	1332.6551	**11**
6	763.3695	**L**	1201.6146	**10**
7	910.4049	**M**	1088.5306	**9**
8	981.4420	**A**	941.4952	**8**
9	1137.5431	**R**	870.4581	**7**
10	1250.6272	**L**	714.3570	**6**
11	1351.6749	**T**	***601.2729***	**5**
12	1537.7542	**W**	500.2252	**4**
13	1608.7913	**A**	314.1459	**3**
14	1695.8233	**S**	***243.1088***	**2**
15		**H**	156.0768	**1**

Figure 3.15: Annotated MS/MS of monomeric rec-oxS100A9 Met_{83}-containing AspN digest peptide. MS/MS of $S100A9_{77-91}$ sequence-specific ions (either as y or b ions) are labelled. Only fragment ions b_7 and y_9 (Met_{83}) showed gain of m/z +16, confirming oxidation of Met_{83} to $Met_{83}(O)$. Masses of individual amino acids are listed in the table. Amino acids in bold italics are those contributing to Mowse scores of isolated peptides.

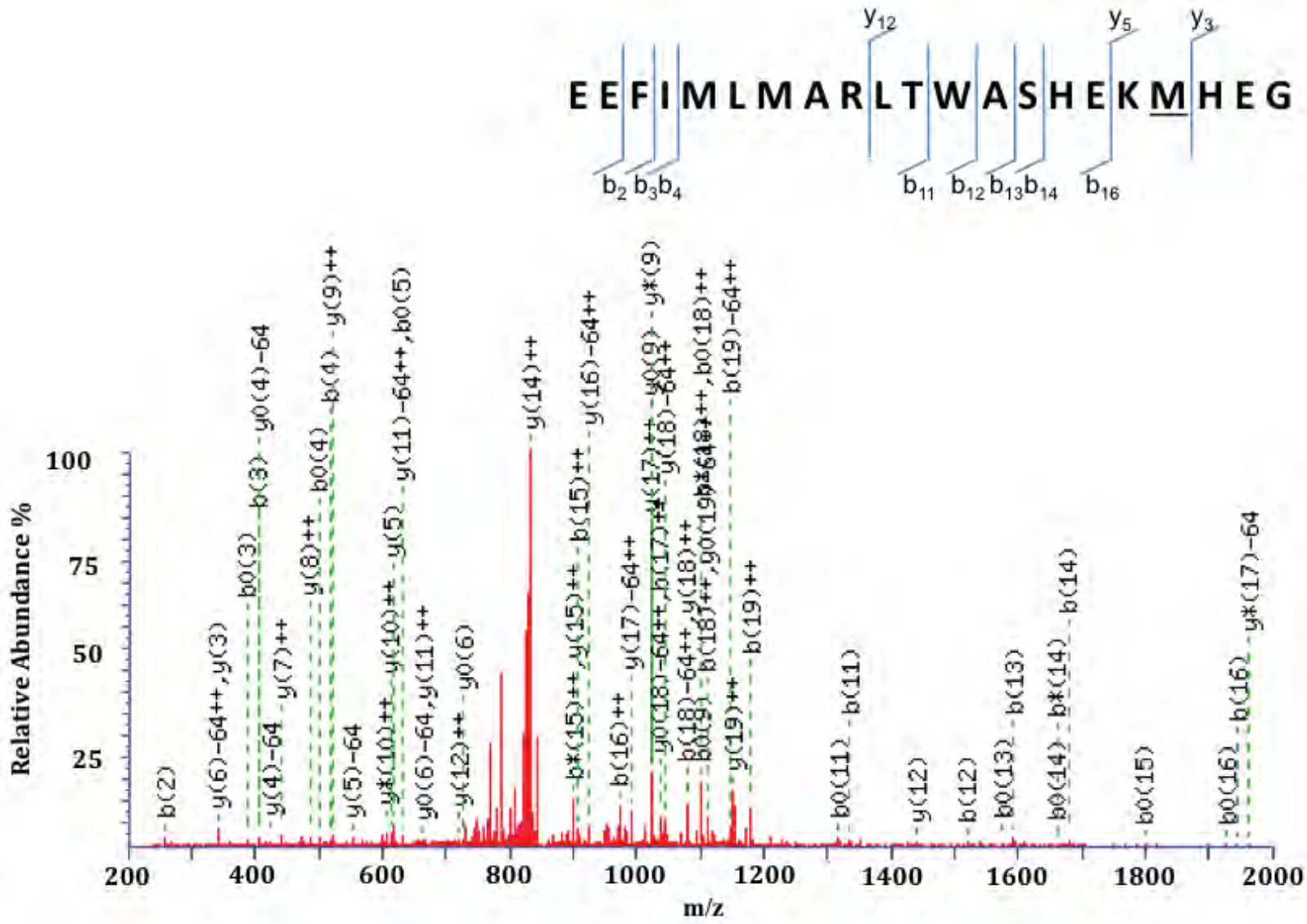
E E F I M L M A R L T W A S H E K M H E G
y12
y5
y3
b2 b3 b4
b11 b12 b13 b14
b16
Relative Abundance %
100
75
50
25
200
400
600
800
1000
1200
1400
1600
1800
2000
m/z
b(2)
y(6)-64++,y(3)
b0(3)
b(3)
y0(4)-64
y(4)-64
y(7)++
y(8)++
b0(4)
b(4)
y(9)++
y(5)-64
y*(10)++
y(10)++
y(5)
y(11)-64++,b0(5)
y0(6)-64,y(11)++
y(12)++
y0(6)
y(14)++
b*(15)++,y(15)++
b(15)++
y(16)-64++
b(16)++
y(17)-64++
y(18)-64++
y*(9)
b(18)-64++,y(18)++
b(19)-64++
y(19)++
b(19)++
b0(11)
b(11)
y(12)
b(12)
b0(13)
b(13)
b0(14)
b*(14)
b(14)
b0(15)
b0(16)
b(16)
y*(17)-64

#	b	Seq.	y	#
1	130.0499	**E**		**21**
2	***259.0925***	**E**	2433.1512	**20**
3	***406.1609***	**F**	2304.1086	**19**
4	***519.2449***	**I**	2157.0402	**18**
5	650.2854	**M**	2043.9561	**17**
6	763.3695	**L**	1912.9157	**16**
7	894.4100	**M**	1799.8316	**15**
8	965.4471	**A**	1668.7911	**14**
9	1121.5482	**R**	1597.7540	**13**
10	1234.6323	**L**	***1441.6529***	**12**
11	***1335.6799***	**T**	1328.5688	**11**
12	***1521.7593***	**W**	1227.5211	**10**
13	***1592.7964***	**A**	1041.4418	**9**
14	***1679.8284***	**S**	970.4047	**8**
15	1816.8873	**H**	883.3727	**7**
16	***1945.9299***	**E**	746.3138	**6**
17	2074.0249	**K**	***617.2712***	**5**
18	2221.0603	**M**	489.1762	**4**
19	2358.1192	**H**	***342.1408***	**3**
20	2487.1618	**E**	205.0819	**2**
21		**G**	76.0393	**1**

Figure 3.16: Annotated MS/MS of monomeric rec-oxS100A9 Met_{94}-containing AspN digest peptide. MS/MS of $S100A9_{77-97}$ sequence-specific ions (either as y or b ions) are labelled. Only fragment ions b_{18} and y_4 (Met_{83}) showed gain of m/z +16, confirming oxidation of Met_{94} to $Met_{94}(O)$. Masses of individual amino acids are listed in the table. Amino acids in bold italics are those contributing to Mowse scores of isolated peptides.

3.4 DISCUSSION

ROS/RNS attack cellular constituents such as lipids and proteins (see Section 1.4.1.7, Chapter 1) resulting in lipid oxidation and degradation, protein cross-linking, aggregation, fragmentation and DNA damage (reviewed in [963]). Oxidative stress is implicated in the pathogenesis of a number of chronic diseases, including atherosclerosis [964], asthma [965] neurodegenerative diseases [966, 967], multiple sclerosis [968], and IBS [969]. Importantly, S100A8 and S100A9 are found in patients with asthma (reviewed in [970]), CVD (reviewed in [971]), multiple sclerosis [463] and IBD [444]. Because S100A8, and S100A9 are sensitive to oxidation, we propose that they may protect against excessive oxidative stress, possibly reducing the severity of inflammatory disorders.

ROS/RNS-induced post-translational modifications in human and murine S100A8 and S100A9 have been reported (see Section 3.1), but modifications to hS100A8 by hypohalous oxidants have not been characterized. Much of the work demonstrated in this chapter draws directly from previous studies by Raftery *et al.*, who described formation of novel sulfinamide bonded rec-mS100A8 after exposure to HOCl [606], and interchain disulfide bonds between Cys_{80} and Cys_{91} in rec-mS100A9 [46]. Modifications observed in mS100A8 were remarkably similar to those identified in LDL peptides after exposure to HOCl (2:1 mol/mol) which generated sulfenamide, sulfinamide, sulfonamide-bonded peptides *in vitro* [904]. Protein carbonylation via oxidation of side chain amino acids such as Lys, Arg, Pro and Thr can also produce high mass aggregates [898, 899]. HOCl oxidation of Tyr side chains produce di-tyrosine and 3-chlorotyrosine [972-974]. We proposed that these types of modifications may contribute to inter- and intra-molecular protein cross-linking [606] and such cross-linked products could potentially propagate inflammation [904].

HOBr is generated by EPO, a major enzyme released by activated eosinophils (Section 1.4.1.2). Reaction of HOBr with proteins results in bromination of aromatic amino acid residues, forming several products and modifications such as 3-bromo-tyrosine and 3,5-dibromo-tyrosine [918, 952-954] are used as specific markers of HOBr reactions in BALF [918] and sputum [920] from patients with asthma. However, amino acid side chains residues such as Cys, Met, Trp, His, Tyr and Lys are regarded as most susceptible to HOBr [922]. HOBr oxidation of BSA can generate protein carbonyls, brominated Tyr residues and the Tyr oxidation products DOPA and di-tyrosine, which result from decay of *N*-bromo species [760]. Oxidative modifications in S100 proteins by

HOBr have not been characterized. This was carried out because we found high amounts of S100A8 in asthmatic sputum (Chapter 4), and it was likely that HOBr could generate oxidative changes in this condition. However, we found no evidence of protein carbonyls, brominated Tyr residues or di-tryrosine in HOBr-oxS100A8. Low abundance of 3-chlorotyrosine on Tyr_{30} was indicated in one peptide generated by from HOCl-oxidized monomeric S100A8 after in-gel, trypsin digestion of HOCl-oxS100A8.

3.4.1 CHARACTERIZATION OF OXIDATION PRODUCTS GENERATED IN S100A8 IN VITRO

Treatment of S100A8 with a 1:1 ratio of HOCl:S100A8 increased the elution time of the unmodified protein from C4-RP-HPLC, suggesting increased hydrophobicity. Compared to the tight elution profile of S100A8 (13.5 min Fig. 3.2A, profile 1), a more complex profile, comprising two apparent peaks, was generated. Silver-staining of fractions eluting at 14.4 and 14.8 min indicated monomer and dimer (Fig. 3.2B). Increasing the concentration of HOCl to a molar ratio of S100A8:HOCl of 1:2 caused aggregation; aggregates could not be separated. Importantly, treatment of Cys_{42}-Ala_{42}S100A8 with equimolar HOCl did not alter elution times or promote dimer formation, indicating involvement of Cys_{42} in structural changes.

Deconvoluted mass analysis of HOCl-oxS100A8 monomer revealed several mass additions, the most abundant of which likely correspond to Cys_{42}-sulfinic and -sulfonic acid, oxidation of Met_{78} to Met_{78}(O) and an unusual mass addition of m/z +30, indicating an as yet unidentified oxidation product. Dimeric forms were more complex; several mass additions were observed, possibly corresponding to oxidation of Cys_{42} and Met_{78}. Two low abundance mass additions of m/z +130 and +26 could not be accurately characterized. As deconvoluted mass analysis revealed only mass increases, specific modifications to Cys_{42} and Met_{78} were confirmed by MS/MS analysis of peptide digests.

Murine and human S100A8 have relatively low amino acid sequence identities. However, the susceptible Cys residue is conserved in both species, as are the $Lys_{35/36}$ residues that are most likely to contribute to inter- and/or intra-molecular cross-links with Cys_{42} (Fig. 3.17)[606]. $Lys_{7/88}$ may also form sulfinamide bonds in mS100A8 [606] and these are conserved in hS100A8. Lys_{31} in mS100A8 does not appear to be involved in inter- and/or intra-molecular sulfinamide bond formation and in hS100A8, there is an Arg in this position [606]. hS100A8 contains six additional Lys residues at positions 18, 23, 48, 49, 56 and 85 (Fig. 3.17) but their involvement in cross-linking is unknown.

Interestingly, several residues within the hinge region of hS100A8 and mS100A8 are not conserved (Fig. 3.17) and the human hinge domain is likely to be less hydrophobic and more charged. Aside from Met_1 in both S100s, hS100A8 contains a single Met residue at position 78, whereas mS100A8 has two at position 37 and 74. We show that Cys_{42} is pivotal in redox reactions involving hS100A8, and that Met_{78} is also oxidized. Moreover, Trp_{54} and $His_{17/27/83}$ were also susceptible to oxidation. Kinetic analysis indicates that Cys and Met residues are the most susceptible to oxidation although His residues also have high reactivity to HOCl [960]. As human S100A8 only has one Cys and one Met residue, identification of oxidized Trp and His residues was unsurprising. In this study, observations relating to His and Trp residues were preliminary and require further analysis, particularly as His oxidation can generate 2-oxo-Histidine, a carbonyl product that can form either by one- or two-electron processes, and may play a role in protein aggregation (reviewed in [948]).

Figure 3.17: Sequence alignment of mS100A8 and hS100A8. Sequence alignment of murine and human S100A8 show that Cys_{42} is conserved, as are $Lys_{7,35,36,84}$. hS100A8 contains six additional Lys residues at postions 18, 23, 48, 49, 56 and 85. mS100A8 contains two Met residues at postion 37 and 74, whereas hS100A8 only contains one Met at position 78. Met_1 is common to both; however, it is not present in the recombinant proteins. Lys residues are indicated by red arrows, Cys by black arrows and Met by green arrows. The hinge region in both proteins is highlighted in blue.

Importantly, the presence of novel oxathiazolidine adducts in hS100A8, and the apparent absence of sulfinamide modifications characteristic of HOCl-oxidized mS100A8 highlight how the structural differences between the human and murine proteins affect the nature of the post-translational modifications. Oxidation of mS100A8 with a 5:1 molar ratio of HOCl, generated $Met_{37/74}$(O) and inter- and intra-molecular sulfinamide bonds between Cys and Lys residues (mass addition, m/z +14) [606]. A summary of these is shown in Fig. 3.18. Sulfinamide bonds were not generated in mS100A8 oxidized with lower ratios of HOCl and other putative products were not characterized (personal communication, A/Prof. Mark Raftery).

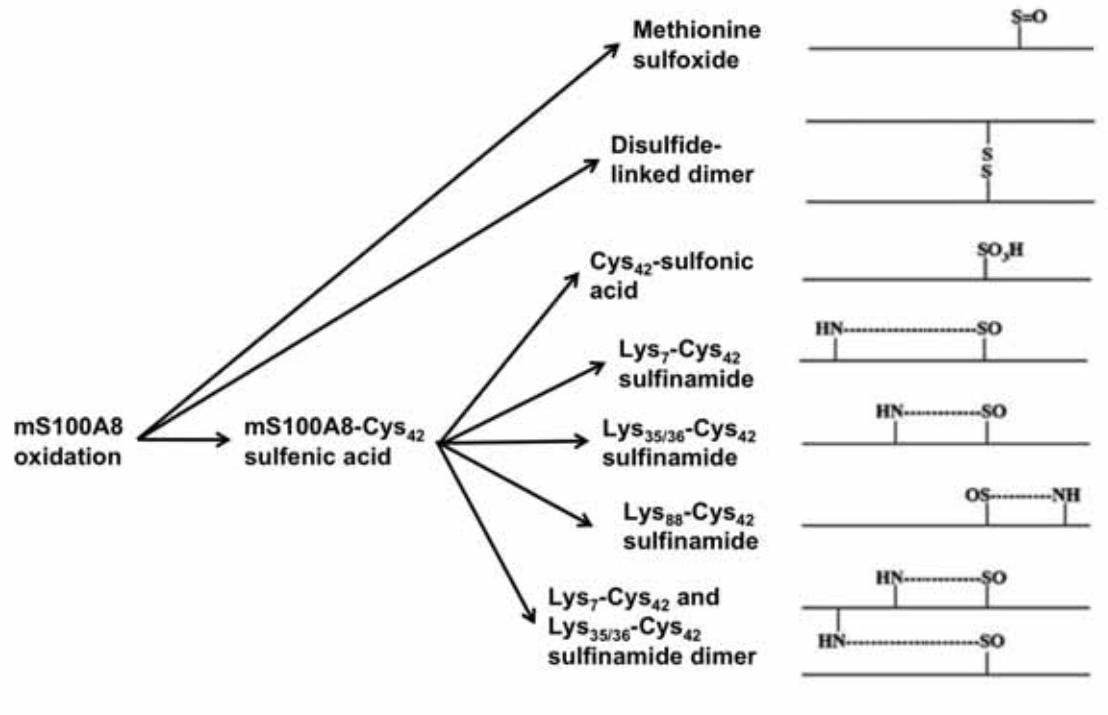

Figure 3.18: Modifications in mS100A8 generated by HOCl. A variety of modifications on $Met_{37/74}$ and Cys_{42} is reported. mS100A8 is irreversibly oxidized to several adducts with inter- and intra-chain sulfinamide-linked complexes. Adapted from [606].

With assistance from Dr. Jesse Goyette (UNSW, Australia), comparative analysis of murine and human S100A8 showed that apart from the conserved amino acids, TECPQ flanking Cys_{42}, murine and human S100A8 have low amino acid sequence identity in this region. This encompasses the hinge domain that contributes to functional diversity in S100 proteins, and we reported functional differences between murine and human S100A8 [317]. In particular, substitution of Gly_{50} in hS100A8 to Asn_{50} in mS100A8 may contribute to differences in sensitivity. Structural analysis of S100A8 homodimers [388] and S100A8/A9 heterodimers [392] indicate that Gly_{50} adopts phi-psi angles that may reduce backbone clashes likely to occur with bulkier residues such as Asn_{50} (Fig. 3.19A and B). Gly_{50} resides within the functional hinge domain, and this region may be more flexible in the human protein, enabling Cys_{42}, which is buried in the core of the protein, to become transiently solvent-exposed and thus more prone to oxidation whereas Asn_{50} in mS100A8 may not afford the same flexibility.

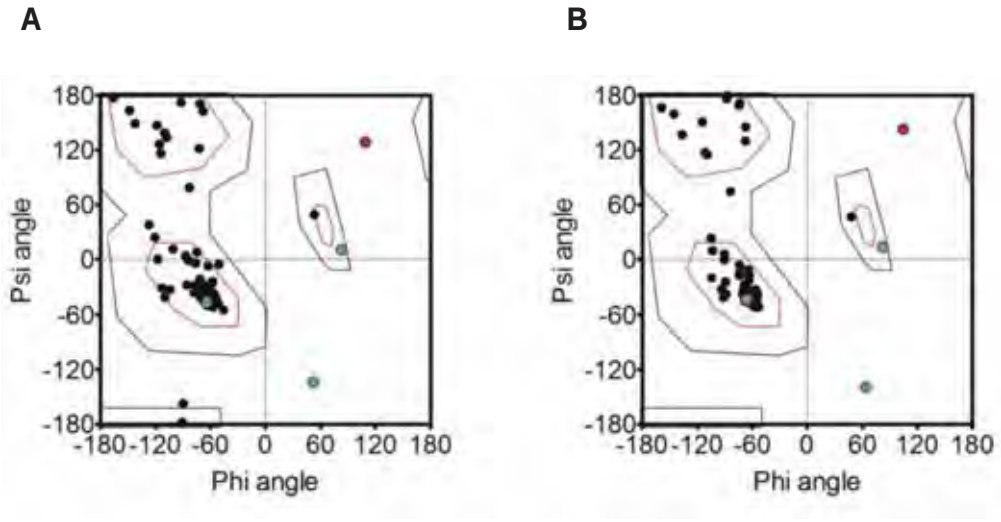

Figure 3.19: Ramachandran plots of human and murine S100A8. (**A**) Based on the structure of the homodimer (protein data bank entry 1MR8) and (**B**) S100A8/S100A9 heterodimer (1XK4) of the human proteins. Glycines are colored green, Gly_{50}in red. Regions of favorable phi/psi angles for residues other than Gly and Pro are outlined in red, allowable regions are outlined in blue. (Ramachandran plot produced by Dr. Jesse Goyette).

Addition of HOBr to S100A8 altered its elution time from C4-RP-HPLC from 13.5 min to 15.1 and 15.6 min; silver-staining revealed predominantly monomeric oxS100A8 eluting at 15.1 min. Insufficient protein was eluted at 15.6 min for further characterization. Deconvoluted mass analysis showed mass additions most likely

corresponding to Met_{78}(O)/Trp(+16) and Cys_{42}-sulfinic or -sulfonic acid, however, only Cys_{42}-sulfonic acid was observed in MS/MS analysis of peptides. In contrast to HOCl, HOBr-oxidized S100A8 indicated Trp_{54} oxidation. Oxidation by HOBr is largely substrate-dependent [803, 922], and Cys and Met residues are generally 10-fold less reactive with HOBr than with HOCl [803], making Trp a more likely target of HOBr-mediated oxidation. This may explain the less efficient oxidation of Met and Cys because the Met(O) and oxathiazolidine-oxide and -dioxide adducts typical of HOCl oxidation were not apparent, and no dimer was formed. A 10-fold higher concentration of HOBr caused aggregation (Fig. 3.2D, profile 3), similar to that observed in S100A8 when treated with an HOCl molar excess of 2:1 (HOCl:S100A8) (Fig. 3.2A, profile 3). More rigourous titration of molar amounts of the hypohalous acids, for various times, may clarify potential differences.

3.4.2 CHARACTERIZATION OF OXS100A8 FROM SILVER- AND COOMASSIE-STAINED IN-GEL DIGESTS

MS analysis of peptides derived from oxidized monomeric and dimeric S100A8 gel slices digested with trypsin indicated only Cys_{42}-sulfonic acid. This modification was also found in the native S100A8 monomer although more careful validation of the mass before processing confirmed no initial modification. Results suggest that the process of separation and generation of peptides in gel slices may have inadvertently caused oxidation. Moreover, despite separating relatively large amounts of protein for analysis, few Cys-containing peptides were obtained by manual inspection of spectra. Speicher *et al*. found that enzyme digestion can cause large losses of peptides from some proteins. Using human spectrin, the authors showed that trypsin digestion resulted in losses of 14-20%, but downstream adsorptive losses further reduced yields [975]. Adsorptive losses, for example in microfuge tubes and with pipette tips used to transfer extracts, or concentration of samples using a SpeediVac results in consistent losses of protein, of between 25-50% [975, 976]. This may have contributed to the low peptide yield found here. In Section 3.3.2, iodoacetamide was added to excised gel bands (covalently binds free thiol groups preventing fortuitous formation of disulfide bonds or other products) after separation by SDS-PAGE to prevent oxidation during peptide generation. Speicher *et al*. suggest that alkylation of proteins with iodoacetamide prior to separation by SDS-PAGE may increase peptide yield [975], and its inclusion at that point may have been beneficial.

Because we were unable to identify putative cross-linked peptides by MS, we made another attempt to determine if sulfinamide bonds were present in higher-order complexes of oxS100A8. S100A8 was mildly oxidized with HOCl *in vitro*, then separated by SDS-PAGE, and gel slices of monomeric, dimeric and trimeric S100A8 digested with trypsin and peptides analyzed by MS. In this case, care was taken to reduce spontaneous oxidation of the protein by alkylation before separation by SDS-PAGE (as recommended by Speicher *et al*. [975]). Despite this, monomeric, native S100A8 contained Cys_{42}-sulfonic acid in the peptide LLETECPQYIR ($S100A8_{37-47}$) in both experiments. The native dimer also contained Cys_{42}-sulfonic acid in the same peptide ($S100A8_{37-47}$). Following oxidation, monomeric S100A8 contained Met_{78}(O) on the peptide MGVAAHK ($S100A8_{78-84}$) in both preparations. Met_{78}-sulfone was also observed in 2/2 preparations, but only on a single peptide, indicating that this was not an abundant modification. Because of its very low abundance, further analysis is required to confirm Met_{78}-sulfone in oxS100A8. Cys_{42}-sulfonic acid and the novel adduct, Cys_{42}-oxathiazolidine-dioxide were also obvious as was oxidation of Trp and His. Interestingly, the oxidized dimer had no obvious Trp or His oxidation, but did contain Cys_{42}-sulfonic acid and Cys_{42}-oxathiazolidine-dioxide modifications in two preparations, and may indicate an intra-molecular Cys_{42}-oxathiazolidine-dioxide dimer, or an as yet uncharacterised modification, possibly involving His (reviewed in [948]). This requires further investigation to confirm this possibility. The trimer was relatively low yield and only Cys_{42}-sulfonic acid was apparent in one preparation (Fig. 3.10).

3.4.3 DETAILED CHARACTERIZATION OF NOVEL OXATHIAZOLIDINE-DIOXIDE MODIFICATIONS IN OXS100A8

Because analysis of in-gel digests of S100A8 with trypsin were unreliable, another method of enrichment was developed to identify oxidized forms of S100A8, and of the oxidized S100A9 monomer formed following HOCl treatment. Isolates were separated by C4-RP-HPLC then digested in solution. HOCl (equimolar ratios) generated Cys_{42}-sulfinic and -sulfonic acid adducts, and the presence of novel derivatives suggested in spectra of the undigested protein (Table 3.1) was confirmed.

Digestion with AspN consistently generated sufficient numbers of peptides to allow analysis of the novel, post-translational modifications. AspN was therefore used as the preferred enzyme in all subsequent in-solution digests.

We propose alternate oxidation of sulfenic acid intermediates, to products that may form between cyclised oxidized Cys_{42} and nitrogen within the peptide backbone, to form oxathiazolidine-dioxide (m/z +46 Da addition). The lesser product, oxathiazolidine-oxide (m/z +30 addition), only obvious in tryptic digests, may be a precursor of the final oxathiazolidine-dioxide (m/z +30 Da addition; Fig. 3.20).

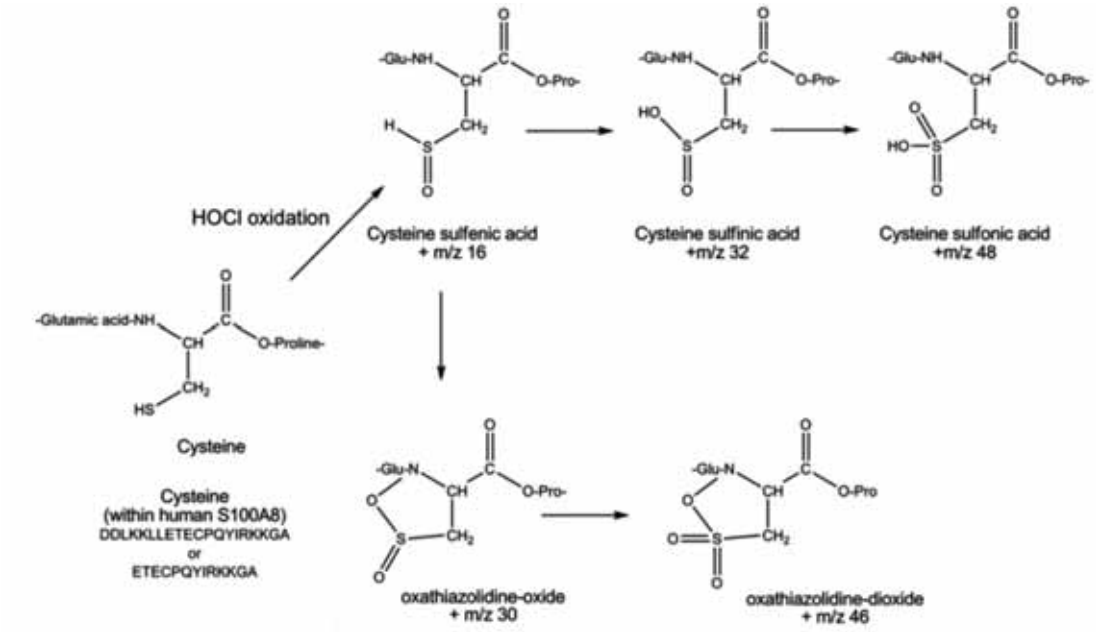

Figure 3.20: The likely products of S100 oxidation by hypohalous acids are summarized. The Cys_{42} adduct, oxathiazolidine-dioxide, (+46 m/z mass addition) may have formed by oxidation of Cys_{42} to sulfinic acid, then further oxidation to sulfinic or sulfonic acids or to the oxathiazolidine-oxide (+30 m/z mass addition). Upon further oxidation, the latter forms a dioxide adduct with a +46 m/z mass addition caused by the neutral loss (of SO_2 and SO_3) to form cyclised products between oxidized Cys_{42} and nitrogen within the peptide backbone (with asistance from A/Prof. Mark Raftery).

Dioxide-containing peptides were plentiful whereas the putative intermediate was less abundant. The same modifications were observed in peptides derived from dimeric oxS100A8. Unlike sulfenic acid and sulfhydryl derivatives that can be reduced by thiol reductases and have high reducing potential, sulfinic and sulfonic acid modifications are irreversible [977] and the oxathiazolidine-dioxide adduct in S100A8 is also likely to be an irreversible modification. Critically, care was taken in preparation and isolation of oxidized proteins (for example, helium-purged RP-HPLC buffers and storage of oxidized protein under argon) to prevent further oxidation. Ideally, preparation and separation of

protein would be best conducted under anaerobic conditions but this was not practical with the current protocol.

Disulfides are often major products of oxy acids (also responsible for producing sulfenic, RSOH; sulfinic, RSO_2H; and sulfonic, RSO_3H (reviewed in [886]) and can be prepared enzymatically (reviewed in [978]). However, in hS100A8 oxidized with HOCl, we saw DTT-resistant oxS100A8 dimer in RP-HPLC-purified preparations and also oligomers formed after direct oxidation (Fig. 3.10). In rec-mS100A8, irreversible oxidative cross-linking occurs via sulfinamide bond formation between Cys_{42} and $Lys_{7/35/36/88}$, resulting in monomeric structures and cross-linked inter- and intra-molecular bonds [606]. However, we found no evidence for sulfinamide bonds in hS100A8 although yields were low and more analysis is necessary, possibly using $Lys_{35/36}$ mutants as for rec-mS100A8 [606]. HOCl can cause dimerization via di-tyrosine formation [979], but no evidence for dimer formation by oxidation of tyrosine residues was observed in rec-mS100A8 [606]. Moreover, no Tyr modifications were obvious in MS analysis of peptides derived from the oxidized dimer or trimer. Formation of 3-chlorotyrosine is an unfavourable reaction of HOCl [764]. Although low amounts of Tyr_{19} oxidation to 3-chlorotyrosine [980] were seen in one peptide of the oxidized monomer derived from in-gel digests and no di-tyrosine was obvious, indicating that dimer formation was unlikely by this mechanism. Analysis of these modifications by could benefit from other types of analyses. For example, identification of 3-chlorotyrosine in proteins is commonly analyzed by stable isotope dilution gas chromatography with mass spectrometry [981, 982] and could be considered for future experiments. More detailed methods for analysis of di-tyrosine and other Tyr related modifications are reviewed in [983].

Carbonyl groups are common markers for measuring protein oxidation in Alzheimer's disease, RA, diabetes and respiratory distress syndrome. They are chemically stable adducts produced on protein side chains, particularly Pro, Arg, Lys and Thr which can form protein aggregates (reviewed in [900, 984]). This type of modification was not apparent in HOCl-oxS100A8, suggesting complex formation independent of carbonyl groups.

Because hS100A8 forms cross-linked multimers with HOCl ([410] and Fig. 3.2B and 3.10), and because Cys_{42} is conserved in both species (Fig 3.17), we may have failed to identify sulfinamide-bonded peptides because the proteases used may not have generated peptides of sufficient length for analysis. For example, pepsin, endoproteinase Lys-C or Glu-C were used by Raftery *et al.* to further digest rec-mS100A8$_{32-57}$ isolated

after an intial cleavage wth AspN, to produce the smaller peptides required for more definitive MSMS analysis [606].

Modifications commonly induced by HOBr include 3-bromotyrosine and 3,5-dibromotyrosine [985]. In proteins, bromamines are generated on the side chain of Lys and His residues, the N-terminal amine group and on side chains of Arg, Asn, Gln (reviewed in [983] these adducts were not identified in any preparation of S100A8. Kinetic studies suggest that HOBr can react 30-100-fold faster than HOCl, however, as stated in Section 3.4.1, Met and Cys residues are 10-fold less reactive. Moreover, HOBr's efficiency as an oxidant is highly dependent on the substrate [803]. Cys_{42} was modified to Cys_{42}-sulfonic acid by HOBr, but this did not generate the oxathiazolidine derivatives. In contrast, Trp_{54} appeared to be readily oxidized and may be a more likely target for oxidation by HOBr [922].

3.4.4 CHARACTERIZATION OF OXS100A9

oxS100A9 readily separated into two peaks from C4-RP-HPLC (14.8 and 15.7 min; Fig. 3.11A, profile 2) that eluted later than native S100A9 (14.1 min; Fig. 3.11A, profile 1), indicating modification. Peak 1 contained monomeric S100A9; peak 2, monomeric S100A9 and high amounts of disulfide-linked dimer. Deconvoluted mass analysis of monomeric oxS100A9 showed evidence of possible modification of Cys_3 and Met residues, whereas the disulfide linked dimer showed no evidence of additional adducts. Previously, we demonstrated that a 25 molar excess of HOCl did not generate covalent mS100A9 dimers, but rather, stepwise increases in mass of the monomer ranging from 1 kDa (with a 4 molar excess of HOCl) to 2 kDa (with a 25 molar excess of HOCl). Sequential oxidation of the seven Met residues and single Cys residue in S100A9 may result in changes in conformation or net charge, and Met residues are preferentially oxidized [605].

Sequence alignment of mS100A9 with hS100A9 shows that $Cys_{80,91,111}$ in mS100A9 are not conserved in hS100A9 (Cys_3). No compelling evidence for Cys_3 modifications were observed in AspN digests. Only one Met residue is conserved among species, Met_{81} (Fig. 3.21). We found that $Met_{63/81/83/94}$ were all oxidized by HOCl to Met(O). Met-sulfone has previously been identified in S100A9 from PMA-treated neutrophils [637], however, in Section 3.3.5, only one contained Met-sulfone (Met_{81} to Met_{81}-sulfone), suggesting that this modification was not abundant. Oxidation of Met residues may have been sufficient to alter elution times from C4-RP-HPLC. Structures

(PDB accession IIRJ and IXK4) show that Met_{63}, Met_{83} and Met_{94} are relatively solvent-exposed and likely prone to oxidation whereas Met_{81} in S100A9 is buried in the interior and contributes to the dimer interface [69].

Oxidation of Trp and His residues was difficult to characterize and requires further analysis. His oxidation would be of particular interest, as the His-x-x-x-His binding motif is implicated in Zn^{2+} binding[621] (see Section 1.1.3.2) and oxidation of these residues may disrupt non-covalent heterocomplex formation with S100A8 and reduce the antimicrobial properties of the heterocomplex [620].

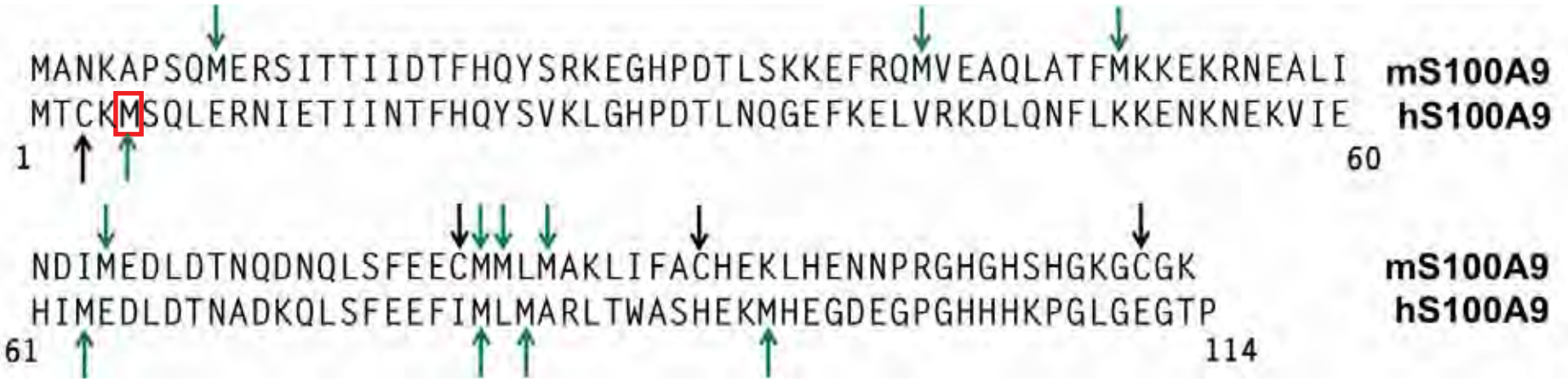

Figure. 3.21: Sequence alignment of mS100A9 and hS100A9. Sequence alignment of murine and human S100A9 shows that mS100A9 contains seven Met residues at positions 9, 41, 50, 64, 81, 82 and 84. hS100A9 contains five Met residues (positions 5, 63, 81, 83 and 94); only Met_{81} is conserved. Cys residues are not conserved; mS100A9 contains three Cys residues at postions 80, 91 and 111, whereas, hS100A9 has one at position 3. Cys residues are indicated by black arrows, Met by green arrows. Met_1 residues are cleaved in the final protein product. The alternate translational start site on Met_5 is indicated with red colour box.

Previously, our lab demonstrated that lysates of neutrophils activated with PMA, ionomycin or opsonized zymosan, contained a number of S100A9 oxidation products including oxidation of Met to Met(O) and Met-sulfone, and glutathionylation of Cys_3 [637]. Met-sulfone was evident in only one peptide in the studies performed here and may require higher amounts of HOCl or more localized oxidation with MPO/H_2O_2 *in situ*.

In summary, this study confirms that S100A8 and S100A9 scavenged hypohalous acid oxidants *in vitro.* These conclusions allowed us to propose that neutrophils and eosinophils activated during episodes of acute inflammation may generate novel adducts, and imply a protective role for these proteins. The results reported in this chapter form the framework for identification of post-translational modifications in S100A8 and S100A9 that may be generated *in vivo* under inflammatory conditions. Because in-gel digests were not considered optimal for generating sufficient peptides for MS analysis, we used the in-solution techniques described to characterize and compare post-translational modifications in S100A8 and S100A9 isolated from human asthmatic sputum (Chapter 4) and from diseased human carotid arteries (Chapter 5). Some functional implications of these modifications will be addressed, however, because analysis of oxidized His and Trp residues in this chapter were preliminary and require further study, these modifications were not studied in biological samples.

CHAPTER 4: S100A8 AND S100A9 ARE OXIDIZED BY HYPOHALOUS ACIDS *IN VIVO*

4.1 INTRODUCTION

Neutrophils are the predominant phagocytes of circulating blood and have various antimicrobial effector functions including production of hydrolytic enzymes, antimicrobial defensins, and cytokines and chemokines that initiate inflammatory responses and regulate leukocyte trafficking (reviewed in [986]). The generation of a respiratory burst, which produces ROS via the NADPH oxidase complex and the MPO system, represents a major antimicrobial function (see Section 1.4.1.5, Chapter 1) [987, 988]. Excess ROS, however, can amplify inflammation, either by non-physiological (such as necrotic) or regulated pathways (apoptotic pathway) [699].

ROS are principally generated by activated granulocytes and macrophages by NADPH oxidase, MPO and EPO. Oxidative stress and an imbalance of anti-oxidant defense mechanisms contribute to the pathogenesis of several lung diseases, including asthma. Oxidative stress contributes to progression, exacerbating inflammation and decreasing lung function [977](Fig. 4.1). ROS such as H_2O_2 can also transfer stimulating signals as critical intracellular second messengers, resulting in modulation of immune responses [989]. In the airways of asthmatics, loss of control of oxidants may bring about initiation of Th2-dominant immunity instead of inducing immune tolerance [990]. Oxidative stress indicators in asthma include excessive production of ROS by macrophages, neutrophils and eosinophils, and increases in exhaled markers of oxidative stress, such as NO, CO and H_2O_2 correlate with airway inflammation [965]. HOCl and HOBr promote common modifications such as 3-chloro/bromo-tyrosine which are associated with asthma severity [407]. As a consequence of these increases, pulmonary extracellular GPx and SOD are increased and there are decreased non-enzymatic anti-oxidants (vitamin C and E) in lung lining fluid. Subsequently, airway hyperresponsiveness is increased as is airway inflammation [965].

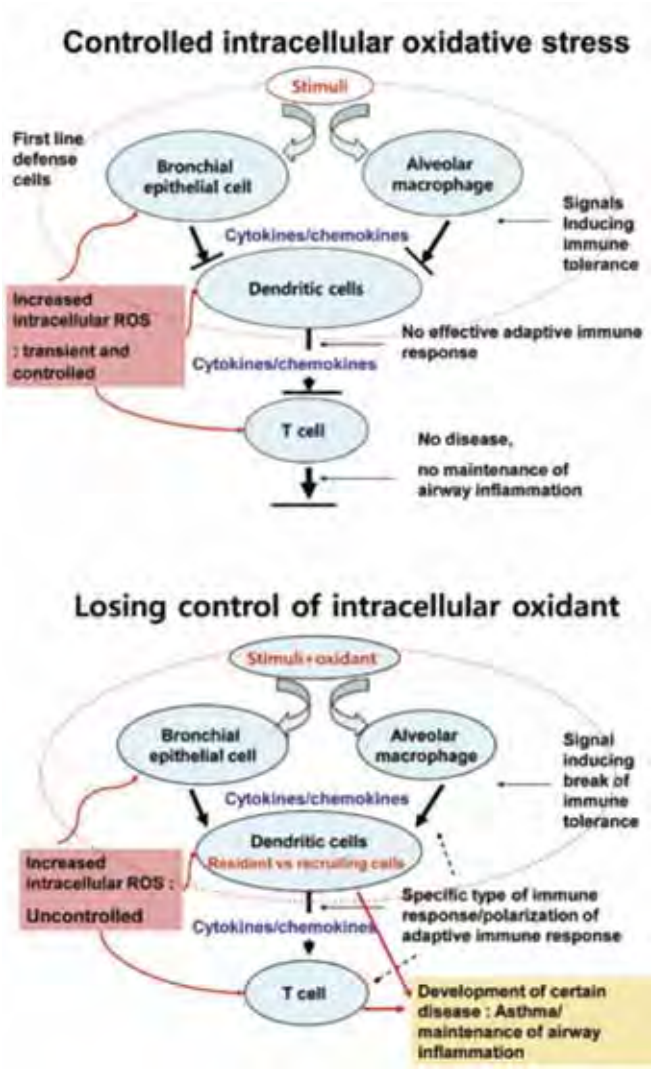

Figure 4.1: Comparison of oxidative stress control in health and disease in the lung. Normal regulation of oxidative stress involves co-ordinated regulation by a number of factors. In disease, the strict set of regulatory mediators is disrupted by excessive oxidant production. From [990].

In the context of bronchiectasis, exhaled H_2O_2 provides novel insights into the extent and severity of disease. Defined as a chronic suppurative airway disease with irreversible dilation of the bronchi, it is characterized by persistent purulent mucus production, with intense neutrophil recruitment into the lumen and tissue infiltration by neutrophils, monocytes and $CD4^+$ T lymphocytes [991-993]. H_2O_2 is increased in exhaled breath from patients with bronchiectasis, but is not decreased by inhaled glucocorticoids or long-term antibiotic treatment. Importantly, chronic colonization by *P. aeruginosa* significantly increases H_2O_2 concentrations in exhaled breath, indicating that bacterial colonization is critical to excess oxidant production in these patients [992]. H_2O_2 levels also provide an indirect indicator of neutrophilic inflammation, impairment of lung function, and extension and severity of disease [992].

ROS/RNS can directly modify signalling proteins through carbonylation, S-nitrosylation, disulfide bond formation and glutathionylation. These modifications can, in turn, also modulate cell signalling, regulating diverse physiological and pathological processes involved in cell development, differentiation, growth and death [994]. Reversible modifications (see Section 1.4.2.1, Chapter 1) may protect against permanent oxidative damage and/or modulate their functions. Other modifications, such as sulfonic acid or sulfinamide formation on Cys residues are irreversible and lead to loss of function, modifying proteins important in cell apoptosis and/or necrosis [995].

High plasma levels of S100A8, S100A9 and the heterocomplex are suggested markers of inflammatory disease activity [393]. Elevated levels of S100A9 (in BALF) and disease activity in subjects with sarcoidosis and IPF, compared to healthy volunteers were found [497, 521]. These proteins are upregulated in numerous cell types [18]. Epithelial cells and tracheal goblet cells from CF patients express S100A8/S100A9 [996] and they are upregulated in LPS-activated bronchial epithelial cells [996], suggesting a role in innate defense of bronchial epithelium. Proteomic studies identified these proteins in sputum from patients with bronchiectasis and CF [443]. Quantitiation of S100A8/A9 in BALF and sputum from patients with acute respiratory distress syndrome or CF indicated elevation compared to controls. Their differential expression is proposed to regulate distinct mechanisms in respiratory inflammation [496].

Because of their abundant expression in inflammation-associated disorders, S100A8 and S100A9 have been considered pro-inflammatory proteins [497, 520, 521, 970]. A recent report showed that a 0.5 Mb region of human chromosome 1q21, which includes S100A8 and S100A9 is significantly associated with elevated serum IgE levels in populations that include atopic asthma patients [997]. Halayko and Ghavami propose that S100A8/A9 may be associated with chronic allergic airway and lung inflammation that may be insensitive to steroid therapy [970].

S100A8 and S100A9 are also increased in CF patients with infective exacerbations, which upon treatment fall [443]. In healthy individuals, ROS-dependent NETs (see Section 1.2.2, Chapter 1) assist in eliminating fungal infections [998]. Neutrophils from patients with chronic granulomatous disease (CGD) are unable to make NETs and consequently these individuals are susceptible to infection with *Aspergillus* species [999]. *In vitro* experiments indicate that S100A8/S100A9 is NET-associated, and critical in antimicrobial and antifungal activity. In addition, NET formation is strictly dependent on NADPH oxidase [999]. Mice lacking S100A9 are also susceptible to

infection possibly due to a lack of Zn^{2+} chelation in the absence of the heterocomplex [999]. Bianchi *et al*. showed that by restoring NADPH oxidase, release of NETs and NET-associated S100A8/S100A9 was also restored, and growth of *Aspergillus nidulans (A. nidulans)* was inhibited *in vitro*. Restoration of NADPH oxidase by human CGD gene therapy with a γ-retroviral SF71gp91^{phox} vector in a patient with CGD resulted in clinical clearance of multifocal therapy-refractory *A. nidulans* lung infection [999], highlighting the unique relationship between S100A8/A9, ROS and antimicrobial function.

S100A8 and S100A9 may be important in oxidant scavenging and products may modulate inflammatory processes. For example, picomolar amounts of mS100A8 are chemotactic for neutrophils [317, 605]. Although rec-mS100A8 lacking Cys_{42} (substituted with Ala: Ala_{42}S100A8) maintains its chemotactic function, oxidation to the disulfide linked dimer reduced its chemotactic activity for leukocytes *in vitro* and *in vivo* [605]. Inhibition of activity is the result of reduced accessibility of the hinge domain, in turn inhibiting receptor interactions, rather than directly modifying amino acids within the chemotactic domain [606]. rec-hS100A8 exerts a fugetactic effect on leukocytes at 10^{-9} M and oxidation of Cys_{42} by HOCl ameliorated this function [612]. The Cys_{42}-Ala_{42}S100A8 mutant generated a form that suppressed leukocyte recruitment to the air-pouch of rats after LPS administration [612]. These observations imply that S100A8 functions may be tightly regulated by its localized tissue concentrations and post-translational modifications, particularly caused by oxidation on Cys_{42}.

S100A8 inhibits MC activation by IgE-antigen by scavenging ROS essential for signalling, and suppressed acute murine asthma by reducing key cytokines affecting eosinophil migration and mucus production [644]. S-nitrosylated S100A8 can trans-nitrosylate hemoglobin. Hemoglobin-SNO, important in maintaining blood vessel tone and formed during inflammation, may contribute to vessel patency in the microcirculation. Thus, S100A8, particularly when expressed in endothelial cells, may modulate vessel tone during inflammation [613].

Some extracellular functions of S100A9 may also be modified by oxidation. For example, Met_{63} and Met_{83} are proposed as necessary for S100A9-mediated migration of neutrophils *in vitro* and Met oxidation may be the main determinant in regulating this process [614]. S100A9 increases neutrophil adhesion to fibronectin [611]. Our lab showed that neutrophils stimulated with rec-hS100A9 or rec-hS100A8/A9 were adherent to levels comparable to activation by fMLP. When the S-glutathionylated S100A9

(S100A9-SSG) was complexed with S100A8, neutrophil adhesion to fibronectin was ablated. Differences in reactivity of the heterocomplexes may be due to conformational changes. S100A9-SSG may protect the protein from further oxidation to higher oligomers and reduce neutrophil binding to the extracellular matrix, regulating the magnitude of neutrophil migration in the extravasculature, thereby limiting tissue damage in acute inflammation [637].

Despite several studies examining expression of S100A8 and S100A9 in asthma and other respiratory diseases [443, 496, 970], the functions of these proteins in these diseases is not well characterized and little attention has been given to the functional consequences of potential post-translational modifications caused by oxidation.

S100A12 is relatively resistant to oxidation because it has no Cys or Met residues, but is associated with respiratory diseases, particularly asthma, CF, COPD and ARDS [131, 443, 496, 996]. Although studies have included patients with bronchiectasis in cohort studies, they are grouped and analyzed in categories that contain other respiratory diseases [131], or are grouped together with subjects who also have CF [493], making comparisons with non-CF bronchiectasis difficult. For this reason, a comparative analysis of S100A12 in saliva and sputum from asthmatic and bronchiectatic subjects was undertaken.

In this chapter, we show hS100A8, ox-hS100A8 and hS100A9 in asthmatic, but not normal human lung; asthmatic sputum had significantly more oxS100A8 than controls. Although S100A12 in sputum and saliva was analyzed by Western blotting and ELISA, levels were not significant relative to samples from control subjects. Since S100A8 and S100A9 were likely to represent the most likely HOCl scavengers, this work focused on characterizing modifications generated *in vivo*. S100A8 from asthmatic sputum contained sulfinic and sulfonic acid intermediates, and novel oxathiazolidine-oxide/dioxide forms, (mass additions, m/z +30 and +46) on the single Cys_{42} residue. Evidence for Cys_{42} oxidation products was weak in control sputum. S100A9 from asthmatic sputum was converted to $Met_{63/81/94}$ (O) *in vivo*. Recombinant oxS100A8/S100A9 abrogated neutrophil adhesion and antimicrobial activity. Results suggest that the oxidant-scavenging capacities, and the oxidation products generated in S100A8 and/or S100A9 may modulate inflammatory responses.

4.2 EXPERIMENTAL PROCEDURES

4.2.1 IMMUNOHISTOCHEMISTRY

Apparently normal portions of lungs from patients undergoing surgery for lung carcinoma (Central Area Health Service, Sydney, Australia) were obtained with consent under ethical guidelines. Asthmatic lung specimens were from Prof. Judy Black (University of Sydney, Australia), obtained with consent. This section of the work was performed in collaboration with Dr.Weixing Yan (UNSW, Australia), formalin-fixed, paraffin-embedded tissues (2-micron serial sections) or cytospin preparations of normal human neutrophils were processed and immunostained as detailed [410]. Rabbit anti-S100A8, anti-oxS100A8, anti-S100A9, or normal rabbit IgG (Dako) (all 5 μg/ml) were used after blocking with normal goat serum (Sigma, MO, USA; 1:5 v/v in PBS). Anti-oxS100A8 IgG, raised against HOCl-oxS100A8, recognizes the oxidized monomer and higher complexes more strongly than does anti-S100A8 [410]. Secondary antibody was biotinylated goat anti-rabbit IgG (Chemicon, Vic, Australia), identified by alkaline phosphatase staining (AP)-red (Vector Laboratory, CA, USA); counterstaining was with Mayer's hematoxylin (Sigma, MO, USA).

4.2.2 PATIENT RECRUITMENT AND SAMPLE PREPARATION

Stable asthmatic, bronchiectatic and control subjects were recruited by A/Prof. Paul Thomas, from the Respiratory Medicine Department, Prince of Wales Hospital Sydney, under protocols approved by the Human Research Ethics Committee of the South Eastern Sydney Area Health Service. After appropriate training, spirometry was performed on each subject to assess airway function, according to American Thoracic Society/European Respiratory Society guidelines. Using a Micro Direct Microlab spirometer (Micro Direct, ME, USA) the best value of three manoeuvres was chosen for FVC, FEV_1 and FEV_1/FVC. Subjects were assessed for smoking history, age, previous/existing medical conditions and current medications and atopy; subjects with allergic exacerbations were excluded. Spirometry confirmed that asthmatic and bronchiectatic patients had reduced lung function compared to control subjects (Table 4.1).

Table 4.1: Subject data

Subject group	Control	Stable asthma	Bronchiectasis
M/F	6/6	5/9	5/5
Age Mean (±SD)	47.75 (±22.85)	51.33 (±19.68)	62.1 (±16.50)
Range (yr)	21-84	24-81	32-84
Smoker	0	3	1
Non-smoker	9	7	7
Ex-smoker	3	4	2
Atopy	3	8	2
FEV_1 (L) (±SD)	2.95 ± 0.25	2.18 ± 0.31	1.38±0.15
FEV_1 (%) (±SD)	98.9 ± 5.33	77.6 ± 7.12	55.00±7.47
FVC (L) (±SD)	3.8 ± 0.29	2.84 ± 0.303	2.096± 0.14
FEV_1/FVC (%) (±SD)	90.93 ± 3.94	73.67 ± 4.63	64.83± 5.18
Steroids	0	14	4

TABLE 4.1: Subject characteristics. Clinical characteristics of control subjects (n=12), and those with stable asthma (n=14) or bronchiectasis (n=10). *Definition of abbreviations:* FEV_1 (L), Forced Expiratory Volume in 1 second, a measurement by a spirometer of the amount of air the lungs can hold; FEV_1 (%), percentage of actual value/predicted value (based on age, height and gender); FVC, Forced Vital Capacity, a measurement by a spirometer of the amount of air the lungs can hold; FEV_1/FVC (%), percentage of FEV_1 to FVC. All asthmatics subjects were on inhaled steroids.

4.2.3 ASSESSMENT OF S100A8, S100A9 AND S100A12 IN SPUTUM

Sputum and saliva from asthmatic, bronchiectatic and control subjects was diluted in PBS/0.1% DTT (1:4 v/v), centrifuged (10 min, 400 x g) and supernatants stored under argon (to prevent spontaneous oxidation) at -80ºC. DTT was required to disperse mucus [1000]. Protein levels were determined by the Bradford assay (Bio-Rad, CA, USA). Sputum proteins (1.5 μg) resolved by 10% SDS-PAGE were silver stained, or Western blotted. As anti-oxS100A8 ELISAs could not be performed, semi-quantitative analysis of anti-oxS100A8 Western blot membranes was performed as follows: images of Western blots were quantified using Gel-Pro Analyzer software (Media Cybernetics, MD, USA). Levels of S100A8 (10 kDa) or oxS100A8 monomer (10 kDa) were quantitated as arbitrary net intensity units, compared to intensities of 250, 100, 50, 25 ng recS100A8 or 500, 250, 100, 50 ng rec-oxS100A8 monomer that were used to contract standard curves for more quantitative measurement. Standards (250 ng) were routinely separated on the same gel. Density of standard bands was given a value of 1; densities of samples expressed as a ratio; bands of density greater than the standard were > 1, and those less than the standard, < 1.

S100A8, S100A9 and S100A12 levels in duplicate sputum samples were quantified by ELISA (see Section 2.1.6, Chapter 2) [410]; recombinant standards contained 0.1% DTT. Amounts were expressed as ratios with respect to total protein (expressed as units). oxS100A8 in sputum could not be quantitated by ELISA because DTT interfered with antibody binding on solid phase.

4.2.4 PREPARATION AND ANALYSIS OF S100A8 AND S100A9 IN SPUTUM

Sputum proteins were initially separated on C8-RP-HPLC (33-59% acetonitrile/0.1% TFA) and then peaks resolved by C4-RP-HPLC (see Section 2.1.4, Chapter 2). The following protocol was developed to detect putative modifications generated in S100A8 and S100A9 *in vivo.* Proteins in sputum (600 μg; n=2 for control and n=5 for asthmatic) were eluted from C8-RP-HPLC in 33-59% acetonitrile/0.1% TFA.

Control samples eluted as three major peaks at 13.8, 14.5 min (which were pooled) and 15-18 min, and asthmatic sputum proteins eluted in a major peak at 11.7-12.6 min that were collected and analyzed; C8-RP-HPLC eluates were lyophilised, suspended in PBS (10 μl) and separated by SDS-PAGE under reducing conditions (0.1% DTT), then Western blotted, with anti-S100A8, anti-oxS100A8 or anti-S100A9 IgG. The pooled

peaks eluting between 12-15 min (control sputum) contained predominantly S100A8, oxS100A8 and minor amounts of S100A9. S100A9 was the major protein in the peak eluting at 15-18 min. Asthmatic sputum contained abundant S100A8, oxS100A8 and S100A9 in the single peak collected. Peaks from control and asthmatic sputum collected from C8-RP-HPLC were further resolved by C4-RP-HPLC (25-70% acetonitrile/0.1% TFA). Western blotting of 500 μl lyophilized C4-RP-HPLC eluate from control sputum (peaks eluted at 15-18 min and 18-21 min) confirmed presence/absence of oxS100A8, S100A8 and S100A9. In asthmatic sputum, S100A8 and S100A9 purified by C4-RP-HPLC were found in peaks eluting at 14.3, 15.3 min, confirmed by Western blotting. Control and asthmatic sputum fractions separated by RP-HPLC were stored under argon at -20°C to prevent spontaneous oxidation.

Due to the varying strengths of the antibodies, and to minimize cross-reactivity, membranes were probed sequentially for anti-oxS100A8, -S100A9 then -S100A8 IgG. Following reactivity with one antibody, membranes were stripped (0.2 M glycine, 0.05% Tween 20, pH 2.5) for 40 min at 80ºC, washed with TBS for 10 min Membranes were then probed with anti-oxS100A8, -S100A8, -S100A9 IgG. Reactions were detected by chemiluminescence as described in Section 2.1.3).

Proteins in the lyophilized peaks (5 μg) were suspended in 20 mM NH_4HCO_3 (100 μl) and digested (50 ng, 4 hrs at 37°C) with AspN or trypsin. Protein mass measurements were acquired as described (see Section 2.1.8, Chapter 2) [637].

4.2.5 CROSS-LINKING OF OXS100A8 AND OXS100A9

To investigate effects of oxidation on heterocomplex formation, equimolar amounts (0.4 μM) of recombinant S100A8, S100A9, oxS100A8 or oxS100A9 were suspended in PBS (with 1 mM $CaCl_2$) and various combinations incubated for 37°C for 30 min, then putative complexes cross-linked with BS_3 cross-linker (1 mM) (Pierce, IL, USA) for an additional 30 min in the dark. Samples without BS_3 were used as controls. Mixtures were separated by 10% SDS-PAGE under non-reducing conditions, then silver-stained.

4.2.6 NEUTROPHIL ADHESION

The S100A8/S100A9 complex does not alter adhesion but is released from transmigrating neutrophils [431]. Effects of oxidation on basal adhesion were tested, with

the assistance of Dr. Su Yin Lim (UNSW, Australia), using the Real-time Cell Analyzer xCELLigence system (Roche, Mannheim, Germany); E-Plates (96-well), containing electrodes measure cell index (CI) based on impedance [1001] were coated with 50 μg/ml fibronectin (Sigma, MO, USA) at 4ºC overnight, then blocked with 1% BSA/PBS for 2 hrs. Neutrophils (10^7/ml) from 5 healthy donors prepared were isolated from citrated blood, using density gradient centrifugation with Ficoll-Paque Plus (GE Healthcare, Rydelmere, Australia) [637]. Neutrophils were mixed with recombinant S100A8/A9, oxS100A8/oxS100A9, oxS100A8/A9, S100A8/oxS100A9 (1 μM) or the positive control, fMLP (Sigma;1 μM) in 1% BSA/RPMI-1640 (Gibco, Invitrogen Australia) in triplicate and immediately transferred to wells (10^6) or were pre-treated with the proteins for 10 min before adding fMLP. Concentrations of oxS100A8 and oxS100A9 (1 μM) were comparable to those used in previous studies [611, 637]. CIs were measured every 15 s for 2 hrs and directly correlated with adherent neutrophil numbers; mean CI values ± SEM were obtained using the software provided.

4.2.7 ANTIBACTERIAL ACTIVITY OF S100A8/S100A9

The antimicrobial activity of S100A8 and S100A9 is optimal as the heterocomplex [18, 620]. Antimicrobial experiments were performed under the guidance of microbiologist, Prof. Hazel Mitchell (UNSW, Australia). Initial experiments focused on *Streptococcus pneumoniae* (*S. pneumoniae*) as this bacterium is commonly found in patients with asthma [1002, 1003] and is sensitive to the antimicrobial properties of calprotectin [9]. However, due to its mucinous properties, *S. pneumoniae* can be difficult to grow as single colonies (personal communication, Prof. Hazel Mitchell), hence it was necessary to first confirm that single colonies could be grown and accurately counted. Briefly, streaked *S. pneumonia* (clinical isolate, stock no. PN66, obtained from Prince of Wales Hospital, Australia) were picked and suspended in 2.5 ml saline (10^5 colony forming units). The mixture was pipetted onto blood agar plates (0.4% agar with 5% horse blood, Oxoid, Hampshire, UK) excess liquid was removed with a pipette and then plates air dried for 20 min at RT, then incubated overnight at 37°C. We found very poor separation of colonies and subsequent serial dilutions (10^4 and 10^3) did not improve separation of colonies. Because these were considered too difficult to quantitate, an alternate bacterium was used.

Because calprotectin elicits an antimicrobial response against *E. coli*, this was chosen for subsequent experiments. The calprotectin complex has better antimicrobial activities than the protein alone [655], so four preparations were used: recombinant S100A8/S100A9, oxS100A8/S100A9, S100A8/oxS100A9 and oxS100A8/oxS100A9. Recombinant S100A8 or oxS100A8 (25 μg), or S100A9 or oxS100A9 (35 μg; 25 μM final concentration) lyophilized with 5 μl PBS, resuspended in 40 μl Luria broth supplemented with 1 mM $CaCl_2$, mixed and incubated for 30 min at 37°C before addition to *E. coli* K12. *E. coli* K12 (stock no. 10798; ATCC) were cultured overnight at 37°C on 1.5% Luria agar plates, then an appropriate number of colonies harvested and resuspended in 1.8 ml Luria broth supplemented with 1 mM $CaCl_2$, to a final concentration of 10^5 colony forming units (CFU)/ml (determined by the optical density of McFarland standards at $A_{450\ nm}$; bioMérieux Australia, NSW, Australia). To determine effects of heterocomplexes on viability, *E. coli* suspensions were diluted 1:4 v/v with Luria broth and added to a sterile Nunc polyethylene tube (Roskilde, Denmark). S100 proteins do not adhere to these tubes, ensuring that observed effects were due to activity of S100 complexes containing the S100s; controls contained 40 μl Luria broth and 10 μl PBS.

To confirm *E. coli* concentrations at assay commencement, 10 μl *E. coli* suspension was removed, diluted to $1x10^{-6}$ CFU, and 50 μl applied to 1.5% Luria broth agar plates incubated for 24 hrs and colonies counted manually. After 24 hrs, 10 μl solution from each assay were diluted to 10^{-6} CFU and 50 μl added to 1.5% Luria broth agar and colony numbers determined after 24 hrs after plating. All assays were conducted in duplicate and results expressed as CFU relative to untreated control.

4.2.8 STATISTICAL ANALYSIS

Comparisons of ELISA results (specific levels) between groups and densitometry were analyzed using a one-way ANOVA in conjunction with Bonferonni's multiple comparison tests, which allowed for comparisons between each of the groups. Comparisons between saliva and sputum protein levels were analyzed by a one-tailed unpaired t-test. For neutrophil adhesion, data were analyzed using repeated measures ANOVA followed by Bonferroni post-test for multiple comparisons. Values are reported as means ± SEM; statistical significance was set at $P < 0.05$. Statistical analysis of the antibacterial experiments was as follows: averages of each replicate condition (2 data

points) (for example, rec-oxS100A8/oxS100A9 vs *E. coli* alone) were divided by the overall average (4 data points) of each replicate from the control condition (*E. coli* alone). Final data was analyzed by one-way ANOVA with Bonferroni post-test for multiple comparisons relative to *E. coli* treated with S100A8/S100A9 (for example, S100A8/S100A9 vs. oxS100A8/oxS100A9).

4.3 RESULTS

4.3.1 S100 EXPRESSION IN ASTHMATIC LUNG

In collaboration with Dr. Weixing Yan (UNSW, Australia), immunostaining showed more intense oxS100A8 reactivity (Fig. 4.2, middle panel) than S100A8 (Fig. 4.2, left panel) in asthmatic lung compared to apparently normal lung (lower panels). Positive eosinophils, some neutrophils and macrophages localized beneath the basement membrane of the airways and within the lung parenchyma. In contrast, immunoreactivity of oxS100A8 in normal human neutrophils (Fig. 4.2, inset middle panel) was negligible, whereas, as expected, reactivity with anti-S100A8 was strong (Fig. 4.2, inset left panel). S100A9 localized in a similar pattern (Fig. 4.2, right panel).

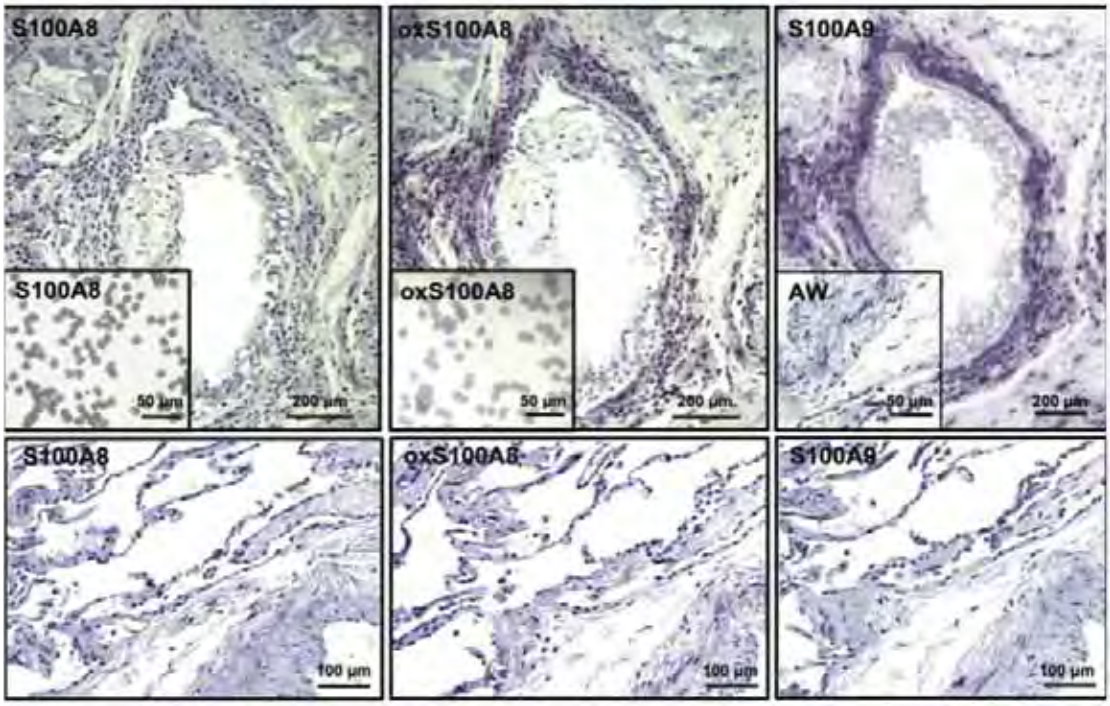

Figure 4.2: S100A8, oxS100A8 and S100A9 in asthmatic lung and sputum. Positive immunoreactivity (indicated by red staining) of S100A8 (left panel) and oxS100A8 (middle panel) was seen in the airway lining in serial sections from an asthmatic lung, representative of five different specimens. Neutrophils, eosinophils and some macrophages were immunoreactive, mostly accumulated beneath the basement membrane of bronchioles and spread within the lung parenchyma; the few immunoreactive cells seen in sections from non-asthmatic lung (lower panels) were confined to leukocytes within blood vessels. Human neutrophils reacted very weakly to anti-oxS100A8 (inset, middle panel) whereas S100A8 reactivity (inset, left panel) was strong. S100A9 (right panel) was expressed in a similar pattern. IgG control of asthmatic lung is shown in inset, right panel.

4.3.2 LEVELS OF S100A8 AND S100A9 IN SPUTUM

Levels of total protein in saliva ($P < 0.01$) and sputum ($P < 0.05$) from subjects with bronchiectasis were significantly higher compared to control and asthmatic subjects (not shown). Control, asthmatic and bronchiectatic subjects had sputum that contained significantly higher amounts of total protein relative to saliva ($P = 0.015$, $P = 0.0006$ and $P = 0.044$) (not shown).

Control saliva contained somewhat more S100A8 (not significant), than control sputum (saliva: 0.015 ± 0.007 units and sputum: 0.0020 ± 0.0009 units; not shown), whereas control saliva contained significantly more S100A9 than sputum (saliva: 0.0036 ± 0.001 units and sputum: 0.0012 ± 0.0003 units, $P = 0.024$; not shown).

Levels of S100A8 in asthmatic saliva were not significantly different to sputum (saliva: 0.0015 ± 0.0006 units and sputum: 0.0026± 0.0015 units; not shown). Similarly, S100A8 levels in bronchiectatic saliva were not different to those in sputum (saliva: 0.00024 ± 0.00006 units and sputum: 0.00045 ± 0.0001 units; not shown). S100A9 levels, although elevated in saliva were not significantly different to those in sputum from asthmatic, because of two outlying samples (saliva: 0.1050582 ± 0.006 units and sputum: 0.0031 ± 0.0008 units; not shown) and amounts in bronchiectatic samples were similar (saliva: 0.0030 ± 0.0007 units and sputum: 0.0033 ± 0.0009 units; not shown).

S100A8 levels in asthmatic, bronchiectatic and control sputum were similar (Fig. 4.3A). Sputum from 2/3 control subjects with atopy had elevated levels whereas this was the case only in 2/8 asthmatic subjects, and increases were marginal. Of two bronchiectatic subjects with atopy, no elevation in S100A8 levels was seen. S100A9 tended to be higher in asthmatic and bronchiectatic sputum, but was not significantly more than controls (Fig. 4.3B). Of these, 4/8 and 1/2 atopic asthmatic and bronchiectatic subjects, respectively, had levels higher than the mean. There was no obvious relationship between smoking and S100A8 or S100A9 levels in sputum from any group tested.

Multimeric S100A8 and S100A9 are present in diseased carotid artery samples that likely were exposed to conditions where excess ROS are generated [410]. Because sputum samples the airways, particular attention was given to identifying monomeric and multimeric S100 protein components in sputum from all subgroups as a means of initially visualizing oxidant-induced, cross-linked protein, which may have formed as a result of oxidizing conditions in the lung. Silver staining of sputum separated by SDS-PAGE showed 10 kDa and 14 kDa components, equivalent to masses of S100A8 and S100A9,

respectively, in most asthmatic, bronchiectatic and some control samples, although amounts varied between groups (Fig. 4.3C). Because of the complex nature of the sputum samples, Western blotting was conducted to identify S100A8, S100A9 and S100A12 (S100A12 protein in sputum is discussed in Section 4.3.3). Anti-S100A8 IgG reacted weakly with 5/12 control samples, and strongly with 9/14 asthmatic samples and 7/10 bronchiectatic samples (Fig. 4.3D). Strong anti-oxS100A8 IgG reactivity was seen in 12/14 asthmatic, 7/10 bronchiectatic and more weakly in 4/12 control sputum samples (Fig. 4.3E). In all samples, only monomeric S100A8 was obvious, with no evidence of DTT-resistant complexes.

Western blotting of control sputum with anti-S100A9 IgG (Fig. 4.3F) indicated strong reactivity in 5/12 samples; reactivity was obvious in 9/14 asthmatic samples but only one contained obvious homodimer. Anti-S100A9 IgG reactivity was strong in sputum from 7/10 bronchiectatic subjects. Other research groups have used the monoclonal antibody 27E10 to detect the heterodimer (non-covalently bound S100A8 and S100A9) [593, 655]. The anti-S100A9 polyclonal IgG generated by us recognizes the 24 kDa heterocomplex although binding epitopes are uncharacterized. This 24 kDa component was found in sputum from 2/12 control, 3/14 asthmatic and 3/10 bronchiectatic subjects. AntiS100A8 IgG did not cross-react with the S100A8/S100A9 complex.

oxS100A8 in sputum could not be quantitated by ELISA as samples contained DTT, which interfered with binding of the antibody in solid phase. Hence, samples were Western blotted with oxS100A8 and S100A8 IgG and semi-quantitated using densitometry. Some 2.3 fold more S100A8 was found in asthmatic sputum and ~ 6.7 times more S100A8 was present in bronchiectatic sputum relative to controls ($P < 0.05$; Fig. 4.3G). In marked contrast, there was significantly more oxS100A8 (14.7 times) in asthmatic sputum compared to control sputum ($P < 0.05$; Fig. 4.3H). Because of the relative abundance of oxidized S100A8 in asthmatic subjects, this subgroup was chosen as the potential source for analysis.

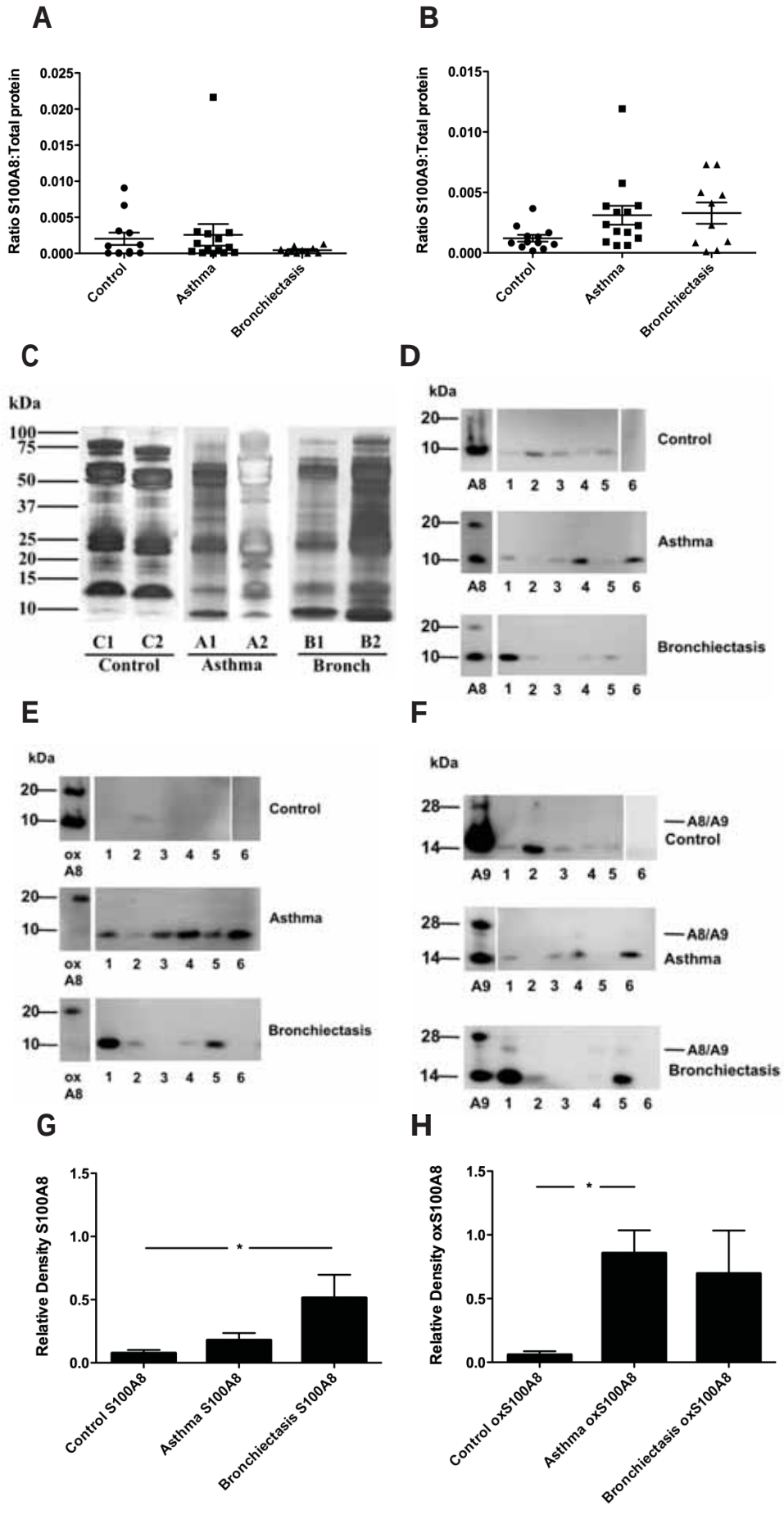
A
Ratio S100A8:Total protein
0.025
0.020
0.015
0.010
0.005
0.000
Control
Asthma
Bronchiectasis
B
Ratio S100A9:Total protein
0.015
0.010
0.005
0.000
Control
Asthma
Bronchiectasis
C
kDa
100
75
50
37
25
20
15
10
C1 C2 A1 A2 B1 B2
Control
Asthma
Bronch
D
kDa
20
10
A8 1 2 3 4 5 6
Control
Asthma
Bronchiectasis
E
kDa
20
10
ox A8 1 2 3 4 5 6
Control
Asthma
Bronchiectasis
F
kDa
28
14
A9 1 2 3 4 5 6
A8/A9
Control
A8/A9
Asthma
A8/A9
Bronchiectasis
G
Relative Density S100A8
1.5
1.0
0.5
0.0
*
Control S100A8
Asthma S100A8
Bronchiectasis S100A8
H
Relative Density oxS100A8
1.5
1.0
0.5
0.0
*
Control oxS100A8
Asthma oxS100A8
Bronchiectasis oxS100A8

Figure 4.3: S100A8 and S100A9 in sputum. (**A**) S100A8 in sputum, measured by ELISA (analyzed by one-way ANOVA in conjunction with Bonferonni's multiple comparison tests), was higher in asthmatic compared to control subjects, but not significantly different. Bronchiectatic sputum had similar S100A8 levels to control subjects; control: n=12; asthma: n=14; bronchiectasis: n=10. (**B**) S100A9 levels in sputum measured by ELISA tended to be higher in samples from asthmatic and bronchiectatic subjects compared to control subjects, although differences were not statistically significant. Results are means ± SEM. (**C**) Sputum (4 μg) from control, asthmatic and bronchiectatic (shown as bronch) subjects was separated by SDS-PAGE and silver-stained. Most samples contained components migrating at 10 kDa and 14 kDa (corresponding to S100A8 and S100A9 respectively). (**D**) Western blotting of sputum (1.5 μg) from asthmatic subjects indicated anti-S100A8 immunoreactivity with a 10 kDa component in 9/14 samples; Western blotting of 7/10 sputum samples from bronchiectatic samples were reactive, whereas immunoreactivity was observed in only 5/12 control subjects (**E**) Positive reactivity with anti-oxS100A8 was obvious in 12/14 asthmatic samples; Samples from 4/12 control subjects reacted relatively weakly with anti-oxS100A8 IgG. Western blotting of sputum from bronchiectatic subjects with anti-oxS100A8 indicated immunoreactivity with a 10 kDa component in 7/10 samples. (**F**) Positive reactivity with anti-S100A9 IgG was apparent in 5/12 control samples. The S100A8/A9 heterodimer was observed in two samples. Anti-S100A9 IgG reactivity was seen in 9/14 asthmatic samples. Anti-S100A9 IgG reactivity was observed in sputum from 7/10 bronchiectatic subjects; 3/10 contained heterocomplex (24 kDa). Results of the 6 subjects shown are representative of all samples analyzed by Western blotting. As samples were blotted on multiple membranes, Western blots shown are intended to illustrate variations in S100 protein amounts and banding patterns within samples from the same subgroup. This is representative of all samples analyzed. (**G**) Intensities of components migrating at 10 kDa were quantified, relative to a 250 ng protein standard of S100A8 or oxS100A8. Although asthmatic and bronchiectatic sputum contained more S100A8, only bronchiectatic sputum had significantly elevated levels compared to control sputum (analyzed by one-way ANOVA in conjunction with Bonferonni's multiple comparison tests; * $P < 0.05$ between control and asthmatic sputum levels of oxS100A8. Results are means ± SEM). (**H**) Intensities of bands migrating at 10 kDa; * $P < 0.05$ between control and asthmatic sputum levels of oxS100A8. Results are means ± SEMof control: n=12; asthma: n=14; bronchiectasis: n=10.

4.3.3 S100A12 IN SPUTUM

Our group showed that S100A12 was significantly raised in sputum from subjects with eosinophilic asthma compared to other types of asthma (e.g. neutrophilic asthma) [131]. Because sputum samples from bronchiectatic subjects were available and these had not been previously analyzed, S100A12 levels in all patient subgroups were investigated by Western blotting and ELISA. Western blotting of saliva and sputum showed little reactivity with anti-S100A12 IgG (Fig. 4.4A).

Quantitation by ELISA indicated that S100A12 levels (control saliva: 0.0089 ± 0.004 units; sputum: 0.0015 ± 0.0006 units; asthma saliva: 0.011 ± 0.007 units; sputum: 0.0054 ± 0.003 units; bronchiectasis saliva: 0.0025 ± 0.0005 units; sputum: 0.0017 ± 0.0003 units, not shown) in saliva, although elevated, were only significantly more than in sputum from control donors (not shown; $P = 0.044$). S100A12 in sputum from asthmatic subjects was higher than in bronchiectatic or control sputum, but levels were not significantly different (Fig. 4.4B). Three control subjects were atopic, but S100A12 levels in these samples were not greater than the mean. Only 1/8 asthmatic subjects with atopy had S100A12 levels higher than the mean (~7.6 times higher). As with S100A8 and S100A9, no relationship between smoking and S100A12 levels in sputum was obvious in any group tested. S100A12 does not have Trp residues, but does contain five His residues that may be susceptible to oxidation by hypohalous acids [948]. However, because of the relatively low levels compared to S100A8, further characterization was not pursued.

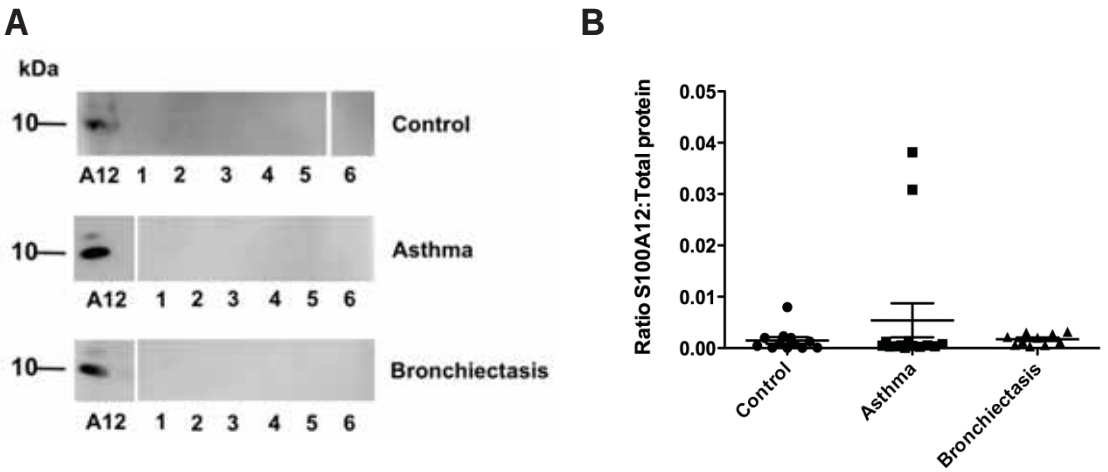

Figure 4.4: S100A12 in sputum. (**A**) Western blotting of sputum showed no visible immunoreactive components in any subgroup tested (250 ng of recS100A12 used as standard). The six subjects shown are representive of all subjects analyzed by Western blotting (**B**) S100A12 in sputum, measured by ELISA, was higher in asthmatic compared to control subjects, but differences did not reach significance. Bronchiectatic sputum had similar S100A12 levels to control subjects; control: n=12; asthma: n=14; bronchiectasis: n=10.

4.3.4 NOVEL OXATHIAZOLIDINE-DIOXIDE MODIFICATIONS IN S100A8

Because there was a relative abundance of oxS100A8 in asthmatic samples, we initially attempted to use in-gel tryptic digests of monomeric anti-S100A8-reactive components from two asthmatic subjects. However, as for native and recombinant oxS100A8, in-gel digests did not generate sufficient quantities of peptides for analysis of oxidative modifications for lower abundance samples (see Section 3.3.2, Chapter 3), although a Cys_{42}-sulfonic acid modification was found on the peptide LLETECPQYIR. No other oxidative modifications were observed. For this reason, S100A8 from control and asthmatic sputum was enriched by RP-HPLC. This new method of enrichment (described in Section 4.2.4) was developed to enable characterization of oxS100A8 fragments after cleavage in solution.

Sputum from 2 control subjects was separated by RP-HPLC. Control sputum contained ~ 14.7-fold less oxS100A8 protein (0.058 ± 0.03 net units) than asthmatic sputum, calculated by densitometry of whole sputum samples (0.86 ± 0.2 net units; see Section 4.3.2, Fig. 4.3H). Control sputum eluted as three poorly-separated broad peaks (12-15 min aliquot comprised two peaks, peak 1 at 13.8 min and peak 2 at 14.5 min, which were pooled, and another eluting at 15-18 min) from C8-RP-HPLC (Fig. 4.5A). Western blotting confirmed that oxS100A8 and S100A8 were predominantly present in the 12-15 min aliquot of C8 RP-HPLC-enriched samples (12-15 min; Fig. 4.5B, left and middle panels); DTT-resistant covalent S100A8 complexes were obvious in both peaks, low levels of dimer (20 kDa) were present in the 12-15 min aliquot and a complex migrating at 34 kDa was present in the 15-18 min aliquot. Although this had a putative mass of 34 kDa, which could indicate $S100A8_2$/S100A9, it did not react with anti-S100A9 IgG, which reacts with S100A8/S100A9 heterocomplexes whereas anti-S100A8 does not, and so may represent S100A8 complexed with another binding partner *in vivo* (Fig. 4.5B, middle panel). Monomeric S100A9 eluted predominantly at 15-18 min from C8-RP-HPLC; low amounts of $S100A9_2$ (28 kDa; Fig. 4.5B, right panel) were present.

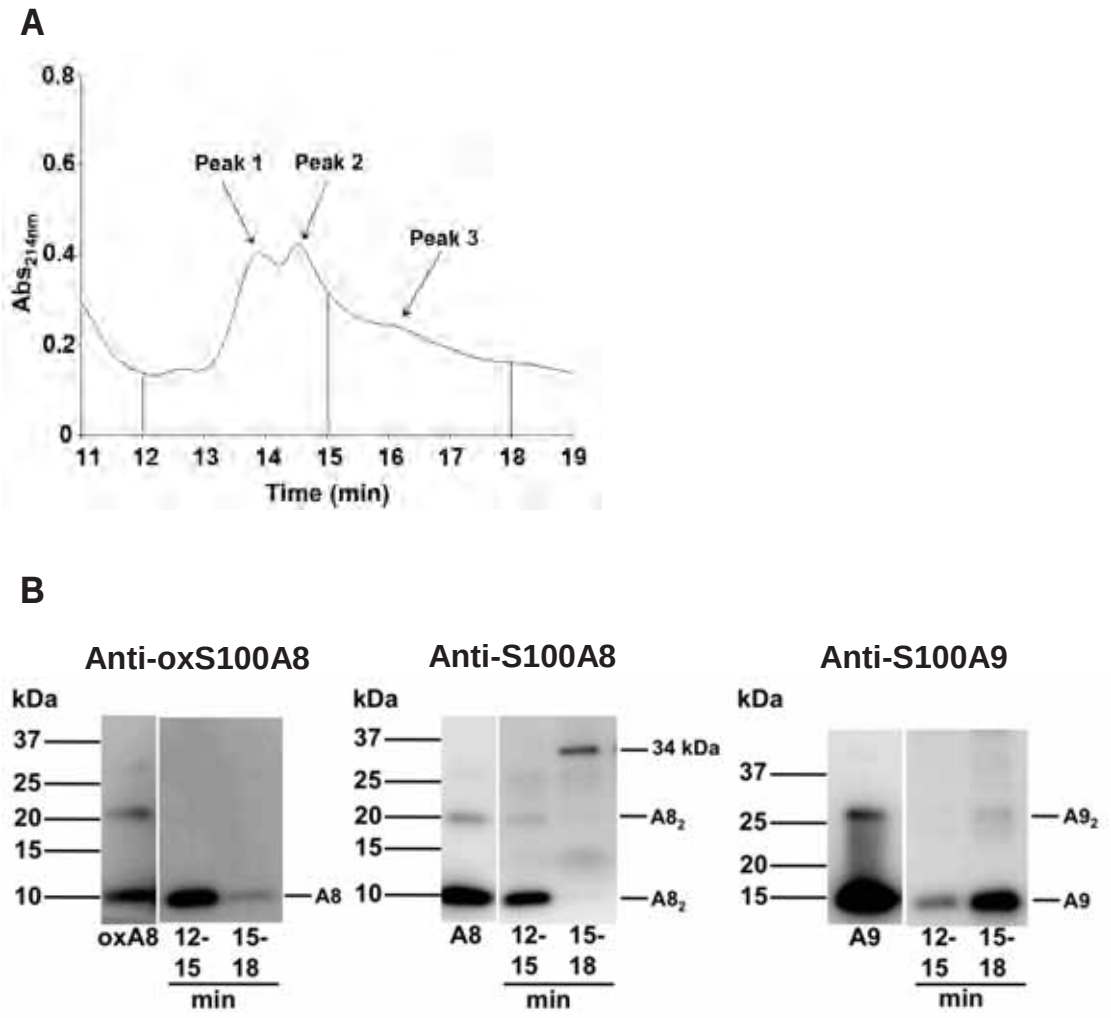

Figure 4.5: S100A8 and S100A9 in control sputum. (**A**) Control sputum (600 μg) eluted from C8-RP-HPLC as three peaks at 13.8 min, 14.5 min (pooled) and 15-18 min. (**B**) Western blotting of Peaks 1 and 2 (12-15 min; 500 μl lyophilized from C8-RP-HPLC) indicated immunoreactivity with anti-oxS100A8, anti-S100A8 and anti-S100A9 antibodies; Peak 3 (15-18 min) indicated monomeric S100A9 and slight reactivity with the dimer (~28 kDa). A complex migrating at 34 kDa was identified by anti-S100A8. Data presented is representative of two samples of enriched control sputum.

Pooled peaks 1 and 2 from C8-RP-HPLC (Fig. 4.5A, 12-15 min) were further separated and enriched by C4-RP-HPLC which resolved a major peak (Fig. 4.6A, profile 1, peak 1: 15-18 min) and a minor peak (Fig. 4.6A, profile 1, peak 2: 18-21 min). Peak 3 from C8-RP-HPLC (Fig. 4.5A, 15-18 min pool) eluted as two minor peaks at 16.5 min and 18-18.5 min (Fig. 4.6A, profile 2). Pools were made of proteins eluting between 15-18 and 18-21 min. Western blotting of C4-RP-HPLC eluate from profile 1 (Fig. 4.6A) confirmed oxS100A8 and S100A8 monomeric, and possibly dimeric (20 kDa), trimeric

(30 kDa) and tetrameric (40 kDa) covalent complexes (Fig. 4.6B left and middle panel, 15-18 min). Monomeric S100A9 (Fig 4.6B right panel, 18-21 min) was found predominantly in peak 2.

Western blotting of C4-RP-HPLC eluate from profile 2 (Fig. 4.6A) indicated low amounts of oxS100A8 monomeric, dimeric complexes (Fig 4.6C, left panel 15-18 min), and possibly dimeric, trimeric and tetrameric complexes of native S100A8 in peaks 1 and 2 (Fig. 4.6C middle panel, 15-18 min). Monomeric S100A9 was enriched from C4-RP-HPLC; minor reactivity with a component which had a size similar to S100A9 dimer (28 kDa) was also apparent (Fig 4.6C right panel, 18-21 min).

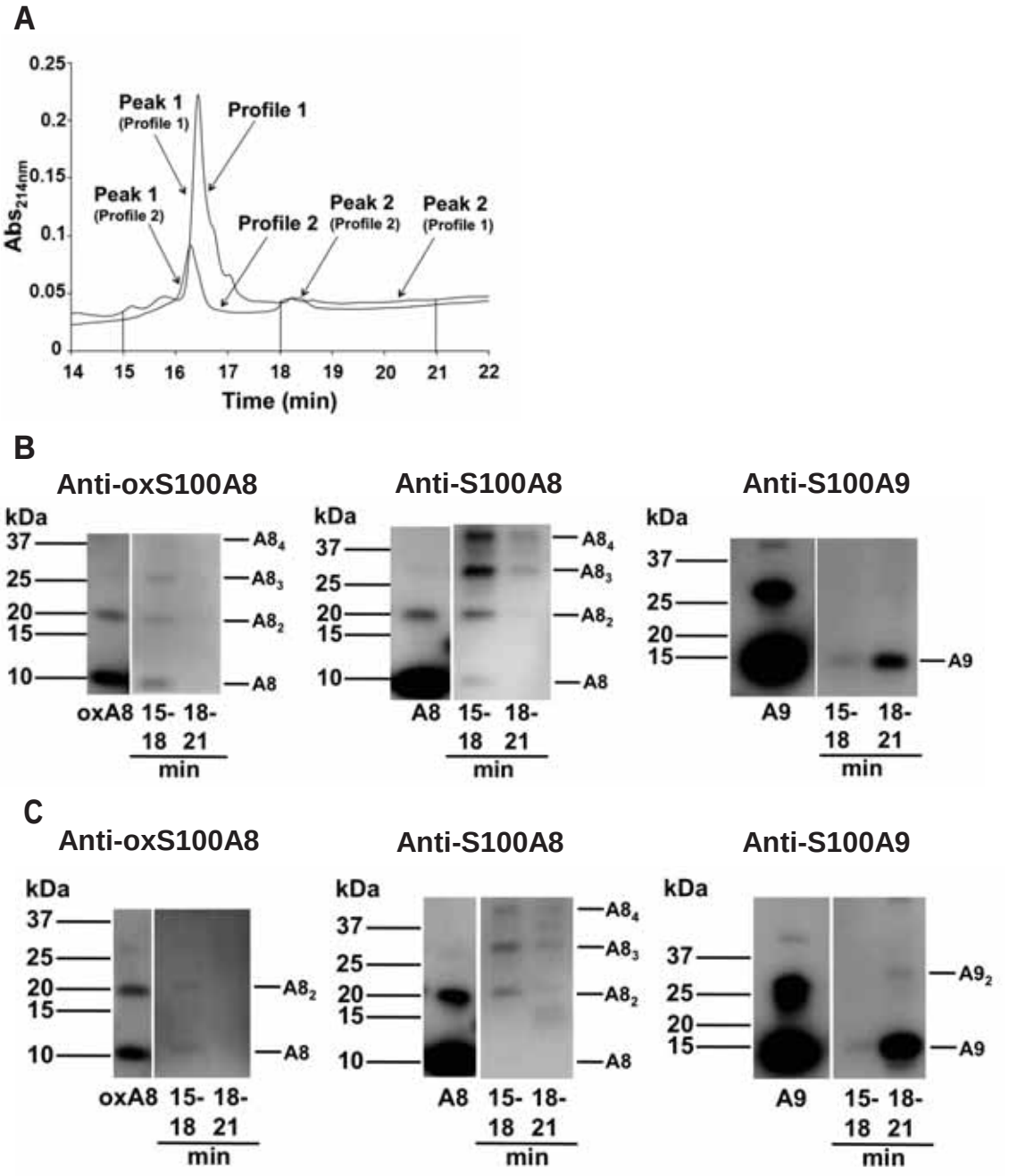

Figure 4.6:S100A8 and S100A9 in control sputum. (**A**) Pooled Peaks 1 and 2, and Peak 3 from C8-RP-HPLC were purified by C4-RP-HPLC, indicated as profiles 1 and 2 respectively. Briefly, profile 1 separated into a major peak (elution time15-18 min) and a minor component between 18-21 min. Profile 2 eluted as small peaks at 15-18 min and 18-21 min. (**B**) Western blotting of profile 1 from Fig 4.6A (500 µl lyophilized from C4-RP-HPLC) showed weak reactivity with anti-oxS100A8; anti-S100A8 reacted with higher-order complexes. Monomeric S100A9 was identified in fractions eluting between 18-21 min. (**C**) Western blotting of profile 2 (Fig 4.6A, 15-18 min) indicated weak reactivity with anti-oxS100A8 and anti-S100A8 IgG; the latter reacted weakly with complexes of the same mass as in 4.6B. Monomeric S100A9 principally eluted between 18-21 min. Western blots included 500 ng rec-oxS100A8, S100A8 or S100A9 as positive controls. Data presented is representative of two samples of enriched control sputum.

Asthmatic sputum from 5 donors was analyzed. These eluted as a broad peak (elution maximum 12.3 min, Fig. 4.7A) from C8-RP-HPLC and contained a 10 kDa anti-S100A8-reactive component and some homodimer (20 kDa), confirmed by Western blotting (not shown). C4-RP-HPLC resolved 3 peaks (elution maxima 14.3, 15.3 and 15.6 min; Fig. 4.7B). Peak 1 (14.3 min) contained strong anti-S100A8 and anti-oxS100A8 IgG-reactive components (Fig. 4.7C) migrating at 10 and 20 kDa; there was little S100A8 in peaks 2 and 3. Peak 1 from C8-RP-HPLC contained components with relatively strong reactivity with anti-S100A9, migrating at 14, 24 and 28 kDa, possibly indicating S100A9 monomer, dimer and the S100A8/S100A9 heterodimer. Minor positive components separated at ~38, 42, 48 kDa and higher masses, resistant to DTT. Peaks 1 and 3 from C4-RP-HPLC-enriched samples contained little S100A9; peak 2 was predominantly S100A9 monomer (14 kDa), dimer (28 kDa) and higher-order complexes (Fig. 4.7D). S100 protein in asthmatic sputum separated by C8-RP-HPLC and C4-RP-HPLC, eluted earlier, with more clearly-defined peaks corresponding to S100A8 and S100A9 than S100 protein in control sputum. RP-HPLC separates proteins based on hydrophobicity; the delayed elution times for S100A8 and S100A9 in control sputum may be due to higher amounts of uncharacterized hydrophobic proteins (compared to asthmatic sputum) that may change elution times.

DTT-resistant complexes were evident in Western blots immuno-stained with anti-oxS100A8 and anti-S100A8; the dimer was most obvious, but only after enrichment by C4-RP-HPLC, and as minor products, these were not characterized further. Because the DTT used to disperse the mucus in sputum could have reduced disulfide-linked dimers, assessment of relative abundance of S100A8 monomers/covalent dimers in sputum was not possible.

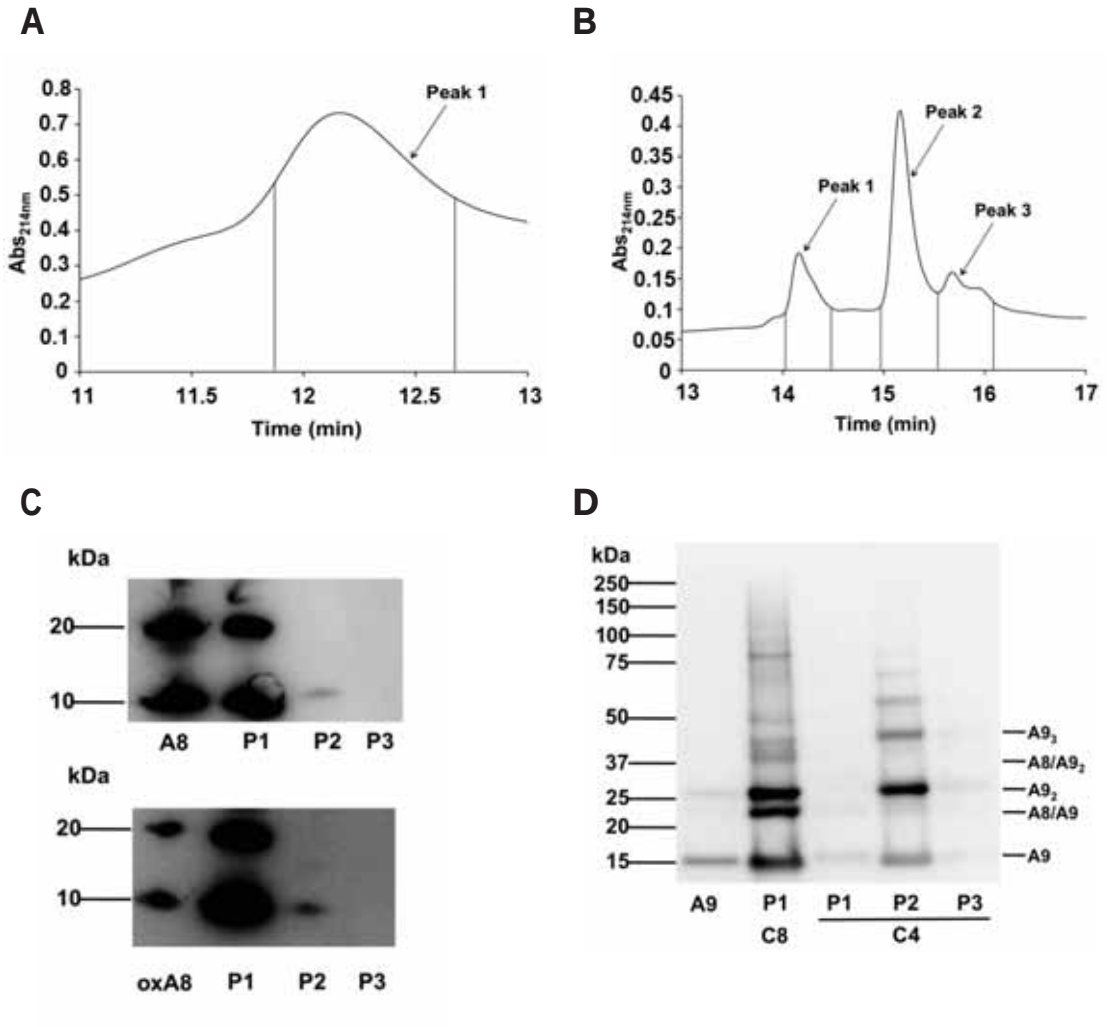

Figure 4.7: Purification of S100A8 and S100A9 from asthmatic sputum. (**A**) Asthmatic sputum (600 μg) eluted from C8-RP-HPLC as a broad peak between 11.7 and 12.6 min. (**B**) Peak 1 from C8-RP-HPLC was purified by C4-RP-HPLC. Peaks eluting at 14.3 (Peak 1), 15.3 (Peak 2) and 15.6 (Peak 3) min were collected. (**C**) Peaks 1, 2 and 3 were immuno-blotted (500 μl, lyophilized to 10 μl) with anti-S100A8 or anti-oxS100A8 IgG under reducing conditions. Peak 1 contained high amounts of 10 and 20 kDa components corresponding to S100A8 monomer and dimer respectively (native and oxidized). Components in Peak 2 had little reactivity with the antibodies; no reactivity was seen in peak 3. (**D**) The single C8-RP-HPLC peak and the three peaks from C4-RP-HPLC were Western blotted with anti-S100A9 IgG. The C8-RP-HPLC eluate contained components migrating at ~14, 24, 28, 38, 42 kDa and minor amounts of large complexes. Purification by C4-RP-HPLC indicated lower amounts of most components, principally in Peak 2, which contained 14, 28, 42 kDa components, corresponding to S100A9, and higher-order complexes. Western blots included 500 ng of each S100 protein as positive control. Data presented is representative of enriched asthmatic sputum from five donors.

Control sputum fractions separated by C4-RP-HPLC (5μg) were analyzed by MS after AspN digestion. Peptides from peaks 1 (pool 15-18 min; Fig 4.6A) indicated oxidation of Met_1 to $Met_1(O)$ in samples from 2/2 control subjects. There was little compelling evidence for Cys_{42} oxidation; only one peptide in 1/2 control samples was modified to Cys_{42}-sulfonic acid (not shown). Peptides of products separated from asthmatic sputum (peak 1, C4-RP-HPLC, 5μg) (Fig 4.7B) contained sulfonic acid intermediates in AspN-specified digests with AspN-specified within Mascot searches from one asthmatic subject. Additional Mascot searches were performed using the same data because some non-specific peptide-bond cleavages were observed previously from similar biological samples (personal communication, A/Prof. Mark Raftery). No-enzyme-specified searches indicated sulfonic acid in peptides from two additional asthmatic subjects and a trypsin-specified digest identified sulfonic acid in another (not shown); no sulfinic acid intermediates were obvious; 3/5 peptides contained $Met_1(O)$ and 1/5 had $Met_{78}(O)$ – see Table 4.2.

The peptide DDLKKLLETECPQYIRKKGA contained oxathiazolidine-dioxide (m/z +46 addition) in one sample digested with AspN (Fig. 4.8), and in the peptide ETECPQYIRKKGA in another sample. The tryptic peptide LLETECPQYIR contained oxathiazolidine-oxide (m/z +30 addition) in one sample digested with trypsin (Fig. 4.9). MS/MS spectra were similar to those generated for digests of recombinant oxS100A8 (see Figs. 3.7C, D and Fig. 3.6A respectively, Section 3.3.3, Chapter 3), although associated Mascot scores for peptides were lower, probably because of the sample complexity and low amounts of S100A8 in the samples.

Table 4.2 summarizes oxidation products identified in S100A8 in enzyme and non-enzyme-specified searches, in peptides generated from sputum products enriched from asthmatic and control donors. Attempts to minimise irrelevant proteins by RP-HPLC enrichment assisted characterization, but contaminating peptides caused high backgrounds in peptide searches, making identification of residues containing novel oxidative modifications more challenging.

Table 4.2 Oxidative modifications in S100A8 identified by MS

Sample	Mass addition (Da)	Modification
Control Sputum (n=2) (15-18 min C4-RP-HPLC)		
AspN digest		
MLTELEKALNSII	+16 (10,850 Da)	$Met_1(O)$
MLTELEKALNSII*	+16 (10,850 Da)	$Met_1(O)$
Asthmatic Sputum (n=5) (peak 1, 14.3 min C4-RP-HPLC)		
AspN digest		
ETECPQYIRKKGA* and DDLKKLLETECP* and DDLKKLLETECPQYIRKKGA	+48 (10,882 Da)	Cys_{42}-sulfonic acid
DDLKKLLETECPQYIRKKGA and ETECPQYIRKKGA	+46 (10,880 Da)	Cys_{42}-oxathiazolidine-dioxide
MLTELEKALNSII	+16 (10,850 Da)	$Met_1(O)$
Trypsin digest		
KLLETECPQYIR	+48 (10,882 Da)	Cys_{42}-sulfonic acid
LLETECPQYIR	+30 (10,864 Da)	Cys_{42}-oxathiazolidine-oxide
	+46 (10,882 Da)	Cys_{42}-oxathiazolidine-dioxide
MGVAAHKK	+16 (10,850 Da)	$Met_{78}(O)$

TABLE 4.2: Oxidative modifications identified in peptides derived from control and asthmatic sputum. Oxidation of Met_1 to $Met_1(O)$ was evident in 2/2 control samples. Little compelling evidence for Cys_{42} modifications were found in control sputum (n=2/2). Masses of modifications are indicated in parentheses, expressed in Daltons (Da). Oxidation products on Cys_{42} of S100A8 were identified by peptide mapping and MS/MS; Oxathiazolidine-oxide (+30 m/z) and dioxide (+46 m/z) adducts were obvious, the former only in tryptic peptides. The oxathiazolidine-dioxide adduct was observed in S100A8-derived peptides separated from asthmatic sputum (n=3/5). Oxidized peptides marked with * indicate sequences identified in non-enzyme specified samples. Modifications observed in these peptides were consistent with modifications identified in enzyme-specified searches.

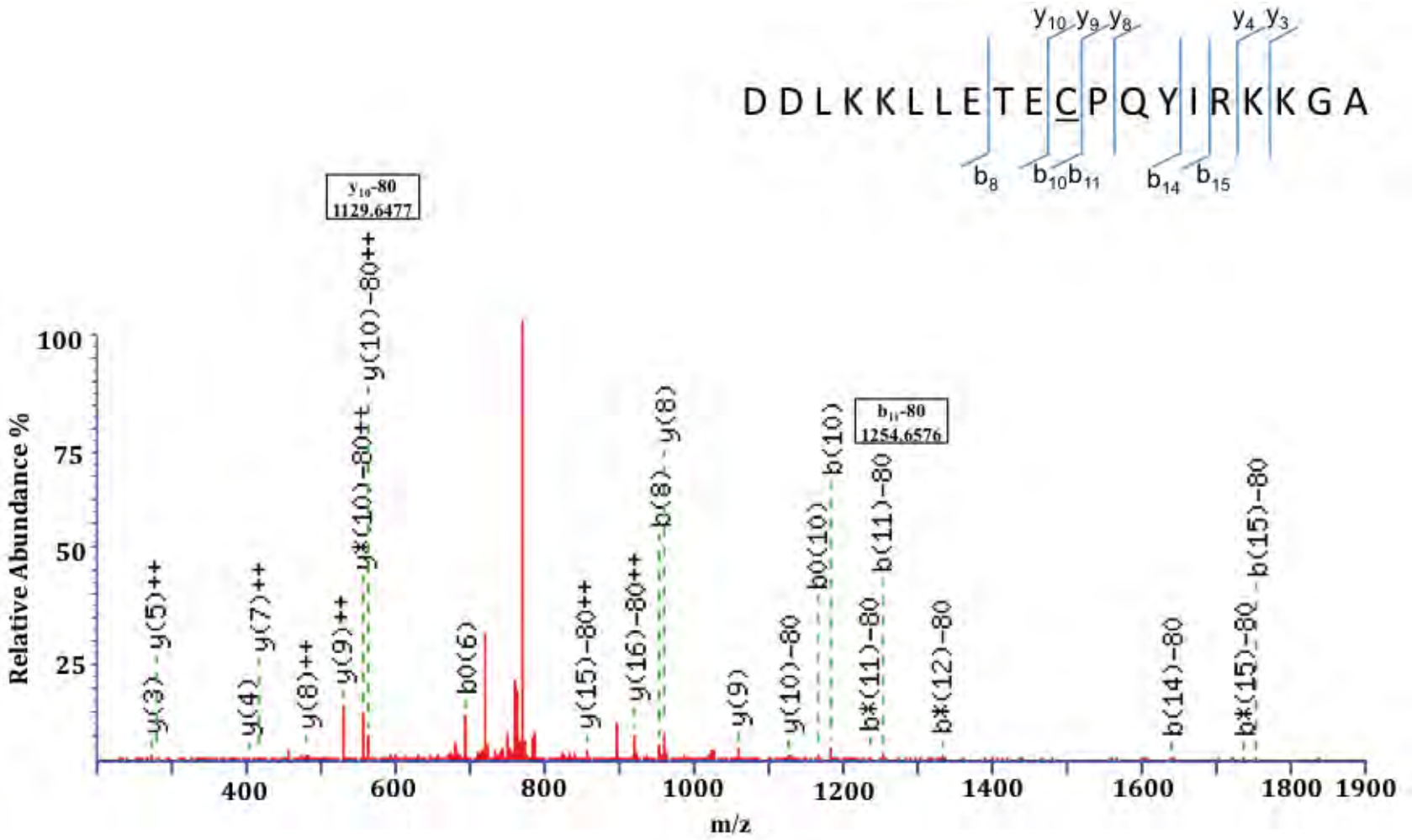
DDLKKLLETECPQYIRKKGA
y10 y9 y8
y4 y3
b8
b10 b11
b14 b15
y10-80
1129.6477
b11-80
1254.6576
Relative Abundance %
100
75
50
25
400
600
800
1000
1200
1400
1600
1800
1900
m/z
y(3)
y(5)++
y(4)
y(7)++
y(8)++
y(9)++
y*(10)-80++
y(10)-80++
b0(6)
y(15)-80++
y(16)-80++
b(8)
y(8)
y(9)
y(10)-80
b0(10)
b(10)
b*(11)-80
b(11)-80
b*(12)-80
b(14)-80
b*(15)-80
b(15)-80

#	b	Seq.	y	#
1	116.0342	**D**		**20**
2	231.0612	**D**	2199.2496	**19**
3	344.1452	**L**	2084.2226	**18**
4	472.2402	**K**	1971.1386	**17**
5	600.3352	**K**	1843.0436	**16**
6	713.4192	**L**	1714.9486	**15**
7	826.5033	**L**	1601.8646	**14**
8	***955.5459***	**E**	1488.7805	**13**
9	1056.5936	**T**	1359.7379	**12**
10	***1185.6361***	**E**	1258.6902	**11**
11	***1254.6576***	**C**	***1129.6477***	**10**
12	1351.7104	**P**	***1060.6262***	**9**
13	1479.7690	**Q**	***963.5734***	**8**
14	***1642.8323***	**Y**	835.5148	**7**
15	***1755.9163***	**I**	672.4515	**6**
16	1912.0175	**R**	559.3675	**5**
17	2040.1124	**K**	***403.2663***	**4**
18	2168.2074	**K**	***275.1714***	**3**
19	2225.2288	**G**	147.0764	**2**
20		**A**	90.0550	**1**

Figure 4.8: Annotated MS/MS of human asthmatic sputum samples eluting at 14.3 min by C4-RP-HPLC digested with AspN. S100A8$_{32-51}$ sequence-specific ions (either as y or b ions) are labelled. Only fragment ions y_{10} and b_{11} (Cys_{42}) showed loss of m/z -80, with concomitant gain of m/z +46 (shown in box), confirming oxidation of Cys_{42} to Cys_{42}-oxathiazolidine-dioxide. Masses of individual amino acids are listed. Amino acids in bold italics are those contributing to Mowse scores of isolated peptides.

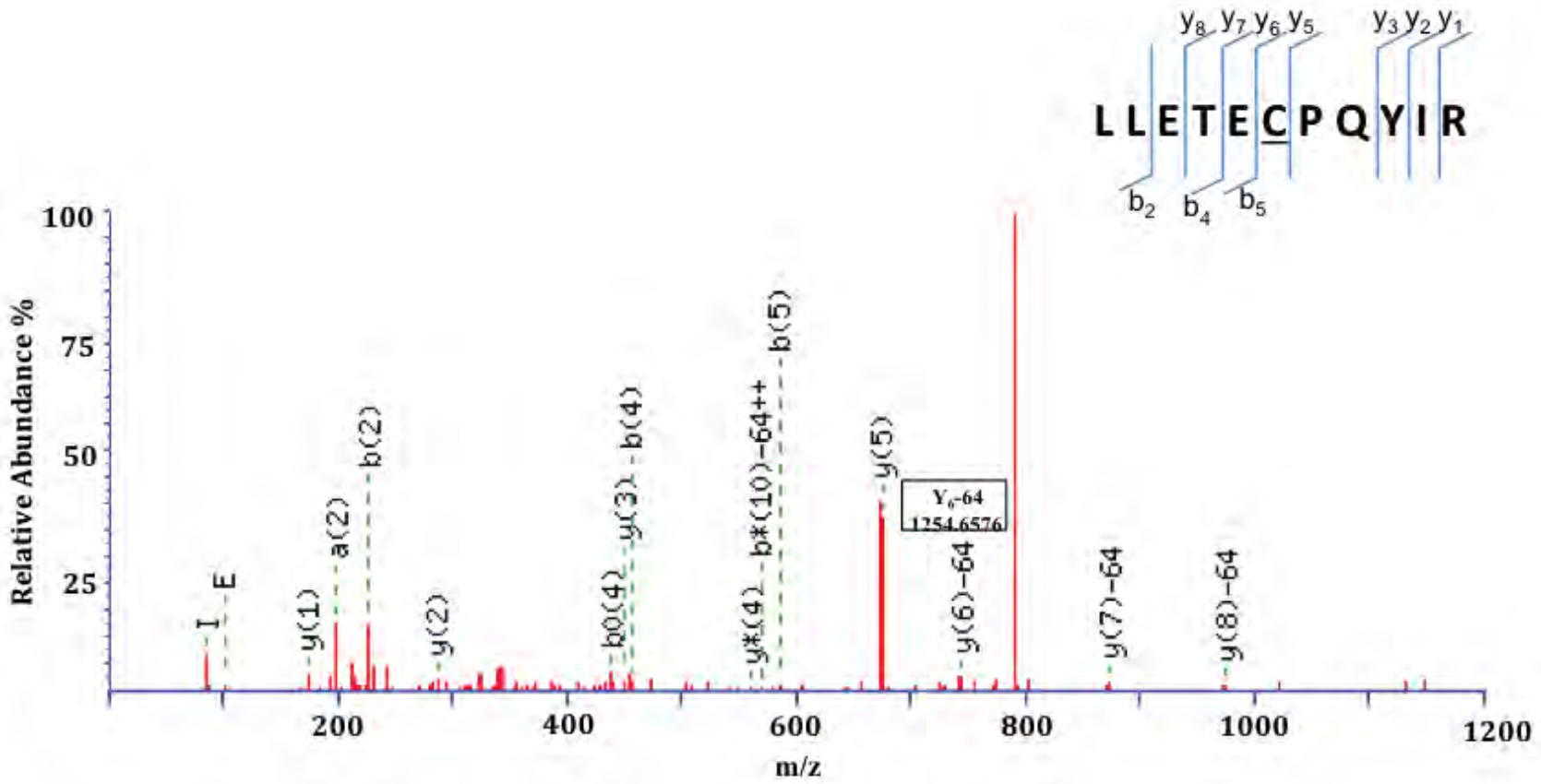
y8 y7 y6 y5 y3 y2 y1
LLETECPQYIR
b2 b4 b5
Relative Abundance %
100
75
50
25
I
E
y(1)
a(2)
b(2)
y(2)
b0(4)
y(3)
b(4)
y*(4)
b*(10)-64++
b(5)
y(5)
Y6-64
1254.6576
y(6)-64
y(7)-64
y(8)-64
200
400
600
800
1000
1200
m/z

#	b	Seq.	y	#
1	114.0913	**L**		**11**
2	***227.1754***	**L**	1217.6161	**10**
3	356.2180	**E**	1104.5320	**9**
4	***457.2657***	**T**	***975.4894***	**8**
5	***586.3083***	**E**	***874.4417***	**7**
6	655.3297	**C**	***745.3992***	**6**
7	752.3825	**P**	***676.3777***	**5**
8	880.4411	**Q**	579.3249	**4**
9	1043.5044	**Y**	***451.2663***	**3**
10	1156.5885	**I**	***288.2030***	**2**
11		**R**	***175.1190***	**1**

Figure 4.9: Annotated MS/MS of human asthmatic sputum samples eluting at 14.3 min by C4-RP-HPLC digested with trypsin. $S100A8_{37-47}$ sequence-specific ions (either as y or b ions) are labelled. Only fragment ions b_6 and y_6 (Cys_{42}) showed loss of m/z -64 with concomitant gain of m/z +30 (y_6 ion shown in box), confirming oxidation of Cys_{42} to Cys_{42}-oxathiazolidine-oxide. Masses of individual amino acids are listed. Amino acids in bold italics are those contributing to Mowse scores of isolated peptides.

4.3.5 MET RESIDUES ARE OXIDIZED IN S100A9 IN VIVO

S100A9 enriched from 2/2 control samples (peak 2, C4-RP-HPLC, Fig. 4.6A, 5μg) only contained Met_{63}(O) (Fig. 4.10). S100A9 from 2/3 asthmatic samples contained only Met_{63}(O) (Fig. 4.11); another contained Met_{63}(O), Met_{81}(O) (Fig. 4.12), and Met_{94}(O) (Fig. 4.13) identified in non-enzyme-specified searches, however, samples had high background interference, complicating analysis (Table 4.3). The single Cys_3 residue of S100A9 was identified in non-enzyme-specified peptide searches from 1/2 control subjects but was not found in peptides from peak 2 of asthmatic sputum. There was no compelling evidence to suggest modifications to Cys_3.

Table 4.3 Oxidative modifications in S100A9 identified by MS

Sample	Mass addition (Da)	Modification
Control Sputum (n=2) (18-21 min C4-RP-HPLC)		
EKVIEHIME	+16 (13,258 Da)	Met_{63}(O)
Asthmatic sputum (n=3) (15.3 min C4-RP-HPLC)		
AspN digest EKVIEHIME and DLQNFLKKENKNEKVIEHIME*	 +16 (13,258 Da)	 Met_{63}(O)
EEFIMLMARLT*	+16 (13,258 Da)	Met_{81}(O)
WASHEKMHEG*	+16 (13,258 Da)	Met_{94}(O)

TABLE 4.3: S100A9 peptides enriched from control and asthmatic sputum. Sputum from 2/2 control and 2/3 asthmatic samples contained Met_{63}(O); of these, one also contained Met_{81} and Met_{94} (O). Oxidized peptides marked with * indicate sequences identified in non-enzyme-specified samples. Modifications observed in these peptides were consistent with those identified in enzyme-specified searches.

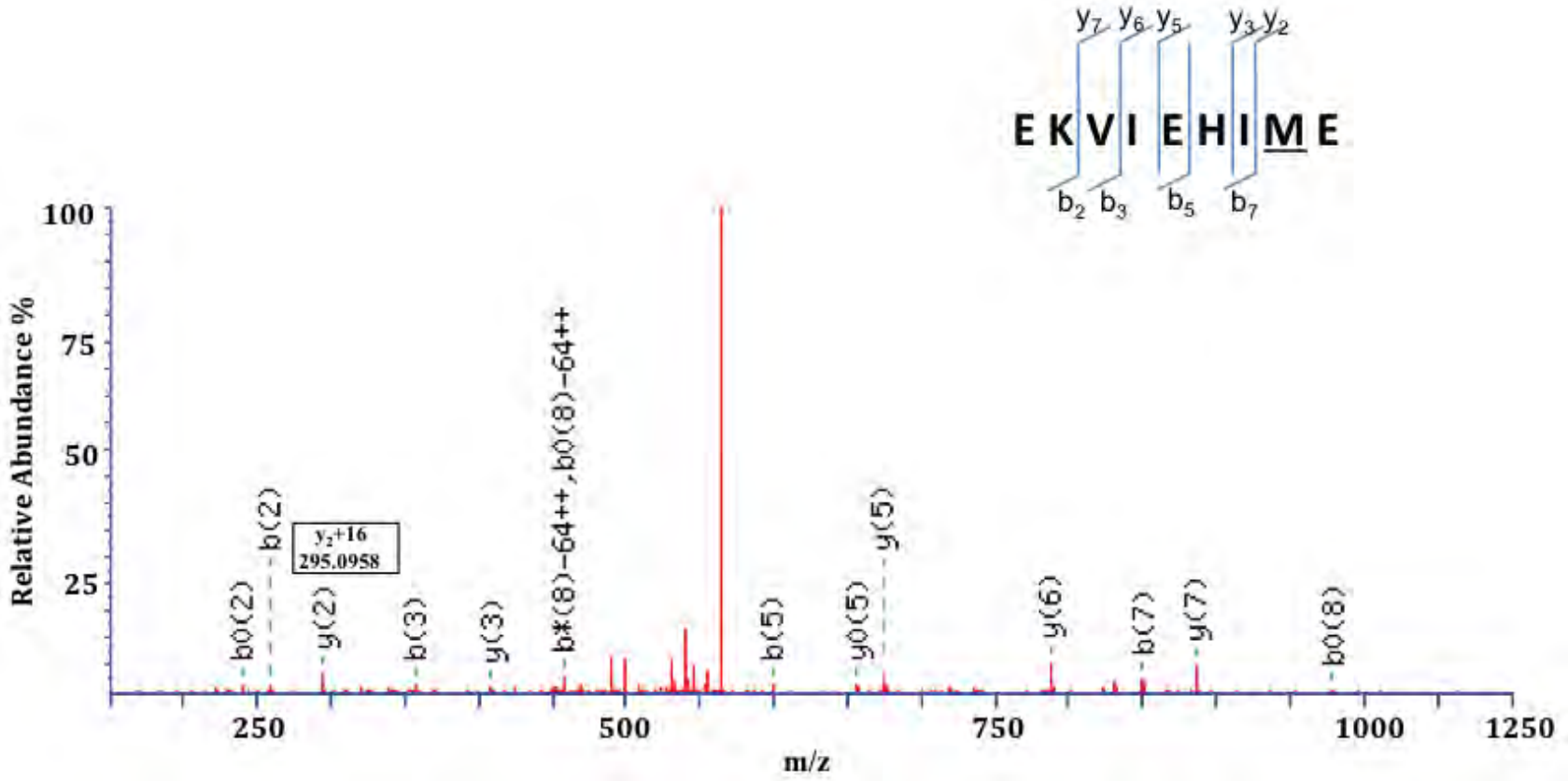
y7 y6 y5 y3 y2
E K V I E H I M E
b2 b3 b5 b7
Relative Abundance %
100
75
50
25
y2+16
295.0958
b0(2)
b(2)
y(2)
b(3)
y(3)
b*(8)-64++,b0(8)-64++
b(5)
y0(5)
y(5)
y(6)
b(7)
y(7)
b0(8)
250
500
750
1000
1250
m/z

#	b	Seq.	y	#
1	130.0499	**E**		**9**
2	***258.1448***	**K**	1014.5288	**8**
3	***357.2132***	**V**	***886.4339***	**7**
4	470.2973	**I**	***787.3655***	**6**
5	***599.3399***	**E**	***674.2814***	**5**
6	736.3988	**H**	545.2388	**4**
7	***849.4829***	**I**	***408.1799***	**3**
8	996.5183	**M**	***295.0958***	**2**
9		**E**	148.0604	**1**

Figure 4.10: Annotated MS/MS of control sputum samples eluting at 18-21 min by C4-RP-HPLC digested with AspN. $S100A9_{56-64}$ sequence-specific ions (either as y or b ions) are labelled. Only fragment ions b_8 and y_2 (Met_{63}) showed loss of m/z +16 (y_2 ion shown in box), confirming oxidation of Met_{63} to $Met_{63}(O)$. Masses of individual amino acids are listed. Amino acids in bold italics are those contributing to Mowse scores of isolated peptides.

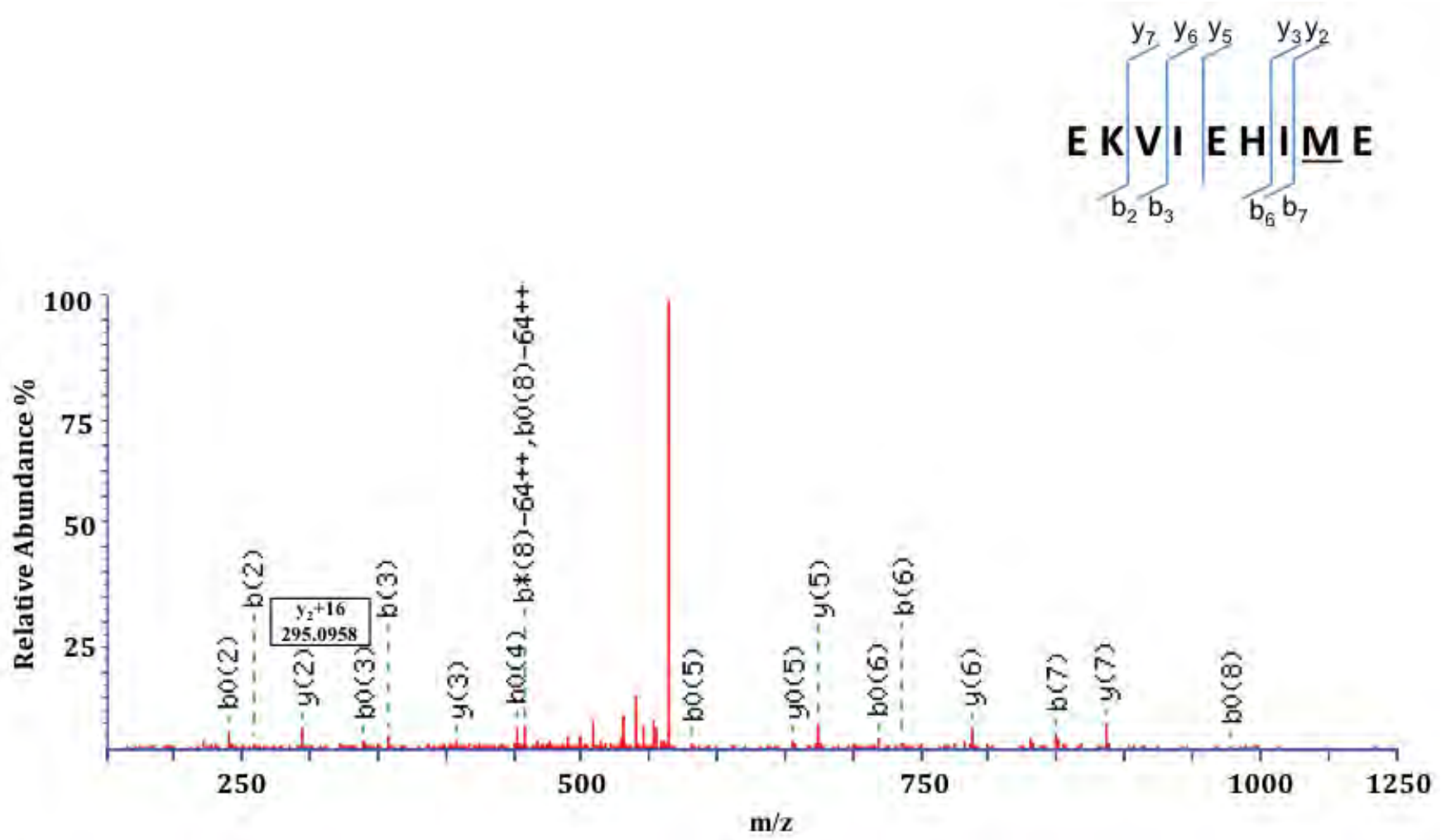
y7 y6 y5 y3 y2
EKVIEHIME
b2 b3 b6 b7
Relative Abundance %
100
75
50
25
y2+16
295.0958
b0(2)
b(2)
y(2)
b0(3)
b(3)
y(3)
b0(4) - b*(8)-64++, b0(8)-64++
b0(5)
y0(5)
y(5)
b0(6)
b(6)
y(6)
b(7)
y(7)
b0(8)
250
500
750
1000
1250
m/z

#	b	Seq.	y	#
1	130.0499	**E**		**9**
2	***258.1448***	**K**	1014.5288	**8**
3	***357.2132***	**V**	***886.4339***	**7**
4	470.2973	**I**	***787.3655***	**6**
5	599.3399	**E**	***674.2814***	**5**
6	***736.3988***	**H**	545.2388	**4**
7	***849.4829***	**I**	***408.1799***	**3**
8	996.5183	**M**	***295.0958***	**2**
9		**E**	148.0604	**1**

Figure 4.11: Annotated MS/MS of asthmatic sputum samples eluting at 15.3 min by C4-RP-HPLC digested with AspN. $S100A9_{56-64}$ sequence-specific ions (either as y or b ions) are labelled. Only fragment ions b_8 and y_2 (Met_{63}) showed loss of m/z +16 (y_2 ion shown in box), confirming oxidation of Met_{63} to $Met_{63}(O)$. Masses of individual amino acids are listed. Amino acids in bold italics are those contributing to Mowse scores of isolated peptides.

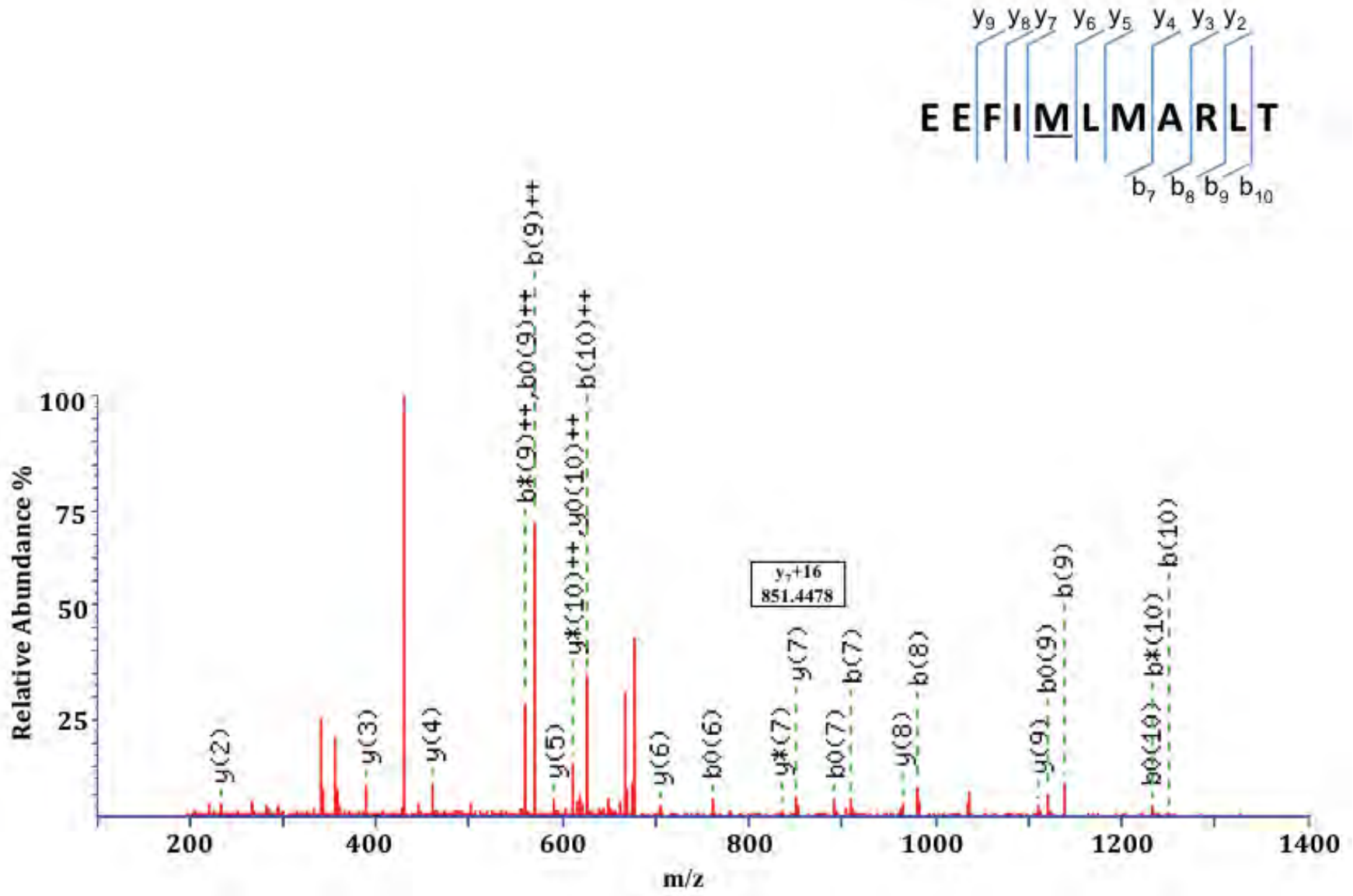
y9 y8 y7 y6 y5 y4 y3 y2
E E F I M L M A R L T
b7 b8 b9 b10
Relative Abundance %
100
75
50
25
y(2)
y(3)
y(4)
b*(9)++,b0(9)++
b(9)++
y(5)
y*(10)++,y0(10)++
b(10)++
y(6)
b0(6)
y7+16
851.4478
y*(7)
y(7)
b0(7)
b(7)
y(8)
b(8)
y(9)
b0(9)
b(9)
b0(10)
b*(10)
b(10)
200
400
600
800
1000
1200
1400
m/z

#	b	Seq.	y	#
1	130.0499	**E**		**11**
2	259.0925	**E**	1240.6428	**10**
3	406.1609	**F**	***1111.6002***	**9**
4	519.2449	**I**	***964.5318***	**8**
5	666.2803	**M**	***851.4478***	**7**
6	779.3644	**L**	***704.4124***	**6**
7	***910.4049***	**M**	***591.3283***	**5**
8	***981.4420***	**A**	***460.2878***	**4**
9	***1137.5431***	**R**	***389.2507***	**3**
10	***1250.6272***	**L**	***233.1496***	**2**
11		**T**	120.0655	**1**

Figure 4.12: Annotated MS/MS of asthmatic sputum samples eluting at 15.3 min by C4-RP-HPLC digested with AspN. S100A9$_{77\text{-}87}$ sequence-specific ions (either as y or b ions) are labelled. Only fragment ions b_5 and y_7 (Met_{81}) showed loss of m/z +16 (y_7 ion shown in box), confirming oxidation of Met_{81} to $Met_{81}(O)$. Masses of individual amino acids are listed. Amino acids in bold italics are those contributing to Mowse scores of isolated peptides from non-enzyme specified searches.

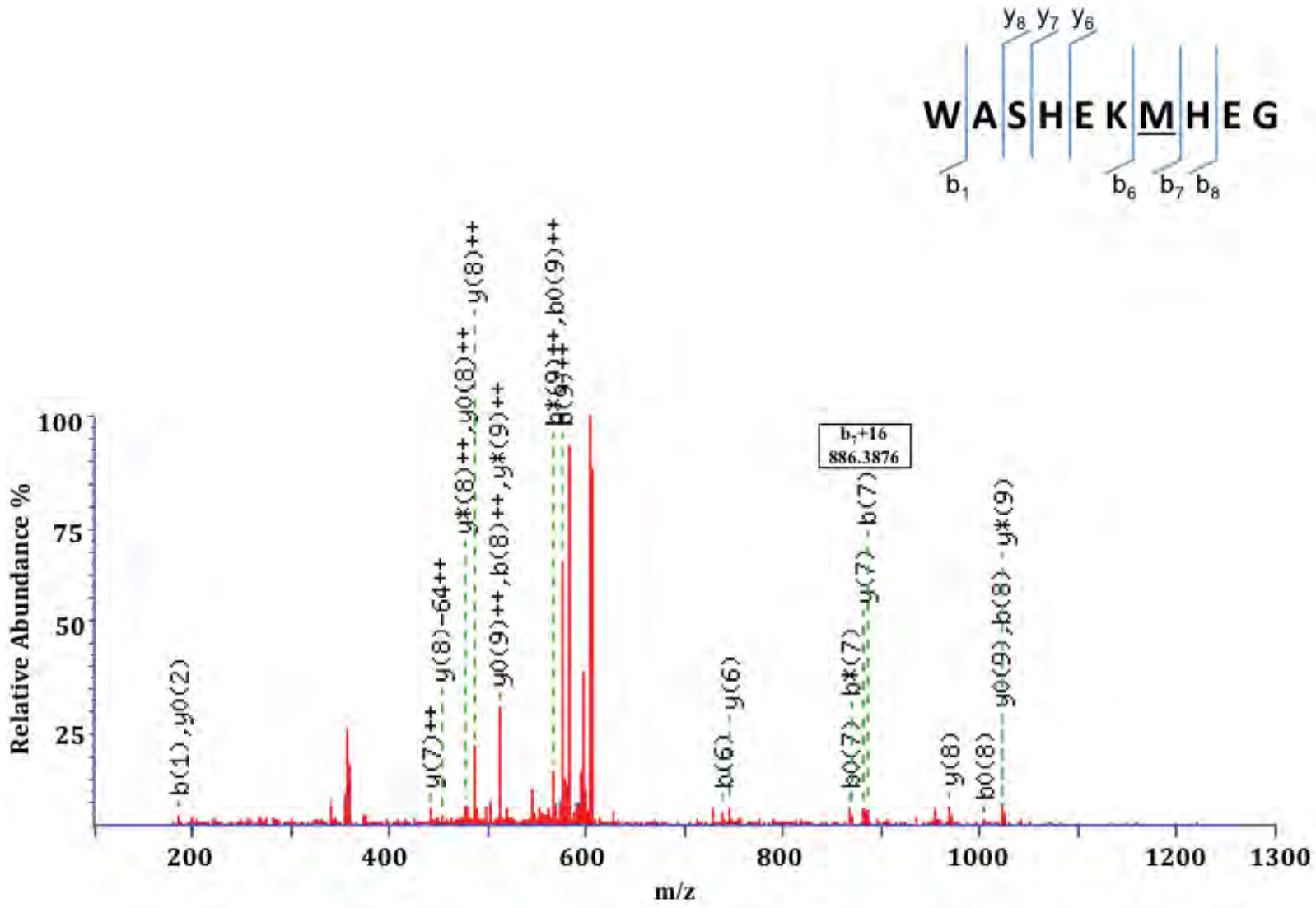
y8 y7 y6
WASHEKMHEG
b1
b6 b7 b8
Relative Abundance %
100
75
50
25
200
400
600
800
1000
1200
1300
m/z
b7+16
886.3876
b(1),y0(2)
y(7)++
y(8)-64++
y*(8)++,y0(8)++
y(8)++
y0(9)++,b(8)++,y*(9)++
b*(9)++,b0(9)++
b(6)-y(6)
b0(7)-b*(7)
y(7)-b(7)
y(8)
b0(8)
y0(9),b(8)-y*(9)

#	b	Seq.	y	#
1	***187.0866***	**W**		10
2	258.1237	**A**	1041.4418	9
3	345.1557	**S**	***970.4047***	8
4	482.2146	**H**	***883.3727***	7
5	611.2572	**E**	***746.3138***	6
6	***739.3522***	**K**	617.2712	5
7	***886.3876***	**M**	489.1762	4
8	***1023.4465***	**H**	342.1408	3
9	1152.4891	**E**	205.0819	2
10		**G**	76.0393	1

Figure 4.13: Annotated MS/MS of asthmatic sputum samples eluting at 15.3 min by C4-RP-HPLC digested with AspN. $S100A9_{88-97}$ sequence-specific ions (either as y or b ions) are labelled. Only fragment ions b_7 and y_4 (Met_{94}) showed loss of m/z +16 (b_7 ion shown in box), confirming oxidation of Met_{94} to $Met_{94}(O)$. Masses of individual amino acids are listed. Amino acids in bold italics are those contributing to Mowse scores of isolated peptides from non-enzyme specified searches.

4.3.6 OXIDATION OF S100A8 AND S100A9 AFFECTS COMPLEX FORMATION

Some functions depend on formation of the S100A8/S100A9 heterocomplex, particularly antimicrobial activity and AA binding [178, 620, 655]. Chemical cross-linking experiments (of rec-hS100 proteins) were performed in an initial attempt to monitor changes in potential structural interactions caused by oxidation. Without cross-linking (Fig. 4.14A), S100A8 and S100A9 separated as monomers, dimers and trimers; oxS100A8 contained only monomer and dimer. The unmodified heterocomplex separated as S100A8 monomers and dimers (10 and 20 kDa), S100A9 monomers and dimers (14 and 28 kDa); the additional complex migrating at 24 kDa indicated heterodimer formation. When oxS100A8 or oxS100A9 (prepared with 1:1 molar ratio S100:HOCl; see Section 2.1.5) were combined with the native counterparts, the same complexes were evident, although heterodimer levels were diminished, and when oxS100A8 and oxS100A9 were combined, the heterodimer was no longer obvious.

Cross-linking indicated additional products (see Fig. 4.14B). oxS100A8 contained dimers, trimers (30 kDa) and tetramers (40 kDa), whereas, oxS100A9 was relatively unchanged. oxS100A8 combined with S100A9 formed the heterodimer, whereas this was less obvious when S100A8 was combined with oxS100A9; in oxS100A8/oxS100A9, heterodimer formation was not obvious.

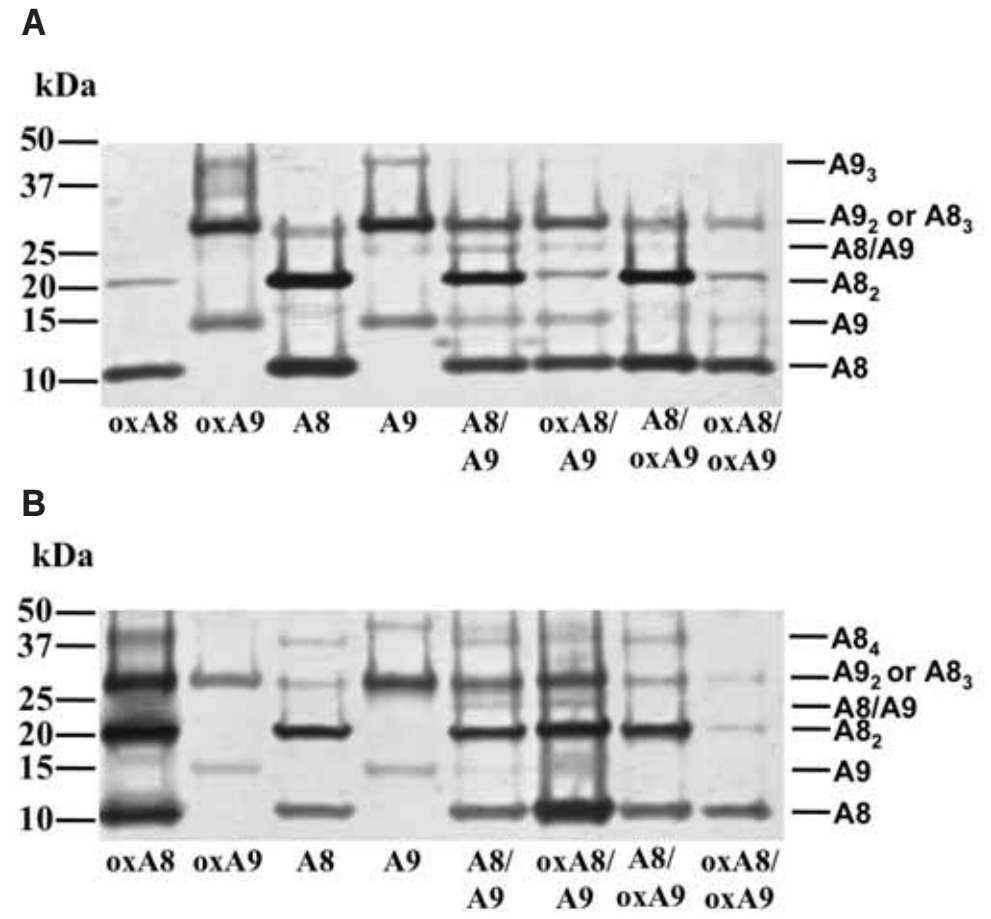

Figure 4.14: Effects of oxidation on heterocomplex formation. Oxidized (see Section 2.1.5) or native recS100 proteins (1 μg of S100A8 or oxS100A8 and 1.4 μg of S100A9 or oxS100A9) were silver stained (under non-reducing conditions) after cross-linking with 1 mM BS_3 cross-linker. **(A)** oxS100A8 comprised oxidized monomer and dimer, and oxS100A9 contained oxidized monomer, dimer and trimer (42 kDa). Unmodifed S100A8 and S100A9 separated as monomers, dimers and trimers. The unmodified S100A8/A9 complex separated into the S100A8 monomer and dimer, S100A9 monomer and dimer and the heterocomplex migrating at 24 kDa. When oxS100A8 or oxS100A9 were combined with the native counterpart (S100A9 or S100A8 respectively), the same complexes were evident, although heterodimer formation was diminished. oxS100A9 monomer was less, when this was combined with native S100A8. When oxS100A8 and oxS100A9 were combined, no heterodimer was obvious. **(B)** When cross-linked, additional products were seen. S100A8 and oxS100A8 separated as dimers, trimers and tetramers; oxS100A9 was predominantly monomeric and dimeric compared to S100A9, which also contained the trimer. When native S100A8 and S100A9 were combined, the heterocomplex at 24 kDa was evident, and S100A8 monomer and dimer, S100A9 monomer, dimer and trimer. When oxS100A8 was combined with S100A9, the heterodimer formed, whereas, when S100A8 was combined with oxS100A9, levels were reduced. When oxS100A8 and oxS100A9 were cross-linked, complex formation was markedly reduced; no heterodimer or oxS100A9 monomer was obvious, indicating that cross-linking may generate complexes that cannot be resolved by SDS-PAGE, or that cross-linking was inefficient.

4.3.7 OXIDATION AFFECTS NEUTROPHIL ADHESION

Transmigrating neutrophils secrete S100A8/S100A9 [431] and hypohalous acids are generated by activated granulocytes. fMLP promoted maximal, saturated adhesion within ~45 min that was significantly above baseline (Fig. 4.15A; $P < 0.01$). recS100A8/S100A9 and oxS100A8/S100A9 caused no change whereas S100A8/oxS100A9 somewhat reduced basal adhesion. Although oxidation of both S100s substantially compromised their ability to form heterocomplexes (see Fig. 4.14), oxS100A8/oxS100A9 (the oxS100A8/oxS100A9 heterodimer was not prepared by oxidizing the native heterocomplex with HOCl. Individual proteins were oxidized prior to Ca^{2+}-induced heterodimer formation) dramatically reduced basal adhesion compared to untreated cells, and cells treated with the unmodified heterocomplex or oxS100A8/S100A9 (n=5, Fig. 4.15A; $P < 0.01$). Unexpectedly, neutrophils pre-treated with native S100A8/S100A9 or oxS100A8/oxS100A9 showed markedly reduced fMLP-induced neutrophil adhesion (n=2, Fig. 4.15B), however further investigation is required to confirm these results.

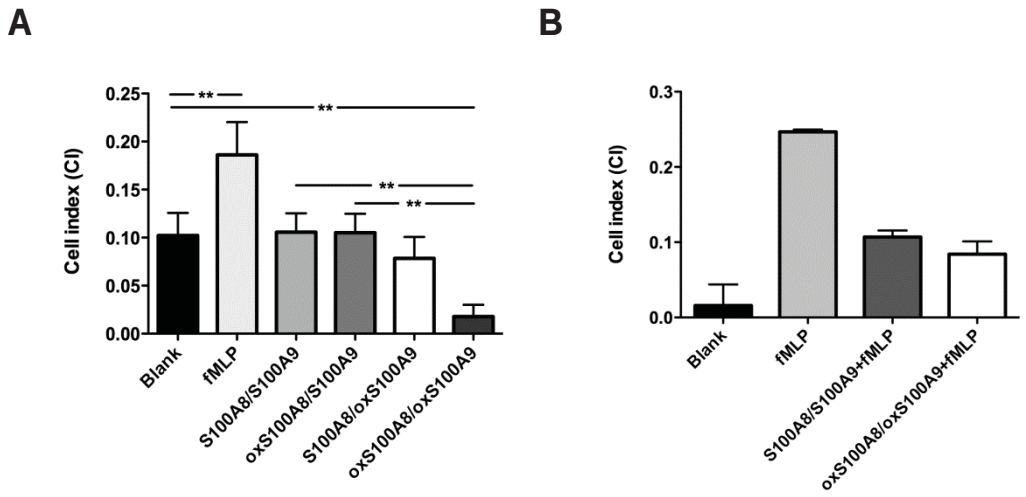

Figure 4.15: Oxidation of recS100A8 and recS100A9 reduced neutrophil adhesion to fibronectin. Adhesion is expressed as cell index (CI). (**A**) The mean CI of neutrophils from 5 donors confirmed that fMLP significantly increased adhesion to fibronectin compared to untreated cells ($P < 0.01$). Adhesion of neutrophils incubated with recS100A8/S100A9 or rec-oxS100A8/S100A9 was not significantly different to basal adhesion. In marked contrast, oxS100A8/oxS100A9 reduced adhesion (** $P < 0.01$) compared to control, the unmodified heterocomplex and oxS100A8/S100A9. Means ± SEM were compared using repeated measures ANOVA with Bonferroni post-test for multiple comparisons. (**B**) Neutrophils from 2 healthy donors pre-treated with recS100A8/S100A9 or oxS100A8/oxS100A9 markedly reduced fMLP-induced neutrophil adhesion by 56.6 ± 5.7% and 65.8 ± 10.5% (means ± SEM) respectively. Statistical analysis was not performed due to insufficient sample size.

4.3.8 OXIDATION AFFECTS ANTIMICROBIAL PROPERTIES

We first tried to test recS100A8/S100A9 antimicrobial activity against *S. pneumoniae*, a common respiratory tract infection, but its mucilaginous properties precluded accurate colony counting (not shown) and *E. coli* was used [9]. Although the antimicrobial activity of S100A8/S100A9 is compromised if Cys_{42} in S100A8 or $Met_{63/83}$ in S100A9 are mutated [655], the impact of oxidation is unknown. When one component of the heterocomplex was oxidized, it remained antimicrobial, although S100A8/oxS100A9 tended to be less effective. When both S100s were oxidized (prepared as described in Section 4.3.7), *E. coli* growth was significantly higher (Fig. 4.16; ***$P < 0.001$) than when incubated with the unmodified heterocomplex.

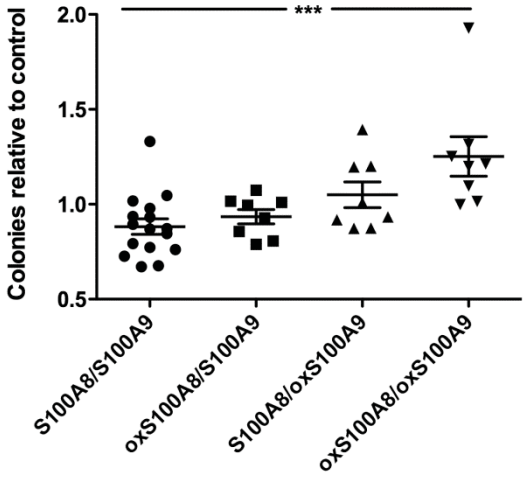

Figure 4.16: Oxidation of recS100 protein affects antimicrobial activity. oxS100A8, or oxS100A9 alone in the heterocomplex mildly reduced antimicrobial activity against *E. coli*; when both components were oxidized, antibacterial activity was significantly abrogated (***$P < 0.001$). Results are means ± SEM from four experiments, analyzed by one-way ANOVA with Bonferroni post-test for multiple comparisons.

4.4 DISCUSSION

S100A8, S100A9 and S100A12 are implicated in respiratory diseases [443, 496, 996], but their functions are largely unexplored. Currently, S100A8 and S100A9 are proposed to act as DAMP molecules that trigger inflammatory responses, possibly via NF-κB activation [393, 421, 1004, 1005]. S100A8 is proposed to propagate inflammation by interacting with TLR-4, with S100A9 reported to negate this effect. The heterocomplex is also reported to promote lethal endotoxin-induced shock and stimulate production of pro-inflammatory cytokines such as TNF-α [435, 1004].

However, emerging evidence suggests that S100A8 and S100A9 may act as anti-inflammatory proteins [613, 637, 644], in part because of their ability to scavenge ROS/RNS, and their subsequent modulation of inflammatory processes as a result of this interaction challenge the current dogma (reviewed in [695]).

For example, S100A8, but not Cys_{42}-Ala_{42}S100A8, suppressed MC activation and production of IL-6, IL-4 and GM-CSF in response to IgE-cross-linking *in vitro*, reducing phosphorylation of downstream LAT and ERK/MAPK, was likely due to inhibition of intracellular production of ROS required for signalling [644]. Significantly, S100A8, but not Cys_{42}-Ala_{42}S100A8, suppressed IL-5, eotaxin and MCP-1 (eosinophil chemoattractants), and eosinophil infiltration in acute murine asthma, when delivered directly to the lung before antigen challenge [644].

Similarly, S-nitrosylated S100A8 suppressed MC activation by compound 48/80 and reduced leukocyte adhesion, and extravasation triggered activated MC in the rat mesenteric microcirculation [613], indicating novel anti-inflammatory properties. Glutathionylation of S100A9 may reduce neutrophil binding to the extracellular matrix, thereby regulating the magnitude of neutrophil sequestration in the extravasculature, which together with S-nitrosylated S100A8 may limit tissue damage in acute inflammation [637].

S100A12 is also regarded as a DAMP [393] because it is a monocyte chemoattractant [320] and activates MCs, resulting in neutrophil and monocyte recruitment *in vivo* [131]. However, S100A12 may be protective because it inhibits MMP-2 and MMP-9 activities via Zn^{2+} sequestration [529]. However, S100A12 was not investigated in the functional experiments described in this chapter because its structural properties indicate that it is unlikely to be an efficient oxidant scavenger.

Here, we proposed a role for S100A8 and S100A9 in anti-oxidant defense [695],

as some adducts were reported to have anti-inflammatory effects [605, 606, 613], but until now, its scavenging capacity in human inflammation is unproven. Because hypohalous acids generated by activated granulocytes are plentiful following their activation, the focus of this work was to address the possibility that S100A8 and/or S100A9 may function as an oxidative sink *in vivo*.

4.4.1 S100A8 AND S100A9 IN ASTHMATIC LUNG

Previous work by Bozinovski *et al*. had shown elevated levels of mS100A8 in BALF from mice challenged for 4 hrs with LPS and treated with corticosteroids chiefly from neutrophils [430]. Similarly, in mice carrying the G551D mutation (confers a CF-like phenotype, by causing a mutation in the CF transmembrane conductance regulator) LPS induced mS100A8 mRNA and protein in the lung, in macrophages and neutrophil accumulation increased [520]. Neutrophilic lung inflammation is an essential component of host defense against a diverse range of pathogens, but in chronic inflammatory lung diseases such as severe asthma, S100A8 and S100A9 were proposed to perpetuate injury (reviewed in [970]). Proteolytic enzymes and oxidants (for example hypohalous acids), when released by activated neutrophils and eosinophils within close proximity to the alveolar walls, extracellular matrix or the small airways and airway mucosa, can severely damage lung tissue.

Here, we show hS100A8 and hS100A9 expression in human asthmatic lung and in infiltrating granulocytes. Matrix-associated S100A8 and S100A9 were apparent. Taken together, most researchers would infer that this expression would confirm the pro-inflammatory role proposed for these proteins [435]. However, immunohistochemical staining with anti-oxS100A8 revealed an important new function associated with S100A8 in asthma. The specificities of the antibodies used were evident in staining of normal human neutrophils, which had little reactivity with anti-oxS100A8 (more strongly recognises S100A8 oxidized by HOCl, compared with the native anti-S100A8 antibody) compared to the strong cytosolic staining seen with anti-S100A8 (Fig. 4.2, insets). Similarly, oxS100A8 expression was particularly strong in eosinophils, neutrophils and epithelial cells lining the airways in human asthmatic lung. Indeed, this was not the first observation of oxidant scavenging *in vivo*. McCormick *et al*. showed anti-oxS100A8 reactivity and evidence of multimeric S100A8 and S100A9 (likely via oxidative-cross-

linking) in atherosclerotic plaque extracts isolated from patients undergoing end arterectomy [410].

This data suggested that S100A8 in asthmatic tissue, instead of perpetuating inflammation, may scavenge ROS generated by activated eosinophils and neutrophils *in vivo*, thus limiting oxidative tissue damage and inferring a protective role in inflammation.

4.4.2 ASSESSMENT OF S100A8, S100A9 AND S100A12 IN ASTHMATIC SPUTUM

Control, asthmatic and bronchiectatic sputum had significantly larger amounts of protein in sputum compared to saliva. In saliva, squamous cells made up more than 99% of the cells, whereas sputum consists of a number of different components, for example, proteins from eosinophils, such as eosinophilic cationic protein, or from neutrophils [131], albumin and fibrinogen [1006], and these would account for the higher protein concentrations in sputum.

Levels of S100A8 were higher in sputum, compared to saliva in all subject groups, except for control samples, although differences were not significant. Levels of S100A9 and S100A12 were significantly elevated in saliva from control subjects, compared to sputum. S100A8, S100A9 and the heterocomplex are present in saliva from patients with bacterial infection, and autoimmune disorders [447, 1007, 1008]. Novel work in the area of protein secretion following stimulation with tastants demonstrated that salty, bitter and sour tastes increased S100A8 in whole saliva [1009]. In our study, no subjects in the two patient groups had a history of oral infection or autoimmune disease, and S100A8 in saliva was not significantly elevated, whereas S100A8 levels were highest in saliva from control subjects. This could possibly indicate a protective function in the oral cavity.

S100A9 concentrations can vary within the different salivary glands of the mouth. Sublingual salivary secretions contain measurable amounts, whereas, S100A9 is absent from submandibular salivary secretions [1010]. Although we have no explanation for the variation, these studies exemplify the very specific nature of S100 protein expression, in particular compartments within the body.

There is little evidence available to explain the elevated amounts of S100A12 found in saliva relative to sputum in all subgroups. Proteomic studies of newborn and adult saliva suggest that S100A12 levels in the acidic soluble fraction of saliva decline with age [1011], but no comparisons of sputum and saliva are available. Because the

three S100 proteins can act as defensins and contribute to antimicrobial defense (see Section 1.3.6.7, Chapter 1), they may form part of normal oral host defense [590, 591].

Sputum from bronchiectasis patients contained significantly elevated amounts of S100A8, compared to controls when analyzed by Western blotting, whereas ELISA indicated no differences. As bronchiectasis is an essentially neutrophilic lesion, we expected high amounts in these samples. oxS100A8, but not S100A8, S100A9 or S100A12, was significantly elevated in asthmatic sputum. Eosinophils in asthmatic patients have high amounts of S100A12 [131], and our studies indicated S100A8 and S100A9 in eosinophils in asthmatic lung and these cells may contribute to the elevated levels found in sputum. Sputum samples the central airways and because its collection is non-invasive, we used this source, and amounts may be underestimated. For example, ~4 fold more IL-8 was found in BALF from CF patients than in sputum [1012]. oxS100A8 monomer was most prominent; only minor amounts of dimer or higher-order complexes that are generated in S100A8 with higher HOCl ratios were found [410]. This may not be unexpected, given that HOBr from eosinophils is likely to predominate.

Greenlee *et al*. showed that MMP-2 and -9 differentially modify particular proteins by proteolytic processing in the asthmatic airway [601], and S100A8 and S100A9 are substrates of MMP-2 and MMP-9 [601]. In chronic inflammation, such as occurs in patients with asthma or bronchiectasis, MMP-2 and MMP-9 were proposed to contribute to retention of a homeostatic environment within the lung [601]. Thus, MMPs, or other granulocyte proteases may modify these, thereby lowering levels detected by Western blotting and ELISA. However, proteins modified by oxidants are resistant to proteases, acting as irreversible inhibitors, resulting in further accumulation of oxidation products (reviewed in [1013]).

In addition, S100A8 and S100A9 bind heparin sulfate [431] that may concentrate their effects at the extracellular matrix, so that our analysis may be an underestimate, particularly given the strong reactivity of anti-oxS100A8 in asthmatic lesions (Fig. 4.2, middle panel).

Asthmatic participants were all on inhaled CSs and effects of this drug would require assessment of naive and treated patients. Moreover, because reactivities of anti-S100A8 and anti-oxS100A8 IgGs are different (anti-oxS100A8 weakly detects unmodified S100A8; anti-S100A8 detects both components (see Fig. 4.3D, E) [410]) a direct comparison between S100A8 and oxS100A8 levels was not possible. However as normal lung does not express S100A8, increased oxS100A8 in asthmatic subjects was

presumably due to increased oxidation of increased amounts of S100A8 in these samples. Hsu *et al*. showed that CS increased murine macrophage S100A8 gene transcription and mRNA half-life. Importantly, CSs also increase constitutive levels of S100A8 and S100A9 mRNA in human monocytes, and S100A8/S100A9-positive macrophages in the synovial membrane of rheumatoid arthritis patients treated with methyl prednisolone [406]. IL-10 may potentiate asthma under some circumstances [1014]. Induction of S100A8 is dependent on IL-10 and is induced by RNA viruses in lung [400], and was associated with resolution. However, in virus-provoked asthma, IL-10 is proposed to increase airway hyper-responsiveness [1015]. Although more work is required, implications in virus-provoked asthma may add to the pro-inflammatory/anti-inflammatory debate surrounding S100A8.

4.4.3 OXIDATIVE POST-TRANSLATIONAL MODIFICATIONS TO S100A8 AND S100A9 GENERATED IN VIVO

Because the oxS100A8 and S100A9 monomers were the major S100 protein products found in asthmatic sputum, we focused on structural changes of these adducts. In Chapter 3 (see Section 3.3.3, Chapter 3) we showed that at equimolar ratios, HOCl generated sulfinic and sulfonic acid adducts, and HOBr generated a sulfonic acid adduct on Cys_{42} of rec-hS100A8. Alternate oxidation of sulfenic acid intermediates to novel products between cyclised oxidized Cys_{42} and nitrogen within the peptide backbone that may form oxathiazolidine-dioxide via an oxathiazolidine-oxide intermediate was principally generated by HOCl (Table 4.2). Met_1 of S100A8 was oxidized in control and asthmatic samples, and $Met_{78}(O)$ was also identified in one sample of asthmatic sputum. There was no compelling evidence to suggest formation of Met-sulfone.

Analysis of control sputum indicated little compelling evidence for modification of Cys_{42} in S100A8, although weak immunoreactivity of enriched fractions suggested low abundance, which is not unexpected, given that the airways are under constant immune surveillance against air-borne pathogens. Met_1 was oxidized to $Met_1(O)$, a modification not observed in recS100A8 as Met_1 is removed by thrombin cleavage from the GST fusion protein [927]. S100A9 from control sputum only contained $Met_{63}(O)$.

Importantly, oxathiazolidine-oxide (1/5 samples) and -dioxide adducts were identified (3/5 samples), confirming oxidation *in vivo*. Peptides containing a free Cys_{42} residue were identified in sputum from 1/2 control subjects, but was not obvious in asthmatic sputum. Oxidation products in Cys_{42}-containing S100A8 peptides from

asthmatic sputum were similar to those generated by HOCl-oxidized recS100A8 (see Table 3.4, Chapter 3 and Section 4.3.4, Table 4.2).

In Section 3.4.1, it was proposed that the Gly_{50} residue in hS100A8 was less bulky than the Asn_{50} residue in mS100A8, which may afford greater flexibility of the hinge region of hS100A8, making Cys_{42} in hS100A8 more prone to oxidation [388, 392]. This may have indeed been the case as we found that rec-hS100A8 aggregated when levels of HOCl above a 1.5:1 molar ratio (HOCl:S100A8) were used for oxidation, whereas rec-mS100A8 was cross-linked but not aggregated with a 5:1 molar ratio (HOCl:mS100A8). Given that the *in vivo* modifications were similar, and the same Cys_{42}-oxathiazolidine-dioxide residues were identified, it is likely that a process similar to the oxidation observed *in vitro* (Chapter 3), also occurs *in vivo*. The oxidative post-translational modifications observed also affected function.

Interestingly, the S100A8/oxS100A8 profile seen in asthmatic sputum is strikingly similar to the anti-oxidant, glutathione. In asthma and other respiratory diseases, the ratio of reduced glutathione relative to the disulfide form (GSH/GSSG) can affect signalling pathways that participate in cell proliferation, autophagy and apoptosis [1016]. Like S100A8, which appeared to be in greater amounts as the oxidized monomer, GSH (from BALF) from patients with severe asthma was lower compared to control subjects, with concomitant increases in GSSG, indicating a shift to the oxidized state [1017]. The large amounts of oxS100A8 in asthmatic sputum suggest that, in asthma, S100A8 has anti-inflammatory effects by scavenging harmful hypohalous acid oxidants.

S100A9 exists in two isoforms, full length and a truncated form, generated from an alternate translation start site at Met_5 [92]. In blood neutrophils the full length isoform predominates, constituting ~70% of total S100A9 [637]. If the truncated form was more prevalent in the lung, for example in eosinophils, this may explain the absence of Cys_3-containing peptides in S100A9 from 1/2 control and 3/3 asthmatic samples. Met_{63}(O) was obvious, and Met_{81}(O) and Met_{94}(O) were found in some peptides from S100A9, although these modifications were only identified in non-enzyme-specified searches. Non-enzyme searches gave more identification in some samples, indicating variations in enzyme cleavage between samples. The weaker-quality data obtained from non-enzyme searches were obtained because of low abundance, but spectra were consistent with the formation of the unusual adducts. Met(O) adducts can be regenerated by reductases such as MSRB2, which is present in the lung [1018]. Met(O) adducts may not have been plentiful in sputum because of MSRB2 activity *in vivo*. Importantly, the oxidation

products found in sputum represent a snapshot of what had occurred, rather than a quantitative measure.

4.4.4 OXIDATION AFFECTS HETEROCOMPLEX FORMATION

Non-covalent S100A8/S100A9 complexes are the preferred structural form in neutrophils but there was little of the predicted 24 or 48 kDa forms [435] in unfractionated sputum (see Section 4.3.2), or in RP-HPLC-enriched fractions (see Section 4.3.4). Chemical cross-linking suggested that when both proteins had been oxidized with HOCl, heterocomplex formation was compromised (Fig 4.14A, B). Although somewhat inaccessible, oxidation of Met_{81} in S100A9 may disrupt the tight packing required for dimerization and/or destabilize the structure [69]. Moreover, the Cys_{42}-Ala_{42}S100A8 mutant does not complex with S100A9 [655]. Our results are consistent with observations reported by Sroussi *et al.* [655]. This inability of the oxidized products to form the heterocomplex would alter functions that are typical of the native heterodimers.

4.4.5 OXIDATION REDUCES NEUTROPHIL ADHESION

Neutrophils accumulate in the airways of patients with more severe airflow obstruction, and are prominent in airway secretions during acute exacerbations [1019]. Adhesion to fibronectin contributes to leukocyte extravasation and retention, and S100A9 promotes this [611] whereas S100A9-GSH is inactive [637]. rec-oxS100A8 and rec-oxS100A9 together almost abolished basal adhesion and the increased adhesion stimulated by the bacterial chemoattractant fMLP. Interestingly, the native complex also reduced adhesion of fMLP-treated neutrophils, uncovering a new anti-inflammatory function that was unaltered by oxidation. Mechanisms mediating this are unclear. However, these results suggest that S100A8/S100A9 may modulate retention of leukocytes at extravascular sites by inhibiting adhesion to fibronectin in the ECM.

4.4.6 OXIDATION OF S100A8 AND S100A9 ABROGATES ANTIMICROBIAL ACTIVITY OF S100A8/S100A9

Patients with chronic asthma are susceptible to lung infections [1003], as are patients with bronchiectasis, although characterization of lower airway microbiology is limited. Children with newly-diagnosed bronchiectasis and adults are commonly positive for *Haemophilus influenzae* (*H. influenzae*) and *P. aeruginosa* [991-993, 1020]. Emerging evidence suggests, however, that development of asthma does not necessarily

precede bacterial colonization in the lungs. Bacterial colonization in the hyperpharyngeal region at one month of age predicts subsequent asthma [1002]. The same may be true of bronchiectasis.

The S100A8/S100A9 heterocomplex is antimicrobial [620], with activity against a number of *Candida* strains, and strains of *Staphylococcus*, *Streptococcus* and *E. coli* [9], but no activity against bacteria associated with bronchiectasis (*H. influenzae* and *P. aeruginosa*) is reported. A Cys_{42}-Ala_{42}S100A8 mutant, abrogates antimicrobial function, suggesting the importance of this oxidation-sensitive residue [612, 655]. Because calprotectin is implicated in host-defense in the lung [1021], which, in areas of concentrated production of ROS may impair function, we tested this possibility.

S. pneumoniae is prevalent in young adults with asthma [1003], and this was initially used to assess potential changes in antimicrobial activity, but its mucinous growth made colony counting difficult and *E. coli* was substituted. Mutation of Met_{63} or Met_{83} in S100A9, or Cys_{42} in S100A8, significantly reduces antimicrobial activity [655]. We found that if either component of the heterocomplex was oxidized, *E. coli* growth was unaffected whereas when both contained HOCl-generated modifications, growth was no longer suppressed. As the antimicrobial effects of calprotectin depend on heterocomplex formation [9, 620], and oxidation of both components compromised heterocomplex formation (Figs. 4.14A, B), this may be the cause of the reduced activity. Met residues are important in anti-oxidant defense [1022] but if Met(O) in S100A9 were regenerated by reductases in lung [1018], its oxidation may not significantly compromise calprotectin's antimicrobial capacity, as oxS100A8/S100A9 remained antimicrobial. This possibly is feasible, given the low abundance of Met oxidation products found in S100A9 isolated from asthmatic sputum, compared to those generated in *in vitro* experiments (Table 3.8, Chapter 3). However, His oxidation of S100A8 or S100A9 (see Chapter 3), particularly within the Zn^{2+} binding motifs (residues 83-87 for S100A8, residues 91-95 for S100A9)[1023] may affect the Zn^{2+} binding capacity of these proteins and this possibility requires further examination.

Taken together, we confirmed that S100A8 scavenges ROS in asthmatic lung, however it may be worthwhile investigating whether other hypohalous acid oxidants such as HOSCN generate the novel oxathiazolidine oxide/dioxide products, to determine whether these were specific for HOCl induced oxidation (these were not generated by HOBr). Oxidation compromised formation of the S100A8/S100A9 heterocomplex, but this did not alter its ability to reduce neutrophil adhesion or to kill *E. coli*, indicating that

some important functions may be maintained. We propose that these S100 proteins contribute to anti-oxidant defense in the lung, particularly in conditions where other anti-oxidant mechanisms are compromised.

CHAPTER 5: S100A8, LIPID BINDING AND ANTI-OXIDANT ACTIVITY IN ATHEROSCLEROSIS

5.1 INTRODUCTION

Atherosclerosis involves chronic stimulation of the endothelial cells that line the intima, the innermost layer of the vessel wall. The inflammatory response is characterized by accumulation of inflammatory cells in the intima, initiating the atherogenic process [1024, 1025].

Oxidation plays a critical role in atherosclerosis and in patients with SLE, who have a higher risk of coronary artery events and carotid artery plaque formation, oxidized high-density lipoprotein (HDL) is increased, creating a pro-inflammatory particle [1026]. Moreover, oxidation of plasma protein by hydroxyl radicals, especially HSA enhances oxidative stress in SLE patients [1027]. These features may accelerate and increase cardiovascular events in these patients.

Specifically, HOCl generated by MPO, co-localizes with macrophages [1028] in human plaque where it oxidizes LDL (oxLDL) to a proatherogenic form, and may regulate proteases contributing to plaque rupture [1029]. Interestingly, increased numbers of MPO-expressing macrophages are seen in eroded or ruptured plaques typical of acute coronary syndromes, whereas macrophages in human fatty streaks contain little or no MPO [1028]. GM-CSF, but not M-CSF appears to regulate the ability of macrophages to express MPO and to produce HOCl *in vitro* [1028].

Approximately 83-96% of the total oxidized proteins in atherosclerotic plaque are localized within the extracellular matrix [1030]. These contain elevated levels of oxidized amino acids, such as DOPA, di-tyrosine, and 2-hydroxyphenylalanine (*o*-Tyr), and these modifications may contribute to advanced atherosclerotic lesions [1030]. More specifically, several studies implicate oxidation of LDL in atherogenesis [1031, 1032]. LDL, modified by ROS, renders the particle pro-inflammatory [1033]. Oxidation of Apolioprotein B-100 (ApoB-100), specifically on Lys residues, increases the net negative charge of the lipoprotein particle [1034, 1035]. Subsequently, LDL becomes susceptible to macrophage uptake, producing cholesterol ester-laden foam cells [1036, 1037]. Gas chromatography-mass spectrometry detected elevated levels of chlorotyrosine [1038] and *o,o'* –dityrosine [972] in human atherosclerotic lesions. HOCl-modified ApoB-100 contains high ratios of 3,5-dichlorotyrosine to 3-chlorotyrosine, indicating local HOCl production and subsequent lipoprotein oxidation [1039].

HDL is the major atheroprotective particle in plasma. It is a complex mixture of cholesterol-carrying lipoprotein particles, built upon a predominantly ApoAI backbone [698], the major lipoprotein of HDL. Other lipoproteins associated with HDL include ApoA-II, apoA-IV, ApoC and ApoE. ApoE and ApoA-IV are metabolised independently of ApoAI within HDL [1040].

HDL regulates RCT, the net transport of cholesterol from peripheral tissues to the liver. Cholesterol is eventually eliminated into the intestinal lumen as biliary cholesterol, where it is ultimately excreted in faeces [1041]. Efflux of cholesterol from foam cells is also mediated by HDL or its apolipoproteins, and represents a vital step in prevention or reversal of atherosclerosis [1042]. ApoAI and HDL are believed to account for the atheroprotective activity, as there is an inverse correlation between HDL cholesterol and ApoAI levels, and cardiovascular risk [698, 1042].

ApoAI is more sensitive to oxidation than LDL, a function that may actually reduce the atherogenecity of oxLDL [1043, 1044]. However, HDL can be rendered pro-inflammatory as a consequence of acute phase responses and chronic inflammatory conditions, and this may negatively affect functions critical for RCT [1045, 1046]. Impairment of HDL function in this context is attributed, in part, to oxidative modification via MPO. MPO binds a specific domain in ApoAI [1047, 1048]. Catalytically-active MPO generates HOCl (see Section 1.4.1.5, Chapter 1) and this can oxidize ApoAI [1042, 1047, 1048]. The pathway leading to dysfunctional HDL is illustrated in Fig. 5.1.

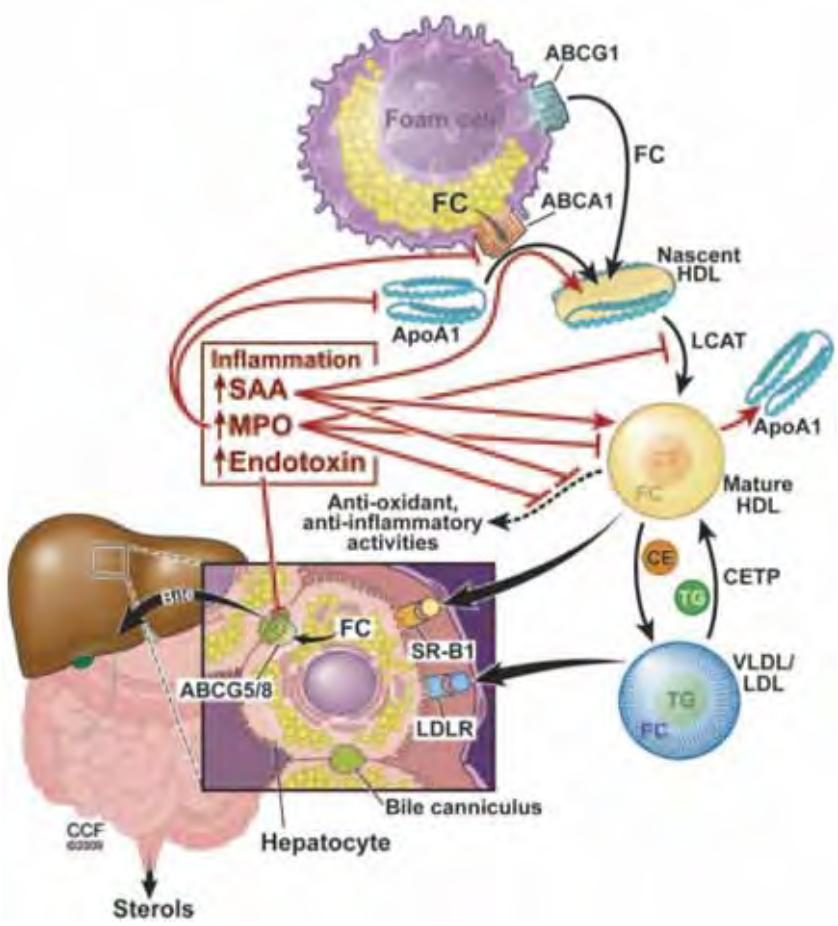

Figure 5.1: Role of inflammation in generating dysfunctional HDL and subsequent disruption of RCT. Cholesterol/sterol trafficking from the foam cell to their excretion is shown in black arrows. Effects of inflammation are shown in red. Under normal circumstances, ATP-binding cassette G member 1 (ABCG1) regulates transport of free cholesterol from foam cells, taken up by HDL. The enzyme lecithin-cholesterol acyltransferase (LCAT) converts free cholesterol into a cholesterol ester. Transfer of plasma protein between very-low-density (VLDL) or LDL in exchange for cholesterol esthers from HDL is then mediated by cholesterol ester transfer protein (CETP). Mature HDL then binds to the scavenger receptor class B member 1 (SR-B1) and LDL binds to the low-density lipoprotein receptor (LDLR) present on hepatocytes. Lipids are then excreted in faeces as sterols. However, inflammatory episodes may upregulate SAA, which displaces ApoAI from mature HDL, and MPO, which impairs LCAT function, binds ApoAI in HDL. Increased endotoxin levels downregulate the ATP-binding cassette G member 5 and 8 (ABCG5/8), impairing transport of lipids from the liver. From [1049].

The most sensitive amino acid cluster in ApoAI contains Met residues; formation of methionine sulfoxides have been identified on $Met_{86/112/148}$ and these were suggested to be a potential surrogate marker of early-stage oxidation of HDL [1042]. Oxidation of all four Trp residues to monohydroxytryptophan at positions, 8, 50, 72 and 108, and dihydroxytryptophan at position 108 within ApoAI may also contribute to MPO-dependent oxidative loss of ApoAI function *in vivo* [670]. Chlorination of Tyr_{192} by HOCl in concert with Met oxidation impairs cholesterol transport by ApoAI. It is proposed that oxidation may alter ApoAI folding, thereby impairing interaction with ABCA1 (reviewed in [1050]). Circular dichroism analysis confirmed that HOCl oxidation of ApoAI caused a dose-dependent loss of α-helical secondary structure in lipid-free, and to a smaller extent, in lipid-associated environments [1051].

Structural intergrity of ApoAI, particularly amphipathic α-helices with high lipid affinity is an important factor for its RCT; modification by reagent or enzymatically-generated HOCl may decrease anti-atherogenic properties of HDL and/or lipid-free ApoAI [1042]. Non-cholesterol efflux-related activities, for example, the HDL modulated reduction of cytotoxic effects generated by oxLDL on endothelial cells and smooth muscle cells [698], are also affected by oxidation which ablates HDL-mediated anti-apoptotic and anti-inflammatory activities. Therefore protection of HDL from oxidation represents an important counter-mechanism to prevent formation of pro-atherogenic particles and to maintain its protective functions.

Anti-oxidants are important in preventing atherosclerosis. Catechin, a natural phenol anti-oxidant [1052] and quercetin, a plant-derived flavanoid [1053], significantly increase paraoxonase 1 (PON1) activity [1054]. PON1 is an HDL-associated esterase/lactonase [1055], and its activity is inversely related to the risk of CVD [1056, 1057]. ApoAI stabilises PON1 by binding with high affinity and stimulates lactonase activity [1055], however, under oxidative stress, PON1 loses its anti-atherogenic properties [1058]. Therefore, oxidation of ApoAI may disrupt binding and subsequent stability of PON1, increasing atherosclerotic plaque formation.

$ApoE^{-/-}$ mice develop advanced atherosclerotic lesions in many locations and these show typical features of those in man, particularly, early fatty streak formation, later calcification and development of necrotic cores and fibrous caps [1059-1061]. Monocytes infiltrating early atherosclerotic lesions, and macrophages within mature plaque of $ApoE^{-/-}$ mice were reported as $mS100A9^{+}$-$S100A8^{-}$ [410, 527]. mS100A8 is a leukocyte

chemoattractant [317]; mS100A8-elicited macrophages had a pro-atherogeneic phenotype [523], expressing high levels of CD11b/CD18, Fc and scavenger receptors [523], which mediate uptake of oxLDL and acetylated LDL [1062]. For this reason, mS100A8 was believed to contribute to foam cell development [523].

In man, McCormick *et al*. showed foam cells and macrophages expressing S100A8 in diseased vessel lesions, whereas the same cells near neovessels were negative for S100A8. S100A9 was present in foam cells and non-foam cells, particularly in $CD68^+$ macrophages surrounding neovessels and endothelial cells and the surrounding extracellular matrix. S100A8 and S100A9 protein and mRNA were also found in macrophages, foam cells and neovessels in human atheroma [410]. S100A9 is also increased in platelets of patients with acute plaque rupture [124]. Moreover, serum levels of S100A8/A9 are 1.5-2.0 fold higher in patients with acute myocardial infarction, compared to those presenting with unstable angina pectoris [1063] and elevated serum levels are suggested to predict increased risk of first and recurrent cardiovascular events [124, 528]. In contrast, Altwegg *et al*. observed only S100A8/A9-positive staining in clustered monocytes/macrophages and neutrophils, but not in platelet aggregates within the coronary thrombi [524]. Ionita *et al.* also found high levels of S100A9 in rupture-prone atherosclerotic lesions, predominantly in non-foamy macrophages, and suggested that it may be a suitable marker for imaging high-risk rupture-prone plaques in humans [1064].

Mice deficient in ApoE and S100A9 had reduced atherosclerotic lesion area and macrophage accumulation in plaque [528]. Moreover, S100A8/A9 enhanced secretion of IL-6, ICAM-1, VCAM-1 and MCP-1 in HUVECs pretreated with advanced glycation end-product-albumin in a MAPK dependent manner, suggesting that these S100s contribute to vascular inflammation [1065]. Pro-inflammatory mediators such as MCP-1 cause changes to the vessel wall inducing adhesion receptors such as ICAM-1 and VCAM-1, thereby initiating stable adhesion of monocytes and their direct migration into the intima at sites of lesion formation [1066, 1067].

S100A8 is some ~200-fold more susceptible to oxidation by HOCl than LDL [410]. Moreover, S100A8 cross-linked covalent complexes were found in extracts of diseased carotid arteries. Thus, S100A8 was proposed to have a protective function by scavenging HOCl, and concomitantly prevent LDL oxidation [410] during atherogenesis. Identification of an association between HDL and S100A8 would strengthen the notion that S100A8 may protect HDL from oxidation by HOCl. S100A8 can also be S-

nitrosylated and this form has important functions that may maintain blood vessel patency and tone [613]. Putative oxidation of $Met_{63/83}$ abrogates S100A9-mediated fugetaxis of neutrophils [614]. In addition, S100A9-SSG reduces neutrophil adhesion to fibronectin [637]. Thus, identification of particular oxidative modifications of these proteins may limit tissue damage and have important implications in atherogenesis.

Preliminary experiments by Dr. Esther Lim and Prof. Carolyn Geczy (UNSW, Australia, unpublished) indicated that S100A8 immunoaffinity columns selectively bound ApoAI, ApoD, ApoE and albumin (see Section 5.3.1). The aim of this study was to characterize putative oxidative modifications to S100A8 and S100A9 in carotid artery plaque extracts, and determine whether S100A8 and/or S100A9 reduced MPO-mediated oxidative damage to endothelial cells. We also attempted to quantitate levels of S100A8, S100A9 and S100A8/A9 and to identify oxidative cross-linked S100A8 and/or S100A9 complexes in serum from subjects with an active inflammatory disorder (SLE) compared to healthy controls, and to confirm an association between S100A8 and ApoAI in HDL. We propose that S100A8, and to a lesser extent S100A9, may scavenge HOCl preferentially, thereby protecting ApoAI from modifications that could render it dysfunctional.

This chapter shows a characteristic multimeric, covalent banding pattern of S100A8 using Western blotting of carotid artery samples. Subsequent analysis indicated post-translational oxidative modifications to Cys_{42} in S100A8, confirming its capacity to scavenge oxidants *in vivo*. Cross-linking studies confirmed that S100A8 may bind ApoAI in HDL. Moreover, no free S100A8 was detected in Western blots of any human serum sample and slot blotting confirmed an association between oxS100A8/S100A8 and HDL. When ApoAI alone was incubated with recS100A8, and subsequently exposed to HOCl, S100A8 protected susceptible Met residues from oxidation, in a dose-dependent manner. Protective effects were reduced when incubated with HDL. The protective effect of the Cys_{42}-Ala_{42}S100A8 mutant, was reduced, indicating the importance of the Cys residue in oxidant scavenging. recS100A8 and/or S100A9 protected endothelial cells from oxidation by the MPO/H_2O_2 system. Taken together, these results suggest a unique relationship between HDL and S100A8. Importantly, S100A8 may prevent excessive oxidation of ApoAI within HDL, suggesting that it plays a protective role in atherogenesis.

5.2 EXPERIMENTAL PROCEDURES

5.2.1 S100A8 AFFINITY CHROMATOGRAPHY

To investigate potential binding partners of S100A8 in serum, recS100A8 (1 mg/ml gel volume) was covalently-coupled to cyanogen bromide (CNBr)-activated Sepharose 4B support (Pharmacia, NY, USA) in carbonate buffer (0.1 M NaHCO3, 0.5 M NaCl, pH 8.3) in a Poly-Prep column (Bio-Rad, MO, USA) according to manufacturer's instruction. Sera from two healthy donors were diluted in Tris buffer (1:1 (v/v) in 50 mM Tris-HCl, 150 mM NaCl, pH 7), loaded onto the S100A8-coupled affinity column or a control (uncoupled) column, washed with 10 x column volume of Tris buffer, and bound proteins eluted with 0.1 M glycine, 150 mM, pH 3. Aliquots (1 ml) of eluted fractions were concentrated by acetone precipitation, resuspended in PBS and proteins resolved by SDS-PAGE, under reducing conditions (10 mM DTT), and silver-stained (Section 2.1.3). Stained protein bands were excised (Section 2.1.7), digested with trypsin, and analyzed by nano-LC and mass spectrometry using LTQ-FT Ultra as previously described [933].

5.2.2 PREPARATION OF SLE AND CONTROL SERUM SAMPLES

In collaboration with Ms. Georgia Margalit and Dr. Sean O'Neill (UNSW, Australia), blood from healthy controls and patients with SLE were obtained with ethics approval and informed consent from patients attending Rheumatology and Immunology clinics at Liverpool Hospital. Serum from clotted blood was centrifuged at 230 x g for 10 min at 25ºC. Supernatants were collected, aliquoted and stored at -80ºC until analysis. The British Isle's Lupus Assessment Group 2004 (BILAG) index measured disease activity in SLE subjects; patients were given a score (A-E) of disease activity for each system; a score of A indicated high activity, with no disease activity defined as E [1068].

5.2.3 MEASUREMENT OF S100A8, S100A9 AND S100A8/A9 IN SERUM

Serum concentrations of S100A8 (diluted 1:50 v/v in PBS) and S100A9 (diluted 1:10 v/v in PBS) in SLE and control samples were determined by ELISA (described in Section 2.1.6). Serum concentration of S100A8/A9 was quantified using a sandwich ELISA kit (Hycult Biotechnology, Uden, the Netherlands) according to the manufacturer's instructions. As directed, serum samples were diluted 1:50 v/v in the dilution buffer provided.

5.2.4 ASSESSMENT OF S100A8, OXS100A8 AND S100A9 IN SERUM, HDL AND LDL

S100A8, oxS100A8 and S100A9 in sera were separated by SDS-PAGE and detected as described [529]. Briefly, sera diluted with PBS (1:10 v/v) were resolved by 10% SDS-PAGE (under reducing conditions; 100 mM DTT) and proteins transferred to a 0.2 μm polyvinylidene difluoride (PVDF) membrane (Section 2.1.3).

To identify oxS100A8, S100A8 and S100A9 in lipoproteins from serum samples, the serum (100 μl) from 3 normal donors and 3 patients with SLE were fractionated by fast protein liquid chromatography (FPLC) using a Superose 6 (1.0 x 300 mm) GL Column (GE Healthcare, PA, USA) [1069]. Dr. Maaike Kockx (UNSW, Australia) and Ms. Georgia Margalit performed the column set up, equilibration and fractionation of samples. Lipoprotein fractions were eluted with 20 mM sodium phosphate buffer, pH 7.8, at 0.25 ml/min and protein levels were monitored at $A_{280\ nm}$; 34 fractions (500 μl each) were collected, beginning after 10 min. Fractions 16-18 and 22-24 contained LDL and HDL respectively as indicated by a cholesterol assay kit (Wako Pure Chemical Industries, Osaka, Japan). Selected fractions were pooled and total protein levels measured using the bicinchoninic acid protein (BCA) assay (Pierce, IL, USA) with BSA standard (Pierce, IL, USA). Detection of S100 proteins in HDL and LDL samples was performed by dot blotting, with assistance from Ms. Georgia Margalit. Briefly, 40 μg from each pooled fraction of LDL were lyophilized and resuspended in 50 μl MilliQ H_2O. HDL eluted immediately before albumin and was contaminated with this protein. Approximately 800 μl of HDL fractions was lyophilized then resuspended in 50 μl Milli Q water. Standard concentrations of recS100A8, S100A9, oxS100A8 and ApoAI were also lyophilized then resuspended in 50 μl PBS. Samples and standards were loaded onto Hybond-ECL nitrocellulose membrane (GE Healthcare, PA, USA) using a Life Technologies Hybrid-slot Manifold (Carlsbad, CA, USA) according to the manufacturer's instructions, the membrane blocked with 5% skim milk in TBS and incubated with anti-oxS100A8, S100A8 or S100A9 IgG (1 μg/ml in 1% skim milk/TBS). A polyclonal goat anti-human ApoAI (1:10000 v/v in 1% skim milk/TBS; BD BioSciences, CA, USA) primary antibody and an HRP-tagged donkey anti-goat IgG (1:5000 v/v in 1% skim milk/TBS; Bio-Rad, CA, USA) secondary antibody were used to detect ApoAI in standards.

Because of varying reactivity of the antibodies, membranes were probed sequentially for oxS100A8, S100A9 then S100A8 minimising cross-reactivity. Following

assessment with oxS100A8 IgG, membranes were stripped (0.2 M glycine, 0.05% Tween 20, pH 2.5) for 40 min at 80ºC, washed with TBS for 2 x 10 min and incubated with HRP-conjugated goat anti-rabbit IgG (1:2000 v/v in 1% skim milk/TBS), as developed (Section 2.1.3) to confirm removal of primary antibody. Membranes were then probed with anti-S100A9, S100A8 or ApoAI IgG. Reactions were detected by chemiluminescence as described in Section 2.1.3.

5.2.5 QUANTITATION OF S100A8, S100A9 AND OXS100A8 BY DENSITOMETRY

Approximate densities of each slot blot band were determined using ImageJ software. Levels of S100A8, S100A9 and oxS100A8 were compared to reactivity of antibodies with 25 ng standard recS100 on each blot. Standards and samples were also compared to a standard curve of each recombinant protein, determined by slot blotting. Because of albumin contamination, amounts of HDL in samples were not quantitated. Results for HDL were expressed as a ratio of total ApoAI by measuring ApoAI density in samples to an ApoAI standard curve developed for the same time (30 s). Results were expressed as ng/100 ng ApoAI.

5.2.6 ISOLATION OF HDL AND APOAI FROM PLASMA

Isolation of HDL was performed with assistance from Dr. Cacang Suarna, and in collaboration with Prof. Roland Stocker (University of Sydney, Australia). Using a two-step density gradient and ultracentrifugation in a TL 100.4 rotor (Beckman Instruments, Palo Alto, Ca) human HDL was isolated rapidly from fresh pooled plasma containing EDTA (1 mg/ml; final concentration) [1070]. Plasma was isolated by low-speed centrifugation (1,500 x g, 30 min; Beckman GS-6R tabletop centrifuge), the density adjusted to 1.24 g/ml with potassium bromide (381.6 mg/ml; Sigma, MO, USA) and then centrifuged for 3 h at 543,000 x g (at 15°C) then HDL (third layer from top) isolated by needle aspiration. Prior to use, low molecular weight compounds were removed by size exclusion chromatography (NAP-10 columns, Sephadex G-25 DNA Grade; GE healthcare, Rydalmere, Australia) conditioned with PBS 3 x bed volume as described [1071]). HDL (1 ml) was passed through the column, followed by 1.5 ml of PBS, which was then collected. The process was repeated until all HDL was collected and purified [1071]. This method does not discriminate between HDL_1, HDL_2 and HDL_3. As these constituents vary among subjects, HDL from a single donor collected from whole blood at a single time was used for all experiments to ensure consistent C18-RP-HPLC profiles

during all experiments. Protein concentration of ApoAI in HDL was calculated by comparing the area under the curve generated at A_{214nm} by C18-RP-HPLC relative to a known protein concentration of ApoAI.

ApoAI was collected and purified from HDL as described [1070, 1071]. Briefly, HDL (300 μl) was separated using gradient RP-HPLC, performed on a Waters alliance 2690 separation module equipped with a Waters 2487 dual absorbance detector (Waters, MA, USA) [1071]. The HPLC-UV system was equipped with a reverse phase semi-preparative C18 column (Vydac, 250 x 10 mm) with guard (5 cm, 4.6 mm ID; Vydac Separations Group, CA, USA). The sample chamber was set to 4°C and the column heated to 50°C after the instrument system was purged with 10% methanol and 10% acetonitrile in H_2O. HDL samples were eluted at 2 ml/min at 50°C, monitored at $A_{214\ nm}$ using the following method. Initial equilibration in 25% solvent A (acetonitrile containing 0.1 vol % TFA) and 75% solvent B (water containing 0.1 vol % TFA) for 10 min, the concentration of solvent A was increased linearly to 45% over 5 min, then to 55% over 32 min, to 95% over 10 min and finally to 100% in 1 min, after which solvent A was decreased to 25% for column re-equilibration. ApoAI had a retention time of 31 min; this peak was collected, lyophilized, resuspended in PBS and quantitated by BCA assay with BSA standard and stored at -80°C.

5.2.7 CROSS-LINKING OF APOAI, HDL AND S100A8

To investigate possible associations between HDL and S100A8, 2 μg recS100A8 or Cys_{42}-Ala_{42}S100A8 and ApoAI or ApoAI in HDL (ApoAI(HDL)) (2 μg) were suspended in PBS (supplemented with 1 mM $CaCl_2$) and incubated for 37°C for 30 mins, then putative complexes cross-linked with BS_3 cross-linker (1 mM) for an additional 30 mins in the dark. Samples without BS_3 were used as controls. Mixtures were separated by 10% SDS-PAGE under non-reducing conditions, then Coomassie-stained. Cross-linked complexes migrating at 38 and 48 kDa (corresponding to masses of S100A8+ApoAI(HDL) and $S100A8_2$+ApoAI(HDL), respectively) were excised and digested according to the method described in Section 2.1.7.

5.2.8 ARTERIAL TISSUE EXTRACTION AND ASSESSMENT OF S100A8, OXS100A8 AND S100A9 IN CAROTID ARTERY

Specimens from three endarterectomy patients (provided by Mr. Victar Hsieh, UNSW, Australia) were pulverized under liquid nitrogen. Because S100 proteins are susceptible to oxidation [410, 606], samples (~500 mg) were prepared in PBS/10 mM EGTA (1.5 ml, pH 7.5) containing protease inhibitor mixture (Roche Applied Science, Mannheim, Germany), 1 mM sodium azide (inhibits MPO that generates HOCl; Sigma, MO, USA) [1072] and 10 mM *N*-ethylmaleimide (NEM; derivatises free thiols; Sigma, MO, USA) [410] were sonicated for 5 min, rotated at 4°C for 2 hrs, then centrifuged (1,600 x g, 20 min, 4°C). Supernatants were pre-cleared with agarose-conjugated caprine anti-rabbit IgG (~1 mg/ml, 1 hr at 4°C; Sigma, MO, USA), centrifuged and total protein measured by BCA assay. Carotid artery proteins (4 μg) were resolved by 10% SDS-PAGE and Western blotted as described in Section 2.1.3.

5.2.9 PEPTIDE GENERATION AND MASS SPECTRAL ANALYSIS OF CAROTID ARTERY SAMPLES

Proteins in carotid artery extracts (250 μg; n=3) were eluted from C8-RP-HPLC in 33-59% acetonitrile/0.1% TFA. Eluates were collected in 3 minute intervals over 30 min and analyzed; C8-RP-HPLC eluates (1 ml from each aliquot, n=10) were lyophilized, suspended in PBS (10 μl) and separated by SDS-PAGE under reducing conditions (100 mM DTT), then Western blotted with anti-S100A8, anti-oxS100A8 or anti-S100A9 IgG (as in Section 2.1.3). Due to insufficient protein yields, membranes were probed sequentially for oxS100A8, S100A9, then S100A8. Following reactivity with one antibody, membranes were stripped and reprobed (Section 5.2.4). Peaks eluting from C8-RP-HPLC between 9-12 and 12-15 min contained predominantly S100A8, oxS100A8 and S100A9. The 9-12 and 12-15 min aliquots were pooled (2 ml from each aliquot) and further resolved by C4-RP-HPLC (25-70% acetonitrile/0.1% TFA).

Western blotting of 1 ml lyophilized C4-RP-HPLC eluate (10 aliquots, each collected over 3 min intervals for 30 min) confirmed presence/absence of oxS100A8, S100A8 and S100A9. Proteins in the lyophilized peaks (5 μg; from 12-15 min, 15-18 min, 18-21 min aliquots) were suspended in 20 mM NH_4HCO_3 (100 μl) and digested (4 hrs at 37°C) with Asp-N and analyzed by MS (Section 2.1.8).

5.2.10 ESTABLISHMENT OF HOCl DOSE REQUIRED FOR APOAI AND APOAI(HDL) OXIDATION

S100A8/A9 associates with lipids in circulation [178] and we found S100A8 associated with HDL (Section 5.3.5). HDL becomes pro-atherogenic following oxidation of ApoAI [698]. recS100A8 was oxidized with HOCl, in the presence of ApoAI or ApoAI(HDL) to assess whether it protected these from oxidation.

Initial dose response experiments were conducted to determine the appropriate concentration of HOCl required to generate a ~50:50 mixture of ApoAI:oxApoAI or ApoAI(HDL):oxApoAI(HDL). Briefly, 3.9 μM ApoAI or ApoAI(HDL) was treated with HOCl diluted in PBS to final molar ratios of 1:0, 1:5, 1:10, 1:15 (ApoAI or ApoAI(HDL): HOCl), in a final volume of 200 μl and incubated for 1 hr at 37°C. Oxidation was stopped with L-Met (final concentration 2.5 mM). All solutions contained 10 μM diethylenetriamine pentaacetic acid (Sigma, MO, USA), to chelate free metal ions and 1 mM $CaCl_2$. Proteins were then analyzed by RP-HPLC as described [1071]. Briefly, oxidized preparations (100 μl) were separated by using a C18 column (250 × 4.6 mm, 5 μm, Vydac Separations Group, CA, USA) with guard column (5 μm, 4.6 ID, Vydac Separations Group, CA, USA) eluted at 50°C and 0.5 ml/min, and $A_{214\ nm}$ monitored. After equilibration in 25% solvent A (acetonitrile containing 0.1 vol % TFA) and 75% solvent B (water containing 0.1 vol % TFA) for 10 min, the concentration of solvent A was increased linearly to 45% over 5 min, then to 55% over 32 min, to 95% over 10 min, and finally to 100% in 1 min. Solvent A was decreased to 25% for column re-equilibration. The area under the curves corresponding to ApoAI or ApoAI(HDL) (retention time ~29 min) and oxApoAI or oxApoAI(HDL) (retention times: ~21 ($Met_{86/112}$(O)), ~22 (Met_{112}(O)) and 28 min (Met_{86}(O))) were quantitated (expressed as net unit area) and expressed as a percentage relative to an unoxidized ApoAI or ApoAI(HDL) protein standard of eqivalent amount (10.9 μg).

5.2.11 LEVELS OF OXIDATION OF APOAI/APOAI(HDL) BY HOCl IN THE PRESENCE OF HSA

HSA is an oxidant scavenger (reviewed in [948]) and was used as a positive control to confirm that ApoAI alone, or as part of HDL, could be protected against oxidation. Briefly, 3.9 μM ApoAI was incubated with increasing molar amounts of HSA (Sigma, MO, USA) (1:0, 1:1, 1:2, 1:4 and 1:10 (ApoAI:HSA)), and incubated for 30 min

at 37°C. HOCl was added in a 5:1 molar excess relative to ApoAI, or a 10:1 molar excess relative to ApoAI(HDL), and incubated for 1 hr at 37°C, and oxidation stopped with a final concentration of 2.5 mM L-Met. A volume of 100 μl was analyzed by RP-HPLC [1071] as described in Section 5.2.10. Total unmodified and oxApoAI was measured (net unit area) and expressed as a percentage relative to unmodified ApoAI (10.9 μg). The same method was used to analyze ApoAI(HDL), however an additional molar ratio of 1:10 (ApoAI(HDL):HSA) was used, as initial experiments suggested that HSA was less efficient at scavenging HOCl when incubated with ApoAI(HDL).

5.2.12 LEVELS OF OXIDATION OF APOAI/HDL(APOAI) BY HOCl IN THE PRESENCE OF S100A8/CYS$_{42}$-ALA$_{42}$S100A8

The oxidant-scavenging capacity of recS100A8 was tested. Cys$_{42}$-Ala$_{42}$S100A8 was analyzed to assess the importance of Cys$_{42}$ in S100A8. The method was identical to that described in Section 5.2.11, using molar ratios of 1:0, 1:1, 1:2, 1:4 and 1:10 (ApoAI/ApoAI(HDL):S100 protein).

5.2.13 OXIDATION OF APOAI WITH OXS100A8

rec-hS100A8 scavenged hypohalous acid oxidants (Chapter 3, Section 3.3.3) and it was important to determine whether the oxidized amino acids (Cys$_{42}$ or Met$_{78}$) in S100A8 could, in turn, oxidize ApoAI. The following protocol was developed to investigate this. Briefly, recS100A8 was oxidized with a 2:1 molar ratio of S100A8:HOCl (HOCl diluted in PBS containing 10 μM DTPA and 1 mM $CaCl_2$) and incubated for 1 hr at 37°C, then the solution added to ApoAI to a final volume of 220 μl. The final molar ratio equated to 1:10:5 of ApoAI:S100A8:HOCl. Volumes of 40 μl were removed after 0, 10, 20, 40, 60 min and 10 μl 50 mM L-Met added to quench any remaining oxidants. Samples were then analyzed by RP-HPLC as in Section 5.2.10. Unoxidized recS100A8 incubated with ApoAI was used as control. Areas under the curves for native and oxApoAI were quantitated as net unit areas and results expressed relative to unoxidized S100A8 and unoxidized ApoAI.

5.2.14 OXIDATION OF BOVINE AORTIC ENDOTHELIAL CELLS BY MPO/H_2O_2

Endothelial dysfunction during inflammatory vascular disease is perpetuated by production of HOCl via endothelium localised MPO (reviewed in [1073]). In

collaboration with Mr. Thuan Thai and Dr. Shane Thomas (UNSW, Australia), we attempted to determine if rec-hS100A8 and/or S100A9 could protect endothelial cells from oxidation by the MPO/H_2O_2 system. Bovine aortic endothelial cells (BAEC) were incubated with HEPES-Krebs buffer (Sigma, MO, USA) with or without 20 nM MPO (Calbiochem, CA, USA) for 2 hrs, then washed and replaced with fresh HEPES-Krebs containing 100 μg/ml S100A8/Cys_{42}-Ala_{42}S100A8, 140 μg/ml S100A9 or both for 30 min. Relevant samples were then incubated with 25 uM H_2O_2 for a further 60 min before lysis with SDS-loading buffer containing 50 mM DTT. Levels of fibronectin (1:5000 v/v, monoclonal mouse anti-fibronectin IgG, BD Transduction Laboratories, CA, USA), hypochlorite-oxidized proteins (HOP); anti-2D10G9 IgG, 1:50 v/v custom-made by Dr. Ernst Malle (Medical University of Graz, Austria) were then assessed by immunoblotting with an HRP-tagged horse anti-mouse IgG secondary antibody (1:2500 v/v; Cell Signaling Technology, MA, USA). Total protein in samples was assessed as total tubulin (monoclonal anti-α tubulin IgG, 1:5000 v/v; Sigma, MO, USA). Western blots were visualized using Western Lightning-ECL enhanced chemiluminescence substrate according to the manufacturer's instructions.

5.2.15 STATISTICAL ANALYSIS

S100 protein concentrations in serum calculated by ELISA were tested for statistical significance using one-way ANOVA in conjunction with Bonferonni's multiple comparison test, which allowed for comparisons between each of the groups. Spearman's correlation, with a confidence level of 95%, was used in experiments analyzing the protective effects of HSA or S100A8 in prevention of ApoAI or ApoAI(HDL) oxidation. Linear regression was used to calculate r^2 values and general trends were reported as a line of best fit. Statistical analysis of slot blot density could not be performed due to insufficient sample size, so only trends are reported. Protein aggregation of S100A8 and Cys_{42}-Ala_{42}S100A8 observed in Section 5.3.8 and 5.3.9 was tested using a one-tailed unpaired t-test.

5.3 RESULTS

5.3.1 S100A8 IMMUNOAFFINITY PULLED DOWN COMPONENTS OF HDL FROM SERUM

Preliminary experiments performed by Dr. Esther Lim and Prof. Carolyn Geczy suggested that S100A8 bound proteins associated with HDL. To enable the work performed in this Chapter to be understood in context, the results are included here.

Putative binding partners of S100A8 in serum were isolated using an S100A8-coupled affinity column (see Section 5.2.1). Four components specifically and consistently bound to the S100A8-coupled column, but not to the control column, in two separate experiments using serum from two healthy donors. Components separated by SDS-PAGE were excised with peptides generated by in-gel trypsin digestion. MS sequencing of digested bands produced high Mascot scores for ApoAI, ApoE, ApoD and albumin (listed in Table 5.1).

Table 5.1: Summary of binding partners of S100A8 in serum

Protein	Molecular weight	MASCOT Score* (peptides matched) Subject 1	MASCOT Score* (peptides matched) Subject 2
Proapolipoprotein (also matched: apoAI preproprotein, ApoAI, Chain A, crystal structure of lipid free human ApoAI)	28,944 kDa	902 (39) [10 kDa band]	638 (21) [14 kDa band]
Apolipoprotein E	36,188 kDa	228 (5) [20 kDa band]	248 (5) [20 kDa band]
Apolipoprotein D	27,975 kDa	203 (7) [20 kDa band]	- 108 (5) [10 kDa band] - 123 (6) [14 kDa band] - 353 (12) [20 kDa band]
Chain A, Prealbumin	13,752 kDa	179 (3) [10 kDa band]	202 (8) [20 kDa band]

*MASCOT score is a non-probabilistic basis for ranking protein hits using the MASCOT program, calculated from the ion score according to -10 x Log(P), where P is the probability that the observed peptide match is a random event [1074]. Results represent serum samples from two healthy donors.

5.3.2 PATIENT CHARACTERISTICS OF SERUM DONORS

Serum from 23 healthy controls and 28 patients with SLE were used. Patients with SLE were divided into two groups: in remission (n=17), or active disease (n=11). BILAG assessment was performed at the time of sample collection [1075]. Patients with active disease had at least one A score or two B scores. Characteristics of serum donors are given in Table 5.2.

Table 5.2: Characteristics of serum donors

	SLE patients in remission (n=17)	**SLE patients with active disease (n=11)**	**Healthy controls (n=23)***
Age (mean ± SD)	41.18 ± 12.39	40.45 ± 10.88	29.14 ± 8.10
Gender ratio (F:M)	16:1	11:0	23:0
ETHNICITY			
South-East Asian	5	5	5
Caucasian	6	2	1
European	3	2	0
African	1	0	0
Middle Eastern	1	1	0
Indian	1	1	8

* Information on age and ethnicity available for n=19 only

5.3.3 SERUM CONCENTRATIONS OF S100A8, S100A9 AND S100A8/A9

Serum concentrations of S100A8, S100A9 and S100A8/A9 were determined by ELISA. No significant differences in S100A8 levels from patients with active SLE (2,685.0 ± 659.5 ng/ml), SLE patients in remission (3,312.1 ± 495.5 ng/ml) or healthy controls (3,951.9 ± 556.4 ng/ml) (Fig. 5.2A) were found. Similarly, no significant differences were observed in serum levels of S100A9 from SLE subjects with active disease (84.2 ± 10.8 ng/ml), SLE subjects in remission (147.3 ± 39.7 ng/ml) or healthy controls (145.7 ± 43.4 ng/ml) (Fig. 5.2B). No significant differences were observed between serum levels of S100A8/A9 in patients with SLE in remission (384.2 ± 40.5 ng/mL), patients with SLE with active disease (305.8 ± 44.9 ng/mL) or healthy controls (348.5 ± 29.8 ng/mL) (Fig. 5.2C).

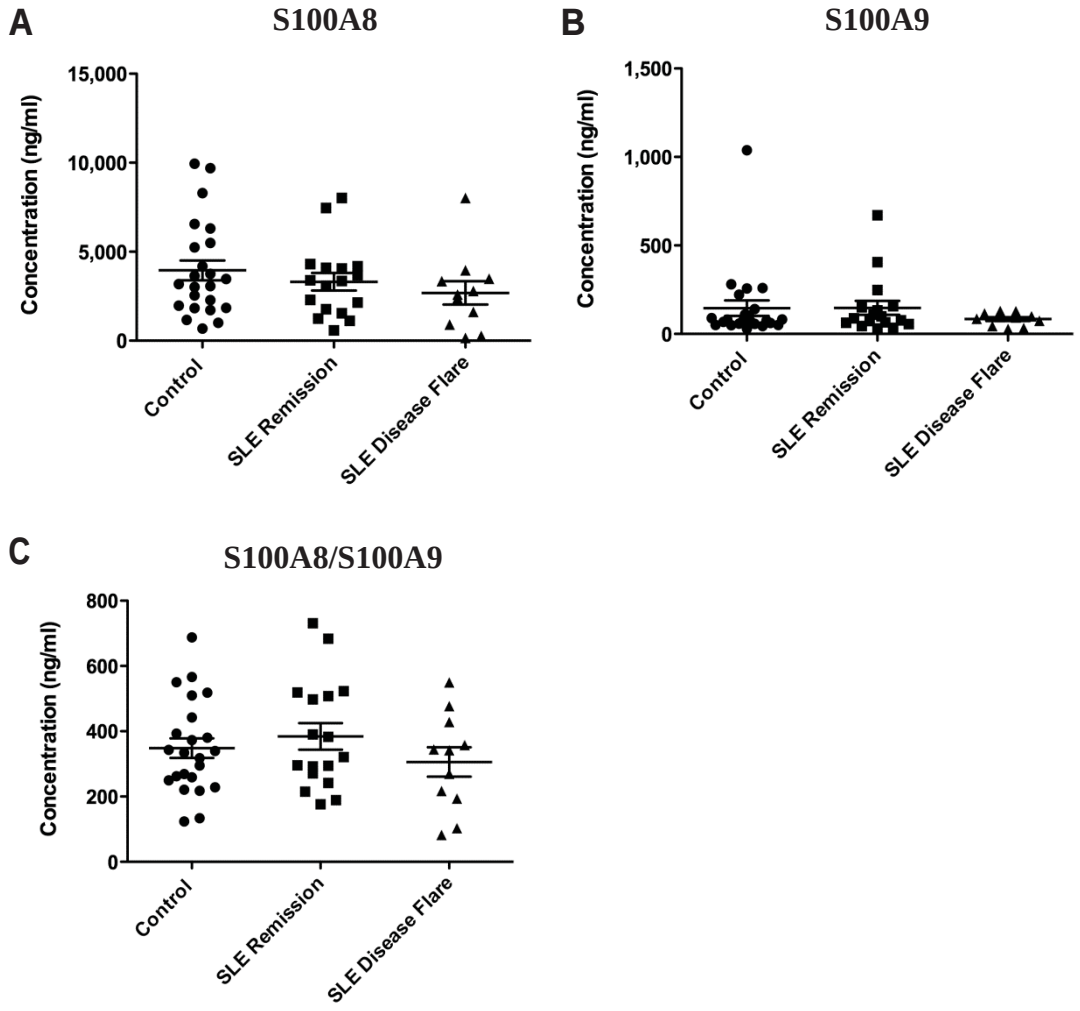

Figure 5.2: Serum concentrations of S100A8, S100A9 and S100A8/A9. (**A**) Levels of S100A8 in serum were not significantly different in any subgroup, although S100A8 was slightly higher in healthy controls. (**B**) Serum concentrations of S100A9 were not significantly different among the subgroups examined. (**C**) Although serum concentrations of S100A8/A9 were somewhat higher in SLE subjects in remission, results were not statistically significant.

5.3.4 S100s IN SERUM WERE NOT DETECTED BY WESTERN BLOTTING

Unfortunately we did not have ready access to serum from patients with CVD, so we used sera from normal donors and those with SLE.

Previous studies reported elevated levels of the S100A8/A9 heterocomplex in serum from patients with SLE [468, 472], but there are no reports defining the likely structure of these proteins in serum. Western blotting was used to identify S100A8, oxS100A8 or S100A9 in serum from normal donors and SLE patients. Anti-S100A8, anti-oxS100A8 and anti-S100A9 IgG failed to detect reactive components in any serum sample (not shown). To ensure that serum proteins were properly transferred to PVDF membranes, one control and one SLE sample were separated by SDS-PAGE and Coomassie-stained to validate effective separation (Fig. 5.3A, left hand gel). The same samples were transferred to PVDF membrane, and then the gel restained to ensure that all protein had been transferred (Fig. 5.3A, right hand gel). The PVDF membrane was Western blotted with anti-S100A8 or anti-oxS100A8 IgG. Again, there was no positive reactivity compared to the strong reactivity seen with the recombinant proteins (Fig. 5.3B).

Interestingly, recombinant HOCl-oxS100A8 appeared less abundant on Coomassie-stained gels and Western blotted PVDF membranes, despite equal amounts of native and oxS100A8 being loaded. This was only observed in C4-HPLC-purified preparations of rec-oxS100A8 and suggests that oxidation may affect electromobility of the oxidized protein.

Because S100A8 could not be detected in whole serum, lipoproteins were isolated and slot blotted to identify S100A8, oxS100A8 and S100A9 in samples.

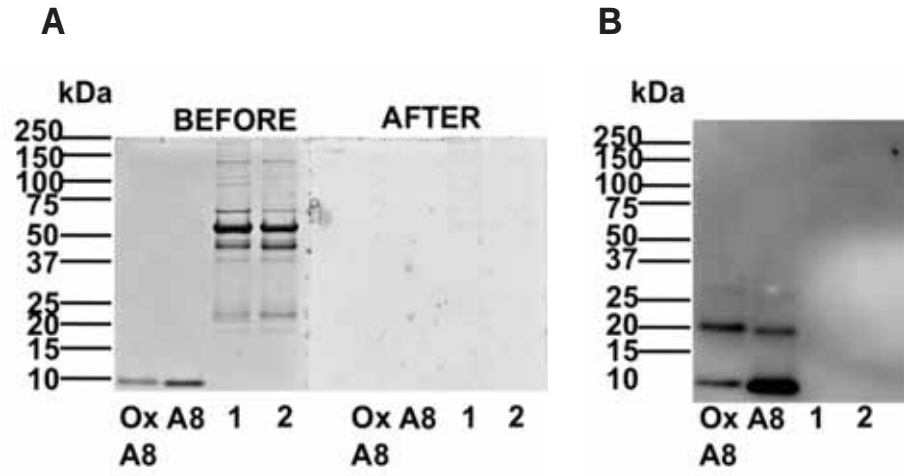

Figure 5.3: Serum protein was transferred to PVDF membranes, but was not immunoreactive. (**A**) 250 ng rec-oxS100A8 or recS100A8 and 1 μg serum (Control: sample 1, SLE: sample 2) was separated by SDS-PAGE and Coomassie-stained, before or after transfer to PVDF membranes. Serum protein was effectively transferred as the re-stained gel (after) had no detectable Coomassie stained bands (**B**) Western blotting of membranes with anti-S100A8 IgG indicated positive reactivity with positive controls, but not serum components.

5.3.5 LIPOPROTEIN FRACTIONS CONTAIN S100 PROTEIN

To standardize levels of S100s or ApoAI to be detected by slot blotting, decreasing concentrations of recombinant proteins were used; 5-10 ng were readily detected (Fig. 5.4). We next used HDL and LDL-enriched fractions from 3 normal and 3 SLE donors to test for S100 content (subject characteristics shown in Table 5.3). S100A8 was detected in all HDL samples, whereas levels in LDL were markedly less. oxS100A8 was also detected in all HDL samples (Fig. 5.5A) although negligible amounts were seen in LDL (Fig. 5.5B). Strong reactivity of HDL samples with anti-ApoAI IgG confirmed its presence in all samples (Fig. 5.5A). In contrast, only LDL samples 3 and 5 had moderate reactivity with anti-ApoAI IgG (Fig. 5.5B), indicating that these were contaminated with HDL and this contamination could be responsible for the weakly positive S100A8/oxS100A8 reactivity in LDL samples. Densities of S100s in slot blots of HDL and LDL fractions were semi-quantitated; levels of the S100s were standardized according to the cholesterol content of each fraction. Using this approach, we confirmed that S100A8 and oxS100A8 were higher in HDL than in LDL. Levels of S100A8 and oxS100A8 tended to be higher in subjects with SLE in HDL and LDL samples (Fig 5.5C, D), particularly in SLE subject 3, who had active disease at the time of collection (Table 5.3). In contrast, S100A9 levels were some 3- to 20-fold lower. For example, SLE2 had 0.52 ng/mg/dL cholesterol of S100A8, but 0.031 ng/ml/dL cholesterol of S100A9; little S100A9 was found in LDL (Fig. 5.5E).

Table 5.3: Characterization of three control and three SLE serum donors used for slot blot experiments

	C1*	C2	C3	SLE1	SLE2	SLE3**
Age	-	34	22	56	53	27
Ethnicity	-	Indian	Middle Eastern	Middle Eastern	Caucasian	Vietnamese
Disease Activity	NA	NA	NA	Remission	Remission	Active
BMI	-	Normal	Overweight	Overweight	Overweight	Normal
Heart Disease	-	No	No	No	No	No
Hypertension	-	No	No	No	No	No
Hypercholesterolaemia	-	No	No	No	No	No
Diabetes	-	No	No	No	No	No
Family History (CVD)	-	No	No	Yes	Yes	-
Smoking	-	No	Yes	No	Ex-smoker	-

* Information on C1 not available

** Some information on SLE3 not available

BMI: Body Mass Index; CVD: cardiovascular disease; NA: not applicable

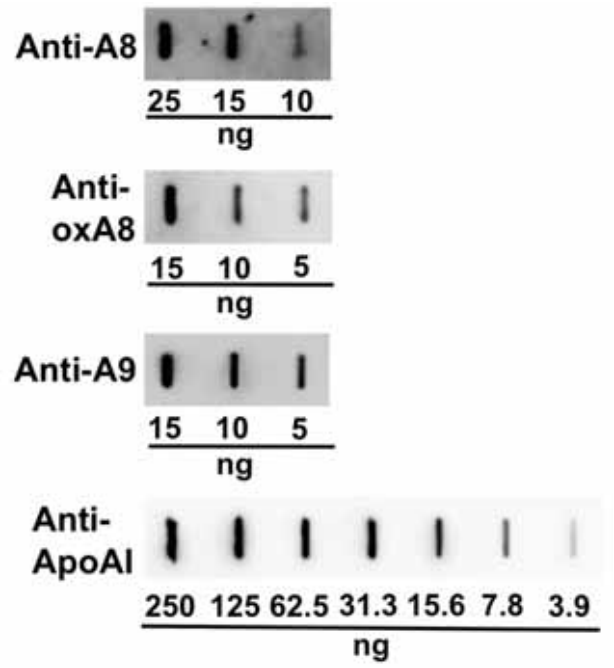

Figure 5.4: Protein standards in slot blots. Slot blots of decreasing concentrations of protein standards of recS100A8, oxS100A8, S100A9, and ApoAI used for semi-quantitation by densitometry.

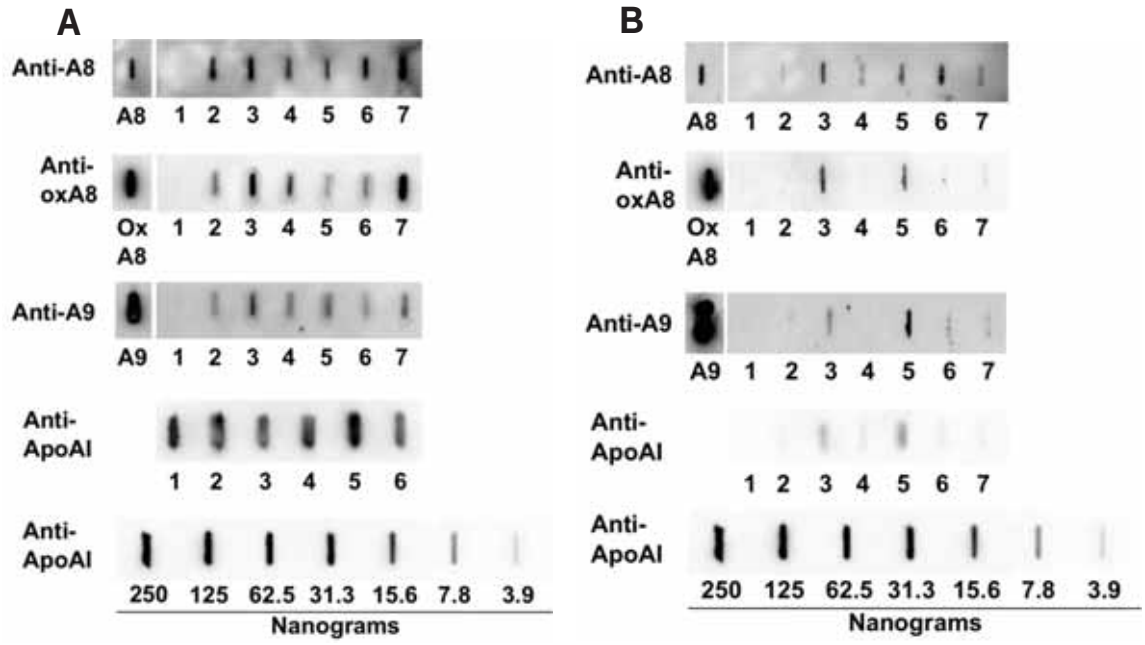
A
Anti-A8
A8 1 2 3 4 5 6 7
Anti-oxA8
Ox A8 1 2 3 4 5 6 7
Anti-A9
A9 1 2 3 4 5 6 7
Anti-ApoAI
1 2 3 4 5 6
Anti-ApoAI
250 125 62.5 31.3 15.6 7.8 3.9
Nanograms
B
Anti-A8
A8 1 2 3 4 5 6 7
Anti-oxA8
Ox A8 1 2 3 4 5 6 7
Anti-A9
A9 1 2 3 4 5 6 7
Anti-ApoAI
1 2 3 4 5 6 7
Anti-ApoAI
250 125 62.5 31.3 15.6 7.8 3.9
Nanograms

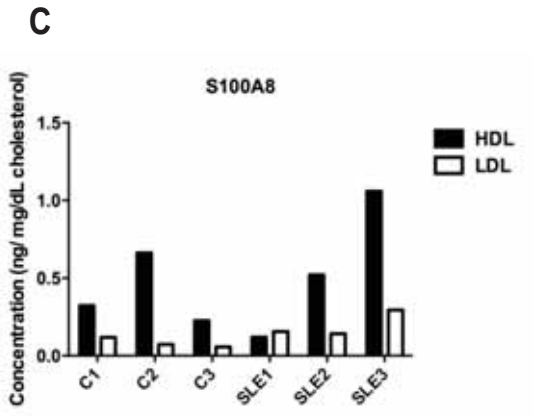
C
S100A8
Concentration (ng/ mg/dL cholesterol)
1.5
1.0
0.5
0.0
HDL
LDL
C1
C2
C3
SLE1
SLE2
SLE3

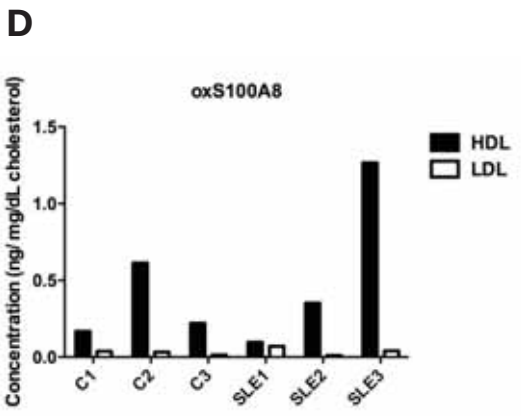
D
oxS100A8
Concentration (ng/ mg/dL cholesterol)
1.5
1.0
0.5
0.0
HDL
LDL
C1
C2
C3
SLE1
SLE2
SLE3

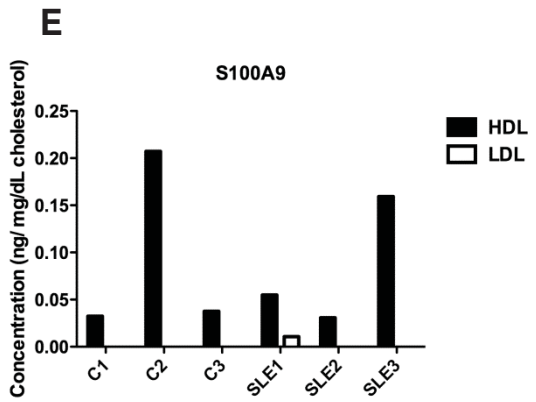
E
S100A9
Concentration (ng/ mg/dL cholesterol)
0.25
0.20
0.15
0.10
0.05
0.00
HDL
LDL
C1
C2
C3
SLE1
SLE2
SLE3

Figure 5.5: Slot blots detecting S100A8, oxS100A8 and S100A9 in HDL and LDL fractions separated from three control and three SLE sera. (**A**) S100A8 and oxS100A8 were detected in all HDL fractions. Low levels of S100A9 were detected in HDL fractions compared to the standard. ApoAI was present in all HDL fractions and used for standardization. Lane 1: PBS, Lane 2: Control 1, Lane 3: Control 2, Lane 4: Control 3, Lane 5: SLE 1, Lane 6: SLE 2, Lane 7: SLE 3. (**B**) S100A8 levels were relatively low in all LDL samples; oxS100A8 was weakly detected or absent. S100A9 levels were very low in LDL fractions compared to the standard. Concentrations of S100A8, oxS100A8 and S100A9 in HDL and LDL fractions from three control and three SLE sera were determined by slot blots, given as ng/S100/mg cholesterol/dL. (**C**) S100A8 levels were higher in all HDL than in LDL fractions except for SLE1. (**D**) oxS100A8 and (**E**) S100A9 levels were higher in HDL than LDL fractions in all samples. S100A9 bars not visible have levels below detection limits. Note that the levels of S100A9 on the Y-ordinate are 0 - 0.25 ng/mg/dL cholesterol compared to S100A8 and oxS100A8 (0 – 1.5 ng/mg/dL cholesterol).

5.3.6 S100A8 FORMS CROSS-LINKED COMPLEXES WITH APOAI AND APOAI IN HDL

Results of S100A8 affinity suggested that it bound ApoAI (Section 5.3.1), and we confirmed the presence of S100A8 and oxS100A8 in HDL fractions. To confirm whether the association between S100A8 and ApoAI alone or in HDL was by direct binding, we performed preliminary cross-linking experiments, paying particular attention to complex migration at 38 and 48 kDa (corresponding to ApoAI + S100A8 and ApoAI + $S100A8_2$ respectively). ApoAI alone was cross-linked with recS100A8 or with $recCys_{42}$-Ala_{42}S100A8 to determine interaction with the Cys_{42} residue. Cross-linking of ApoAI alone generated multiple complexes migrating at ≥ 75 kDa. Only when ApoAI was cross-linked with S100A8, was a complex at 38 kDa (ApoAI + S100A8) evident and the preparation containing Cys_{42}-Ala_{42}S100A8 had a similar component. ApoAI + $S100A8_2$ was also evident in ApoAI + S100A8/Cys_{42}-Ala_{42}S100A8 cross-linked preparations (Fig. 5.6). Results indicate that ApoAI binds S100A8 independently of the Cys_{42} residue.

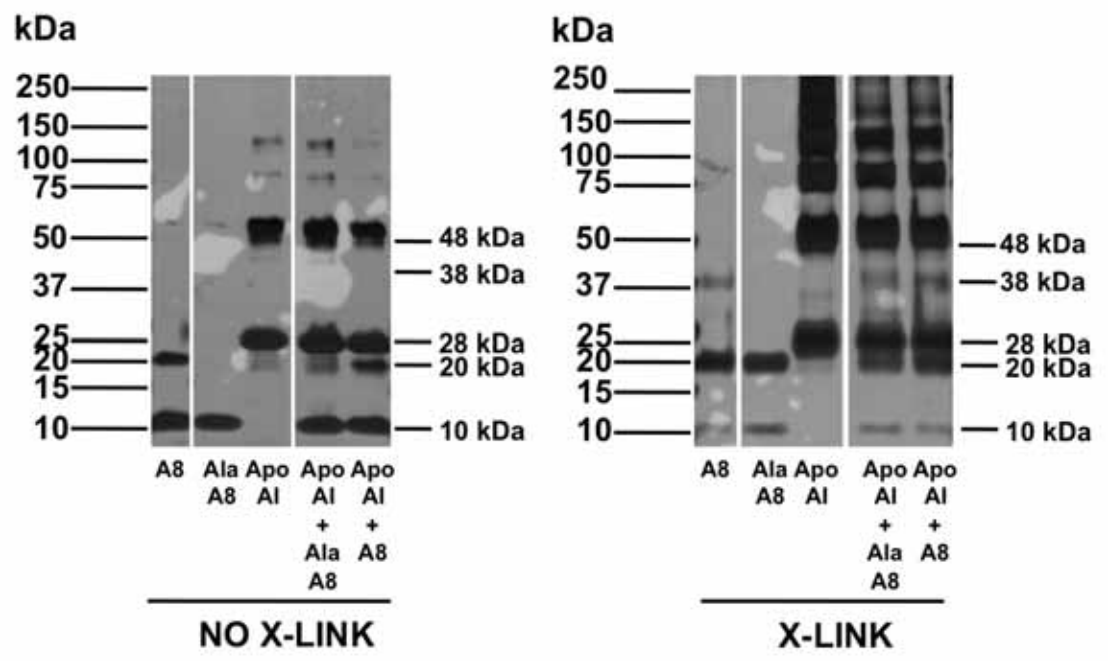

Figure 5.6: ApoAI forms cross-linked products with S100A8. ApoAI was cross-linked with recS100A8 (A8) or $recCys_{42}$-Ala_{42}S100A8 (AlaA8) and separated by SDS-PAGE (10% PAGE gel) under non-reducing conditions then silver-stained. Cross-linked S100A8 or Cys_{42}-Ala_{42}S100A8 and ApoAI formed complexes at 38 kDa (S100A8 + ApoAI) and 48 kDa ($S100A8_2$ + ApoAI), which were not immediately apparent in non-cross-linked preparations.

Because S100A8 may have interacted with other components of HDL *in vivo*, ApoAI(HDL) was cross-linked with recS100A8 or with Cys_{42}-Ala_{42}S100A8. Uncross-linked ApoAI(HDL) contained a 38 kDa component and a marginal increase in this was seen in cross-linked preparations containing ApoAI(HDL) and S100A8. A second product was also observed at 48 kDa (ApoAI + $S100A8_2$) in cross-linked preparations of ApoAI(HDL) and S100A8 or Cys_{42}-Ala_{42}S100A8 (Fig. 5.7).

To confirm putative ApoAI-S100A8 interactions, components migrating at 38 and 48 kDa were excised from cross-linked gels from the three preparations, digested with trypsin and peptides analyzed by MS sequencing.

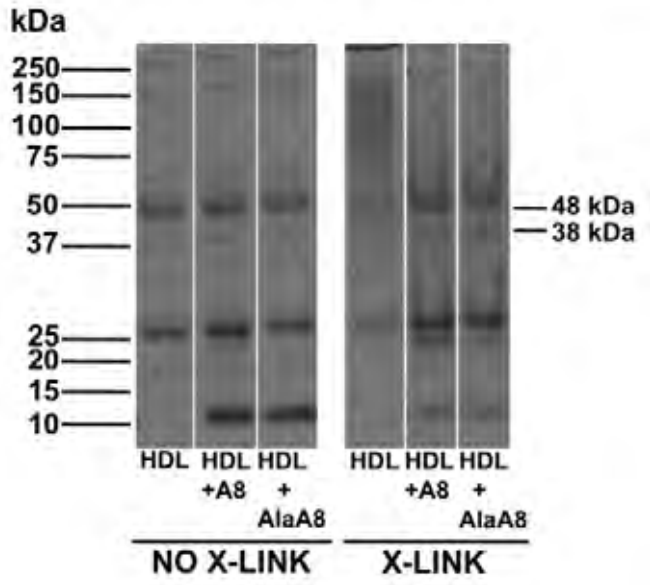

Figure 5.7: ApoAI(HDL) forms cross-linked products with S100A8. ApoAI**(**HDL) was cross-linked with S100A8 (A8) or Cys_{42}-Ala_{42}S100A8 (AlaA8) and separation by SDS-PAGE (10% PAGE gel) under non-reducing conditions then silver-stained. Cross-linked S100A8 or Cys_{42}-Ala_{42}S100A8 and ApoAI(HDL) formed complexes at 38 kDa (S100A8 + ApoAI) and 48 kDa ($S100A8_2$ + ApoAI).

MS sequencing confirmed peptides derived from ApoAI(HDL) in components that migrated at 38 and 48 kDa. The Mascot scores were higher in gel bands migrating at 48 kDa, with larger numbers of positive peptides (Table 5.4) Mascot scores of S100A8 in HDL samples were statistically significant ($P < 0.05$), however, only a single peptide was identified in both components. This suggests that S100A8 was bound to ApoAI in HDL preparations, but in small amounts.

MS sequencing of peptides derived from HDL to which S100A8 had been added and cross-linked, indicated increases in Mascot scores, and in the number of peptide matches for S100A8 in components that migrated at 38 and 48 kDa. Scores for peptides matching ApoAI sequences were also strong in both, confirming likely associations between S100A8 and ApoAI in HDL. The high Mascot score for ApoAI in the 48 kDa band may indicate that the S100A8 dimer may react more readily with ApoAI.

Preparations using the Cys_{42}-Ala_{42}S100A8 mutant had similar Mascot scores to those obtained with S100A8, again indicating that the single Cys_{42} residue in S100A8 is not necessary for ApoAI/S100A8 interactions, leaving it available for oxidant scavenging.

Table 5.4: Summary of MS analysis of cross-linked HDL and recS100A8

Protein	Molecular weight	MASCOT Score* (sequences matched) Sample 1	MASCOT Score* (sequences matched) Sample 2
HDL	**38 kDa**		
	ApoAI	177 (13)	389 (23)
	S100A8	34 (1)	182 (3)
	48 kDa		
	ApoAI	550 (17)	1765 (35)
	S100A8	47 (1)	211 (6)
HDL+A8	**38 kDa**		
	ApoAI	330 (20)	967 (30)
	S100A8	245 (4)	88 (4)
	48 kDa		
	ApoAI	1289 (34)	606 (26)
	S100A8	199 (4)	63 (2)
HDL+AlaA8	**38 kDa**		
	ApoAI	560 (25)	517 (12)
	AlaS100A8	52 (3)	107 (2)
	48 kDa		
	ApoAI	1843 (34)	823 (22)
	AlaS100A8	67 (5)	184 (4)

*Mascot score is a non-probabilistic basis for ranking protein hits using the MASCOT program, calculated from the ion score according to -10 x Log(P), where P is the probability that the observed peptide match is a random event [1074]. Only statistically significant protein matches ($P < 0.05$) were included in this final summary of results. Results are representative of two experiments.

5.3.7 S100A8 AND S100A9 MAY SCAVENGE OXIDANTS DURING PLAQUE FORMATION IN VIVO

S100A8/oxS100A8 and S100A9 are present in macrophages, foam cells and neovessels in human atheroma [410]. Monomeric and DTT-resistant complexed forms of S100A8 and S100A9 were apparent in plaque extracts and based on experiments *in vitro* were suggested to form by oxidation-induced protein cross-linking, leading to the proposal that S100A8 and S100A9 may influence redox-dependent processes during atherogenesis [410]. S100 proteins in carotid artery have not been analyzed for putative oxidative modifications. We aimed to confirm the presence of S100 protein in carotid artery samples from patients with CVD and to enrich these for S100A8 and S100A9 in order to analyze potential modifications.

In contrast to McCormick *et al*. [410], the unfractionated carotid artery extracts used in this study reacted only very weakly with anti-S100A8, anti-oxS100A8 or anti-S100A9 IgG in Western blots (not shown). Amounts of protein that were loaded in the previous study were unclear, making it difficult to conclude whether samples used contained lower amounts of S100 than those reported [410], or whether insufficient total protein was loaded for Western blot analysis.

To enrich the S100 proteins, carotid artery extracts from three subjects were separated by C8-RP-HPLC. Unlike asthmatic sputum, which had an obvious peak corresponding to S100 eluates (Section 4.3.4, Fig. 4.7A), these were not seen in carotid artery samples (Fig. 5.8A). Because of this, aliquots were collected over three minute intervals (in total, 10 aliquots for each sample) and each aliquot was subjected to Western blotting with anti-S100A8, anti-oxS100A8 or anti-S100A9 IgG to determine which eluate contained the highest levels.

Aliquots 4 and 5 (elution times 9-12 min and 12-15 min, respectively) contained the highest amounts of S100A8 and oxS100A8. Extracts contained components indicating dimer and trimer forms of S100A8 and because these were stable in DTT, may indicate oxidative cross-linking (Fig. 5.8B, C). Only very low amounts of S100A9 were detected (elution time 12-15 min) and this was monomeric. There were no obvious S100A8/S100A9 complexes (Fig. 5.8D). Because most protein eluted between 9 and 15 min, the two aliquots (2 ml each aliquot) were pooled and further enriched by C4-RP-HPLC.

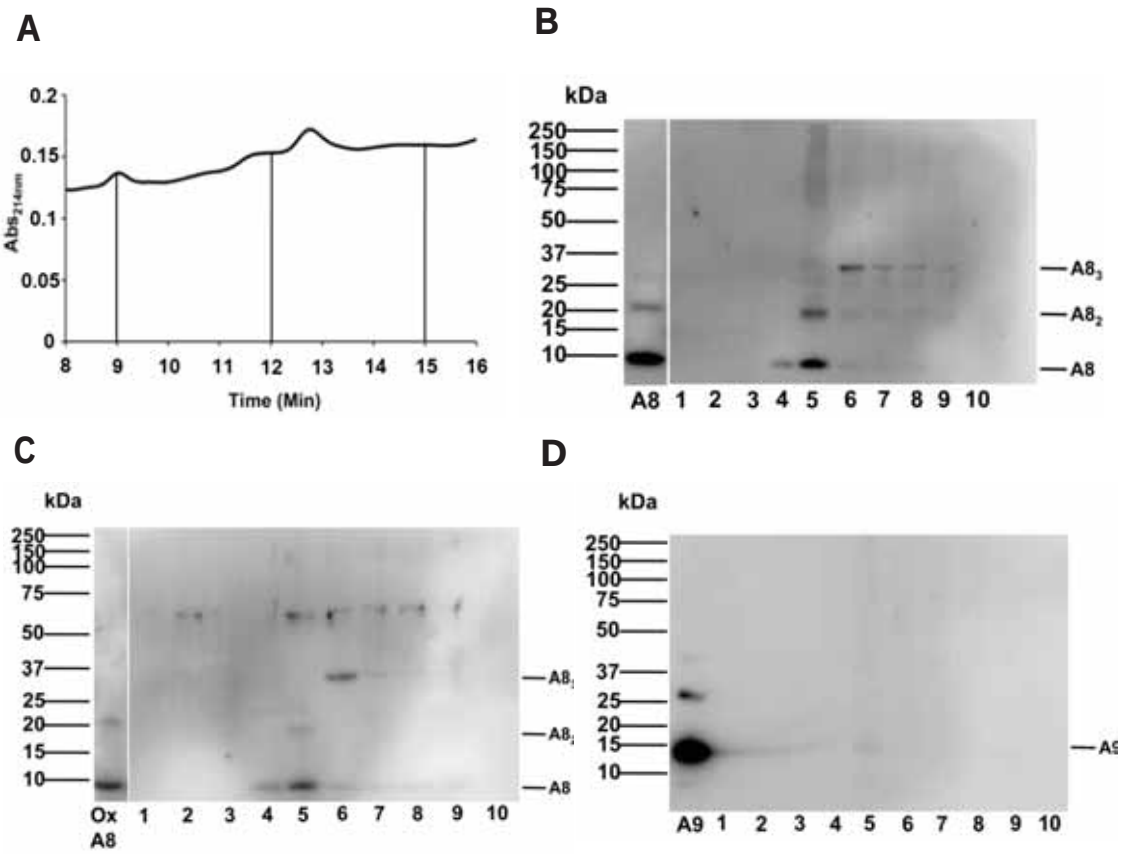

Figure 5.8: Separation of carotid artery extracts by C8-RP-HPLC and detection of S100s by Western blotting. (**A**) S100A8 and S100A9 in carotid artery specimens (250 μg) were enriched by C8-RP-HPLC; no identifiable peaks were obvious. (**B**) Aliquots of eluates (1 ml, lyophilized and suspended in 10 μl PBS) were Western blotted with anti-S100A8 IgG. Each lane represents one 3-minute aliquot, starting from 0 min. Aliquots with the most abundant S100A8 were seen in lanes 4 and 5, corresponding to elution times of 9-12 mins and 12-15 mins. Lane 5 indicates higher order covalent complexes, possibly of $S100A8_3$ (~30 kDa) (**C**) Anti-oxS100A8 also reacted with components in these eluates; lanes 4 and 5 contain the most abundant amounts. (**D**) Western blotting with anti-S100A9 IgG also detected monomeric S100A9 in lane 5, although reactivity was extremely low.

C4-RP-HPLC resolved three peaks eluting at 14.9, 15.1 and 17 min; 10 aliquots were collected in three minute intervals from 0 min to 30 min (Fig. 5.9A). Western blotting of aliquots (1 ml from each aliquot lyophilized and suspended in 10 μl) with anti-S100A8 IgG detected strong reactivity with components in aliquots that eluted at 15-18 min (10 and 20 kDa; S100A8 monomer and dimer respectively), and at 18-21 min (10, 20, 30, 40 kDa, corresponding to putative S100A8 monomers, dimers, trimers and tetramers; lanes 6 and 7 respectively), weak reactivity with similar components was observed in aliquots that eluted at 21-24 min, 24-27 min and 27-30 min (lanes 8-10) (Fig. 5.9B). Western blotting with anti-oxS100A8 IgG also indicated strong reactivity in lanes 6 and 7, with a less intense banding pattern seen in lanes 8-10 (Fig. 5.9C). Importantly, monomers (10 kDa) and dimers (20 kDa) indicated in lanes 6 and 7; lane 7 contained anti-S100A8- and oxS100A8-reactive components migrating at 20, 30 and 40 kDa. These were resistant to reduction by DTT, strongly suggesting oxidative cross-linking. These components were observed in extracts from 2/3 subjects. Western blotting with anti-S100A9 IgG only indicated very weak/no reactivity in samples. (Fig. 5.9D). As lanes 6 and 7 contained the most abundant S100A8 aliquots corresponding to these were digested in-solution by AspN (Section 5.2.9).

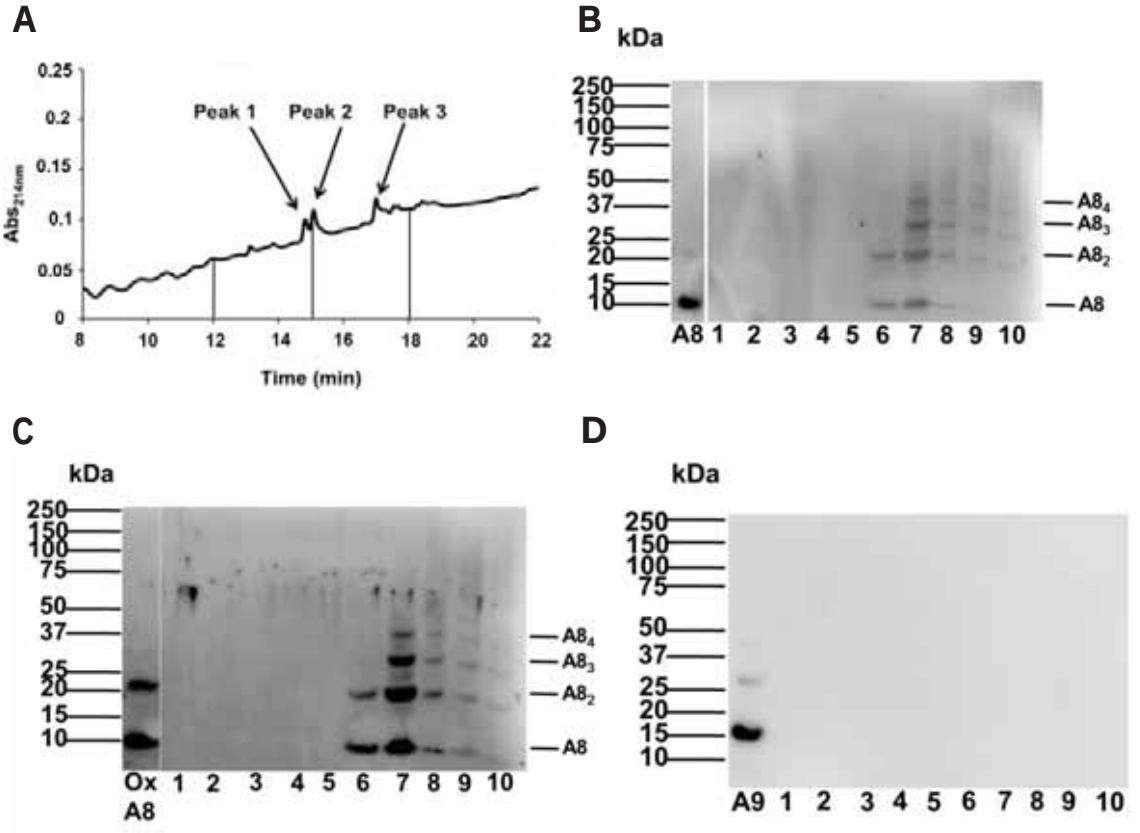

Figure 5.9: Isolation and purification of S100A8 and S100A9 by C4-RP-HPLC and Western blotting. Eluate pooled from 9-12 and 12-15 min aliquots (2 ml from each aliquot) was lyophilised to a final volume of 500 µl and separated by C4 RP-HPLC. (**A**) Three distinct peaks were evident at 14.9, 15.1 and 17 min (Peaks 1-3 respectively). Western blotting of eluate (1 ml) with (**B**) anti-S100A8 IgG, (**C**) anti-oxS100A8 IgG, indicates monomeric and multimeric S100A8 that were stable in DTT reducing gels; (**D**) anti-S100A9 IgG showed little/no reactivity in any sample.

MS analysis of peptides derived from digests of C4-RP-HPLC aliquots 12-15, 15-18, 18-21 min (eluates 5-7) indicated S100A8-containing peptides (oxidized peptides summarized in Table 5.5) in samples from 2/3 subjects, however, only one of these contained an oxidized Cys_{42} residue in the peptide sequence $S100A8_{32-44}$. These peptides were derived from aliquot 6, which eluted between 15-18 min. The modification identified was sulfonic acid.

S100A9 was only found in samples derived from Subject 2. S100A9 peptides were found in aliquot 6 which eluted between 15-18 min; one contained a single Met residue at position 63 that had been oxidized to Met (O), within the peptide $S100A9_{56-64}$.

Carotid extract from Subject 3 contained no S100A8 or S100A9-derived peptides, despite a second enrichment by C4-RP-HPLC; Western blotting of enriched samples also detected no reactivity with anti-S100A8, anti-oxS100A8 or anti-S100A9 IgG, suggesting insufficient protein for analysis.

No other variable modifications were observed and no Tyr containing peptides were seen in any MS spectra. MS analysis indicated that relative to other proteins, such as albumin (Mascot score range: 41-134), S100A8 and S100A9 (Mascot score range: 20-50) were of relatively low abundance, which may have contributed to the poor spectral data seen with these samples.

Table 5.5 Summary of oxidized peptides in carotid artery extracts

Sample	Mass addition (Da)	Modification
Carotid artery Sample 1		
S100A8 (15-18 min) DDLKKLLETE<u>C</u>PQ* **S100A9** No native or oxidized peptides identified	+48 (10,882 Da)	Cys_{42} sulfonic acid
Carotid artery Sample 2		
S100A8 GNFHAVYR* DDLKKLLETE* **S100A9 (15-18 min)** EKVIEHI<u>M</u>E	- (10,834 Da) +16 (13,258 Da)	No oxidized products Met_{63} (O)
Carotid artery Sample 3		
No oxidized or native S100A8 or S100A9 peptides due to low yield		

TABLE 5.5: Oxidative modifications identified in peptides derived from carotid artery extracts. Oxidation products in S100A8 and S100A9 were identified by peptide mapping and MS/MS; masses of modifications are indicated in parentheses, expressed in Daltons (Da). Peptides marked with * indicate sequences identified in non-enzyme specified samples. The oxidation products found in these peptides were consistent with modifications identified in enzyme-specified searches.

5.3.8 S100A8 PROTECTS APOAI FROM OXIDATION BY HOCl

We proposed that S100A8 may protect ApoAI from oxidation. S100A8 can complex with ApoAI in HDL (Section 5.3.6), and because ApoAI can be oxidized by HOCl to change the protective properties of HDL [698], we next asked whether S100A8 could protect ApoAI from oxidation by HOCl *in vitro*.

Before experiments were conducted, unmodified ApoAI, ApoAI(HDL), recS100A8, HSA and the corresponding oxidized protein were separated by C18-RP-HPLC to determine elution times for each. ApoAI had a retention time of 29.6 min with no evidence of oxidized products (Fig. 5.10A, solid line). Separation of ApoAI oxidized with a molar ratio of 5:1 HOCl:ApoAI confirmed conversion of some unmodified ApoAI, with a concomitant rise in Met_{86}(O) and Met_{112}(O) in ApoAI (28.4 and 22.3 min, respectively). A third product, $Met_{86/112}$(O) eluted at 21.7 min (Fig. 5.10A, broken line). Unmodified ApoAI(HDL) eluted slightly earlier than unmodified ApoAI, with a retention time of 29.3 min (Fig 5.10B, solid line). Separation of oxidized ApoAI(HDL) (10:1 molar ratio of HOCl:ApoAI(HDL)) confirmed less native ApoAI(HDL) (elution time 28.3 min), and elevated amounts of Met_{86}(O), Met_{112}(O) and $Met_{86/112}$(O) in ApoAI(HDL) (elution times 27.3, 21.7 and 21 min, respectively, Fig. 5.10B, broken line). HSA had a similar elution time (16.0 min, Fig. 5.10C, solid line) after oxidation with a 5:1 molar excess of HOCl:HSA, although unmodified HSA was somewhat diminished (16.0 min, Fig. 5.10C, broken line). recS100A8 eluted from C18-RP-HPLC after 17.1 min. The second small peak eluting at 16.2 min was present in control PBS (Fig. 5.10D, solid line). Following oxidation with a 5:1 molar ratio of HOCl:S100A8, S100A8 levels were dramatically diminished, with only low levels eluting as a broad peak between 16.6-17.5 min, likely due to aggregation (see Section 3.3.1, Chapter 3) (Fig. 5.10D, broken line). The recCys$_{42}$-Ala$_{42}$S100A8 mutant eluted at the same time as native S100A8, with similar protein loss following oxidation with HOCl, indicating that concentrations of HOCl used in these experiments resulted in Cys$_{42}$-independent aggregation (not shown).

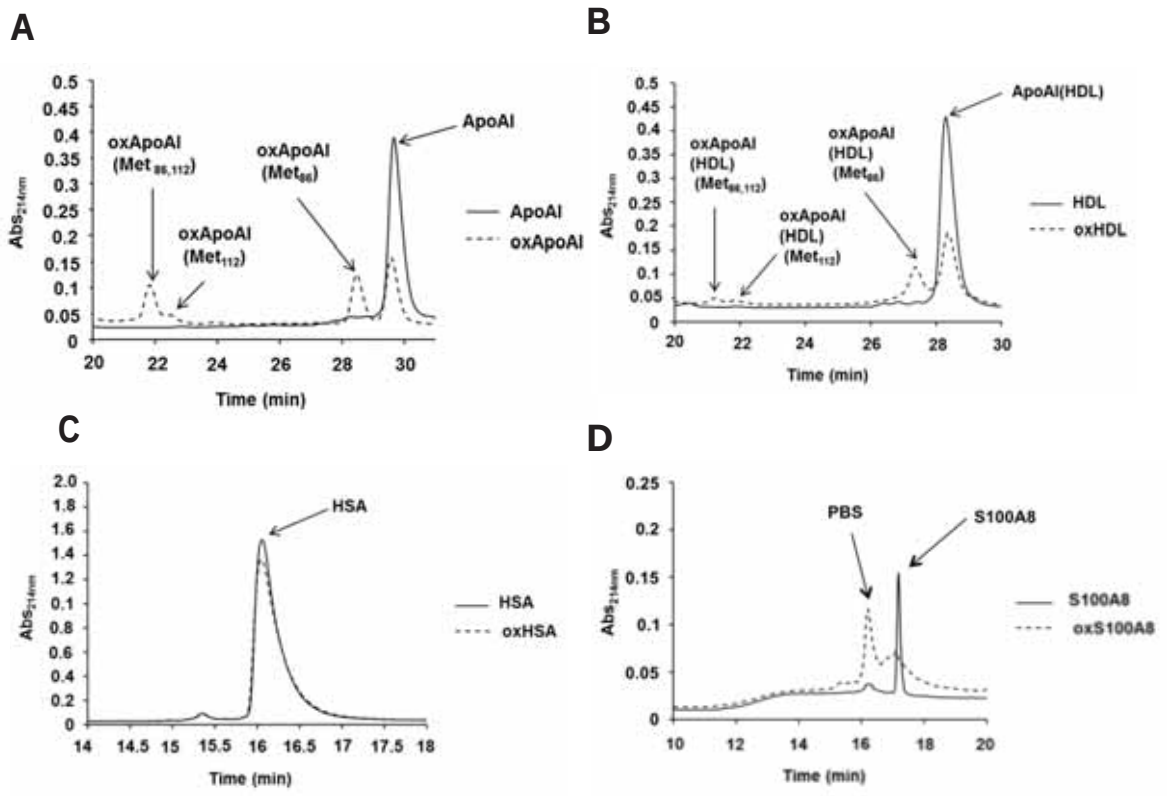

Figure 5.10: C18-RP-HPLC elution profiles of native ApoAI, (ApoAI)HDL, HSA and recS100A8 (solid lines) and oxidized proteins (broken lines). (**A**) Unmodified ApoAI eluted at 29.6 min. After HOCl oxidation of ApoAI (5:1 molar ratios of HOCl:ApoAI), oxApoAI (Met_{86}) eluted at 28.4 min, oxApoAI (Met_{112}) at 22.3 min and oxApoAI ($Met_{86/112}$) at 21.7 min. (**B**) ApoAI from HDL eluted at 28.3 min. oxApoAI (Met_{86}) eluted at 27.3, oxApoAI (Met_{112}) at 21.7 min and oxApoAI ($Met_{86/112}$) at 21 min. (**C**) Unmodified HSA eluted at 16.0 min and oxidized HSA eluted at 16 min. (**D**) Native S100A8 eluted at 17.1 min. After HOCl oxidation, S100A8 levels were dramatically diminished and eluted as a broad peak between 16.6 and 17.5 min.

Initial dose response experiments were carried out to determine the optimal concentration of HOCl required to oxidize ApoAI by ~50%. This was chosen so that any oxidized protein present prior to addition of an oxidant scavenger could be accurately quantified by C18-RP-HPLC. A molar excess of 5:1 (HOCl:ApoAI) was determined to be most appropriate because it reduced native unmodified ApoAI, relative to total protein, by ~45% (Fig. 5.11A).

We also needed to confirm that any oxidized moieties present in S100A8 would not subsequently oxidize native ApoAI, even though Cys_{42}-sulfonic acid, Cys_{42}-oxathiazolidine-oxide and Cys_{42}-oxathiazolidine-dioxide are irreversible modifications.

As a molar ratio of 10:1 (S100A8:ApoAI) was to be the highest used in all experiments, this was used to determine any oxidation of ApoAI in the presence of oxS100A8; aliquots were analyzed every 20 min over 60 min. Native S100A8 was used as control. C18-RP-HPLC chromatograms showed no evidence of formation of the oxidized ApoAI components that eluted at 21.7, 22.3 or 28.4 min, confirming that oxidized S100A8 did not oxidize ApoAI (not shown).

To determine whether ApoAI could be protected against oxidation, we next analyzed the protective effects of HSA, a known oxidant scavenger [948]. Because HOCl oxidation of ApoAI promoted some aggregation, or there was loss in the C18-RP-HPLC separation, values for conversion of ApoAI to oxApoAI could not be calculated as absolute percentages. Approximately 27% of native ApoAI remained after treatment with a 5:1 molar ratio of HOCl:ApoAI (Fig. 5.11B). A molar ratio of 1:1:5 (HSA:ApoAI:HOCl) allowed retention of ~98% native ApoAI. Increasing molar amounts of HSA positively correlated with protection of native ApoAI (r^2 = 0.58, *P* = 0.042; Fig. 5.11B). In contrast, we found no significant change in levels of detectable oxApoAI which were low, even with HSA:ApoAI ratios of 1:1 (Fig. 5.11B).

We next substituted S100A8 for HSA and monitored its potential to protect ApoAI from oxidation. In this experiment, HOCl oxidized ~75% of the available ApoAI. Of the oxApoAI, ~35% was detected by C18-RP-HPLC. Increasing molar amounts of S100A8 correlated with decreasing levels of oxApoAI and increased protection of ApoAI (r^2 = 0.61, *P* = 0.0083). Increasing concentrations of S100A8 inversely correlated with reduced amounts (~13%) of oxApoAI (r^2 = 0.63, *P* = 0.0083; Fig. 5.11C). Results indicate that S100A8 protected ApoAI from oxidation. Its efficiency cannot be compared with HSA because at the molar ratio of HOCl used to promote ApoAI oxidation, much of the S100A8 aggregated (Fig. 5.10D, broken line).

To examine the role of Cys_{42} in oxidant scavenging, Cys_{42}-Ala_{42}S100A8 was tested. In this experiment, HOCl oxidized ~81% of native ApoAI. Increasing concentrations of Cys_{42}-Ala_{42}S100A8 positively correlated with increased protection of native ApoAI (r^2 = 0.59, *P* = 0.0083; Fig. 5.11D), and ~27% more native ApoAI. Increasing ratios of Cys_{42}-Ala_{42}S100A8 inversely correlated with a loss of oxApoAI (r^2 = 0.26, *P* = 0.0083), with ~12% reduction in detectable oxApoAI, relative to oxidized ApoAI control. Although higher molar ratios of the mutant protein were somewhat protective, Cys_{42}-Ala_{42}S100A8 was less effective than S100A8 (relative to retention of native ApoAI). Interestingly, two peaks eluting at 16.8 and 17.1 min were evident with

increased molar amounts of Cys_{42}-Ala_{42}S100A8, after addition of ApoAI and HOCl (contrasting with native S100A8, which eluted as a single broad peak, not shown) and likely corresponds to Cys_{42}-Ala_{42}S100A8+Met_{78}(O)/sulfone and Cys_{42}-Ala_{42}S100A8, respectively. Results indicate that Cys_{42}-Ala_{42}S100A8 retained some anti-oxidant capacity via Met_{78} (see Section 3.3.3, Chapter 3). The absence of oxidized Cys_{42} residues in these preparations may have allowed better separation of oxidized Met_{78} adducts from Cys_{42}-Ala_{42}S100A8.

S100A8 aggregated after addition of a 5 molar ratio of HOCl and the amount of protein eluted from C18-RP-HPLC was markedly reduced (Figure 5.10D, broken line). Cys_{42}-Ala_{42}S100A8 also aggregated following treatment with this amount of HOCl. However, in the presence of ApoAI, Cys_{42}-Ala_{42}S100A8 was significantly more resistant to aggregation than S100A8. Table 5.6 shows the percentage loss of S100A8 relative to Cys_{42}-Ala_{42}S100A8. Higher molar amounts of S100A8 were more resistant to aggregation by HOCl when in the presence of ApoAI. The S100A8 aggregation that occured with the high molar ratios of HOCl used in these experiments would not have allowed a true assessment of its ability to protect ApoAI from oxidation.

Table 5.6: Percentage loss of S100A8 relative to Cys_{42}-Ala_{42}S100A8

Preparation (ApoAI:S100A8:HOCl)	Percentage loss (relative to Ala_{42}S100A8)	*P* value
1:1:5	43.7% loss	0.0337
1:2:5	56.7% loss	0.0014
1:4:5	51.5% loss	0.0001
1:10:5	29.7% loss	0.0192

Table 5.6: S100A8 underwent significant aggregation after addition of a 5 molar excess of HOCl relative to Cys_{42}-Ala_{42}S100A8. S100A8 protected ApoAI from oxidation by HOCl. However, relative to Cys_{42}-Ala_{42}S100A8, the native protein underwent significantly more aggregation. Aggregation of native S100A8 is expressed as a percentage loss relative to similarly ox Cys_{42}-Ala_{42}S100A8. Experimental conditions are given in the left hand column, expressed as a ratio of ApoAI:S100A8:HOCl. Aggregation of S100A8 decreased as molar amounts increased (middle column). Significance was determined as $P < 0.05$ (right column).

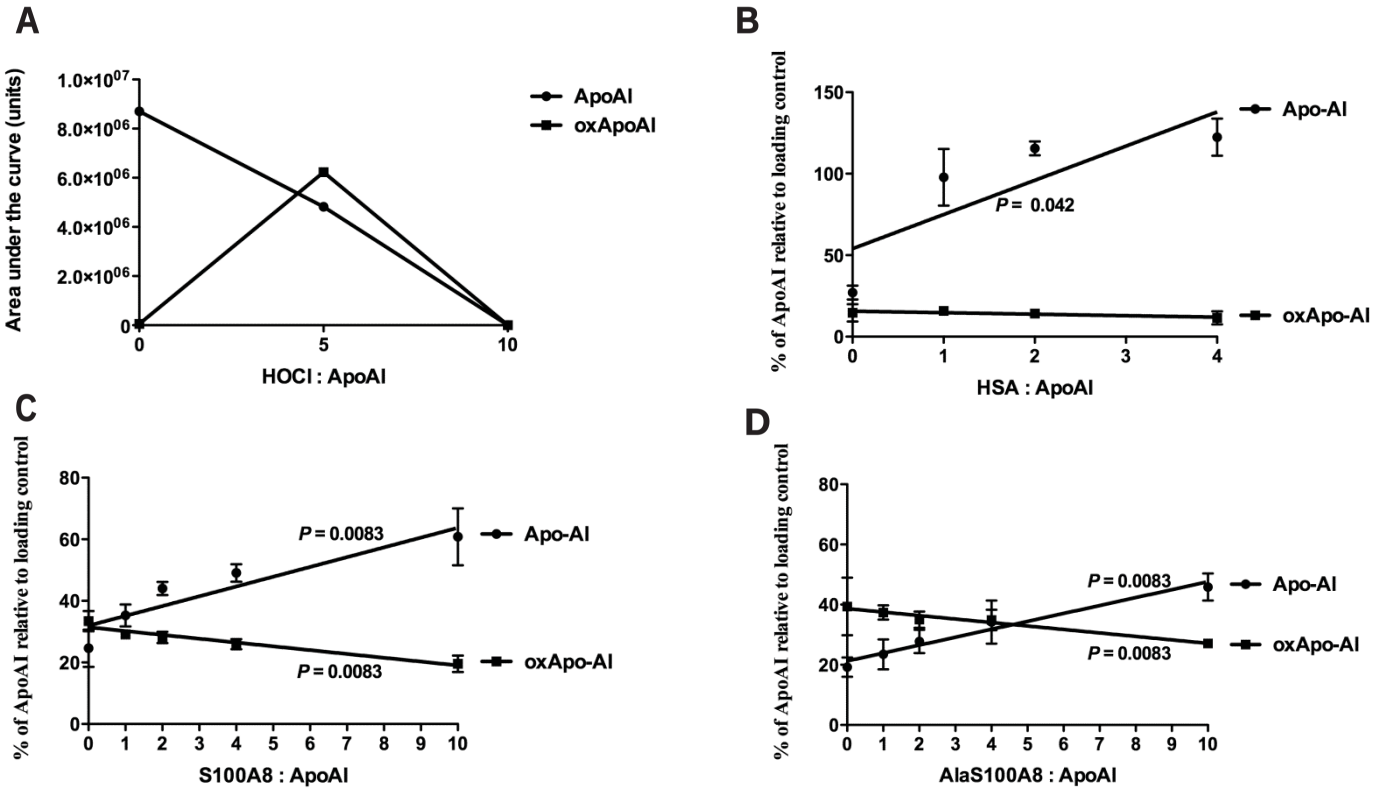

Figure 5.11: HOCl promotes concentration-dependent formation of oxApoAI, but is protected by oxidant scavengers. (**A**) A 5 molar excess of HOCl resulted in a ~45% reduction in unmodified ApoAI. Higher amounts of HOCl caused aggregation, and the protein could not be separated by C18-RP-HPLC. (**B**) Increasing concentrations of HSA correlated with increased protection of native ApoAI (r^2 = 0.58, *P* = 0.042). (**C**) Increasing molar amounts of S100A8 positively correlated with increased protection of native ApoAI (r^2 = 0.61, *P* = 0.0083), and inversely correlated with loss of oxApoAI (r^2 = 0.63, *P* = 0.0083) (**D**) In contrast, Cys_{42}-Ala_{42}S100A8 (AlaS100A8) was less efficient, although increasing amounts correlated with increased protection of native ApoAI (r^2 = 0.59, *P* = 0.0083). Similarly, increased amounts of Ala_{42}S100A8 inversely correlated to loss of oxApoAI (r^2 = 0.26, *P* = 0.0083) Graphs are mean representations ± SEM of three experiments, except for Figure 5.11A which was only conducted once. General trends in Figs. 5.11B-D are illustrated as a line of best fit. r^2 values are only given where significant correlations were observed.

5.3.9 S100A8 PROTECTION OF APOAI IN HDL

The anti-inflammatory properties of HDL can be changed by oxidation. VCAM-1 induction on endothelial cells is involved in development of atherosclerosis, as this mediates the migration and extravasation of leukocytes across the vascular endothelium [1076, 1077]. HDL inhibits TNF-α induced VCAM-1 expression in endothelial cells [1078] whereas oxHDL enhanced TNF-α induced VCAM-1 expression in HUVEC. Importantly, these observations were not observed with lipid-poor ApoAI or with HDL lipids [698], suggesting that lipid or lipid-protein interactions are important in regulating HDL functions.

Because lipid is functionally important, we next tested the oxidant-scavenging potential of S100A8 on lipid-associated ApoAI *in vitro*. For this, we used HDL in which levels of ApoAI were validated by C18-RP-HPLC. As with lipid-poor ApoAI, a dose response experiment was carried out to determine the optimal HOCl concentration required for ~50% oxidation (Section 5.3.8). A molar excess of 10:1 (HOCl:ApoAI(HDL)) oxidized ~57% of native ApoAI(HDL) (Fig. 5.12A). This contrasts with lipid-free ApoAI, which was not detected on C18-RP-HPLC chromatograms after addition of a 10:1 molar excess of HOCl:ApoAI, due to aggregation (Fig. 5.11A). These results confirmed that the lipid component of HDL reduced the efficiency of HOCl to oxidize ApoAI.

HSA was added to ApoAI(HDL) to determine whether other HDL components altered its oxidant-scavenging potential. In this experiment, a 10:1 molar ratio of HOCl:ApoAI(HDL) reduced native ApoAI(HDL) levels by ~74%. However, unlike lipid-free ApoAI which was protected by a 1:1 ratio of HSA:ApoAI in the presence of HOCl (Fig 5.11B), protection in ApoAI(HDL) was less, and the highest molar ratio (10:1, HSA:ApoAI(HDL)) was required for ~100% protection. Increased protection of native lipid-associated ApoAI correlated with increasing ratios of HSA (r^2 = 0.86, P = 0.0083; Fig. 5.12B) with a concomitant, inversely correlated, decrease in oxApoAI (r^2 = 0.81, P = 0.0083). Overall, detectable levels of oxApoAI(HDL) were reduced by ~26% with a 10:1 molar ratio of HSA:ApoAI(HDL) (relative to oxApoAI(HDL) control, Fig. 5.12B).

To test effects of S100A8, we first established that HOCl oxidized ~61% of ApoAI in HDL in this experiment (Fig. 5.12C). In contrast to the significant S100A8-mediated protection of ApoAI alone (Fig. 5.11C), increasing molar amounts of S100A8 ony promoted modest protection, which was not significant (Fig. 5.12C).

In lipid-free preparations of ApoAI, Cys_{42}-Ala_{42}S100A8 also protected against HOCl-induced oxidation. However, in ApoAI(HDL) preparations, increasing amounts of Cys_{42}-Ala_{42}S100A8 caused a ~14% loss of native ApoAI in HDL and oxApoAI(HDL) increased by ~25% with the higher amounts of Cys_{42}-Ala_{42}S100A8. The two peaks eluting at 16.8 and 17.1 min that were found in lipid-free experiments were also observed (not shown), suggesting some oxidant-scavenging by Met_{78}. It was unexpected that increased amounts of Cys_{42}-Ala_{42}S100A8 positively correlated with increased oxApoAI(HDL) (r^2 = 0.69, P = 0.0083; Fig. 5.12D) indicating that it did not protect ApoAI in HDL from oxidation.

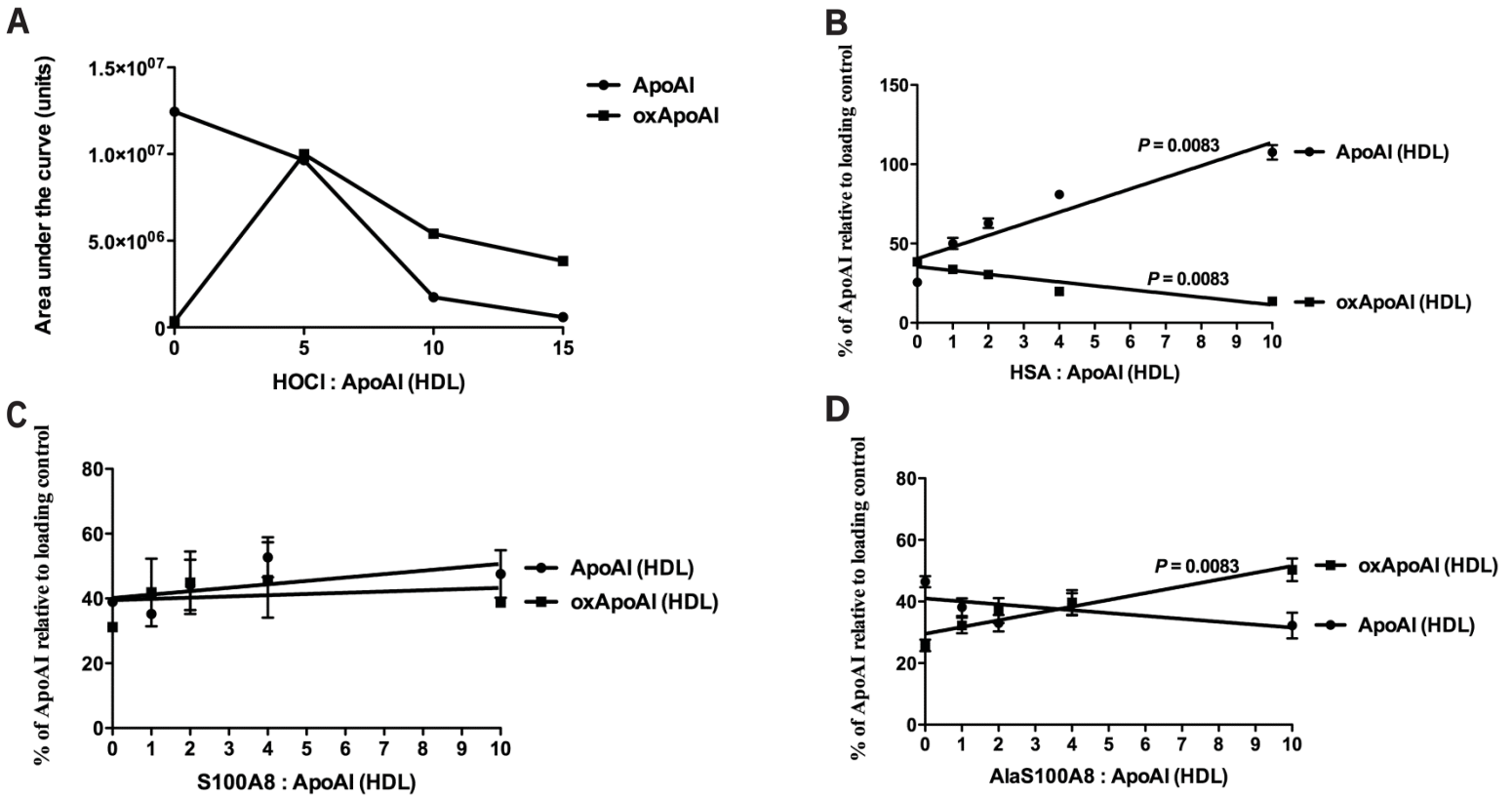

Figure 5.12: Dose response experiments using a molar excess of HOCl against ApoAI(HDL). (**A**) A 10-fold molar excess of HOCl resulted in a ~60% reduction in unmodified apoAI. (**B**) Increased concentrations of HSA correlated with increased retention of native ApoAI(HDL) (r^2 = 0.86, *P* = 0.0083). Increased amounts of HSA inversely correlated with reduction of oxApoAI(HDL) (r^2 = 0.81, *P* = 0.0083). (**C**) Increased levels of S100A8 promoted modest protection of ApoAI(HDL), with no observable decrease in oxApoAI. (**D**) Increased amounts of Cys_{42}-Ala_{42}S100A8 positively correlated with an increase of oxApoAI(HDL) (r^2 = 0.69, *P* = 0.0083), and a concomitant loss of native ApoAI(HDL) (not significant). Graphs are mean representations ± SEM of three experiments, except for Figure 5.12A which was only conducted once. General trends in Figs. 5.12B-D are illustrated as a line of best fit. r^2 values are only given where significant correlations were observed.

5.3.10 S100A8/A9 REDUCED FORMATION OF HOCl-OXIDIZED PROTEIN IN BAEC

Products of MPO can cause endothelial dysfunction during inflammatory vascular disease. MPO is released by activated phagocytes and deposits into the vascular endothelium, associating with the extracellular matrix protein, fibronectin. S100A8/A9 also binds to the endothelium, facilitated by strong binding to heparin and heparan sulfate GAGs [431]. Because of this association, we proposed that S100A8/A9 and/or the individual subunits may protect endothelial cells from excessive oxidation by MPO/H_2O_2.

Control experiments showed that MPO or H_2O_2 alone, did not promote oxidation of BAEC proteins whereas, strong anti-HOP IgG reactivity was obvious in lysates of cells treated with MPO + H_2O_2. 2D10G9 is a monoclonal antibody that reacts with many proteins that have been oxidized with HOCl [1079] defined as HOP, although it does not react with HOCl-oxS100A8 [410]. The S100 proteins did not contain any HOP and reactivity was similar to control samples (Fig. 5.13A). However, when S100 proteins were included in cells treated with MPO/H_2O_2 there was marked reduction in HOP reactivity. In contrast to the suppression seen with recS100A8, recCys_{42}-Ala_{42}S100A8 did not protect BAEC from generation of HOP-positive components, strongly supporting our proposal that Cys_{42} in S100A8 is the redox-reactive residue. recS100A9 protected from HOCl-oxidation in a similar manner, as did the recS100A8/S100A9 complex. When Cys_{42}-Ala_{42}S100A8+S100A9 were included, this also reduced generation of HOP, suggesting that if Cys_{42} in S100A8 were oxidized, S100A9 alone, or in the heterocomplex may still be protective; this would be worth exploring.

Effects of S100 protein preparations on fibronectin retention were less clear. MPO alone reduced basal levels of fibronectin, whereas H_2O_2 did not, and it was difficult to compare any protection afforded by the S100 proteins after adding H_2O_2 (Fig. 5.13B). The S100 proteins alone did not cause fibronectin breakdown when probed with monoclonal mouse anti-fibronectin IgG.

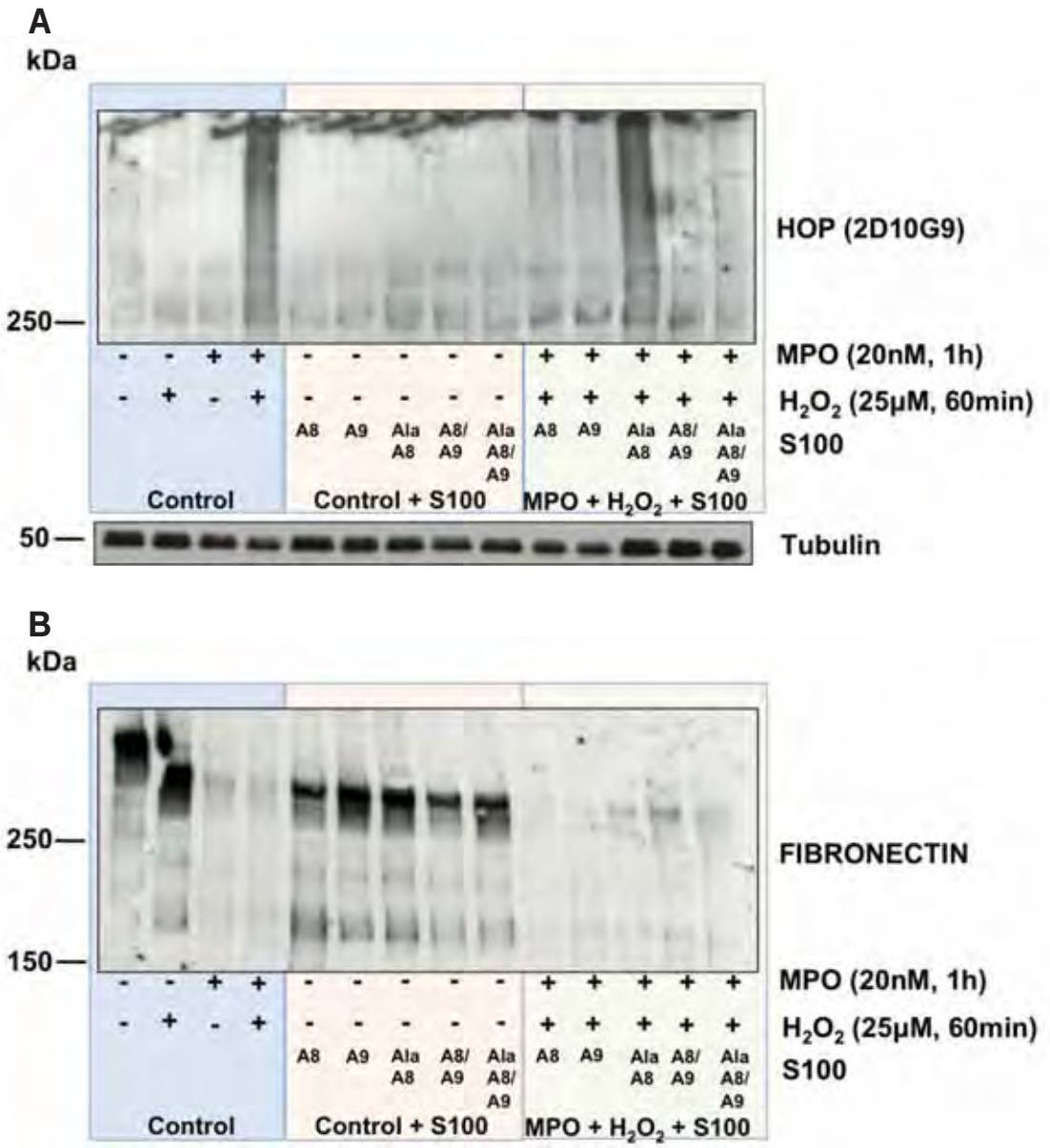

Figure 5.13: recS100A8 and recS100A9 prevent formation of HOP but effects on fibronectin degradation were unclear. (**A**) HOCl-modified proteins detected in BAEC by the anti-HOP mAb were only apparent after incubation with MPO/H_2O_2. S100 protein alone did not promote HOP reactivity. S100A8 and S100A9 preparations prevented formation of HOP in the presence of MPO/H_2O_2, whereas Cys_{42}-Ala_{42}S100A8 did not, indicating that Cys_{42} was important for oxidant scavenging. Western blotting of tubulin in cell lysates indicated consistant sample loading. Results are representative of two experiments. (**B**) Effects of S100 proteins on fibronectin, using anti-fibronectin IgG, were less clear. MPO alone reduced basal levels of fibronectin. Results are representative of two separate experiments.

5.4 DISCUSSION

S100A8 and S100A9's involvement in CVD has been steadily emerging (reviewed in [971]). Elevated serum levels of S100A8/A9 are reported in patients with unstable angina and acute myocardial infarction [483, 1063] and correlated with increased severity of carotid artery disease and carotid intima-media thickness in patients with type 2 diabetes. Levels also correlated with increased expression of Mac-1 on peripheral blood monocytes and enhanced monocyte adhesion to extracellular matrix proteins such as fibronectin [1080, 1081].

MPO is associated with inflammation and oxidative stress (see Sections 1.4.1.6 and 1.4.1.7, respectively, Chapter 1) and its activity is strongly associated with CVD (reviewed in [1082]). Specifically, elevated circulating concentrations of MPO are associated with increased disease risk [1083, 1084]. In chronic inflammatory diseases such as SLE, MPO is elevated in serum [1085]. ApoAI is selectively targeted by MPO, with subsequent oxidation by HOCl and this may reduce the anti-inflammatory properties of HDL and thereby accelerate CVD development, a major cause of mortality in SLE patients [698, 1026, 1086].

MPO is deposited onto the vascular endothelium [1087, 1088], and like S100A8 and S100A9, binds GAGS and heparin sulfates [431]. In a murine model of acute vascular inflammation, MPO accumulated in the aortic endothelium, significantly impairing endothelium-dependent relaxation [1089]. After binding, MPO is subsequently internalized and transcytosed into the endothelial basement membrane where it associates with fibronectin, a target of nitration by active MPO [1087, 1088]. Exposure of endothelial cells to low levels of HOCl promotes expression and activity of tissue factor thereby promoting thrombosis, and promotes endothelial cell apoptosis that contributes to endothelial dysfunction [1090].

S100A8 and S100A9 are expressed in macrophages and foam cells in human atheroma and are particularly sensitive to HOCl oxidation compared to LDL [410, 483, 524]. S100A8/A9 is also found in infiltrating neutrophils and macrophages in infarcted myocardium [1063]. Expression of S100A8 and S100A9 in atherosclerotic lesions from SLE patients has not been reported, but would be expected. S100A8 and S100A9 are detected in the glomerulus of patients presenting with glomerular nephritis [683].

Oxidation of HDL is evident in serum from patients with SLE and has been associated with development of atherosclerosis possibly by generating pro-inflammatory

HDL [698, 1026]. Together with oxidation of LDL and phospholipids, these factors are likely to accelerate atherosclerosis and promote the increased cardiovascular events seen in SLE patients [1086]. Because of their sensitivity to oxidation, S100A8 and S100A9 proteins may help reduce oxidant-induced damage to HDL, allowing it to maintain its protective functions.

5.4.1 S100 LEVELS IN SLE SERUM

No significant differences between S100A8, S100A9 or S100A8/A9 levels in serum from patients with SLE in remission or with active disease, and healthy controls were seen. However, S100A8 levels were in the range 1-10 μg/ml whereas S100A9 levels were some 10-fold lower, and mean calprotectin levels were ~0.4 μg/ml, indicating predominance of S100A8. In this study control subjects were predominantly Indian whereas there were more Caucasian SLE subjects. The incidence of SLE is reported to be higher in Black, Asian and Indian populations [1091] and this study would have benefited from a more representative control subgroup. However this was a pilot study, and more patients and controls need to be included to improve statistical significance and analysis of trends between subgroups (for example control vs disease flare/remission).

Our results for calprotectin contrast markedly with earlier studies [468, 472]. Discrepancies between results presented here and those reported may be explained by antibody specificities and/or serum preparation techniques. An uncharacterized antibody was used by Haga *et al.* that detected much higher levels (1050.83 ± 542.08 ng/mL) of S100A8/A9 in control sera [472] compared to those presented in here (348.5 ± 29.8 ng/mL), or by Soyfoo *et al*. (339 ± 35 ng/mL). The high serum concentrations found by Haga *et al*. suggest that the anti-S100A8/A9 antibody was not specific for the heterocomplex.

Soyfoo *et al.* used an in-house ELISA assay and the monoclonal antibody 27E10. This antibody recognises a specific epitope in the S100A8/A9 complex. Serum calprotectin concentrations determined here were determined using a commercial ELISA kit previously used in our laboratory and by others [1092]. This detected elevated S100A8/A9 levels in RA sera compared to controls (personal communication, Dr. Chandi Perera), validating the method. In addition, levels of S100A8 and S100A9 were determined using in-house antibodies that have been validated for cross-reactivity, and detected differences in S100A8 and S100A9 levels in RA and control sera [533].

The SLE and control serum samples used here were processed in an identical manner, ensuring that no cells/cell debris were present. Contamination by neutrophils or their lysis products, possibly generated following centrifugation at inappropriate speed, could increase S100 protein levels, as these contain ~40% cytoplasmic S100A8 and S100A9 [588]. We found that sera from three individuals from the SLE subgroup contained high amounts of S100A8 and S100A9; all but one, were in remission.

5.4.2 DETECTION OF S100s IN SERUM BY WESTERN BLOT

Western blotting of serum protein with anti-S100A8 (Fig. 5.3B), -oxS100A8, -S100A9 IgG, failed to detect immunoreactive components even though the proteins were effectively transferred to PVDF membranes. Western blotting is less sensitive than the ELISA but S100A8 levels in control and SLE samples, determined by ELISA (~1-10 μg/ml; see Section 5.3.2) indicated that S100s should be detected by Western blotting.

Samples were diluted 1:10 v/v because separation of neat serum was poor due to excess albumin. However, the samples used would still have contained ~250 ng/ml S100A8 which should have been detected by anti-oxS100A8 or anti-S100A8 IgG as these reacted with 250 ng standard recS100A8 preparations (see Fig. 5.3B), and anti-S100A8 readily reacts with S100A8 levels as low as 40 ng [410]. Removal of albumin and separation of neat samples may have allowed detection. However, in accordance with our results, an analysis of putative serum glycoprotein markers for human lung adenocarcinoma, indicated that in 100 μg serum separated by SDS-PAGE, no S100A8 was detected using an antibody specific for S100A8, despite serum from lung cancer patients having 4.5-fold higher spectral counts (a method of quantitating relative protein concentrations in pre-digested protein mixtures using MS [1093]), compared to healthy controls when analyzed by MS [1094]. This suggests that in serum, antibodies that recognize epitopes on S100A8 and S100A9 in ELISA fail to do so in Western blotting. Results presented in Fig. 5.5 suggest that S100A8 in serum may be complexed in HDL and may explain the inability to detect these in Western blots.

Interestingly, equivalent amounts of rec-oxS100A8 compared to recS100A8 appeared to have lower intensity in Coomassie-stained PAGE-gels and reduced chemiluminescence when immunoblotted with anti-oxS100A8 or anti-S100A8 IgGs. Although we reported that anti-oxS100A8 antibodies react more strongly with rec-oxS100A8 than do anti-S100A8 antibodies in ELISA [410], those experiments used non-

C4-RP-HPLC purifed rec-oxS100A8. Diminished reactivity of rec-oxS100A8 was only observed with HPLC-purified monomeric and dimeric oxS100A8. Repeated exposure to solvents such as acetonitrile of trifluoroacetic acid or repeated lyophilization may denature epitopes reducing reactivity if anti-oxS100A8 and anti-S100A8 IgG in Western blots.

5.4.3 S100 PROTEIN IS PRESENT IN HDL

An affinity S100A8 column pulled out ApoAI and ApoD from normal serum (see Section 5.3.1). S100A8 also binds lipids [178] and these components are all present in HDL. We confirmed S100A8 association with HDL in sera from controls and SLE patients using enriched LDL and HDL fractions separated by FPLC. S100A8 levels in HDL were higher than in LDL and the LDL fractions that were positive, contained contaminating HDL, as indicated by positive reactivity with anti-ApoAI (Fig. 5.5B). oxS100A8 also associated with HDL (Fig. 5.5A), whereas S100A9 was much less abundant (Fig. 5.5A), possibly because S100A9 levels in serum were relatively low. Interestingly, SLE subject 3 (Fig. 5.5A) had high amounts of oxS100A8 associated with HDL. At the time of collection subject 3 had active disease, whereas subjects 1 and 2 were in remission, suggesting that S100A8 may moderate oxidation of HDL and more patients are required to test this. However, this study was preliminary, and not aimed at investigating SLE patient populations in detail, but rather to determine whether S100A8 complexed with lipoproteins. Increasing the number of SLE subjects and appropriately age- and gender-matched controls to more accurately compare lipid binding of S100 protein would be beneficial. A concurrent study of SLE patients in remission or disease flare could indicate levels of lipid binding of S100A8 and S100A9 in active disease.

HDL and LDL do not separate well on SDS-PAGE as they are large complexes with several structural forms (discoidal, spherical). According to Santucci *et al*., 2D-electrophoresis in non-denaturing gels that resolve large protein and macro-aggregates are required for purification [1095]. Although slot blots have limitations (e.g. only allow semi-quantitative analysis, and the suction used for sample loading can create artificial banding patterns), results presented strongly suggest that S100A8 in the circulation was part of the HDL particle. Unfortunately, because of the small sample size (normal: n=3, SLE: n=3) statistical analysis was not possible, and only general trends are reported. A larger cohort study is needed to confirm these results.

5.4.4 S100A8 COMPLEXES WITH APOAI AND APOAI(HDL)

S100A8 was predominantly found in HDL fractions from healthy and SLE subjects, and associated with ApoAI when used as an affinity support (see Section 5.3.1). Using the BS_3 cross-linker we found that S100A8 bound ApoAI, in the presence of Ca^{2+}. When HDL was separated by SDS-PAGE, low levels of a 48 kDa component were obvious, suggesting the presence of ApoAI/$S100A8_2$ (Fig. 5.7). This component increased when S100A8 was added to HDL. Peptide sequencing confirmed that these complexes comprised of S100A8 and ApoAI (Table 5.4).

Upon Ca^{2+}-binding, S100 proteins, for example S100A8, undergo a ~40° alteration, exposing the hydrophobic surface that enables interaction with target proteins [159]. From our experiments it is unclear if ApoAI-S100A8 binding requires Ca^{2+} to expose the hydrophobic surface, or if lipids facilitate interactions. ApoAI would not bind Cys_{42} by disulfide bridging as it has no Cys residues and this was confirmed using the mutant Cys_{42}-Ala_{42}S100A8 which also interacted with ApoAI. In S100A8/A9, Ca^{2+} and His residues in the extended C-terminal of S100A9 are necessary for binding of the complex to AA [581], although non-covalent heterocomplex formation of S100A8 with S100A9 appears to require Cys_{42} [655]. Experiments analyzing complex formation between ApoAI/ApoAI(HDL) and S100A8 in the presence/absence of Ca^{2+} and surface plasmon resonance studies may provide more in-depth detail of interactions and binding affinities.

The studies reported here confirm associations with HDL, likely by binding ApoAI and support the notion of a separate function of S100A8 independent of S100A9 and the S100A8/S100A9 heterocomplex.

5.4.5 S100A8 AND S100A9 IN CAROTID EXTRACTS

S100A8 and S100A9 are expressed in macrophages and foam cells in human atheroma and in areas of vascular calcification. Western blotting of carotid artery extracts detected monomeric and complexed forms of S100A8 and S100A9, suggesting possible oxidative cross-linking *in vivo* [410]. This was considered to be a consequence of inter-molecular sulfinamide cross-links between Cys and Lys residues [606]. Here we confirmed the presence of multimeric S100A8 (probed with anti-S100A8 and anti-oxS100A8 IgG) in carotid artery extracts, but these were only obvious after enrichment by C8- and C4-RP-HPLC. The enriched samples had little reactivity with anti-S100A9

IgG. Moreover, we found no evidence of S100A8/A9 complexes, using anti-S100A9 IgG, which detects the heterodimer. Putative ApoAI-S100A8 complexes 38 and 48 kDa, Figs. 5.6 and 5.7) were not apparent.

In an attempt to determine whether the complexes seen in artery extracts were cross-linked, a modified method to extract protein was used; NEM and sodium azide were included in the buffer to prevent fortuitous oxidation of protein during the extraction procedure. This may have reduced protein yield, although, McCormick *et al*. found that these reagents did not affect the mobility of S100A8 and S100A9 complexes separated by SDS-PAGE [410].

MS sequencing of peptides derived from carotid artery extracts identified Cys_{42} in oxS100A8 peptides in 1/3 samples. This was Cys_{42}-sulfonic acid. S100A9 was found in one peptide from 1/3 extracts and contained $Met_{63}(O)$. Our failure to identify oxidized peptides, despite evidence implicating oxidation as the likely reason for protein cross-linking in 2/3 samples, was unexpected. MS analysis of samples indicated relatively low abundance of S100A8 and S100A9 compared to other proteins identified. As impressed by Qian *et al*., the diverse range of human bodily fluid and tissue proteomes makes detection of low-abundance proteins difficult [1096]. Despite advances, detection of low ng/ml - sub-ng/ml protein concentrations is still difficult to achieve (reviewed in [1097]). For example, in human plasma, 22 proteins are responsible for 99% of the bulk mass of total protein, creating a "masking" effect that limits accurate analysis of proteins that constitute 1% of the rest. [1098, 1099]. Removal of high abundance proteins, such as albumin prior to peptide generation and MS sequencing may improve detection. Notwithstanding, here we present evidence for the same modifications identified in S100A8 derived from asthmatic sputum.

5.4.6 S100A8 PROTECTS APOAI FROM OXIDATION

Protection of lipoproteins against oxidation is largely mediated by tocopherol and carotenoid classes of lipid-soluble anti-oxidants, although tocopherol is not effective against 2-electron oxidants (reviewed in [1100]). HDL is more susceptible to oxidation than LDL [1101] and protects LDL from oxidation *in vitro* [1102]. Molar excesses ~800:1 (HOCl:LDL) were required to fully oxidize LDL [1079]. S100A8 was markedly more sensitive to oxidation by HOCl than either BSA or LDL. rec-mS100A8 is readily oxidized with 5:1 molar excess HOCl [606], whereas hS100A8 was sensitive to equimolar ratios (Chapter 3, Table 3.4).

We confirmed that increasing molar amounts of HSA, which can scavenge oxidants [764] protected ApoAI from HOCl oxidation of Met_{86} and Met_{112}. A 10-fold molar excess of HSA was required to achieve ~100% retention of native ApoAI in HDL. S100A8 also provided significant protection, particularly when in a pure system. However, when HSA and rec-hS100A8 were added to ApoAI(HDL) they were apparently less protective and it is possible the lipid component alters their effectiveness or that the 10:1 molar ratio of HOCl required to assess ApoAI(HDL) oxidation promoted excessive aggregation, making analysis unreliable. More studies in pure systems with addition of appropriate lipids, and of MPO and H_2O_2 rather than reagent HOCl may clarify this.

HSA has several oxidant-sensitive amino acids. In particular, Met_{147}, Trp_{238}, Met_{353} and Met_{572} undergo addition of a single oxygen after exposure to HOCl. Protection by HSA may be important. For example, at less than physiological concentrations, HSA protects inactivation of α_1-anti-trypsin, a protease inhibitor, which can be inactivated by HOCl [1103]. Interestingly, HSA has a single free Cys residue at position 58 but the mass of this residue remains unchanged [1104]. In contrast, human recS100A8 contains a single Cys residue and two Met residues. Cys_{42} modulates several oxidant-sensitive functions of S100A8. For example, the fugetactic activity for human neutrophils is abrogated by oxidation of Cys_{42} [612]. Similarly, substitution of Cys_{42} in S100A8 inhibited heterocomplex formation with S100A9 and dimished antimicrobial activity of the complex [655]. Here, we show that the recCys_{42}-Ala_{42}S100A8 mutant was less efficient in preventing oxidation, confirming that Cys_{42} contributed to protection of lipid-free ApoAI from oxidation by HOCl.

Aggregation of recS100A8 in lipid-free ApoAI preparations was significantly more than aggregation of recCys_{42}-Ala_{42}S100A8. In Chapter 3 (see Section 3.3.1, Fig. 3.2A, profile 3), we showed that a 2:1 molar ratio of HOCl:S100A8 promoted aggregation. The concentrations of HOCl used in Section 5.3.8 and 5.3.9 (20 μM and 40 μM respectively) were high, because of the need to generate oxApoAI, but levels may not represent HOCl concentrations generated locally. For example, 10^6 activated neutrophils produce approximately 2 x 10^{-7} mol of HOCl during a 2 hr period [1105], and S100A8 may be less susceptible to aggregation *in vivo* when exposed to the lower levels of HOCl that may be generated locally.

HDL contains several lipids, including palmitoyl-oleoyl-phosphatidylcholine, palmitoylphosphatidylcholine, cholesterol esters, free cholesterol and triglyceride [1106, 1107]. Triglycerides and cholesterol esters constitute a hydrophobic interior, with phospholipids covering the surface of the particle [1108]. Aggregation of S100A8 in ApoAI(HDL) preparations was somewhat less, suggesting that lipids stabilize these proteins and/or that HOCl may preferentially interact with lipid. In healthy, fasting donors HDL particles carry ~85% of detectable oxidized lipids [1109]. It is noteworthy that slot blotting indicated oxS100A8 in HDL (Fig. 5.5A).

The reduced protection seen with HSA and S100A8 in ApoAI(HDL) preparations may in part be mediated by their binding of lipid components. Albumin binds phosphatidylcholine [1110] and free fatty acids by hydrophobic interactions [1111, 1112], which might alter its oxidant-scavenging capacity. S100A8 (in complex with S100A9) also binds lipids [580], possibly via hydrophobic domains [1113], and this could potentially reduce its protective effects. Lipids also stabilize ApoAI [698], and could stabilize S100A8 and more studies to investigate S100A8-ApoAI interactions in HDL are warranted.

Here, we show that S100A8 in the circulation is principally within the HDL particle and this may have important functional consequences. HDL is preferentially oxidized in the presence of LDL because HDL lacks anti-oxidants such as α-tocopherol and ubiquinol and increased amounts of S100A8 generated as a consequence of inflammation could provide initial protection [1109]. Normal HDL is considered anti-inflammatory [1114-1119]. However, MPO is also present in HDL and binds a specific domain in ApoAI [1047, 1048]. Association of S100A8 in close proximity may be an important inflammation-specific defense mechanism, where it can act locally to scavenge low amounts of HOCl. Chronic inflammatory diseases such as SLE promote and increase in MPO activity in the circulation [1085], increasing HDL oxidation and accelerating CVD [1026]. Results here suggest that S100A8, possibly by interaction with ApoAI may protect ApoAI from oxidation, thereby reducing the potential for HDL to form a pro-inflammatory particle.

5.4.7 S100A8/A9 REDUCED FORMATION OF HOP ON ENDOTHELIAL CELLS

MPO localized to endothelium promotes endothelial dysfunction by producing HOCl (summarized in Fig. 5.14) (reviewed in [1073]).

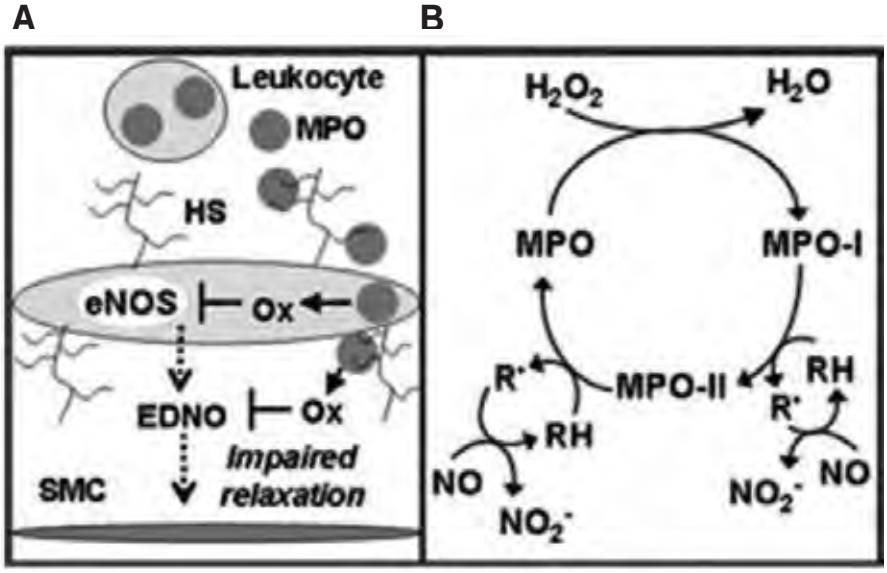

Figure. 5.14: MPO and endothelial dysfunction. (**A**) MPO is released by activated leukocytes and binds to heparan sulfates expressed on the endothelium. Binding results in enzyme transcytosis to the sub-endothelial space where the enzyme catalyses oxidative reactions that impair endothelium-derived nitric oxide (EDNO) activity. (**B**) MPO in the presence of H_2O_2 catalytically consumes NO through the production of substrate radicals (R*) generated by compound I (MPO-I) or II (MPO-II) of the enzyme. Heparan sulfate; HS and smooth muscle cell; SMC. From [1073].

Recombinant S100A8, S100A9 or the heterocomplex inhibited formation of HOP from BAEC treated with MPO and H_2O_2, whereas Cys_{42}-Ala_{42}S100A8 failed to do so. A heterocomplex of Cys_{42}-Ala_{42}S100A8/A9 also prevented oxidation, probably due to the scavenging capacity of S100A9. Although BAEC are a convenient cell for analyzing functional effects of S100 proteins, a homologous system using human cells (for example HUVEC or the HMEC would be more appropriate. Using these cells, it would be interesting to determine if MPO and S100A8, S100A9 or the heterocomplex co-localize, and are obvious in the extracellular matrix in human atheroma [410]. Moreover, it would be worth studying whether S100A8 and/or S100A9 prevented inhibition of GAPDH or loss of GSH in endothelial cells after exposure to MPO-derived oxidants [1120].

A pathological role for MPO in CVD is implicated (see Section 5.4). MPO and increased levels of S100A8/A9 in the circulation are reported in patients with unstable angina and acute myocardial infarction and correlate with increased disease severity [483, 1063, 1080, 1081]. MPO rapidly binds heparin sulfate GAGs on endothelial cells [1087], where the enzyme associates with the basement membrane, particularly targeting

fibronectin. Interestingly, S100A8/A9 binds endothelial cells by a similar mechanism [431]. Thus MPO and S100s are found together and may co-localize on the endothelium and in HDL. S100A8 was protective in both compartments. This is functionally important as it suggests that S100A8 and S100A9 may protect against ROS-induced damage in atherosclerosis, not only by binding and reducing HOCl-induced oxidation of ApoAI (see Section 5.3.8 and 5.3.9) [698], but also by reducing oxidant levels generated by MPO on the endothelium, and by modulating leukocyte transmigration and accumulation by regulating adhesion to fibronectin (see Fig. 4.15, Chapter 4).

CHAPTER 6: GENERAL DISCUSSION

Oxidative stress contributes to progression and exacerbation of inflammation, and excess ROS/RNS reduce lung function [977] or accelerate atherosclerosis following oxidation of HDL [698, 1042]. Three members of the S100 family, S100A8, S100A9 and S100A12 are highly expressed in lung disorders [443] and in cardiovascular disease [410, 1063], and because of this association, were designated inflammation-associated S100 proteins. However, increasing evidence suggests that S100A8 and S100A9 play protective roles in inflammation, principally through oxidant scavenging [410, 606, 613, 644, 695].

S100A8 and S100A9 are highly sensitive to oxidation by several ROS, including HOCl [410, 605, 606], derived from the MPO/H_2O_2 system, subsequent to neutrophil activation (reviewed in [1073]). However, ROS can also modify lipids and proteins irreversibly (reviewed in [695, 1121]). S100A8 and S100A9 are preferentially oxidized compared to the molar ratios required to promote structural changes in BSA or LDL and were proposed to have a protective role in oxidative stress [410]. The structural modifications to mS100A8 and mS100A9 generated by HOCl have been reported [605, 606, 957] whereas, *in vitro* or *in vivo* modifications to hS100A8 and hS100A9 have not been examined in depth. Studies presented in Chapter 3 investigated putative modifications to monomeric and dimeric hypohalous acid-oxidized hS100A8 and hS100A9 *in vitro* and identified novel post-translational modifications in S100A8.

Mild oxidation of Cys residues is reversible in biological systems (reviewed in [613]) and H_2O_2 or Cu^{2+}-oxidation generates the S100A8 disulfide-linked homodimer [605], whereas HOCl can irreversibly modify this amino acid [606]. Such modifications are likely to regulate function. HOCl-oxidation of hS100A8 [612], or site-directed mutagenesis of $Met_{63/83}$ in hS100A9 abrogates neutrophil fugetaxis [614] and substitution of Cys and Met residues in S100A8 and S100A9 alters antifungal activity because of impaired heterocomplex formation [655]. Oxidation impacts on the chemotactic activity of mS100A8 [605, 606] and S-nitrosylation may regulate leukocyte-endothelial cell interactions in the microcirculation, and suppress mast cell-mediated inflammation [613]. Moreover, the ROS-scavenging capacity of S100A8 may regulate mast cell activation and be protective in asthma [644]. S-glutathionylation of S100A9 may regulate neutrophil sequestration in the extravasculature [637]. Studies presented in Chapters 4 and 5

characterize oxidative modifications to S100A8 and S100A9 in two chronic inflammatory conditions, asthma and atherosclerosis, and describes some functional outcomes.

This thesis aimed to identify putative oxidation products in S100A8 and S100A9 in samples from human disease. This information would confirm their ROS scavenging capacity *in vivo*, a possibility indicated by experiments performed with mS100A8 [606, 644]. However hypohalous acid oxidation products of the native protein had not been characterized. Here we show that equimolar ratios of protein:HOCl generated novel oxathiazolidine adducts on the single Cys residue of rec-hS100A8, a unique product. Next, we used sputum from asthmatic patients as a source of oxidized S100A8 because our studies using an antibody that recognized oxS100A8 indicated strong reactivity in the lung (Fig. 4.2, Chapter 4) and sputum contained the oxidized product (Fig. 4.3E, Chapter 4). This is the first report of an excess of oxidized S100A8, compared to S100A8, in any human disease. Because we could not satisfactorily use in-gel digests of bands separated by SDS-PAGE to identify the novel adducts, we developed a purification scheme using RP-HPLC to enrich the S100 proteins before digesting them in solution. Here we present the first evidence that S100A8, and to a lesser extent S100A9, scavenge hypohalous acid oxidants in asthma.

We next used carotid artery samples from patients with atherosclerosis because our earlier studies indicated that S100A8 was oxidized in such samples [410]. Analysis proved more difficult because of the calcified nature of the samples and extraction was not ideal. However our results suggest that in these samples, S100A8 has a similar scavenging function.

Because oxidation of mS100A8 by peroxide or HOCl modified its chemotactic properties [605, 606], and S-nitrosylation of mS100A8 inhibited mast cell activation and neutrophil recruitment in the rat mesenteric circulation [613], we postulated that the HOCl-oxidized hS100A8 may have altered function. We show for the first time, that rec-oxS100A8 and rec-oxS100A9 did not form heterocomplexes (Fig. 4.14, Chapter 4) and this affected their antimicrobial activity (Fig. 4.16, Chapter 4) whereas fMLP- provoked neutrophil adhesion to fibronectin was reduced by the native and oxidized complexes (Fig. 4.15B, Chapter 4). These properties may contribute to the suppression observed with S100A8 in acute murine asthma [644].

Importantly, we show here that S100A8 is a component of HDL in plasma (Fig. 5.5A), again implicating it in host protection. We show that S100A8 protected ApoAI from oxidation by HOCl (Fig. 5.11C), an important new function for host defense in

cardiovascular disease, and other conditions, such as SLE that have increased cardiovascular risk. Preliminary experiments also showed that S100A8 reduced endothelial cell oxidation by HOCl derived from MPO/H_2O_2 although more experiments are required to identify other functions that may be maintained.

The following sections describe these aspects in more detail, and limitations of the study are discussed.

6.1 HYPOHALOUS ACID OXIDATION INDUCES POST-TRANSLATIONAL MODIFICATIONS TO HUMAN S100A8 AND S100A9

Sulfinamide bond formation in mS100A8 [606] by HOCl underpinned the work presented in Chapter 3. HOCl was used to compare the structures generated murine and human orthologs. Products generated by HOBr were also analyzed, because this is prevalent in asthmatic lung [918].

Results in Section 3.3 indicated that a molar ratio of 1:1, HOCl:S100A8 readily generated the oxidized monomer and dimer whereas higher molar ratios promoted aggregation. In contrast, a 1:1 ratio of HOBr:S100A8 only generated monomeric oxS100A8, with little evidence of the dimer. Monomeric oxS100A8 contained Met_{78}(O), Trp_{54}(+16) and $His_{17/27/83}$(+16), Cys_{42}-sulfonic acid and two novel modifications, oxathiazolidine oxide, (m/z +30 Da mass addition) and oxathiazolidine dioxide (m/z +46 Da mass addition) on the Cys_{42} residue. Oxidation of Met_{78} to Met_{78}-sulfone and chlorination of $Tyr_{16/19}$ were observed in monomeric samples of HOCl-oxS100A8 but these were present in very minor amounts, indicating that the Cys and Met oxidation products were preferentially generated.

In contrast to HOCl, oxidation of Cys_{42} by HOBr only generated Cys_{42}-sulfonic acid and Trp_{54}(+16). The relative reaction rates of some amino acids with HOCl reported by Winterbourn *et al*. indicate an order of reactivity, Cys > Met > Cystine > His > Ser > Leu [960]. Reaction rates with HOBr are substrate-dependent, but, in general Cys and Met residues are approximately 10-fold less reactive to HOBr than to HOCl [922]. These rate constants may contribute to the ready formation of HOCl-oxidized Cys adducts, and Met residues in S100A8 relative to formation of Cys_{42}-sulfonic acid and Trp_{54}(+16) that were more prominent following HOBr treatment. However the oxidation products generated would not only depend on the type of hypohalous acid oxidant generated, but

its concentration and time of exposure, factors that would be important *in vivo*. Kinetic experiments with lower doses of the oxidants would be informative in this respect. Moreover, characterization of His and Trp oxidation was preliminary and further analysis to accurately characterise other potential modifications is required.

Fig. 6.1 shows the proposed sequence of oxidation products generated by HOCl or HOBr. Reactions of HOCl with Cys begin with chlorination of the thiol group which yields unstable sulfenyl chloride intermediates [943], ultimately forming sulfonic acid (RSO_3H) and relies on reactions with sulfenic (RSOH) and sulfinic (RSO_2H) acids as intermediates [942]. Sulfenyl chloride intermediates can react with the thiol group of a second Cys molecule to generate disulfide bonded cystine [943], however, the oxidized multimers of S100A8 (after treatment with 1.5:1 M HOCl:S100A8; see Fig. 3.10, Chapter 3) were resistant to DTT, suggesting that oxidized S100A8 dimers were not disulfide-bonded Cys residues.

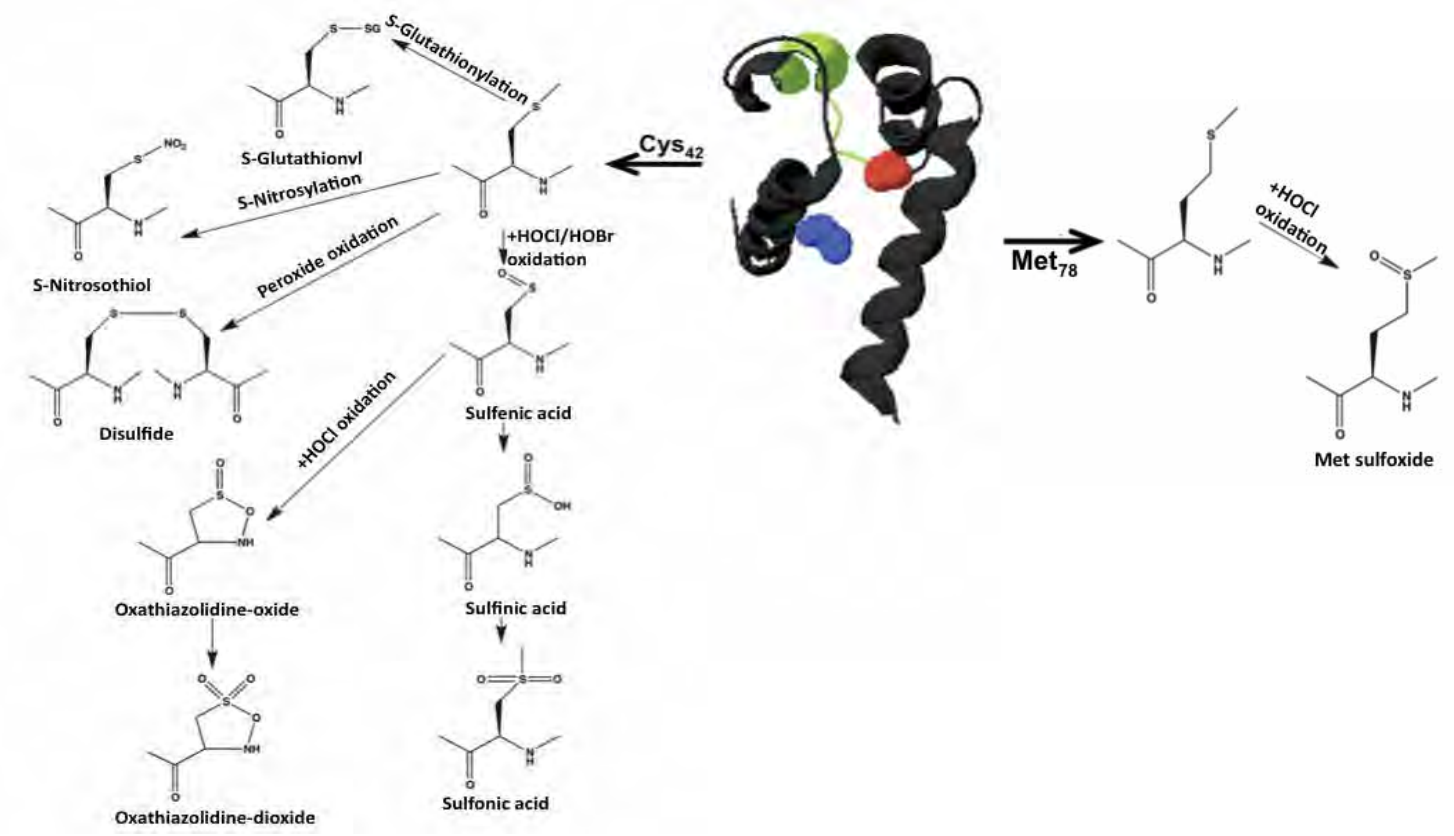

Figure 6.1: Putative *in vitro* products of S100A8 oxidation are summarized. For HOCl oxidation, the Cys_{42} (backbone of the Cys residue shown in red) adduct, oxathiazolidine-dioxide, (+46 m/z mass addition) may have formed by oxidation of Cys to sulfenic acid, then further oxidation to sulfinic or sulfonic acids, or to the oxathiazolidine-oxide (+30 m/z mass addition). Further oxidation of the latter generates a dioxide adduct with a +46 m/z mass addition caused by the neutral loss (of SO_2 and SO_3), to form cyclised products between oxidized Cys and nitrogen within the peptide backbone. The Met adduct (backbone of the Met residue shown in blue), methionine sulfoxide (+16) is formed by oxidation of Met_{78}. The hinge region (residues 43-55) is highlighted in green. Products of His and Trp oxidation are not included in this schematic, as oxidation products require further analysis. Drawn using Swiss-PDB Viewer 4.04.

Because HOCl-oxS100A8 dimers were apparently not disulfide-bonded Cys residues, other mechanisms were investigated. Dimerization via Tyr residues is a product of HOCl cross-linking, the result of one-electron oxidation of L-Tyr to generate a tyrosyl radical [979]. Dimer formation as a consequence of oxidation of Tyr residues does not occur in mS100A8 [606] and we found no evidence for this in MS analysis of peptides derived from HOCl-oxS100A8, making this an unlikely mechanism. Similarly, oxidation of Trp and His residues in S100A8 were not identified in the oxidized dimer or trimer, however, His can be oxidised to 2-oxo-histidine, which can contribute to cross-linked complexes (reviewed in [948]), and further work is required to fully elicidate the process of multimer formation.

Another mechanism of oxidative cross-linking is carbonylation although we found no evidence for this. Protein carbonylation is metal-catalyzed oxidation, typically with reduced metal ions such as Fe^{2+} or Cu^{2+} [1122]. The Fenton reaction produces a highly reactive hydroxyl radical, which interacts with amino acid side chains, generating carbonyl groups [1123]. Our group demonstrated that rec-mS100A8 is susceptible to oxidation by Cu^{2+} [605], which generated the disulfide dimer, but not multimeric components. More carefully controlled studies with appropriate reagents would be useful to determine whether carbonyl groups could contribute to cross-linking of hS100A8 and/or hS100A9.

In rec-mS100A8, for which 5:1 molar ratios of HOCl:mS100A8 generated sufficient peptides for analysis [606], inter- and intra-molecular covalent sulfinamide cross-links formed between Cys_{42} and ε-amine groups on Lys residues after oxidation by reagent or MPO-derived HOCl [606]. Sulfenyl chloride intermediates react with nitrogen centres, via two-electron processes forming sulfenamide crosslinks (RSN-). Further exposure of sulfenamides to oxygen generates sulfinamides (RS(O)N-) [606] and sulfonamides ($RS(O)_2N$-) [904]. Previous work by Fu *et al*. used synthetic peptides to demonstrate intra-molecular sulfenamide, sulfinamide and sulfonamide cross-linked peptides in LDL. These products formed via thiol groups and Lys residues, whereas sulfur-nitrogen cross-links occurred between guanidine groups (produced by HOCl oxidation of guanine) and arginine residues [904].

We found no evidence for sulfinamide bonds in rec-hS100A8 even though multimeric DTT-resistant complexes were generated with 1.5:1 molar ratios of HOCl (see Fig. 3.10, Chapter 3). We were unable to identify sulfinamide bonds in these adducts,

possibly because of the low yields, as increasing HOCl concentrations promoted rapid aggregation (see Fig. 3.2A, profile 3, Chapter 3). $Lys_{35/36}$ were necessary for initiation of sulfinamide bond complexing in murine oxS100A8 [606]. Oxidation of a $Lys_{35/36}$-$Ala_{35/36}$S100A8 mutant may help identify whether these amino acids contribute to complex formation, particularly as these residues are conserved in the murine and human proteins (see Fig. 3.17, Chapter 3). The presence of Cys_{42}-oxathiazolidine-dioxide in oxidized dimer may indicate possible involvement of this bond in dimer formation. Increased incubation times with low levels of HOCl may increase the abundance of oxidized multimers, allowing for more definitive analysis. Notwithstanding, neither Cys_{42}-sulfonic acid nor the oxathiazoldine derivatives are likely to contribute to sulfinamide cross-linking, and these products were the dominant oxidation products, suggesting that this product is unique to hS100A8. We propose that the Cys_{42}-oxathiazolidine adducts form following oxidation of Cys_{42}-sulfenic acid by HOCl (Fig. 6.1) and represent a new type of irreversible modification.

Oxidized proteins are thermodynamically unstable and can form partially unfolded tertiary structures, resulting in cross-linking (see Fig. 5.9C, Chapter 5). Approximately 20% of newly synthesized protein is rapidly degraded by the proteasome, minimizing formation of incorrectly folded proteins that could form protein aggregates [1124, 1125], however, prolonged exposure to ROS can increase production of misfolded proteins, overwhelming proteases. When protein aggregates form ordered filaments, amyloid formation results, which are protease resistant (reviewed in [1126]), thereby reducing clearance. We found that molar ratios of HOCl > 1.5 M, or HOBr > 5 M rapidly generated aggregation in rec-hS100A8 (see Fig. 3.2A, profile 3 and Fig. 3.2D, profile 3, Chapter 3), whereas rec-mS100A9 is more stable [605].

S100A8 and S100A9 were implicated in *corpora amylacea* formation in prostate glands of patients with prostate cancer, facilitated by Ca^{2+} and Zn^{2+}. Activated macrophages with elevated levels of S100A8/A9 in surrounding tissue were also observed, and these proteins are proposed to increase the risk of malignancy in the ageing prostate [1127]. Amyloid formation is sometimes associated with bacterial infection. We also found S100A9 in brain extracts from Alzheimer's disease patients [418]. Recently, Fritz *et al*. proposed that other S100 proteins (such as S100A2 and S100B) in conditions of oxidative stress, or alterations in metal homeostasis, may also form amyloid fibrils, and these authors suggest that amyloid formation may serve as a sink for inflammation-promoting proteins [396]. The presence of multimeric S100A8 seen here (see Fig. 3.10,

Chapter 3 and Fig. 5.9C, Chapter 5) and by others [410] suggests that S100A8 may form amyloid structures and so excess oxidation could potentially turn a protective mechanism into a pathogenic process.

S100A9 appeared somewhat less sensitive to oxidation by HOCl and did not aggregate. The 1:1 molar ratio generated oxidized monomer and disulfide-linked dimer, which was reduced after addition of DTT (see Fig. 3.11B, Chapter 3). No compelling evidence for peptides containing oxidized Cys_3 in S100A9 were identified indicating that that the amino acids in the helical loops surrounding S100A9 contribute to its reactivity. However, peptides containing Cys_3 were only seen in one non-enzyme specified digested sample. The absence of Cys_3 peptides in enzyme specified searches could be due to the choice of protease, and appropriate protease cleavage sites within S100A9 (cleavage sites for AspN and trypsin are shown in Figs. 6.2A and 6.2B respectively).

AspN cleaves Asp residues from the N-terminal side [1128]. hS100A9 contains six Asp residues - the closest to the N-terminus is at position 30. Although the resultant peptide would contain the Cys residue at position 4, the length of this peptide would make analysis of Cys modifications by MS difficult (personal communication, A/Prof. Mark Raftery). Conversely, trypsin cleaves at Arg and Lys residues from the C-terminal side [1129]. Unfortunately human S100A9 contains a Lys residue at position 4, creating a peptide too small for analysis (personal communication, A/Prof. Mark Raftery). The enzyme Arg-C endopeptidase cleaves specifically at Arg residues; the closest Arg residue to Cys_3 is at position 10, and this may generate a peptide more appropriate for MS sequencing and analysis of putative Cys_3 modifications. hS100A9 contains only three Arg residues at positions 10, 42 and 85, and as S100A9 has 114 amino acid residues, use of Arg-C endopeptidase alone would not create sufficiently small peptides for accurate analysis of the Met residues, but would be useful as an additional reagent. Analysis by double enzyme digests is commonly used to analyze complex samples by MS and may be appropriate to analyze Cys modifications in S100A9 [1130]. Fig. 6.2C shows that a primary digest with Arg-C endopeptidase would produce a peptide of appropriate length for Cys_3 residue analysis. A secondary digest with AspN would then cleave the larger peptides into smaller peptides for analysis of Met oxidation products.

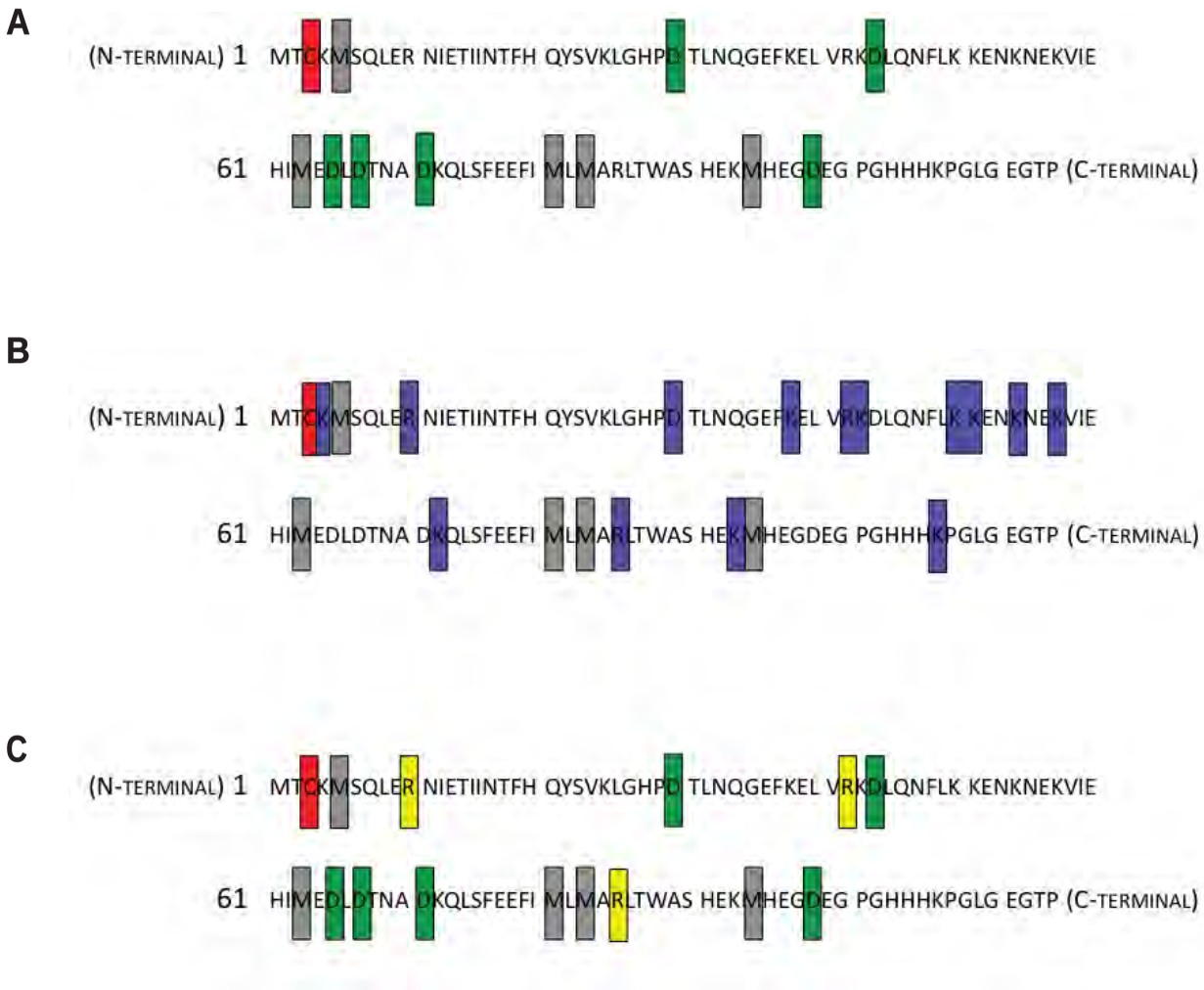

Figure 6.2: Amino acid cleavage sites in hS100A9. (A) Endoproteinase AspN cleaves Asp residues (highlighted in green) from the N-terminal. Digestion with AspN would yield a peptide 29 amino acids in length, too large for accurate MS analysis of Cys_3 (highlighted in red) modifications. Digestion with AspN generates peptides of sufficient length for analysis of the five Met residues (highlighted in grey; Met_1 is not highlighted as this residue is cleaved during purification of recombinant protein). **(B)** Trypsin cleaves at Lys and Arg residues (highlighted in purple) from the C-terminal and would generate a Cys_3-containing peptide of four amino acids, too small for analysis by MS. As with AspN, trypsin digests would be appropriate for MS analysis of Met residues. **(C)** Double enzyme digest may be the most adequate method of generating Cys_3-containing peptides of appropriate size for analysis. A primary digest using Arg-C endopeptidase, which cleaves arginine residues (highlighted in yellow) from the C-terminal would result in a Cys containg peptide of nine amino acids that would be adequate for MS analysis. A secondary digest with AspN would ensure that Met residues would be present in peptides small enough for analysis.

The rec-oxS100A9 monomer (from C4-RP-HPLC, see Fig. 3.11A, profile 2, Chapter 3) contained $Met_{63/81/83/94}(O)$, whereas, the peak containing high amounts of disulfide-linked dimer (eluted at 15.7 min) only indicated conversion of Met_{63} to $Met_{63}(O)$. Met oxidation to Met(O) generates a stable product, but this can be reversed by methionine sulfoxide reductase [1131]. As potential oxidant scavengers, this reversibility may represent an inefficient defense mechanism but such reactions are proposed to protect functions of some proteins under oxidative stress (reviewed in [1132]). In contrast, Met-sulfone, an irreversible modification which forms following treatment of S100A9 with glutathione-SNO [637], was only observed in one peptide from oxS100A9, suggesting that this is not a preferred product. Interestingly, treatment of S100A8 with glutathione-SNO generates S100A8-SNO whereas the predominant product in S100A9 is glutathionylated [613]. Together with the results presented here, these studies indicate that each S100 may preferentially regulate particular redox pathways.

The studies presented here focused on HOCl and HOBr, however, it would be interesting to analyze how HOSCN, the other major MPO-derived oxidant (reviewed in [1133]), could protentially modify the structure of S100A8 and S100A9. In this context, use of HOSCN to oxidize rec-hS100A8 and rec-hS100A9 *in vitro* would be interesting, as HOSCN targets Cys residues but does not modify Met [1134]. Moreover, comparisons of putative oxidation products with HOCl may indicate that the novel oxathiazolidine adducts found in HOCl-oxidized protein were unique to this oxidant.

The *in vitro* modifications to S100A8 and S100A9 characterized in Chapter 3 enhance understanding of how hypohalous acid oxidants alter the structures of these proteins and confirm the proposal that these human S100 proteins can indeed scavenge oxidants, a theory proposed by McCormick *et al*. after identification of multimeric structures in human atheroma [410].

6.2 S100A8 AND S100A9 ARE OXIDIZED IN VIVO AND OXIDATION REGULATES INFLAMMATORY FUNCTIONS

S100A8/S100A9 are implicated in respiratory diseases [443, 496, 996], but their functions are largely unexplored. S100A8 suppresses MC activation and leukocyte infiltration and production of some relevant cytokines in acute murine asthma, when delivered directly to the lung before antigen challenge [644]. We identified Cys_{42} adducts formed as a result of HOCl-oxidation in recS100A8 (Fig. 6.1) and oxidation of Met

residues in S100A9, but until now, the scavenging capacity of these proteins in human inflammation was unproven.

Many oxidative modifications of S100A8 and S100A9 have important functional consequences as some mediate anti-inflammatory effects [605, 606, 613, 644]. These can be grouped into reversible and irreversible modifications. Disulfide bond formation between Cys residues, and Met oxidation to Met(O) are reversible due to the activities of specific reductases such as peroxiredoxins and Met(O) reducatases [885]. However, oxidation to Cys-sulfinic or sulfonic acids is irreversible [1135] and it is likely that sulfinamide formation is as well, because of amino acid cross-linking [606]; Met oxidation to Met-sulfone is also irreversible [958]. In Section 4.3, we identified similar oxidative post-translational modifications in oxS100A8 in sputum from subjects with asthma and explored some potential consequences using *in vitro* tests.

An antibody that reacts strongly with HOCl-oxS100A8 was strongly reactive in some eosinophils, neutrophils and macrophages localized beneath the basement membrane of airways, and within the lung parenchyma in asthmatic lung (see Fig. 4.2, Chapter 4). Accumulation of neutrophils in the lung is important in host defense against a diverse range of pathogens. Proteolytic enzymes and hypohalous acids oxidants are released by activated neutrophils. When released within close proximity to the alveolar walls, extracellular matrix or the small airways and airway mucosa, these can severely damage lung tissue [1136, 1137]. In chronic inflammatory lung diseases, such as severe asthma, S100A8 and S100A9 were proposed to perpetuate injury. For example, Halayko and Ghavami propose that S100A8/A9 induces receptor-mediated signalling pathways in airway mesenchymal cells, and independent intracellular activation of signalling pathways via RAGE and TLR-4. Specifically, S100A8/A9 is proposed to induce secretion of HMGB1, a ligand for RAGE, working in concert with LPS to potentiate activation of TLR-4, promoting local inflammation and tissue repair, resulting in progression of airway remodelling (reviewed in [970]).

Previously our group showed that asthmatic lung contains S100A12-positive leukocytes in the sub-mucosal region, and S100A12-positive eosinophils within mucus plugs from asthmatic airways, not seen in healthy controls [131]. S100A12 is regarded as a DAMP [393] and is a monocyte chemoattractant [320]. It can potentiate MC activation [131], resulting in neutrophil and monocyte recruitment *in vivo*, and is itself a MC chemoattractant and may sequester MC in asthmatic lung [298]. Serum concentrations of S100A12 correlate with disease activity in some inflammatory disorders [442, 537] and

S100A12 was prominent in sputum from patients with eosinophilic asthma [131]. The strong anti-S100A8 and S100A9 reactivity in asthmatic lung may initially suggest pro-inflammatory roles for these proteins in asthma, and certainly for S100A12 this appears to be true [131], even though recent studies suggest a protective role in asthma [669]. The strong reactivity to anti-oxS100A8 IgG in asthmatic lung, however, suggested that S100A8 may scavenge hypohalous acids generated from activated eosinophils and neutrophils, particularly in patients with infections such as *H. influenzae* and *P. aeruginosa* [991-993, 1020], thereby limiting tissue damage.

Semi-quantitative Western blotting of control, asthmatic and bronchiectatic sputum showed that oxS100A8 (largely monomeric) was significantly raised in asthmatic subjects compared to healthy control subjects. Although S100A8, S100A9 and S100A12 (detected by ELISA) were elevated in asthmatic sputum relative to control subjects, levels were not significantly higher (see Section 4.3.2 and 4.3.3, Chapter 4).

Sputum samples the central airways, hence amounts of S100 protein may be underestimated. Moreover, S100A8 and S100A9 bind heparan sulfate [431] and may concentrate effects at the extracellular matrix, and this may contribute to the lower concentrations in sputum. In addition, collection of spontaneous sputum, or induction of sputum has been used to study pathological processes in the larger airways, whereas there is limited data on how large airway inflammation relates to pathological processes at sites of airflow obstruction: the small airways and the alveolar region [1138]. A limiting factor in collecting spontaneous sputum is a productive cough prior to collection. Subjects with a productive cough in the days preceding collection expectorate readily for collection and produce larger samples, enabling better inflammatory cell analysis, than those subjects without a productive cough before [1139]. As expectoration of sputum varies among subjects, induction by inhalation of hypertonic saline may have been a more appropriate method to ensure more consistent sample collection among subjects. Inhalation of hypertonic saline to induce sputum has been used since the 1980s, originally to diagnose *Pneumocystis catrinii* pneumonia in patients infected with HIV [1140] and was adapted by Pin *et al*. for examining cell populations in asthma [1141]. However, hypertonic saline increased (although not significant) levels of IL-6 and TNF-α in exhaled breath condensate in asthmatic, COPD and healthy subjects [1142] and we chose not to use this method.

BALF may be the most appropriate means of measuring S100 protein levels. For

example, ~4 fold more IL-8 was found in BALF from CF patients than in sputum [1012]. Nebulized hypertonic saline treatment disrupts interactions between GAGs and IL-8, rendering IL-8 susceptible to proteolytic degradation, thereby underestimating levels in sputum [1012]. Future studies comparing S100 protein levels and oxidation products in spontaneous sputum, induced sputum, and BALF, and correlation with disease activity in various lung disorders may allow us to better understand how these proteins may regulate the inflammatory response in different respiratory diseases.

All asthmatic subjects were on inhaled corticosteroids. Corticosteroids upregulate S100A8 mRNA and protein in macrophages in an IL-10 dependent manner and this mechanism of induction suggests an anti-inflammatory role for S100A8 [406]. Steroids increase S100A8 levels in lungs of mice treated with LPS [430] and S100A8 positive-macrophage numbers increase in the synovium of RA patients treated with high dose steroids [406]. Thus, comparisons of sputum from a subgroup of steroid-naïve asthmatics with those on inhaled corticosteroids would be informative. In addition, the sample size of each subgroup was relatively small (n=10-14), as this work was originally conducted as a pilot study to identify a likely source of S100A8 for structural characterization and numbers could be increased. Levels of S100A8, S100A9 and S100A12 detected by ELISA in asthmatic sputum trended towards significance compared to control subjects, and greater cohort numbers, may clarify statistical significance.

Given the strong reactivity of oxS100A8 in the lung, oxidized complexes were predicted in sputum but Western blotting indicated only monomeric forms. Studies by other groups would assume that as S100A8 migrated in SDS-PAGE as a single component of 10 kDa, a size typical of the native monomer, no modification was indicated. However, the *in vitro* studies in Chapter 3 identified mainly recS100A8 monomeric oxidation products that until now, have never been characterized. Because this was elevated in asthmatic sputum, this was used as a source for analysis.

In control sputum, oxidation of Met_1 to $Met_1(O)$ in S100A8 and formation of $Met_{63}(O)$ in S100A9 were the only obvious modifications. The novel oxathiazolidine-dioxide adducts and its intermediates were only identified in S100A8 isolated from asthmatic sputum. The presence of Cys_{42}-oxathiazolidine-dioxide in asthmatic sputum indicates hypohalous acid generation in asthmatic lung and confirms the oxidant-scavenging potential of S100A8 *in vivo*. In asthmatic sputum, $Met_{1/78}$ in S100A8 (see Table 6.1 for a comparison of post-translational modifications found *in vitro* and *in vivo*.) and $Met_{63/81/94}$ in S100A9 were oxidized to Met(O).

Table 6.1: *In vitro* and *in vivo* oxidative modifications to S100A8

Recombinant Sample	Mass addition (Da)	Modification
HOCl-oxidized S100A8 (1:1)		
AspN digest		
DDLKKLLETE<u>C</u>PQYIRKKGA	+32 (10,876 Da)	Cys_{42}-sulfinic acid
ETE<u>C</u>PQYIRKKGA		
DDLKKLLETE<u>C</u>PQYIRKKGA	+48 (10,892 Da)	Cys_{42}-sulfonic acid
ETE<u>C</u>PQYIRKKGA		
DDLKKLLETE<u>C</u>PQYIRKKGA	+46 (10,890 Da)	Cys_{42}-oxathiazolide-dioxide
ETE<u>C</u>PQYIRKKGA		
EFLILVIK<u>M</u>GVAAHKKSHE	+16 (10,860 Da)	Met_{78}(O)
DV<u>W</u>FKEL	+16 (10,860 Da)	Trp_{54}(+16)
DVY<u>H</u>KYSLIKGNFHAVYR	+16 (10,860 Da)	His_{17}(+16)
DVYHKYSLIKGNF<u>H</u>AVYR	+16 (10,860 Da)	His_{27}(+16)
GVAA<u>H</u>KKSHEESHKE*	+16 (10,860 Da)	His_{83}(+16)
Trypsin digest		
LLETE<u>C</u>PQYIR	+30 (10,874 Da)	Cys_{42}-oxathiazolidine-oxide
	+46 (10,890 Da)	Cys_{42}-oxathiazolidine-dioxide
	+48 (10,892 Da)	Cys_{42}-sulfonic acid
HOBr-oxidized S100A8 (1:1)		
AspN digest		
ETE<u>C</u>PQYIRKKGA	+48 (10,892 Da)	Cys_{42}-sulfonic acid
DV<u>W</u>FKEL	+16 (10,860 Da)	Trp_{54}(+16)
Sputum Sample	Mass addition (Da)	Modification
***Control Sputum (n=2) (15-18 min C4-RP-HPLC*)**		
AspN digest		
<u>M</u>LTELEKALNSII	+16 (10,850 Da)	Met_1(O)
<u>M</u>LTELEKALNSII*	+16 (10,850 Da)	Met_1(O)
Asthmatic Sputum (n=5) (peak 1, 14.3 min C4-RP-HPLC)		
AspN digest		
ETE<u>C</u>PQYIRKKGA* and	+48 (10,882 Da)	Cys_{42}-sulfonic acid
DDLKKLLETE<u>C</u>P* and		
DDLKKLLETE<u>C</u>PQYIRKKGA		
DDLKKLLETE<u>C</u>PQYIRKKGA	+46 (10,880 Da)	Cys_{42}-oxathiazolidine-dioxide
and		
ETE<u>C</u>PQYIRKKGA		
<u>M</u>LTELEKALNSII	+16 (10,850 Da)	Met_1(O)
Trypsin digest		
KLLETE<u>C</u>PQYIR	+48 (10,882 Da)	Cys_{42}-sulfonic acid
LLETE<u>C</u>PQYIR	+30 (10,864 Da)	Cys_{42}-oxathiazolidine-oxide
	+46 (10,882 Da)	Cys_{42}-oxathiazolidine-dioxide
<u>M</u>GVAAHKK	+16 (10,850 Da)	Met_{78}(O)

* denotes non-enzyme specified searches

Oxidation of critical Met residues can be functionally important [663, 1143]. S100A9 oxidation by HOCl alters its affects on neutrophil migration, and mutation of Met_{63} and Met_{83} to Ala resulted in an oxidation-resistant protein [614]. However, if Met(O) in S100A8 and S100A9 are regenerated by reductases such as MSRB2 that is present in lung [1018], these adducts may not be plentiful. A comparison of the oxidative products identified in S100A9 *in vitro* and *in vivo* is presented in Table 6.2.

Table 6.2: *In vitro* and *in vivo* oxidative modifications to S100A9

Recombinant Sample	**Mass addition (Da)**	**Modification**
HOCl-oxidized S100A9 (1:1) (Fig. 3.11A, peak 1, 14.8 min)		
AspN digest		
EKVIEHIM	+16 (13,268 Da)	$Met_{63}(O)$
EEFIMLMARLTWASH	+16	$Met_{81}(O)$
EEFIMLMARLTWASH	+16	$Met_{83}(O)$
EEFIMLMARLTWASHEKMHEG	+16	$Met_{94}(O)$
HOCl-oxidized S100A9 (1:1) (Fig. 3.11A, peak 2, 15.7 min)		
EKVIEHIM	+16 (13,268 Da)	$Met_{63}(O)$
Sputum Sample	**Mass addition (Da)**	**Modification**
***Control Sputum (n=2) (18-21 min C4-RP-HPLC*)**		
EKVIEHIME	+16 (13,258 Da)	$Met_{63}(O)$
Asthmatic sputum (n=3) (15.3 min C4-RP-HPLC)		
AspN digest		
EKVIEHIME and DLQNFLKKENKNEKVIEHIME*	+16 (13,258 Da)	$Met_{63}(O)$
EEFIMLMARLT*	+16 (13,258 Da)	$Met_{81}(O)$
WASHEKMHEG*	+16 (13,258 Da)	$Met_{94}(O)$

* denotes non-enzyme specified searches

Patients with asthma have granulocyte accumulation in the airways, and in acute exacerbation, neutrophil become prominent in airway secretions [1019]. An essential component of granulocyte migration from the blood to inflammatory sites is their adhesion to endothelial cells and to extracellular matrix proteins. S100A9 induces neutrophil adhesion to fibronectin through activation of the cell surface adhesion molecule, β2 integrin, which mediates cell-cell interactions [611, 1144]. When S100A9 is S-glutathionylated, adhesion is significantly increased, however, when the same protein is in the presense of S100A8, adhesion is significantly decreased [637]. Conformational changes may account for differences in reactivity of the S100A8/A9-SSG heterocomplex and S100A8 was required for negative regulation. This suggests that post-translational modifications such as S-glutathionylation may limit neutrophil accumulation in the extravascular compartment, another protective process that could limit the extent of inflammatory exudates [637]. Here, we show that HOCl oxidation of both S100 proteins significantly impaired basal adhesion of neutrophils to fibronectin (see Section 4.3.7, Chapter 4) suggesting suppression of upregulation of Mac-1 on neutrophils [316, 1145]. Unexpectedly, rec-oxS100A8/oxS100A9 significantly reduced fMLP-induced neutrophil adhesion. As this experiment was carried out using cells from two healthy donors additional experiments are required to confirm activity and because only the oxS100A8/oxS100A9 treatment was tested, further work is required using the individual proteins (oxidized/native), and oxS100A8/S100A9 and S100A8/oxS100A9 preparations to fully understand the contributions of each oxidized protein in mediating this effect. However, S100A8/S100A9 also dramatically reduced fMLP-induced adhesion, indicating a new anti-inflammatory pathway mediated by the complex.

More generally, it would be interesting to compare effects on adhesion using different cell types. For example, peripheral blood eosinophils from asthmatic patients have a pre-activated phenotype which facilitates recruitment of eosinophils from the blood to the airways, a property not characteristic of eosinophils from healthy individuals [1146-1149]. Behaviour of neutrophils in response to allergen appears to be more subtle, with a similar allergen-primed phenotype observed only after activation with fMLP [1150]. Comparisons between eosinophil and neutrophil migration to appropriate chemoattractants such as IL-5, and adhesion of cells from healthy and asthmatic subjects could further highlight the functional importance of oxidative modifications to S100A8 and S100A9 on other properties of these cells in inflammation.

Some functions are dependent on the S100A8/S100A9 heterocomplex, particularly antimicrobial activity [620]. Cross-linking experiments showed that oxidation of recS100A8 and recS100A9 impaired heterocomplex formation, however, heterocomplexes were still apparent when only one protein in the complex was oxidized (see Section 4.3.8, Chapter 4). Using a Cys_{42}-Ala_{42}S100A8 mutant Sroussi *et al*. showed that Cys_{42} was critical for forming the heterocomplex with S100A9 [655]. However, here we found that oxS100A8 may still complex with native S100A9, and native S100A8 with oxS100A9, although levels were diminished, relative to amounts found in chemically cross-linked samples of native S100A8 and S100A9. Our results suggest that oxS100A8 retained some capacity to form the heterocomplex. We suggest that appropriately-oxidized (e.g. oxidation with hypohalous acid) S100 protein should be used to investigate potential changes in function, rather than to predict these using amino acid substitution mutants [614, 655].

Here, we show that rec-oxS100A8 and rec-oxS100A9 no longer inhibited *E. coli* growth. The antimicrobial activity appeared to depend on Cys_{42} in S100A8, as the Cys_{42}-Ala_{42} mutant significantly reduced the antifungal activity of the heterocomplex against *C. albicans*, possibly because of reduced complex formation [655]. However, Fig. 4.16 (see Chapter 4) shows that when only one component of the complex was oxidized, there was no significant reduction in antimicrobial activity. Although bacterial counts were higher in samples treated with S100A8/oxS100A9, this may not compromise the host significantly. In recS100A9 and in S100A9 isolated from asthmatic sputum, the predominant modification was Met(O), a reversible modification. If Met(O) in S100A9 is regenerate by reductases, such as MSRB2 in lung [1018], antimicrobial activity may be maintained.

Bacterial colonization by *S. pneumoniae* [1003] in asthmatics and *H. influenzae* and *P. aeruginosa* in subjects with bronchiectasis is reported [991-993, 1020]. In Section 4.2.7 a reproducible assay to test antimicrobial activity of the heterocomplex against *S. pneumoniae* could not be produced. Further work is required to develop an assay that effectively measures S100A8/S100A9 antimicrobial activity against a broader range of microbes; calprotectin activity against *H. influenzae* and *P. aeruginosa* is not reported. Investigations that focus on these species, which are common in lung conditions, including CF, could define whether the S100 proteins, either alone or in complex contribute to surveillance.

S100A8 suppresses acute murine asthma. Eosinophil chemoattractants (IL-5,

eotaxin, MCP-1), and eosinophil infiltration is suppressed in lungs of mice treated intranasally with S100A8 just before antigen challenge [644], possibly via ROS-scavenging, which may suppress MC activation. Furthermore, S-nitrosylated S100A8 markedly reduces mast cell activation and leukocyte transmigration in the inflamed mesenteric microcirculation [613]. Results here suggest key modulatory roles for S100A8, and effects of oxS100A8 monomer on expression of inflammatory genes and Th2-modulated responses are currently under investigation in our laboratory.

Interestingly, HOSCN, can inactivate bacteria, with no apparent damage to lung tissue [1151, 1152]. Moreover, SCN^- can scavenge HOCl and/or HOBr and protect human lung epithelial cells from damage induced by HOCl [1153, 1154]. As HOSCN targets Cys residues [1134], it would be worth studying whether oxidation of rec-hS100A8 and rec-hS100A9 by HOSCN could modify heterocomplex formation and its subsequent antimicrobial function or anti-adhesive properties in a manner similar to the HOCl-oxidized proteins.

In chronic asthma an oxidative environment predominates. Non-enzymatic (vitamin E, vitamin C and glutathione) and enzymatic anti-oxidants such as SOD and catalase are important first lines of defense against pathologic oxidizing process. However, the anti-oxidant capacity of the more ubiquitous anti-oxidants (for example SOD) can be lost following oxidative modification and anti-oxidant defense is reduced (reviewed in [977]. Results reported here suggest that S100A8 and S100A9 may contribute to redox homeostasis in this disease. These proteins are not normally present, but induced in epithelial cells lining the airways (see Fig. 4.2, Chapter 4) and in macrophages, and in granulocytes infiltrating the lung. The enhanced local concentrations of the S100s could counter-balance effects of hypohalous acids generated locally. Together with results reported here, and because S100A8 suppresses murine asthma, these studies provide a promising foundation for additional experiments using animal models to unravel mechanisms. For example, inhibition of MPO by a 2-thioxanthine MPO inhibitor, AZ1, in a 6-month cigarette smoke exposure model stopped progression of experimental COPD in guinea pigs [1155]. It would be interesting to examine effects of S100A8 and/or S100A9 in other respiratory disease models, to better understand their functions.

6.3 S100A8 IN ATHEROSCLEROSIS

Inflammation is associated with risk of CVD and with chronic autoimmune diseases such as RA and SLE [1156, 1157]. Interestingly, coronary artery disease is the major cardiovascular condition associated with asthma [1158], and ApoAI mimetics attenuate airway inflammation and may represent a novel treatment in asthma [1159].

HDL has anti-inflammatory and atheroprotective functions but in chronic inflammatory diseases, increased oxidative stress can oxidize ApoAI, a key protein in HDL, producing a pro-inflammatory particle [698, 1160]. Oxidation of HDL is increased in patients with SLE, with oxidized HDL characterized by lower content of the cholesterol transport lipoprotein ApoAI [1026], which can accelerate atherosclerosis and promote increased cardiovascular events in SLE patients [1157]. Moreover, hydroxyl radicals form neoantigens such as hydroxyl radical-damaged HSA, which may initiate autoimmunity in SLE [1027]. Increased serum concentrations of the S100A8/A9 heterocomplex are associated with increased severity of coronary artery disease and increases in carotid intima media thickness in subjects with type II diabetes [1080]. S100A8/A9 is also eluted in serum from patients with acute myocardial infarction [1063]. S100A8 may bind proteins associated with HDL (Section 5.3, Chapter 5), and S100A8 and S100A9 form oxidant-induced cross-linked complexes in atherosclerotic plaque, suggesting oxidant-scavenging *in vivo* [410]. Given these properties, and its association with ApoAI, we proposed a protective role for S100A8 in vascular disease.

Patients with SLE are also predisposed to CVD [1157], but in Section 5.3 (see Chapter 5) we show that S100A8, S100A9 and S100A8/A9 serum concentrations in patients with SLE were no different to healthy serum, contrasting with previous studies [468, 472]; antibody specificities and/or serum preparation may contribute to the variations seen between investigators. With our antibodies, S100A8, oxS100A8 and S100A9 in SLE serum could not be detected by Western blotting. Heo *et al*. also found that S100A8 could not be identified by Western blotting, despite using a 100-fold higher amount of serum protein relative to our own experiments [1094]. Reactivity with anti-S100A8, anti-oxS100A8 and anti-S100A9 antibodies was only apparent after separation of serum by FPLC into HDL and LDL fractions and slot blotting of the lipoproteins. S100A8 and oxS100A8 were predominant in HDL, with lower levels in LDL, possibly due to HDL contamination (Figs. 5.5A, B, Chapter 5). There was little S100A9 in either fraction.

Serum from control and SLE subjects was separated by FPLC to isolate HDL and LDL lipoproteins. A disadvantage of this method is that LDL and HDL elute in consecutive peaks, increasing the likelihood of contamination of each. Moreover, albumin partially co-elutes with HDL fractions [1161]. Using the same S100A8 affinity support column, our laboratory found that albumin may also bind S100A8 (see Section 5.3, Chapter 5). Separation of HDL and LDL by sequential gradient density ultracentrifugation may be a better method of purification. Although this is time-consuming [1071], contamination by albumin and cross-contamination of LDL with ApoAI from HDL is less [1070]. Consequently, reduction of albumin in samples, and more efficient separation of lipoproteins could provide a more accurate assessment of S100A8 in HDL or LDL. Statistical analysis could not be performed on semi-quantified slot blots due to insufficient sample numbers. Analysis of serum from a larger number of patients and controls, and from patients with active SLE and CVD, would clarify associations.

ApoAI bound an S100A8 affinity column and SDS-PAGE separated a 38 kDa component containing ApoAI/S100A8 (see Figs. 5.6 and 5.7, Chapter 5). S100A8 Cross-linking experiments with recS100A8 or recCys$_{42}$-Ala$_{42}$S100A8 strongly support the proposal that these bound ApoAI and ApoAI(HDL). Additional experiments are required to analyze precise mechanisms of complex formation. Because binding of Cys$_{42}$-Ala$_{42}$S100A8 to ApoAI and ApoAI(HDL) was similar to that of S100A8, and as ApoAI contains no Cys residues, non-covalent interactions may be involved. When S100 proteins bind Ca^{2+} conformational changes occur, exposing hydrophobic residues, enabling the protein to interact with its target [159]. Our experiments were performed in the presence of Ca^{2+}, making non-covalent binding a possibility. However, S100 proteins also bind some target proteins in the absence of Ca^{2+} (reviewed in [159]). S100A8/A9 binds CD36 and *phox* proteins, facilitating inflammatory responses, fatty acid uptake and providing a scaffold for *phox* and NADPH oxidase activation [179, 182, 619, 1162]. Comparisons with and without calcium would provide more insights into binding mechanics and surface plasmon resonance studies would validate affinities.

Despite strong evidence indicating an association between S100A8 and HDL, further work is required to accurately characterize interactions. HDL and LDL are large complexes with several structural forms (discoidal, spherical) which do not separate well on SDS-PAGE [1095]. 2D-electrophoresis in non-denaturing gels would resolve the large protein and macro-aggregates [1095] that may interfere with antibody reactivity in

Western blots and would enable observation of co-migration of ApoAI and S100A8 in serum. S100A8 has subsequently been validated in HDL by 2D-PAGE and Western blotting (Prof. Kerry-Anne Rye, Lincoln Gomes *et al*. unpublished) and this is currently being analyzed.

The S100A8/A9 complex is expressed in macrophages and foam cells in atherosclerotic plaques in coronary and carotid arteries [410, 483, 524]. High levels of S100A9 are associated with rupture-prone lesions [1064] and are associated with calcification [410]. Enrichment of carotid artery samples revealed multimeric covalent complexes of S100A8. Despite the strong reactivity with anti-oxS100A8 and anti-S100A8 IgG in C8- and C4-RP-HPLC purified samples, MS analysis indicated that S100A8 was less abundant relative to albumin, making characterization of oxidative modifications difficult. Detection of protein in ng/ml amounts is difficult, particularly in the presence of highly abundant proteins such as albumin (reviewed in [1097]). Future studies require more purification to enable more accurate analysis of the post-translational modifications in these low abundance proteins.

recS100A8 was oxidized with equimolar ratios of HOCl whereas significantly more was required to readily detect oxidation of ApoAI (see Fig. 5.10A, Chapter 5) or to oxidize LDL [1079], suggesting that S100A8 may be preferentially oxidized. Binding of MPO to ApoAI in HDL renders the particle pro-inflammatory [698], but ApoAI may also bind S100A8. We propose that S100A8 within the particle may protect ApoAI from oxidation by HOCl, thereby reducing oxidation-induced loss of function of HDL. In Section 5.3 (see Chapter 5) we demonstrated that S100A8 protected ApoAI from oxidation by HOCl but effects were less when ApoAI was added to HDL. The anti-oxidant potential of S100A8 appeared to be mediated largely by the single Cys_{42} residue. However, the 1:5 M ratio of S100A8/HOCl that had to be used to allow detection of oxidized ApoAI, promoted S100A8 aggregation, so its efficiency cannot be compared with HSA. A limitation of this study is that only S100A8 was used for analysis of effects on ApoAI protection. Although we found little evidence of S100A9 in HDL (see Fig. 5.5A, Chapter 5), experiments using recS100A9 and the recombinant heterocomplex may provide a better understanding of how these S100s regulate oxidative damage to ApoAI.

In situations where S100A8 is secreted by activated macrophages in lesions, it is unlikely to encounter such high local concentrations of HOCl and so may be highly protective locally, if in sufficient quantities in HDL. Indeed, we found oxS100A8 in HDL (see Fig. 5.5A, Chapter 5), and its characterization in HDL from patients, compared to

controls, would validate its capacity to scavenge HOCl generated by elevated MPO levels in the circulation (reviewed in [1163]). In addition, effects on HDL function particularly relating to endothelial cells [1164], could be assessed following oxidation with MPO/H_2O_2 rather than reagent HOCl.

MPO binds heparin sulfate GAGs on the surface of endothelial cells, particularly targeting fibronectin [1087]. In Section 5.3 (Chapter 5), we showed that recS100A8, recS100A9 or the recombinant heterocomplex inhibited generation of HOP in endothelial cells treated with MPO and H_2O_2. Again, Cys_{42}-Ala_{42}S100A8 was inactive, confirming the importance of Cys_{42}. S100A8/A9 also binds endothelial cells by a similar GAG-binding mechanism [431]. We propose that these S100 proteins protect against HOP formation in the vessel wall, by binding in close proximity to MPO on endothelial cells, or in HDL, thereby affording localized protection.

Fibronectin is important in vascular integrity and is a substrate for leukocyte adhesion (see Section 4.4.5, Chapter 4 and reviewed in [1073]). S100A8/S100A9 or the oxidized form, reduced leukocyte adhesion to fibronectin, particularly after treatment with a chemoattractant (see Fig. 4.15, Chapter 4). These results strongly indicate an anti-inflammatory role for these proteins in and complement earlier work on atherosclerosis by our group [410]. Studies could be expanded by testing the individual S100 proteins and the complex, oxidized or not, in other functional assays, such as endothelial cell transmigration of monocytes with or without activation by the relevant chemokine, MCP-1 using trans-well chambers. Other aspects of endothelial cell activation, such as the ability of the S100s/adducts to influence expression of adhesion molecules, NO generation and production of selected growth factors would be informative.

We next investigated whether the S100s protected fibronectin from oxidative cleavage by MPO/H_2O_2 [949]. However, results were unclear because our MPO preparation promoted fibronectin loss. Loss of fibronectin can reduce leukocyte attachment and subsequent transmigration and sequestration, and can promote vascular leakage and initiate local thrombosis (reviewed in [1165]), and effects of S100A8 and/or S100A9 should be tested, and may indicate new mechanisms that contribute to blood vessel homeostasis.

There is evidence that the complex has anti-inflammatory properties in cardiac disease. In an experimental rat model of autoimmune myocarditis, addition of recS100A8/A9 bound IL-1β, IL-6 and TNF-α in the myocardium, suggesting that these

cytokines are immobilized by the heterocomplex, thereby reduced the severity of myocarditis [1166]. On the other hand, calprotectin is proposed to promote vascular inflammation and propagate vascular injury by promoting leukocyte recruitment [528]. However, our laboratory finds no activation of endothelial cells by these proteins (personal communication, Prof. Carolyn Geczy), and S100A8 is not a monocyte chemoattractant [317]. Moreover high amounts of oxS100A8 are seen in macrophages and foam cells in human atheroma and in microvessels [410]. More functional studies are required to clarify the roles of S100A8 and S100A9, and their oxidized forms, in CVD.

6.4 S100A8 AND S100A9 IN REDOX BALANCE

S100A8 and S100A9 were recently described as DAMPs, suggested to exert extracellular, pro-inflammatory effects via interactions with TLRs and RAGE [393]. This thesis provides strong evidence that these proteins also exert anti-inflammatory effects, principally through oxidant scavenging. Several functions of S100A8 and S100A9 were proposed to be regulated by oxidation [605, 606, 612, 614, 957], but this is the first in-depth characterization of oxidized S100 adducts derived from inflammatory sources. S100A8 and S100A9 are readily secreted by neutrophils, eosinophils and macrophages following cellular activation or necrosis [144, 230, 407, 633]. ROS-induced post-translational modifications to recS100A8 and/or recS100A9 (by HOCl) impaired heterocomplex formation and negatively regulated leukocyte transmigration and antimicrobial activity. We show novel interactions of recS100A8 with ApoAI and localized the protein to the HDL particle in serum. recS100A8 reduced oxidation of ApoAI alone and, and to some extent, in HDL. The findings reported in this thesis, in the context of the known functions of these proteins are illustrated in Figs. 6.3A and B.

A

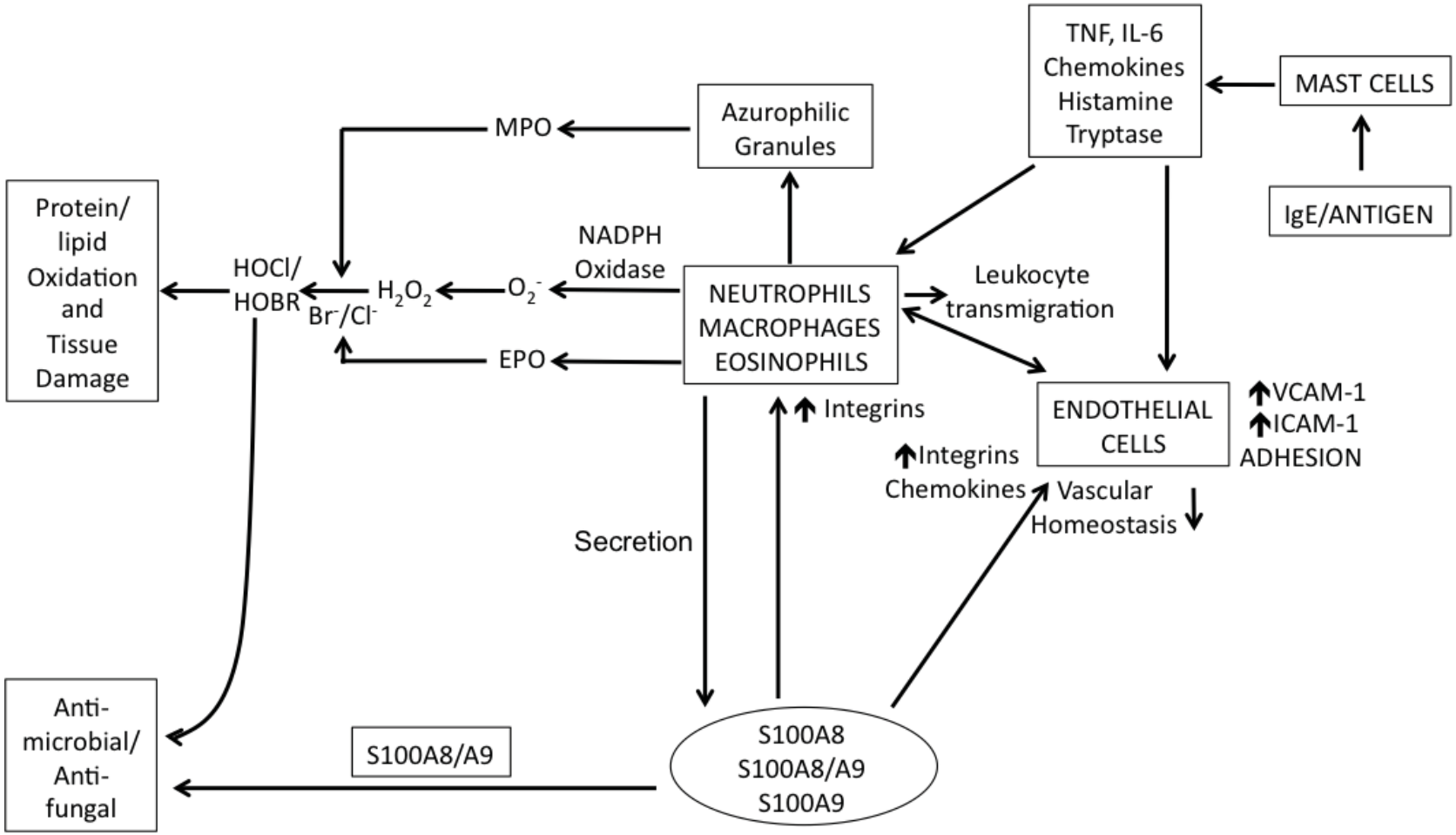
TNF, IL-6
Chemokines
Histamine
Tryptase
MAST CELLS
IgE/ANTIGEN
Azurophilic
Granules
MPO
Protein/
lipid
Oxidation
and
Tissue
Damage
HOCl/
HOBR
H_2O_2
O_2^-
NADPH
Oxidase
Br^-/Cl^-
NEUTROPHILS
MACROPHAGES
EOSINOPHILS
Leukocyte
transmigration
EPO
Integrins
ENDOTHELIAL
CELLS
VCAM-1
ICAM-1
ADHESION
Integrins
Chemokines
Vascular
Homeostasis
Secretion
Anti-
microbial/
Anti-
fungal
S100A8/A9
S100A8
S100A8/A9
S100A9

B

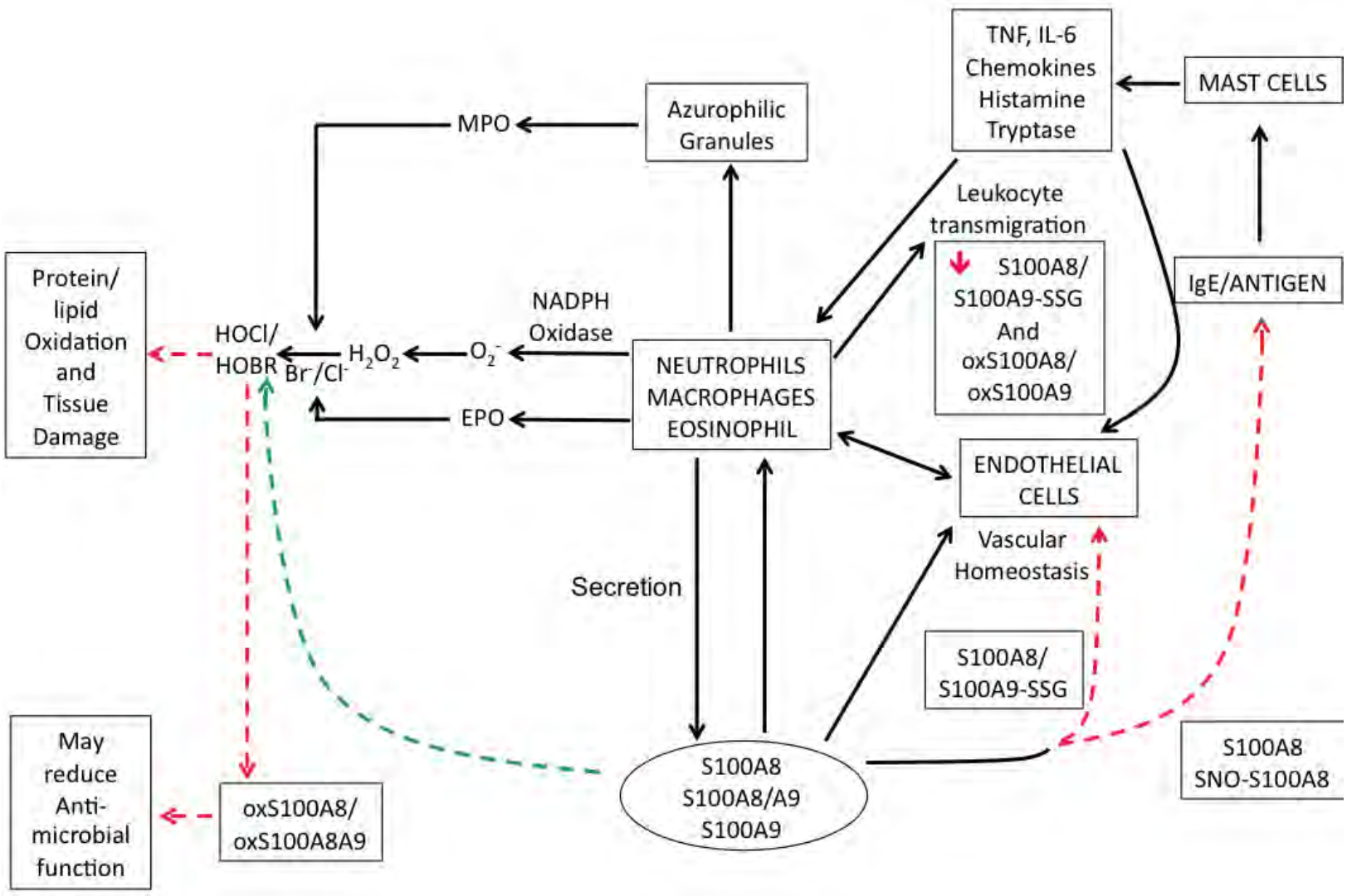
TNF, IL-6
Chemokines
Histamine
Tryptase
MAST CELLS
Azurophilic
Granules
MPO
Leukocyte
transmigration
S100A8/
S100A9-SSG
And
oxS100A8/
oxS100A9
IgE/ANTIGEN
Protein/
lipid
Oxidation
and
Tissue
Damage
HOCl/
HOBR
Br⁻/Cl⁻
H2O2
O2⁻
NADPH
Oxidase
EPO
NEUTROPHILS
MACROPHAGES
EOSINOPHIL
ENDOTHELIAL
CELLS
Vascular
Homeostasis
Secretion
S100A8/
S100A9-SSG
May
reduce
Anti-
microbial
function
oxS100A8/
oxS100A8A9
S100A8
S100A8/A9
S100A9
S100A8
SNO-S100A8

Figure 6.3: Potential extracellular roles of S100A8 and S100A9 in promoting and regulating inflammation. (**A**) Neutrophils, eosinophils and macrophages are a primary source of S100A8 and S100A9, which are secreted following cellular activation or necrosis. S100A8 and S100A9 may participate in positive feedback loops by upregulating integrin expression and/or mediating chemotaxis of neutrophils, respectively. S100A8, S100A9 and the heterocomplex may act on endothelial cells to also facilitate leukocyte recruitment. The heterocomplex also has functions in antimicrobial defense. Phagocytes, particularly neutrophils mediate tissue damage and lipid/protein oxidation via the NADPH oxidase system, converting H_2O_2 to HOCl in an MPO-dependent manner or HOBr in an EPO-dependent manner. (**B**) However, ROS-induced structural changes to S100A8 and/or S100A9 (either by H_2O_2, HOCl, NO, or glutathione) may also negatively regulate inflammation (red broken arrows). S100A8 and S100A8-SNO inhibit mast cell activation and regulate vascular homoeostasis. S100A9 can be glutathionylated by the physiological donor S-nitrosoglutathione to S100A9-SSG, and this downregulates neutrophil adhesion to the ECM complex with S100A8. S100A8, and to a lesser extent S100A9, are potent anti-oxidants and limit tissue damage by actively scavenging HOBr/HOCl (green broken arrow). Oxidation of the heterocomplex can also inhibit neutrophil adhesion to the ECM possibly limiting leukocyte sequestration in the extravasculature. However, under conditions of excessive oxidation, HOCl also oxidizes the heterocomplex, and may reduce its antimicrobial function (red broken arrow).

Although this thesis describes new and novel functions and modifications of hypohalous acid-oxidized S100A8 and S100A9, the heavy reliance on MS must be acknowledged. The majority of the work presented in this thesis relied on what Yates *et al*. define as a "Bottom-up Approach" (reviewed in [1167]), whereby proteins are digested into peptides prior to analysis, with resultant peptide masses and sequences used to identify corresponding proteins. This approach relies on tandem data acquisition, whereby peptides are subjected to collision-activated dissociation, and database searches are the main tool for identifying tandem MS data [1074]. This approach is data-dependent, that is, the user is responsible for defining which post-translational modifications are to be analyzed; potential disadvantages include limited protein sequence coverage by identified peptides and failure to identify stable or labile post-translational modifications (reviewed in [1167]). In the studies reported here, efforts were made to be as inclusive as possible in data-acquisition. However a more multi-disciplinary approach may have identified additional components. For example, gas chromatography coupled with MS, combined with immunological methods (for example Western blotting or ELISA) (reviewed in [983]) may identify chlorotyrosine derivatives, although these approaches rely on the specificities of the antibodies used. Moreover, some antibodies to oxidized proteins prepared by others (e.g. anti-2D10G9) did not react with HOCl-oxidized S100A8 [410].

Despite these limitations, we were able to confirm the HOCl and HOBr-scavenging capacity of recS100A8 and recS100A9 *in vitro* in Chapter 3, and Chapters 4 and 5 confirmed that these proteins likely scavenged hypohalous acids generated in lung or arteries from patients with asthma and atherosclerosis respectively. A new paradigm is indicated by the potential protective effects of S100A8 in HDL and more detailed studies of its role in the protective function of the HDL particle in the context of atherosclerosis may indicate new ways to protect vessels from oxidative damage.

In the past decade, the protective effects of the calgranulins has gained more attention. In asthma, S100A8 reduced MC activation and eosinophil recruitment by oxidant scavenging [644]. The heterocomplex is implicated in intra- and extracellular defense against fungi [655], and in regulating keratinocyte and oral epithelial cell resistance to *L. monocytogenes* [593] and *P. gingivalis* [590] respectively. In RA, calprotectin injected into joints of rats before onset of avridine-induced arthritis, had lower scores for cellular infiltration, though not significant, suggesting that the complex regulates joint inflammation [648]. More recently, transgenic mice expressing hS100A12

showed reduced peribronchial and perivascular inflammation, mucus production and reduced airway hyperresponsiveness [669]. S100A12 binds Zn^{2+}, forming a hexamer, which co-localized with MMP-2 and MMP-9 and may protect plaque from rupture by inhibiting MMP activity [529]. Thus, the calgranulins may have pleiotropic roles, and this may depend on their local concentration and environmental factors.

Data presented in this thesis extend the anti-inflammatory functions of S100A8 and S100A9, and confirm that they are oxidatively sensitive targets. Post-translational modifications generated may abrogate pro-inflammatory activities, such as chemotaxis and consequently induce anti-inflammatory activities (for example, suppression of leukocyte transmigration and accumulation), thereby preventing excessive tissue damage and restoring homeostasis, particularly during acute inflammatory responses. However, excessive accumulation of cross-linked S100A8 and/or S100A9 complexes, for example in human atheroma [410] may contribute to amyloid formation [1127] and propagate chronic inflammatory conditions.

These studies possibly have far-reaching consequences in conditions where levels of these proteins are elevated in the circulation or in tissues. They may reduce the amount of ROS and could modulate intracellular functions as well (reviewed in [695]) by impacting on ROS-sensitive transcriptional events, particularly under conditions of oxidative stress. In this context, effects on energy metabolism, cell survival and activation, such as S100A8's ability to reduce mast cell activation by suppressing ROS-mediated LAT phosphorylation [644] are worthy of investigation. S100A8 and S100A9 are inflammation-specific proteins that may contribute to the fine-tuning of redox in leukocytes and modulate the host response in acute and chronic conditions.

REFERENCES

1. Moore, B.W., *A soluble protein characteristic of the nervous system.* Biochem Biophys Res Commun, 1965. **19**(6): p. 739-44.
2. Schafer, B.W., et al., *Isolation of a YAC clone covering a cluster of nine S100 genes on human chromosome 1q21: rationale for a new nomenclature of the S100 calcium-binding protein family.* Genomics, 1995. **25**(3): p. 638-43.
3. Marenholz, I., R.C. Lovering, and C.W. Heizmann, *An update of the S100 nomenclature.* Biochim Biophys Acta, 2006. **1763**(11): p. 1282-3.
4. Kratz, C.P., et al., *Candidate gene isolation and comparative analysis of a commonly deleted segment of 7q22 implicated in myeloid malignancies.* Genomics, 2001. **77**(3): p. 171-80.
5. Marenholz, I., C.W. Heizmann, and G. Fritz, *S100 proteins in mouse and man: from evolution to function and pathology (including an update of the nomenclature).* Biochem Biophys Res Commun, 2004. **322**(4): p. 1111-22.
6. Kulski, J.K., et al., *Genomic and phylogenetic analysis of the S100A7 (Psoriasin) gene duplications within the region of the S100 gene cluster on human chromosome 1q21.* J Mol Evol, 2003. **56**(4): p. 397-406.
7. Ravasi, T., et al., *Probing the S100 protein family through genomic and functional analysis.* Genomics, 2004. **84**(1): p. 10-22.
8. Burmeister, G., L. Tarcsay, and C. Sorg, *Generation and characterization of a monoclonal antibody (1C5) to human migration inhibitory factor (MIF).* Immunobiology, 1986. **171**(4-5): p. 461-74.
9. Steinbakk, M., et al., *Antimicrobial actions of calcium binding leucocyte L1 protein, calprotectin.* Lancet, 1990. **336**(8718): p. 763-5.
10. Ridinger, K., et al., *Clustered organization of S100 genes in human and mouse.* Biochim Biophys Acta, 1998. **1448**(2): p. 254-63.
11. Glenney, J.R., Jr., M.S. Kindy, and L. Zokas, *Isolation of a new member of the S100 protein family: amino acid sequence, tissue, and subcellular distribution.* J Cell Biol, 1989. **108**(2): p. 569-78.
12. Engelkamp, D., et al., *Six S100 genes are clustered on human chromosome 1q21: identification of two genes coding for the two previously unreported calcium-binding proteins S100D and S100E.* Proc Natl Acad Sci U S A, 1993. **90**(14): p. 6547-51.
13. Jackson-Grusby, L.L., J. Swiergiel, and D.I. Linzer, *A growth-related mRNA in cultured mouse cells encodes a placental calcium binding protein.* Nucleic Acids Res, 1987. **15**(16): p. 6677-90.
14. Calabretta, B., et al., *Molecular cloning of the cDNA for a growth factor-inducible gene with strong homology to S-100, a calcium-binding protein.* J Biol Chem, 1986. **261**(27): p. 12628-32.
15. Madsen, P., et al., *Molecular cloning, occurrence, and expression of a novel partially secreted protein "psoriasin" that is highly up-regulated in psoriatic skin.* J Invest Dermatol, 1991. **97**(4): p. 701-12.
16. Odink, K., et al., *Two calcium-binding proteins in infiltrate macrophages of rheumatoid arthritis.* Nature, 1987. **330**(6143): p. 80-2.
17. Yonekawa, K., et al., *Myeloid related proteins activate Toll-like receptor 4 in human acute coronary syndromes.* Atherosclerosis, 2011. **218**(2): p. 486-92.
18. Hsu, K., et al., *Anti-Infective Protective Properties of S100 Calgranulins.* Antiinflamm Antiallergy Agents Med Chem, 2009. **8**(4): p. 290-305.

19. Kocher, M., et al., *Functional chemotactic factor CP-10 and MRP-14 are abundant in murine abscesses.* Infect Immun, 1996. **64**(4): p. 1342-50.
20. Glenney, J.R., Jr. and B.F. Tack, *Amino-terminal sequence of p36 and associated p10: identification of the site of tyrosine phosphorylation and homology with S-100.* Proc Natl Acad Sci U S A, 1985. **82**(23): p. 7884-8.
21. Todoroki, H., et al., *Purification, characterization, and partial sequence analysis of a newly identified EF-hand type 13-kDa Ca(2+)-binding protein from smooth muscle and non-muscle tissues.* J Biol Chem, 1991. **266**(28): p. 18668-73.
22. Dell'Angelica, E.C., C.H. Schleicher, and J.A. Santome, *Primary structure and binding properties of calgranulin C, a novel S100-like calcium-binding protein from pig granulocytes.* J Biol Chem, 1994. **269**(46): p. 28929-36.
23. Wicki, R., et al., *Characterization of the human S100A12 (calgranulin C, p6, CAAF1, CGRP) gene, a new member of the S100 gene cluster on chromosome 1q21.* Cell Calcium, 1996. **20**(6): p. 459-64.
24. Pietas, A., et al., *Molecular cloning and characterization of the human S100A14 gene encoding a novel member of the S100 family.* Genomics, 2002. **79**(4): p. 513-22.
25. Emoto, Y., et al., *Purification and characterization of a new member of the S-100 protein family from human placenta.* Biochem Biophys Res Commun, 1992. **182**(3): p. 1246-53.
26. Gribenko, A.V., J.E. Hopper, and G.I. Makhatadze, *Molecular characterization and tissue distribution of a novel member of the S100 family of EF-hand proteins.* Biochemistry, 2001. **40**(51): p. 15538-48.
27. Kallfelz, F.A., A.N. Taylor, and R.H. Wasserman, *Vitamin D-induced calcium binding factor in rat intestinal mucosa.* Proc Soc Exp Biol Med, 1967. **125**(1): p. 54-8.
28. Moncrief, N.D., R.H. Kretsinger, and M. Goodman, *Evolution of EF-hand calcium-modulated proteins. I. Relationships based on amino acid sequences.* J Mol Evol, 1990. **30**(6): p. 522-62.
29. Donato, R., *S100: a multigenic family of calcium-modulated proteins of the EF-hand type with intracellular and extracellular functional roles.* Int J Biochem Cell Biol, 2001. **33**(7): p. 637-68.
30. Kawasaki, H., S. Nakayama, and R.H. Kretsinger, *Classification and evolution of EF-hand proteins.* Biometals, 1998. **11**(4): p. 277-95.
31. Mischke, D., et al., *Genes encoding structural proteins of epidermal cornification and S100 calcium-binding proteins form a gene complex ("epidermal differentiation complex") on human chromosome 1q21.* J Invest Dermatol, 1996. **106**(5): p. 989-92.
32. Heizmann, C.W., G. Fritz, and B.W. Schafer, *S100 proteins: structure, functions and pathology.* Front Biosci, 2002. **7**: p. d1356-68.
33. Heizmann, C.W., *The multifunctional S100 protein family.* Methods Mol Biol, 2002. **172**: p. 69-80.
34. Fano, G., et al., *The S-100: a protein family in search of a function.* Prog Neurobiol, 1995. **46**(1): p. 71-82.
35. Wicki, R., et al., *Characterization of the human and mouse cDNAs coding for S100A13, a new member of the S100 protein family.* Biochem Biophys Res Commun, 1996. **227**(2): p. 594-9.
36. South, A.P., et al., *Human epidermal differentiation complex in a single 2.5 Mbp long continuum of overlapping DNA cloned in bacteria integrating physical and transcript maps.* J Invest Dermatol, 1999. **112**(6): p. 910-8.

37. Zimmer, D.B., et al., *The S100 protein family: history, function, and expression.* Brain Res Bull, 1995. **37**(4): p. 417-29.
38. Albertazzi, E., F. Cajone, and G.V. Sherbet, *Characterization of a splice variant of metastasis-associated h-mts1 (S100A4) gene expressed in human infiltrating carcinomas of the breast.* DNA Cell Biol, 1998. **17**(12): p. 1003-8.
39. Schafer, B.W., et al., *Brain S100A5 is a novel calcium-, zinc-, and copper ion-binding protein of the EF-hand superfamily.* J Biol Chem, 2000. **275**(39): p. 30623-30.
40. Nakamura, T., et al., *A unique exon-intron organization of a porcine S100C gene: close evolutionary relationship to calmodulin genes.* Biochem Biophys Res Commun, 1998. **243**(3): p. 647-52.
41. Kerkhoff, C., M. Klempt, and C. Sorg, *Novel insights into structure and function of MRP8 (S100A8) and MRP14 (S100A9).* Biochim Biophys Acta, 1998. **1448**(2): p. 200-11.
42. Ambartsumian, N., et al., *Characterization of two splice variants of metastasis-associated human mts1 gene.* Gene, 1995. **159**(1): p. 125-30.
43. Wolf, R., et al., *Molecular cloning and characterization of alternatively spliced mRNA isoforms from psoriatic skin encoding a novel member of the S100 family.* FASEB J, 2003. **17**(13): p. 1969-71.
44. Wolf, R., et al., *Human S100A15 splice variants are differentially expressed in inflammatory skin diseases and regulated through Th1 cytokines and calcium.* Exp Dermatol, 2007. **16**(8): p. 685-91.
45. Edgeworth, J., et al., *Identification of p8,14 as a highly abundant heterodimeric calcium binding protein complex of myeloid cells.* J Biol Chem, 1991. **266**(12): p. 7706-13.
46. Raftery, M.J., et al., *Isolation of the murine S100 protein MRP14 (14 kDa migration-inhibitory-factor-related protein) from activated spleen cells: characterization of post-translational modifications and zinc binding.* Biochem J, 1996. **316 (Pt 1)**: p. 285-93.
47. Vogl, T., et al., *Calcium-induced noncovalently linked tetramers of MRP8 and MRP14 detected by ultraviolet matrix-assisted laser desorption/ionization mass spectrometry.* J Am Soc Mass Spectrom, 1999. **10**(11): p. 1124-30.
48. Hakansson, M. and S. Linse, *Protein reconstitution and 3D domain swapping.* Curr Protein Pept Sci, 2002. **3**(6): p. 629-42.
49. Ostermeier, M. and S.J. Benkovic, *Evolution of protein function by domain swapping.* Adv Protein Chem, 2000. **55**: p. 29-77.
50. Kraemer, A.M., L.R. Saraiva, and S.I. Korsching, *Structural and functional diversification in the teleost S100 family of calcium-binding proteins.* BMC Evol Biol, 2008. **8**: p. 48.
51. Fuellen, G., et al., *Computational searches for missing orthologs: the case of S100A12 in mice.* OMICS, 2004. **8**(4): p. 334-40.
52. Murphy, P.M., *Molecular mimicry and the generation of host defense protein diversity.* Cell, 1993. **72**(6): p. 823-6.
53. Morgenstern, B. and W.R. Atchley, *Evolution of bHLH transcription factors: modular evolution by domain shuffling?* Mol Biol Evol, 1999. **16**(12): p. 1654-63.
54. Ravasi, T., et al., *Systematic characterization of the zinc-finger-containing proteins in the mouse transcriptome.* Genome Res, 2003. **13**(6B): p. 1430-42.
55. Oram, S., et al., *Regulation of calcium homeostasis by S100RVP, an androgen-regulated S100 protein in the rat ventral prostate.* Prostate, 2006. **66**(7): p. 768-78.

56. Wang, Z., et al., *Genes regulated by androgen in the rat ventral prostate.* Proc Natl Acad Sci U S A, 1997. **94**(24): p. 12999-3004.
57. Gifford, J.L., M.P. Walsh, and H.J. Vogel, *Structures and metal-ion-binding properties of the Ca2+-binding helix-loop-helix EF-hand motifs.* Biochem J, 2007. **405**(2): p. 199-221.
58. Schaffer, C.J. and L.B. Nanney, *Cell biology of wound healing.* Int Rev Cytol, 1996. **169**: p. 151-81.
59. Heizmann, C.W. and J.A. Cox, *New perspectives on S100 proteins: a multi-functional Ca(2+)-, Zn(2+)- and Cu(2+)-binding protein family.* Biometals, 1998. **11**(4): p. 383-97.
60. Hilt, D.C., and D. Kligman, *The S100 protein family: a biochemical and functional overview*, 1991, Springer-Velrag, Berlin.
61. Krebs, J., M. Quadroni, and L.J. Van Eldik, *Dance of the dimers.* Nat Struct Biol, 1995. **2**(9): p. 711-4.
62. Donato, R., *S-100 proteins.* Cell Calcium, 1986. **7**(3): p. 123-45.
63. Kligman, D. and D.C. Hilt, *The S100 protein family.* Trends Biochem Sci, 1988. **13**(11): p. 437-43.
64. Smith, S.P. and G.S. Shaw, *A change-in-hand mechanism for S100 signalling.* Biochem Cell Biol, 1998. **76**(2-3): p. 324-33.
65. Szebenyi, D.M. and K. Moffat, *The refined structure of vitamin D-dependent calcium-binding protein from bovine intestine. Molecular details, ion binding, and implications for the structure of other calcium-binding proteins.* J Biol Chem, 1986. **261**(19): p. 8761-77.
66. Zimmer, D.B., P. Wright Sadosky, and D.J. Weber, *Molecular mechanisms of S100-target protein interactions.* Microsc Res Tech, 2003. **60**(6): p. 552-9.
67. Maler, L., M. Sastry, and W.J. Chazin, *A structural basis for S100 protein specificity derived from comparative analysis of apo and Ca(2+)-calcyclin.* J Mol Biol, 2002. **317**(2): p. 279-90.
68. Brodersen, D.E., et al., *EF-hands at atomic resolution: the structure of human psoriasin (S100A7) solved by MAD phasing.* Structure, 1998. **6**(4): p. 477-89.
69. Itou, H., et al., *The crystal structure of human MRP14 (S100A9), a Ca(2+)-dependent regulator protein in inflammatory process.* J Mol Biol, 2002. **316**(2): p. 265-76.
70. McClintock, K.A. and G.S. Shaw, *A novel S100 target conformation is revealed by the solution structure of the Ca2+-S100B-TRTK-12 complex.* J Biol Chem, 2003. **278**(8): p. 6251-7.
71. Rety, S., et al., *The crystal structure of a complex of p11 with the annexin II N-terminal peptide.* Nat Struct Biol, 1999. **6**(1): p. 89-95.
72. Fohr, U.G., et al., *Purification and cation binding properties of the recombinant human S100 calcium-binding protein A3, an EF-hand motif protein with high affinity for zinc.* J Biol Chem, 1995. **270**(36): p. 21056-61.
73. Fritz, G., C.W. Heizmann, and P.M. Kroneck, *Probing the structure of the human Ca2+- and Zn2+-binding protein S100A3: spectroscopic investigations of its transition metal ion complexes, and three-dimensional structural model.* Biochim Biophys Acta, 1998. **1448**(2): p. 264-76.
74. Baudier, J., et al., *Zinc ion binding to human brain calcium binding proteins, calmodulin and S100b protein.* Biochem Biophys Res Commun, 1983. **114**(3): p. 1138-46.
75. Brodersen, D.E., J. Nyborg, and M. Kjeldgaard, *Zinc-binding site of an S100 protein revealed. Two crystal structures of Ca2+-bound human psoriasin*

(S100A7) in the Zn2+-loaded and Zn2+-free states. Biochemistry, 1999. **38**(6): p. 1695-704.
76. Baudier, J., N. Glasser, and D. Gerard, *Ions binding to S100 proteins. I. Calcium- and zinc-binding properties of bovine brain S100 alpha alpha, S100a (alpha beta), and S100b (beta beta) protein: Zn2+ regulates Ca2+ binding on S100b protein.* J Biol Chem, 1986. **261**(18): p. 8192-203.
77. Kerkhoff, C., et al., *Zinc binding reverses the calcium-induced arachidonic acid-binding capacity of the S100A8/A9 protein complex.* FEBS Lett, 1999. **460**(1): p. 134-8.
78. Moroz, O.V., et al., *Structure of the human S100A12-copper complex: implications for host-parasite defence.* Acta Crystallogr D Biol Crystallogr, 2003. **59**(Pt 5): p. 859-67.
79. Moroz, O.V., et al., *Crystallization and preliminary X-ray diffraction analysis of human calcium-binding protein S100A12.* Acta Crystallogr D Biol Crystallogr, 2000. **56**(Pt 2): p. 189-91.
80. Deloulme, J.C., B.J. Gentil, and J. Baudier, *Monitoring of S100 homodimerization and heterodimeric interactions by the yeast two-hybrid system.* Microsc Res Tech, 2003. **60**(6): p. 560-8.
81. Donato, R., *Intracellular and extracellular roles of S100 proteins.* Microsc Res Tech, 2003. **60**(6): p. 540-51.
82. Kilby, P.M., L.J. Van Eldik, and G.C. Roberts, *Identification of the binding site on S100B protein for the actin capping protein CapZ.* Protein Sci, 1997. **6**(12): p. 2494-503.
83. Rety, S., et al., *Structural basis of the Ca(2+)-dependent association between S100C (S100A11) and its target, the N-terminal part of annexin I.* Structure, 2000. **8**(2): p. 175-84.
84. Garbuglia, M., et al., *S100A1 and S100B interactions with annexins.* Biochim Biophys Acta, 2000. **1498**(2-3): p. 192-206.
85. Sopkova-de Oliveira Santos, J., et al., *S100 protein-annexin interactions: a model of the (Anx2-p11)(2) heterotetramer complex.* Biochim Biophys Acta, 2000. **1498**(2-3): p. 181-91.
86. Berntzen, H.B. and M.K. Fagerhol, *L1, a major granulocyte protein: antigenic properties of its subunits.* Scand J Clin Lab Invest, 1988. **48**(7): p. 647-52.
87. Gribenko, A.V. and G.I. Makhatadze, *Oligomerization and divalent ion binding properties of the S100P protein: a Ca2+/Mg2+-switch model.* J Mol Biol, 1998. **283**(3): p. 679-94.
88. Kizawa, K., et al., *Specific citrullination causes assembly of a globular S100A3 homotetramer: a putative Ca2+ modulator matures human hair cuticle.* J Biol Chem, 2008. **283**(8): p. 5004-13.
89. Ostendorp, T., et al., *Structural and functional insights into RAGE activation by multimeric S100B.* EMBO J, 2007. **26**(16): p. 3868-78.
90. Propper, C., et al., *Analysis of the MRP8-MRP14 protein-protein interaction by the two-hybrid system suggests a prominent role of the C-terminal domain of S100 proteins in dimer formation.* J Biol Chem, 1999. **274**(1): p. 183-8.
91. Strupat, K., et al., *Calcium-induced noncovalently linked tetramers of MRP8 and MRP14 are confirmed by electrospray ionization-mass analysis.* J Am Soc Mass Spectrom, 2000. **11**(9): p. 780-8.
92. Teigelkamp, S., et al., *Calcium-dependent complex assembly of the myeloic differentiation proteins MRP-8 and MRP-14.* J Biol Chem, 1991. **266**(20): p. 13462-7.

93. Moroz, O.V., et al., *The structure of S100A12 in a hexameric form and its proposed role in receptor signalling.* Acta Crystallogr D Biol Crystallogr, 2002. **58**(Pt 3): p. 407-13.
94. Xie, J., et al., *Hexameric calgranulin C (S100A12) binds to the receptor for advanced glycated end products (RAGE) using symmetric hydrophobic target-binding patches.* J Biol Chem, 2007. **282**(6): p. 4218-31.
95. Koch, M., et al., *Implications on zinc binding to S100A2.* Biochim Biophys Acta, 2007. **1773**(3): p. 457-70.
96. Novitskaya, V., et al., *Oligomeric forms of the metastasis-related Mts1 (S100A4) protein stimulate neuronal differentiation in cultures of rat hippocampal neurons.* J Biol Chem, 2000. **275**(52): p. 41278-86.
97. Sturchler, E., et al., *S100A16, a novel calcium-binding protein of the EF-hand superfamily.* J Biol Chem, 2006. **281**(50): p. 38905-17.
98. Moroz, O.V., et al., *The crystal structures of human S100A12 in apo form and in complex with zinc: new insights into S100A12 oligomerisation.* J Mol Biol, 2009. **391**(3): p. 536-51.
99. Hoyaux, D., et al., *S100 proteins in Corpora amylacea from normal human brain.* Brain Res, 2000. **867**(1-2): p. 280-8.
100. McNutt, N.S., *The S100 family of multipurpose calcium-binding proteins.* J Cutan Pathol, 1998. **25**(10): p. 521-9.
101. Gonzalez-Martinez, T., et al., *S-100 proteins in the human peripheral nervous system.* Microsc Res Tech, 2003. **60**(6): p. 633-8.
102. Mandinova, A., et al., *Distinct subcellular localization of calcium binding S100 proteins in human smooth muscle cells and their relocation in response to rises in intracellular calcium.* J Cell Sci, 1998. **111 (Pt 14)**: p. 2043-54.
103. Heizmann, C.W. and W. Hunziker, *Intracellular calcium-binding proteins: more sites than insights.* Trends Biochem Sci, 1991. **16**(3): p. 98-103.
104. Tsoporis, J.N., et al., *The myocardial protein S100A1 plays a role in the maintenance of normal gene expression in the adult heart.* Mol Cell Biochem, 2003. **242**(1-2): p. 27-33.
105. Zimmer, D.B., et al., *S100A1 and S100B expression and target proteins in type I diabetes.* Endocrinology, 1997. **138**(12): p. 5176-83.
106. Ackermann, G.E., et al., *S100A1-deficient male mice exhibit increased exploratory activity and reduced anxiety-related responses.* Biochim Biophys Acta, 2006. **1763**(11): p. 1307-19.
107. Schafer, B.W. and C.W. Heizmann, *The S100 family of EF-hand calcium-binding proteins: functions and pathology.* Trends Biochem Sci, 1996. **21**(4): p. 134-40.
108. Randazzo, A., et al., *Structural insight into human Zn(2+)-bound S100A2 from NMR and homology modeling.* Biochem Biophys Res Commun, 2001. **288**(2): p. 462-7.
109. Sato, N. and J. Hitomi, *S100P expression in human esophageal epithelial cells: Human esophageal epithelial cells sequentially produce different S100 proteins in the process of differentiation.* Anat Rec, 2002. **267**(1): p. 60-9.
110. Santin, A.D., et al., *Gene expression profiles in primary ovarian serous papillary tumors and normal ovarian epithelium: identification of candidate molecular markers for ovarian cancer diagnosis and therapy.* Int J Cancer, 2004. **112**(1): p. 14-25.
111. Kizawa, K., et al., *Gene expression of mouse S100A3, a cysteine-rich calcium-binding protein, in developing hair follicle.* J Invest Dermatol, 1998. **111**(5): p. 879-86.

112. Rogers, G. and K. Koike, *Laser capture microscopy in a study of expression of structural proteins in the cuticle cells of human hair.* Exp Dermatol, 2009. **18**(6): p. 541-7.
113. Barraclough, R., *Calcium-binding protein S100A4 in health and disease.* Biochim Biophys Acta, 1998. **1448**(2): p. 190-9.
114. Mazzucchelli, L., *Protein S100A4: too long overlooked by pathologists?* Am J Pathol, 2002. **160**(1): p. 7-13.
115. Chan, W.Y., et al., *Differential expression of S100 proteins in the developing human hippocampus and temporal cortex.* Microsc Res Tech, 2003. **60**(6): p. 600-13.
116. Teratani, T., et al., *Restricted expression of calcium-binding protein S100A5 in human kidney.* Biochem Biophys Res Commun, 2002. **291**(3): p. 623-7.
117. Stradal, T.B. and M. Gimona, *Ca(2+)-dependent association of S100A6 (Calcyclin) with the plasma membrane and the nuclear envelope.* J Biol Chem, 1999. **274**(44): p. 31593-6.
118. Watson, P.H., E.R. Leygue, and L.C. Murphy, *Psoriasin (S100A7).* Int J Biochem Cell Biol, 1998. **30**(5): p. 567-71.
119. Cross, S.S., et al., *Expression of S100 proteins in normal human tissues and common cancers using tissue microarrays: S100A6, S100A8, S100A9 and S100A11 are all overexpressed in common cancers.* Histopathology, 2005. **46**(3): p. 256-69.
120. Goyette, J. and C.L. Geczy, *Inflammation-associated S100 proteins: new mechanisms that regulate function.* Amino Acids, 2011. **41**(4): p. 821-42.
121. Wilkinson, M.M., et al., *Expression pattern of two related cystic fibrosis-associated calcium-binding proteins in normal and abnormal tissues.* J Cell Sci, 1988. **91 (Pt 2)**: p. 221-30.
122. Zreiqat, H., et al., *S100A8/S100A9 and their association with cartilage and bone.* J Mol Histol, 2007. **38**(5): p. 381-91.
123. Kumar, A., A. Steinkasserer, and S. Berchtold, *Interleukin-10 influences the expression of MRP8 and MRP14 in human dendritic cells.* Int Arch Allergy Immunol, 2003. **132**(1): p. 40-7.
124. Healy, A.M., et al., *Platelet expression profiling and clinical validation of myeloid-related protein-14 as a novel determinant of cardiovascular events.* Circulation, 2006. **113**(19): p. 2278-84.
125. Kaczan-Bourgois, D., et al., *Increased content of annexin II (p36) and p11 in human placenta brush-border membrane vesicles during syncytiotrophoblast maturation and differentiation.* Placenta, 1996. **17**(8): p. 669-76.
126. Munz, B., et al., *Differential expression of the calpactin I subunits annexin II and p11 in cultured keratinocytes and during wound repair.* J Invest Dermatol, 1997. **108**(3): p. 307-12.
127. Wu, T., et al., *P11, a unique member of the S100 family of calcium-binding proteins, interacts with and inhibits the activity of the 85-kDa cytosolic phospholipase A2.* J Biol Chem, 1997. **272**(27): p. 17145-53.
128. Sakaguchi, M., et al., *Up-regulation of S100C in normal human fibroblasts in the process of aging in vitro.* Exp Gerontol, 2001. **36**(8): p. 1317-25.
129. Kondo, A., et al., *Localization of S100C immunoreactivity in various human tissues.* Acta Med Okayama, 2002. **56**(1): p. 31-4.
130. Hitomi, J., et al., *Novel S100 proteins in human esophageal epithelial cells: CAAF1 expression is associated with cell growth arrest.* Arch Histol Cytol, 1998. **61**(2): p. 163-78.

131. Yang, Z., et al., *S100A12 provokes mast cell activation: a potential amplification pathway in asthma and innate immunity.* J Allergy Clin Immunol, 2007. **119**(1): p. 106-14.
132. Ridinger, K., et al., *S100A13. Biochemical characterization and subcellular localization in different cell lines.* J Biol Chem, 2000. **275**(12): p. 8686-94.
133. Wolf, R., et al., *Chemotactic activity of S100A7 (Psoriasin) is mediated by the receptor for advanced glycation end products and potentiates inflammation with highly homologous but functionally distinct S100A15.* J Immunol, 2008. **181**(2): p. 1499-506.
134. Buchau, A.S., et al., *S100A15, an antimicrobial protein of the skin: regulation by E. coli through Toll-like receptor 4.* J Invest Dermatol, 2007. **127**(11): p. 2596-604.
135. Shiras, A., et al., *S100 expression in primary mouse fibroblast cultures.* In Vitro Cell Dev Biol Anim, 2001. **37**(3): p. 172-4.
136. Bobryshev, Y.V. and R.S. Lord, *Mapping of vascular dendritic cells in atherosclerotic arteries suggests their involvement in local immune-inflammatory reactions.* Cardiovasc Res, 1998. **37**(3): p. 799-810.
137. Bobryshev, Y.V. and R.S. Lord, *Detection of vascular dendritic cells accumulating calcified deposits in their cytoplasm.* Tissue Cell, 1998. **30**(3): p. 383-8.
138. Bobryshev, Y.V. and R.S. Lord, *S-100 positive cells in human arterial intima and in atherosclerotic lesions.* Cardiovasc Res, 1995. **29**(5): p. 689-96.
139. Glaser, R., et al., *The antimicrobial protein psoriasin (S100A7) is upregulated in atopic dermatitis and after experimental skin barrier disruption.* J Invest Dermatol, 2009. **129**(3): p. 641-9.
140. Becker, T., et al., *S100P, a novel Ca(2+)-binding protein from human placenta. cDNA cloning, recombinant protein expression and Ca2+ binding properties.* Eur J Biochem, 1992. **207**(2): p. 541-7.
141. Yusenko, M.V., D. Zubakov, and G. Kovacs, *Gene expression profiling of chromophobe renal cell carcinomas and renal oncocytomas by Affymetrix GeneChip using pooled and individual tumours.* Int J Biol Sci, 2009. **5**(6): p. 517-27.
142. Rothermundt, M., et al., *S100B in brain damage and neurodegeneration.* Microsc Res Tech, 2003. **60**(6): p. 614-32.
143. Hu, S.P., et al., *Induction of the chemotactic S100 protein, CP-10, in monocyte/macrophages by lipopolysaccharide.* Blood, 1996. **87**(9): p. 3919-28.
144. Xu, K., T. Yen, and C.L. Geczy, *Il-10 up-regulates macrophage expression of the S100 protein S100A8.* J Immunol, 2001. **166**(10): p. 6358-66.
145. Gladwin, M.T., et al., *Retinoic acid reduces p11 protein levels in bronchial epithelial cells by a posttranslational mechanism.* Am J Physiol Lung Cell Mol Physiol, 2000. **279**(6): p. L1103-9.
146. He, K.L., et al., *Endothelial cell annexin A2 regulates polyubiquitination and degradation of its binding partner S100A10/p11.* J Biol Chem, 2008. **283**(28): p. 19192-200.
147. Donato, R., *Functional roles of S100 proteins, calcium-binding proteins of the EF-hand type.* Biochim Biophys Acta, 1999. **1450**(3): p. 191-231.
148. Baudier, J., et al., *Characterization of the tumor suppressor protein p53 as a protein kinase C substrate and a S100b-binding protein.* Proc Natl Acad Sci U S A, 1992. **89**(23): p. 11627-31.

149. Scotto, C., et al., *Calcium and S100B regulation of p53-dependent cell growth arrest and apoptosis.* Mol Cell Biol, 1998. **18**(7): p. 4272-81.
150. Rustandi, R.R., D.M. Baldisseri, and D.J. Weber, *Structure of the negative regulatory domain of p53 bound to S100B(betabeta).* Nat Struct Biol, 2000. **7**(7): p. 570-4.
151. Kolber, A.R., et al., *Drug-induced differentiation of a rat glioma in vitro: II. the expression of S-100, a glial specific protein and steroid sulfatase.* Brain Res, 1978. **143**(3): p. 513-20.
152. Labourdette, G. and A. Marks, *Synthesis of S-100 protein in monolayer cultures of rat-glial cells.* Eur J Biochem, 1975. **58**(1): p. 73-9.
153. Moussavi, R.S., C.A. Kelley, and R.S. Adelstein, *Phosphorylation of vertebrate nonmuscle and smooth muscle myosin heavy chains and light chains.* Mol Cell Biochem, 1993. **127-128**: p. 219-27.
154. Sakaguchi, M., et al., *Relationship between contact inhibition and intranuclear S100C of normal human fibroblasts.* J Cell Biol, 2000. **149**(6): p. 1193-206.
155. Grigorian, M., et al., *Tumor suppressor p53 protein is a new target for the metastasis-associated Mts1/S100A4 protein: functional consequences of their interaction.* J Biol Chem, 2001. **276**(25): p. 22699-708.
156. Takenaga, K., et al., *Binding of pEL98 protein, an S100-related calcium-binding protein, to nonmuscle tropomyosin.* J Cell Biol, 1994. **124**(5): p. 757-68.
157. Watanabe, Y., et al., *Calvasculin, as a factor affecting the microfilament assemblies in rat fibroblasts transfected by src gene.* FEBS Lett, 1993. **324**(1): p. 51-5.
158. Slomnicki, L.P. and W. Lesniak, *S100A6 (calcyclin) deficiency induces senescence-like changes in cell cycle, morphology and functional characteristics of mouse NIH 3T3 fibroblasts.* J Cell Biochem, 2010. **109**(3): p. 576-84.
159. Santamaria-Kisiel, L., A.C. Rintala-Dempsey, and G.S. Shaw, *Calcium-dependent and -independent interactions of the S100 protein family.* Biochem J, 2006. **396**(2): p. 201-14.
160. Most, P., et al., *The C terminus (amino acids 75-94) and the linker region (amino acids 42-54) of the Ca2+-binding protein S100A1 differentially enhance sarcoplasmic Ca2+ release in murine skinned skeletal muscle fibers.* J Biol Chem, 2003. **278**(29): p. 26356-64.
161. Treves, S., et al., *Interaction of S100A1 with the Ca2+ release channel (ryanodine receptor) of skeletal muscle.* Biochemistry, 1997. **36**(38): p. 11496-503.
162. Prosser, B.L., et al., *S100A1 binds to the calmodulin-binding site of ryanodine receptor and modulates skeletal muscle excitation-contraction coupling.* J Biol Chem, 2008. **283**(8): p. 5046-57.
163. Xiong, Z., et al., *Enhanced calcium transients in glial cells in neonatal cerebellar cultures derived from S100B null mice.* Exp Cell Res, 2000. **257**(2): p. 281-9.
164. Petzold, A., et al., *Cerebrospinal fluid (CSF) and serum S100B: release and wash-out pattern.* Brain Res Bull, 2003. **61**(3): p. 281-5.
165. Zimmer, D.B. and L.J. Van Eldik, *Identification of a molecular target for the calcium-modulated protein S100. Fructose-1,6-bisphosphate aldolase.* J Biol Chem, 1986. **261**(24): p. 11424-8.
166. Landar, A., et al., *Identification of an S100A1/S100B target protein: phosphoglucomutase.* Cell Calcium, 1996. **20**(3): p. 279-85.
167. Heierhorst, J., et al., *Ca2+/S100 regulation of giant protein kinases.* Nature, 1996. **380**(6575): p. 636-9.

168. Millward, T.A., et al., *Calcium regulation of Ndr protein kinase mediated by S100 calcium-binding proteins.* EMBO J, 1998. **17**(20): p. 5913-22.
169. Duda, T., R.M. Goraczniak, and R.K. Sharma, *Molecular characterization of S100A1-S100B protein in retina and its activation mechanism of bovine photoreceptor guanylate cyclase.* Biochemistry, 1996. **35**(20): p. 6263-6.
170. Margulis, A., N. Pozdnyakov, and A. Sitaramayya, *Activation of bovine photoreceptor guanylate cyclase by S100 proteins.* Biochem Biophys Res Commun, 1996. **218**(1): p. 243-7.
171. Pozdnyakov, N., et al., *Structural and functional characterization of retinal calcium-dependent guanylate cyclase activator protein (CD-GCAP): identity with S100beta protein.* Biochemistry, 1997. **36**(46): p. 14159-66.
172. Pozdnyakov, N., A. Margulis, and A. Sitaramayya, *Identification of effector binding sites on S100 beta: studies with guanylate cyclase and p80, a retinal phosphoprotein.* Biochemistry, 1998. **37**(30): p. 10701-8.
173. Rambotti, M.G., et al., *S100B and S100A1 proteins in bovine retina:their calcium-dependent stimulation of a membrane-bound guanylate cyclase activity as investigated by ultracytochemistry.* Neuroscience, 1999. **92**(3): p. 1089-101.
174. Yamasaki, R., et al., *Titin-actin interaction in mouse myocardium: passive tension modulation and its regulation by calcium/S100A1.* Biophys J, 2001. **81**(4): p. 2297-313.
175. Zimmer, D.B. and J.G. Dubuisson, *Identification of an S100 target protein: glycogen phosphorylase.* Cell Calcium, 1993. **14**(4): p. 323-32.
176. Boerries, M., et al., *Ca2+ -dependent interaction of S100A1 with F1-ATPase leads to an increased ATP content in cardiomyocytes.* Mol Cell Biol, 2007. **27**(12): p. 4365-73.
177. Murao, S., F.R. Collart, and E. Huberman, *A protein containing the cystic fibrosis antigen is an inhibitor of protein kinases.* J Biol Chem, 1989. **264**(14): p. 8356-60.
178. Kerkhoff, C., et al., *The arachidonic acid-binding protein S100A8/A9 promotes NADPH oxidase activation by interaction with p67phox and Rac-2.* FASEB J, 2005. **19**(3): p. 467-9.
179. Berthier, S., et al., *Changing the conformation state of cytochrome b558 initiates NADPH oxidase activation: MRP8/MRP14 regulation.* J Biol Chem, 2003. **278**(28): p. 25499-508.
180. Doussiere, J., F. Bouzidi, and P.V. Vignais, *A phenylarsine oxide-binding protein of neutrophil cytosol, which belongs to the S100 family, potentiates NADPH oxidase activation.* Biochem Biophys Res Commun, 2001. **285**(5): p. 1317-20.
181. Paclet, M.H., et al., *Regulation of phagocyte NADPH oxidase activity: identification of two cytochrome b558 activation states.* FASEB J, 2007. **21**(4): p. 1244-55.
182. Doussiere, J., F. Bouzidi, and P.V. Vignais, *The S100A8/A9 protein as a partner for the cytosolic factors of NADPH oxidase activation in neutrophils.* Eur J Biochem, 2002. **269**(13): p. 3246-55.
183. Rosenberger, S., et al., *A novel regulator of telomerase. S100A8 mediates differentiation-dependent and calcium-induced inhibition of telomerase activity in the human epidermal keratinocyte line HaCaT.* J Biol Chem, 2007. **282**(9): p. 6126-35.
184. Zimmer, D.B. and A. Landar, *Analysis of S100A1 expression during skeletal muscle and neuronal cell differentiation.* J Neurochem, 1995. **64**(6): p. 2727-36.

185. Kassam, G., et al., *The p11 subunit of the annexin II tetramer plays a key role in the stimulation of t-PA-dependent plasminogen activation.* Biochemistry, 1998. **37**(48): p. 16958-66.
186. Zhao, X.Q., et al., *Ca(2+)-dependent inhibition of actin-activated myosin ATPase activity by S100C (S100A11), a novel member of the S100 protein family.* Biochem Biophys Res Commun, 2000. **267**(1): p. 77-9.
187. Tsoporis, J.N., et al., *S100beta inhibits alpha1-adrenergic induction of the hypertrophic phenotype in cardiac myocytes.* J Biol Chem, 1997. **272**(50): p. 31915-21.
188. Tsoporis, J.N., et al., *Inhibition of norepinephrine-induced cardiac hypertrophy in s100beta transgenic mice.* J Clin Invest, 1998. **102**(8): p. 1609-16.
189. Yu, W.H. and P.E. Fraser, *S100beta interaction with tau is promoted by zinc and inhibited by hyperphosphorylation in Alzheimer's disease.* J Neurosci, 2001. **21**(7): p. 2240-6.
190. Sheu, F.S., F.L. Huang, and K.P. Huang, *Differential responses of protein kinase C substrates (MARCKS, neuromodulin, and neurogranin) phosphorylation to calmodulin and S100.* Arch Biochem Biophys, 1995. **316**(1): p. 335-42.
191. Hagiwara, M., et al., *Modulation of tyrosine phosphorylation of p36 and other substrates by the S-100 protein.* J Biol Chem, 1988. **263**(13): p. 6438-41.
192. Sheu, F.S., et al., *Glial-derived S100b protein selectively inhibits recombinant beta protein kinase C (PKC) phosphorylation of neuron-specific protein F1/GAP43.* Brain Res Mol Brain Res, 1994. **21**(1-2): p. 62-6.
193. Lin, L.H., et al., *Inhibition of protein kinase C- and casein kinase II-mediated phosphorylation of GAP-43 by S100 beta.* Brain Res Mol Brain Res, 1994. **25**(3-4): p. 297-304.
194. Fujii, T., et al., *Calcium-dependent control of caldesmon-actin interaction by S100 protein.* J Biochem, 1990. **107**(1): p. 133-7.
195. Pritchard, K. and S.B. Marston, *Ca(2+)-dependent regulation of vascular smooth-muscle caldesmon by S.100 and related smooth-muscle proteins.* Biochem J, 1991. **277 (Pt 3)**: p. 819-24.
196. Frizzo, J.K., et al., *S100B-mediated inhibition of the phosphorylation of GFAP is prevented by TRTK-12.* Neurochem Res, 2004. **29**(4): p. 735-40.
197. Lin, J., et al., *Inhibition of p53 transcriptional activity by the S100B calcium-binding protein.* J Biol Chem, 2001. **276**(37): p. 35037-41.
198. Baudier, J., et al., *Interactions of myogenic bHLH transcription factors with calcium-binding calmodulin and S100a (alpha alpha) proteins.* Biochemistry, 1995. **34**(24): p. 7834-46.
199. Onions, J., S. Hermann, and T. Grundstrom, *Basic helix-loop-helix protein sequences determining differential inhibition by calmodulin and S-100 proteins.* J Biol Chem, 1997. **272**(38): p. 23930-7.
200. Wright, N.T., et al., *S100A1: Structure, Function, and Therapeutic Potential.* Curr Chem Biol, 2009. **3**(2): p. 138-145.
201. Dulyaninova, N.G., et al., *Regulation of myosin-IIA assembly and Mts1 binding by heavy chain phosphorylation.* Biochemistry, 2005. **44**(18): p. 6867-76.
202. Kriajevska, M., et al., *Metastasis-associated protein Mts1 (S100A4) inhibits CK2-mediated phosphorylation and self-assembly of the heavy chain of nonmuscle myosin.* Biochim Biophys Acta, 2000. **1498**(2-3): p. 252-63.
203. Li, Z.H. and A.R. Bresnick, *The S100A4 metastasis factor regulates cellular motility via a direct interaction with myosin-IIA.* Cancer Res, 2006. **66**(10): p. 5173-80.

204. Rescher, U. and V. Gerke, *S100A10/p11: family, friends and functions.* Pflugers Arch, 2008. **455**(4): p. 575-82.
205. Sakaguchi, M., et al., *Truncation of annexin A1 is a regulatory lever for linking epidermal growth factor signaling with cytosolic phospholipase A2 in normal and malignant squamous epithelial cells.* J Biol Chem, 2007. **282**(49): p. 35679-86.
206. Sorci, G., A.L. Agneletti, and R. Donato, *Effects of S100A1 and S100B on microtubule stability. An in vitro study using triton-cytoskeletons from astrocyte and myoblast cell lines.* Neuroscience, 2000. **99**(4): p. 773-83.
207. Garbuglia, M., et al., *The calcium-modulated proteins, S100A1 and S100B, as potential regulators of the dynamics of type III intermediate filaments.* Braz J Med Biol Res, 1999. **32**(10): p. 1177-85.
208. Gimona, M., et al., *Ca2+-dependent interaction of S100A2 with muscle and nonmuscle tropomyosins.* J Cell Sci, 1997. **110 (Pt 5)**: p. 611-21.
209. Garbuglia, M., et al., *Effects of calcium-binding proteins (S-100a(o), S-100a, S-100b) on desmin assembly in vitro.* FASEB J, 1996. **10**(2): p. 317-24.
210. Bianchi, R., et al., *Mechanism of S100 protein-dependent inhibition of glial fibrillary acidic protein (GFAP) polymerization.* Biochim Biophys Acta, 1994. **1223**(3): p. 354-60.
211. Garbuglia, M., et al., *Characterization of type III intermediate filament regulatory protein target epitopes: S-100 (beta and/or alpha) binds the N-terminal head domain; annexin II2-p11(2) binds the rod domain.* Biochim Biophys Acta, 1996. **1313**(3): p. 268-76.
212. Garbuglia, M., et al., *Annexin II2-p11(2) (calpactin I) stimulates the assembly of GFAP in a calcium- and pH-dependent manner.* Biochem Biophys Res Commun, 1995. **208**(3): p. 901-9.
213. Heierhorst, J., R.J. Mann, and B.E. Kemp, *Interaction of the recombinant S100A1 protein with twitchin kinase, and comparison with other Ca2+-binding proteins.* Eur J Biochem, 1997. **249**(1): p. 127-33.
214. Kriajevska, M., et al., *Metastasis-associated Mts1 (S100A4) protein modulates protein kinase C phosphorylation of the heavy chain of nonmuscle myosin.* J Biol Chem, 1998. **273**(16): p. 9852-6.
215. Donato, R., *Calcium-sensitivity of brain microtubule proteins in the presence of S-100 proteins.* Cell Calcium, 1985. **6**(4): p. 343-61.
216. Donato, R., *Calcium-independent, pH-regulated effects of S-100 proteins on assembly-disassembly of brain microtubule protein in vitro.* J Biol Chem, 1988. **263**(1): p. 106-10.
217. Sorci, G., et al., *Association of S100B with intermediate filaments and microtubules in glial cells.* Biochim Biophys Acta, 1998. **1448**(2): p. 277-89.
218. Skripnikova, E.V. and N.B. Gusev, *Interaction of smooth muscle caldesmon with S-100 protein.* FEBS Lett, 1989. **257**(2): p. 380-2.
219. Wills, F.L., W.D. McCubbin, and C.M. Kay, *Characterization of the smooth muscle calponin and calmodulin complex.* Biochemistry, 1993. **32**(9): p. 2321-8.
220. Donato, R., et al., *S100B's double life: intracellular regulator and extracellular signal.* Biochim Biophys Acta, 2009. **1793**(6): p. 1008-22.
221. Ivanenkov, V.V., et al., *Characterization of S-100b binding epitopes. Identification of a novel target, the actin capping protein, CapZ.* J Biol Chem, 1995. **270**(24): p. 14651-8.
222. Ivanenkov, V.V., R.V. Dimlich, and G.A. Jamieson, Jr., *Interaction of S100a0 protein with the actin capping protein, CapZ: characterization of a putative*

S100a0 binding site in CapZ alpha-subunit. Biochem Biophys Res Commun, 1996. **221**(1): p. 46-50.
223. Badyal, S.K., et al., *Mechanism of the Ca(2)+-dependent interaction between S100A4 and tail fragments of nonmuscle myosin heavy chain IIA.* J Mol Biol, 2011. **405**(4): p. 1004-26.
224. Chen, H., et al., *Binding to intracellular targets of the metastasis-inducing protein, S100A4 (p9Ka).* Biochem Biophys Res Commun, 2001. **286**(5): p. 1212-7.
225. Ford, H.L. and S.B. Zain, *Interaction of metastasis associated Mts1 protein with nonmuscle myosin.* Oncogene, 1995. **10**(8): p. 1597-605.
226. Gibbs, F.E., et al., *Interactions in vitro of p9Ka, the rat S-100-related, metastasis-inducing, calcium-binding protein.* J Biol Chem, 1994. **269**(29): p. 18992-9.
227. Kriajevska, M.V., et al., *Non-muscle myosin heavy chain as a possible target for protein encoded by metastasis-related mts-1 gene.* J Biol Chem, 1994. **269**(31): p. 19679-82.
228. Golitsina, N.L., et al., *Ca2+-dependent binding of calcyclin to muscle tropomyosin.* Biochem Biophys Res Commun, 1996. **220**(2): p. 360-5.
229. Mani, R.S., W.D. McCubbin, and C.M. Kay, *Calcium-dependent regulation of caldesmon by an 11-kDa smooth muscle calcium-binding protein, caltropin.* Biochemistry, 1992. **31**(47): p. 11896-901.
230. Rammes, A., et al., *Myeloid-related protein (MRP) 8 and MRP14, calcium-binding proteins of the S100 family, are secreted by activated monocytes via a novel, tubulin-dependent pathway.* J Biol Chem, 1997. **272**(14): p. 9496-502.
231. Roth, J., et al., *MRP8 and MRP14, S-100-like proteins associated with myeloid differentiation, are translocated to plasma membrane and intermediate filaments in a calcium-dependent manner.* Blood, 1993. **82**(6): p. 1875-83.
232. Vogl, T., et al., *MRP8 and MRP14 control microtubule reorganization during transendothelial migration of phagocytes.* Blood, 2004. **104**(13): p. 4260-8.
233. Goebeler, M., et al., *Increase of calcium levels in epithelial cells induces translocation of calcium-binding proteins migration inhibitory factor-related protein 8 (MRP8) and MRP14 to keratin intermediate filaments.* Biochem J, 1995. **309 (Pt 2)**: p. 419-24.
234. Benaud, C., et al., *AHNAK interaction with the annexin 2/S100A10 complex regulates cell membrane cytoarchitecture.* J Cell Biol, 2004. **164**(1): p. 133-44.
235. Broome, A.M. and R.L. Eckert, *Microtubule-dependent redistribution of a cytoplasmic cornified envelope precursor.* J Invest Dermatol, 2004. **122**(1): p. 29-38.
236. Vogl, T., et al., *S100A12 is expressed exclusively by granulocytes and acts independently from MRP8 and MRP14.* J Biol Chem, 1999. **274**(36): p. 25291-6.
237. Sherbet, G.V., *Metastasis promoter S100A4 is a potentially valuable molecular target for cancer therapy.* Cancer Lett, 2009. **280**(1): p. 15-30.
238. Mueller, A., et al., *The calcium-binding protein S100A2 interacts with p53 and modulates its transcriptional activity.* J Biol Chem, 2005. **280**(32): p. 29186-93.
239. Wang, X., L. Chen, and Y. Zeng, *[Calcium-binding protein S100A2 in the retardation of growth and proliferation of hepatocellular carcinoma cells].* Zhonghua Zhong Liu Za Zhi, 2001. **23**(5): p. 363-5.
240. Landriscina, M., et al., *Copper induces the assembly of a multiprotein aggregate implicated in the release of fibroblast growth factor 1 in response to stress.* J Biol Chem, 2001. **276**(27): p. 25549-57.

241. Prudovsky, I., et al., *The intracellular translocation of the components of the fibroblast growth factor 1 release complex precedes their assembly prior to export.* J Cell Biol, 2002. **158**(2): p. 201-8.
242. Mouta Carreira, C., et al., *S100A13 is involved in the regulation of fibroblast growth factor-1 and p40 synaptotagmin-1 release in vitro.* J Biol Chem, 1998. **273**(35): p. 22224-31.
243. Urban, C.F., et al., *Neutrophil extracellular traps contain calprotectin, a cytosolic protein complex involved in host defense against Candida albicans.* PLoS Pathog, 2009. **5**(10): p. e1000639.
244. Kligman, D. and D.R. Marshak, *Purification and characterization of a neurite extension factor from bovine brain.* Proc Natl Acad Sci U S A, 1985. **82**(20): p. 7136-9.
245. Winningham-Major, F., et al., *Neurite extension and neuronal survival activities of recombinant S100 beta proteins that differ in the content and position of cysteine residues.* J Cell Biol, 1989. **109**(6 Pt 1): p. 3063-71.
246. Van Eldik, L.J., et al., *Neurotrophic activity of S-100 beta in cultures of dorsal root ganglia from embryonic chick and fetal rat.* Brain Res, 1991. **542**(2): p. 280-5.
247. Ueda, S., et al., *Serotonergic sprouting into transplanted C-6 gliomas is blocked by S-100 beta antisense gene.* Brain Res Mol Brain Res, 1995. **29**(2): p. 365-8.
248. Haglid, K.G., et al., *S-100beta stimulates neurite outgrowth in the rat sciatic nerve grafted with acellular muscle transplants.* Brain Res, 1997. **753**(2): p. 196-201.
249. Huttunen, H.J., et al., *Coregulation of neurite outgrowth and cell survival by amphoterin and S100 proteins through receptor for advanced glycation end products (RAGE) activation.* J Biol Chem, 2000. **275**(51): p. 40096-105.
250. Bhattacharyya, A., et al., *S100 is present in developing chicken neurons and Schwann cells and promotes motor neuron survival in vivo.* J Neurobiol, 1992. **23**(4): p. 451-66.
251. Barger, S.W., L.J. Van Eldik, and M.P. Mattson, *S100 beta protects hippocampal neurons from damage induced by glucose deprivation.* Brain Res, 1995. **677**(1): p. 167-70.
252. Iwasaki, Y., T. Shiojima, and M. Kinoshita, *S100 beta prevents the death of motor neurons in newborn rats after sciatic nerve section.* J Neurol Sci, 1997. **151**(1): p. 7-12.
253. Businaro, R., et al., *S100B protects LAN-5 neuroblastoma cells against Abeta amyloid-induced neurotoxicity via RAGE engagement at low doses but increases Abeta amyloid neurotoxicity at high doses.* J Neurosci Res, 2006. **83**(5): p. 897-906.
254. Ahlemeyer, B., et al., *S-100beta protects cultured neurons against glutamate- and staurosporine-induced damage and is involved in the antiapoptotic action of the 5 HT(1A)-receptor agonist, Bay x 3702.* Brain Res, 2000. **858**(1): p. 121-8.
255. Kogel, D., et al., *S100B potently activates p65/c-Rel transcriptional complexes in hippocampal neurons: Clinical implications for the role of S100B in excitotoxic brain injury.* Neuroscience, 2004. **127**(4): p. 913-20.
256. Pichiule, P., et al., *Hypoxia-inducible factor-1 mediates neuronal expression of the receptor for advanced glycation end products following hypoxia/ischemia.* J Biol Chem, 2007. **282**(50): p. 36330-40.

257. Nishi, M., P.M. Whitaker-Azmitia, and E.C. Azmitia, *Enhanced synaptophysin immunoreactivity in rat hippocampal culture by 5-HT 1A agonist, S100b, and corticosteroid receptor agonists.* Synapse, 1996. **23**(1): p. 1-9.
258. Ciccarelli, R., et al., *Activation of A(1) adenosine or mGlu3 metabotropic glutamate receptors enhances the release of nerve growth factor and S-100beta protein from cultured astrocytes.* Glia, 1999. **27**(3): p. 275-81.
259. Arcuri, C., et al., *S100B increases proliferation in PC12 neuronal cells and reduces their responsiveness to nerve growth factor via Akt activation.* J Biol Chem, 2005. **280**(6): p. 4402-14.
260. Selinfreund, R.H., et al., *Neurotrophic protein S100 beta stimulates glial cell proliferation.* Proc Natl Acad Sci U S A, 1991. **88**(9): p. 3554-8.
261. Mariggio, M.A., et al., *The brain protein S-100ab induces apoptosis in PC12 cells.* Neuroscience, 1994. **60**(1): p. 29-35.
262. Hu, J., A. Ferreira, and L.J. Van Eldik, *S100beta induces neuronal cell death through nitric oxide release from astrocytes.* J Neurochem, 1997. **69**(6): p. 2294-301.
263. Fulle, S., et al., *Calcium and fos involvement in brain-derived Ca(2+)-binding protein (S100)-dependent apoptosis in rat phaeochromocytoma cells.* Exp Physiol, 2000. **85**(3): p. 243-53.
264. Fano, G., et al., *The S-100 protein causes an increase of intracellular calcium and death of PC12 cells.* Neuroscience, 1993. **53**(4): p. 919-25.
265. Li, Y., et al., *S100beta induction of the proinflammatory cytokine interleukin-6 in neurons.* J Neurochem, 2000. **74**(1): p. 143-50.
266. Adami, C., et al., *S100B expression in and effects on microglia.* Glia, 2001. **33**(2): p. 131-42.
267. Petrova, T.V., J. Hu, and L.J. Van Eldik, *Modulation of glial activation by astrocyte-derived protein S100B: differential responses of astrocyte and microglial cultures.* Brain Res, 2000. **853**(1): p. 74-80.
268. Nishiyama, H., et al., *Glial protein S100B modulates long-term neuronal synaptic plasticity.* Proc Natl Acad Sci U S A, 2002. **99**(6): p. 4037-42.
269. Tsoporis, J.N., et al., *S100B expression modulates left ventricular remodeling after myocardial infarction in mice.* Circulation, 2005. **111**(5): p. 598-606.
270. Sorci, G., et al., *S100B inhibits myogenic differentiation and myotube formation in a RAGE-independent manner.* Mol Cell Biol, 2003. **23**(14): p. 4870-81.
271. Sorci, G., et al., *S100B causes apoptosis in a myoblast cell line in a RAGE-independent manner.* J Cell Physiol, 2004. **199**(2): p. 274-83.
272. Sorci, G., et al., *Amphoterin stimulates myogenesis and counteracts the antimyogenic factors basic fibroblast growth factor and S100B via RAGE binding.* Mol Cell Biol, 2004. **24**(11): p. 4880-94.
273. Riuzzi, F., G. Sorci, and R. Donato, *S100B stimulates myoblast proliferation and inhibits myoblast differentiation by independently stimulating ERK1/2 and inhibiting p38 MAPK.* J Cell Physiol, 2006. **207**(2): p. 461-70.
274. Most, P., et al., *Extracellular S100A1 protein inhibits apoptosis in ventricular cardiomyocytes via activation of the extracellular signal-regulated protein kinase 1/2 (ERK1/2).* J Biol Chem, 2003. **278**(48): p. 48404-12.
275. Komada, T., et al., *Novel specific chemtactic receptor for S100L protein on guinea pig eosinophils.* Biochem Biophys Res Commun, 1996. **220**(3): p. 871-4.
276. Nagy, N., et al., *S100A2, a putative tumor suppressor gene, regulates in vitro squamous cell carcinoma migration.* Lab Invest, 2001. **81**(4): p. 599-612.

277. Schneider, M., et al., *S100A4 is upregulated in injured myocardium and promotes growth and survival of cardiac myocytes.* Cardiovasc Res, 2007. **75**(1): p. 40-50.
278. Schmidt-Hansen, B., et al., *Extracellular S100A4(mts1) stimulates invasive growth of mouse endothelial cells and modulates MMP-13 matrix metalloproteinase activity.* Oncogene, 2004. **23**(32): p. 5487-95.
279. Semov, A., et al., *Metastasis-associated protein S100A4 induces angiogenesis through interaction with Annexin II and accelerated plasmin formation.* J Biol Chem, 2005. **280**(21): p. 20833-41.
280. Belot, N., et al., *Extracellular S100A4 stimulates the migration rate of astrocytic tumor cells by modifying the organization of their actin cytoskeleton.* Biochim Biophys Acta, 2002. **1600**(1-2): p. 74-83.
281. Leclerc, E., et al., *S100B and S100A6 differentially modulate cell survival by interacting with distinct RAGE (receptor for advanced glycation end products) immunoglobulin domains.* J Biol Chem, 2007. **282**(43): p. 31317-31.
282. Jinquan, T., et al., *Psoriasin: a novel chemotactic protein.* J Invest Dermatol, 1996. **107**(1): p. 5-10.
283. Emberley, E.D., L.C. Murphy, and P.H. Watson, *S100 proteins and their influence on pro-survival pathways in cancer.* Biochem Cell Biol, 2004. **82**(4): p. 508-15.
284. Lee, K.C. and R.L. Eckert, *S100A7 (Psoriasin)--mechanism of antibacterial action in wounds.* J Invest Dermatol, 2007. **127**(4): p. 945-57.
285. Sakaguchi, M., et al., *S100A11, an dual mediator for growth regulation of human keratinocytes.* Mol Biol Cell, 2008. **19**(1): p. 78-85.
286. Sakaguchi, M. and N.H. Huh, *S100A11, a dual growth regulator of epidermal keratinocytes.* Amino Acids, 2011. **41**(4): p. 797-807.
287. Cecil, D.L., et al., *Inflammation-induced chondrocyte hypertrophy is driven by receptor for advanced glycation end products.* J Immunol, 2005. **175**(12): p. 8296-302.
288. Cecil, D.L. and R. Terkeltaub, *Transamidation by transglutaminase 2 transforms S100A11 calgranulin into a procatabolic cytokine for chondrocytes.* J Immunol, 2008. **180**(12): p. 8378-85.
289. Arumugam, T., et al., *S100P stimulates cell proliferation and survival via receptor for activated glycation end products (RAGE).* J Biol Chem, 2004. **279**(7): p. 5059-65.
290. Fuentes, M.K., et al., *RAGE activation by S100P in colon cancer stimulates growth, migration, and cell signaling pathways.* Dis Colon Rectum, 2007. **50**(8): p. 1230-40.
291. Leclerc, E., et al., *Binding of S100 proteins to RAGE: an update.* Biochim Biophys Acta, 2009. **1793**(6): p. 993-1007.
292. Zimmer, D.B., et al., *S100A1 regulates neurite organization, tubulin levels, and proliferation in PC12 cells.* J Biol Chem, 1998. **273**(8): p. 4705-11.
293. Huttunen, H.J., C. Fages, and H. Rauvala, *Receptor for advanced glycation end products (RAGE)-mediated neurite outgrowth and activation of NF-kappaB require the cytoplasmic domain of the receptor but different downstream signaling pathways.* J Biol Chem, 1999. **274**(28): p. 19919-24.
294. Ghavami, S., et al., *S100A8/A9 at low concentration promotes tumor cell growth via RAGE ligation and MAP kinase-dependent pathway.* J Leukoc Biol, 2008. **83**(6): p. 1484-92.
295. Wolf, R., T. Ruzicka, and S.H. Yuspa, *Novel S100A7 (psoriasin)/S100A15 (koebnerisin) subfamily: highly homologous but distinct in regulation and function.* Amino Acids, 2011. **41**(4): p. 789-96.

296. Cornish, C.J., et al., *S100 protein CP-10 stimulates myeloid cell chemotaxis without activation.* J Cell Physiol, 1996. **166**(2): p. 427-37.
297. Newton, R.A. and N. Hogg, *The human S100 protein MRP-14 is a novel activator of the beta 2 integrin Mac-1 on neutrophils.* J Immunol, 1998. **160**(3): p. 1427-35.
298. Yan, W.X., et al., *Mast cell and monocyte recruitment by S100A12 and its hinge domain.* J Biol Chem, 2008. **283**(19): p. 13035-43.
299. Sorci, G., et al., *S100B Protein, A Damage-Associated Molecular Pattern Protein in the Brain and Heart, and Beyond.* Cardiovasc Psychiatry Neurol, 2010. **2010**.
300. Donato, R., *RAGE: a single receptor for several ligands and different cellular responses: the case of certain S100 proteins.* Curr Mol Med, 2007. **7**(8): p. 711-24.
301. Greene, L.A. and A.S. Tischler, *Establishment of a noradrenergic clonal line of rat adrenal pheochromocytoma cells which respond to nerve growth factor.* Proc Natl Acad Sci U S A, 1976. **73**(7): p. 2424-8.
302. Yui, S., et al., *Implication of extracellular zinc exclusion by recombinant human calprotectin (MRP8 and MRP14) from target cells in its apoptosis-inducing activity.* Mediators Inflamm, 2002. **11**(3): p. 165-72.
303. Ribeiro, J.M. and D.A. Carson, *Ca2+/Mg(2+)-dependent endonuclease from human spleen: purification, properties, and role in apoptosis.* Biochemistry, 1993. **32**(35): p. 9129-36.
304. Marini, M., et al., *Modulation of caspase-3 activity by zinc ions and by the cell redox state.* Exp Cell Res, 2001. **266**(2): p. 323-32.
305. McCabe, M.J., Jr., S.A. Jiang, and S. Orrenius, *Chelation of intracellular zinc triggers apoptosis in mature thymocytes.* Lab Invest, 1993. **69**(1): p. 101-10.
306. Chai, F., et al., *Regulation of caspase activation and apoptosis by cellular zinc fluxes and zinc deprivation: A review.* Immunol Cell Biol, 1999. **77**(3): p. 272-8.
307. Nakatani, T., et al., *Apoptosis induced by chelation of intracellular zinc is associated with depletion of cellular reduced glutathione level in rat hepatocytes.* Chem Biol Interact, 2000. **125**(3): p. 151-63.
308. Hyun, H.J., et al., *Depletion of intracellular zinc induces macromolecule synthesis- and caspase-dependent apoptosis of cultured retinal cells.* Brain Res, 2000. **869**(1-2): p. 39-48.
309. Pedersen, K.B., et al., *Sensitization of interferon-gamma induced apoptosis in human osteosarcoma cells by extracellular S100A4.* BMC Cancer, 2004. **4**: p. 52.
310. Liu, D., et al., *Expression of calcium-binding protein S100A2 in breast lesions.* Br J Cancer, 2000. **83**(11): p. 1473-9.
311. Vos, J.B., et al., *Transcriptional response of bronchial epithelial cells to Pseudomonas aeruginosa: identification of early mediators of host defense.* Physiol Genomics, 2005. **21**(3): p. 324-36.
312. Glaser, R., et al., *Antimicrobial psoriasin (S100A7) protects human skin from Escherichia coli infection.* Nat Immunol, 2005. **6**(1): p. 57-64.
313. Michalek, M., et al., *The human antimicrobial protein psoriasin acts by permeabilization of bacterial membranes.* Dev Comp Immunol, 2009. **33**(6): p. 740-6.
314. Lackmann, M., et al., *Purification and structural analysis of a murine chemotactic cytokine (CP-10) with sequence homology to S100 proteins.* J Biol Chem, 1992. **267**(11): p. 7499-504.
315. Geczy, C., *Regulation and proinflammatory properties of the chemotactic protein, CP-10.* Biochim Biophys Acta, 1996. **1313**(3): p. 246-52.

316. Ryckman, C., et al., *Proinflammatory activities of S100: proteins S100A8, S100A9, and S100A8/A9 induce neutrophil chemotaxis and adhesion.* J Immunol, 2003. **170**(6): p. 3233-42.
317. Lackmann, M., et al., *Identification of a chemotactic domain of the pro-inflammatory S100 protein CP-10.* J Immunol, 1993. **150**(7): p. 2981-91.
318. Nishimura, F., et al., *Migration inhibitory factor related protein-8 (MRP-8) is an autocrine chemotactic factor for periodontal ligament cells.* J Dent Res, 1999. **78**(6): p. 1251-5.
319. Rouleau, P., et al., *The calcium-binding protein S100A12 induces neutrophil adhesion, migration, and release from bone marrow in mouse at concentrations similar to those found in human inflammatory arthritis.* Clin Immunol, 2003. **107**(1): p. 46-54.
320. Yang, Z., et al., *Proinflammatory properties of the human S100 protein S100A12.* J Leukoc Biol, 2001. **69**(6): p. 986-94.
321. Sakaguchi, T., et al., *Central role of RAGE-dependent neointimal expansion in arterial restenosis.* J Clin Invest, 2003. **111**(7): p. 959-72.
322. Bian, L., et al., *S100A4 deficiency is associated with efficient bacterial clearance and protects against joint destruction during Staphylococcal infection.* J Infect Dis, 2011. **204**(5): p. 722-30.
323. Bin, L., et al., *Inhibition of S100A11 gene expression impairs keratinocyte response against vaccinia virus through downregulation of the IL-10 receptor 2 chain.* J Allergy Clin Immunol, 2009. **124**(2): p. 270-7, 277 e1.
324. McLachlan, J.L., et al., *S100 and cytokine expression in caries.* Infect Immun, 2004. **72**(7): p. 4102-8.
325. Salama, I., et al., *A review of the S100 proteins in cancer.* Eur J Surg Oncol, 2008. **34**(4): p. 357-64.
326. Sheikh, A.A., et al., *The expression of S100A8 in pancreatic cancer-associated monocytes is associated with the Smad4 status of pancreatic cancer cells.* Proteomics, 2007. **7**(11): p. 1929-40.
327. Hermani, A., et al., *Calcium-binding proteins S100A8 and S100A9 as novel diagnostic markers in human prostate cancer.* Clin Cancer Res, 2005. **11**(14): p. 5146-52.
328. Heizmann, C.W., *Multistep calcium signalling in health and disease.* Mol Cells, 1996. **6**(629).
329. Sen, J. and A. Belli, *S100B in neuropathologic states: the CRP of the brain?* J Neurosci Res, 2007. **85**(7): p. 1373-80.
330. Sheng, J.G., R.E. Mrak, and W.S. Griffin, *S100 beta protein expression in Alzheimer disease: potential role in the pathogenesis of neuritic plaques.* J Neurosci Res, 1994. **39**(4): p. 398-404.
331. Van Eldik, L.J. and W.S. Griffin, *S100 beta expression in Alzheimer's disease: relation to neuropathology in brain regions.* Biochim Biophys Acta, 1994. **1223**(3): p. 398-403.
332. Sussmuth, S.D., et al., *Amyotrophic lateral sclerosis: disease stage related changes of tau protein and S100 beta in cerebrospinal fluid and creatine kinase in serum.* Neurosci Lett, 2003. **353**(1): p. 57-60.
333. Griffin, W.S., et al., *Overexpression of the neurotrophic cytokine S100 beta in human temporal lobe epilepsy.* J Neurochem, 1995. **65**(1): p. 228-33.
334. Remppis, A., et al., *Altered expression of the Ca(2+)-binding protein S100A1 in human cardiomyopathy.* Biochim Biophys Acta, 1996. **1313**(3): p. 253-7.

335. Ehlermann, P., et al., *Right ventricular upregulation of the Ca(2+) binding protein S100A1 in chronic pulmonary hypertension.* Biochim Biophys Acta, 2000. **1500**(2): p. 249-55.
336. Kiewitz, R., et al., *S100A1, a new marker for acute myocardial ischemia.* Biochem Biophys Res Commun, 2000. **274**(3): p. 865-71.
337. Bartling, B., et al., *S100A2-S100P expression profile and diagnosis of non-small cell lung carcinoma: impairment by advanced tumour stages and neoadjuvant chemotherapy.* Eur J Cancer, 2007. **43**(13): p. 1935-43.
338. Hsieh, H.L., et al., *Expression analysis of S100 proteins and RAGE in human tumors using tissue microarrays.* Biochem Biophys Res Commun, 2003. **307**(2): p. 375-81.
339. Wicki, R., et al., *Repression of the candidate tumor suppressor gene S100A2 in breast cancer is mediated by site-specific hypermethylation.* Cell Calcium, 1997. **22**(4): p. 243-54.
340. Nagy, N., et al., *The Ca2+-binding S100A2 protein is differentially expressed in epithelial tissue of glandular or squamous origin.* Histol Histopathol, 2002. **17**(1): p. 123-30.
341. Heighway, J., et al., *Expression profiling of primary non-small cell lung cancer for target identification.* Oncogene, 2002. **21**(50): p. 7749-63.
342. El-Rifai, W., et al., *Gastric cancers overexpress S100A calcium-binding proteins.* Cancer Res, 2002. **62**(23): p. 6823-6.
343. Lee, S.W., et al., *Down-regulation of a member of the S100 gene family in mammary carcinoma cells and reexpression by azadeoxycytidine treatment.* Proc Natl Acad Sci U S A, 1992. **89**(6): p. 2504-8.
344. Feng, G., et al., *Diminished expression of S100A2, a putative tumor suppressor, at early stage of human lung carcinogenesis.* Cancer Res, 2001. **61**(21): p. 7999-8004.
345. Shrestha, P., et al., *Localization of Ca(2+)-binding S100 proteins in epithelial tumours of the skin.* Virchows Arch, 1998. **432**(1): p. 53-9.
346. Hough, C.D., et al., *Coordinately up-regulated genes in ovarian cancer.* Cancer Res, 2001. **61**(10): p. 3869-76.
347. Ohuchida, K., et al., *Over-expression of S100A2 in pancreatic cancer correlates with progression and poor prognosis.* J Pathol, 2007. **213**(3): p. 275-82.
348. Kizawa, K., et al., *Aberrantly differentiated cells in benign pilomatrixoma reflect the normal hair follicle: immunohistochemical analysis of Ca-binding S100A2, S100A3 and S100A6 proteins.* Br J Dermatol, 2005. **152**(2): p. 314-20.
349. Lee, O.J., et al., *Expression of calcium-binding proteins S100A2 and S100A4 in Barrett's adenocarcinomas.* Neoplasia, 2006. **8**(10): p. 843-50.
350. Pelc, P., et al., *Differential expression of S100 calcium-binding proteins in epidermoid cysts, branchial cysts, craniopharyngiomas and cholesteatomas.* Histopathology, 2003. **42**(4): p. 387-94.
351. Ambartsumian, N.S., et al., *Metastasis of mammary carcinomas in GRS/A hybrid mice transgenic for the mts1 gene.* Oncogene, 1996. **13**(8): p. 1621-30.
352. Ambartsumian, N., et al., *The metastasis-associated Mts1(S100A4) protein could act as an angiogenic factor.* Oncogene, 2001. **20**(34): p. 4685-95.
353. Platt-Higgins, A.M., et al., *Comparison of the metastasis-inducing protein S100A4 (p9ka) with other prognostic markers in human breast cancer.* Int J Cancer, 2000. **89**(2): p. 198-208.

354. Pedrocchi, M., et al., *Expression of Ca(2+)-binding proteins of the S100 family in malignant human breast-cancer cell lines and biopsy samples.* Int J Cancer, 1994. **57**(5): p. 684-90.
355. Tang, Y., et al., *Effect of hypoxic preconditioning on brain genomic response before and following ischemia in the adult mouse: identification of potential neuroprotective candidates for stroke.* Neurobiol Dis, 2006. **21**(1): p. 18-28.
356. Lusis, E. and D.H. Gutmann, *Meningioma: an update.* Curr Opin Neurol, 2004. **17**(6): p. 687-92.
357. Hancq, S., et al., *S100A5: a marker of recurrence in WHO grade I meningiomas.* Neuropathol Appl Neurobiol, 2004. **30**(2): p. 178-87.
358. Vimalachandran, D., et al., *High nuclear S100A6 (Calcyclin) is significantly associated with poor survival in pancreatic cancer patients.* Cancer Res, 2005. **65**(8): p. 3218-25.
359. Guo, X.J., et al., *Identification of a serum-inducible messenger RNA (5B10) as the mouse homologue of calcyclin: tissue distribution and expression in metastatic, ras-transformed NIH 3T3 cells.* Cell Growth Differ, 1990. **1**(7): p. 333-8.
360. Cheng, C.W., et al., *Calcium-binding proteins annexin A2 and S100A6 are sensors of tubular injury and recovery in acute renal failure.* Kidney Int, 2005. **68**(6): p. 2694-703.
361. Hoyaux, D., et al., *S100A6 overexpression within astrocytes associated with impaired axons from both ALS mouse model and human patients.* J Neuropathol Exp Neurol, 2002. **61**(8): p. 736-44.
362. Kim, J., et al., *S100A6 protein as a marker for differential diagnosis of cholangiocarcinoma from hepatocellular carcinoma.* Hepatol Res, 2002. **23**(4): p. 274.
363. Luu, H.H., et al., *Increased expression of S100A6 is associated with decreased metastasis and inhibition of cell migration and anchorage independent growth in human osteosarcoma.* Cancer Lett, 2005. **229**(1): p. 135-48.
364. Maelandsmo, G.M., et al., *Differential expression patterns of S100A2, S100A4 and S100A6 during progression of human malignant melanoma.* Int J Cancer, 1997. **74**(4): p. 464-9.
365. Shekouh, A.R., et al., *Application of laser capture microdissection combined with two-dimensional electrophoresis for the discovery of differentially regulated proteins in pancreatic ductal adenocarcinoma.* Proteomics, 2003. **3**(10): p. 1988-2001.
366. Weterman, M.A., et al., *Expression of calcyclin in human melanoma cell lines correlates with metastatic behavior in nude mice.* Cancer Res, 1992. **52**(5): p. 1291-6.
367. Yang, Y.Q., et al., *Upregulated expression of S100A6 in human gastric cancer.* J Dig Dis, 2007. **8**(4): p. 186-93.
368. Ohuchida, K., et al., *The role of S100A6 in pancreatic cancer development and its clinical implication as a diagnostic marker and therapeutic target.* Clin Cancer Res, 2005. **11**(21): p. 7785-93.
369. Lee, J.G. and E.P. Kay, *FGF-2-mediated signal transduction during endothelial mesenchymal transformation in corneal endothelial cells.* Exp Eye Res, 2006. **83**(6): p. 1309-16.
370. Broome, A.M., D. Ryan, and R.L. Eckert, *S100 protein subcellular localization during epidermal differentiation and psoriasis.* J Histochem Cytochem, 2003. **51**(5): p. 675-85.

371. Al-Haddad, S., et al., *Psoriasin (S100A7) expression and invasive breast cancer.* Am J Pathol, 1999. **155**(6): p. 2057-66.
372. Karvonen, S.L., et al., *Psoriasis and altered calcium metabolism: downregulated capacitative calcium influx and defective calcium-mediated cell signaling in cultured psoriatic keratinocytes.* J Invest Dermatol, 2000. **114**(4): p. 693-700.
373. Zhou, G., et al., *Reciprocal negative regulation between S100A7/psoriasin and beta-catenin signaling plays an important role in tumor progression of squamous cell carcinoma of oral cavity.* Oncogene, 2008. **27**(25): p. 3527-38.
374. Wolf, R., et al., *Highly homologous hS100A15 and hS100A7 proteins are distinctly expressed in normal breast tissue and breast cancer.* Cancer Lett, 2009. **277**(1): p. 101-7.
375. Emberley, E.D., et al., *Psoriasin (S100A7) expression is associated with poor outcome in estrogen receptor-negative invasive breast cancer.* Clin Cancer Res, 2003. **9**(7): p. 2627-31.
376. Emberley, E.D., L.C. Murphy, and P.H. Watson, *S100A7 and the progression of breast cancer.* Breast Cancer Res, 2004. **6**(4): p. 153-9.
377. Svenningsson, P., et al., *Alterations in 5-HT1B receptor function by p11 in depression-like states.* Science, 2006. **311**(5757): p. 77-80.
378. Svenningsson, P. and P. Greengard, *p11 (S100A10)--an inducible adaptor protein that modulates neuronal functions.* Curr Opin Pharmacol, 2007. **7**(1): p. 27-32.
379. Inada, H., et al., *Balance between activities of Rho kinase and type 1 protein phosphatase modulates turnover of phosphorylation and dynamics of desmin/vimentin filaments.* J Biol Chem, 1999. **274**(49): p. 34932-9.
380. Polans, A.S., et al., *Calcium-binding proteins and their assessment in ocular diseases.* Methods Enzymol, 2000. **316**: p. 103-21.
381. Tanaka, M., et al., *Human calgizzarin; one colorectal cancer-related gene selected by a large scale random cDNA sequencing and northern blot analysis.* Cancer Lett, 1995. **89**(2): p. 195-200.
382. Ohuchida, K., et al., *S100A11, a putative tumor suppressor gene, is overexpressed in pancreatic carcinogenesis.* Clin Cancer Res, 2006. **12**(18): p. 5417-22.
383. Rehman, I., et al., *Dysregulated expression of S100A11 (calgizzarin) in prostate cancer and precursor lesions.* Hum Pathol, 2004. **35**(11): p. 1385-91.
384. Landriscina, M., et al., *S100A13 participates in the release of fibroblast growth factor 1 in response to heat shock in vitro.* J Biol Chem, 2001. **276**(25): p. 22544-52.
385. Hayrabedyan, S., S. Kyurkchiev, and I. Kehayov, *FGF-1 and S100A13 possibly contribute to angiogenesis in endometriosis.* J Reprod Immunol, 2005. **67**(1-2): p. 87-101.
386. Guerreiro Da Silva, I.D., et al., *S100P calcium-binding protein overexpression is associated with immortalization of human breast epithelial cells in vitro and early stages of breast cancer development in vivo.* Int J Oncol, 2000. **16**(2): p. 231-40.
387. Valenzuela, S.M., Berkhan, M. , Porkovich, A. , Huynh, T. , Goyette, J. , Martin, D.M. , Geczy, C.L., *Soluble Structure of CLIC and S100 Proteins investigated by Atomic Force Microscopy.* Journal of Biomaterials and Nanotechnology, 2011. **2**(1): p. 8-17.
388. Ishikawa, K., et al., *The structure of human MRP8, a member of the S100 calcium-binding protein family, by MAD phasing at 1.9 A resolution.* Acta Crystallogr D Biol Crystallogr, 2000. **56**(Pt 5): p. 559-66.
389. Raftery, M.J. and C.L. Geczy, *Identification of noncovalent dimeric complexes of the recombinant murine S100 protein CP10 by electrospray ionization mass*

spectrometry and chemical cross-linking. J Am Soc Mass Spectrom, 1998. **9**(5): p. 533-9.
390. Hessian, P.A. and L. Fisher, *The heterodimeric complex of MRP-8 (S100A8) and MRP-14 (S100A9). Antibody recognition, epitope definition and the implications for structure.* Eur J Biochem, 2001. **268**(2): p. 353-63.
391. Hunter, M.J. and W.J. Chazin, *High level expression and dimer characterization of the S100 EF-hand proteins, migration inhibitory factor-related proteins 8 and 14.* J Biol Chem, 1998. **273**(20): p. 12427-35.
392. Korndorfer, I.P., F. Brueckner, and A. Skerra, *The crystal structure of the human (S100A8/S100A9)2 heterotetramer, calprotectin, illustrates how conformational changes of interacting alpha-helices can determine specific association of two EF-hand proteins.* J Mol Biol, 2007. **370**(5): p. 887-98.
393. Foell, D., et al., *S100 proteins expressed in phagocytes: a novel group of damage-associated molecular pattern molecules.* J Leukoc Biol, 2007. **81**(1): p. 28-37.
394. Clohessy, P.A. and B.E. Golden, *His-X-X-X-His motif in S100 protein, calprotectin: relation to microbiostatic activity.* J Leukoc Biol, 1996. **60**(5): p. 674.
395. Vogl, T., et al., *Biophysical characterization of S100A8 and S100A9 in the absence and presence of bivalent cations.* Biochim Biophys Acta, 2006. **1763**(11): p. 1298-306.
396. Fritz, G., et al., *Natural and amyloid self-assembly of S100 proteins: structural basis of functional diversity.* FEBS J, 2010. **277**(22): p. 4578-90.
397. Hessian, P.A., J. Edgeworth, and N. Hogg, *MRP-8 and MRP-14, two abundant Ca(2+)-binding proteins of neutrophils and monocytes.* J Leukoc Biol, 1993. **53**(2): p. 197-204.
398. Kumar, R.K., et al., *Dimeric S100A8 in human neutrophils is diminished after phagocytosis.* J Leukoc Biol, 2001. **70**(1): p. 59-64.
399. Kerkhoff, C., et al., *Binding of two nuclear complexes to a novel regulatory element within the human S100A9 promoter drives the S100A9 gene expression.* J Biol Chem, 2002. **277**(44): p. 41879-87.
400. Endoh, Y., et al., *IL-10-dependent S100A8 gene induction in monocytes/macrophages by double-stranded RNA.* J Immunol, 2009. **182**(4): p. 2258-68.
401. Kuruto, R., et al., *Myeloid calcium binding proteins: expression in the differentiated HL-60 cells and detection in sera of patients with connective tissue diseases.* J Biochem, 1990. **108**(4): p. 650-3.
402. Passey, R.J., et al., *S100A8: emerging functions and regulation.* J Leukoc Biol, 1999. **66**(4): p. 549-56.
403. Gebhardt, C., et al., *S100A8 and S100A9 in inflammation and cancer.* Biochem Pharmacol, 2006. **72**(11): p. 1622-31.
404. Cheng, P., et al., *Inhibition of dendritic cell differentiation and accumulation of myeloid-derived suppressor cells in cancer is regulated by S100A9 protein.* J Exp Med, 2008. **205**(10): p. 2235-49.
405. Roth, J., et al., *Phagocyte-specific S100 proteins: a novel group of proinflammatory molecules.* Trends Immunol, 2003. **24**(4): p. 155-8.
406. Hsu, K., et al., *Regulation of S100A8 by glucocorticoids.* J Immunol, 2005. **174**(4): p. 2318-26.
407. Xu, K. and C.L. Geczy, *IFN-gamma and TNF regulate macrophage expression of the chemotactic S100 protein S100A8.* J Immunol, 2000. **164**(9): p. 4916-23.

408. Zwadlo, G., et al., *Two calcium-binding proteins associated with specific stages of myeloid cell differentiation are expressed by subsets of macrophages in inflammatory tissues.* Clin Exp Immunol, 1988. **72**(3): p. 510-5.
409. Hogg, N., C. Allen, and J. Edgeworth, *Monoclonal antibody 5.5 reacts with p8,14, a myeloid molecule associated with some vascular endothelium.* Eur J Immunol, 1989. **19**(6): p. 1053-61.
410. McCormick, M.M., et al., *S100A8 and S100A9 in human arterial wall. Implications for atherogenesis.* J Biol Chem, 2005. **280**(50): p. 41521-9.
411. Yen, T., et al., *Induction of the S100 chemotactic protein, CP-10, in murine microvascular endothelial cells by proinflammatory stimuli.* Blood, 1997. **90**(12): p. 4812-21.
412. Coleman, N. and M.A. Stanley, *Expression of the myelomonocytic antigens CD36 and L1 by keratinocytes in squamous intraepithelial lesions of the cervix.* Hum Pathol, 1994. **25**(1): p. 73-9.
413. Eckert, R.L., et al., *S100 proteins in the epidermis.* J Invest Dermatol, 2004. **123**(1): p. 23-33.
414. Eversole, L.R., K.T. Miyasaki, and R.E. Christensen, *The distribution of the antimicrobial protein, calprotectin, in normal oral keratinocytes.* Arch Oral Biol, 1992. **37**(11): p. 963-8.
415. Eversole, L.R., K.T. Miyasaki, and R.E. Christensen, *Keratinocyte expression of calprotectin in oral inflammatory mucosal diseases.* J Oral Pathol Med, 1993. **22**(7): p. 303-7.
416. Grimbaldeston, M.A., et al., *S100A8 induction in keratinocytes by ultraviolet A irradiation is dependent on reactive oxygen intermediates.* J Invest Dermatol, 2003. **121**(5): p. 1168-74.
417. Akiyama, H., et al., *Expression of MRP14, 27E10, interferon-alpha and leukocyte common antigen by reactive microglia in postmortem human brain tissue.* J Neuroimmunol, 1994. **50**(2): p. 195-201.
418. Shepherd, C.E., et al., *Inflammatory S100A9 and S100A12 proteins in Alzheimer's disease.* Neurobiol Aging, 2006. **27**(11): p. 1554-63.
419. Rahimi, F., et al., *FGF-2, IL-1beta and TGF-beta regulate fibroblast expression of S100A8.* FEBS J, 2005. **272**(11): p. 2811-27.
420. Passey, R.J., et al., *A null mutation in the inflammation-associated S100 protein S100A8 causes early resorption of the mouse embryo.* J Immunol, 1999. **163**(4): p. 2209-16.
421. Vogl, T., et al., *Mrp8 and Mrp14 are endogenous activators of Toll-like receptor 4, promoting lethal, endotoxin-induced shock.* Nat Med, 2007. **13**(9): p. 1042-9.
422. Garcia, M.A., et al., *Impact of protein kinase PKR in cell biology: from antiviral to antiproliferative action.* Microbiol Mol Biol Rev, 2006. **70**(4): p. 1032-60.
423. Gebhardt, C., et al., *Calgranulins S100A8 and S100A9 are negatively regulated by glucocorticoids in a c-Fos-dependent manner and overexpressed throughout skin carcinogenesis.* Oncogene, 2002. **21**(27): p. 4266-76.
424. Murao, S., F. Collart, and E. Huberman, *A protein complex expressed during terminal differentiation of monomyelocytic cells is an inhibitor of cell growth.* Cell Growth Differ, 1990. **1**(10): p. 447-54.
425. Bai, B., et al., *Complex regulation of S100A8 by IL-17, dexamethasone, IL-4 and IL-13 in HaCat cells (human keratinocyte cell line).* J Dermatol Sci, 2007. **47**(3): p. 259-62.

426. Sellmayer, A., et al., *1 alpha,25-(OH)2 vitamin D3 enhances expression of the genes encoding Ca(2+)-binding proteins MRP-8 and MRP-14.* Am J Physiol, 1992. **262**(1 Pt 1): p. C235-42.
427. Lugering, N., et al., *Importance of combined treatment with IL-10 and IL-4, but not IL-13, for inhibition of monocyte release of the Ca(2+)-binding protein MRP8/14.* Immunology, 1997. **91**(1): p. 130-4.
428. Suryono, et al., *Norepinephrine stimulates calprotectin expression in human monocytic cells.* J Periodontal Res, 2006. **41**(3): p. 159-64.
429. Mork, G., et al., *Proinflammatory cytokines upregulate expression of calprotectin (L1 protein, MRP-8/MRP-14) in cultured human keratinocytes.* Br J Dermatol, 2003. **149**(3): p. 484-91.
430. Bozinovski, S., et al., *S100A8 chemotactic protein is abundantly increased, but only a minor contributor to LPS-induced, steroid resistant neutrophilic lung inflammation in vivo.* J Proteome Res, 2005. **4**(1): p. 136-45.
431. Robinson, M.J., et al., *The S100 family heterodimer, MRP-8/14, binds with high affinity to heparin and heparan sulfate glycosaminoglycans on endothelial cells.* J Biol Chem, 2002. **277**(5): p. 3658-65.
432. Brandtzaeg, P., I. Dale, and M.K. Fagerhol, *Distribution of a formalin-resistant myelomonocytic antigen (L1) in human tissues. II. Normal and aberrant occurrence in various epithelia.* Am J Clin Pathol, 1987. **87**(6): p. 700-7.
433. Dale, I. and P. Brandtzaeg, *Expression of the epithelial L1 antigen as an immunohistochemical marker of squamous cell carcinoma of the lung.* Histopathology, 1989. **14**(5): p. 493-502.
434. Gabrielsen, T.O., et al., *Epidermal and dermal distribution of a myelomonocytic antigen (L1) shared by epithelial cells in various inflammatory skin diseases.* J Am Acad Dermatol, 1986. **15**(2 Pt 1): p. 173-9.
435. Ehrchen, J.M., et al., *The endogenous Toll-like receptor 4 agonist S100A8/S100A9 (calprotectin) as innate amplifier of infection, autoimmunity, and cancer.* J Leukoc Biol, 2009. **86**(3): p. 557-66.
436. Bando, M., et al., *Interleukin-1alpha regulates antimicrobial peptide expression in human keratinocytes.* Immunol Cell Biol, 2007. **85**(7): p. 532-7.
437. Marionnet, C., et al., *Modulation of gene expression induced in human epidermis by environmental stress in vivo.* J Invest Dermatol, 2003. **121**(6): p. 1447-58.
438. Robinson, M.J. and N. Hogg, *A comparison of human S100A12 with MRP-14 (S100A9).* Biochem Biophys Res Commun, 2000. **275**(3): p. 865-70.
439. Hasegawa, T., et al., *The regulation of EN-RAGE (S100A12) gene expression in human THP-1 macrophages.* Atherosclerosis, 2003. **171**(2): p. 211-8.
440. Hofmann, M.A., et al., *RAGE mediates a novel proinflammatory axis: a central cell surface receptor for S100/calgranulin polypeptides.* Cell, 1999. **97**(7): p. 889-901.
441. Perera, C., H.P. McNeil, and C.L. Geczy, *S100 Calgranulins in inflammatory arthritis.* Immunol Cell Biol, 2010. **88**(1): p. 41-9.
442. Foell, D. and J. Roth, *Proinflammatory S100 proteins in arthritis and autoimmune disease.* Arthritis Rheum, 2004. **50**(12): p. 3762-71.
443. Gray, R.D., et al., *Sputum proteomics in inflammatory and suppurative respiratory diseases.* Am J Respir Crit Care Med, 2008. **178**(5): p. 444-52.
444. Leach, S.T., et al., *Serum and mucosal S100 proteins, calprotectin (S100A8/S100A9) and S100A12, are elevated at diagnosis in children with inflammatory bowel disease.* Scand J Gastroenterol, 2007. **42**(11): p. 1321-31.

445. Tibble, J.A. and I. Bjarnason, *Fecal calprotectin as an index of intestinal inflammation.* Drugs Today (Barc), 2001. **37**(2): p. 85-96.
446. Andersen, E., et al., *Myeloid-related protein (MRP8/14) expression in gingival crevice fluid in periodontal health and disease and after treatment.* J Periodontal Res, 2010. **45**(4): p. 458-63.
447. Kojima, T., et al., *Human gingival crevicular fluid contains MRP8 (S100A8) and MRP14 (S100A9), two calcium-binding proteins of the S100 family.* J Dent Res, 2000. **79**(2): p. 740-7.
448. Edgeworth, J.D., A. Abiose, and B.R. Jones, *An immunohistochemical analysis of onchocercal nodules: evidence for an interaction between macrophage MRP8/MRP14 and adult Onchocerca volvulus.* Clin Exp Immunol, 1993. **92**(1): p. 84-92.
449. Marti, T., K.D. Erttmann, and M.Y. Gallin, *Host-parasite interaction in human onchocerciasis: identification and sequence analysis of a novel human calgranulin.* Biochem Biophys Res Commun, 1996. **221**(2): p. 454-8.
450. Pechkovsky, D.V., et al., *Calprotectin (MRP8/14 protein complex) release during mycobacterial infection in vitro and in vivo.* FEMS Immunol Med Microbiol, 2000. **29**(1): p. 27-33.
451. Schweyer, S. and A. Fayyazi, *Activation and apoptosis of macrophages in cat scratch disease.* J Pathol, 2002. **198**(4): p. 534-40.
452. Bordmann, G., et al., *MRP 8/14 as marker for Plasmodium falciparum-induced malaria episodes in individuals in a holoendemic area.* Clin Diagn Lab Immunol, 1997. **4**(4): p. 435-9.
453. Goto, Y., et al., *Adhesion of MRP8/14 to amastigotes in skin lesions of Leishmania major-infected mice.* Exp Parasitol, 2008. **119**(1): p. 80-6.
454. Muller, F., et al., *Elevated serum calprotectin levels in HIV-infected patients: the calprotectin response during ZDV treatment is associated with clinical events.* J Acquir Immune Defic Syndr, 1994. **7**(9): p. 931-9.
455. Hashemi, F.B., et al., *Myeloid-related protein (MRP)-8 from cervico-vaginal secretions activates HIV replication.* AIDS, 2001. **15**(4): p. 441-9.
456. Strasser, F., P.L. Gowland, and C. Ruef, *Elevated serum macrophage inhibitory factor-related protein (MRP) 8/14 levels in advanced HIV infection and during disease exacerbation.* J Acquir Immune Defic Syndr Hum Retrovirol, 1997. **16**(4): p. 230-8.
457. Akpek, E.K., et al., *Identification of paramyosin as a binding protein for calgranulin C in experimental helminthic keratitis.* Invest Ophthalmol Vis Sci, 2002. **43**(8): p. 2677-84.
458. Russell, D.G., *Staphylococcus and the healing power of pus.* Cell Host Microbe, 2008. **3**(3): p. 115-6.
459. Sunderkotter, C.H., et al., *High expression of myeloid-related proteins 8 and 14 characterizes an inflammatorily active but ineffective response of macrophages during leprosy.* Immunology, 2004. **111**(4): p. 472-80.
460. Kane, D., et al., *Increased perivascular synovial membrane expression of myeloid-related proteins in psoriatic arthritis.* Arthritis Rheum, 2003. **48**(6): p. 1676-85.
461. Kiefer, R., et al., *Macrophage differentiation antigens in acute and chronic autoimmune polyneuropathies.* Brain, 1998. **121 (Pt 3)**: p. 469-79.
462. Lawrance, I.C., L. Maxwell, and W. Doe, *Altered response of intestinal mucosal fibroblasts to profibrogenic cytokines in inflammatory bowel disease.* Inflamm Bowel Dis, 2001. **7**(3): p. 226-36.

463. Floris, S., et al., *Monocyte activation and disease activity in multiple sclerosis. A longitudinal analysis of serum MRP8/14 levels.* J Neuroimmunol, 2004. **148**(1-2): p. 172-7.
464. Mikkelsen, S.E., et al., *S100A12 protein is a strong inducer of neurite outgrowth from primary hippocampal neurons.* J Neurochem, 2001. **79**(4): p. 767-76.
465. Shiose, A. and H. Sumimoto, *Arachidonic acid and phosphorylation synergistically induce a conformational change of p47phox to activate the phagocyte NADPH oxidase.* J Biol Chem, 2000. **275**(18): p. 13793-801.
466. Frosch, M., et al., *Expression of MRP8 and MRP14 by macrophages is a marker for severe forms of glomerulonephritis.* J Leukoc Biol, 2004. **75**(2): p. 198-206.
467. Lood, C., et al., *Protein synthesis of the pro-inflammatory S100A8/A9 complex in plasmacytoid dendritic cells and cell surface S100A8/A9 on leukocyte subpopulations in systemic lupus erythematosus.* Arthritis Res Ther, 2011. **13**(2): p. R60.
468. Soyfoo, M.S., et al., *Phagocyte-specific S100A8/A9 protein levels during disease exacerbations and infections in systemic lupus erythematosus.* J Rheumatol, 2009. **36**(10): p. 2190-4.
469. Ebihara, T., et al., *Differential gene expression of S100 protein family in leukocytes from patients with Kawasaki disease.* Eur J Pediatr, 2005. **164**(7): p. 427-31.
470. Foell, D., et al., *S100A12 (EN-RAGE) in monitoring Kawasaki disease.* Lancet, 2003. **361**(9365): p. 1270-2.
471. Hirono, K., et al., *Expression of myeloid-related protein-8 and -14 in patients with acute Kawasaki disease.* J Am Coll Cardiol, 2006. **48**(6): p. 1257-64.
472. Haga, H.J., et al., *Calprotectin in patients with systemic lupus erythematosus: relation to clinical and laboratory parameters of disease activity.* Lupus, 1993. **2**(1): p. 47-50.
473. Mirmohammadsadegh, A., et al., *Calgranulin C is overexpressed in lesional psoriasis.* J Invest Dermatol, 2000. **114**(6): p. 1207-8.
474. Semprini, S., et al., *Evidence for differential S100 gene over-expression in psoriatic patients from genetically heterogeneous pedigrees.* Hum Genet, 2002. **111**(4-5): p. 310-3.
475. Benoit, S., et al., *Elevated serum levels of calcium-binding S100 proteins A8 and A9 reflect disease activity and abnormal differentiation of keratinocytes in psoriasis.* Br J Dermatol, 2006. **155**(1): p. 62-6.
476. Wolk, K., et al., *IL-22 regulates the expression of genes responsible for antimicrobial defense, cellular differentiation, and mobility in keratinocytes: a potential role in psoriasis.* Eur J Immunol, 2006. **36**(5): p. 1309-23.
477. Kunz, M., et al., *Epidermal expression of the calcium binding surface antigen 27E10 in inflammatory skin diseases.* Arch Dermatol Res, 1992. **284**(7): p. 386-90.
478. Kim, M.H., et al., *The expression of RAGE and EN-RAGE in leprosy.* Br J Dermatol, 2006. **154**(4): p. 594-601.
479. Foell, D., et al., *Phagocyte-specific calcium-binding S100 proteins as clinical laboratory markers of inflammation.* Clin Chim Acta, 2004. **344**(1-2): p. 37-51.
480. Ye, F., et al., *Neutrophil-derived S100A12 is profoundly upregulated in the early stage of acute Kawasaki disease.* Am J Cardiol, 2004. **94**(6): p. 840-4.
481. Nijhuis, J., et al., *Neutrophil activation in morbid obesity, chronic activation of acute inflammation.* Obesity (Silver Spring), 2009. **17**(11): p. 2014-8.

482. Foell, D., et al., *Early recruitment of phagocytes contributes to the vascular inflammation of giant cell arteritis.* J Pathol, 2004. **204**(3): p. 311-6.
483. Miyamoto, S., et al., *Increased serum levels and expression of S100A8/A9 complex in infiltrated neutrophils in atherosclerotic plaque of unstable angina.* Heart, 2008. **94**(8): p. 1002-7.
484. Barthe, C., et al., *Identification of 'cystic fibrosis protein' as a complex of two calcium-binding proteins present in human cells of myeloid origin.* Biochim Biophys Acta, 1991. **1096**(2): p. 175-7.
485. Clohessy, P.A. and B.E. Golden, *Elevated plasma levels of L1L and L1H in CF patients.* Biochem Soc Trans, 1996. **24**(2): p. 310S.
486. Foell, D., et al., *Expression of S100A12 (EN-RAGE) in cystic fibrosis.* Thorax, 2003. **58**(7): p. 613-7.
487. Renaud, W., M. Merten, and C. Figarella, *Increased coexpression of CFTR and S100 calcium binding proteins MRP8 and MRP14 mRNAs in cystic fibrosis human tracheal gland cells.* Biochem Biophys Res Commun, 1994. **201**(3): p. 1518-25.
488. Golden, B.E., et al., *Calprotectin as a marker of inflammation in cystic fibrosis.* Arch Dis Child, 1996. **74**(2): p. 136-9.
489. Hayward, C., et al., *Serum concentrations of a granulocyte-derived calcium-binding protein in cystic fibrosis patients and heterozygotes.* Clin Chim Acta, 1987. **170**(1): p. 45-55.
490. Roth, J., et al., *Complex pattern of the myelo-monocytic differentiation antigens MRP8 and MRP14 during chronic airway inflammation.* Immunobiology, 1992. **186**(3-4): p. 304-14.
491. Tirkos, S., et al., *Expression of S100A8 correlates with inflammatory lung disease in congenic mice deficient of the cystic fibrosis transmembrane conductance regulator.* Respir Res, 2006. **7**: p. 51.
492. Gray, R.D., et al., *Sputum and serum calprotectin are useful biomarkers during CF exacerbation.* J Cyst Fibros, 2010. **9**(3): p. 193-8.
493. McMorran, B.J., et al., *Novel neutrophil-derived proteins in bronchoalveolar lavage fluid indicate an exaggerated inflammatory response in pediatric cystic fibrosis patients.* Clin Chem, 2007. **53**(10): p. 1782-91.
494. Buhling, F., et al., *MRP8/MRP14, CD11b and HLA-DR expression of alveolar macrophages in pneumonia.* Immunol Lett, 2000. **71**(3): p. 185-90.
495. Foell, D., H. Wittkowski, and J. Roth, *Mechanisms of disease: a 'DAMP' view of inflammatory arthritis.* Nat Clin Pract Rheumatol, 2007. **3**(7): p. 382-90.
496. Lorenz, E., et al., *Different expression ratio of S100A8/A9 and S100A12 in acute and chronic lung diseases.* Respir Med, 2008. **102**(4): p. 567-73.
497. Bargagli, E., et al., *Calgranulin B (S100A9/MRP14): a key molecule in idiopathic pulmonary fibrosis?* Inflammation, 2011. **34**(2): p. 85-91.
498. Schluesener, H.J., P.G. Kremsner, and R. Meyermann, *Widespread expression of MRP8 and MRP14 in human cerebral malaria by microglial cells.* Acta Neuropathol, 1998. **96**(6): p. 575-80.
499. Schwab, J.M., et al., *Selective accumulation of cyclooxygenase-1-expressing microglial cells/macrophages in lesions of human focal cerebral ischemia.* Acta Neuropathol, 2000. **99**(6): p. 609-14.
500. Engel, S., et al., *Dynamics of microglial activation after human traumatic brain injury are revealed by delayed expression of macrophage-related proteins MRP8 and MRP14.* Acta Neuropathol, 2000. **100**(3): p. 313-22.

501. Schweyer, S., et al., *Continuous recruitment, co-expression of tumour necrosis factor-alpha and matrix metalloproteinases, and apoptosis of macrophages in gout tophi.* Virchows Arch, 2000. **437**(5): p. 534-9.
502. Greitemann, B., et al., *Inflammatory reactions in primary osteoarthritis of the hip and total hip prosthesis loosening.* Arch Orthop Trauma Surg, 1992. **111**(3): p. 138-41.
503. Burkhardt, K., et al., *An increase in myeloid-related protein serum levels precedes acute renal allograft rejection.* J Am Soc Nephrol, 2001. **12**(9): p. 1947-57.
504. Zali, H., et al., *On the mechanism of apoptosis-inducing activity of human calprotectin: zinc sequestration, induction of a signaling pathway, or something else?* Med Hypotheses, 2007. **68**(5): p. 1012-5.
505. Fessatou, S., et al., *Severe anemia and neutropenia associated with hyperzincemia and hypercalprotectinemia.* J Pediatr Hematol Oncol, 2005. **27**(9): p. 477-80.
506. Boso, M., et al., *Alterations of circulating endogenous secretory RAGE and S100A9 levels indicating dysfunction of the AGE-RAGE axis in autism.* Neurosci Lett, 2006. **410**(3): p. 169-73.
507. Tong, L., et al., *Association of tear proteins with Meibomian gland disease and dry eye symptoms.* Br J Ophthalmol, 2011. **95**(6): p. 848-52.
508. Li, C., F. Zhang, and Y. Wang, *S100A proteins in the pathogenesis of experimental corneal neovascularization.* Mol Vis, 2010. **16**: p. 2225-35.
509. Zhou, L., et al., *Elevation of human alpha-defensins and S100 calcium-binding proteins A8 and A9 in tear fluid of patients with pterygium.* Invest Ophthalmol Vis Sci, 2009. **50**(5): p. 2077-86.
510. Kaiser, T., et al., *Faecal S100A12 as a non-invasive marker distinguishing inflammatory bowel disease from irritable bowel syndrome.* Gut, 2007. **56**(12): p. 1706-13.
511. Abtin, A., et al., *The antimicrobial heterodimer S100A8/S100A9 (calprotectin) is upregulated by bacterial flagellin in human epidermal keratinocytes.* J Invest Dermatol, 2010. **130**(10): p. 2423-30.
512. Corbin, B.D., et al., *Metal chelation and inhibition of bacterial growth in tissue abscesses.* Science, 2008. **319**(5865): p. 962-5.
513. Lugering, N., et al., *Serum 27E10 antigen: a new potential marker for staging HIV disease.* Clin Exp Immunol, 1995. **101**(2): p. 249-53.
514. Nakatani, Y., et al., *Regulation of S100A8/A9 (calprotectin) binding to tumor cells by zinc ion and its implication for apoptosis-inducing activity.* Mediators Inflamm, 2005. **2005**(5): p. 280-92.
515. Martin, S.J., et al., *Programmed cell death (apoptosis) in lymphoid and myeloid cell lines during zinc deficiency.* Clin Exp Immunol, 1991. **83**(2): p. 338-43.
516. Jaramillo, M., et al., *Hemozoin-inducible proinflammatory events in vivo: potential role in malaria infection.* J Immunol, 2004. **172**(5): p. 3101-10.
517. Dorin, J.R., et al., *A clue to the basic defect in cystic fibrosis from cloning the CF antigen gene.* Nature, 1987. **326**(6113): p. 614-7.
518. Stockley, R.A., et al., *Relationship of neutrophil cytoplasmic protein (L1) to acute and chronic lung disease.* Scand J Clin Lab Invest, 1984. **44**(7): p. 629-34.
519. MacGregor, G., et al., *Biomarkers for cystic fibrosis lung disease: application of SELDI-TOF mass spectrometry to BAL fluid.* J Cyst Fibros, 2008. **7**(5): p. 352-8.
520. Thomas, G.R., et al., *G551D cystic fibrosis mice exhibit abnormal regulation of inflammation in lungs and macrophages.* J Immunol, 2000. **164**(7): p. 3870-7.
521. Korthagen, N.M., et al., *MRP14 is elevated in the bronchoalveolar lavage fluid of fibrosing interstitial lung diseases.* Clin Exp Immunol, 2010. **161**(2): p. 342-7.

522. Nacken, W., et al., *S100A9/S100A8: Myeloid representatives of the S100 protein family as prominent players in innate immunity.* Microsc Res Tech, 2003. **60**(6): p. 569-80.
523. Lau, W., J.M. Devery, and C.L. Geczy, *A chemotactic S100 peptide enhances scavenger receptor and Mac-1 expression and cholesteryl ester accumulation in murine peritoneal macrophages in vivo.* J Clin Invest, 1995. **95**(5): p. 1957-65.
524. Altwegg, L.A., et al., *Myeloid-related protein 8/14 complex is released by monocytes and granulocytes at the site of coronary occlusion: a novel, early, and sensitive marker of acute coronary syndromes.* Eur Heart J, 2007. **28**(8): p. 941-8.
525. Morrow, D.A., et al., *Myeloid-related protein 8/14 and the risk of cardiovascular death or myocardial infarction after an acute coronary syndrome in the Pravastatin or Atorvastatin Evaluation and Infection Therapy: Thrombolysis in Myocardial Infarction (PROVE IT-TIMI 22) trial.* Am Heart J, 2008. **155**(1): p. 49-55.
526. Brugada, P. and J. Brugada, *Right bundle branch block, persistent ST segment elevation and sudden cardiac death: a distinct clinical and electrocardiographic syndrome. A multicenter report.* J Am Coll Cardiol, 1992. **20**(6): p. 1391-6.
527. Eue, I., et al., *Myeloid related protein (MRP) 14 expressing monocytes infiltrate atherosclerotic lesions of ApoE null mice.* Atherosclerosis, 2000. **151**(2): p. 593-7.
528. Croce, K., et al., *Myeloid-related protein-8/14 is critical for the biological response to vascular injury.* Circulation, 2009. **120**(5): p. 427-36.
529. Goyette, J., et al., *Pleiotropic roles of S100A12 in coronary atherosclerotic plaque formation and rupture.* J Immunol, 2009. **183**(1): p. 593-603.
530. Burke, A.P., et al., *Morphologic findings of coronary atherosclerotic plaques in diabetics: a postmortem study.* Arterioscler Thromb Vasc Biol, 2004. **24**(7): p. 1266-71.
531. Mori, Y., et al., *Increased plasma S100A12 (EN-RAGE) levels in hemodialysis patients with atherosclerosis.* Am J Nephrol, 2009. **29**(1): p. 18-24.
532. Kleemann, R., S. Zadelaar, and T. Kooistra, *Cytokines and atherosclerosis: a comprehensive review of studies in mice.* Cardiovasc Res, 2008. **79**(3): p. 360-76.
533. Chen, Y.S., et al., *Serum levels of soluble receptor for advanced glycation end products and of S100 proteins are associated with inflammatory, autoantibody, and classical risk markers of joint and vascular damage in rheumatoid arthritis.* Arthritis Res Ther, 2009. **11**(2): p. R39.
534. Frosch, M., et al., *Myeloid-related proteins 8 and 14 are specifically secreted during interaction of phagocytes and activated endothelium and are useful markers for monitoring disease activity in pauciarticular-onset juvenile rheumatoid arthritis.* Arthritis Rheum, 2000. **43**(3): p. 628-37.
535. Foell, D., et al., *Expression of the pro-inflammatory protein S100A12 (EN-RAGE) in rheumatoid and psoriatic arthritis.* Rheumatology (Oxford), 2003. **42**(11): p. 1383-9.
536. Hofmann, M.A., et al., *RAGE and arthritis: the G82S polymorphism amplifies the inflammatory response.* Genes Immun, 2002. **3**(3): p. 123-35.
537. Foell, D., et al., *Neutrophil derived human S100A12 (EN-RAGE) is strongly expressed during chronic active inflammatory bowel disease.* Gut, 2003. **52**(6): p. 847-53.
538. Leach, S.T. and A.S. Day, *S100 proteins in the pathogenesis and diagnosis of inflammatory bowel disease.* Expert Rev Clin Immunol, 2006. **2**(3): p. 471-80.

539. Sidler, M.A., S.T. Leach, and A.S. Day, *Fecal S100A12 and fecal calprotectin as noninvasive markers for inflammatory bowel disease in children.* Inflamm Bowel Dis, 2008. **14**(3): p. 359-66.
540. Koon, N., et al., *Clustering of molecular alterations in gastroesophageal carcinomas.* Neoplasia, 2004. **6**(2): p. 143-9.
541. Sy, S.M., et al., *Regional over-representations on chromosomes 1q, 3q and 7q in the progression of hepatitis B virus-related hepatocellular carcinoma.* Mod Pathol, 2005. **18**(5): p. 686-92.
542. Moinzadeh, P., et al., *Chromosome alterations in human hepatocellular carcinomas correlate with aetiology and histological grade--results of an explorative CGH meta-analysis.* Br J Cancer, 2005. **92**(5): p. 935-41.
543. Knosel, T., et al., *Incidence of chromosomal imbalances in advanced colorectal carcinomas and their metastases.* Virchows Arch, 2002. **440**(2): p. 187-94.
544. Petersen, S., et al., *Chromosomal alterations in the clonal evolution to the metastatic stage of squamous cell carcinomas of the lung.* Br J Cancer, 2000. **82**(1): p. 65-73.
545. Sy, S.M., et al., *Distinct patterns of genetic alterations in adenocarcinoma and squamous cell carcinoma of the lung.* Eur J Cancer, 2004. **40**(7): p. 1082-94.
546. Goeze, A., et al., *Chromosomal imbalances of primary and metastatic lung adenocarcinomas.* J Pathol, 2002. **196**(1): p. 8-16.
547. Jee, K.J., et al., *Gain in 1q is a common abnormality in phyllodes tumours of the breast.* Anal Cell Pathol, 2003. **25**(2): p. 89-93.
548. Hayashi, M., et al., *Genomic alterations detected by comparative genomic hybridization in primary lung adenocarcinomas with special reference to the relationship with DNA ploidy.* Oncol Rep, 2005. **14**(6): p. 1429-35.
549. Bridge, J.A., et al., *Cytogenetic findings in 73 osteosarcoma specimens and a review of the literature.* Cancer Genet Cytogenet, 1997. **95**(1): p. 74-87.
550. Lamb, J.A., et al., *JunD mediates survival signaling by the JNK signal transduction pathway.* Mol Cell, 2003. **11**(6): p. 1479-89.
551. Lau, C.C., et al., *Frequent amplification and rearrangement of chromosomal bands 6p12-p21 and 17p11.2 in osteosarcoma.* Genes Chromosomes Cancer, 2004. **39**(1): p. 11-21.
552. Letson, G.D. and C.A. Muro-Cacho, *Genetic and molecular abnormalities in tumors of the bone and soft tissues.* Cancer Control, 2001. **8**(3): p. 239-51.
553. Ozaki, T., et al., *Genetic imbalances revealed by comparative genomic hybridization in osteosarcomas.* Int J Cancer, 2002. **102**(4): p. 355-65.
554. Glinsky, G.V., Y.A. Ivanova, and A.B. Glinskii, *Common malignancy-associated regions of transcriptional activation (MARTA) in human prostate, breast, ovarian, and colon cancers are targets for DNA amplification.* Cancer Lett, 2003. **201**(1): p. 67-77.
555. Glinsky, G.V., A. Krones-Herzig, and A.B. Glinskii, *Malignancy-associated regions of transcriptional activation: gene expression profiling identifies common chromosomal regions of a recurrent transcriptional activation in human prostate, breast, ovarian, and colon cancers.* Neoplasia, 2003. **5**(3): p. 218-28.
556. Ju, W., et al., *Identification of genes with differential expression in chemoresistant epithelial ovarian cancer using high-density oligonucleotide microarrays.* Oncol Res, 2009. **18**(2-3): p. 47-56.
557. Hermani, A., et al., *S100A8 and S100A9 activate MAP kinase and NF-kappaB signaling pathways and trigger translocation of RAGE in human prostate cancer cells.* Exp Cell Res, 2006. **312**(2): p. 184-97.

558. Li, C., et al., *Induction of S100A9 gene expression by cytokine oncostatin M in breast cancer cells through the STAT3 signaling cascade.* Breast Cancer Res Treat, 2004. **87**(2): p. 123-34.
559. Arai, K., et al., *S100A9 expression in invasive ductal carcinoma of the breast: S100A9 expression in adenocarcinoma is closely associated with poor tumour differentiation.* Eur J Cancer, 2004. **40**(8): p. 1179-87.
560. Talmadge, J.E., *Pathways mediating the expansion and immunosuppressive activity of myeloid-derived suppressor cells and their relevance to cancer therapy.* Clin Cancer Res, 2007. **13**(18 Pt 1): p. 5243-8.
561. Varga, G., et al., *Glucocorticoids induce an activated, anti-inflammatory monocyte subset in mice that resembles myeloid-derived suppressor cells.* J Leukoc Biol, 2008. **84**(3): p. 644-50.
562. Kaplan, R.N., et al., *VEGFR1-positive haematopoietic bone marrow progenitors initiate the pre-metastatic niche.* Nature, 2005. **438**(7069): p. 820-7.
563. Hiratsuka, S., et al., *MMP9 induction by vascular endothelial growth factor receptor-1 is involved in lung-specific metastasis.* Cancer Cell, 2002. **2**(4): p. 289-300.
564. Hiratsuka, S., et al., *Tumour-mediated upregulation of chemoattractants and recruitment of myeloid cells predetermines lung metastasis.* Nat Cell Biol, 2006. **8**(12): p. 1369-75.
565. Thorey, I.S., et al., *The Ca2+-binding proteins S100A8 and S100A9 are encoded by novel injury-regulated genes.* J Biol Chem, 2001. **276**(38): p. 35818-25.
566. Schmidt, M., et al., *Selective expression of calcium-binding proteins S100a8 and S100a9 at distinct sites of hair follicles.* J Invest Dermatol, 2001. **117**(3): p. 748-50.
567. Ribe, A. and N.S. McNutt, *S100A6 protein expression is different in Spitz nevi and melanomas.* Mod Pathol, 2003. **16**(5): p. 505-11.
568. Hume, D.A., S.J. Monkley, and B.J. Wainwright, *Detection of c-fms protooncogene in early mouse embryos by whole mount in situ hybridization indicates roles for macrophages in tissue remodelling.* Br J Haematol, 1995. **90**(4): p. 939-42.
569. Brandon, J.M., *Leucocyte distribution in the uterus during the preimplantation period of pregnancy and phagocyte recruitment to sites of blastocyst attachment in mice.* J Reprod Fertil, 1993. **98**(2): p. 567-76.
570. Orlando-Mathur, C.E. and T.G. Kennedy, *An investigation into the role of neutrophils in decidualization and early pregnancy in the rat.* Biol Reprod, 1993. **48**(6): p. 1258-65.
571. Hobbs, J.A., et al., *Myeloid cell function in MRP-14 (S100A9) null mice.* Mol Cell Biol, 2003. **23**(7): p. 2564-76.
572. Manitz, M.P., et al., *Loss of S100A9 (MRP14) results in reduced interleukin-8-induced CD11b surface expression, a polarized microfilament system, and diminished responsiveness to chemoattractants in vitro.* Mol Cell Biol, 2003. **23**(3): p. 1034-43.
573. Kuwayama, A., et al., *Appearance of nuclear factors that interact with genes for myeloid calcium binding proteins (MRP-8 and MRP-14) in differentiated HL-60 cells.* Blood, 1993. **81**(11): p. 3116-21.
574. Lagasse, E. and R.G. Clerc, *Cloning and expression of two human genes encoding calcium-binding proteins that are regulated during myeloid differentiation.* Mol Cell Biol, 1988. **8**(6): p. 2402-10.

575. Goebeler, M., et al., *Expression and complex assembly of calcium-binding proteins MRP8 and MRP14 during differentiation of murine myelomonocytic cells.* J Leukoc Biol, 1993. **53**(1): p. 11-8.
576. Yousefi, R., et al., *Investigation on the surface hydrophobicity and aggregation kinetics of human calprotectin in the presence of calcium.* J Biochem Mol Biol, 2005. **38**(4): p. 407-13.
577. Nacken, W., et al., *S100A9 deficiency alters adenosine-5'-triphosphate induced calcium signalling but does not generally interfere with calcium and zinc homeostasis in murine neutrophils.* Int J Biochem Cell Biol, 2005. **37**(6): p. 1241-53.
578. Lodie, T.A., et al., *Stimulation of macrophages by lipopolysaccharide alters the phosphorylation state, conformation, and function of PU.1 via activation of casein kinase II.* J Immunol, 1997. **158**(4): p. 1848-56.
579. Siegenthaler, G., et al., *A heterocomplex formed by the calcium-binding proteins MRP8 (S100A8) and MRP14 (S100A9) binds unsaturated fatty acids with high affinity.* J Biol Chem, 1997. **272**(14): p. 9371-7.
580. Kerkhoff, C., et al., *The two calcium-binding proteins, S100A8 and S100A9, are involved in the metabolism of arachidonic acid in human neutrophils.* J Biol Chem, 1999. **274**(46): p. 32672-9.
581. Sopalla, C., et al., *Evidence for the involvement of the unique C-tail of S100A9 in the binding of arachidonic acid to the heterocomplex S100A8/A9.* Biol Chem, 2002. **383**(12): p. 1895-905.
582. Roulin, K., et al., *The fatty acid-binding heterocomplex FA-p34 formed by S100A8 and S100A9 is the major fatty acid carrier in neutrophils and translocates from the cytosol to the membrane upon stimulation.* Exp Cell Res, 1999. **247**(2): p. 410-21.
583. Hii, C.S. and A. Ferrante, *Regulation of the NADPH oxidase activity and anti-microbial function of neutrophils by arachidonic acid.* Arch Immunol Ther Exp (Warsz), 2007. **55**(2): p. 99-110.
584. Benedyk, M., et al., *HaCaT keratinocytes overexpressing the S100 proteins S100A8 and S100A9 show increased NADPH oxidase and NF-kappaB activities.* J Invest Dermatol, 2007. **127**(8): p. 2001-11.
585. Lemarchand, P., et al., *Translocation of a small cytosolic calcium-binding protein (MRP-8) to plasma membrane correlates with human neutrophil activation.* J Biol Chem, 1992. **267**(27): p. 19379-82.
586. Bhardwaj, R.S., et al., *The calcium-binding proteins MRP8 and MRP14 form a membrane-associated heterodimer in a subset of monocytes/macrophages present in acute but absent in chronic inflammatory lesions.* Eur J Immunol, 1992. **22**(7): p. 1891-7.
587. Lominadze, G., et al., *Myeloid-related protein-14 is a p38 MAPK substrate in human neutrophils.* J Immunol, 2005. **174**(11): p. 7257-67.
588. Edgeworth, J., P. Freemont, and N. Hogg, *Ionomycin-regulated phosphorylation of the myeloid calcium-binding protein p14.* Nature, 1989. **342**(6246): p. 189-92.
589. Leukert, N., et al., *Calcium-dependent tetramer formation of S100A8 and S100A9 is essential for biological activity.* J Mol Biol, 2006. **359**(4): p. 961-72.
590. Nisapakultorn, K., K.F. Ross, and M.C. Herzberg, *Calprotectin expression in vitro by oral epithelial cells confers resistance to infection by Porphyromonas gingivalis.* Infect Immun, 2001. **69**(7): p. 4242-7.

591. Nisapakultorn, K., K.F. Ross, and M.C. Herzberg, *Calprotectin expression inhibits bacterial binding to mucosal epithelial cells.* Infect Immun, 2001. **69**(6): p. 3692-6.
592. Zaia, A.A., et al., *Subversion of antimicrobial calprotectin (S100A8/S100A9 complex) in the cytoplasm of TR146 epithelial cells after invasion by Listeria monocytogenes.* Mucosal Immunol, 2009. **2**(1): p. 43-53.
593. Champaiboon, C., et al., *Calprotectin S100A9 calcium-binding loops I and II are essential for keratinocyte resistance to bacterial invasion.* J Biol Chem, 2009. **284**(11): p. 7078-90.
594. Watt, K.W., I.L. Brightman, and E.J. Goetzl, *Isolation of two polypeptides comprising the neutrophil-immobilizing factor of human leucocytes.* Immunology, 1983. **48**(1): p. 79-86.
595. Sohnle, P.G. and B.L. Hahn, *Effect of zinc-reversible growth-inhibitory activity in human empyema fluid on antibiotic microbicidal activity.* Antimicrob Agents Chemother, 2000. **44**(1): p. 139-42.
596. van den Bos, C., et al., *Phosphorylation of MRP14, an S100 protein expressed during monocytic differentiation, modulates Ca(2+)-dependent translocation from cytoplasm to membranes and cytoskeleton.* J Immunol, 1996. **156**(3): p. 1247-54.
597. Leslie, C.C., *Regulation of arachidonic acid availability for eicosanoid production.* Biochem Cell Biol, 2004. **82**(1): p. 1-17.
598. Wu, N. and J.M. Davidson, *Migration inhibitory factor-related protein (MRP)8 and MRP14 are differentially expressed in free-electron laser and scalpel incisions.* Wound Repair Regen, 2004. **12**(3): p. 327-36.
599. Isaksen, B. and M.K. Fagerhol, *Calprotectin inhibits matrix metalloproteinases by sequestration of zinc.* Mol Pathol, 2001. **54**(5): p. 289-92.
600. Nacken, W. and C. Kerkhoff, *The hetero-oligomeric complex of the S100A8/S100A9 protein is extremely protease resistant.* FEBS Lett, 2007. **581**(26): p. 5127-30.
601. Greenlee, K.J., et al., *Proteomic identification of in vivo substrates for matrix metalloproteinases 2 and 9 reveals a mechanism for resolution of inflammation.* J Immunol, 2006. **177**(10): p. 7312-21.
602. Gold, L.I., et al., *Type I (RI) and type II (RII) receptors for transforming growth factor-beta isoforms are expressed subsequent to transforming growth factor-beta ligands during excisional wound repair.* Am J Pathol, 1997. **150**(1): p. 209-22.
603. Pierce, G.F., et al., *Platelet-derived growth factor (BB homodimer), transforming growth factor-beta 1, and basic fibroblast growth factor in dermal wound healing. Neovessel and matrix formation and cessation of repair.* Am J Pathol, 1992. **140**(6): p. 1375-88.
604. Ueda, Y., et al., *Inhibition of FGF-induced alphaA-crystallin promoter activity in lens epithelial explants by TGFbeta.* Invest Ophthalmol Vis Sci, 2000. **41**(7): p. 1833-9.
605. Harrison, C.A., et al., *Oxidation regulates the inflammatory properties of the murine S100 protein S100A8.* J Biol Chem, 1999. **274**(13): p. 8561-9.
606. Raftery, M.J., et al., *Novel intra- and inter-molecular sulfinamide bonds in S100A8 produced by hypochlorite oxidation.* J Biol Chem, 2001. **276**(36): p. 33393-401.
607. Hatakeyama, T., et al., *Identification of intracellular target proteins of the calcium-signaling protein S100A12.* Eur J Biochem, 2004. **271**(18): p. 3765-75.
608. Pietzsch, J. and S. Hoppmann, *Human S100A12: a novel key player in inflammation?* Amino Acids, 2009. **36**(3): p. 381-9.

609. Hofmann Bowman, M., et al., *S100A12 mediates aortic wall remodeling and aortic aneurysm.* Circ Res, 2010. **106**(1): p. 145-54.
610. Hofmann Bowman, M.A., et al., *S100A12 in vascular smooth muscle accelerates vascular calcification in apolipoprotein E-null mice by activating an osteogenic gene regulatory program.* Arterioscler Thromb Vasc Biol, 2011. **31**(2): p. 337-44.
611. Anceriz, N., K. Vandal, and P.A. Tessier, *S100A9 mediates neutrophil adhesion to fibronectin through activation of beta2 integrins.* Biochem Biophys Res Commun, 2007. **354**(1): p. 84-9.
612. Sroussi, H.Y., et al., *S100A8 triggers oxidation-sensitive repulsion of neutrophils.* J Dent Res, 2006. **85**(9): p. 829-33.
613. Lim, S.Y., et al., *S-nitrosylated S100A8: novel anti-inflammatory properties.* J Immunol, 2008. **181**(8): p. 5627-36.
614. Sroussi, H.Y., J. Berline, and J.M. Palefsky, *Oxidation of methionine 63 and 83 regulates the effect of S100A9 on the migration of neutrophils in vitro.* J Leukoc Biol, 2007. **81**(3): p. 818-24.
615. Hessian, P.A., L. Wilkinson, and N. Hogg, *The S100 family protein MRP-14 (S100A9) has homology with the contact domain of high molecular weight kininogen.* FEBS Lett, 1995. **371**(3): p. 271-5.
616. Pagano, R.L., et al., *Neutrophils and the calcium-binding protein MRP-14 mediate carrageenan-induced antinociception in mice.* Mediators Inflamm, 2002. **11**(4): p. 203-10.
617. Pagano, R.L., M. Mariano, and R. Giorgi, *Neutrophilic cell-free exudate induces antinociception mediate by the protein S100A9.* Mediators Inflamm, 2006. **2006**(4): p. 36765.
618. Aguiar-Passeti, T., et al., *Epithelioid cells from foreign-body granuloma selectively express the calcium-binding protein MRP-14, a novel down-regulatory molecule of macrophage activation.* J Leukoc Biol, 1997. **62**(6): p. 852-8.
619. Kerkhoff, C., et al., *Interaction of S100A8/S100A9-arachidonic acid complexes with the scavenger receptor CD36 may facilitate fatty acid uptake by endothelial cells.* Biochemistry, 2001. **40**(1): p. 241-8.
620. Murthy, A.R., et al., *In vitro candidastatic properties of the human neutrophil calprotectin complex.* J Immunol, 1993. **151**(11): p. 6291-301.
621. Sohnle, P.G., et al., *Zinc-reversible antimicrobial activity of recombinant calprotectin (migration inhibitory factor-related proteins 8 and 14).* J Infect Dis, 2000. **182**(4): p. 1272-5.
622. Viemann, D., et al., *MRP8/MRP14 impairs endothelial integrity and induces a caspase-dependent and -independent cell death program.* Blood, 2007. **109**(6): p. 2453-60.
623. Viemann, D., et al., *Myeloid-related proteins 8 and 14 induce a specific inflammatory response in human microvascular endothelial cells.* Blood, 2005. **105**(7): p. 2955-62.
624. Yong, H.Y. and A. Moon, *Roles of calcium-binding proteins, S100A8 and S100A9, in invasive phenotype of human gastric cancer cells.* Arch Pharm Res, 2007. **30**(1): p. 75-81.
625. van Lent, P.L., et al., *Myeloid-related proteins S100A8/S100A9 regulate joint inflammation and cartilage destruction during antigen-induced arthritis.* Ann Rheum Dis, 2008. **67**(12): p. 1750-8.
626. Pouliot, P., et al., *Myeloid-related proteins rapidly modulate macrophage nitric oxide production during innate immune response.* J Immunol, 2008. **181**(5): p. 3595-601.

627. van Lent, P.L., et al., *Stimulation of chondrocyte-mediated cartilage destruction by S100A8 in experimental murine arthritis.* Arthritis Rheum, 2008. **58**(12): p. 3776-87.
628. Raftery, M.J. and C.L. Geczy, *Electrospray low energy CID and MALDI PSD fragmentations of protonated sulfinamide cross-linked peptides.* J Am Soc Mass Spectrom, 2002. **13**(6): p. 709-18.
629. Dale, C.S., et al., *The C-terminus of murine S100A9 inhibits hyperalgesia and edema induced by jararhagin.* Peptides, 2004. **25**(1): p. 81-9.
630. Dale, C.S., et al., *Effect of the C-terminus of murine S100A9 protein on experimental nociception.* Peptides, 2006. **27**(11): p. 2794-802.
631. Ikemoto, M., et al., *Intrinsic function of S100A8/A9 complex as an anti-inflammatory protein in liver injury induced by lipopolysaccharide in rats.* Clin Chim Acta, 2007. **376**(1-2): p. 197-204.
632. Cole, A.M., et al., *Calcitermin, a novel antimicrobial peptide isolated from human airway secretions.* FEBS Lett, 2001. **504**(1-2): p. 5-10.
633. Voganatsi, A., et al., *Mechanism of extracellular release of human neutrophil calprotectin complex.* J Leukoc Biol, 2001. **70**(1): p. 130-4.
634. Kido, J., et al., *Calprotectin release from human neutrophils is induced by Porphyromonas gingivalis lipopolysaccharide via the CD-14-Toll-like receptor-nuclear factor kappaB pathway.* J Periodontal Res, 2003. **38**(6): p. 557-63.
635. Hetland, G., G.J. Talgo, and M.K. Fagerhol, *Chemotaxins C5a and fMLP induce release of calprotectin (leucocyte L1 protein) from polymorphonuclear cells in vitro.* Mol Pathol, 1998. **51**(3): p. 143-8.
636. Devery, J.M., N.J. King, and C.L. Geczy, *Acute inflammatory activity of the S100 protein CP-10. Activation of neutrophils in vivo and in vitro.* J Immunol, 1994. **152**(4): p. 1888-97.
637. Lim, S.Y., et al., *S-glutathionylation regulates inflammatory activities of S100A9.* J Biol Chem, 2010. **285**(19): p. 14377-88.
638. Eue, I., et al., *Transendothelial migration of 27E10+ human monocytes.* Int Immunol, 2000. **12**(11): p. 1593-604.
639. Poltorak, A., et al., *Defective LPS signaling in C3H/HeJ and C57BL/10ScCr mice: mutations in Tlr4 gene.* Science, 1998. **282**(5396): p. 2085-8.
640. Schnekenburger, J., et al., *The calcium binding protein S100A9 is essential for pancreatic leukocyte infiltration and induces disruption of cell-cell contacts.* J Cell Physiol, 2008. **216**(2): p. 558-67.
641. McNeill, E., et al., *Defective chemoattractant-induced calcium signalling in S100A9 null neutrophils.* Cell Calcium, 2007. **41**(2): p. 107-21.
642. Galli, S.J., S. Nakae, and M. Tsai, *Mast cells in the development of adaptive immune responses.* Nat Immunol, 2005. **6**(2): p. 135-42.
643. Robbie-Ryan, M. and M. Brown, *The role of mast cells in allergy and autoimmunity.* Curr Opin Immunol, 2002. **14**(6): p. 728-33.
644. Zhao, J., et al., *S100A8 modulates mast cell function and suppresses eosinophil migration in acute asthma.* Antioxid Redox Signal, 2011. **14**(9): p. 1589-600.
645. Suzuki, Y., et al., *Fc epsilon RI signaling of mast cells activates intracellular production of hydrogen peroxide: role in the regulation of calcium signals.* J Immunol, 2003. **171**(11): p. 6119-27.
646. Forsythe, P. and A.D. Befus, *Inhibition of calpain is a component of nitric oxide-induced down-regulation of human mast cell adhesion.* J Immunol, 2003. **170**(1): p. 287-93.

647. Coleman, J.W., *Nitric oxide: a regulator of mast cell activation and mast cell-mediated inflammation.* Clin Exp Immunol, 2002. **129**(1): p. 4-10.
648. Brun, J.G., et al., *Effects of calprotectin in avridine-induced arthritis.* APMIS, 1995. **103**(3): p. 233-40.
649. Dale, C.S., et al., *The C-terminus of murine S100A9 protein inhibits hyperalgesia induced by the agonist peptide of protease-activated receptor 2 (PAR2).* Br J Pharmacol, 2006. **149**(4): p. 374-84.
650. Mitchell, K., et al., *Localization of S100A8 and S100A9 expressing neutrophils to spinal cord during peripheral tissue inflammation.* Pain, 2008. **134**(1-2): p. 216-31.
651. van Zoelen, M.A., et al., *Expression and role of myeloid-related protein-14 in clinical and experimental sepsis.* Am J Respir Crit Care Med, 2009. **180**(11): p. 1098-106.
652. Sohnle, P.G., B.L. Hahn, and V. Santhanagopalan, *Inhibition of Candida albicans growth by calprotectin in the absence of direct contact with the organisms.* J Infect Dis, 1996. **174**(6): p. 1369-72.
653. Geerlings, S.E., et al., *Effect of glucose and pH on uropathogenic and non-uropathogenic Escherichia coli: studies with urine from diabetic and non-diabetic individuals.* J Med Microbiol, 1999. **48**(6): p. 535-9.
654. Lulloff, S.J., B.L. Hahn, and P.G. Sohnle, *Fungal susceptibility to zinc deprivation.* J Lab Clin Med, 2004. **144**(4): p. 208-14.
655. Sroussi, H.Y., et al., *Substitution of methionine 63 or 83 in S100A9 and cysteine 42 in S100A8 abrogate the antifungal activities of S100A8/A9: potential role for oxidative regulation.* FEMS Immunol Med Microbiol, 2009. **55**(1): p. 55-61.
656. Guerfali, F.Z., et al., *Simultaneous gene expression profiling in human macrophages infected with Leishmania major parasites using SAGE.* BMC Genomics, 2008. **9**: p. 238.
657. Yui, S., M. Mikami, and M. Yamazaki, *Induction of apoptotic cell death in mouse lymphoma and human leukemia cell lines by a calcium-binding protein complex, calprotectin, derived from inflammatory peritoneal exudate cells.* J Leukoc Biol, 1995. **58**(6): p. 650-8.
658. Yui, S., Y. Nakatani, and M. Mikami, *Calprotectin (S100A8/S100A9), an inflammatory protein complex from neutrophils with a broad apoptosis-inducing activity.* Biol Pharm Bull, 2003. **26**(6): p. 753-60.
659. Yui, S., M. Mikami, and M. Yamazaki, *Purification and characterization of the cytotoxic factor in rat peritoneal exudate cells: its identification as the calcium binding protein complex, calprotectin.* J Leukoc Biol, 1995. **58**(3): p. 307-16.
660. Yui, S., et al., *Growth-inhibitory and apoptosis-inducing activities of calprotectin derived from inflammatory exudate cells on normal fibroblasts: regulation by metal ions.* J Leukoc Biol, 1997. **61**(1): p. 50-7.
661. Seeliger, S., et al., *Expression of calcium-binding proteins MRP8 and MRP14 in inflammatory muscle diseases.* Am J Pathol, 2003. **163**(3): p. 947-56.
662. Ghavami, S., et al., *S100A8/9 induces cell death via a novel, RAGE-independent pathway that involves selective release of Smac/DIABLO and Omi/HtrA2.* Biochim Biophys Acta, 2008. **1783**(2): p. 297-311.
663. Li, C., et al., *A novel p53 target gene, S100A9, induces p53-dependent cellular apoptosis and mediates the p53 apoptosis pathway.* Biochem J, 2009. **422**(2): p. 363-72.

664. Rampersad, R.R., et al., *S100A9 is not essential for disease expression in an acute (K/BxN) or chronic (CIA) model of inflammatory arthritis.* Scand J Rheumatol, 2009. **38**(6): p. 445-9.
665. Dessing, M.C., et al., *S100A8/A9 is not involved in host defense against murine urinary tract infection.* PLoS One, 2010. **5**(10): p. e13394.
666. Bjork, P., et al., *Identification of human S100A9 as a novel target for treatment of autoimmune disease via binding to quinoline-3-carboxamides.* PLoS Biol, 2009. **7**(4): p. e97.
667. Ziegler, G., et al., *Mrp-8 and -14 mediate CNS injury in focal cerebral ischemia.* Biochim Biophys Acta, 2009. **1792**(12): p. 1198-204.
668. Solway, J., et al., *Structure and expression of a smooth muscle cell-specific gene, SM22 alpha.* J Biol Chem, 1995. **270**(22): p. 13460-9.
669. Hofmann Bowman, M.A., et al., *Transgenic expression of human S100A12 induces structural airway abnormalities and limited lung inflammation in a mouse model of allergic inflammation.* Clin Exp Allergy, 2011. **41**(6): p. 878-89.
670. Peng, D.Q., et al., *Apolipoprotein A-I tryptophan substitution leads to resistance to myeloperoxidase-mediated loss of function.* Arterioscler Thromb Vasc Biol, 2008. **28**(11): p. 2063-70.
671. Gottsch, J.D., et al., *Calgranulin C has filariacidal and filariastatic activity.* Infect Immun, 1999. **67**(12): p. 6631-6.
672. Handel, T.M., et al., *Regulation of protein function by glycosaminoglycans--as exemplified by chemokines.* Annu Rev Biochem, 2005. **74**: p. 385-410.
673. Johnson, Z., A.E. Proudfoot, and T.M. Handel, *Interaction of chemokines and glycosaminoglycans: a new twist in the regulation of chemokine function with opportunities for therapeutic intervention.* Cytokine Growth Factor Rev, 2005. **16**(6): p. 625-36.
674. Aviezer, D., M. Safran, and A. Yayon, *Heparin differentially regulates the interaction of fibroblast growth factor-4 with FGF receptors 1 and 2.* Biochem Biophys Res Commun, 1999. **263**(3): p. 621-6.
675. Srikrishna, G., et al., *Two proteins modulating transendothelial migration of leukocytes recognize novel carboxylated glycans on endothelial cells.* J Immunol, 2001. **166**(7): p. 4678-88.
676. Sinha, P., et al., *Proinflammatory S100 proteins regulate the accumulation of myeloid-derived suppressor cells.* J Immunol, 2008. **181**(7): p. 4666-75.
677. Striz, I. and I. Trebichavsky, *Calprotectin - a pleiotropic molecule in acute and chronic inflammation.* Physiol Res, 2004. **53**(3): p. 245-53.
678. Abumrad, N.A., et al., *Cloning of a rat adipocyte membrane protein implicated in binding or transport of long-chain fatty acids that is induced during preadipocyte differentiation. Homology with human CD36.* J Biol Chem, 1993. **268**(24): p. 17665-8.
679. Jerala, R., *Structural biology of the LPS recognition.* Int J Med Microbiol, 2007. **297**(5): p. 353-63.
680. Miyake, K., *Roles for accessory molecules in microbial recognition by Toll-like receptors.* J Endotoxin Res, 2006. **12**(4): p. 195-204.
681. Bours, M.J., et al., *Adenosine 5'-triphosphate and adenosine as endogenous signaling molecules in immunity and inflammation.* Pharmacol Ther, 2006. **112**(2): p. 358-404.
682. Schelbergen, R.F., et al., *Alarmins S100A8 and S100A9 elicit a catabolic effect in human osteoarthritic chondrocytes that is dependent on Toll-like receptor 4.* Arthritis Rheum, 2012. **64**(5): p. 1477-87.

683. Loser, K., et al., *The Toll-like receptor 4 ligands Mrp8 and Mrp14 are crucial in the development of autoreactive CD8+ T cells.* Nat Med, 2010. **16**(6): p. 713-7.
684. Simard, J.C., et al., *Damage-associated molecular pattern S100A9 increases bactericidal activity of human neutrophils by enhancing phagocytosis.* J Immunol, 2011. **186**(6): p. 3622-31.
685. Ichikawa, M., et al., *S100A8/A9 activate key genes and pathways in colon tumor progression.* Mol Cancer Res, 2011. **9**(2): p. 133-48.
686. Boyd, J.H., et al., *S100A8 and S100A9 mediate endotoxin-induced cardiomyocyte dysfunction via the receptor for advanced glycation end products.* Circ Res, 2008. **102**(10): p. 1239-46.
687. Tian, J., et al., *Toll-like receptor 9-dependent activation by DNA-containing immune complexes is mediated by HMGB1 and RAGE.* Nat Immunol, 2007. **8**(5): p. 487-96.
688. Ghavami, S., et al., *Possible Involvement of a Specific Cell Surface Receptor for Calprotectin-Induced Apoptosis in Colon Adenocarcinoma and Carcinam Cell Lines (SW742 and HT29/219).* Journal of Sciences, Islamic Republic of Iran, 2004. **15**(1): p. 3-11.
689. Sato, S., et al., *Galectins in innate immunity: dual functions of host soluble beta-galactoside-binding lectins as damage-associated molecular patterns (DAMPs) and as receptors for pathogen-associated molecular patterns (PAMPs).* Immunol Rev, 2009. **230**(1): p. 172-87.
690. Correa, S.G., et al., *Opposite effects of galectin-1 on alternative metabolic pathways of L-arginine in resident, inflammatory, and activated macrophages.* Glycobiology, 2003. **13**(2): p. 119-28.
691. La, M., et al., *A novel biological activity for galectin-1: inhibition of leukocyte-endothelial cell interactions in experimental inflammation.* Am J Pathol, 2003. **163**(4): p. 1505-15.
692. Barondes, S.H., et al., *Galectins: a family of animal beta-galactoside-binding lectins.* Cell, 1994. **76**(4): p. 597-8.
693. Rubartelli, A., et al., *A novel secretory pathway for interleukin-1 beta, a protein lacking a signal sequence.* EMBO J, 1990. **9**(5): p. 1503-10.
694. Jaffrey, S.R., et al., *Protein S-nitrosylation: a physiological signal for neuronal nitric oxide.* Nat Cell Biol, 2001. **3**(2): p. 193-7.
695. Lim, S.Y., et al., *Oxidative modifications of S100 proteins: functional regulation by redox.* J Leukoc Biol, 2009. **86**(3): p. 577-87.
696. Hensley, K., et al., *Reactive oxygen species, cell signaling, and cell injury.* Free Radic Biol Med, 2000. **28**(10): p. 1456-62.
697. Apel, K. and H. Hirt, *Reactive oxygen species: metabolism, oxidative stress, and signal transduction.* Annu Rev Plant Biol, 2004. **55**: p. 373-99.
698. Undurti, A., et al., *Modification of high density lipoprotein by myeloperoxidase generates a pro-inflammatory particle.* J Biol Chem, 2009. **284**(45): p. 30825-35.
699. Ryter, S.W., et al., *Mechanisms of cell death in oxidative stress.* Antioxid Redox Signal, 2007. **9**(1): p. 49-89.
700. Finkel, T. and N.J. Holbrook, *Oxidants, oxidative stress and the biology of ageing.* Nature, 2000. **408**(6809): p. 239-47.
701. Spitz, D.R., et al., *Metabolic oxidation/reduction reactions and cellular responses to ionizing radiation: a unifying concept in stress response biology.* Cancer Metastasis Rev, 2004. **23**(3-4): p. 311-22.
702. Kulmacz, R.J., W.A. van der Donk, and A.L. Tsai, *Comparison of the properties of prostaglandin H synthase-1 and -2.* Prog Lipid Res, 2003. **42**(5): p. 377-404.

703. Lotzer, K., C.D. Funk, and A.J. Habenicht, *The 5-lipoxygenase pathway in arterial wall biology and atherosclerosis.* Biochim Biophys Acta, 2005. **1736**(1): p. 30-7.
704. Finkel, T., *Signal transduction by reactive oxygen species.* J Cell Biol, 2011. **194**(1): p. 7-15.
705. Leto, T.L. and M. Geiszt, *Role of Nox family NADPH oxidases in host defense.* Antioxid Redox Signal, 2006. **8**(9-10): p. 1549-61.
706. Lambeth, J.D., *NOX enzymes and the biology of reactive oxygen.* Nat Rev Immunol, 2004. **4**(3): p. 181-9.
707. Cui, W., et al., *NOX1/nicotinamide adenine dinucleotide phosphate, reduced form (NADPH) oxidase promotes proliferation of stellate cells and aggravates liver fibrosis induced by bile duct ligation.* Hepatology, 2011. **54**(3): p. 949-58.
708. Won, H.Y., et al., *Enhancement of Allergen-induced Airway Inflammation by NOX2 Deficiency.* Immune Netw, 2011. **11**(3): p. 169-74.
709. Paffenholz, R., et al., *Vestibular defects in head-tilt mice result from mutations in Nox3, encoding an NADPH oxidase.* Genes Dev, 2004. **18**(5): p. 486-91.
710. Carnesecchi, S., et al., *A key role for NOX4 in epithelial cell death during development of lung fibrosis.* Antioxid Redox Signal, 2011. **15**(3): p. 607-19.
711. Bedard, K., V. Jaquet, and K.H. Krause, *NOX5: from basic biology to signaling and disease.* Free Radic Biol Med, 2012. **52**(4): p. 725-34.
712. Bedard, K. and K.H. Krause, *The NOX family of ROS-generating NADPH oxidases: physiology and pathophysiology.* Physiol Rev, 2007. **87**(1): p. 245-313.
713. El-Benna, J., et al., *Phagocyte NADPH oxidase: a multicomponent enzyme essential for host defenses.* Arch Immunol Ther Exp (Warsz), 2005. **53**(3): p. 199-206.
714. Davies, M.J., et al., *Mammalian heme peroxidases: from molecular mechanisms to health implications.* Antioxid Redox Signal, 2008. **10**(7): p. 1199-234.
715. Wink, D.A., et al., *Nitric oxide and redox mechanisms in the immune response.* J Leukoc Biol, 2011. **89**(6): p. 873-91.
716. Bogdan, C., *Nitric oxide and the immune response.* Nat Immunol, 2001. **2**(10): p. 907-16.
717. Fialkow, L., Y. Wang, and G.P. Downey, *Reactive oxygen and nitrogen species as signaling molecules regulating neutrophil function.* Free Radic Biol Med, 2007. **42**(2): p. 153-64.
718. Alderton, W.K., C.E. Cooper, and R.G. Knowles, *Nitric oxide synthases: structure, function and inhibition.* Biochem J, 2001. **357**(Pt 3): p. 593-615.
719. MacMicking, J., Q.W. Xie, and C. Nathan, *Nitric oxide and macrophage function.* Annu Rev Immunol, 1997. **15**: p. 323-50.
720. Forstermann, U. and T. Munzel, *Endothelial nitric oxide synthase in vascular disease: from marvel to menace.* Circulation, 2006. **113**(13): p. 1708-14.
721. Fang, F.C., *Antimicrobial reactive oxygen and nitrogen species: concepts and controversies.* Nat Rev Microbiol, 2004. **2**(10): p. 820-32.
722. Brenman, J.E. and D.S. Bredt, *Synaptic signaling by nitric oxide.* Curr Opin Neurobiol, 1997. **7**(3): p. 374-8.
723. Johnstone, V.P. and C.R. Raymond, *A protein synthesis and nitric oxide-dependent presynaptic enhancement in persistent forms of long-term potentiation.* Learn Mem, 2011. **18**(10): p. 625-33.
724. Beckman, J.S. and W.H. Koppenol, *Nitric oxide, superoxide, and peroxynitrite: the good, the bad, and ugly.* Am J Physiol, 1996. **271**(5 Pt 1): p. C1424-37.

725. Pacher, P., et al., *Role of nitrosative stress and peroxynitrite in the pathogenesis of diabetic complications. Emerging new therapeutical strategies.* Curr Med Chem, 2005. **12**(3): p. 267-75.
726. Kim, K.M., et al., *Regulation of apoptosis by nitrosative stress.* J Biochem Mol Biol, 2002. **35**(1): p. 127-33.
727. Korhonen, R., et al., *Nitric oxide production and signaling in inflammation.* Curr Drug Targets Inflamm Allergy, 2005. **4**(4): p. 471-9.
728. Finkel, T., *Redox-dependent signal transduction.* FEBS Lett, 2000. **476**(1-2): p. 52-4.
729. Touyz, R.M., *Reactive oxygen species as mediators of calcium signaling by angiotensin II: implications in vascular physiology and pathophysiology.* Antioxid Redox Signal, 2005. **7**(9-10): p. 1302-14.
730. Swain, S.D., T.T. Rohn, and M.T. Quinn, *Neutrophil priming in host defense: role of oxidants as priming agents.* Antioxid Redox Signal, 2002. **4**(1): p. 69-83.
731. Brumell, J.H., et al., *Endogenous reactive oxygen intermediates activate tyrosine kinases in human neutrophils.* J Biol Chem, 1996. **271**(3): p. 1455-61.
732. Chiarugi, P. and P. Cirri, *Redox regulation of protein tyrosine phosphatases during receptor tyrosine kinase signal transduction.* Trends Biochem Sci, 2003. **28**(9): p. 509-14.
733. Monteiro, H.P., R.J. Arai, and L.R. Travassos, *Protein tyrosine phosphorylation and protein tyrosine nitration in redox signaling.* Antioxid Redox Signal, 2008. **10**(5): p. 843-89.
734. Bae, Y.S., et al., *Epidermal growth factor (EGF)-induced generation of hydrogen peroxide. Role in EGF receptor-mediated tyrosine phosphorylation.* J Biol Chem, 1997. **272**(1): p. 217-21.
735. Sundaresan, M., et al., *Requirement for generation of H2O2 for platelet-derived growth factor signal transduction.* Science, 1995. **270**(5234): p. 296-9.
736. Moreno-Lopez, B., C.R. Sunico, and D. Gonzalez-Forero, *NO orchestrates the loss of synaptic boutons from adult "sick" motoneurons: modeling a molecular mechanism.* Mol Neurobiol, 2011. **43**(1): p. 41-66.
737. Imlay, J.A. and S. Linn, *Bimodal pattern of killing of DNA-repair-defective or anoxically grown Escherichia coli by hydrogen peroxide.* J Bacteriol, 1986. **166**(2): p. 519-27.
738. Imlay, J.A. and S. Linn, *DNA damage and oxygen radical toxicity.* Science, 1988. **240**(4857): p. 1302-9.
739. McCormick, M.L., G.R. Buettner, and B.E. Britigan, *Endogenous superoxide dismutase levels regulate iron-dependent hydroxyl radical formation in Escherichia coli exposed to hydrogen peroxide.* J Bacteriol, 1998. **180**(3): p. 622-5.
740. Stadler, N., M. Hofer, and K. Sigler, *Mechanisms of Saccharomyces cerevisiae PMA1 H+-ATPase inactivation by Fe2+, H2O2 and Fenton reagents.* Free Radic Res, 2001. **35**(6): p. 643-53.
741. van den Berg, J.M., et al., *Chronic granulomatous disease: the European experience.* PLoS One, 2009. **4**(4): p. e5234.
742. Babior, B.M., *NADPH oxidase.* Curr Opin Immunol, 2004. **16**(1): p. 42-7.
743. Quinn, M.T. and K.A. Gauss, *Structure and regulation of the neutrophil respiratory burst oxidase: comparison with nonphagocyte oxidases.* J Leukoc Biol, 2004. **76**(4): p. 760-81.

744. Minakami, R. and H. Sumimotoa, *Phagocytosis-coupled activation of the superoxide-producing phagocyte oxidase, a member of the NADPH oxidase (nox) family.* Int J Hematol, 2006. **84**(3): p. 193-8.
745. Schapiro, J.M., S.J. Libby, and F.C. Fang, *Inhibition of bacterial DNA replication by zinc mobilization during nitrosative stress.* Proc Natl Acad Sci U S A, 2003. **100**(14): p. 8496-501.
746. Pacelli, R., et al., *Nitric oxide potentiates hydrogen peroxide-induced killing of Escherichia coli.* J Exp Med, 1995. **182**(5): p. 1469-79.
747. Stevanin, T.M., et al., *Flavohemoglobin Hmp affords inducible protection for Escherichia coli respiration, catalyzed by cytochromes bo' or bd, from nitric oxide.* J Biol Chem, 2000. **275**(46): p. 35868-75.
748. Voskuil, M.I., et al., *Inhibition of respiration by nitric oxide induces a Mycobacterium tuberculosis dormancy program.* J Exp Med, 2003. **198**(5): p. 705-13.
749. Shi, L., et al., *Expression of Th1-mediated immunity in mouse lungs induces a Mycobacterium tuberculosis transcription pattern characteristic of nonreplicating persistence.* Proc Natl Acad Sci U S A, 2003. **100**(1): p. 241-6.
750. Lepoivre, M., et al., *Inactivation of ribonucleotide reductase by nitric oxide.* Biochem Biophys Res Commun, 1991. **179**(1): p. 442-8.
751. Nathan, C. and M.U. Shiloh, *Reactive oxygen and nitrogen intermediates in the relationship between mammalian hosts and microbial pathogens.* Proc Natl Acad Sci U S A, 2000. **97**(16): p. 8841-8.
752. Klebanoff, S.J., *Iodination of bacteria: a bactericidal mechanism.* J Exp Med, 1967. **126**(6): p. 1063-78.
753. Thomas, E.L. and T.M. Aune, *Oxidation of Escherichia coli sulfhydryl components by the peroxidase-hydrogen peroxide-iodide antimicrobial system.* Antimicrob Agents Chemother, 1978. **13**(6): p. 1006-10.
754. Rakita, R.M., B.R. Michel, and H. Rosen, *Myeloperoxidase-mediated inhibition of microbial respiration: damage to Escherichia coli ubiquinol oxidase.* Biochemistry, 1989. **28**(7): p. 3031-6.
755. Miyakawa, H., et al., *Effects of inducible nitric oxide synthase and xanthine oxidase inhibitors on SEB-induced interstitial pneumonia in mice.* Eur Respir J, 2002. **19**(3): p. 447-57.
756. Moorhouse, P.C., et al., *Allopurinol and oxypurinol are hydroxyl radical scavengers.* FEBS Lett, 1987. **213**(1): p. 23-8.
757. Frayha, R.A., et al., *Hereditary xanthinuria: report on three patients and short review of the literature.* Nephron, 1977. **19**(6): p. 328-32.
758. Vorbach, C., A. Scriven, and M.R. Capecchi, *The housekeeping gene xanthine oxidoreductase is necessary for milk fat droplet enveloping and secretion: gene sharing in the lactating mammary gland.* Genes Dev, 2002. **16**(24): p. 3223-35.
759. Weiss, S.J., et al., *Brominating oxidants generated by human eosinophils.* Science, 1986. **234**(4773): p. 200-3.
760. Hawkins, C.L. and M.J. Davies, *The role of reactive N-bromo species and radical intermediates in hypobromous acid-induced protein oxidation.* Free Radic Biol Med, 2005. **39**(7): p. 900-12.
761. Senthilmohan, R. and A.J. Kettle, *Bromination and chlorination reactions of myeloperoxidase at physiological concentrations of bromide and chloride.* Arch Biochem Biophys, 2006. **445**(2): p. 235-44.
762. Jong, E.C., W.R. Henderson, and S.J. Klebanoff, *Bactericidal activity of eosinophil peroxidase.* J Immunol, 1980. **124**(3): p. 1378-82.

763. Pattison, D.I. and M.J. Davies, *Reactions of myeloperoxidase-derived oxidants with biological substrates: gaining chemical insight into human inflammatory diseases.* Curr Med Chem, 2006. **13**(27): p. 3271-90.
764. Pattison, D.I. and M.J. Davies, *Absolute rate constants for the reaction of hypochlorous acid with protein side chains and peptide bonds.* Chem Res Toxicol, 2001. **14**(10): p. 1453-64.
765. Albrich, J.M., C.A. McCarthy, and J.K. Hurst, *Biological reactivity of hypochlorous acid: implications for microbicidal mechanisms of leukocyte myeloperoxidase.* Proc Natl Acad Sci U S A, 1981. **78**(1): p. 210-4.
766. Rosen, H. and S.J. Klebanoff, *Oxidation of Escherichia coli iron centers by the myeloperoxidase-mediated microbicidal system.* J Biol Chem, 1982. **257**(22): p. 13731-35.
767. Schraufstatter, I.U., et al., *Mechanisms of hypochlorite injury of target cells.* J Clin Invest, 1990. **85**(2): p. 554-62.
768. Woods, A.A. and M.J. Davies, *Fragmentation of extracellular matrix by hypochlorous acid.* Biochem J, 2003. **376**(Pt 1): p. 219-27.
769. Celec, P., *Nuclear factor kappa B--molecular biomedicine: the next generation.* Biomed Pharmacother, 2004. **58**(6-7): p. 365-71.
770. van den Berg, R., et al., *Transcription factor NF-kappaB as a potential biomarker for oxidative stress.* Br J Nutr, 2001. **86 Suppl 1**: p. S121-7.
771. Hansen, J.M., H. Zhang, and D.P. Jones, *Mitochondrial thioredoxin-2 has a key role in determining tumor necrosis factor-alpha-induced reactive oxygen species generation, NF-kappaB activation, and apoptosis.* Toxicol Sci, 2006. **91**(2): p. 643-50.
772. Kim, J.H., et al., *The non-provitamin A carotenoid, lutein, inhibits NF-kappaB-dependent gene expression through redox-based regulation of the phosphatidylinositol 3-kinase/PTEN/Akt and NF-kappaB-inducing kinase pathways: role of H(2)O(2) in NF-kappaB activation.* Free Radic Biol Med, 2008. **45**(6): p. 885-96.
773. Jacobs, A.T. and L.J. Ignarro, *Nuclear factor-kappa B and mitogen-activated protein kinases mediate nitric oxide-enhanced transcriptional expression of interferon-beta.* J Biol Chem, 2003. **278**(10): p. 8018-27.
774. Van Dervort, A.L., et al., *Nitric oxide regulates endotoxin-induced TNF-alpha production by human neutrophils.* J Immunol, 1994. **152**(8): p. 4102-9.
775. Wu, F., et al., *Nitric oxide attenuates but superoxide enhances iNOS expression in endotoxin- and IFNgamma-stimulated skeletal muscle endothelial cells.* Microcirculation, 2001. **8**(6): p. 415-25.
776. Li, Q. and J.F. Engelhardt, *Interleukin-1beta induction of NFkappaB is partially regulated by H2O2-mediated activation of NFkappaB-inducing kinase.* J Biol Chem, 2006. **281**(3): p. 1495-505.
777. Grumbach, I.M., et al., *A negative feedback mechanism involving nitric oxide and nuclear factor kappa-B modulates endothelial nitric oxide synthase transcription.* J Mol Cell Cardiol, 2005. **39**(4): p. 595-603.
778. Lee, J.S., et al., *Modulation of monocyte chemokine production and nuclear factor kappa B activity by oxidants.* J Interferon Cytokine Res, 1999. **19**(7): p. 761-7.
779. Schreck, R., K. Albermann, and P.A. Baeuerle, *Nuclear factor kappa B: an oxidative stress-responsive transcription factor of eukaryotic cells (a review).* Free Radic Res Commun, 1992. **17**(4): p. 221-37.

780. Midwinter, R.G., et al., *IkappaB is a sensitive target for oxidation by cell-permeable chloramines: inhibition of NF-kappaB activity by glycine chloramine through methionine oxidation.* Biochem J, 2006. **396**(1): p. 71-8.
781. Ray, R. and A.M. Shah, *NADPH oxidase and endothelial cell function.* Clin Sci (Lond), 2005. **109**(3): p. 217-26.
782. Witting, P.K., et al., *Hydrogen peroxide promotes endothelial dysfunction by stimulating multiple sources of superoxide anion radical production and decreasing nitric oxide bioavailability.* Cell Physiol Biochem, 2007. **20**(5): p. 255-68.
783. Balla, J., et al., *Heme, heme oxygenase, and ferritin: how the vascular endothelium survives (and dies) in an iron-rich environment.* Antioxid Redox Signal, 2007. **9**(12): p. 2119-37.
784. Graca-Souza, A.V., et al., *Neutrophil activation by heme: implications for inflammatory processes.* Blood, 2002. **99**(11): p. 4160-5.
785. Negre-Salvayre, A., et al., *Advanced lipid peroxidation end products in oxidative damage to proteins. Potential role in diseases and therapeutic prospects for the inhibitors.* Br J Pharmacol, 2008. **153**(1): p. 6-20.
786. Sugihara, N., et al., *Anti- and pro-oxidative effects of flavonoids on metal-induced lipid hydroperoxide-dependent lipid peroxidation in cultured hepatocytes loaded with alpha-linolenic acid.* Free Radic Biol Med, 1999. **27**(11-12): p. 1313-23.
787. Feeney, L. and E.R. Berman, *Oxygen toxicity: membrane damage by free radicals.* Invest Ophthalmol, 1976. **15**(10): p. 789-92.
788. Weinberg, R.B., et al., *Pro-oxidant effect of vitamin E in cigarette smokers consuming a high polyunsaturated fat diet.* Arterioscler Thromb Vasc Biol, 2001. **21**(6): p. 1029-33.
789. Ford, D.A., *Lipid oxidation by hypochlorous acid: chlorinated lipids in atherosclerosis and myocardial ischemia.* Clin Lipidol, 2010. **5**(6): p. 835-852.
790. Hazen, S.L., et al., *Molecular chlorine generated by the myeloperoxidase-hydrogen peroxide-chloride system of phagocytes converts low density lipoprotein cholesterol into a family of chlorinated sterols.* J Biol Chem, 1996. **271**(38): p. 23080-8.
791. Heinecke, J.W., et al., *Cholesterol chlorohydrin synthesis by the myeloperoxidase-hydrogen peroxide-chloride system: potential markers for lipoproteins oxidatively damaged by phagocytes.* Biochemistry, 1994. **33**(33): p. 10127-36.
792. Arnhold, J., et al., *Effects of hypochlorous acid on unsaturated phosphatidylcholines.* Free Radic Biol Med, 2001. **31**(9): p. 1111-9.
793. Robaszkiewicz, A., et al., *Effect of phosphatidylcholine chlorohydrins on human erythrocytes.* Chem Phys Lipids, 2010. **163**(7): p. 639-47.
794. Spickett, C.M., *Chlorinated lipids and fatty acids: an emerging role in pathology.* Pharmacol Ther, 2007. **115**(3): p. 400-9.
795. Carr, A.C., J.J. van den Berg, and C.C. Winterbourn, *Chlorination of cholesterol in cell membranes by hypochlorous acid.* Arch Biochem Biophys, 1996. **332**(1): p. 63-9.
796. Messner, M.C., et al., *Selective plasmenylcholine oxidation by hypochlorous acid: formation of lysophosphatidylcholine chlorohydrins.* Chem Phys Lipids, 2006. **144**(1): p. 34-44.
797. Messner, M.C., et al., *Identification of lysophosphatidylcholine-chlorohydrin in human atherosclerotic lesions.* Lipids, 2008. **43**(3): p. 243-9.
798. Flemmig, J., et al., *Modification of phosphatidylserine by hypochlorous acid.* Chem Phys Lipids, 2009. **161**(1): p. 44-50.

799. Kawai, Y., et al., *Hypochlorous acid-derived modification of phospholipids: characterization of aminophospholipids as regulatory molecules for lipid peroxidation.* Biochemistry, 2006. **45**(47): p. 14201-11.
800. Hazell, L.J., M.J. Davies, and R. Stocker, *Secondary radicals derived from chloramines of apolipoprotein B-100 contribute to HOCl-induced lipid peroxidation of low-density lipoproteins.* Biochem J, 1999. **339 (Pt 3)**: p. 489-95.
801. Carr, A.C., J.J. van den Berg, and C.C. Winterbourn, *Differential reactivities of hypochlorous and hypobromous acids with purified Escherichia coli phospholipid: formation of haloamines and halohydrins.* Biochim Biophys Acta, 1998. **1392**(2-3): p. 254-64.
802. Carr, A.C., et al., *Comparison of low-density lipoprotein modification by myeloperoxidase-derived hypochlorous and hypobromous acids.* Free Radic Biol Med, 2001. **31**(1): p. 62-72.
803. Skaff, O., D.I. Pattison, and M.J. Davies, *Kinetics of hypobromous acid-mediated oxidation of lipid components and antioxidants.* Chem Res Toxicol, 2007. **20**(12): p. 1980-8.
804. Vissers, M.C., A.C. Carr, and A.L. Chapman, *Comparison of human red cell lysis by hypochlorous and hypobromous acids: insights into the mechanism of lysis.* Biochem J, 1998. **330 (Pt 1)**: p. 131-8.
805. Spalteholz, H., O.M. Panasenko, and J. Arnhold, *Formation of reactive halide species by myeloperoxidase and eosinophil peroxidase.* Arch Biochem Biophys, 2006. **445**(2): p. 225-34.
806. Spalteholz, H., K. Wenske, and J. Arnhold, *Interaction of hypohalous acids and heme peroxidases with unsaturated phosphatidylcholines.* Biofactors, 2005. **24**(1-4): p. 67-76.
807. Sayre, L.M., et al., *4-Hydroxynonenal-derived advanced lipid peroxidation end products are increased in Alzheimer's disease.* J Neurochem, 1997. **68**(5): p. 2092-7.
808. Smith, M.A., et al., *Cytochemical demonstration of oxidative damage in Alzheimer disease by immunochemical enhancement of the carbonyl reaction with 2,4-dinitrophenylhydrazine.* J Histochem Cytochem, 1998. **46**(6): p. 731-5.
809. Wataya, T., et al., *High molecular weight neurofilament proteins are physiological substrates of adduction by the lipid peroxidation product hydroxynonenal.* J Biol Chem, 2002. **277**(7): p. 4644-8.
810. Yoritaka, A., et al., *Immunohistochemical detection of 4-hydroxynonenal protein adducts in Parkinson disease.* Proc Natl Acad Sci U S A, 1996. **93**(7): p. 2696-701.
811. Jenner, P., *Oxidative stress in Parkinson's disease.* Ann Neurol, 2003. **53 Suppl 3**: p. S26-36; discussion S36-8.
812. Brown, B.E., R.T. Dean, and M.J. Davies, *Glycation of low-density lipoproteins by methylglyoxal and glycolaldehyde gives rise to the in vitro formation of lipid-laden cells.* Diabetologia, 2005. **48**(2): p. 361-9.
813. Weber, L.W., M. Boll, and A. Stampfl, *Hepatotoxicity and mechanism of action of haloalkanes: carbon tetrachloride as a toxicological model.* Crit Rev Toxicol, 2003. **33**(2): p. 105-36.
814. Morquette, B., et al., *Production of lipid peroxidation products in osteoarthritic tissues: new evidence linking 4-hydroxynonenal to cartilage degradation.* Arthritis Rheum, 2006. **54**(1): p. 271-81.

815. Shi, Q., et al., *Alterations of metabolic activity in human osteoarthritic osteoblasts by lipid peroxidation end product 4-hydroxynonenal.* Arthritis Res Ther, 2006. **8**(6): p. R159.
816. Boldogh, I., et al., *ROS generated by pollen NADPH oxidase provide a signal that augments antigen-induced allergic airway inflammation.* J Clin Invest, 2005. **115**(8): p. 2169-79.
817. Castro, S.M., et al., *Antioxidant treatment ameliorates respiratory syncytial virus-induced disease and lung inflammation.* Am J Respir Crit Care Med, 2006. **174**(12): p. 1361-9.
818. Pryor, W.A., *Oxy-radicals and related species: their formation, lifetimes, and reactions.* Annu Rev Physiol, 1986. **48**: p. 657-67.
819. Henle, E.S. and S. Linn, *Formation, prevention, and repair of DNA damage by iron/hydrogen peroxide.* J Biol Chem, 1997. **272**(31): p. 19095-8.
820. Cadet, J., et al., *Hydroxyl radicals and DNA base damage.* Mutat Res, 1999. **424**(1-2): p. 9-21.
821. Marnett, L.J., *Oxyradicals and DNA damage.* Carcinogenesis, 2000. **21**(3): p. 361-70.
822. Stanley, N.R., D.I. Pattison, and C.L. Hawkins, *Ability of hypochlorous acid and N-chloramines to chlorinate DNA and its constituents.* Chem Res Toxicol, 2010. **23**(7): p. 1293-302.
823. Vertuani, S., A. Angusti, and S. Manfredini, *The antioxidants and pro-antioxidants network: an overview.* Curr Pharm Des, 2004. **10**(14): p. 1677-94.
824. Zelko, I.N., T.J. Mariani, and R.J. Folz, *Superoxide dismutase multigene family: a comparison of the CuZn-SOD (SOD1), Mn-SOD (SOD2), and EC-SOD (SOD3) gene structures, evolution, and expression.* Free Radic Biol Med, 2002. **33**(3): p. 337-49.
825. Elchuri, S., et al., *CuZnSOD deficiency leads to persistent and widespread oxidative damage and hepatocarcinogenesis later in life.* Oncogene, 2005. **24**(3): p. 367-80.
826. Li, Y., et al., *Dilated cardiomyopathy and neonatal lethality in mutant mice lacking manganese superoxide dismutase.* Nat Genet, 1995. **11**(4): p. 376-81.
827. Kirkman, H.N. and G.F. Gaetani, *Mammalian catalase: a venerable enzyme with new mysteries.* Trends Biochem Sci, 2007. **32**(1): p. 44-50.
828. Ho, Y.S., et al., *Mice lacking catalase develop normally but show differential sensitivity to oxidant tissue injury.* J Biol Chem, 2004. **279**(31): p. 32804-12.
829. Schriner, S.E., et al., *Extension of murine life span by overexpression of catalase targeted to mitochondria.* Science, 2005. **308**(5730): p. 1909-11.
830. Brown, K.K., A.G. Cox, and M.B. Hampton, *Mitochondrial respiratory chain involvement in peroxiredoxin 3 oxidation by phenethyl isothiocyanate and auranofin.* FEBS Lett, 2010. **584**(6): p. 1257-62.
831. Wood, Z.A., et al., *Structure, mechanism and regulation of peroxiredoxins.* Trends Biochem Sci, 2003. **28**(1): p. 32-40.
832. Meyer, Y., et al., *Thioredoxins and glutaredoxins: unifying elements in redox biology.* Annu Rev Genet, 2009. **43**: p. 335-67.
833. Kalinina, E.V., N.N. Chernov, and A.N. Saprin, *Involvement of thio-, peroxi-, and glutaredoxins in cellular redox-dependent processes.* Biochemistry (Mosc), 2008. **73**(13): p. 1493-510.
834. Sadek, C.M., et al., *Characterization of human thioredoxin-like 2. A novel microtubule-binding thioredoxin expressed predominantly in the cilia of lung*

airway epithelium and spermatid manchette and axoneme. J Biol Chem, 2003. **278**(15): p. 13133-42.
835. Rhee, S.G., et al., *Peroxiredoxin, a novel family of peroxidases.* IUBMB Life, 2001. **52**(1-2): p. 35-41.
836. Das, K.C. and C.K. Das, *Thioredoxin, a singlet oxygen quencher and hydroxyl radical scavenger: redox independent functions.* Biochem Biophys Res Commun, 2000. **277**(2): p. 443-7.
837. Powis, G. and W.R. Montfort, *Properties and biological activities of thioredoxins.* Annu Rev Pharmacol Toxicol, 2001. **41**: p. 261-95.
838. Takagi, Y., et al., *Overexpression of thioredoxin in transgenic mice attenuates focal ischemic brain damage.* Proc Natl Acad Sci U S A, 1999. **96**(7): p. 4131-6.
839. Nakamura, H., et al., *Enhanced resistancy of thioredoxin-transgenic mice against influenza virus-induced pneumonia.* Immunol Lett, 2002. **82**(1-2): p. 165-70.
840. Kasuno, K., et al., *Protective roles of thioredoxin, a redox-regulating protein, in renal ischemia/reperfusion injury.* Kidney Int, 2003. **64**(4): p. 1273-82.
841. Das, K.C., *Thioredoxin system in premature and newborn biology.* Antioxid Redox Signal, 2004. **6**(1): p. 177-84.
842. Pedrajas, J.R., et al., *Mitochondria of Saccharomyces cerevisiae contain one-conserved cysteine type peroxiredoxin with thioredoxin peroxidase activity.* J Biol Chem, 2000. **275**(21): p. 16296-301.
843. Chen, Y., et al., *Overexpressed human mitochondrial thioredoxin confers resistance to oxidant-induced apoptosis in human osteosarcoma cells.* J Biol Chem, 2002. **277**(36): p. 33242-8.
844. Lundberg, M., et al., *Cloning and expression of a novel human glutaredoxin (Grx2) with mitochondrial and nuclear isoforms.* J Biol Chem, 2001. **276**(28): p. 26269-75.
845. Wingert, R.A., et al., *Deficiency of glutaredoxin 5 reveals Fe-S clusters are required for vertebrate haem synthesis.* Nature, 2005. **436**(7053): p. 1035-39.
846. Holmgren, A., *Thioredoxin and glutaredoxin systems.* J Biol Chem, 1989. **264**(24): p. 13963-6.
847. Takashima, Y., et al., *Differential expression of glutaredoxin and thioredoxin during monocytic differentiation.* Immunol Lett, 1999. **68**(2-3): p. 397-401.
848. Bandyopadhyay, S., et al., *Thioltransferase (glutaredoxin) reactivates the DNA-binding activity of oxidation-inactivated nuclear factor I.* J Biol Chem, 1998. **273**(1): p. 392-7.
849. Hirota, K., et al., *Nucleoredoxin, glutaredoxin, and thioredoxin differentially regulate NF-kappaB, AP-1, and CREB activation in HEK293 cells.* Biochem Biophys Res Commun, 2000. **274**(1): p. 177-82.
850. Nakamura, T., et al., *Mouse glutaredoxin - cDNA cloning, high level expression in E. coli and its possible implication in redox regulation of the DNA binding activity in transcription factor PEBP2.* Free Radic Res, 1999. **31**(4): p. 357-65.
851. Chrestensen, C.A., D.W. Starke, and J.J. Mieyal, *Acute cadmium exposure inactivates thioltransferase (Glutaredoxin), inhibits intracellular reduction of protein-glutathionyl-mixed disulfides, and initiates apoptosis.* J Biol Chem, 2000. **275**(34): p. 26556-65.
852. Daily, D., et al., *Glutaredoxin protects cerebellar granule neurons from dopamine-induced apoptosis by activating NF-kappa B via Ref-1.* J Biol Chem, 2001. **276**(2): p. 1335-44.

853. Okuda, M., et al., *Expression of glutaredoxin in human coronary arteries: its potential role in antioxidant protection against atherosclerosis.* Arterioscler Thromb Vasc Biol, 2001. **21**(9): p. 1483-7.
854. Barry-Lane, P.A., et al., *p47phox is required for atherosclerotic lesion progression in ApoE(-/-) mice.* J Clin Invest, 2001. **108**(10): p. 1513-22.
855. Adachi, T., et al., *S-glutathiolation of Ras mediates redox-sensitive signaling by angiotensin II in vascular smooth muscle cells.* J Biol Chem, 2004. **279**(28): p. 29857-62.
856. Johansson, C., C.H. Lillig, and A. Holmgren, *Human mitochondrial glutaredoxin reduces S-glutathionylated proteins with high affinity accepting electrons from either glutathione or thioredoxin reductase.* J Biol Chem, 2004. **279**(9): p. 7537-43.
857. Beer, S.M., et al., *Glutaredoxin 2 catalyzes the reversible oxidation and glutathionylation of mitochondrial membrane thiol proteins: implications for mitochondrial redox regulation and antioxidant DEFENSE.* J Biol Chem, 2004. **279**(46): p. 47939-51.
858. Taylor, E.R., et al., *Reversible glutathionylation of complex I increases mitochondrial superoxide formation.* J Biol Chem, 2003. **278**(22): p. 19603-10.
859. Enoksson, M., et al., *Overexpression of glutaredoxin 2 attenuates apoptosis by preventing cytochrome c release.* Biochem Biophys Res Commun, 2005. **327**(3): p. 774-9.
860. Rodriguez-Manzaneque, M.T., et al., *Grx5 is a mitochondrial glutaredoxin required for the activity of iron/sulfur enzymes.* Mol Biol Cell, 2002. **13**(4): p. 1109-21.
861. Fernandes, A.P., et al., *A novel monothiol glutaredoxin (Grx4) from Escherichia coli can serve as a substrate for thioredoxin reductase.* J Biol Chem, 2005. **280**(26): p. 24544-52.
862. Tamarit, J., et al., *Biochemical characterization of yeast mitochondrial Grx5 monothiol glutaredoxin.* J Biol Chem, 2003. **278**(28): p. 25745-51.
863. Margis, R., et al., *Glutathione peroxidase family - an evolutionary overview.* FEBS J, 2008. **275**(15): p. 3959-70.
864. Toppo, S., et al., *Evolutionary and structural insights into the multifaceted glutathione peroxidase (Gpx) superfamily.* Antioxid Redox Signal, 2008. **10**(9): p. 1501-14.
865. Blankenberg, S., et al., *Glutathione peroxidase 1 activity and cardiovascular events in patients with coronary artery disease.* N Engl J Med, 2003. **349**(17): p. 1605-13.
866. Gonzales, R., et al., *Superoxide dismutase, catalase, and glutathione peroxidase in red blood cells from patients with malignant diseases.* Cancer Res, 1984. **44**(9): p. 4137-9.
867. Voetsch, B., et al., *Promoter polymorphisms in the plasma glutathione peroxidase (GPx-3) gene: a novel risk factor for arterial ischemic stroke among young adults and children.* Stroke, 2007. **38**(1): p. 41-9.
868. Raza, H., *Dual localization of glutathione S-transferase in the cytosol and mitochondria: implications in oxidative stress, toxicity and disease.* FEBS J, 2011. **278**(22): p. 4243-51.
869. Chaudiere, J. and R. Ferrari-Iliou, *Intracellular antioxidants: from chemical to biochemical mechanisms.* Food Chem Toxicol, 1999. **37**(9-10): p. 949-62.
870. Gerard-Monnier, D. and J. Chaudiere, *[Metabolism and antioxidant function of glutathione]*. Pathol Biol (Paris), 1996. **44**(1): p. 77-85.

871. Lakhtakia, R., Ramji, M.T. , Lavanya, K. , Rajesh, K. , Jayakumar, K. , Sneha, C. , Narayan, A. , Ramya, B. , Ramana, G. , Chari, P. V. B. , Chaitanya, K.V. , *The role of antioxidants in human health maintenance: small molecules with infinite functions.* International Journal of Pharmaceutical Sciences and Research, 2011. **2**(6): p. 1395-1402.
872. Otterbein, L.E., et al., *Heme oxygenase-1: unleashing the protective properties of heme.* Trends Immunol, 2003. **24**(8): p. 449-55.
873. Stocker, R., *Antioxidant activities of bile pigments.* Antioxid Redox Signal, 2004. **6**(5): p. 841-9.
874. Minamino, T., et al., *Targeted expression of heme oxygenase-1 prevents the pulmonary inflammatory and vascular responses to hypoxia.* Proc Natl Acad Sci U S A, 2001. **98**(15): p. 8798-803.
875. Nakahira, K., et al., *Carbon monoxide differentially inhibits TLR signaling pathways by regulating ROS-induced trafficking of TLRs to lipid rafts.* J Exp Med, 2006. **203**(10): p. 2377-89.
876. Stevens, B. and R.D. Small, Jr., *The photoperoxidation of unsaturated organic molecules--XV. O21Delta g quenching by bilirubin and biliverdin.* Photochem Photobiol, 1976. **23**(1): p. 33-6.
877. Brodersen, R. and P. Bartels, *Enzymatic oxidation of bilirubin.* Eur J Biochem, 1969. **10**(3): p. 468-73.
878. Jacobsen, J. and O. Fedders, *Determination of non-albumin-bound bilirubin in human serum.* Scand J Clin Lab Invest, 1970. **26**(3): p. 237-41.
879. Reed, G.A., et al., *Peroxidative oxidation of bilirubin during prostaglandin biosynthesis.* Prostaglandins, 1985. **30**(1): p. 153-65.
880. Stocker, R., A.N. Glazer, and B.N. Ames, *Antioxidant activity of albumin-bound bilirubin.* Proc Natl Acad Sci U S A, 1987. **84**(16): p. 5918-22.
881. Abraham, N.G. and A. Kappas, *Pharmacological and clinical aspects of heme oxygenase.* Pharmacol Rev, 2008. **60**(1): p. 79-127.
882. Ren, H., et al., *Induction of haem oxygenase-1 causes cortical non-haem iron increase in experimental pneumococcal meningitis: evidence that concomitant ferritin up-regulation prevents iron-induced oxidative damage.* J Neurochem, 2007. **100**(2): p. 532-44.
883. Balla, G., et al., *Ferritin: a cytoprotective antioxidant strategem of endothelium.* J Biol Chem, 1992. **267**(25): p. 18148-53.
884. Taylor, J.L., M.S. Carraway, and C.A. Piantadosi, *Lung-specific induction of heme oxygenase-1 and hyperoxic lung injury.* Am J Physiol, 1998. **274**(4 Pt 1): p. L582-90.
885. Forman, H.J., J.M. Fukuto, and M. Torres, *Redox signaling: thiol chemistry defines which reactive oxygen and nitrogen species can act as second messengers.* Am J Physiol Cell Physiol, 2004. **287**(2): p. C246-56.
886. Biswas, S., A.S. Chida, and I. Rahman, *Redox modifications of protein-thiols: emerging roles in cell signaling.* Biochem Pharmacol, 2006. **71**(5): p. 551-64.
887. Claiborne, A., et al., *Protein-sulfenic acids: diverse roles for an unlikely player in enzyme catalysis and redox regulation.* Biochemistry, 1999. **38**(47): p. 15407-16.
888. Biteau, B., J. Labarre, and M.B. Toledano, *ATP-dependent reduction of cysteine-sulphinic acid by S. cerevisiae sulphiredoxin.* Nature, 2003. **425**(6961): p. 980-4.
889. Stamler, J.S., et al., *(S)NO signals: translocation, regulation, and a consensus motif.* Neuron, 1997. **18**(5): p. 691-6.
890. Hess, D.T., et al., *Protein S-nitrosylation: purview and parameters.* Nat Rev Mol Cell Biol, 2005. **6**(2): p. 150-66.

891. Kelleher, Z.T., et al., *NOS2 regulation of NF-kappaB by S-nitrosylation of p65.* J Biol Chem, 2007. **282**(42): p. 30667-72.
892. Benhar, M., M.T. Forrester, and J.S. Stamler, *Nitrosative stress in the ER: a new role for S-nitrosylation in neurodegenerative diseases.* ACS Chem Biol, 2006. **1**(6): p. 355-8.
893. Davis, D.A., et al., *Reversible oxidation of HIV-2 protease.* Methods Enzymol, 2002. **348**: p. 249-59.
894. D'Autreaux, B. and M.B. Toledano, *ROS as signalling molecules: mechanisms that generate specificity in ROS homeostasis.* Nat Rev Mol Cell Biol, 2007. **8**(10): p. 813-24.
895. Ghezzi, P., *Regulation of protein function by glutathionylation.* Free Radic Res, 2005. **39**(6): p. 573-80.
896. Moskovitz, J., *Methionine sulfoxide reductases: ubiquitous enzymes involved in antioxidant defense, protein regulation, and prevention of aging-associated diseases.* Biochim Biophys Acta, 2005. **1703**(2): p. 213-9.
897. Moller, I.M., A. Rogowska-Wrzesinska, and R.S. Rao, *Protein carbonylation and metal-catalyzed protein oxidation in a cellular perspective.* J Proteomics, 2011. **74**(11): p. 2228-42.
898. Levine, R.L., *Carbonyl modified proteins in cellular regulation, aging, and disease.* Free Radic Biol Med, 2002. **32**(9): p. 790-6.
899. Stadtman, E.R. and R.L. Levine, *Protein oxidation.* Ann N Y Acad Sci, 2000. **899**: p. 191-208.
900. Dalle-Donne, I., et al., *Protein carbonylation, cellular dysfunction, and disease progression.* J Cell Mol Med, 2006. **10**(2): p. 389-406.
901. Andersen, J.K., *Oxidative stress in neurodegeneration: cause or consequence?* Nat Med, 2004. **10 Suppl**: p. S18-25.
902. Barnham, K.J., C.L. Masters, and A.I. Bush, *Neurodegenerative diseases and oxidative stress.* Nat Rev Drug Discov, 2004. **3**(3): p. 205-14.
903. O'Connell, A.M., S.P. Gieseg, and K.K. Stanley, *Hypochlorite oxidation causes cross-linking of Lp(a).* Biochim Biophys Acta, 1994. **1225**(2): p. 180-6.
904. Fu, X., D.M. Mueller, and J.W. Heinecke, *Generation of intramolecular and intermolecular sulfenamides, sulfinamides, and sulfonamides by hypochlorous acid: a potential pathway for oxidative cross-linking of low-density lipoprotein by myeloperoxidase.* Biochemistry, 2002. **41**(4): p. 1293-301.
905. Radi, R., *Nitric oxide, oxidants, and protein tyrosine nitration.* Proc Natl Acad Sci U S A, 2004. **101**(12): p. 4003-8.
906. Kuo, W.N. and J.M. Kocis, *Nitration/S-nitrosation of proteins by peroxynitrite-treatment and subsequent modification by glutathione S-transferase and glutathione peroxidase.* Mol Cell Biochem, 2002. **233**(1-2): p. 57-63.
907. Peluffo, G. and R. Radi, *Biochemistry of protein tyrosine nitration in cardiovascular pathology.* Cardiovasc Res, 2007. **75**(2): p. 291-302.
908. Elfering, S.L., et al., *Aspects, mechanism, and biological relevance of mitochondrial protein nitration sustained by mitochondrial nitric oxide synthase.* Am J Physiol Heart Circ Physiol, 2004. **286**(1): p. H22-9.
909. Yakovlev, V.A. and R.B. Mikkelsen, *Protein tyrosine nitration in cellular signal transduction pathways.* J Recept Signal Transduct Res, 2010. **30**(6): p. 420-9.
910. Aulak, K.S., et al., *Dynamics of protein nitration in cells and mitochondria.* Am J Physiol Heart Circ Physiol, 2004. **286**(1): p. H30-8.

911. Koeck, T., et al., *Rapid and selective oxygen-regulated protein tyrosine denitration and nitration in mitochondria.* J Biol Chem, 2004. **279**(26): p. 27257-62.
912. Yakovlev, V.A., et al., *Nitration of the tumor suppressor protein p53 at tyrosine 327 promotes p53 oligomerization and activation.* Biochemistry, 2010. **49**(25): p. 5331-9.
913. Yakovlev, V.A., et al., *Tyrosine nitration of IkappaBalpha: a novel mechanism for NF-kappaB activation.* Biochemistry, 2007. **46**(42): p. 11671-83.
914. Csibi, A., et al., *Angiotensin II inhibits insulin-stimulated GLUT4 translocation and Akt activation through tyrosine nitration-dependent mechanisms.* PLoS One, 2010. **5**(4): p. e10070.
915. Monti, M., et al., *deltaPKC inhibition or varepsilonPKC activation repairs endothelial vascular dysfunction by regulating eNOS post-translational modification.* J Mol Cell Cardiol, 2010. **48**(4): p. 746-56.
916. Domigan, N.M., et al., *Chlorination of tyrosyl residues in peptides by myeloperoxidase and human neutrophils.* J Biol Chem, 1995. **270**(28): p. 16542-8.
917. Kettle, A.J., *Detection of 3-chlorotyrosine in proteins exposed to neutrophil oxidants.* Methods Enzymol, 1999. **300**: p. 111-20.
918. Wu, W., et al., *Eosinophils generate brominating oxidants in allergen-induced asthma.* J Clin Invest, 2000. **105**(10): p. 1455-63.
919. Wu, W., et al., *3-Bromotyrosine and 3,5-dibromotyrosine are major products of protein oxidation by eosinophil peroxidase: potential markers for eosinophil-dependent tissue injury in vivo.* Biochemistry, 1999. **38**(12): p. 3538-48.
920. Aldridge, R.E., et al., *Eosinophil peroxidase produces hypobromous acid in the airways of stable asthmatics.* Free Radic Biol Med, 2002. **33**(6): p. 847-56.
921. MacPherson, J.C., et al., *Eosinophils are a major source of nitric oxide-derived oxidants in severe asthma: characterization of pathways available to eosinophils for generating reactive nitrogen species.* J Immunol, 2001. **166**(9): p. 5763-72.
922. Pattison, D.I. and M.J. Davies, *Kinetic analysis of the reactions of hypobromous acid with protein components: implications for cellular damage and use of 3-bromotyrosine as a marker of oxidative stress.* Biochemistry, 2004. **43**(16): p. 4799-809.
923. Fukuda, K., et al., *Free amino acid content of lymphocytes nd granulocytes compared.* Clin Chem, 1982. **28**(8): p. 1758-61.
924. Schuller-Levis, G.B. and E. Park, *Taurine and its chloramine: modulators of immunity.* Neurochem Res, 2004. **29**(1): p. 117-26.
925. Cunningham, C., K.F. Tipton, and H.B. Dixon, *Conversion of taurine into N-chlorotaurine (taurine chloramine) and sulphoacetaldehyde in response to oxidative stress.* Biochem J, 1998. **330 (Pt 2)**: p. 939-45.
926. Wright, C.E., et al., *Taurine: Biological Actions and Clinical Perspectives.* 1985: p. 137-147.
927. Iismaa, S.E., et al., *Recombinant and cellular expression of the murine chemotactic protein, CP-10.* DNA Cell Biol, 1994. **13**(2): p. 183-92.
928. Hoad, R.B. and C.L. Geczy, *Characterisation of monoclonal antibodies to human factor X/Xa. Initial observations with a quantitative ELISA procedure.* J Immunol Methods, 1991. **136**(2): p. 269-78.
929. Schagger, H., *Tricine-SDS-PAGE.* Nat Protoc, 2006. **1**(1): p. 16-22.
930. Schagger, H. and G. von Jagow, *Tricine-sodium dodecyl sulfate-polyacrylamide gel electrophoresis for the separation of proteins in the range from 1 to 100 kDa.* Anal Biochem, 1987. **166**(2): p. 368-79.

931. Shevchenko, A., et al., *Mass spectrometric sequencing of proteins silver-stained polyacrylamide gels.* Anal Chem, 1996. **68**(5): p. 850-8.
932. Gatlin, C.L., et al., *Protein identification at the low femtomole level from silver-stained gels using a new fritless electrospray interface for liquid chromatography-microspray and nanospray mass spectrometry.* Anal Biochem, 1998. **263**(1): p. 93-101.
933. Raftery, M.J., *Enrichment by organomercurial agarose and identification of cys-containing peptides from yeast cell lysates.* Anal Chem, 2008. **80**(9): p. 3334-41.
934. Davies, M.J., *Myeloperoxidase-derived oxidation: mechanisms of biological damage and its prevention.* J Clin Biochem Nutr, 2011. **48**(1): p. 8-19.
935. Schultz, J. and K. Kaminker, *Myeloperoxidase of the leucocyte of normal human blood. I. Content and localization.* Arch Biochem Biophys, 1962. **96**: p. 465-7.
936. Ikitimur, B. and B. Karadag, *Role of myeloperoxidase in cardiology.* Future Cardiol, 2010. **6**(5): p. 693-702.
937. Abu-Ghazaleh, R.I., et al., *Eosinophil granule proteins in peripheral blood granulocytes.* J Leukoc Biol, 1992. **52**(6): p. 611-8.
938. Ten, R.M., et al., *Molecular cloning of the human eosinophil peroxidase. Evidence for the existence of a peroxidase multigene family.* J Exp Med, 1989. **169**(5): p. 1757-69.
939. Furtmuller, P.G., et al., *Active site structure and catalytic mechanisms of human peroxidases.* Arch Biochem Biophys, 2006. **445**(2): p. 199-213.
940. Ueda, T., et al., *Molecular cloning and characterization of the chromosomal gene for human lactoperoxidase.* Eur J Biochem, 1997. **243**(1-2): p. 32-41.
941. Klebanoff, S.J., *Myeloperoxidase-halide-hydrogen peroxide antibacterial system.* J Bacteriol, 1968. **95**(6): p. 2131-8.
942. Capozzi, G. and G. Modena, *Oxidation of thiols.* In: Patai S (ed) The chemistry of the thiol group, Part 2, 1974: p. 785-839.
943. Drozdz, R., J.W. Naskalski, and J. Sznajd, *Oxidation of amino acids and peptides in reaction with myeloperoxidase, chloride and hydrogen peroxide.* Biochim Biophys Acta, 1988. **957**(1): p. 47-52.
944. Pereira, W.E., et al., *Chlorination studies. II. The reaction of aqueous hypochlorous acid with alpha-amino acids and dipeptides.* Biochim Biophys Acta, 1973. **313**(1): p. 170-80.
945. Zgliczynski, J.M., et al., *Myeloperoxidase of human leukaemic leucocytes. Oxidation of amino acids in the presence of hydrogen peroxide.* Eur J Biochem, 1968. **4**(4): p. 540-7.
946. Clark, R.A., et al., *Oxidation of lysine side-chains of elastin by the myeloperoxidase system and by stimulated human neutrophils.* Biochem Biophys Res Commun, 1986. **135**(2): p. 451-7.
947. Hazell, L.J., J.J. van den Berg, and R. Stocker, *Oxidation of low-density lipoprotein by hypochlorite causes aggregation that is mediated by modification of lysine residues rather than lipid oxidation.* Biochem J, 1994. **302 (Pt 1)**: p. 297-304.
948. Hawkins, C.L., D.I. Pattison, and M.J. Davies, *Hypochlorite-induced oxidation of amino acids, peptides and proteins.* Amino Acids, 2003. **25**(3-4): p. 259-74.
949. Vissers, M.C. and C.C. Winterbourn, *Oxidative damage to fibronectin. I. The effects of the neutrophil myeloperoxidase system and HOCl.* Arch Biochem Biophys, 1991. **285**(1): p. 53-9.

950. Thomas, E.L., *Myeloperoxidase, hydrogen peroxide, chloride antimicrobial system: nitrogen-chlorine derivatives of bacterial components in bactericidal action against Escherichia coli.* Infect Immun, 1979. **23**(2): p. 522-31.
951. Prutz, W.A., *Consecutive halogen transfer between various functional groups induced by reaction of hypohalous acids: NADH oxidation by halogenated amide groups.* Arch Biochem Biophys, 1999. **371**(1): p. 107-14.
952. Nieder, M. and L. Hager, *Conversion of alpha-amino acids and peptides to nitriles and aldehydes by bromoperoxidase.* Arch Biochem Biophys, 1985. **240**(1): p. 121-7.
953. Knight, L.C. and M.J. Welch, *Sites of direct and indirect halogenation of albumin.* Biochim Biophys Acta, 1978. **534**(2): p. 185-95.
954. Buchberger, W., *Investigations into lactoperoxidase-catalysed bromination of tyrosine and thyroglobulin.* J Chromatogr, 1988. **432**: p. 57-63.
955. Fang, Y.Z., S. Yang, and G. Wu, *Free radicals, antioxidants, and nutrition.* Nutrition, 2002. **18**(10): p. 872-9.
956. Schoneich, C., *Methionine oxidation by reactive oxygen species: reaction mechanisms and relevance to Alzheimer's disease.* Biochim Biophys Acta, 2005. **1703**(2): p. 111-9.
957. Raftery, M.J., L. Collinson, and C.L. Geczy, *Overexpression, oxidative refolding, and zinc binding of recombinant forms of the murine S100 protein MRP14 (S100A9).* Protein Expr Purif, 1999. **15**(2): p. 228-35.
958. Vogt, W., *Oxidation of methionyl residues in proteins: tools, targets, and reversal.* Free Radic Biol Med, 1995. **18**(1): p. 93-105.
959. Maiti, P., et al., *Surprising toxicity and assembly behaviour of amyloid beta-protein oxidized to sulfone.* Biochem J, 2011. **433**(2): p. 323-32.
960. Winterbourn, C.C., *Comparative reactivities of various biological compounds with myeloperoxidase-hydrogen peroxide-chloride, and similarity of the oxidant to hypochlorite.* Biochim Biophys Acta, 1985. **840**(2): p. 204-10.
961. Boersema, P.J., et al., *Straightforward and de novo peptide sequencing by MALDI-MS/MS using a Lys-N metalloendopeptidase.* Mol Cell Proteomics, 2009. **8**(4): p. 650-60.
962. Pappin, D.J., P. Hojrup, and A.J. Bleasby, *Rapid identification of proteins by peptide-mass fingerprinting.* Curr Biol, 1993. **3**(6): p. 327-32.
963. Valko, M., et al., *Free radicals and antioxidants in normal physiological functions and human disease.* Int J Biochem Cell Biol, 2007. **39**(1): p. 44-84.
964. Lakshmi, S.V., et al., *Oxidative stress in cardiovascular disease.* Indian J Biochem Biophys, 2009. **46**(6): p. 421-40.
965. Riedl, M.A. and A.E. Nel, *Importance of oxidative stress in the pathogenesis and treatment of asthma.* Curr Opin Allergy Clin Immunol, 2008. **8**(1): p. 49-56.
966. Sorolla, M.A., et al., *Protein oxidation in Huntington disease.* Biofactors, 2012.
967. Venkateshappa, C., et al., *Elevated oxidative stress and decreased antioxidant function in the human hippocampus and frontal cortex with increasing age: implications for neurodegeneration in Alzheimer's disease.* Neurochem Res, 2012. **37**(8): p. 1601-14.
968. Acar, A., et al., *Evaluation of serum oxidant/antioxidant balance in multiple sclerosis.* Acta Neurol Belg, 2012.
969. Zhu, H. and Y.R. Li, *Oxidative stress and redox signaling mechanisms of inflammatory bowel disease: updated experimental and clinical evidence.* Exp Biol Med (Maywood), 2012. **237**(5): p. 474-80.

970. Halayko, A.J. and S. Ghavami, *S100A8/A9: a mediator of severe asthma pathogenesis and morbidity?* Can J Physiol Pharmacol, 2009. **87**(10): p. 743-55.
971. Averill, M.M., C. Kerkhoff, and K.E. Bornfeldt, *S100A8 and S100A9 in cardiovascular biology and disease.* Arterioscler Thromb Vasc Biol, 2012. **32**(2): p. 223-9.
972. Hazen, S.L. and J.W. Heinecke, *3-Chlorotyrosine, a specific marker of myeloperoxidase-catalyzed oxidation, is markedly elevated in low density lipoprotein isolated from human atherosclerotic intima.* J Clin Invest, 1997. **99**(9): p. 2075-81.
973. Heinecke, J.W., et al., *Dityrosine, a specific marker of oxidation, is synthesized by the myeloperoxidase-hydrogen peroxide system of human neutrophils and macrophages.* J Biol Chem, 1993. **268**(6): p. 4069-77.
974. Kettle, A.J., *Neutrophils convert tyrosyl residues in albumin to chlorotyrosine.* FEBS Lett, 1996. **379**(1): p. 103-6.
975. Speicher, K.D., et al., *Systematic analysis of peptide recoveries from in-gel digestions for protein identifications in proteome studies.* J Biomol Tech, 2000. **11**(2): p. 74-86.
976. Stewart, II, T. Thomson, and D. Figeys, *18O labeling: a tool for proteomics.* Rapid Commun Mass Spectrom, 2001. **15**(24): p. 2456-65.
977. Comhair, S.A. and S.C. Erzurum, *Redox control of asthma: molecular mechanisms and therapeutic opportunities.* Antioxid Redox Signal, 2010. **12**(1): p. 93-124.
978. Mary, J., et al., *Enzymatic reactions involved in the repair of oxidized proteins.* Exp Gerontol, 2004. **39**(8): p. 1117-23.
979. McCormick, M.L., et al., *Electron paramagnetic resonance detection of free tyrosyl radical generated by myeloperoxidase, lactoperoxidase, and horseradish peroxidase.* J Biol Chem, 1998. **273**(48): p. 32030-7.
980. Malle, E., et al., *Immunohistochemical evidence for the myeloperoxidase/H2O2/halide system in human atherosclerotic lesions: colocalization of myeloperoxidase and hypochlorite-modified proteins.* Eur J Biochem, 2000. **267**(14): p. 4495-503.
981. Heinecke, J.W., et al., *Detecting oxidative modification of biomolecules with isotope dilution mass spectrometry: sensitive and quantitative assays for oxidized amino acids in proteins and tissues.* Methods Enzymol, 1999. **300**: p. 124-44.
982. Buss, I.H., et al., *3-Chlorotyrosine as a marker of protein damage by myeloperoxidase in tracheal aspirates from preterm infants: association with adverse respiratory outcome.* Pediatr Res, 2003. **53**(3): p. 455-62.
983. Hawkins, C.L., P.E. Morgan, and M.J. Davies, *Quantification of protein modification by oxidants.* Free Radic Biol Med, 2009. **46**(8): p. 965-88.
984. Dalle-Donne, I., et al., *Protein carbonyl groups as biomarkers of oxidative stress.* Clin Chim Acta, 2003. **329**(1-2): p. 23-38.
985. Schoneich, C. and V.S. Sharov, *Mass spectrometry of protein modifications by reactive oxygen and nitrogen species.* Free Radic Biol Med, 2006. **41**(10): p. 1507-20.
986. Monteseirin, J., *Neutrophils and asthma.* J Investig Allergol Clin Immunol, 2009. **19**(5): p. 340-54.
987. Smith, G.C., D.G. Tew, and C.R. Wolf, *Dissection of NADPH-cytochrome P450 oxidoreductase into distinct functional domains.* Proc Natl Acad Sci U S A, 1994. **91**(18): p. 8710-4.

988. Hampton, M.B., A.J. Kettle, and C.C. Winterbourn, *Inside the neutrophil phagosome: oxidants, myeloperoxidase, and bacterial killing.* Blood, 1998. **92**(9): p. 3007-17.
989. Stone, J.R. and S. Yang, *Hydrogen peroxide: a signaling messenger.* Antioxid Redox Signal, 2006. **8**(3-4): p. 243-70.
990. Cho, Y.S. and H.B. Moon, *The role of oxidative stress in the pathogenesis of asthma.* Allergy Asthma Immunol Res, 2010. **2**(3): p. 183-7.
991. Angrill, J., C. Agusti, and A. Torres, *Bronchiectasis.* Curr Opin Infect Dis, 2001. **14**(2): p. 193-7.
992. Loukides, S., et al., *Exhaled H(2)O(2) in steady-state bronchiectasis: relationship with cellular composition in induced sputum, spirometry, and extent and severity of disease.* Chest, 2002. **121**(1): p. 81-7.
993. Wilson, C.B., et al., *Systemic markers of inflammation in stable bronchiectasis.* Eur Respir J, 1998. **12**(4): p. 820-4.
994. England, K. and T.G. Cotter, *Direct oxidative modifications of signalling proteins in mammalian cells and their effects on apoptosis.* Redox Rep, 2005. **10**(5): p. 237-45.
995. Niwa, T., *Protein glutathionylation and oxidative stress.* J Chromatogr B Analyt Technol Biomed Life Sci, 2007. **855**(1): p. 59-65.
996. Henke, M.O., et al., *Up-regulation of S100A8 and S100A9 protein in bronchial epithelial cells by lipopolysaccharide.* Exp Lung Res, 2006. **32**(8): p. 331-47.
997. Sharma, M., et al., *Association of a chromosome 1q21 locus in close proximity to a late cornified envelope-like proline-rich 1 (LELP1) gene with total serum IgE levels.* J Hum Genet, 2007. **52**(4): p. 378-83.
998. Brinkmann, V., et al., *Neutrophil extracellular traps kill bacteria.* Science, 2004. **303**(5663): p. 1532-5.
999. Bianchi, M., et al., *Restoration of anti-Aspergillus defense by neutrophil extracellular traps in human chronic granulomatous disease after gene therapy is calprotectin-dependent.* J Allergy Clin Immunol, 2011. **127**(5): p. 1243-1252 e7.
1000. Efthimiadis, A., et al., *Induced sputum cell and fluid-phase indices of inflammation: comparison of treatment with dithiothreitol vs phosphate-buffered saline.* Eur Respir J, 1997. **10**(6): p. 1336-40.
1001. Atienza, J.M., et al., *Dynamic and label-free cell-based assays using the real-time cell electronic sensing system.* Assay Drug Dev Technol, 2006. **4**(5): p. 597-607.
1002. Bisgaard, H., et al., *Childhood asthma after bacterial colonization of the airway in neonates.* N Engl J Med, 2007. **357**(15): p. 1487-95.
1003. Klemets, P., et al., *Risk of invasive pneumococcal infections among working age adults with asthma.* Thorax, 2010. **65**(8): p. 698-702.
1004. Sunahori, K., et al., *The S100A8/A9 heterodimer amplifies proinflammatory cytokine production by macrophages via activation of nuclear factor kappa B and p38 mitogen-activated protein kinase in rheumatoid arthritis.* Arthritis Res Ther, 2006. **8**(3): p. R69.
1005. Bianchi, M.E., *DAMPs, PAMPs and alarmins: all we need to know about danger.* J Leukoc Biol, 2007. **81**(1): p. 1-5.
1006. Fahy, J.V., et al., *Cellular and biochemical analysis of induced sputum from asthmatic and from healthy subjects.* Am Rev Respir Dis, 1993. **147**(5): p. 1126-31.
1007. Sweet, S.P., A.N. Denbury, and S.J. Challacombe, *Salivary calprotectin levels are raised in patients with oral candidiasis or Sjogren's syndrome but decreased by HIV infection.* Oral Microbiol Immunol, 2001. **16**(2): p. 119-23.

1008. Haigh, B.J., et al., *Alterations in the salivary proteome associated with periodontitis.* J Clin Periodontol, 2010. **37**(3): p. 241-7.
1009. Neyraud, E., et al., *Proteomic analysis of human whole and parotid salivas following stimulation by different tastes.* J Proteome Res, 2006. **5**(9): p. 2474-80.
1010. Hu, S., et al., *Differentially expressed protein markers in human submandibular and sublingual secretions.* Int J Oncol, 2004. **25**(5): p. 1423-30.
1011. Castagnola, M., et al., *The surprising composition of the salivary proteome of preterm human newborn.* Mol Cell Proteomics, 2011. **10**(1): p. M110 003467.
1012. Reeves, E.P., et al., *Nebulized hypertonic saline decreases IL-8 in sputum of patients with cystic fibrosis.* Am J Respir Crit Care Med, 2011. **183**(11): p. 1517-23.
1013. Davies, K.J., *Degradation of oxidized proteins by the 20S proteasome.* Biochimie, 2001. **83**(3-4): p. 301-10.
1014. Hawrylowicz, C.M. and A. O'Garra, *Potential role of interleukin-10-secreting regulatory T cells in allergy and asthma.* Nat Rev Immunol, 2005. **5**(4): p. 271-83.
1015. Busse, W.W. and J.E. Gern, *Is interleukin-10 a "10" in virus-provoked asthma?* Am J Respir Crit Care Med, 2005. **172**(4): p. 405-6.
1016. Biswas, S.K. and I. Rahman, *Environmental toxicity, redox signaling and lung inflammation: the role of glutathione.* Mol Aspects Med, 2009. **30**(1-2): p. 60-76.
1017. Fitzpatrick, A.M., et al., *Airway glutathione homeostasis is altered in children with severe asthma: evidence for oxidant stress.* J Allergy Clin Immunol, 2009. **123**(1): p. 146-152 e8.
1018. Hansel, A., et al., *A second human methionine sulfoxide reductase (hMSRB2) reducing methionine-R-sulfoxide displays a tissue expression pattern distinct from hMSRB1.* Redox Rep, 2003. **8**(6): p. 384-8.
1019. Fahy, J.V., *Eosinophilic and neutrophilic inflammation in asthma: insights from clinical studies.* Proc Am Thorac Soc, 2009. **6**(3): p. 256-9.
1020. Kapur, N., et al., *Lower airway microbiology and cellularity in children with newly diagnosed non-CF bronchiectasis.* Pediatr Pulmonol, 2012. **47**(3): p. 300-7.
1021. Herndon, B.L., et al., *Calcium-binding proteins MRP 8 and 14 in a Staphylococcus aureus infection model: role of therapy, inflammation, and infection persistence.* J Lab Clin Med, 2003. **141**(2): p. 110-20.
1022. Luo, S. and R.L. Levine, *Methionine in proteins defends against oxidative stress.* FASEB J, 2009. **23**(2): p. 464-72.
1023. Berthier, S., et al., *Molecular Interface of S100A8 with Cytochrome b and NADPH Oxidase Activation.* PLoS One, 2012. **7**(7): p. e40277.
1024. Libby, P., *Inflammation in atherosclerosis.* Nature, 2002. **420**(6917): p. 868-74.
1025. Ross, R., *Atherosclerosis--an inflammatory disease.* N Engl J Med, 1999. **340**(2): p. 115-26.
1026. Hahn, B.H. and M. McMahon, *Atherosclerosis and systemic lupus erythematosus: the role of altered lipids and of autoantibodies.* Lupus, 2008. **17**(5): p. 368-70.
1027. Sheikh, Z., et al., *Enhanced recognition of reactive oxygen species damaged human serum albumin by circulating systemic lupus erythematosus autoantibodies.* Autoimmunity, 2007. **40**(7): p. 512-20.
1028. Sugiyama, S., et al., *Macrophage myeloperoxidase regulation by granulocyte macrophage colony-stimulating factor in human atherosclerosis and implications in acute coronary syndromes.* Am J Pathol, 2001. **158**(3): p. 879-91.
1029. Heinecke, J.W., *Oxidative stress: new approaches to diagnosis and prognosis in atherosclerosis.* Am J Cardiol, 2003. **91**(3A): p. 12A-16A.

1030. Woods, A.A., S.M. Linton, and M.J. Davies, *Detection of HOCl-mediated protein oxidation products in the extracellular matrix of human atherosclerotic plaques.* Biochem J, 2003. **370**(Pt 2): p. 729-35.
1031. Heinecke, J.W., *Mechanisms of oxidative damage of low density lipoprotein in human atherosclerosis.* Curr Opin Lipidol, 1997. **8**(5): p. 268-74.
1032. Steinberg, D., *Lewis A. Conner Memorial Lecture. Oxidative modification of LDL and atherogenesis.* Circulation, 1997. **95**(4): p. 1062-71.
1033. Niki, E., *Do free radicals play causal role in atherosclerosis? Low density lipoprotein oxidation and vitamin E revisited.* J Clin Biochem Nutr, 2011. **48**(1): p. 3-7.
1034. Oorni, K., et al., *Oxidation of low density lipoprotein particles decreases their ability to bind to human aortic proteoglycans. Dependence on oxidative modification of the lysine residues.* J Biol Chem, 1997. **272**(34): p. 21303-11.
1035. Haberland, M.E., A.M. Fogelman, and P.A. Edwards, *Specificity of receptor-mediated recognition of malondialdehyde-modified low density lipoproteins.* Proc Natl Acad Sci U S A, 1982. **79**(6): p. 1712-6.
1036. Pentikainen, M.O., et al., *Modified LDL - trigger of atherosclerosis and inflammation in the arterial intima.* J Intern Med, 2000. **247**(3): p. 359-70.
1037. Aviram, M., *Review of human studies on oxidative damage and antioxidant protection related to cardiovascular diseases.* Free Radic Res, 2000. **33 Suppl**: p. S85-97.
1038. Leeuwenburgh, C., et al., *Mass spectrometric quantification of markers for protein oxidation by tyrosyl radical, copper, and hydroxyl radical in low density lipoprotein isolated from human atherosclerotic plaques.* J Biol Chem, 1997. **272**(6): p. 3520-6.
1039. Upston, J.M., et al., *Disease stage-dependent accumulation of lipid and protein oxidation products in human atherosclerosis.* Am J Pathol, 2002. **160**(2): p. 701-10.
1040. Asztalos, B.F., M. Tani, and E.J. Schaefer, *Metabolic and functional relevance of HDL subspecies.* Curr Opin Lipidol, 2011. **22**(3): p. 176-85.
1041. Fielding, C.J. and P.E. Fielding, *Molecular physiology of reverse cholesterol transport.* J Lipid Res, 1995. **36**(2): p. 211-28.
1042. Malle, E., et al., *Myeloperoxidase-mediated oxidation of high-density lipoproteins: fingerprints of newly recognized potential proatherogenic lipoproteins.* Arch Biochem Biophys, 2006. **445**(2): p. 245-55.
1043. Christison, J., et al., *Rapid reduction and removal of HDL- but not LDL-associated cholesteryl ester hydroperoxides by rat liver perfused in situ.* Biochem J, 1996. **314 (Pt 3)**: p. 739-42.
1044. Navab, M., et al., *Normal high density lipoprotein inhibits three steps in the formation of mildly oxidized low density lipoprotein: steps 2 and 3.* J Lipid Res, 2000. **41**(9): p. 1495-508.
1045. Nicholls, S.J., L. Zheng, and S.L. Hazen, *Formation of dysfunctional high-density lipoprotein by myeloperoxidase.* Trends Cardiovasc Med, 2005. **15**(6): p. 212-9.
1046. Navab, M., et al., *The role of dysfunctional HDL in atherosclerosis.* J Lipid Res, 2009. **50 Suppl**: p. S145-9.
1047. Zheng, L., et al., *Apolipoprotein A-I is a selective target for myeloperoxidase-catalyzed oxidation and functional impairment in subjects with cardiovascular disease.* J Clin Invest, 2004. **114**(4): p. 529-41.
1048. Zheng, L., et al., *Localization of nitration and chlorination sites on apolipoprotein A-I catalyzed by myeloperoxidase in human atheroma and associated oxidative*

impairment in ABCA1-dependent cholesterol efflux from macrophages. J Biol Chem, 2005. **280**(1): p. 38-47.
1049. Smith, J.D., *Dysfunctional HDL as a diagnostic and therapeutic target.* Arterioscler Thromb Vasc Biol, 2010. **30**(2): p. 151-5.
1050. Shao, B. and J.W. Heinecke, *Impact of HDL oxidation by the myeloperoxidase system on sterol efflux by the ABCA1 pathway.* J Proteomics, 2011. **74**(11): p. 2289-99.
1051. Cogny, A., et al., *High-density lipoprotein 3 physicochemical modifications induced by interaction with human polymorphonuclear leucocytes affect their ability to remove cholesterol from cells.* Biochem J, 1996. **314 (Pt 1)**: p. 285-92.
1052. Vinas, P., et al., *Determination of phenols in wines by liquid chromatography with photodiode array and fluorescence detection.* J Chromatogr A, 2000. **871**(1-2): p. 85-93.
1053. Zsila, F., Z. Bikadi, and M. Simonyi, *Probing the binding of the flavonoid, quercetin to human serum albumin by circular dichroism, electronic absorption spectroscopy and molecular modelling methods.* Biochem Pharmacol, 2003. **65**(3): p. 447-56.
1054. Hayek, T., et al., *Reduced progression of atherosclerosis in apolipoprotein E-deficient mice following consumption of red wine, or its polyphenols quercetin or catechin, is associated with reduced susceptibility of LDL to oxidation and aggregation.* Arterioscler Thromb Vasc Biol, 1997. **17**(11): p. 2744-52.
1055. Gaidukov, L. and D.S. Tawfik, *High affinity, stability, and lactonase activity of serum paraoxonase PON1 anchored on HDL with ApoA-I.* Biochemistry, 2005. **44**(35): p. 11843-54.
1056. Tsuzura, S., et al., *Correlation of plasma oxidized low-density lipoprotein levels to vascular complications and human serum paraoxonase in patients with type 2 diabetes.* Metabolism, 2004. **53**(3): p. 297-302.
1057. Getz, G.S. and C.A. Reardon, *Paraoxonase, a cardioprotective enzyme: continuing issues.* Curr Opin Lipidol, 2004. **15**(3): p. 261-7.
1058. Aviram, M., et al., *Human serum paraoxonase (PON 1) is inactivated by oxidized low density lipoprotein and preserved by antioxidants.* Free Radic Biol Med, 1999. **26**(7-8): p. 892-904.
1059. Nakashima, Y., et al., *ApoE-deficient mice develop lesions of all phases of atherosclerosis throughout the arterial tree.* Arterioscler Thromb, 1994. **14**(1): p. 133-40.
1060. Reddick, R.L., S.H. Zhang, and N. Maeda, *Atherosclerosis in mice lacking apo E. Evaluation of lesional development and progression.* Arterioscler Thromb, 1994. **14**(1): p. 141-7.
1061. Zhang, S.H., et al., *Spontaneous hypercholesterolemia and arterial lesions in mice lacking apolipoprotein E.* Science, 1992. **258**(5081): p. 468-71.
1062. Goldstein, J.L., et al., *Binding site on macrophages that mediates uptake and degradation of acetylated low density lipoprotein, producing massive cholesterol deposition.* Proc Natl Acad Sci U S A, 1979. **76**(1): p. 333-7.
1063. Katashima, T., et al., *Enhanced expression of the S100A8/A9 complex in acute myocardial infarction patients.* Circ J, 2010. **74**(4): p. 741-8.
1064. Ionita, M.G., et al., *High levels of myeloid-related protein 14 in human atherosclerotic plaques correlate with the characteristics of rupture-prone lesions.* Arterioscler Thromb Vasc Biol, 2009. **29**(8): p. 1220-7.

1065. Ehlermann, P., et al., *Increased proinflammatory endothelial response to S100A8/A9 after preactivation through advanced glycation end products.* Cardiovasc Diabetol, 2006. **5**: p. 6.
1066. Gu, L., et al., *Absence of monocyte chemoattractant protein-1 reduces atherosclerosis in low density lipoprotein receptor-deficient mice.* Mol Cell, 1998. **2**(2): p. 275-81.
1067. Boring, L., et al., *Decreased lesion formation in CCR2-/- mice reveals a role for chemokines in the initiation of atherosclerosis.* Nature, 1998. **394**(6696): p. 894-7.
1068. Yee, C.S., et al., *Revised British Isles Lupus Assessment Group 2004 index: a reliable tool for assessment of systemic lupus erythematosus activity.* Arthritis Rheum, 2006. **54**(10): p. 3300-5.
1069. Glaros, E.N., et al., *Inhibition of atherosclerosis by the serine palmitoyl transferase inhibitor myriocin is associated with reduced plasma glycosphingolipid concentration.* Biochem Pharmacol, 2007. **73**(9): p. 1340-6.
1070. Sattler, W., D. Mohr, and R. Stocker, *Rapid isolation of lipoproteins and assessment of their peroxidation by high-performance liquid chromatography postcolumn chemiluminescence.* Methods Enzymol, 1994. **233**: p. 469-89.
1071. Wang, X.S., et al., *A sensitive and specific ELISA detects methionine sulfoxide-containing apolipoprotein A-I in HDL.* J Lipid Res, 2009. **50**(3): p. 586-94.
1072. Panasenko, O.M., et al., *Myeloperoxidase-induced formation of chlorohydrins and lysophospholipids from unsaturated phosphatidylcholines.* Free Radic Biol Med, 2003. **34**(5): p. 553-62.
1073. Thomas, S.R., P.K. Witting, and G.R. Drummond, *Redox control of endothelial function and dysfunction: molecular mechanisms and therapeutic opportunities.* Antioxid Redox Signal, 2008. **10**(10): p. 1713-65.
1074. Perkins, D.N., et al., *Probability-based protein identification by searching sequence databases using mass spectrometry data.* Electrophoresis, 1999. **20**(18): p. 3551-67.
1075. Yee, C.S., et al., *BILAG-2004 index captures systemic lupus erythematosus disease activity better than SLEDAI-2000.* Ann Rheum Dis, 2008. **67**(6): p. 873-6.
1076. Cybulsky, M.I. and M.A. Gimbrone, Jr., *Endothelial expression of a mononuclear leukocyte adhesion molecule during atherogenesis.* Science, 1991. **251**(4995): p. 788-91.
1077. Nakashima, Y., et al., *Upregulation of VCAM-1 and ICAM-1 at atherosclerosis-prone sites on the endothelium in the ApoE-deficient mouse.* Arterioscler Thromb Vasc Biol, 1998. **18**(5): p. 842-51.
1078. Kimura, T., et al., *Induction of scavenger receptor class B type I is critical for simvastatin enhancement of high-density lipoprotein-induced anti-inflammatory actions in endothelial cells.* J Immunol, 2008. **181**(10): p. 7332-40.
1079. Hazell, L.J., et al., *Presence of hypochlorite-modified proteins in human atherosclerotic lesions.* J Clin Invest, 1996. **97**(6): p. 1535-44.
1080. Peng, W.H., et al., *Increased serum myeloid-related protein 8/14 level is associated with atherosclerosis in type 2 diabetic patients.* Cardiovasc Diabetol, 2011. **10**: p. 41.
1081. Bouma, G., et al., *Increased serum levels of MRP-8/14 in type 1 diabetes induce an increased expression of CD11b and an enhanced adhesion of circulating monocytes to fibronectin.* Diabetes, 2004. **53**(8): p. 1979-86.
1082. Schindhelm, R.K., et al., *Myeloperoxidase: a useful biomarker for cardiovascular disease risk stratification?* Clin Chem, 2009. **55**(8): p. 1462-70.

1083. Brevetti, G., et al., *Myeloperoxidase, but not C-reactive protein, predicts cardiovascular risk in peripheral arterial disease.* Eur Heart J, 2008. **29**(2): p. 224-30.
1084. Dominguez-Rodriguez, A., et al., *Prognostic value of admission myeloperoxidase levels in patients with ST-segment elevation myocardial infarction and cardiogenic shock.* Am J Cardiol, 2008. **101**(11): p. 1537-40.
1085. Zhang, Q., et al., *Oxidative protein damage and antioxidant status in systemic lupus erythematosus.* Clin Exp Dermatol, 2010. **35**(3): p. 287-94.
1086. Svenungsson, E., et al., *Risk factors for cardiovascular disease in systemic lupus erythematosus.* Circulation, 2001. **104**(16): p. 1887-93.
1087. Baldus, S., et al., *Endothelial transcytosis of myeloperoxidase confers specificity to vascular ECM proteins as targets of tyrosine nitration.* J Clin Invest, 2001. **108**(12): p. 1759-70.
1088. Eiserich, J.P., et al., *Myeloperoxidase, a leukocyte-derived vascular NO oxidase.* Science, 2002. **296**(5577): p. 2391-4.
1089. Zhang, C., et al., *Interaction of myeloperoxidase with vascular NAD(P)H oxidase-derived reactive oxygen species in vasculature: implications for vascular diseases.* Am J Physiol Heart Circ Physiol, 2003. **285**(6): p. H2563-72.
1090. Sugiyama, S., et al., *Hypochlorous acid, a macrophage product, induces endothelial apoptosis and tissue factor expression: involvement of myeloperoxidase-mediated oxidant in plaque erosion and thrombogenesis.* Arterioscler Thromb Vasc Biol, 2004. **24**(7): p. 1309-14.
1091. Kaslow, R.A. and A.T. Masi, *Age, sex, and race effects on mortality from systemic lupus erythematosus in the United States.* Arthritis Rheum, 1978. **21**(4): p. 473-9.
1092. de Seny, D., et al., *Monomeric calgranulins measured by SELDI-TOF mass spectrometry and calprotectin measured by ELISA as biomarkers in arthritis.* Clin Chem, 2008. **54**(6): p. 1066-75.
1093. Carvalho, P.C., et al., *Identifying differences in protein expression levels by spectral counting and feature selection.* Genet Mol Res, 2008. **7**(2): p. 342-56.
1094. Heo, S.H., et al., *Identification of putative serum glycoprotein biomarkers for human lung adenocarcinoma by multilectin affinity chromatography and LC-MS/MS.* Proteomics, 2007. **7**(23): p. 4292-302.
1095. Santucci, L., et al., *Protein-protein interaction heterogeneity of plasma apolipoprotein A1 in nephrotic syndrome.* Mol Biosyst, 2011. **7**(3): p. 659-66.
1096. Qian, W.J., et al., *Enhanced detection of low abundance human plasma proteins using a tandem IgY12-SuperMix immunoaffinity separation strategy.* Mol Cell Proteomics, 2008. **7**(10): p. 1963-73.
1097. Qian, W.J., et al., *Advances and challenges in liquid chromatography-mass spectrometry-based proteomics profiling for clinical applications.* Mol Cell Proteomics, 2006. **5**(10): p. 1727-44.
1098. Anderson, N.L. and N.G. Anderson, *The human plasma proteome: history, character, and diagnostic prospects.* Mol Cell Proteomics, 2002. **1**(11): p. 845-67.
1099. Liu, T., et al., *Evaluation of multiprotein immunoaffinity subtraction for plasma proteomics and candidate biomarker discovery using mass spectrometry.* Mol Cell Proteomics, 2006. **5**(11): p. 2167-74.
1100. Stocker, R. and J.F. Keaney, Jr., *Role of oxidative modifications in atherosclerosis.* Physiol Rev, 2004. **84**(4): p. 1381-478.
1101. Francis, G.A., *High density lipoprotein oxidation: in vitro susceptibility and potential in vivo consequences.* Biochim Biophys Acta, 2000. **1483**(2): p. 217-35.

1102. Mackness, B., et al., *Paraoxonase-1 inhibits oxidised LDL-induced MCP-1 production by endothelial cells.* Biochem Biophys Res Commun, 2004. **318**(3): p. 680-3.
1103. Wasil, M., et al., *The antioxidant action of human extracellular fluids. Effect of human serum and its protein components on the inactivation of alpha 1-antiproteinase by hypochlorous acid and by hydrogen peroxide.* Biochem J, 1987. **243**(1): p. 219-23.
1104. Salavej, P., H. Spalteholz, and J. Arnhold, *Modification of amino acid residues in human serum albumin by myeloperoxidase.* Free Radic Biol Med, 2006. **40**(3): p. 516-25.
1105. Weiss, S.J., *Tissue destruction by neutrophils.* N Engl J Med, 1989. **320**(6): p. 365-76.
1106. Maldonado, E.N., et al., *Lipid and fatty acid composition of canine lipoproteins.* Comp Biochem Physiol B Biochem Mol Biol, 2001. **128**(4): p. 719-29.
1107. Kotronen, A., et al., *Serum saturated fatty acids containing triacylglycerols are better markers of insulin resistance than total serum triacylglycerol concentrations.* Diabetologia, 2009. **52**(4): p. 684-90.
1108. Edelstein, C., et al., *Apolipoproteins and the structural organization of plasma lipoproteins: human plasma high density lipoprotein-3.* J Lipid Res, 1979. **20**(2): p. 143-53.
1109. Bowry, V.W., K.K. Stanley, and R. Stocker, *High density lipoprotein is the major carrier of lipid hydroperoxides in human blood plasma from fasting donors.* Proc Natl Acad Sci U S A, 1992. **89**(21): p. 10316-20.
1110. Jonas, A., *Interaction of phosphatidylcholine with bovine serum albumin. Specificity and properties of the complexes.* Biochim Biophys Acta, 1976. **427**(1): p. 325-36.
1111. Voshol, P.J., et al., *Effect of plasma triglyceride metabolism on lipid storage in adipose tissue: studies using genetically engineered mouse models.* Biochim Biophys Acta, 2009. **1791**(6): p. 479-85.
1112. Teusink, B., et al., *Contribution of fatty acids released from lipolysis of plasma triglycerides to total plasma fatty acid flux and tissue-specific fatty acid uptake.* Diabetes, 2003. **52**(3): p. 614-20.
1113. Leukert, N., C. Sorg, and J. Roth, *Molecular basis of the complex formation between the two calcium-binding proteins S100A8 (MRP8) and S100A9 (MRP14).* Biol Chem, 2005. **386**(5): p. 429-34.
1114. Baker, P.W., et al., *Ability of reconstituted high density lipoproteins to inhibit cytokine-induced expression of vascular cell adhesion molecule-1 in human umbilical vein endothelial cells.* J Lipid Res, 1999. **40**(2): p. 345-53.
1115. Barter, P.J., et al., *Antiinflammatory properties of HDL.* Circ Res, 2004. **95**(8): p. 764-72.
1116. Hessler, J.R., A.L. Robertson, Jr., and G.M. Chisolm, 3rd, *LDL-induced cytotoxicity and its inhibition by HDL in human vascular smooth muscle and endothelial cells in culture.* Atherosclerosis, 1979. **32**(3): p. 213-29.
1117. Van Lenten, B.J., et al., *Anti-inflammatory HDL becomes pro-inflammatory during the acute phase response. Loss of protective effect of HDL against LDL oxidation in aortic wall cell cocultures.* J Clin Invest, 1995. **96**(6): p. 2758-67.
1118. Van Lenten, B.J., et al., *High-density lipoprotein loses its anti-inflammatory properties during acute influenza a infection.* Circulation, 2001. **103**(18): p. 2283-8.

1119. Cockerill, G.W., et al., *Elevation of plasma high-density lipoprotein concentration reduces interleukin-1-induced expression of E-selectin in an in vivo model of acute inflammation.* Circulation, 2001. **103**(1): p. 108-12.
1120. Bozonet, S.M., et al., *Hypothiocyanous acid is a potent inhibitor of apoptosis and caspase 3 activation in endothelial cells.* Free Radic Biol Med, 2010. **49**(6): p. 1054-63.
1121. Halliwell, B., *Phagocyte-derived reactive species: salvation or suicide?* Trends Biochem Sci, 2006. **31**(9): p. 509-15.
1122. Valentine, J.S., *Biological Inorganic Chemistry Structure and Reactivity*. Sausalito: Univeristy Science Books, 2007: p. 31-41.
1123. Maisonneuve, E., et al., *Rules governing selective protein carbonylation.* PLoS One, 2009. **4**(10): p. e7269.
1124. Turner, G.C. and A. Varshavsky, *Detecting and measuring cotranslational protein degradation in vivo.* Science, 2000. **289**(5487): p. 2117-20.
1125. Wickner, S., M.R. Maurizi, and S. Gottesman, *Posttranslational quality control: folding, refolding, and degrading proteins.* Science, 1999. **286**(5446): p. 1888-93.
1126. Squier, T.C., *Oxidative stress and protein aggregation during biological aging.* Exp Gerontol, 2001. **36**(9): p. 1539-50.
1127. Yanamandra, K., et al., *Amyloid formation by the pro-inflammatory S100A8/A9 proteins in the ageing prostate.* PLoS One, 2009. **4**(5): p. e5562.
1128. Rauhamaki, V., et al., *Identification of a histidine-tyrosine cross-link in the active site of the cbb3-type cytochrome c oxidase from Rhodobacter sphaeroides.* Proc Natl Acad Sci U S A, 2006. **103**(44): p. 16135-40.
1129. Olsen, J.V., S.E. Ong, and M. Mann, *Trypsin cleaves exclusively C-terminal to arginine and lysine residues.* Mol Cell Proteomics, 2004. **3**(6): p. 608-14.
1130. Oetjen, J., S. Rexroth, and B. Reinhold-Hurek, *Mass spectrometric characterization of the covalent modification of the nitrogenase Fe-protein in Azoarcus sp. BH72.* FEBS J, 2009. **276**(13): p. 3618-27.
1131. Moskovitz, J., et al., *Methionine sulfoxide reductase (MsrA) is a regulator of antioxidant defense and lifespan in mammals.* Proc Natl Acad Sci U S A, 2001. **98**(23): p. 12920-5.
1132. Stadtman, E.R. and R.L. Levine, *Free radical-mediated oxidation of free amino acids and amino acid residues in proteins.* Amino Acids, 2003. **25**(3-4): p. 207-18.
1133. Pattison, D.I., M.J. Davies, and C.L. Hawkins, *Reactions and reactivity of myeloperoxidase-derived oxidants: Differential biological effects of hypochlorous and hypothiocyanous acids.* Free Radic Res, 2012. **46**(8): p. 975-95.
1134. Skaff, O., D.I. Pattison, and M.J. Davies, *Hypothiocyanous acid reactivity with low-molecular-mass and protein thiols: absolute rate constants and assessment of biological relevance.* Biochem J, 2009. **422**(1): p. 111-7.
1135. Ying, J., et al., *Thiol oxidation in signaling and response to stress: detection and quantification of physiological and pathophysiological thiol modifications.* Free Radic Biol Med, 2007. **43**(8): p. 1099-108.
1136. Stockley, R.A., *Neutrophils and the pathogenesis of COPD.* Chest, 2002. **121**(5 Suppl): p. 151S-155S.
1137. Stockley, R.A., *Neutrophils and protease/antiprotease imbalance.* Am J Respir Crit Care Med, 1999. **160**(5 Pt 2): p. S49-52.
1138. Hill, A., S. Gompertz, and R. Stockley, *Factors influencing airway inflammation in chronic obstructive pulmonary disease.* Thorax, 2000. **55**(11): p. 970-7.

1139. Bartoli, M.L., et al., *Some factors influencing quality of spontaneous or induced sputum for inflammatory cell analysis.* Monaldi Arch Chest Dis, 2007. **67**(2): p. 81-3.
1140. Pitchenik, A.E., et al., *Sputum examination for the diagnosis of Pneumocystis carinii pneumonia in the acquired immunodeficiency syndrome.* Am Rev Respir Dis, 1986. **133**(2): p. 226-9.
1141. Pin, I., et al., *Use of induced sputum cell counts to investigate airway inflammation in asthma.* Thorax, 1992. **47**(1): p. 25-9.
1142. Carpagnano, G.E., et al., *Use of exhaled breath condensate in the study of airway inflammation after hypertonic saline solution challenge.* Chest, 2005. **128**(5): p. 3159-66.
1143. Manzanares, D., et al., *Modification of tryptophan and methionine residues is implicated in the oxidative inactivation of surfactant protein B.* Biochemistry, 2007. **46**(18): p. 5604-15.
1144. van der Flier, A. and A. Sonnenberg, *Function and interactions of integrins.* Cell Tissue Res, 2001. **305**(3): p. 285-98.
1145. Ryckman, C., et al., *Role of S100A8 and S100A9 in neutrophil recruitment in response to monosodium urate monohydrate crystals in the air-pouch model of acute gouty arthritis.* Arthritis Rheum, 2003. **48**(8): p. 2310-20.
1146. Luijk, B., et al., *Gradual increase in priming of human eosinophils during extravasation from peripheral blood to the airways in response to allergen challenge.* J Allergy Clin Immunol, 2005. **115**(5): p. 997-1003.
1147. Warringa, R.A., et al., *Upregulation of formyl-peptide and interleukin-8-induced eosinophil chemotaxis in patients with allergic asthma.* J Allergy Clin Immunol, 1993. **91**(6): p. 1198-205.
1148. Moser, R., et al., *Migration of primed human eosinophils across cytokine-activated endothelial cell monolayers.* Blood, 1992. **79**(11): p. 2937-45.
1149. Ebisawa, M., et al., *Eosinophil transendothelial migration induced by cytokines. II. Potentiation of eosinophil transendothelial migration by eosinophil-active cytokines.* J Immunol, 1994. **152**(9): p. 4590-6.
1150. Kanters, D., et al., *Expression of activated Fc gamma RII discriminates between multiple granulocyte-priming phenotypes in peripheral blood of allergic asthmatic subjects.* J Allergy Clin Immunol, 2007. **120**(5): p. 1073-81.
1151. Moskwa, P., et al., *A novel host defense system of airways is defective in cystic fibrosis.* Am J Respir Crit Care Med, 2007. **175**(2): p. 174-83.
1152. Minarowski, L., et al., *Thiocyanate concentration in saliva of cystic fibrosis patients.* Folia Histochem Cytobiol, 2008. **46**(2): p. 245-6.
1153. Xu, Y., S. Szep, and Z. Lu, *The antioxidant role of thiocyanate in the pathogenesis of cystic fibrosis and other inflammation-related diseases.* Proc Natl Acad Sci U S A, 2009. **106**(48): p. 20515-9.
1154. Gould, N.S., et al., *Hypertonic saline increases lung epithelial lining fluid glutathione and thiocyanate: two protective CFTR-dependent thiols against oxidative injury.* Respir Res, 2010. **11**: p. 119.
1155. Churg, A., et al., *Late intervention with a myeloperoxidase inhibitor stops progression of experimental chronic obstructive pulmonary disease.* Am J Respir Crit Care Med, 2012. **185**(1): p. 34-43.
1156. Turesson, C., A. Jarenros, and L. Jacobsson, *Increased incidence of cardiovascular disease in patients with rheumatoid arthritis: results from a community based study.* Ann Rheum Dis, 2004. **63**(8): p. 952-5.

1157. Roman, M.J., et al., *Prevalence and correlates of accelerated atherosclerosis in systemic lupus erythematosus.* N Engl J Med, 2003. **349**(25): p. 2399-406.
1158. Lee, H.M., S.T. Truong, and N.D. Wong, *Association of adult-onset asthma with specific cardiovascular conditions.* Respir Med, 2012. **106**(7): p. 948-53.
1159. Yao, X., et al., *Apolipoprotein mimetic peptides: a new approach for the treatment of asthma.* Front Pharmacol, 2012. **3**: p. 37.
1160. Ansell, B.J., et al., *Inflammatory/antiinflammatory properties of high-density lipoprotein distinguish patients from control subjects better than high-density lipoprotein cholesterol levels and are favorably affected by simvastatin treatment.* Circulation, 2003. **108**(22): p. 2751-6.
1161. Wiesner, P., et al., *Lipid profiling of FPLC-separated lipoprotein fractions by electrospray ionization tandem mass spectrometry.* J Lipid Res, 2009. **50**(3): p. 574-85.
1162. Srikrishna, G., et al., *Carboxylated glycans mediate colitis through activation of NF-kappa B.* J Immunol, 2005. **175**(8): p. 5412-22.
1163. Nicholls, S.J. and S.L. Hazen, *Myeloperoxidase and cardiovascular disease.* Arterioscler Thromb Vasc Biol, 2005. **25**(6): p. 1102-11.
1164. Vaisman, B.L., et al., *Endothelial expression of human ABCA1 in mice increases plasma HDL cholesterol and reduces diet-induced atherosclerosis.* J Lipid Res, 2012. **53**(1): p. 158-67.
1165. Pober, J.S., W. Min, and J.R. Bradley, *Mechanisms of endothelial dysfunction, injury, and death.* Annu Rev Pathol, 2009. **4**: p. 71-95.
1166. Otsuka, K., et al., *Suppression of inflammation in rat autoimmune myocarditis by S100A8/A9 through modulation of the proinflammatory cytokine network.* Eur J Heart Fail, 2009. **11**(3): p. 229-37.
1167. Yates, J.R., C.I. Ruse, and A. Nakorchevsky, *Proteomics by mass spectrometry: approaches, advances, and applications.* Annu Rev Biomed Eng, 2009. **11**: p. 49-79.

APPENDIX I: COMMON CHEMICALS AND REAGENTS

General chemicals	Suppliers
3,3´,5,5´-tetramethyl benzidine (TMB)	Pierce (IL, USA)
40% acrylamine/Bis Solution, 29:1 (3.3% C)	Bio-Rad (CA, USA)
Acetic acid	Ajac (Taren Point, Australia)
Acetonitrile	Ajax
Ammonium persulfate	Bio-Rad
Ampicillin	Sigma (MO, USA)
Biotinylated goat anti-rabbit IgG	Chemicon (Vic, Australia)
Bis (sulfosuccinimidyl) suberate (BS_3)	Pierce (IL, USA)
Bovine serum albumin (BSA)	Sigma
Bicinchoninic acid (BCA) assay reagent	Thermo Fisher Scientific
Bradford Protein Assay	Bio-Rad
Brilliant Blue R	Sigma
Bromophenol Blue	Bio-Rad
$CaCl_2$	Sigma
CNBr-activated sepharose	Amersham (Buckinghamshire, UK)
Colloidal Blue Staining kit	Invitrogen (NY, USA)
Complete® proteinase inhibitors	Roche (Mannheim, Germany)
Dithiothreitol (DTT)	Bio-Rad
Endoproteinase AspN	Roche
Enhanced chemiluminescence reagents	Perkin Elmer (Waverly,
Ethylenediaminetetraacetic acid (EDTA)	Sigma
Ethylene-glycol-bis[beta-aminoethylether]-N,N,N´,N´-tetraacetic acid (EGTA)	Sigma
EZ-link sulfo-NHS LC-biotin	Pierce
Filter syringes	Millipore (MA, USA)
Formic acid	Honeywell Riedel de Haen (NJ, USA)
Freud's adjuvant (complete and incomplete)	Sigma
Glutathione-agarose	Sigma
Glycerol, for molecular biology, minimum 99%	Sigma
Glycine for electrophoresis, purity 99%	MP Biomedicals (OH, USA)
Goat anti-rabbit IgG-HRP conjugate	Bio-Rad
HCl	VWR International (QLD, Australia)
Horseradish peroxidase conjugated goat anti-rabbit IgG	Bio-Rad
Human serum albumin (HSA)	Sigma
Iodoacetamide	Sigma
Isopropyl-β-D-thiogalactoside (IPTG)	Invitrogen
Lennox broth (LB)	Sigma
L-methionine	Sigma
Methanol	Ajax
N,N,N´,N´-tetramethylethylene-diamine (TEMED)	Sigma
NaCl	Sigma
NaH_2PO_4	Ajax

$NaHCO_3$	Ajax
NH_4HCO_3	Sigma
Polyoxyethylenesorbitan monolaurate (Tween 20)	Sigma
Potassium bromide	Sigma
Polyvinylidene difluoride (PVDF) membranes	Millipore
Protein-A sepharose CL-4B	Pharmacia, NY, USA
Sodium dodecyl sulphate (SDS)	Sigma
SDS-PAGE and Western blot apparatus	Bio-Rad
Sodium hypochlorite	Sigma
Streptavidin-conjugated HRP	R&D Systems (MN, USA)
Sulfo-NHS-LC-biotin	Pierce
Thrombin	Sigma
Triton X-100	Sigma
Tricine	Sigma
Trifluoroacetic acid	Sigma
Tris	MP Biomedicals
Trypsin	Roche Diagnostics